UNCLASSIFIED

AD NUMBER
AD903305
LIMITATION CHANGES
TO: **Approved for public release; distribution is unlimited.**
FROM: **Distribution authorized to U.S. Gov't. agencies only; Test and Evaluation; 11 JUL 1972. Other requests shall be referred to Air Force Cambridge Research Laboratories, Attn: OPI, L. G. Hanscom Field, Bedford MA 01730.**
AUTHORITY
AFGL ltr, 15 Jan 1981

THIS PAGE IS UNCLASSIFIED

AFCRL-72-0353

ATMOSPHERIC EMISSION AT HIGH LATITUDES

by

David G. Murcray, D. Boyd Barker, James N. Brooks
John J. Kosters, Frank H. Murcray and Walter J. Williams

Department of Physics
University of Denver
Denver, Colorado 80210

Contract: F19628-71-C-0171
Project No. 8692

FINAL REPORT

Period Covered: 1 April 1971 to 1 April 1972

June 1972

Contract Monitor: Robert A. McClatchey
Optical Physics Laboratory

Sponsored by
Defense Advanced Research Project Agency
ARPA Order No. 1366
Monitored by
Air Force Cambridge Research Laboratories

BEST
AVAILABLE COPY

THIS REPORT HAS BEEN DELIMITED AND CLEARED FOR PUBLIC RELEASE UNDER DOD DIRECTIVE 5200.20 AND NO RESTRICTIONS ARE IMPOSED UPON ITS USE AND DISCLOSURE.

DISTRIBUTION STATEMENT A

APPROVED FOR PUBLIC RELEASE;
DISTRIBUTION UNLIMITED.

ARPA Order No. 1366

Program Code No. 1E50

Contractor: University of Denver

Effective Date of Contract:
26 March 1971

Contract No. F19628-71-C-0171

Principal investigator and phone no.
Dr. David G. Murcray/303 753-2627

AFCRL project scientist and phone no.
Dr. Robert A. McClatchey/617 861-3224

Contract expiration date: 29 February 1972

AFCRL-72-0353

ATMOSPHERIC EMISSION AT HIGH LATITUDES

by

David G. Murcray, D. Boyd Barker, James N. Brooks
John J. Kosters, Frank H. Murcray and Walter J. Williams

Department of Physics
University of Denver
Denver, Colorado 80210

Contract: F19628-71-C-0171
Project No. 8692

FINAL REPORT

Period Covered: 1 April 1971 to 1 April 1972

June 1972

Contract Monitor: Robert A. McClatchey
Optical Physics Laboratory

Distribution limited to U.S. Government agencies only; Test and Evaluation, 11 July 1972. Other requests for this document must be referred to AFCRL (OPI), L.G. Hanscom Field, Bedford Massachusetts 01730.

Sponsored by
Defense Advanced Research Project Agency
ARPA Order No. 1366
Monitored by
Air Force Cambridge Research Laboratories

ABSTRACT

The primary emphasis under this contract has been to obtain infrared emission measurements during known auroral activity. Three balloon flights were made from Fairbanks, Alaska to accomplish this. On two of these flights moderate auroral activity occurred, but there was no enhancement in the emission spectrum from 9-14μm. The time of night that these measurements were made was several hours earlier than the time when observations of enhanced infrared emission were made on 13 September 1969.

A total of six balloon flights was conducted during the contract period. Data from four of these flights is presented in this report and a summary of the data reports covering the other two flights is also included.

TABLE OF CONTENTS

LIST OF FIGURES

I. INTRODUCTION

This program was a continuation of the work performed under contract F19628-68-C-0233. The object has been to investigate the spectral nature of the absorption and radiant emittance of the lower stratosphere as a function of altitude and geographic location on an absolute basis. The primary emphasis has been on the atmospheric emission in the 16-30μm region and on the possible emission in that region and in the 9-13μm region by aurorally excited phenomena. In addition, transmittance data for the 3-5μm region were obtained.

A basic question exists concerning the nature of the atmospheric "windows" in the infrared at observational latitudes within the auroral oval: Are the properties of these "windows" the same at auroral latitudes as at mid-latitudes or is there a radiant enhancement? In September 1969 such an enhancement was observed in the 11-12μm region. To understand this phenomenon, it is first necessary to define it through measurement. Such measurement should include magnitude, spectral nature, temporal properties, spatial properties and any related, defined auroral activities.

An experimental program designed to measure these parameters constituted the primary effort under this contract. The infrared instruments necessary for these measurements were developed on a previous contract. Auxiliary experiments to define the auroral activity during the infrared observations were developed under this contract. Each of these is discussed separately. The purpose of each flight is stated, the instruments flown are described and the results along with any analysis are either presented or summarized. All the data collected under this contract have been presented in Data Reports or are being presented here. In addition, tapes on all these flights have been completed. On the 18 January 1972 flight, selected records only are presented here and on tape. When additional records from that flight are available, they will be supplied to the contract monitor.

II. INSTRUMENTATION

Some of the instruments and instrumentation used on this contract were built on earlier contracts. These instruments are described here briefly. A set of filter photometers was designed and constructed for this contract and described in an earlier report. A brief description from that report is included here.

The data obtained with the instruments were recorded on board the balloon payload by means of two digital magnetic tape recorders. Parallel outputs were also telemetered by means of an FM/FM telemetry system, which monitored the system performance in real time and also was a backup in case of a malfunction of the on board recorders. Power for operation of the various units was supplied by means of a 28 vdc silver-zinc primary battery pack. All mechanical operations were accomplished by means of 400 Hz motors. The instrumentation was mounted in a gondola constructed of electrical conduit. The following instruments were used during the flight program.

1. D.U. Filter Radiometer. This instrument was built on the previous contract and described in detail in reports under that contract. A brief description is included here. To attain the required sensitivity, all of the optical components in the field of view of the detector are cooled to 77° K. The boil off gas from the liquid nitrogen coolant is vented into the back of the instrument. This flushing gas flows out through the entrance aperture and over a series of baffles which are used to reduce the stray radiation in the system and also to keep ambient air from reaching the cold optical surfaces of the radiometer and frosting them. The system employs a tuning fork chopper which interrupts the incoming radiation at a 156 Hz rate. The radiation passes through a filter wheel with positions for 5 filters after which it is focused onto the Ge:Cu detector. The ac signal out of the detector is synchronously rectified and amplified. The dc signal is

brought out at three levels of amplification for recording.

2. D. U. Spectral Radiometer. The spectral radiometer employs a cassegrainian design with a Bausch and Lomb replica grating used as a dispersing element. Incoming radiation is interrupted at a 150 Hz rate with a tuning fork chopper just in front of the spectrometer entrance slit. Radiation passing through the exit slit is imaged onto the Ge:Cu detector and the ac output is rectified and recorded. The whole unit is enclosed in a container which is cooled to 77° K by liquid nitrogen. As in the filter instrument, the boil off nitrogen gas is again vented into the back of the instrument and used for anti-frost.

3. Transmission Instrumentation. The preceeding two units are designed to measure the atmospheric emission in selected wavelength regions. The transmittance instrumentation is designed to measure the atmospheric transmittance at various altitudes. These data are obtained by studying the variation of the solar spectrum in various wavelength intervals with altitude. The system consists of a biaxial pointing control which is used to maintain the solar radiation on the entrance slit of the spectrometer and a Czerny Turner 1/2 meter grating spectrometer which uses a small Littrow prism spectrometer as a predisperser and employs a Ge:Cu detector. The radiation is double passed after being interrupted by a tuning fork chopper at a 750 Hz rate after the first pass. This reduces the scattered light and also increases the resolution while keeping the spectrometer small. This instrumentation is described in an article in Applied Optics.[1]

4. Photometers. A six channel visible photometer system was constructed and calibrated for use on the Alaskan auroral flights. The visible photometers are designed to have the same field of view as the infrared instruments and are positioned on the gondola so that they are optically aligned with the infrared instruments. These units

employ photomultiplier tubes as detectors. Two different tubes are used in order to get good responses over the full wavelength range desired. An RCA 4516 equipped with a bialkali photocathode No. 115 is used for the wavelength regions from 3200 to 6000Å and an RCA 8644 with an S-20 spectral response is used for the regions from 6000 to 7800Å. During the flights, the following filters were used in the photometers: 3914Å BW25Å, 4229Å BW10Å, 4280Å BW10Å, 5725Å BW50Å, 6300Å BW25Å and 7625Å BW30Å. The photometers were operated in the dc mode and were calibrated at the AFCRL Optical Physics Laboratory facility. This facility uses a high temperature blackbody source equipped with various apertures as the calibration source. The calibration included the range of radiance values to be expected from both weak and strong auroral events.

All photometer components were chosen so as to minimize any variation in sensitivity with temperature. Since the filter band pass is temperature dependent, the unit was designed so that all filters were mounted on a common plate and the temperature of the plate was thermostatically controlled. As a result of these factors, the temperature of the total system did not vary significantly during the flights.

All units are built for balloon use and are designed to operate automatically in the environment to which they are subjected during a balloon flight. This includes being constructed so as to withstand the accelerations normally encountered during a balloon flight.

III. FLIGHT PROGRAM

Six balloon flights were completed under this contract. Five of these were made with the cold radiometer instrumentation. Three of these were flown from Fairbanks, Alaska and one from Holloman AFB in preparation for the Alaskan flights. The other cold radiometer flight was made earlier from Holloman AFB. The sixth flight contained instrumentation to study atmospheric transmittance from 3-5μm in the

lower stratosphere.

A discussion of each flight is contained below. Included is a summary of wavelengths covered, results obtained and any spectral features noted. Some of the data are contained in data reports and these are not shown again here. The remainder of the data are presented for the first time here.

23 April 1971 Flight. The cold filter radiometer and the cold spectral readiometer were set to operate in the 16.3 to 29.3 μm region for this flight. This was the second flight with the cold radiometers covering this region. The filter radiometer functioned properly throughout the flight and altitude profiles for all five filters were obtained. The region covered by these filters is shown in Figure 172. Unfortunately, the drive assembly for the grating spectrometer froze up just after launch and no data were obtained with this instrument.

Filter data from this flight are presented in a Data Report (Balloon Flight 23 April 1971). Several features were discussed about the data, two of which are briefly mentioned here. The radiance height profiles agreed closely with similar data for 22 February 1971 and the radiance levels diminished rapidly above 92 kft for all filters by roughly the same absolute amount, indicating an aerosol or "dust" layer. When the instrument was valved down from float altitude this "dust" layer was confirmed by the reproducibility of the radiance height profile. Earlier flights showed variability at float altitude in the 12μm "window". The magnitude of this variation was larger, but when normalized with a blackbody function for an appropriate atmospheric temperature, it represented very similar emissivities. Thus there is strong evidence of atmospheric "dust" or particulates between 90 and 100 kft. Any radiometric system operating at these altitudes and using the atmospheric "windows" can expect occasional variability due to this source.

29 June 1971 Flight. Instrumentation for the Alaskan flights was completed and a test flight was conducted at Holloman AFB. The 16.3 to 29.3μ m region was selected for this flight since both this region and the 9-13μm region were to be observed on different flights in Alaska and since there was no spectral data obtained on the previous flight covering this region. Data were obtained with both cold radiometers during the ascent portion of the flight and are presented in a Data Report (Balloon Flight 29 June 1971).

The photometers were set to look at some night glow features to test their response. A preliminary calibration was performed prior to the flight. Several minor problems developed with the photometers during the flight and were corrected before going to Alaska.

To handle all the data anticipated from the Alaskan flights, it was necessary to include two on board digital recorders. These changes were made before the test flight in June so that the complete data system could be checked out.

The filter radiometer data were very similar in their altitude radiance profiles to the profiles observed on 22 February 1971 and 23 April 1971. Radiance values from appropriate regions of the spectral data agreed to within 10% of the filter data for the entire altitude profile. The combination of values from two instruments and three flights fairly well establishes the absolute radiance values to be expected in this spectral region in the lower stratosphere. Some analysis of the water lines near 25μm has been made and may be reported on at a later time.

12 September 1971 Flight. This was the first of three flights from Fairbanks, Alaska. A completely instrumented payload had been prepared to measure infrared emissions as well as visible emissions and also record the gondola orientation with magnetometers. In addition, two ground based photometer systems were set to operate during the times the balloon instrumentation was airborne. The one

remaining parameter of the experiment (time) contained several conflicts. The balloon observational time above 50 kft is limited on most nights to 3 to 4 hours due to trajectory considerations. Maximum auroral activity occurs shortly before through a few hours following midnight. The infrared enhancements observed in September of 1969 occurred between 0700 and 0900 ADT--after sunrise. Therefore, it was decided to launch the balloon shortly after midnight local time so that if the aurora was active, it would be possible to observe it during the latter part of the peak period. In addition, if the float winds were light, it would be possible to remain at float through the early morning hours.

For the first flight the spectral regions were set to include from 8.5 to 14.7μm. Thus including the regions of earlier auroral observation. The filters used in the filter radiometer are shown in Figure 1. These filters monitored radiance from the 11 and 12μm "windows", (filters 3 and 7), radiance from the shorter wavelength region near 8.5μm (filter H) and radiance from the O_3 band and the HNO_3 band (filters 8 and 7).

The grating spectrometer scanned from 9.3 to 14.7μm with a resolution of about 0.07μm. With this spectral range, data were obtained for the O_3 band the HNO_3 band and part of several CO_2 bands as well as the two "windows" at 11 and 12μm. It has been suggested that the auroral enhancement in the infrared might be associated either with excited O_3 or excited CO_2.

The flight proceeded in a normal manner. The balloon was launched at 0132 ADT and arrived at float altitude at about 0400 ADT. The balloon altitude profile is shown in Figure 2 and the temperature altitude profile is shown in Figure 3. Shortly after 0600 ADT, the balloon started descending due to a failure somewhere in the balloon. It was not possible to control the descent by releasing ballast; therefore, the flight was terminated at 0643 ADT at an altitude of 65 kft. Impact occurred north of Fairbanks on the side of a mountain. The Army

helicopter recovery team returned the equipment a few hours later without serious damage.

The instruments were calibrated before and after the flight and both calibrations were in close agreement. Data were obtained with both instruments during ascent and at float altitude. No data are presented for times after 0440 ADT, because the main battery voltage dropped below 24 vdc at that time and about one half hour later the recorders began to drop out due to the falling voltage.

The filter data are presented in Figures 4 to 8. These data show a very monotomic decrease in radiance values during ascent even though there was significant auroral activity in the field of view (as will be noted later). The float data were carefully examined for time fluxuations, and the only significant variation in the data occurred when the moon passed through the field of view. The records where this occurred are shown in Figures 9 through 19. Each record is shown separately with all 5 filters on the same plot in the time sequence in which they were observed. Each record is about 1.9 minutes long. The moon is always observed at the proper angle as shown by the magnetometer data which is plotted above the filter data. There was no evidence during this flight of the type of radiance variation observed in September 1969.

The radiance height profile of the various filters can be compared with previous flights. The radiance level of filter 7 is about 2 1/2 times higher than the 13 September 1969 data for filter F and about 6 times higher than the 20 September data. It is very similar to the data observed at Holloman AFB on 23 September 1970 and 18 October 1970.

The spectral radiometer data are presented in Figures 20 to 85. A mean altitude and time are associated with each scan which takes about 1.9 minutes. Because of the large dynamic range required to include the O_3, CO_2 and the window regions, it is necessary to plot

radiance on a log scale. On this flight there was some interference from the barocoder transmitter and some complete records plus portions of others have been omitted as a result. Radiance levels from the spectral data when averaged over appropriate regions agree well with the radiance values of the 5 filters. The only significant variation which occurs in the float data is again attributable to the moon passing through the field of view.

The photometer data are presented in Figures 86 through 95. There were moderate emissions in the northern half of the sky during the entire time period covered by these data. The peak values represent an IBC I type aurora. However, during this period no variation was observed with either radiometer.

There was some difficulty with the time-sharing circuitry used to record the photometer data. Some of the photometer channels are not useable during the entire flight and most of the later data was not useable for all channels. A similar problem developed on the 15 September flight; however, one of the channels was working when the moon passed through the field of view of the radiometers. At this point the photometer was saturated.

15 September 1971 Flight. This flight was similar to the flight of 12 September. All spectral regions were the same and identical calibrations were used in reducing the radiometer and photometer data. Again a launch time was set for shortly after midnight with the hope of measuring both active aurora near midnight and any post break-up activity which might occur during the early morning hours.

The balloon was launched at 0055 ADT and reached its peak altitude of 94 kft at 0246 ADT. At that time there was a balloon failure of unknown origin and the parachute was automatically separated from the balloon. The payload impacted in the dark but was located shortly after sunrise and returned in good condition to the assembly area a few hours later. The balloon altitude profile is shown in Figure 96 and the temperature altitude profile is shown in Figure 97.

Both radiometers operated throughout the flight and continuous data are presented here. The filter data are shown in Figures 98 through 102. The height radiance profiles are similar to the 12 September data with most variations being attributable to the slight differences in the temperature altitude profiles for the two dates. The moon was too low to be in the field of view and no significant variations were observed in the data. Auroral activity, however, was greater on 15 September than on the 12th. This can be seen in the photometer data presented in Figures 161 through 171.

The spectral radiometer data (Figures 103 to 160) show a detailed height profile of the spectral structure of the 9.3 to 14.7μm region. A great deal of information is available from analysis of this data concerning the height profile of several atmospheric constituents. This analysis is being undertaken but does not form a part of this report. However, there is no evidence of enhanced emission at any wavelength in these data even though the auroral activity at times approached IBC II levels.

<u>23 September 1971 Flight.</u> For this flight the spectral region covered by the radiometers was shifted to the long wavelength. The filter wheel in the filter radiometer was replaced with one containing the same filters that were flown in March, April and June 1971. Curves for these filters are shown in Figure 172. The spectral radiometer was set to scan from 16.3 to 29.3μm with a resolution of about 0.1μm.

The flight was planned for the same time frame as the preceeding two flights; however, a problem with a wire from the main battery delayed the launch. The balloon was finally launched at 0251 ADT and reached a maximum altitude of 94 kft at 0449 ADT. The balloon again failed at this point due to unknown causes and the payload was automatically separated. The payload impact was before sunrise, but the parachute was spotted a little later and the instruments were returned in good condition. The balloon ascent profile is shown in Figure 173

and the temperature altitude profile is shown in Figure 174.

Both instruments were calibrated before and after the flight with good agreement. Due to a problem with the digital recorders, some spectral data are missing around 20 kft and 50 kft. The rest of the data are presented here.

The filter data are shown in Figures 175 through 179 and the spectral data in Figures 180 through 215. Three different radiance scales are used for the spectral data due to the dynamic range of the data at the lower altitudes and the relatively constant values at the higher altitudes. Figures 180 to 182 use a log radiance scale from 10^{-6} to 10^{-3} w cm^{-2} sr^{-1} μ^{-1}. Similarly, Figures 183 through 188 use a log scale from 10^{-7} to 10^{-4} w cm^{-2} sr^{-1} μ^{-1}. Finally, Figures 189 through 215 use a linear radiance scale.

Due to the late launch time there was little auroral activity when the balloon was above 50 kft; the photometer data was very low, dropping into noise at times. The 3914Å data seldom got above 50 Rayleighs. Due to the low values these data are not presented in this report. It should also be pointed out that the filter and spectral radiometer data showed no evidence of auroral activity during the ascent portion of the flight.

<u>18 January 1972 Flight</u>. On 11 July 1970 a flight was made from Holloman AFB on which the 3-5μm region was scanned using the solar pointer and the high resolution grating spectrometer. The atmospheric transmittance was measured at various altitudes and with the setting sun from 100 kft. There was considerable difficulty with the pointing control on this flight and only a few useful records were obtained. Therefore the flight was repeated on 18 January 1972. A large number of useful records were obtained including a few with relatively long optical paths observed during sunset from 100 kft.

The reduction of this data is very time consuming, and at this time nearly all the records have initial envelopes on them to convert

the voltage readings to transmittance. However, these must be checked against each other to verify the choice of envelope and to eliminate any region effected by pointing control perturbations.

A few of the data were selected to be presented here. They represent a sampling of altitudes and a few records with different optical paths at float altitude. These records are fairly free of the required corrections mentioned above; however, care should be exercised in interpreting these data. The seven spectra are shown in Figures 216 through 236.

IV. CONCLUSIONS

The primary emphasis of this contract has been on the measurement of infrared auroral phenomena. On two flights in September of 1971, infrared measurements were made in the 9-14μm region during moderate auroral activity. No enhancement of the infrared data was observed. Previously, on 13 September 1969, enhanced infrared data were obtained, but at a different time of day (0800ADT) than when the recent observations took place. Unfortunately, it is difficult to correlate the infrared data with known auroral phenomena during daylight hours. However, it seems that the emphasis on the next measurements of this type should beon a period of time overlapping the 0800 ADT.

V. ACKNOWLEDGMENTS

The investigations reported here are the results of the efforts of a number of individuals and groups in addition to the authors. The following individuals at the University of Denver assisted in the program: Carolyn Bauer. W. Cochran, T. Dow, A. Goldman, F. J. Murcray and J. VanAllen. The launch and recovery of the balloon payloads were handled very capably by the Air Force Cambridge Research Laboratories balloon groups at Holloman AFB, and Chico, California.

REFERENCES

1. D. G. Murcray, F. H. Murcray, and W. J. Williams, "A Balloon Borne Grating Spectrometer", Applied Optics 6, 191 (1967).

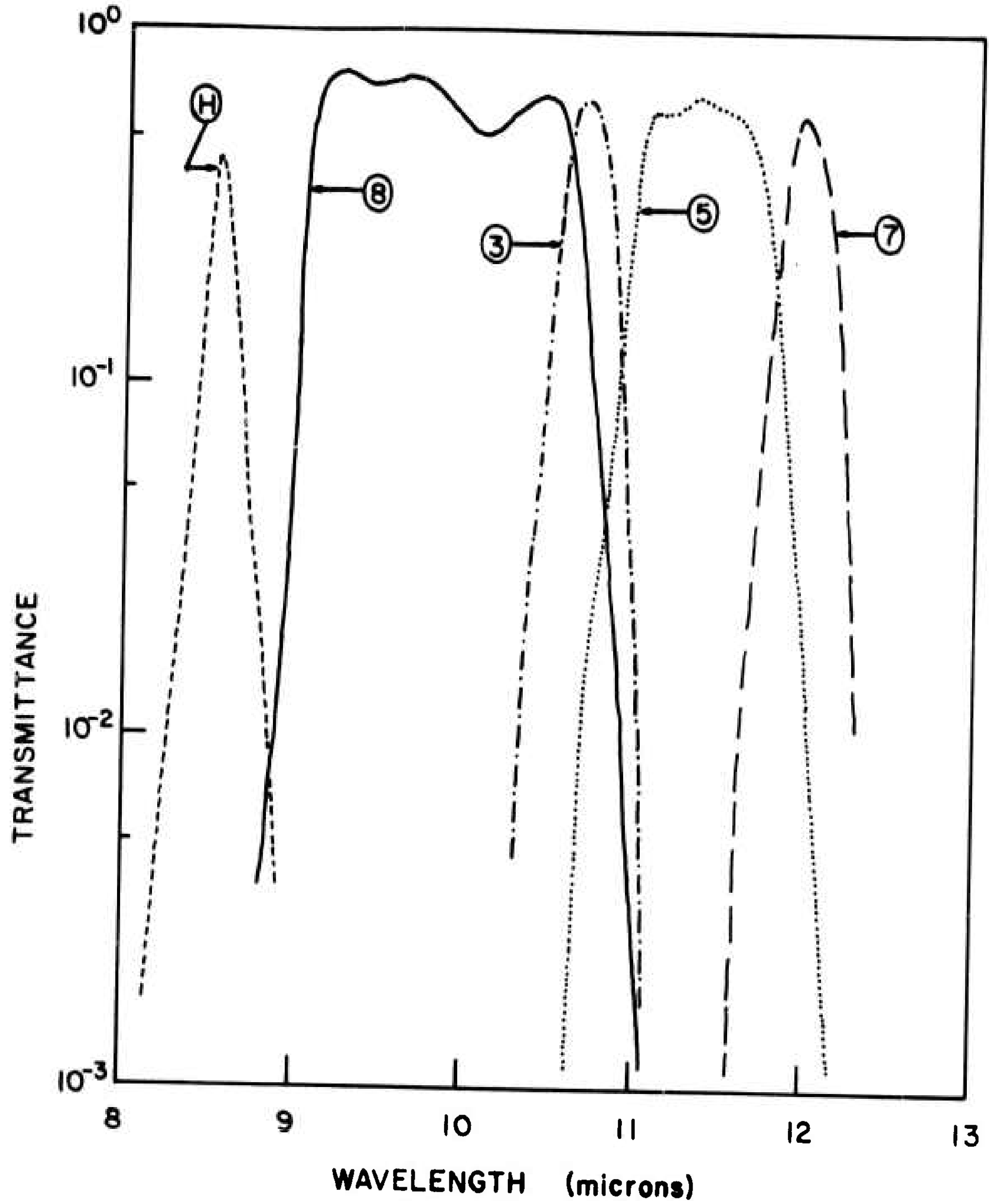

Figure 1. D.U. Filter Radiometer curves for 12 and 15 September 1971, Fairbanks, Alaska.

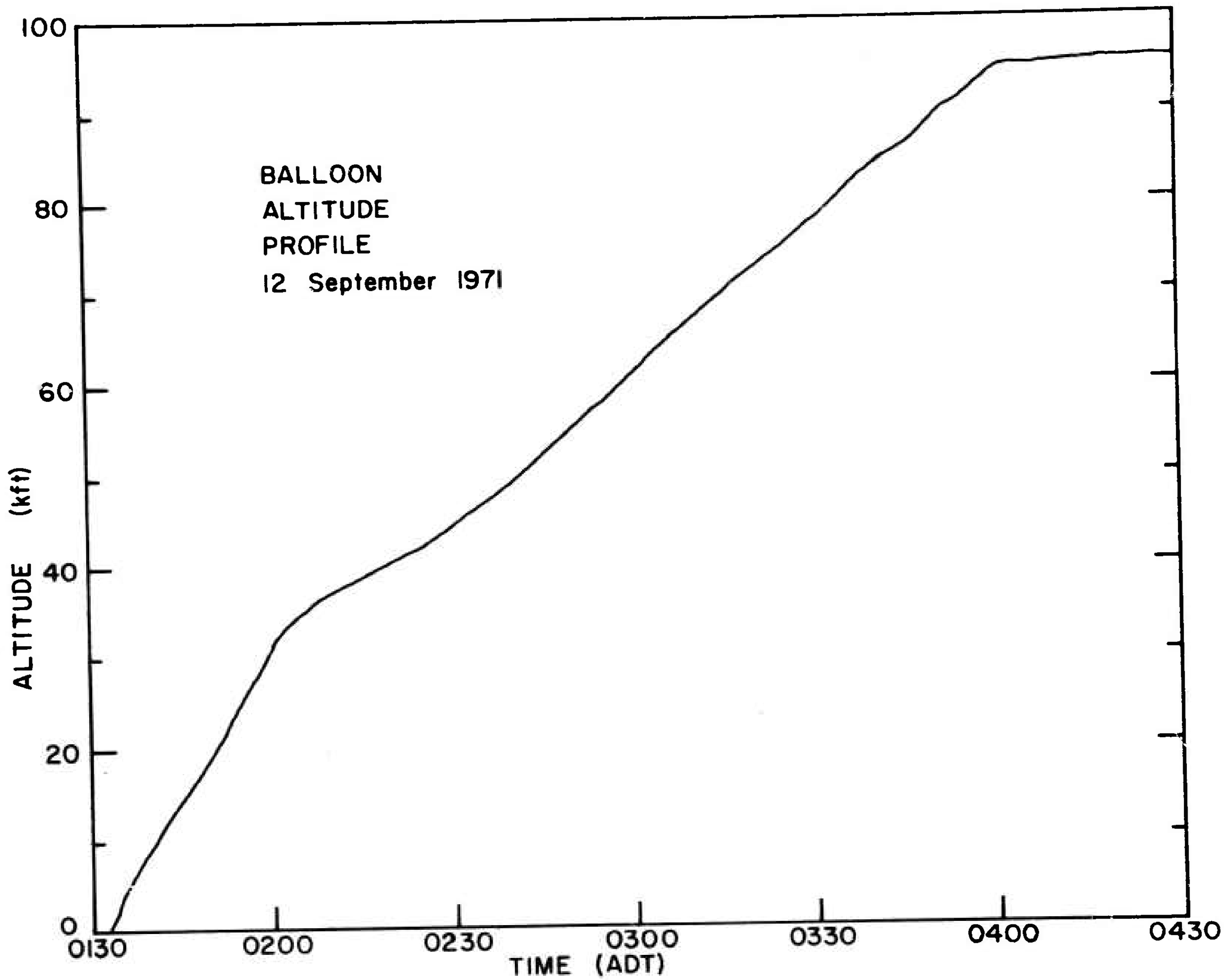

Figure 2. Time vs Altitude Profile of 12 September 1971 Balloon.

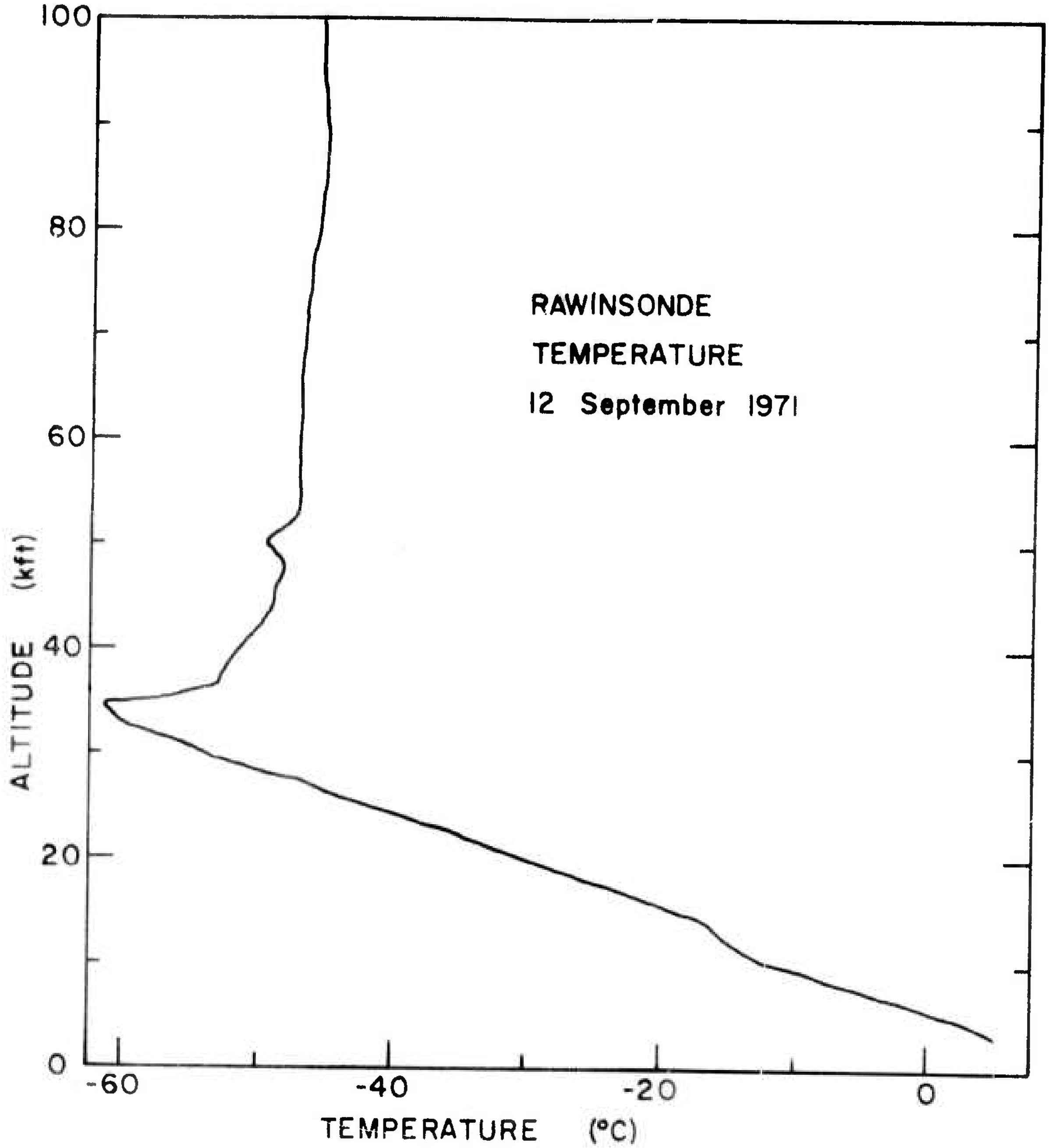

Figure 3. Rawinsonde Temperature vs Altitude for 12 September 1971, Fairbanks, Alaska.

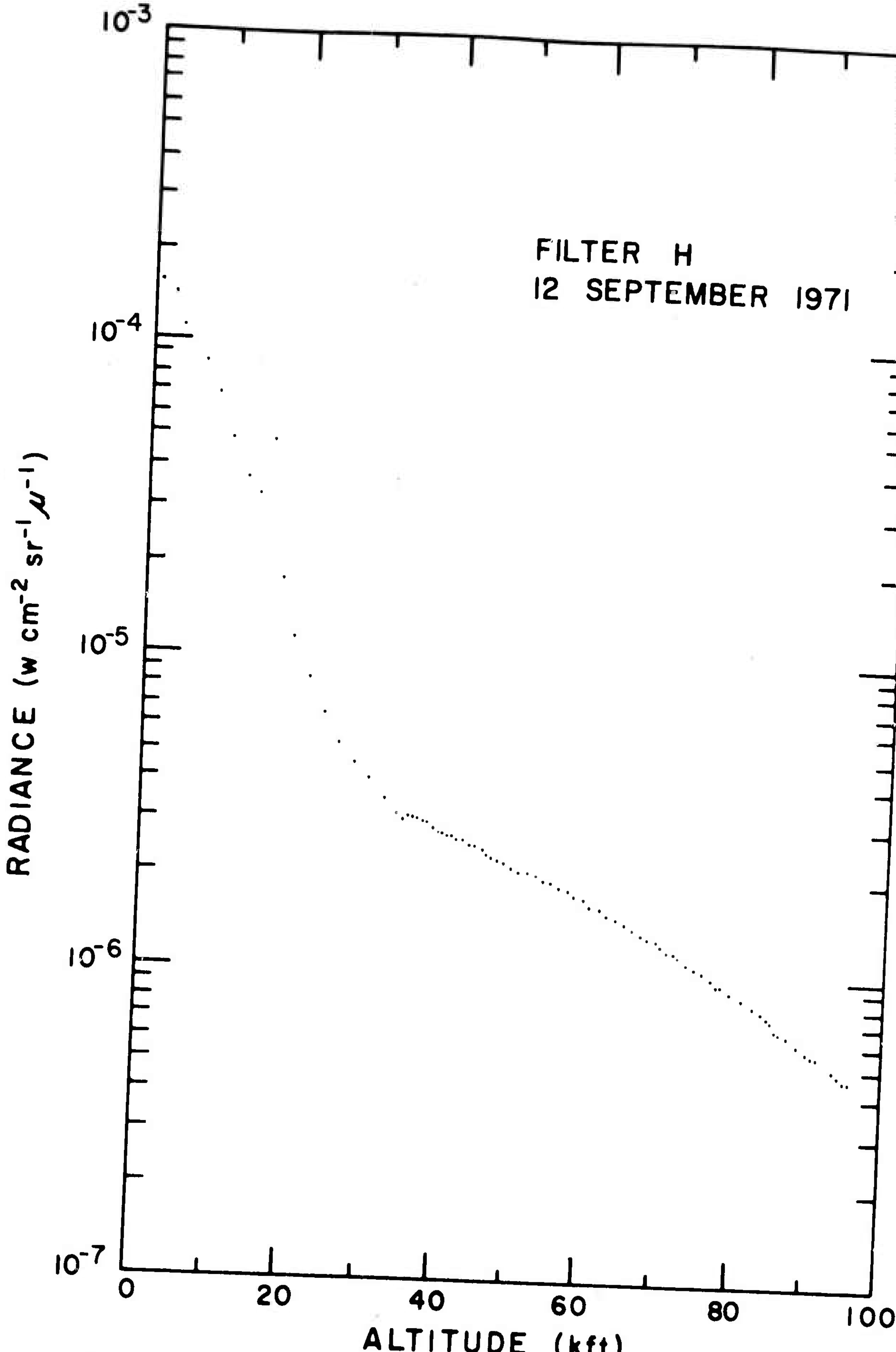

Figure 4. Radiance vs Altitude for Filter H, 12 September 1971.

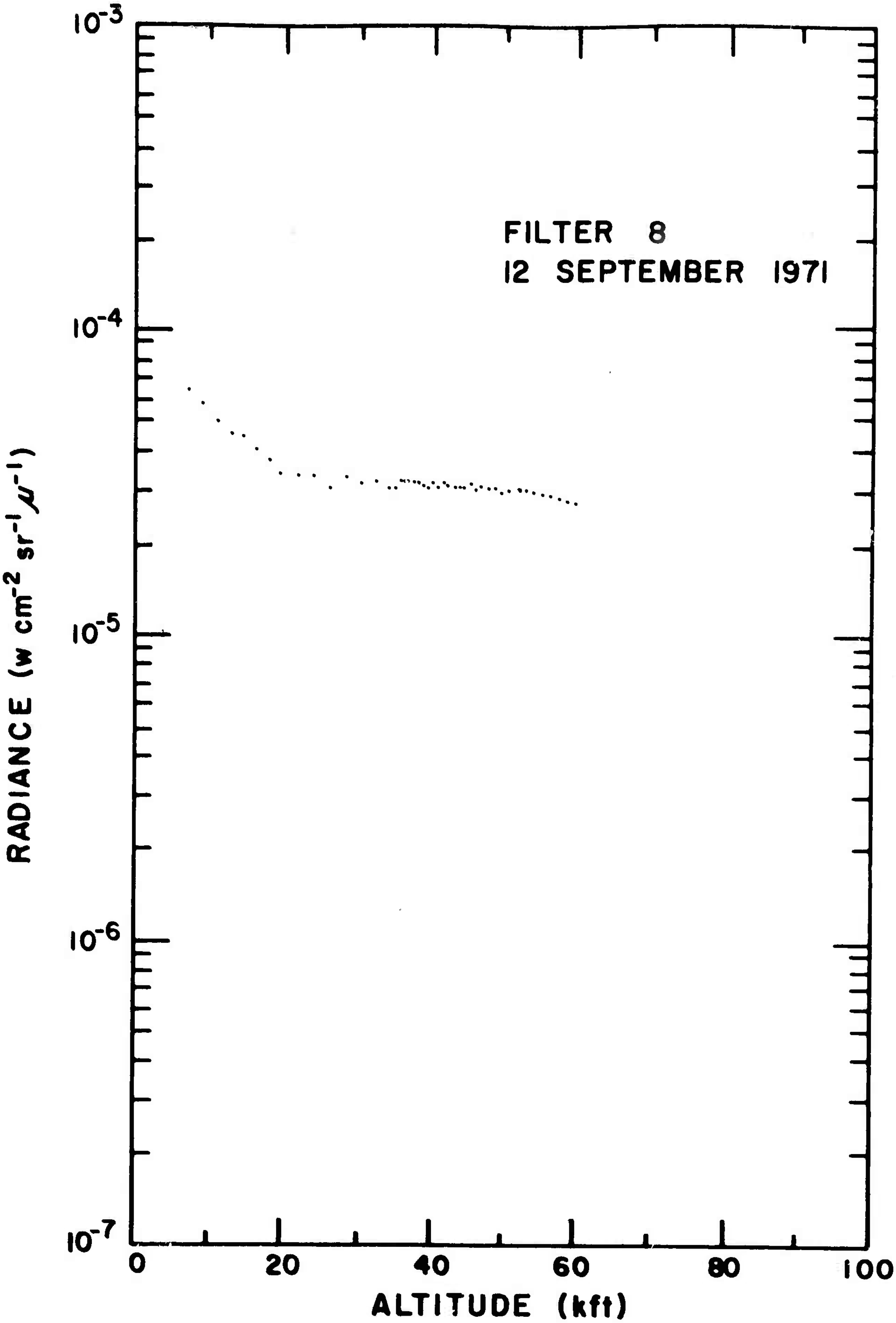

Figure 5. Radiance vs Altitude for Filter 8, 12 September 1971.

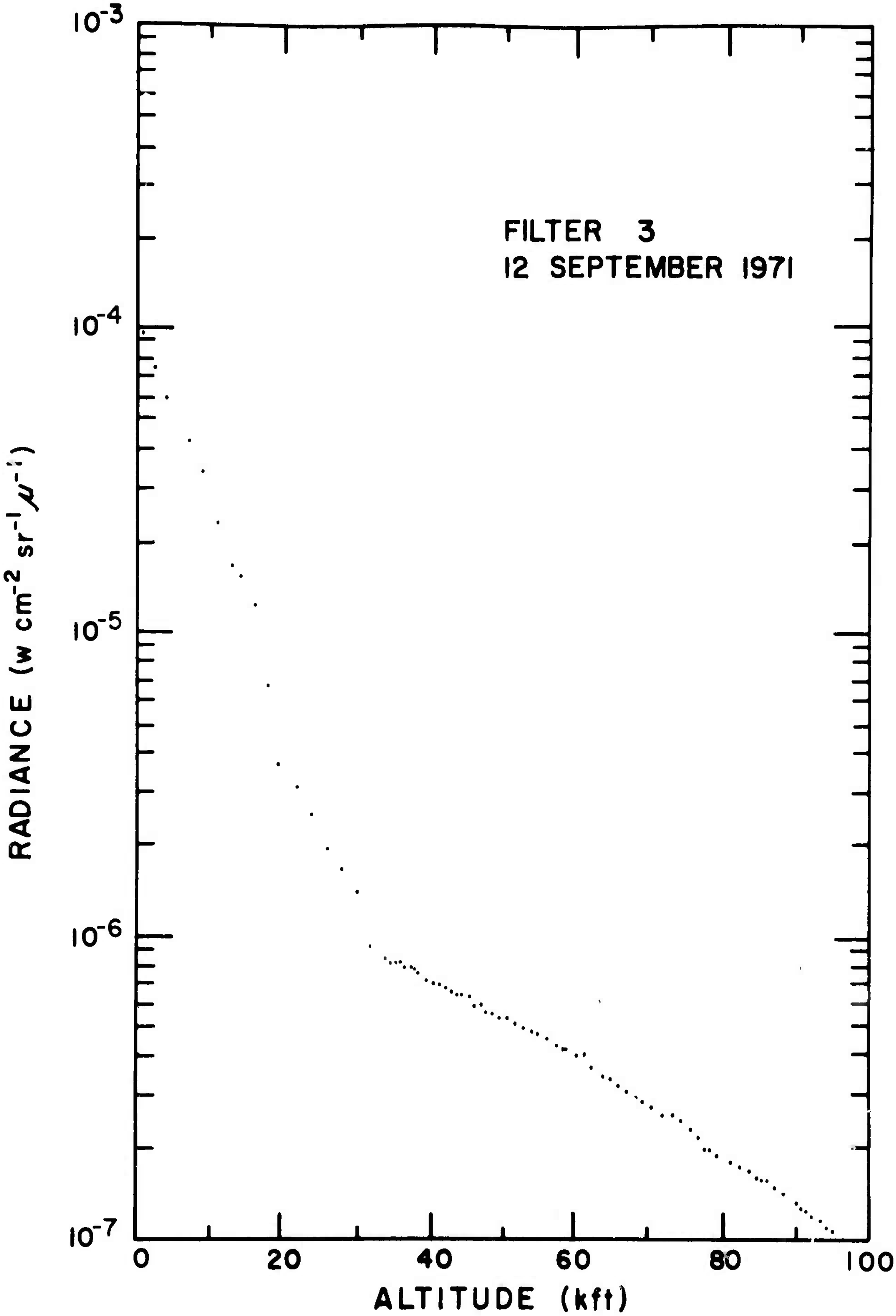

Figure 6. Radiance vs Altitude for Filter 3, 12 September 1971.

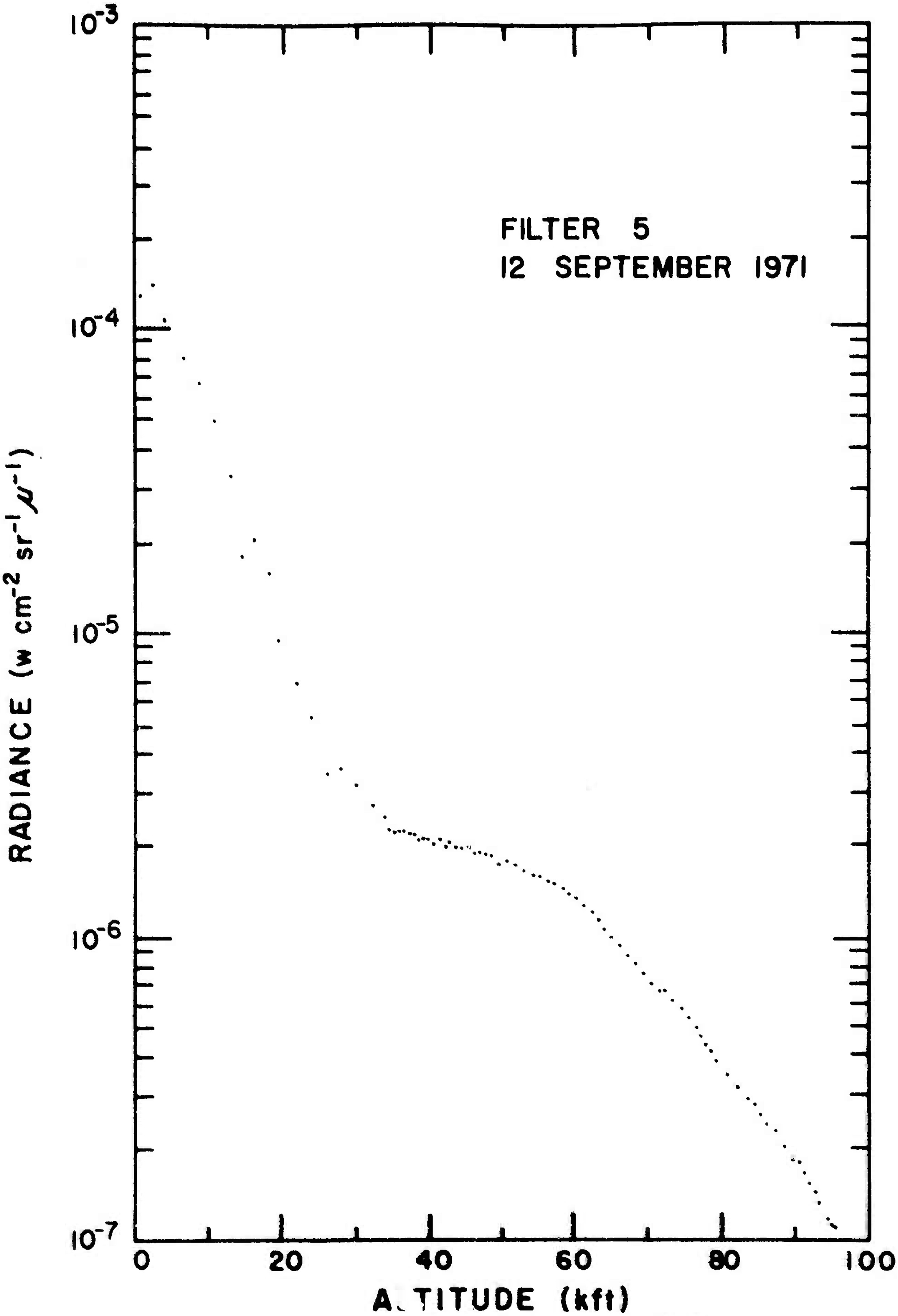

Figure 7. Radiance vs Altitude for Filter 5, 12 September 1971.

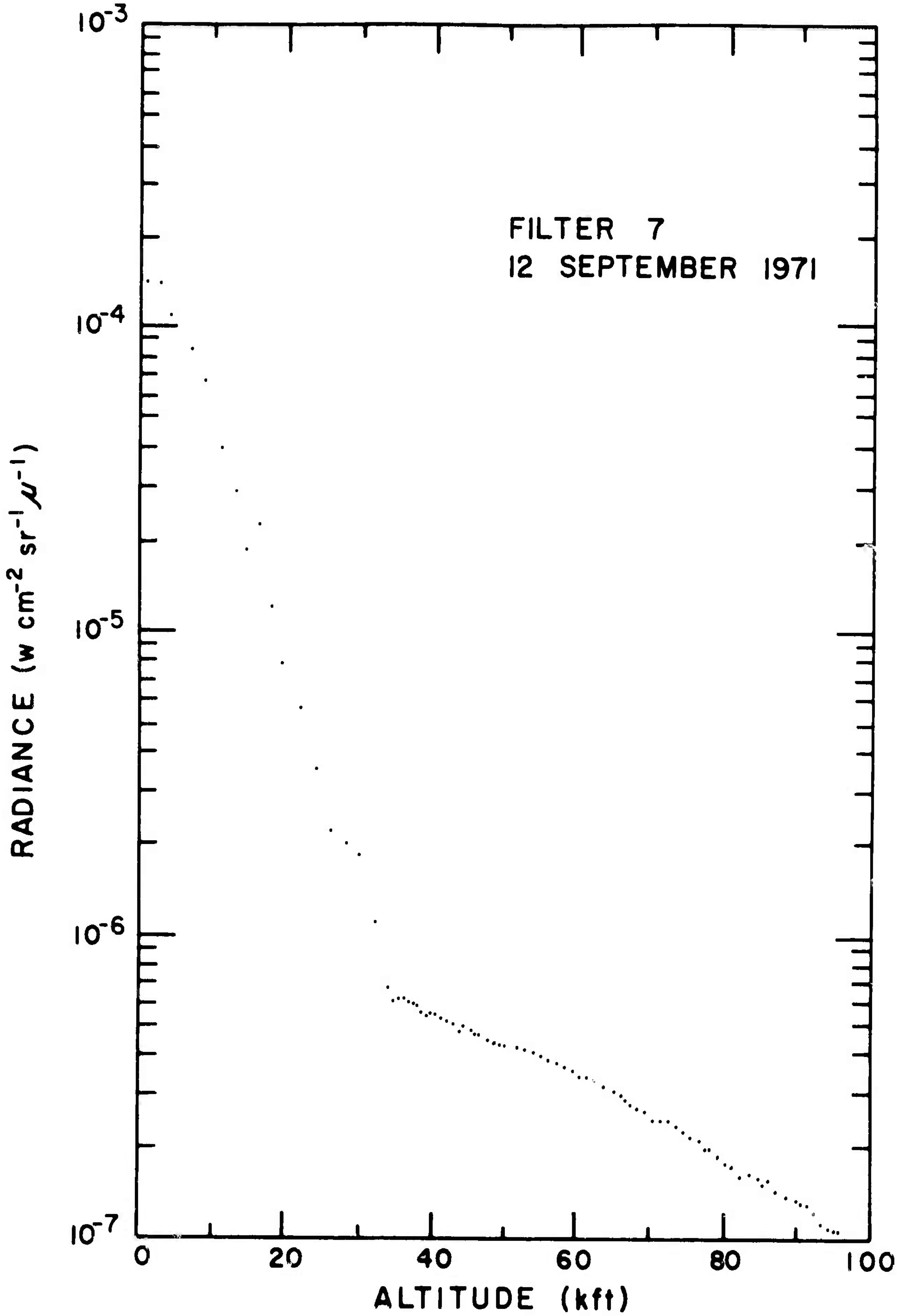

Figure 8. Radiance vs Altitude for Filter 7, 12 September 1971.

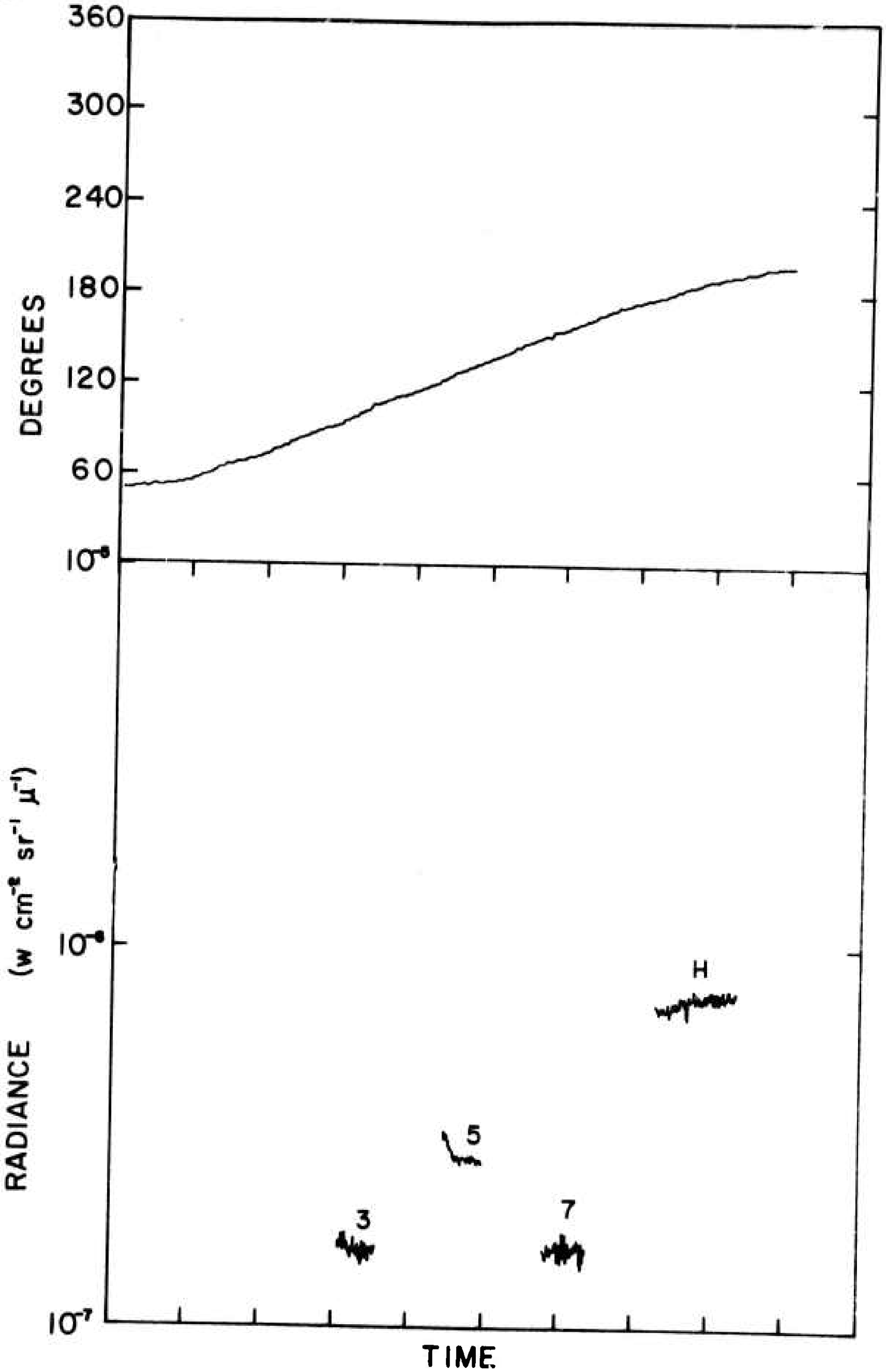

Figure 9. Filter radiance vs time showing inclusion of moon in radiometer field of view. 0330 ADT, 12 September 1971.

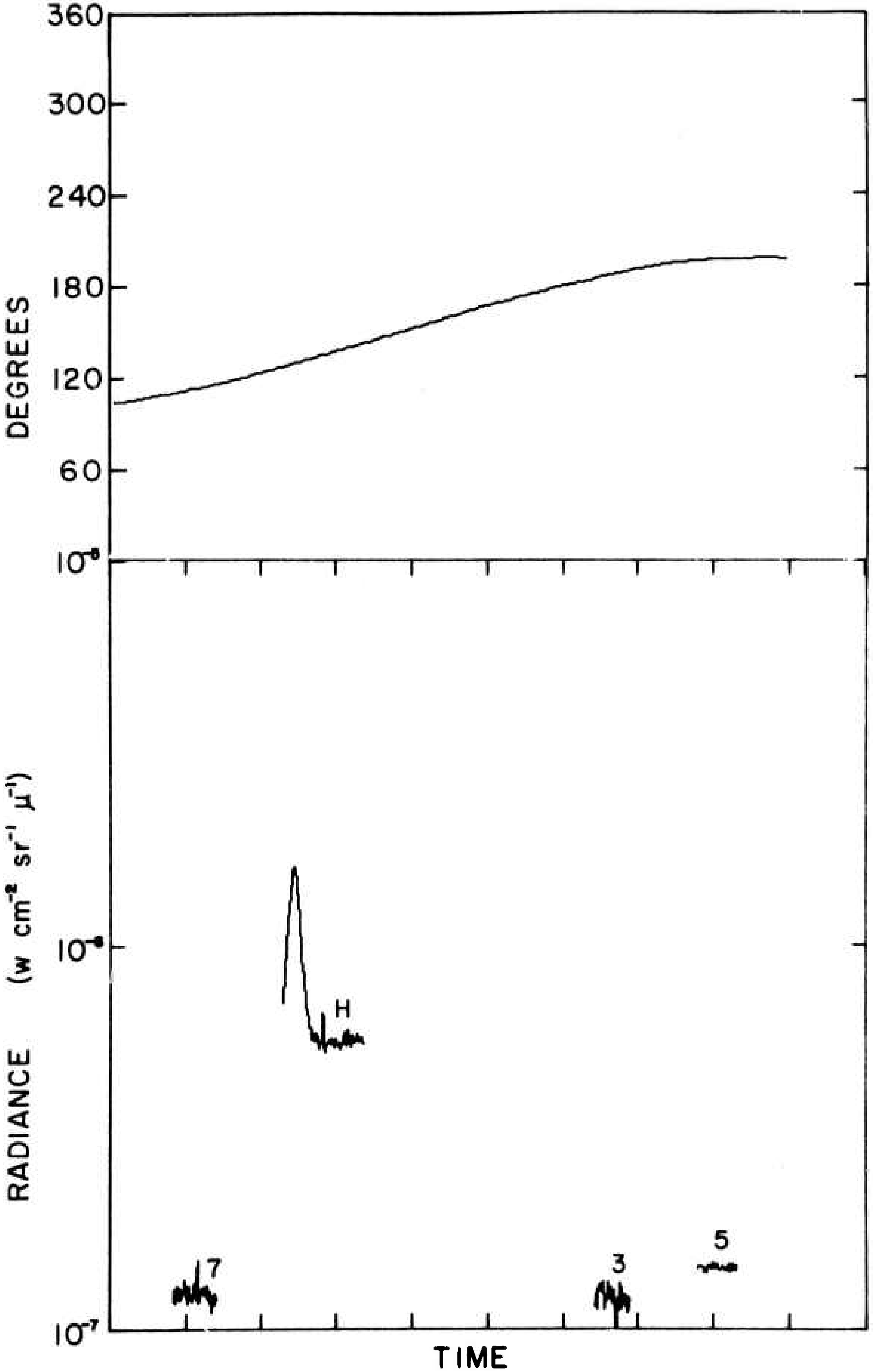

Figure 10. Filter radiance vs time showing inclusion of moon in radiometer field of view. 0344 ADT, 12 September 1971.

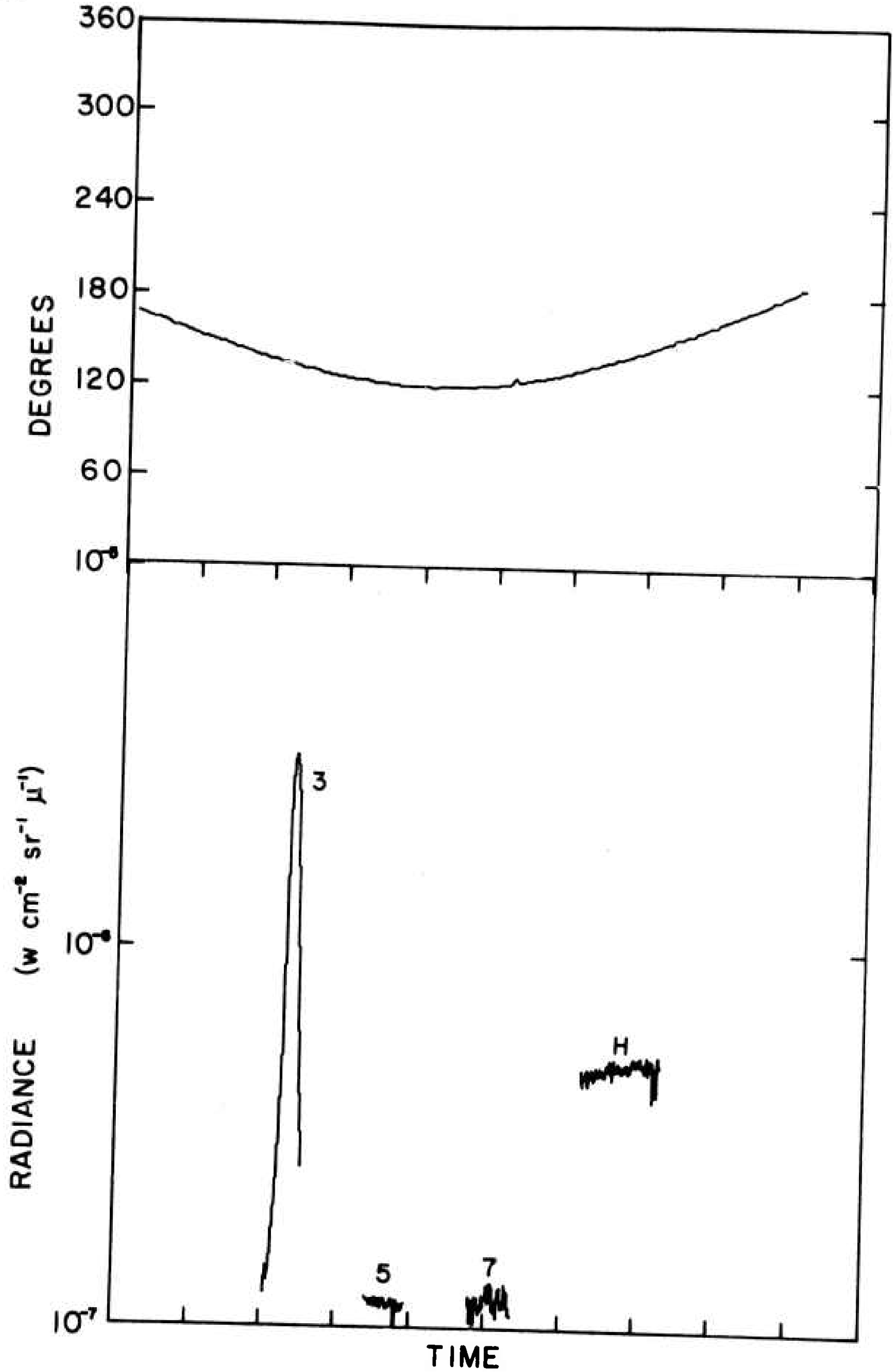

Figure 11. Filter radiance vs time showing inclusion of moon in radiometer field of view. 0356 ADT, 12 September 1971.

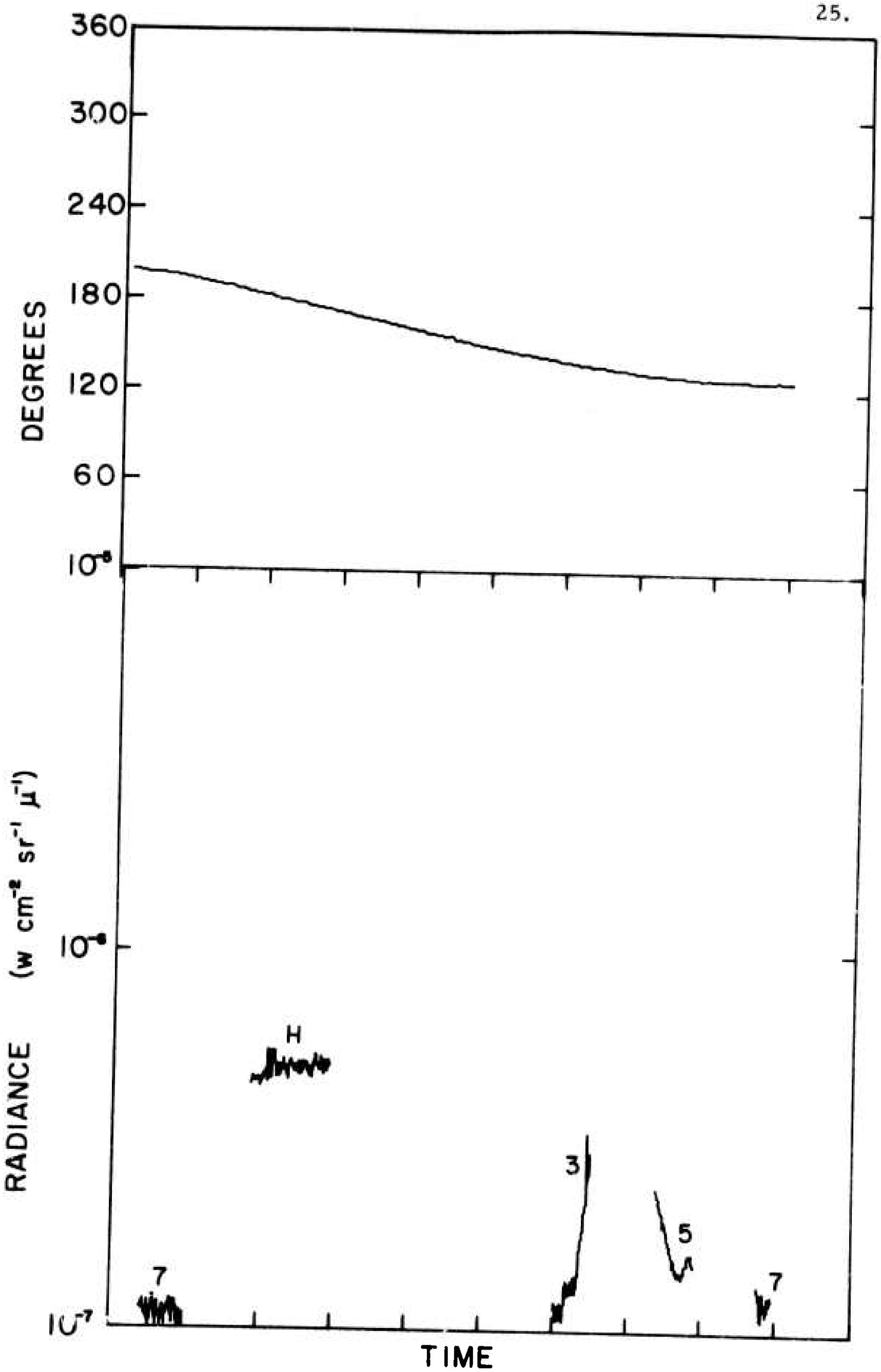

Figure 12. Filter radiance vs time showing inclusion of moon in radiometer field of view. 0409 ADT, 12 September 1971.

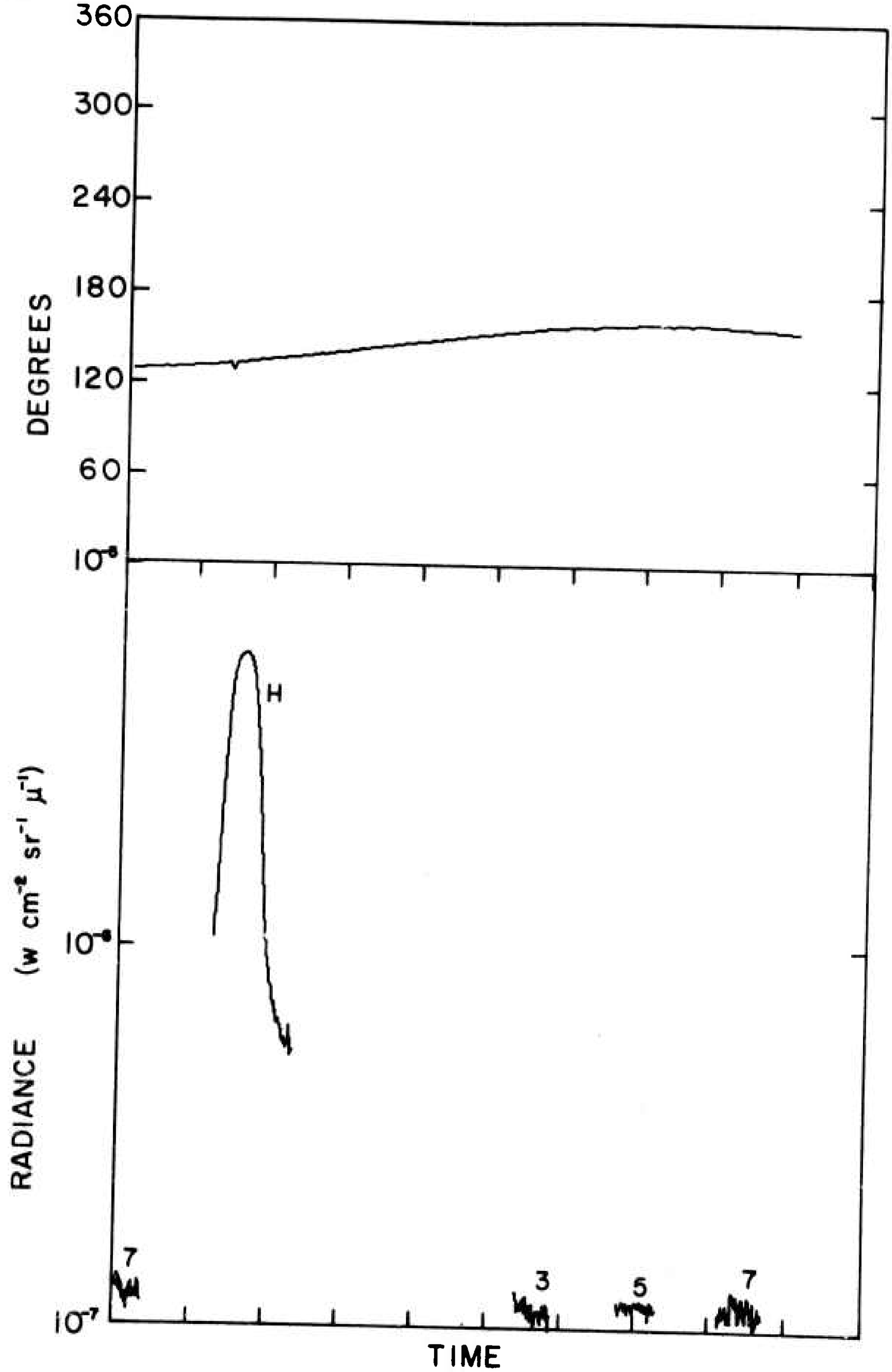

Figure 13. Filter radiance vs time showing inclusion of moon in radiometer field of view. 0411 ADT, 12 September 1971.

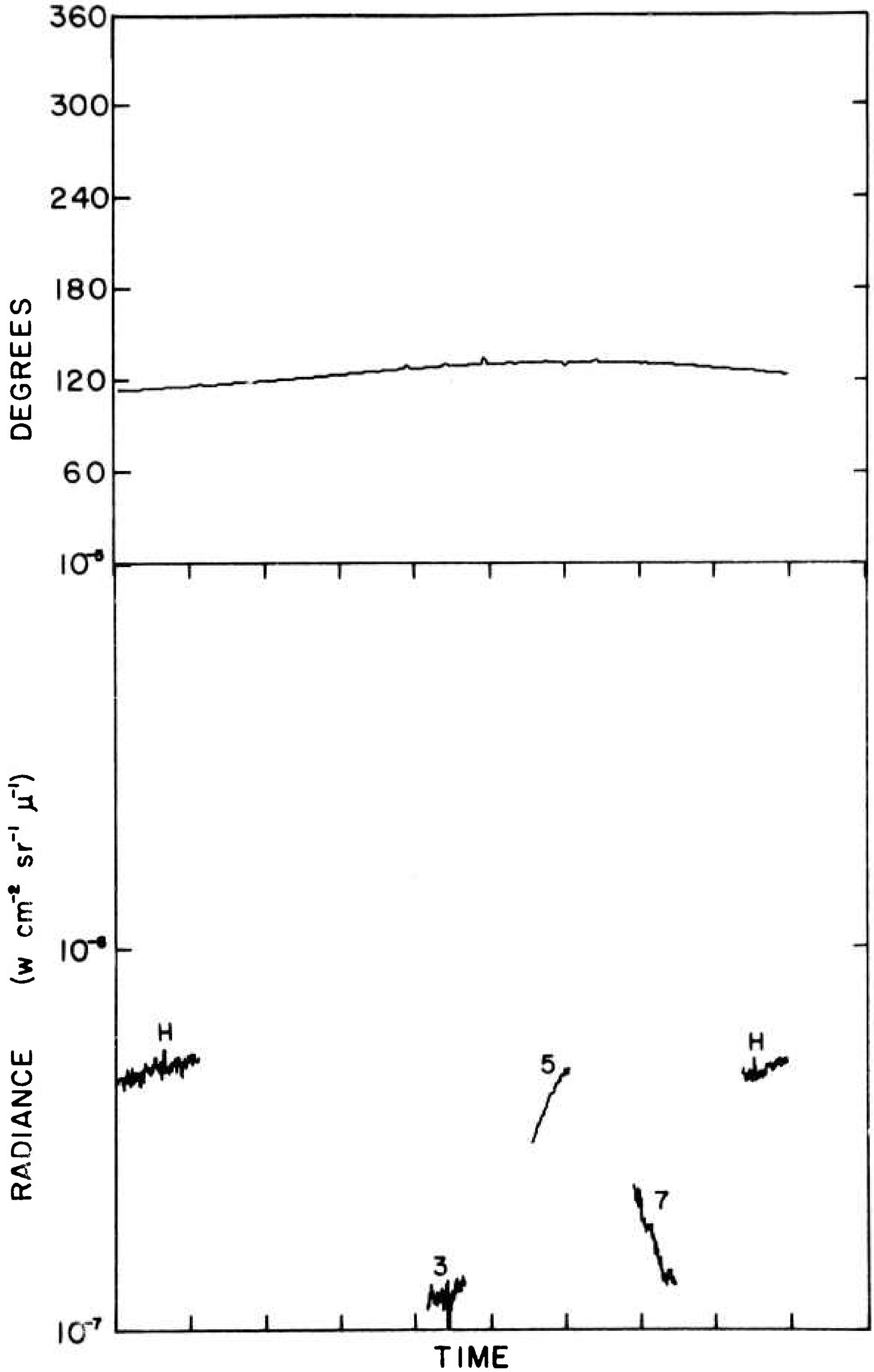

Figure 14. Filter radiance vs time showing inclusion of moon in radiometer field of view. 0414 ADT, 12 September 1971.

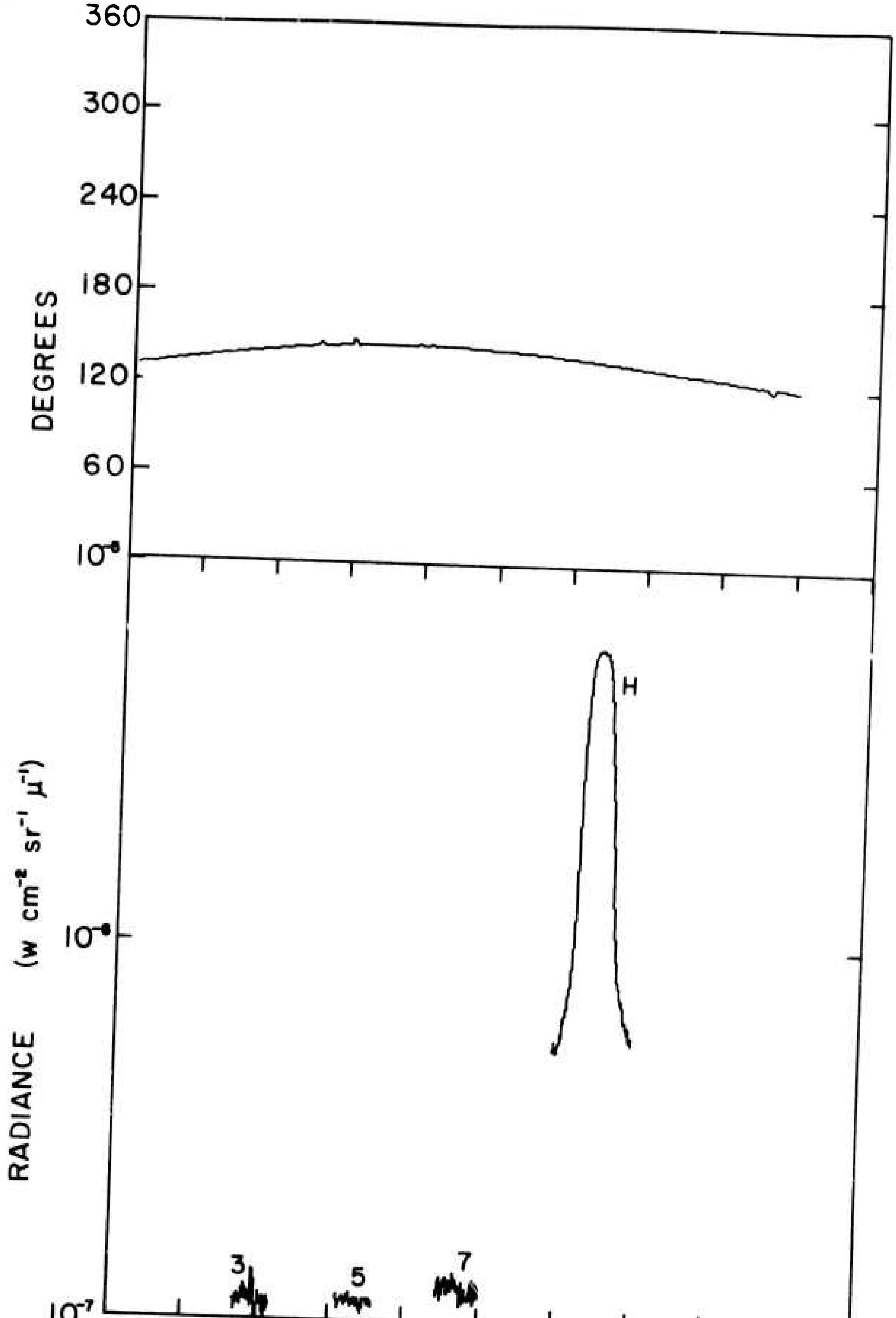

Figure 15. Filter radiance vs time showing inclusion of moon in radiometer field of view. 0422 ADT, 12 September 1971.

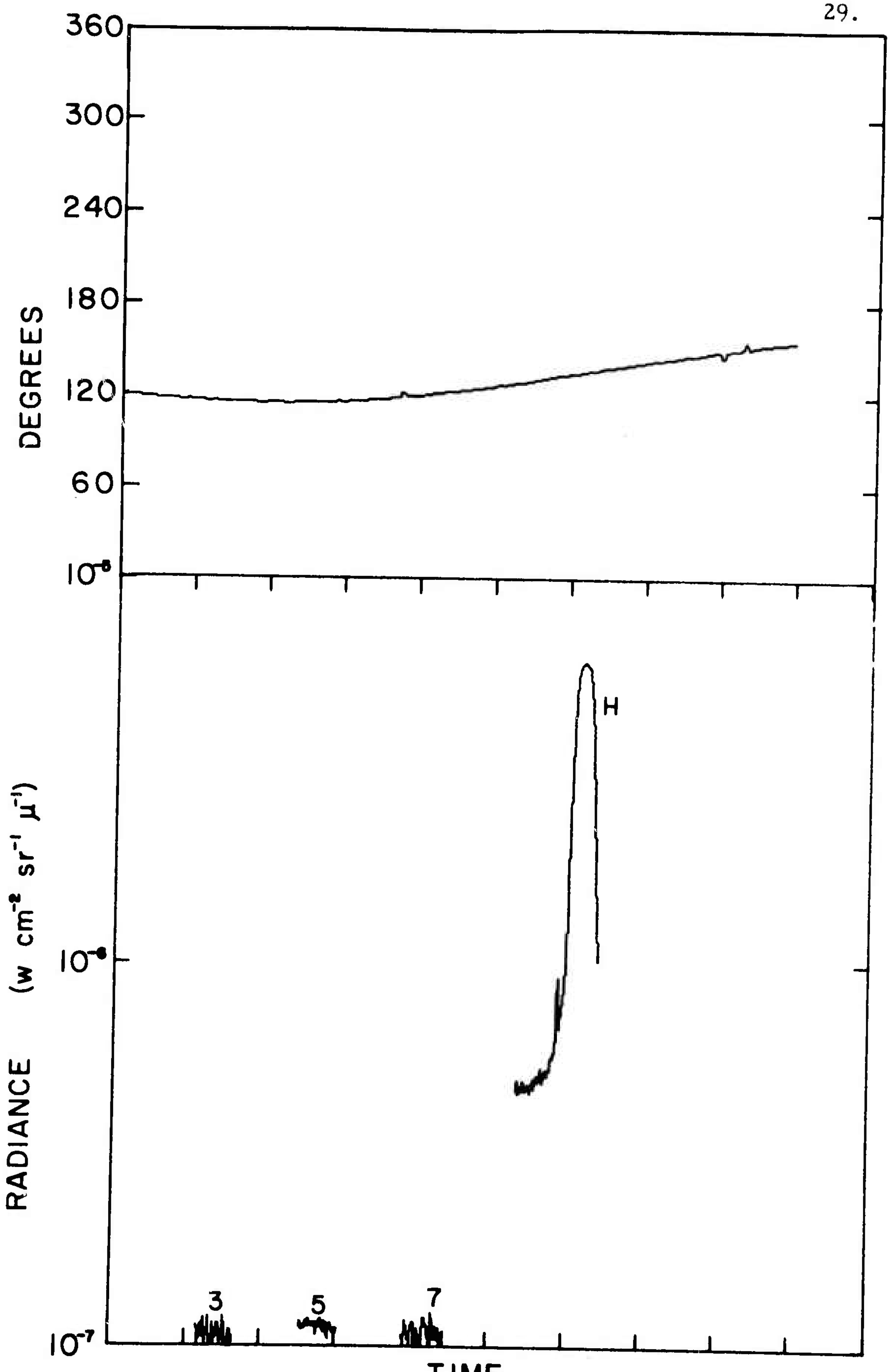

Figure 16. Filter radiance vs time showing inclusion of moon in radiometer field of view. 0423 ADT, 12 September 1971.

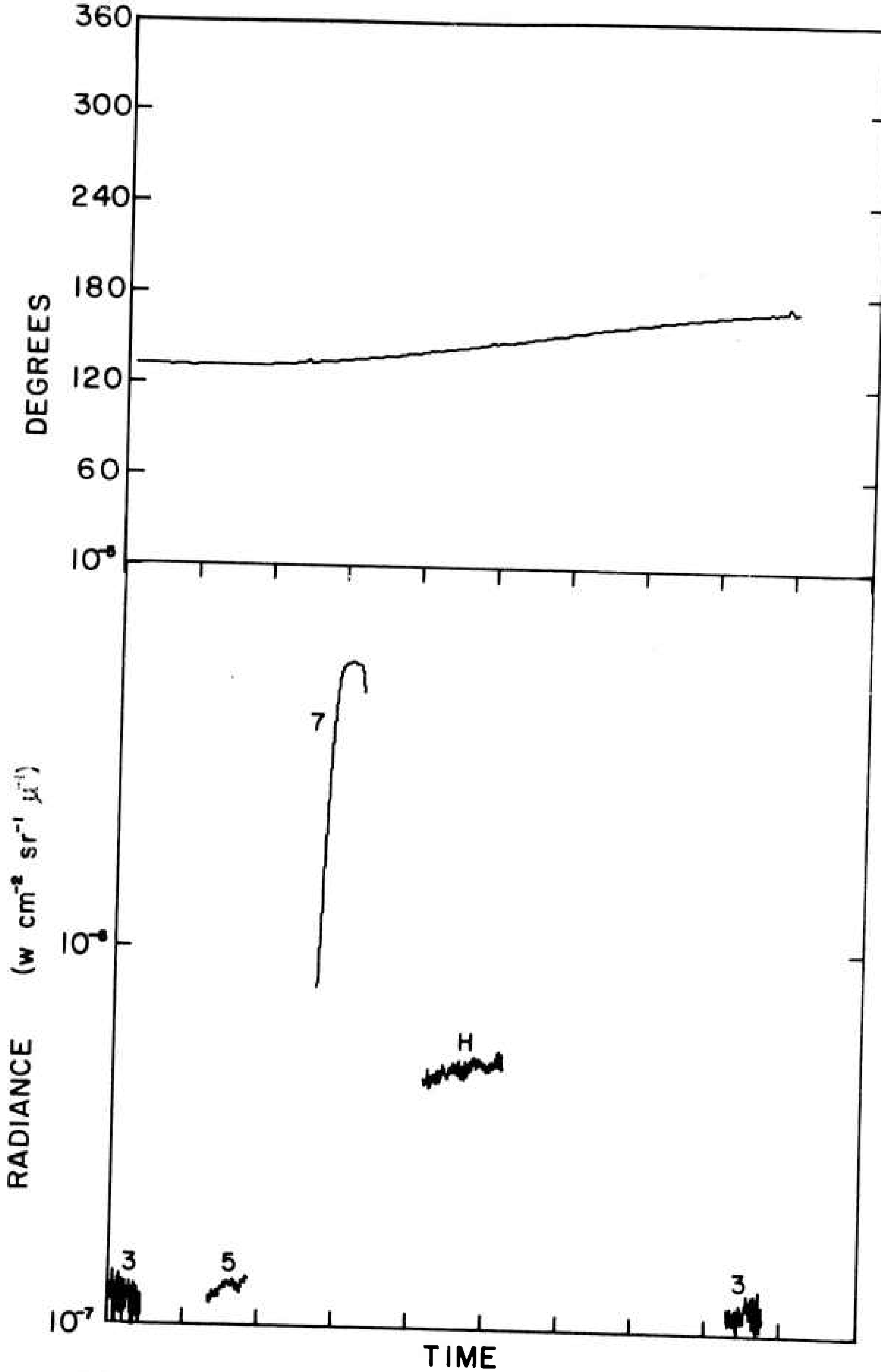

Figure 17. Filter radiance vs time showing inclusion of moon in radiometer field of view. 0427 ADT, 12 September 1971.

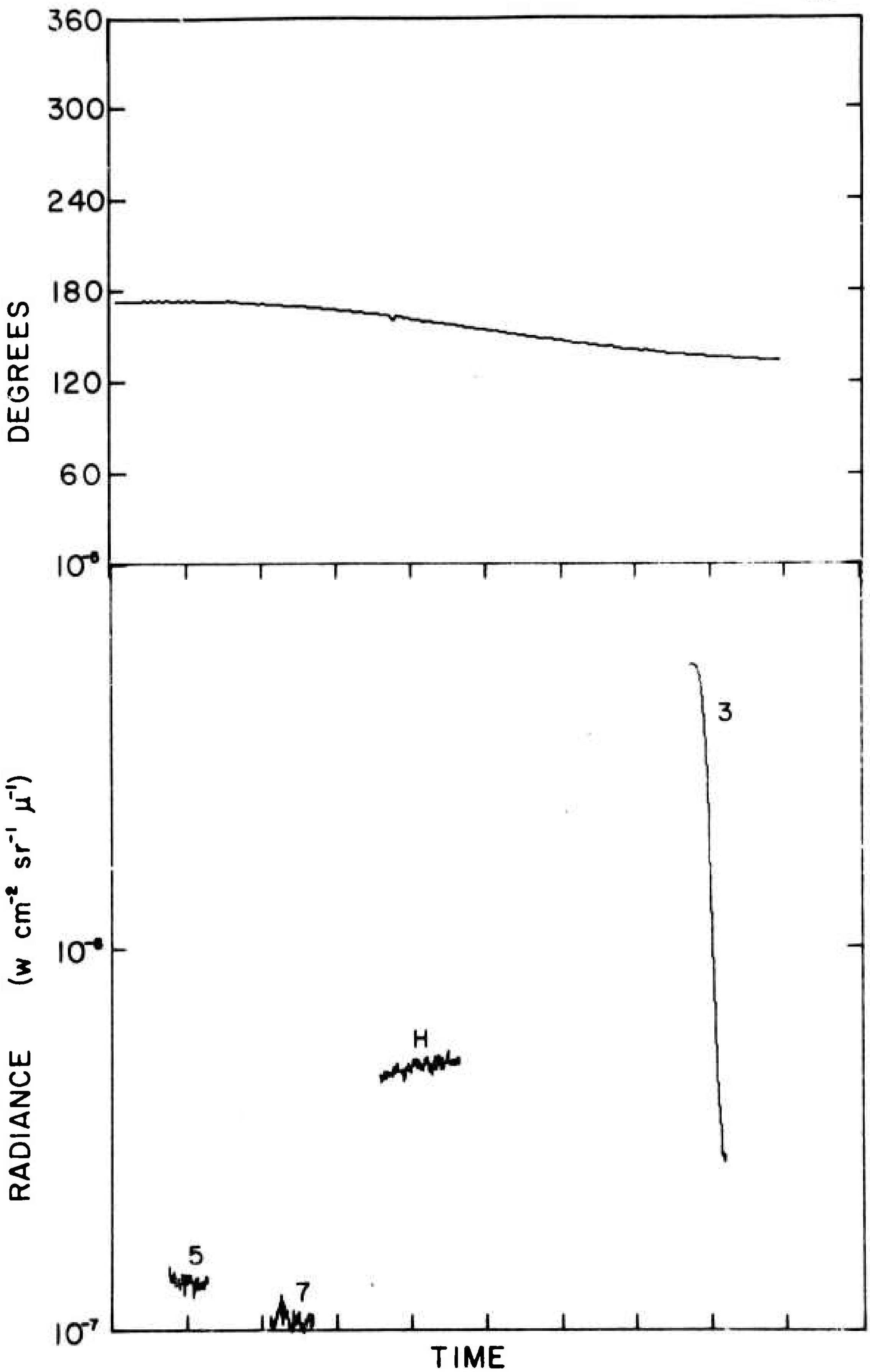

Figure 18. Filter radiance vs time showing inclusion of moon in radiometer field of view. 0429 ADT, 12 September 1971.

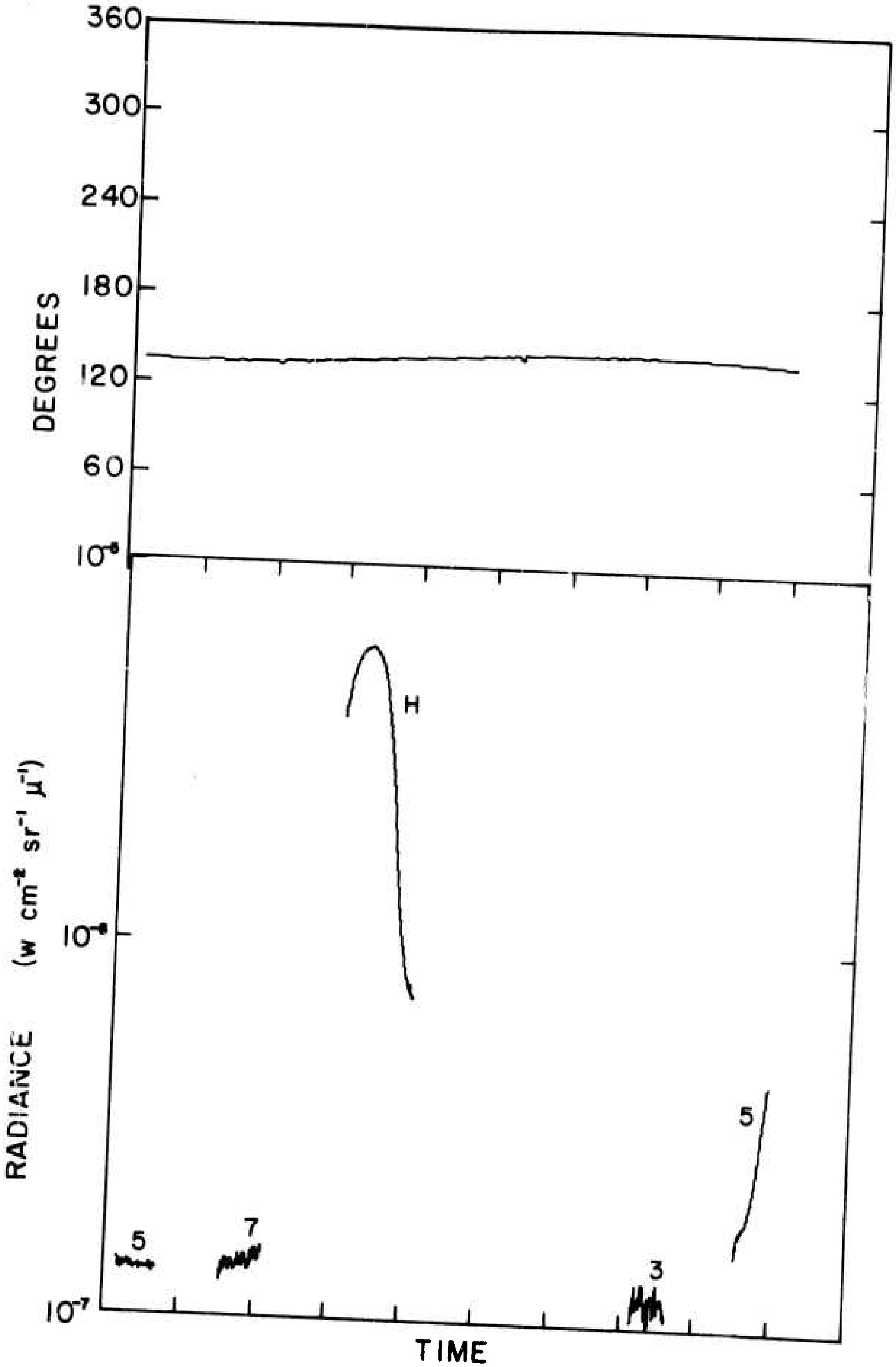

Figure 19. Filter radiance vs time showing inclusion of moon in radiometer field of view. 0431 ADT, 12 September 1971.

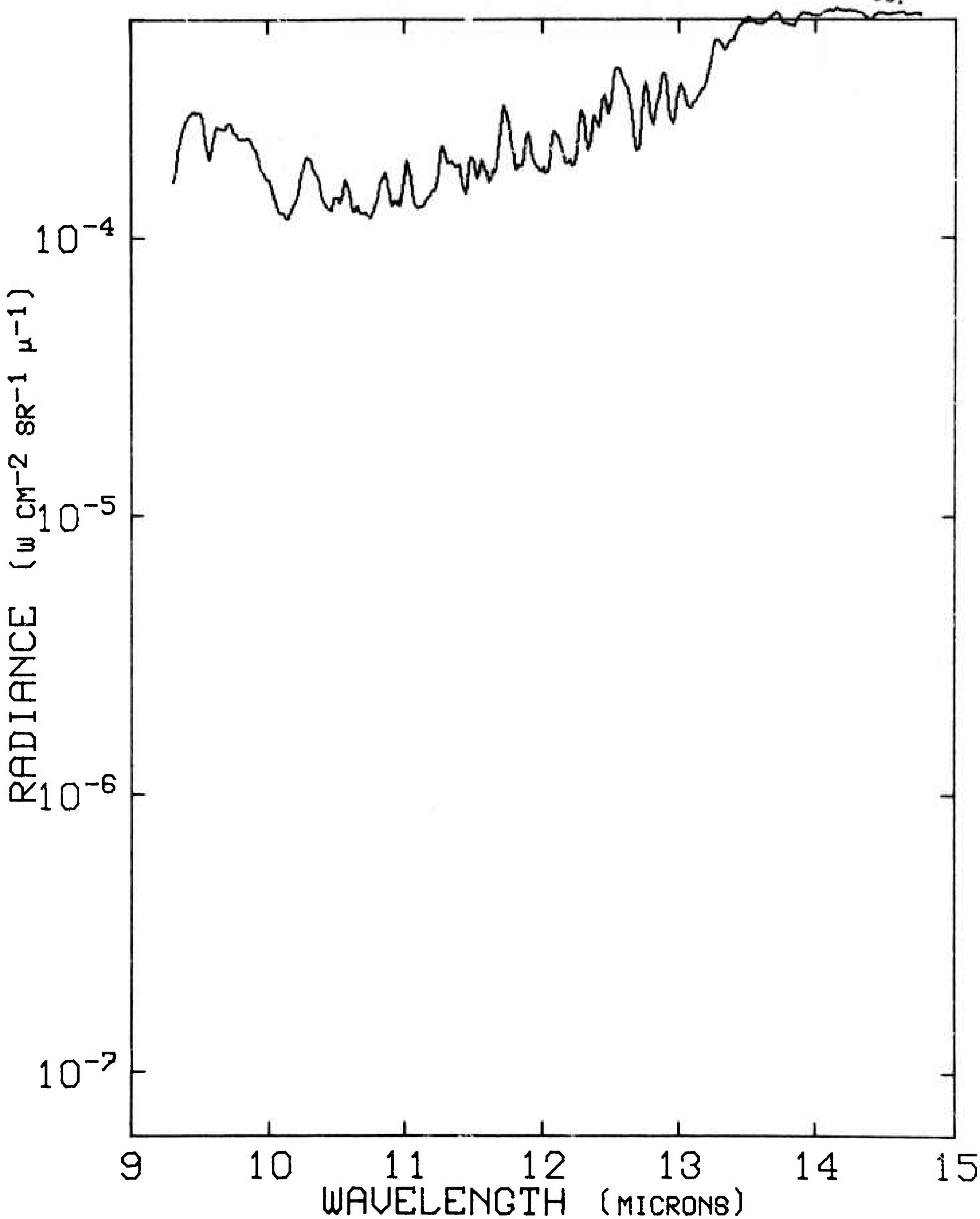

Figure 20. Radiance vs Wavelength at 0.4 kft and 0132 ADT, 12 September 1971.

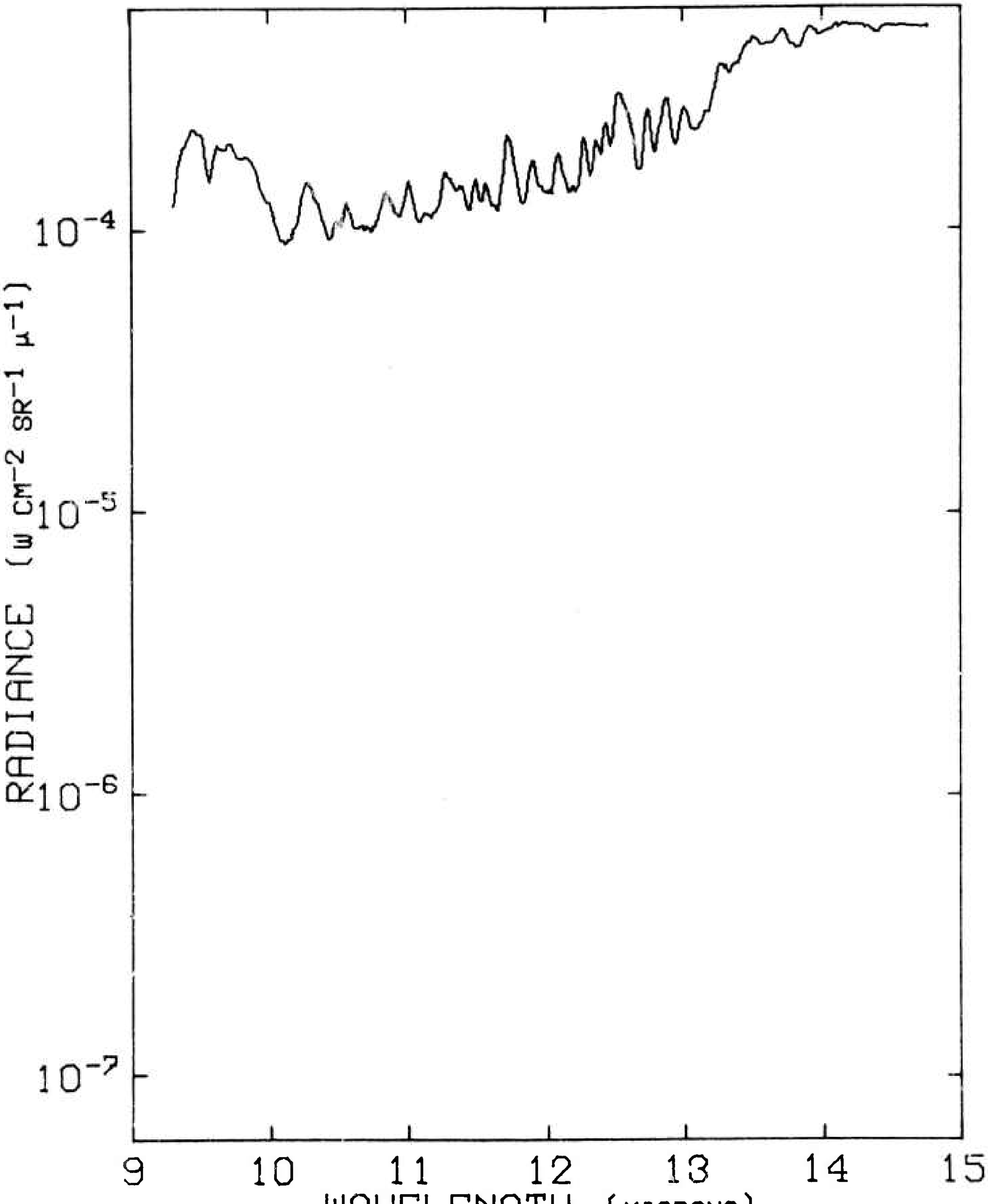

Figure 21. Radiance vs Wavelength at 1.8 kft and 0134 ADT, 12 September 1971.

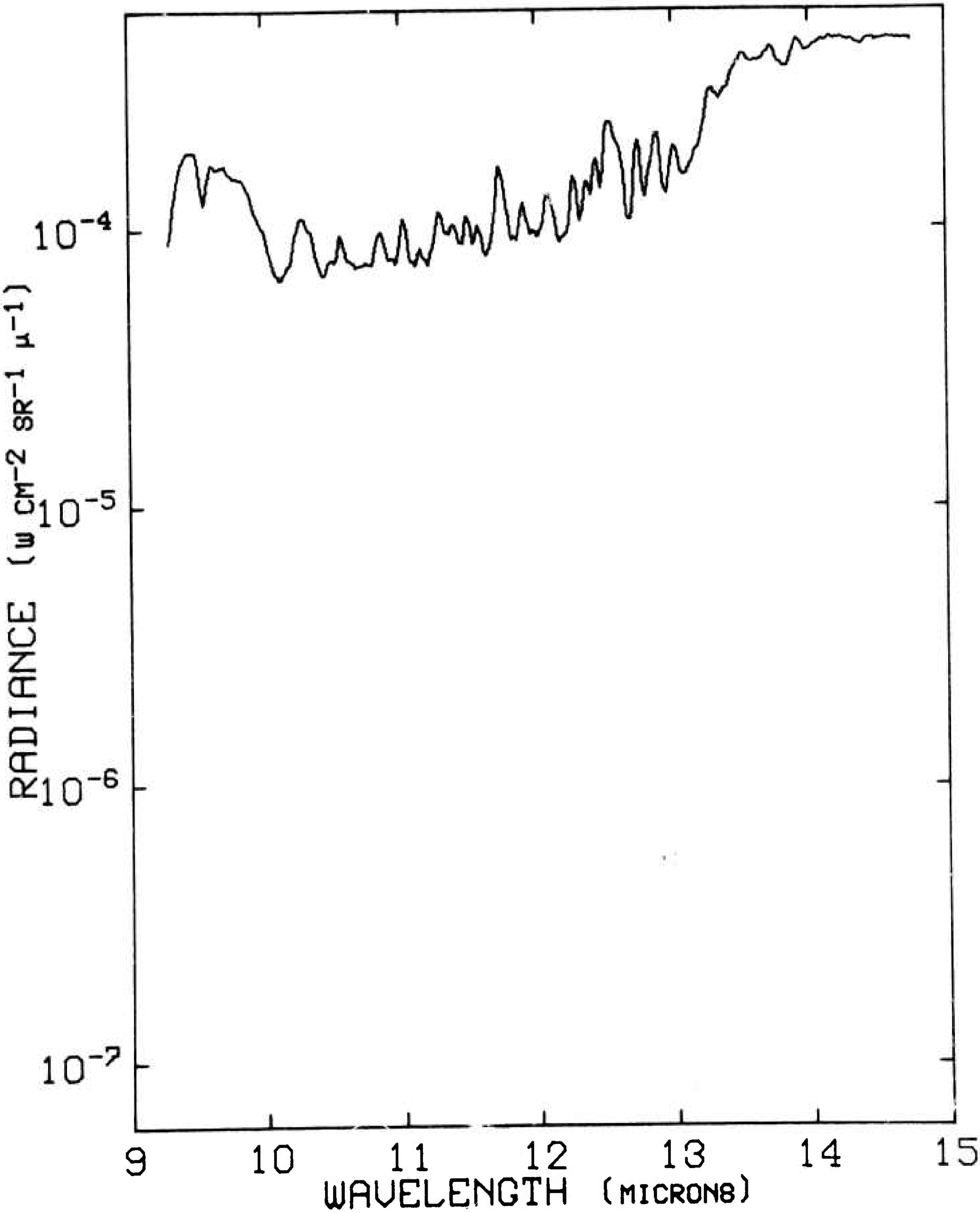

Figure 22. Radiance vs Wavelength at 4.2 kft and 0135 ADT, 12 September 1971.

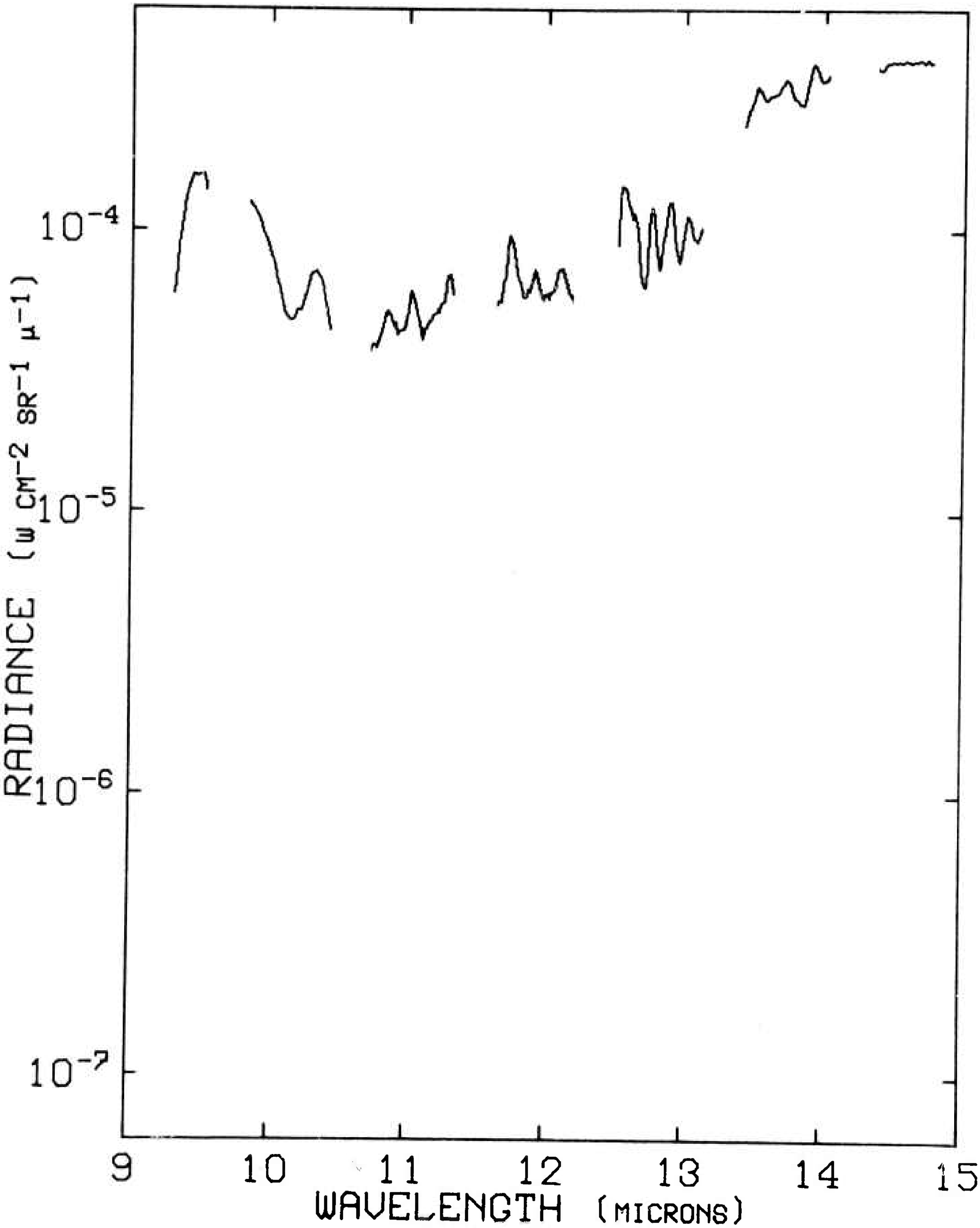

Figure 23. Radiance vs Wavelength at 8.9 kft and 0139 ADT, 12 September 1971.

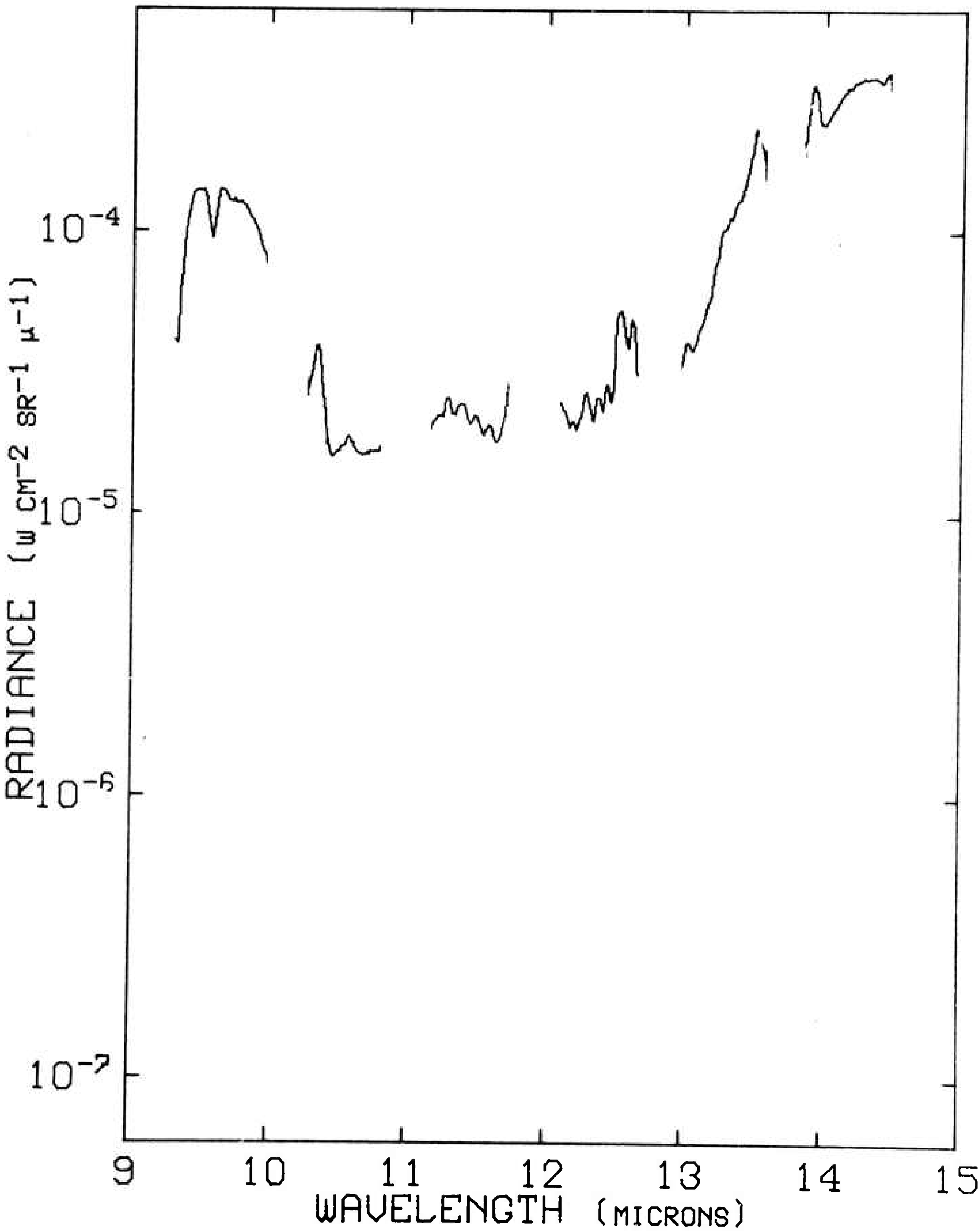

Figure 24. Radiance vs Wavelength at 16.3 kft and 0147 ADT, 12 September 1971.

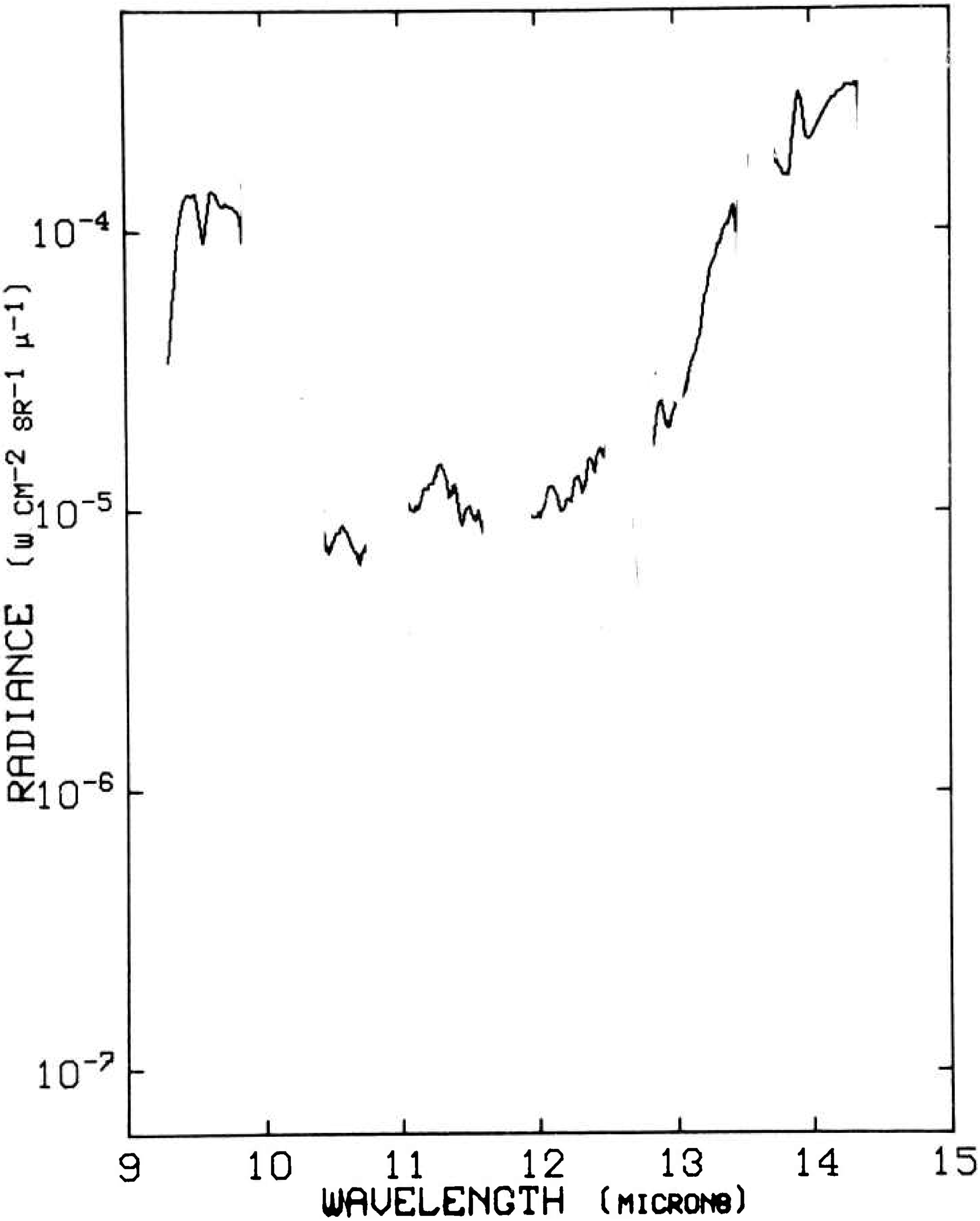

Figure 25. Radiance vs Wavelength at 18.6 kft and 0149 ADT, 12 September 1971.

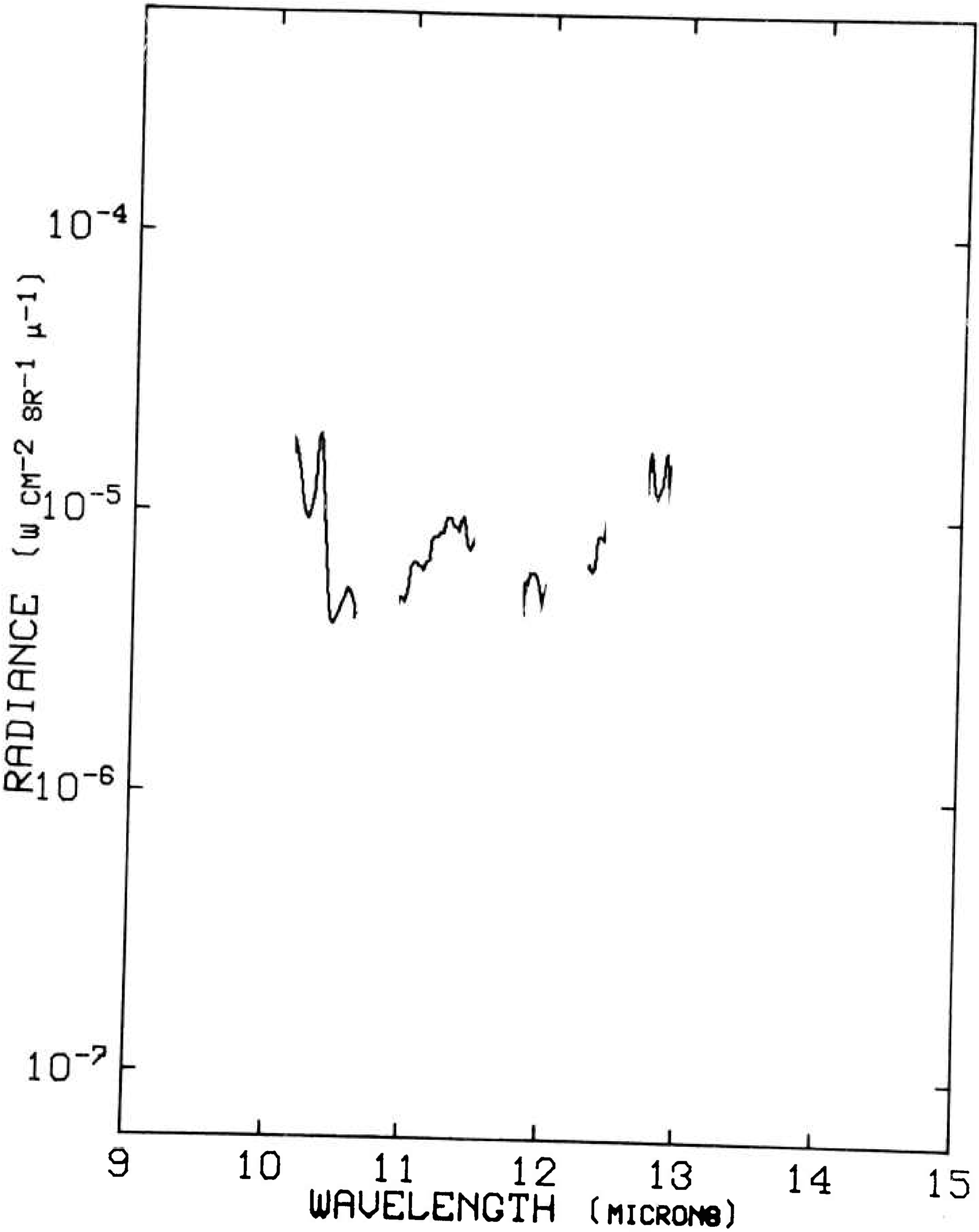

Figure 26. Radiance vs Wavelength at 20.7 kft and 0151 ADT, 12 September 1971.

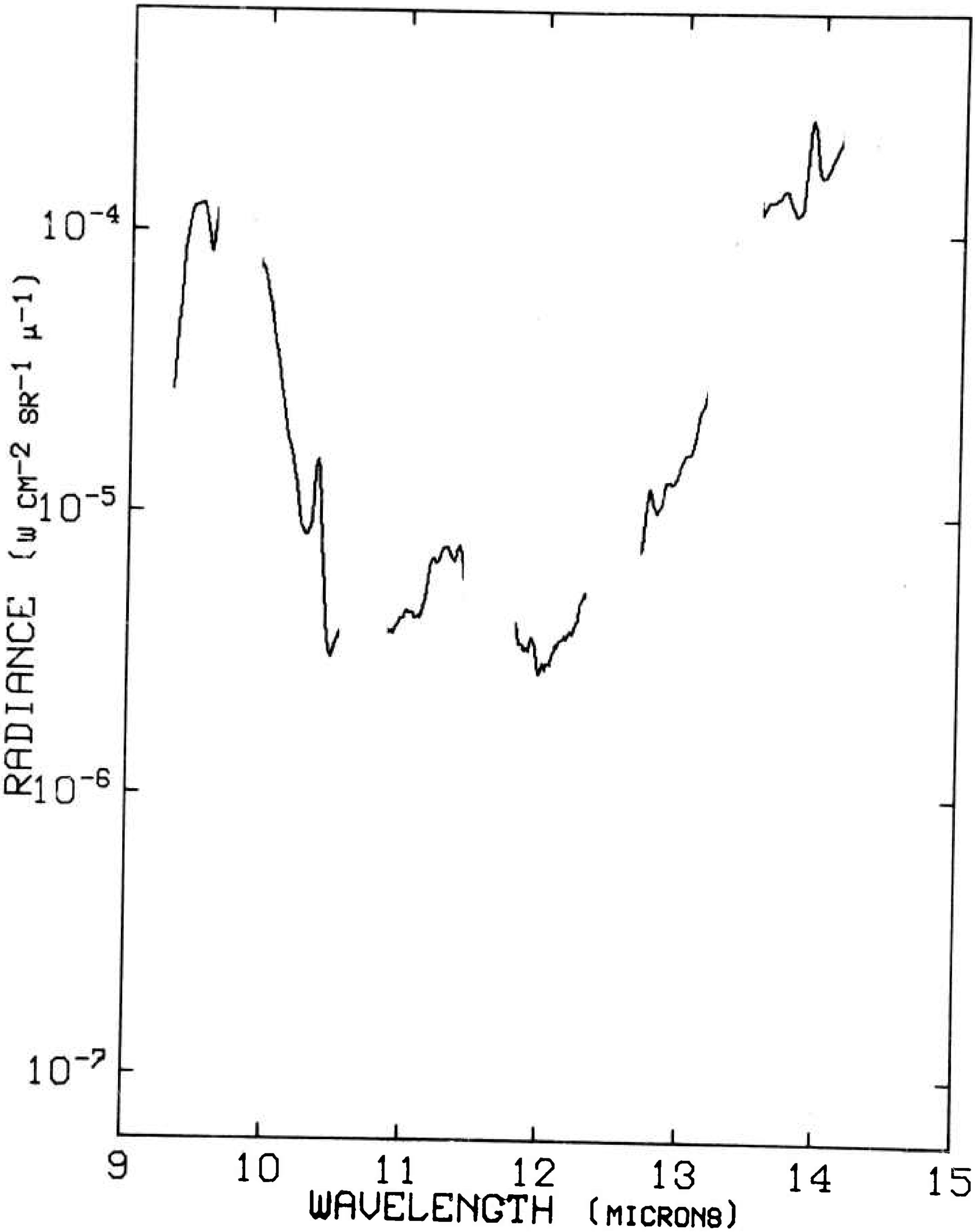

Figure 27. Radiance vs Wavelength at 22.6 kft and 0153 ADT, 12 September 1971.

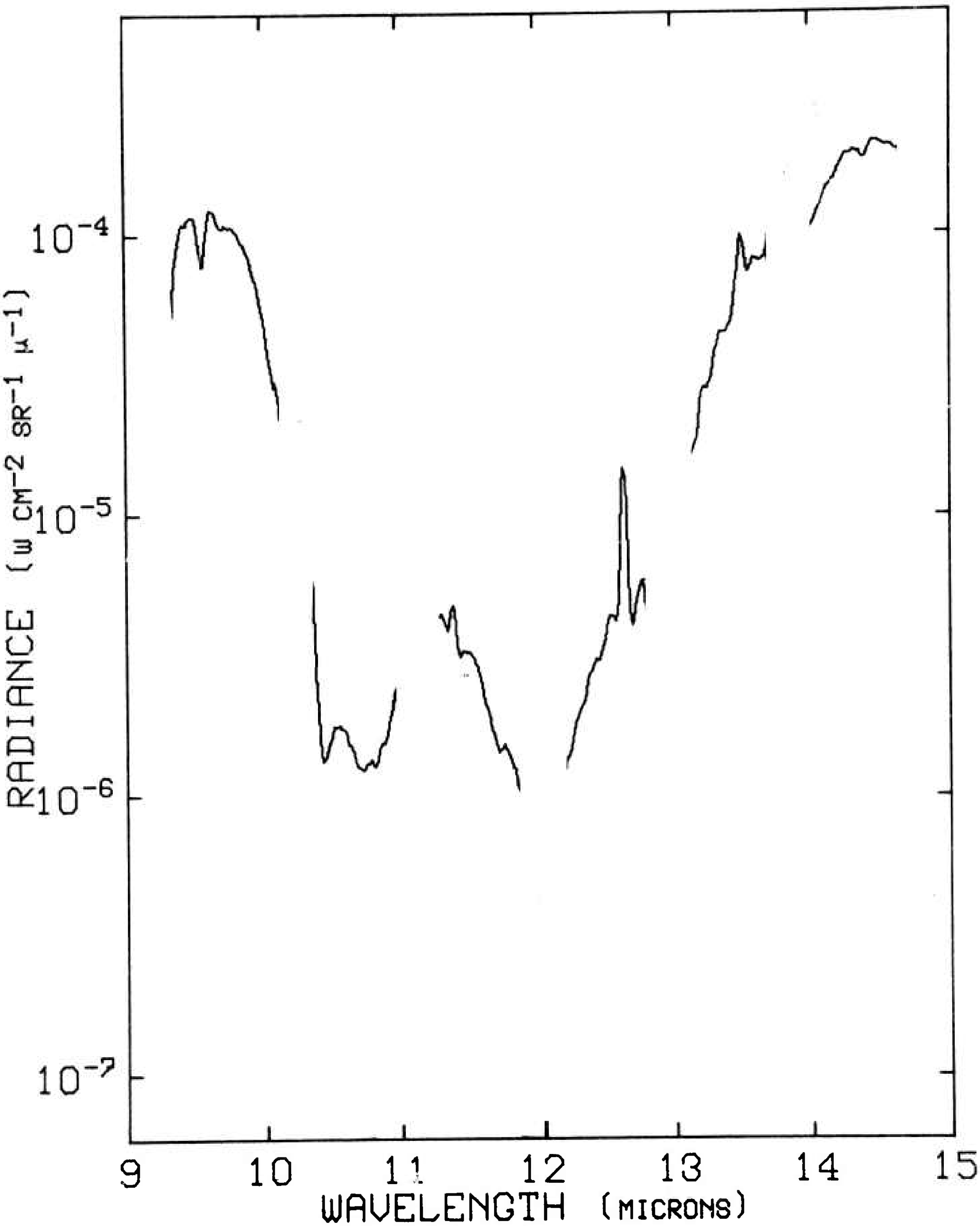

Figure 28. Radiance vs Wavelength at 32.0 kft and 0201 ADT, 12 September 1971.

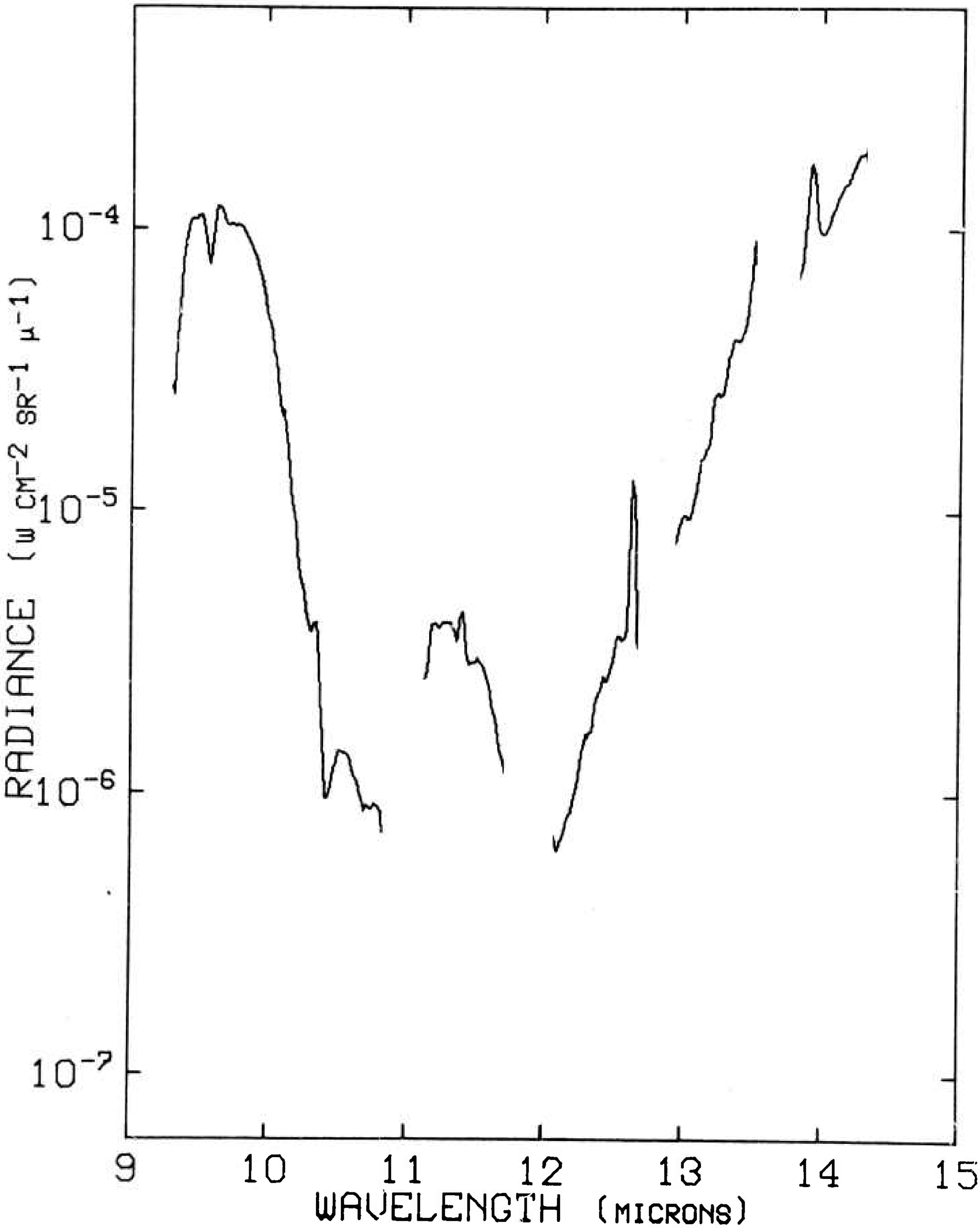

Figure 29. Radiance vs Wavelength at 34.6 kft and 0204 ADT, 12 September 1971.

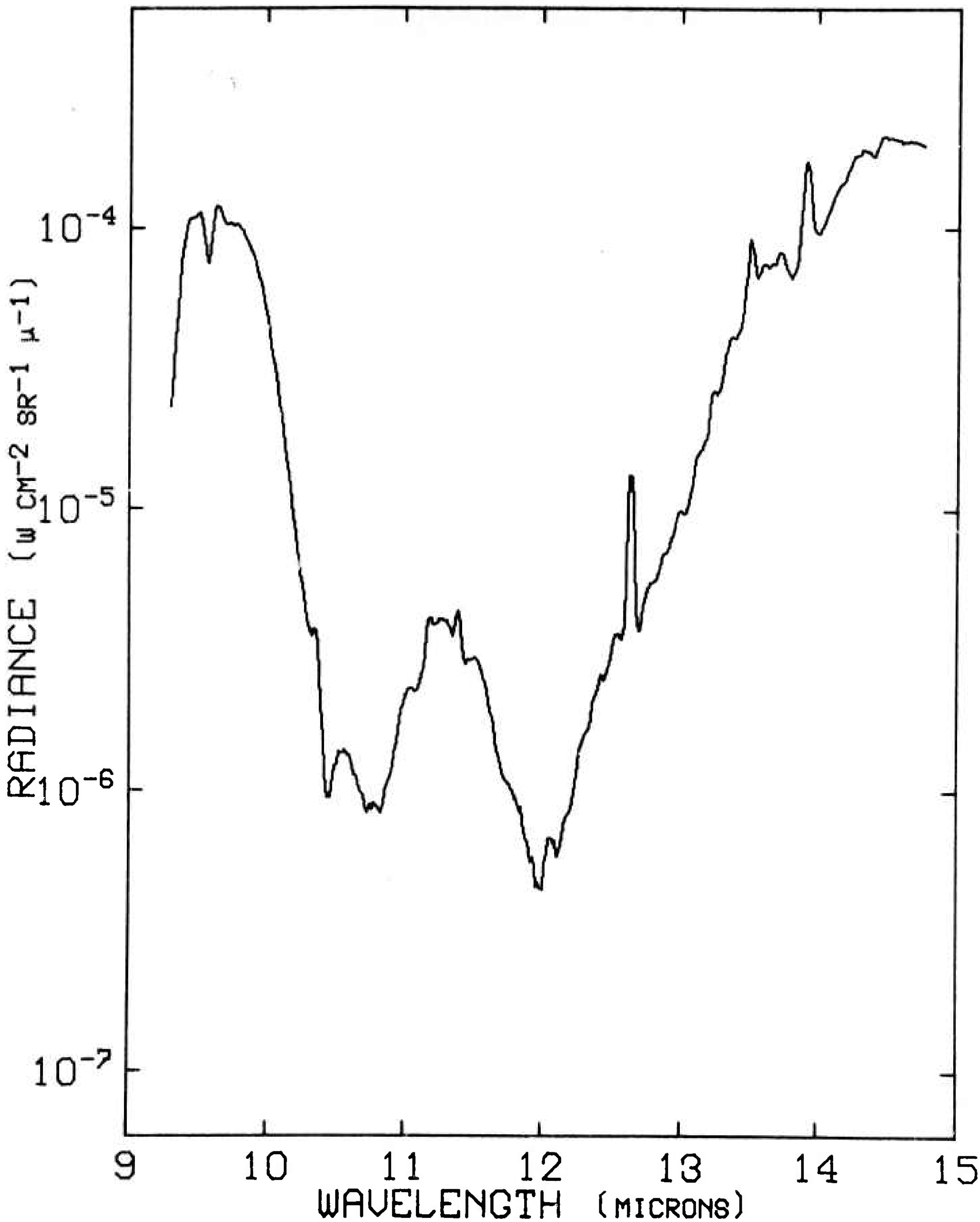

Figure 30. Radiance vs Wavelength at 35.5 kft and 0206 ADT, 12 September 1971.

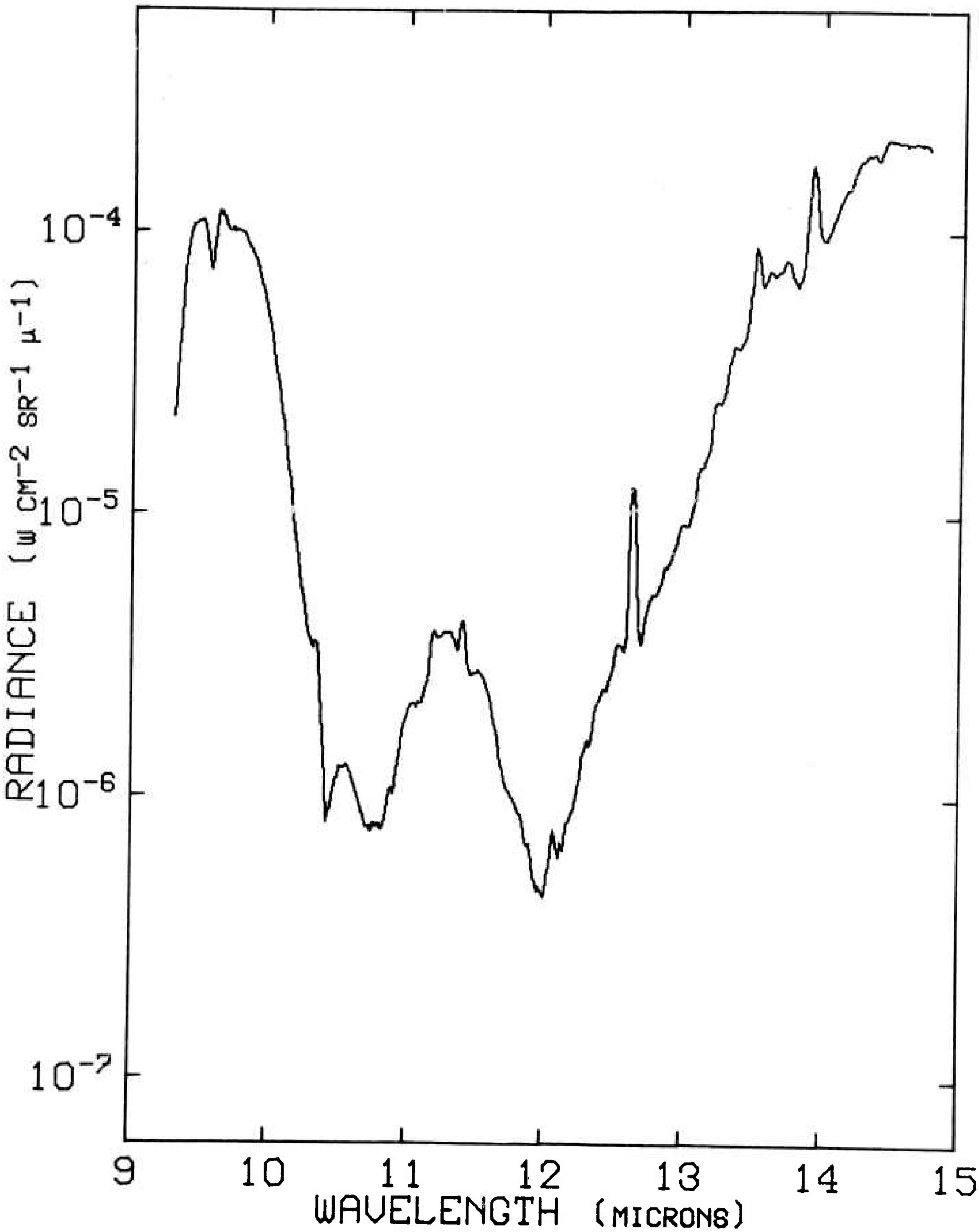

Figure 31. Radiance vs Wavelength at 36.3 kft and 0208 ADT, 12 September 1971.

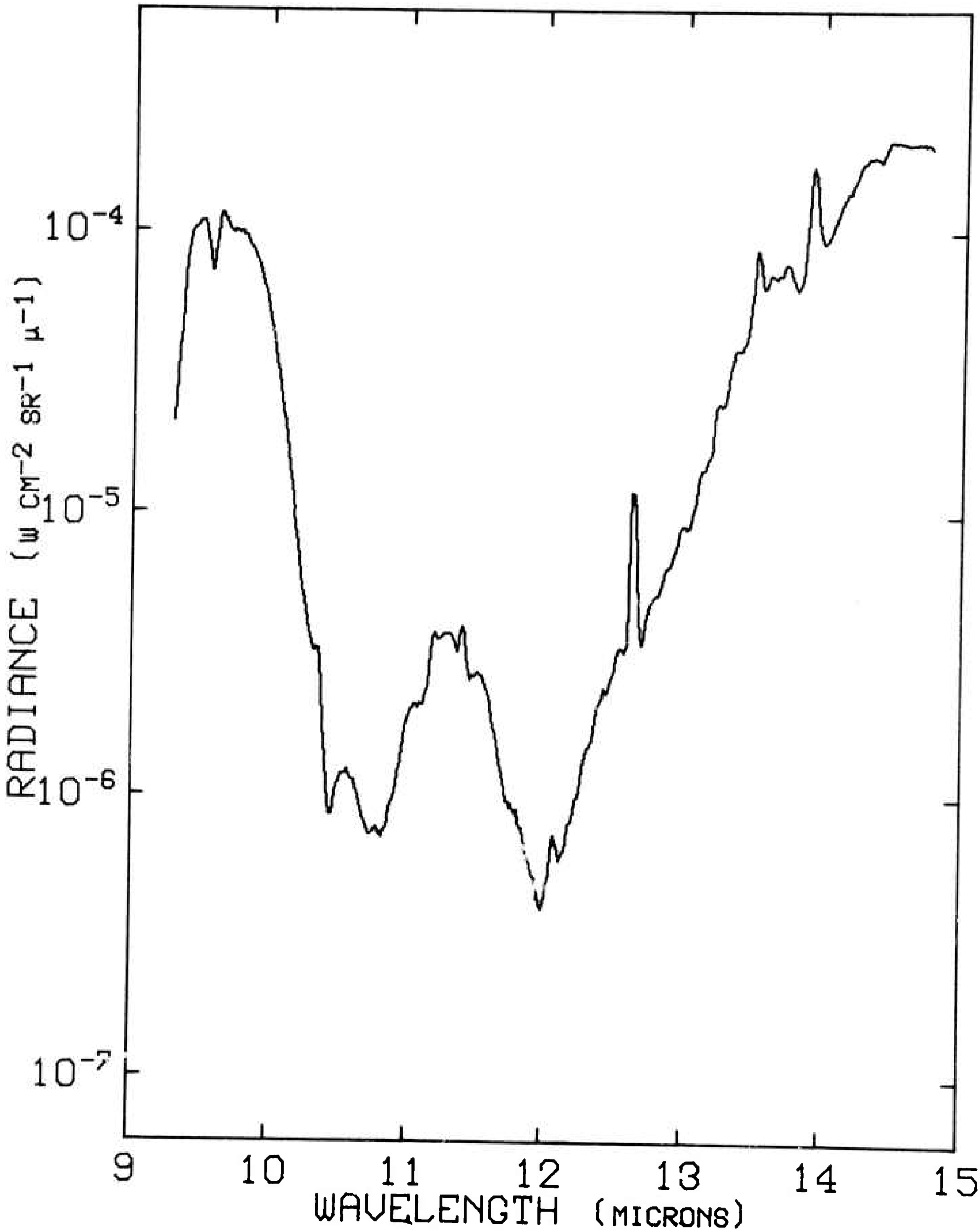

Figure 32. Radiance vs Wavelength at 37.0 kft and 0210 ADT, 12 September 1971.

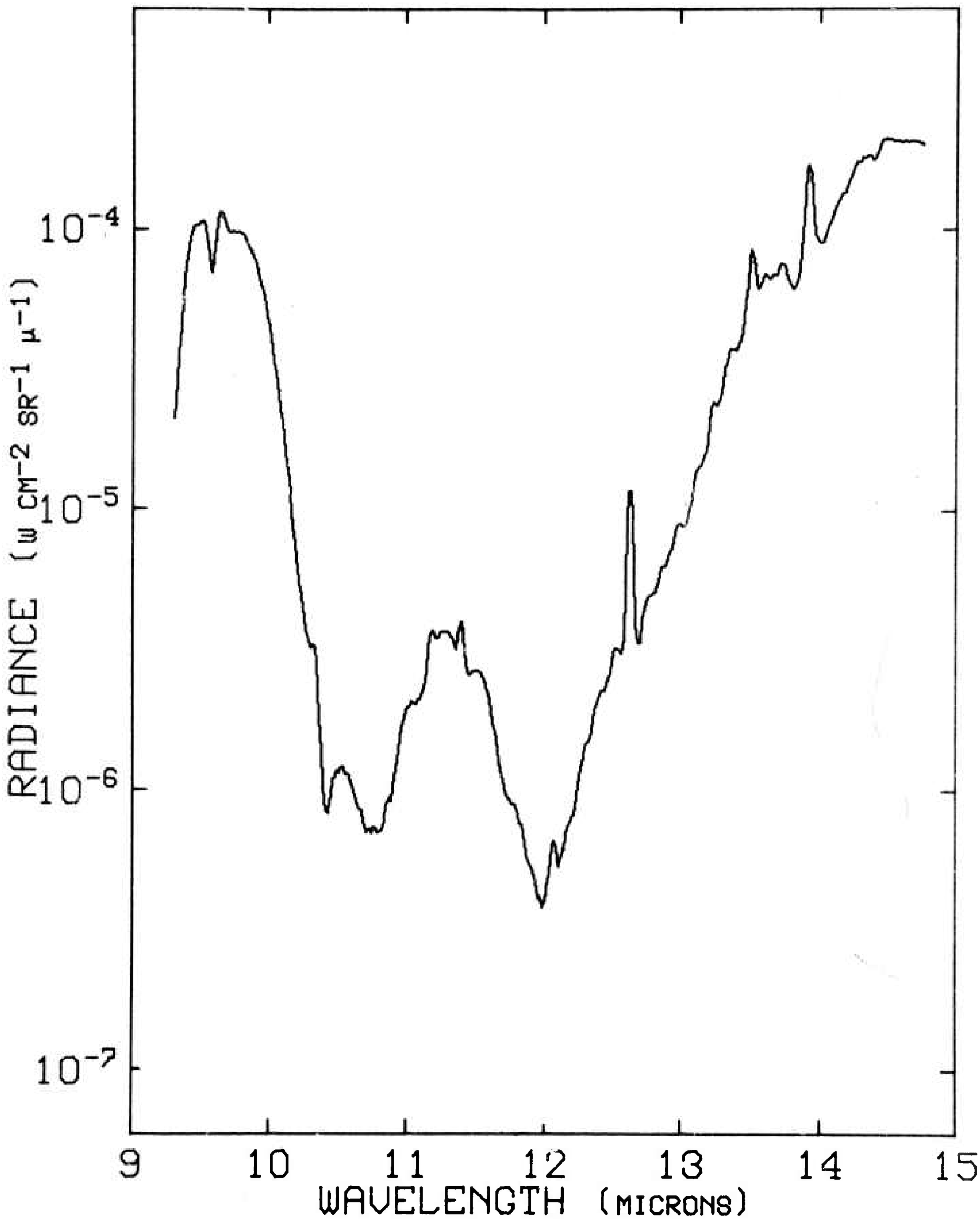

Figure 33. Radiance vs Wavelength at 37.7 kft and 0210 ADT, 12 September 1971.

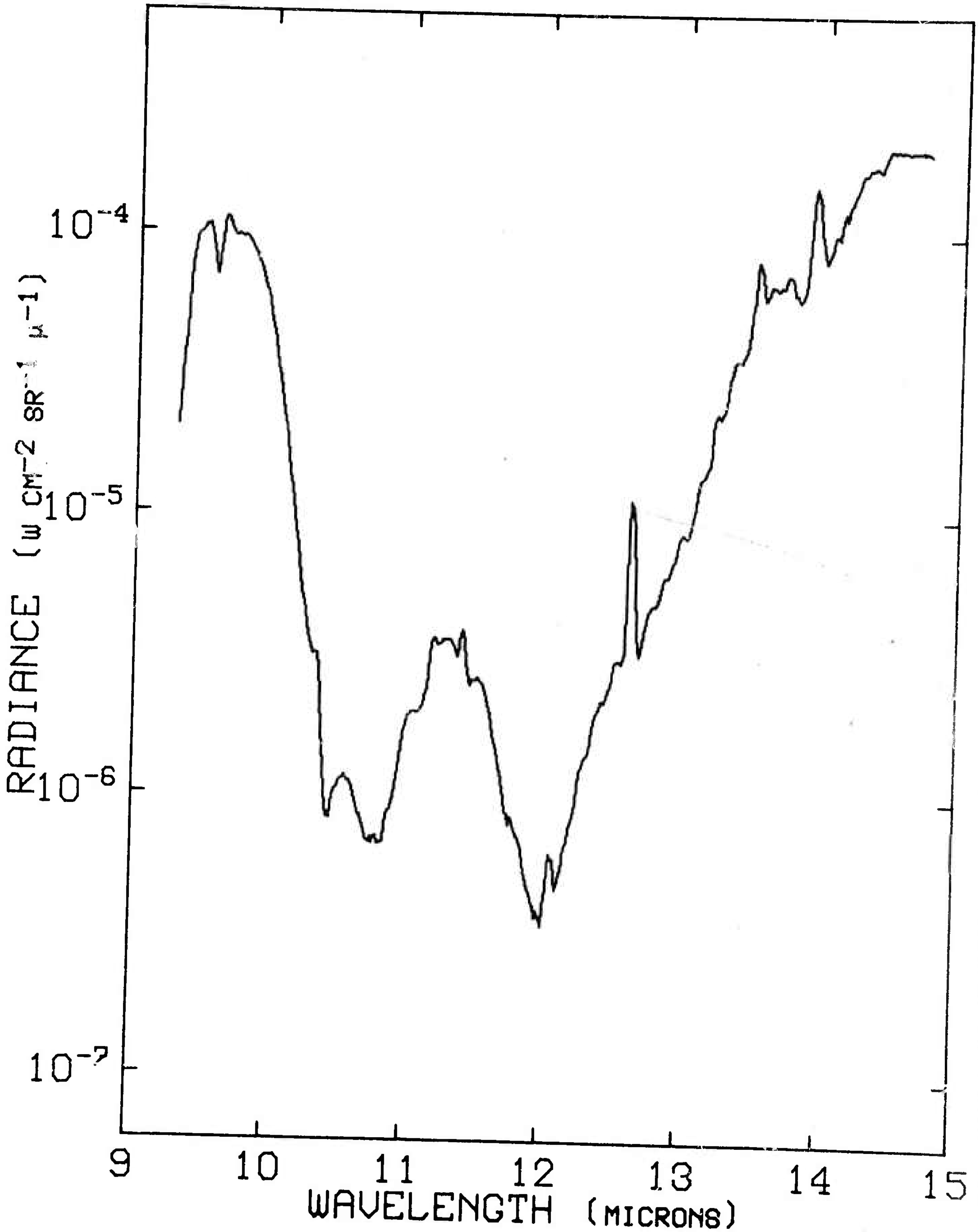

Figure 34. Radiance vs Wavelength at 38.3 kft and 0214 ADT, 12 September 1971.

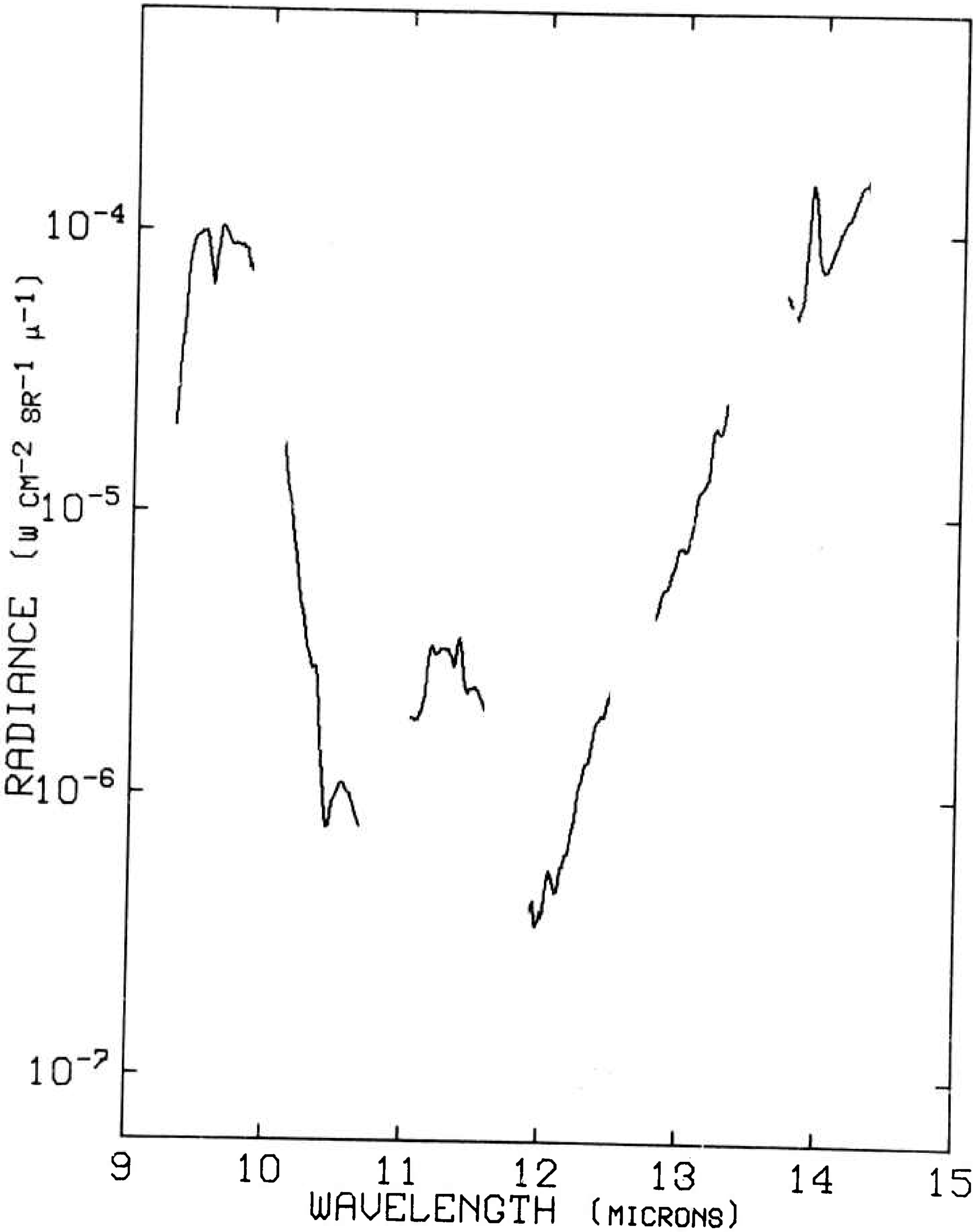

Figure 35. Radiance vs Wavelength at 41.0 kft and 0222 ADT, 12 September 1971.

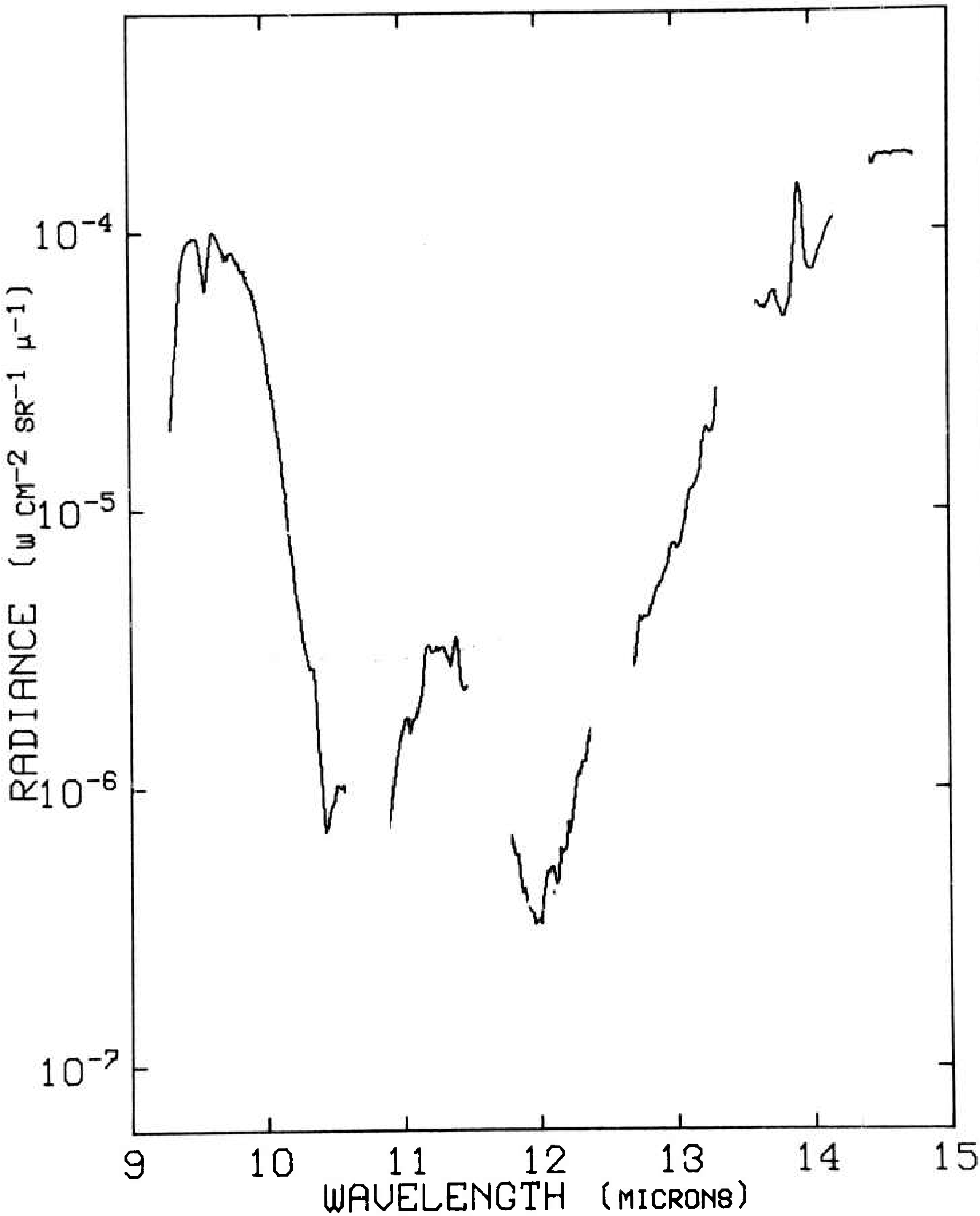

Figure 36. Radiance vs Wavelength at 41.9 kft and 0224 ADT, 12 September 1971.

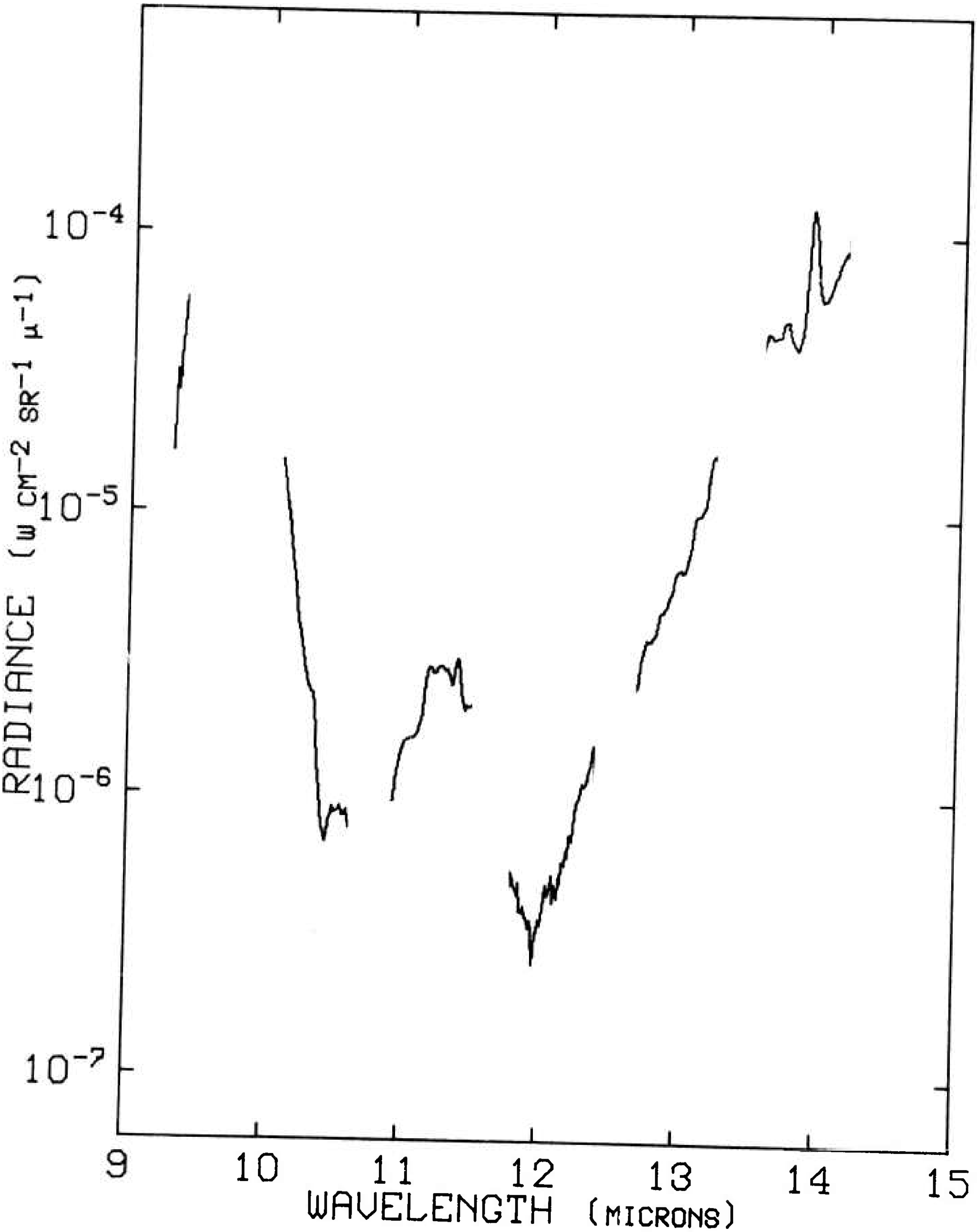

Figure 37. Radiance vs Wavelength at 44.3 kft and 0230 ADT, 12 September 1971.

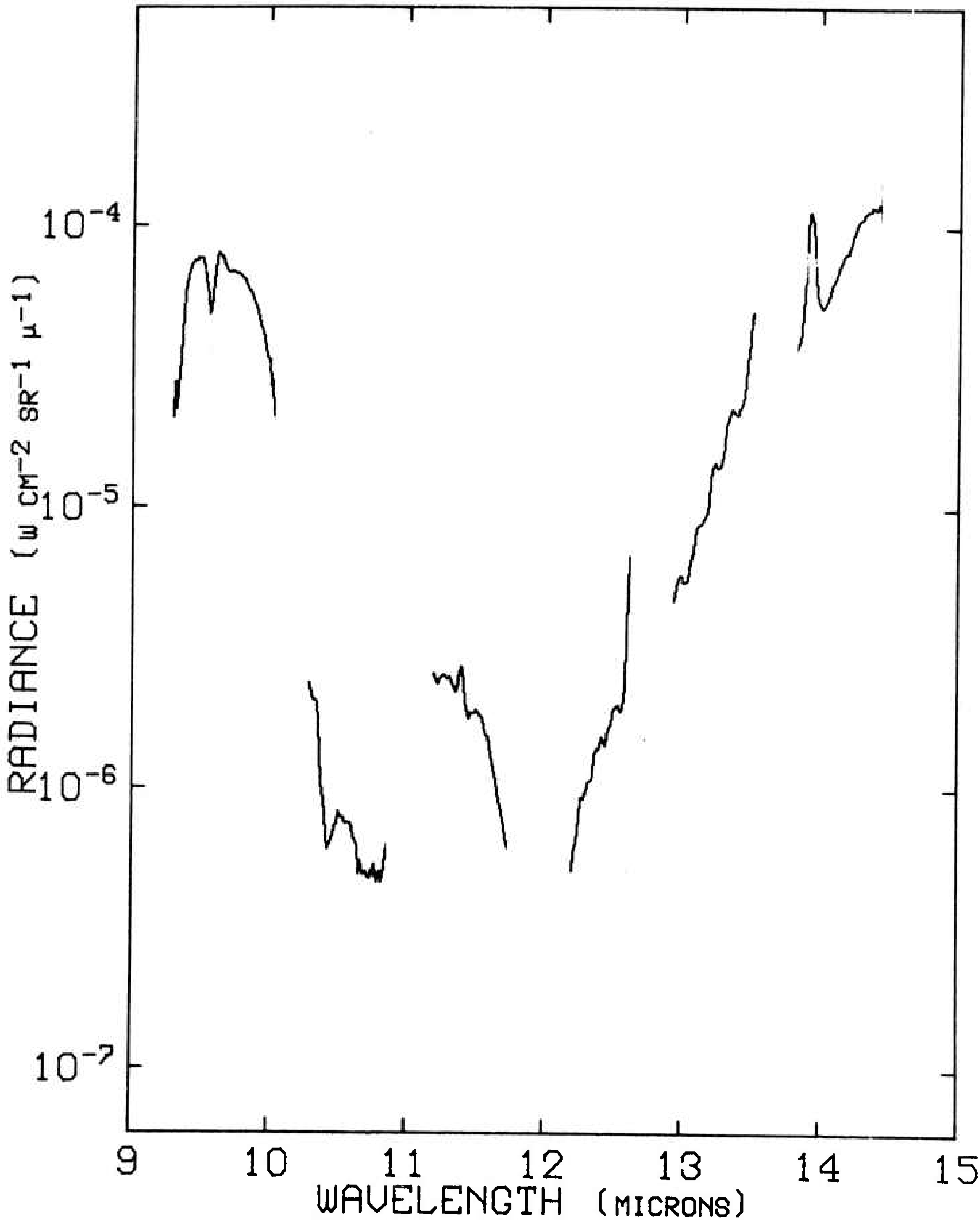

Figure 38. Radiance vs Wavelength at 46.1 kft and 0233 ADT, 12 September 1971.

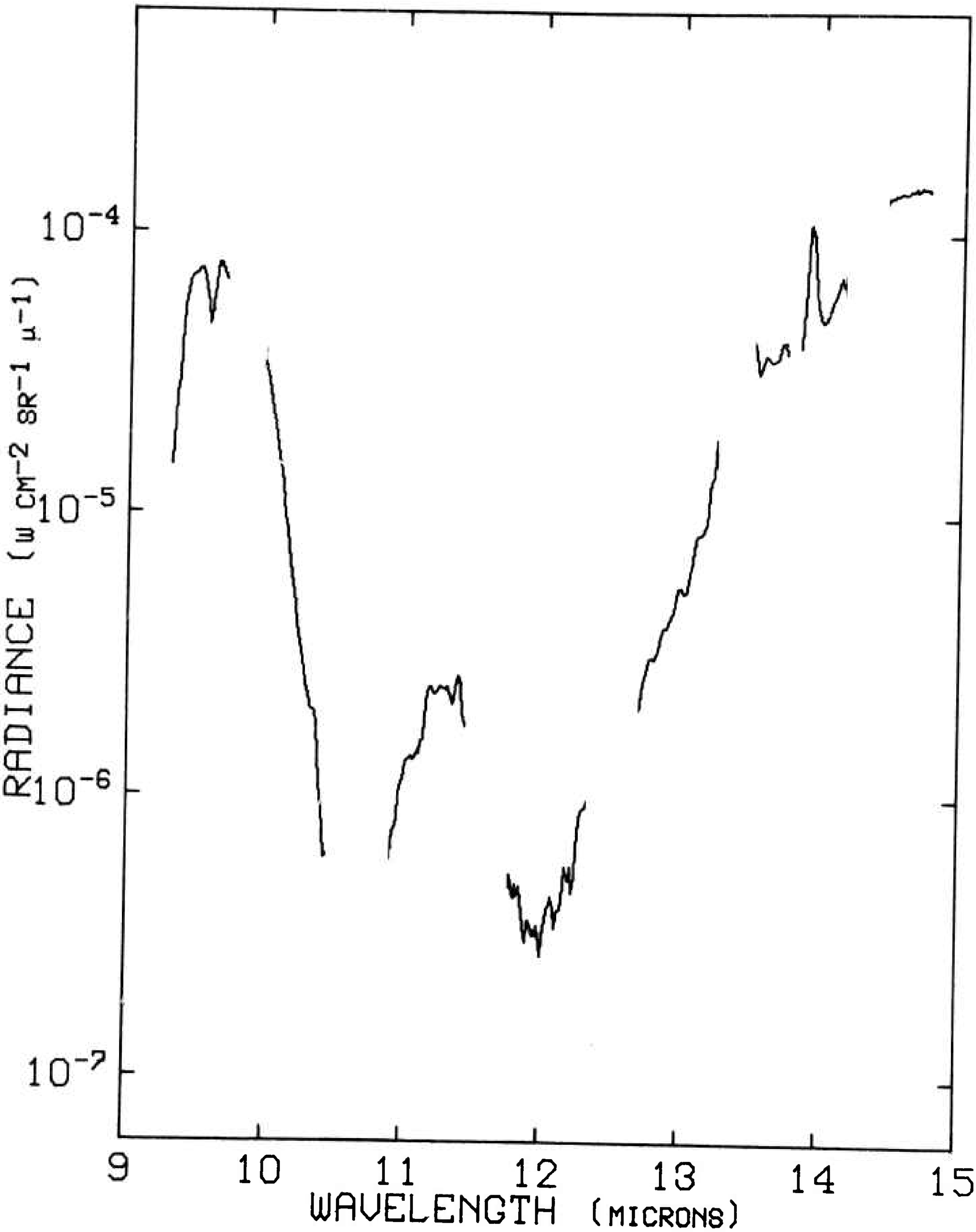

Figure 39. Radiance vs Wavelength at 47.0 kft and 0235 ADT, 12 September 1971.

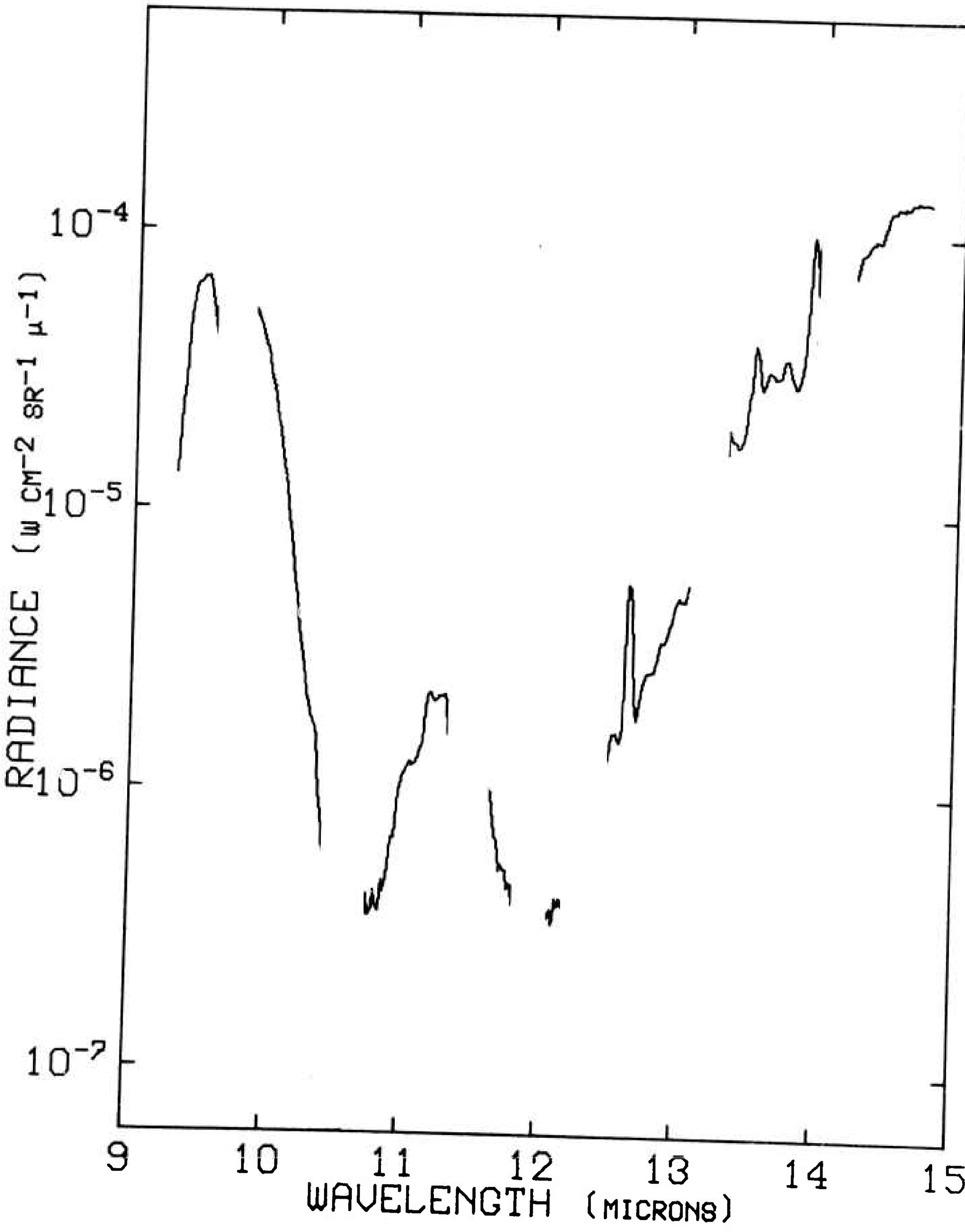

Figure 40. Radiance vs Wavelength at 48.9 kft and 0239 ADT, 12 September 1971.

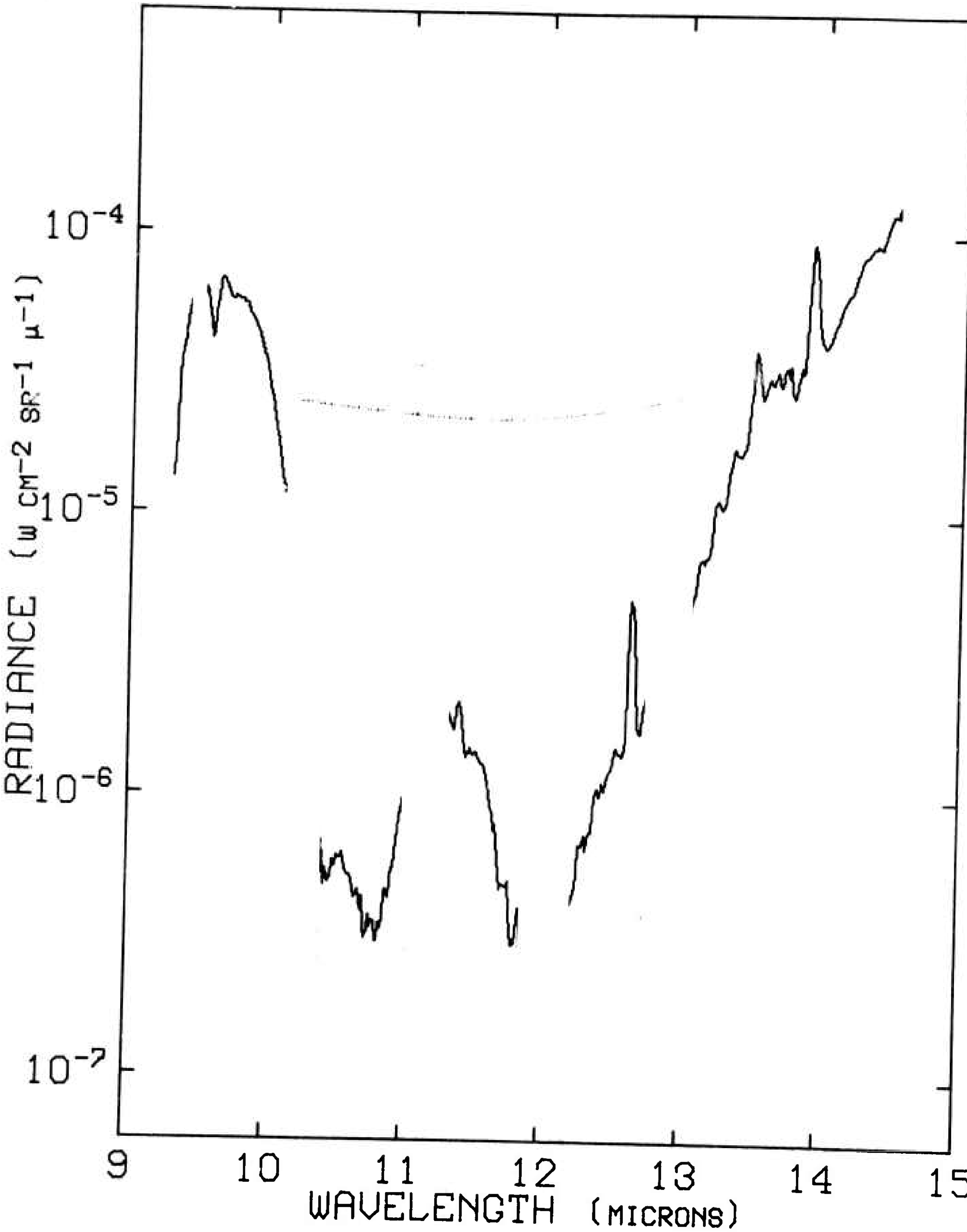

Figure 41. Radiance vs Wavelength at 50.0 kft and 0241 ADT, 12 September 1971.

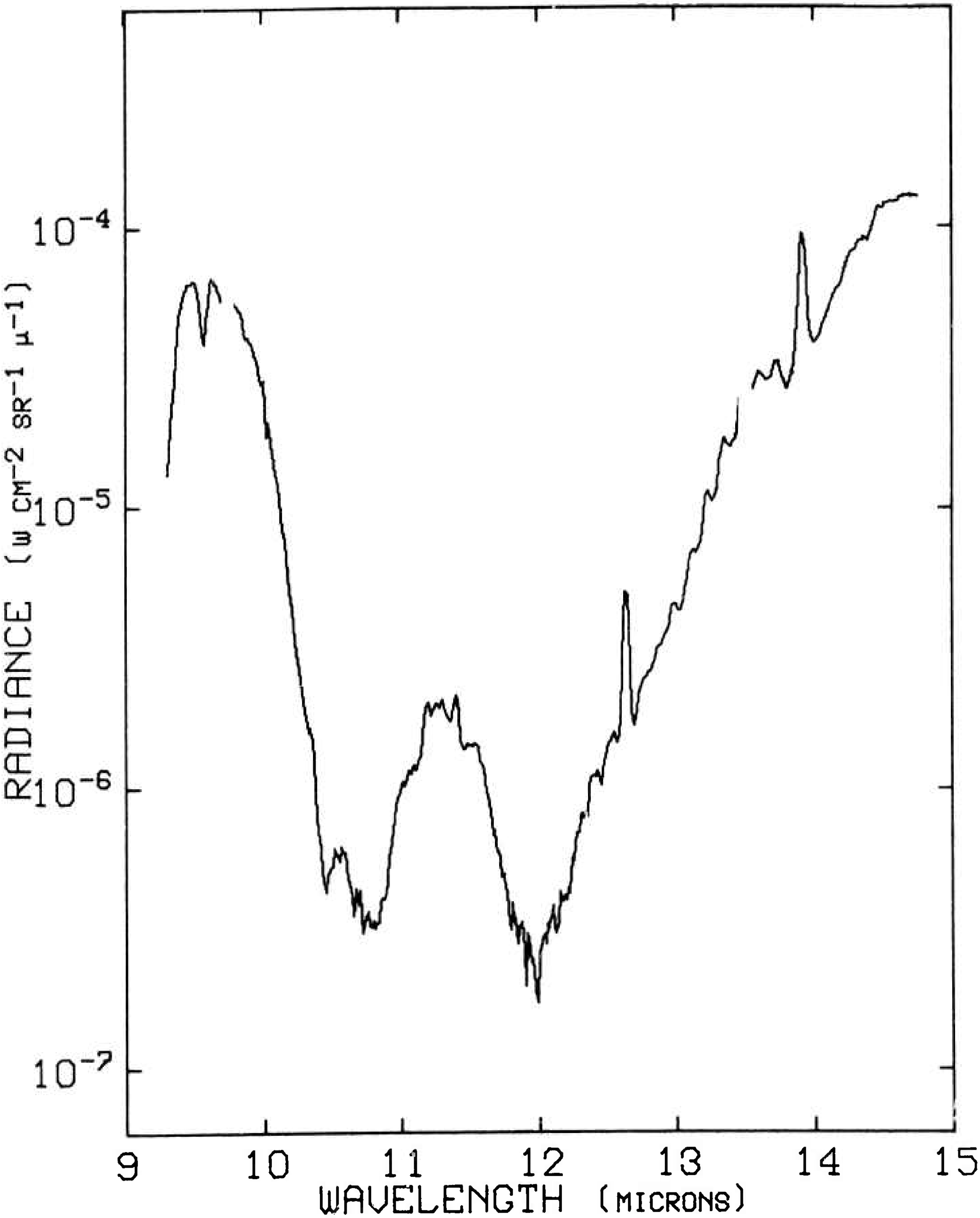

Figure 42. Radiance vs Wavelength at 51.1 kft and 0243 ADT, 12 September 1971.

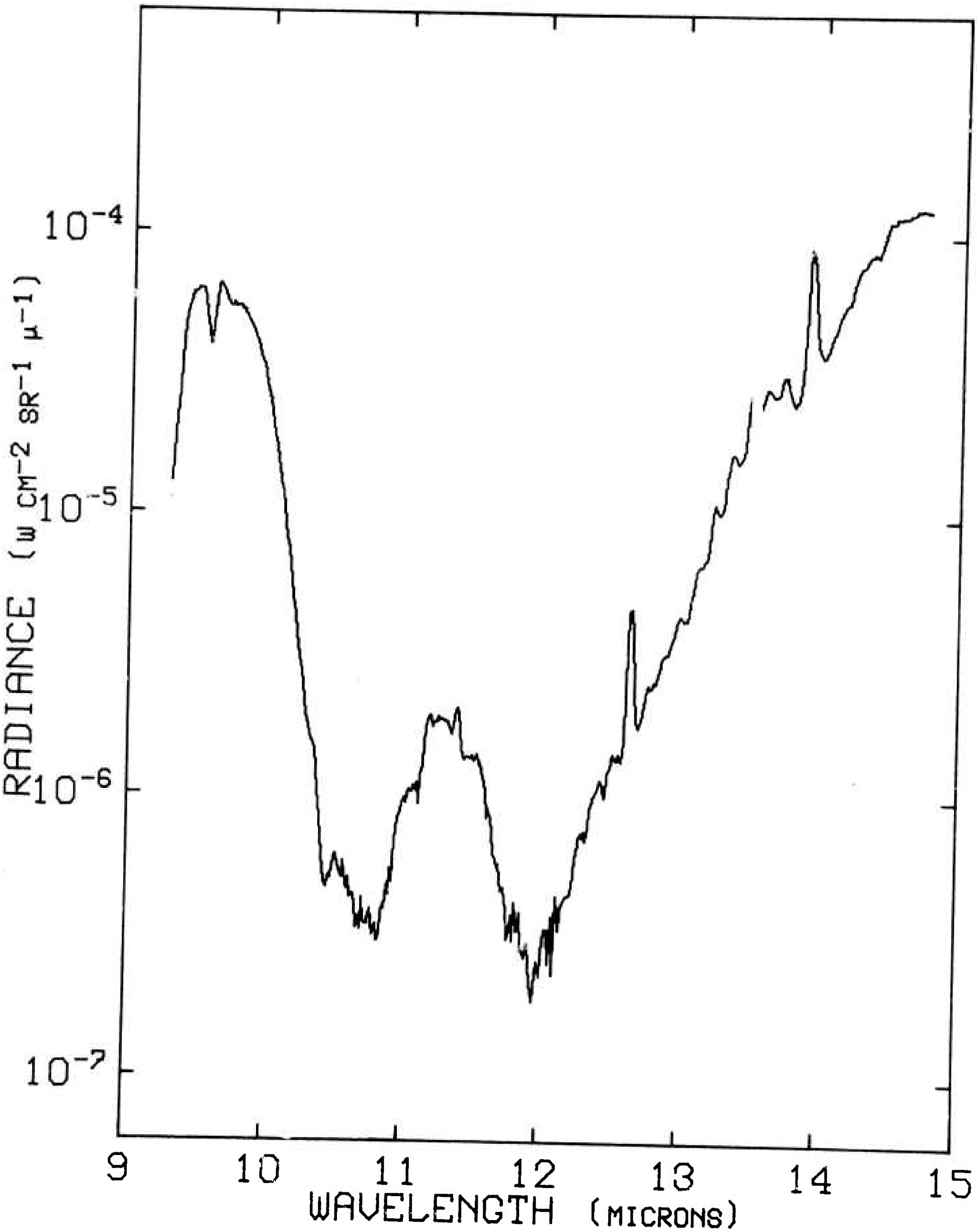

Figure 43. Radiance vs Wavelength at 52.2 kft and 0245 ADT, 12 September 1971.

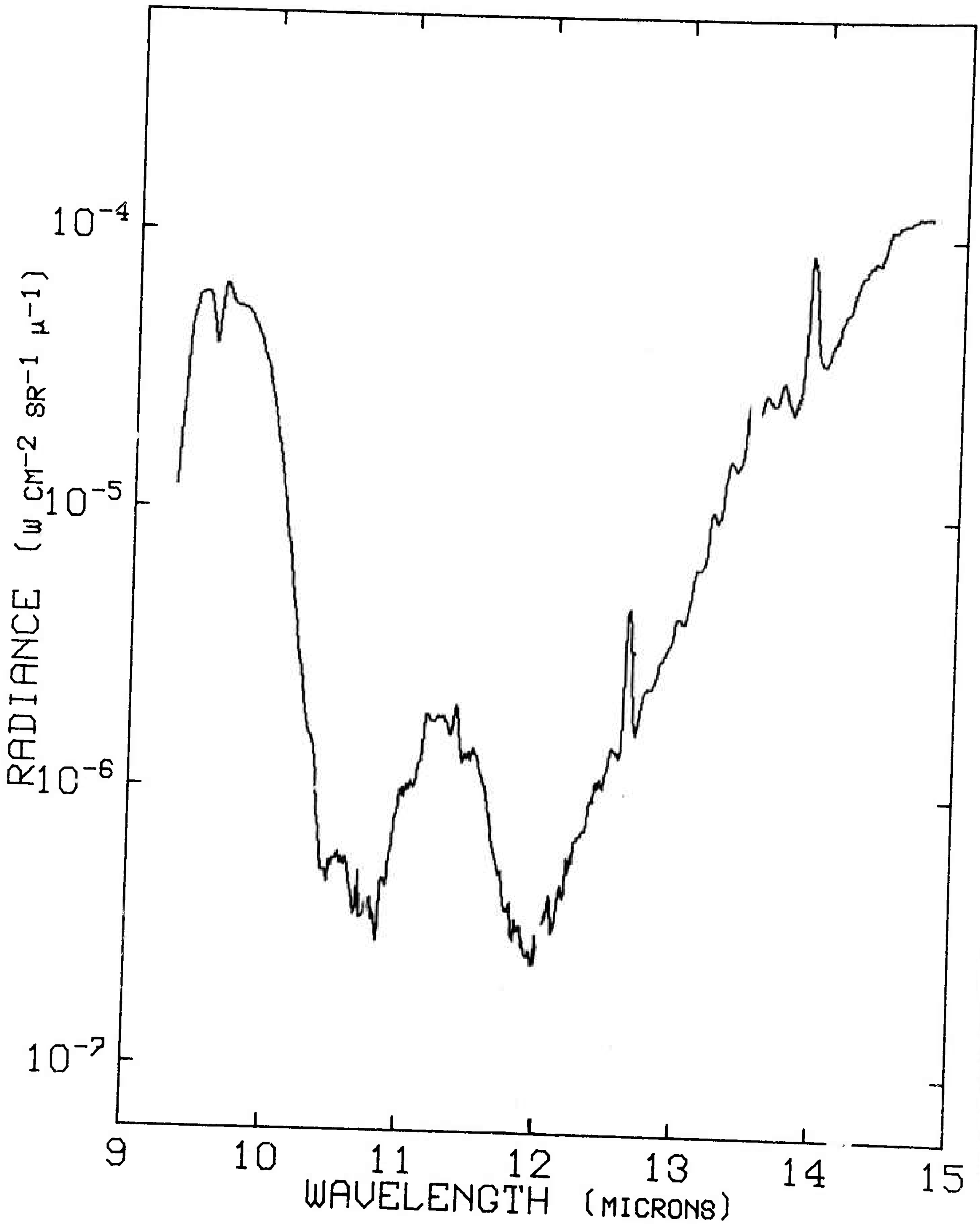

Figure 44. Radiance vs Wavelength at 53.4 kft and 0247 ADT, 12 September 1971.

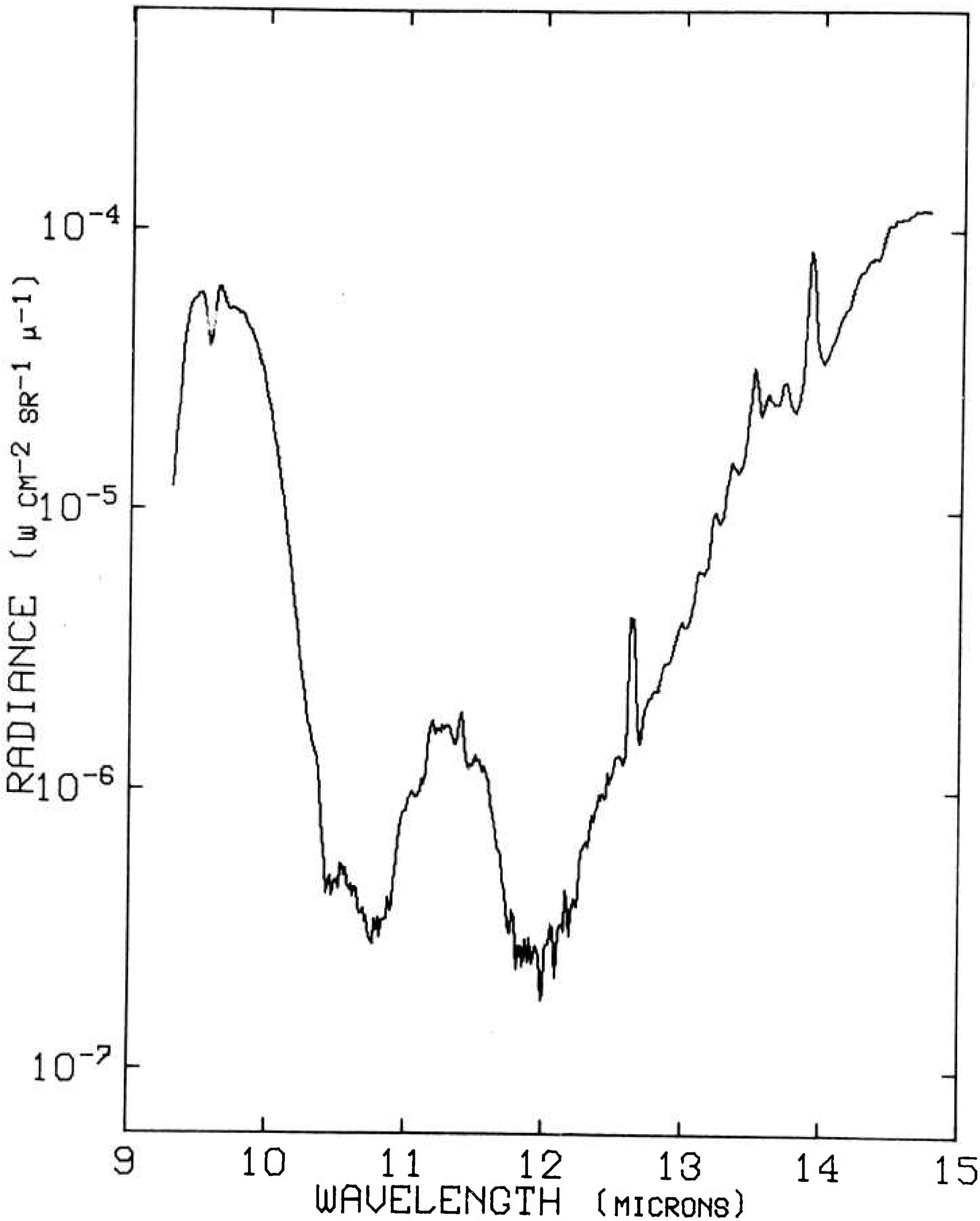

Figure 45. Radiance vs Wavelength at 54.2 kft and 0249 ADT, 12 September 1971.

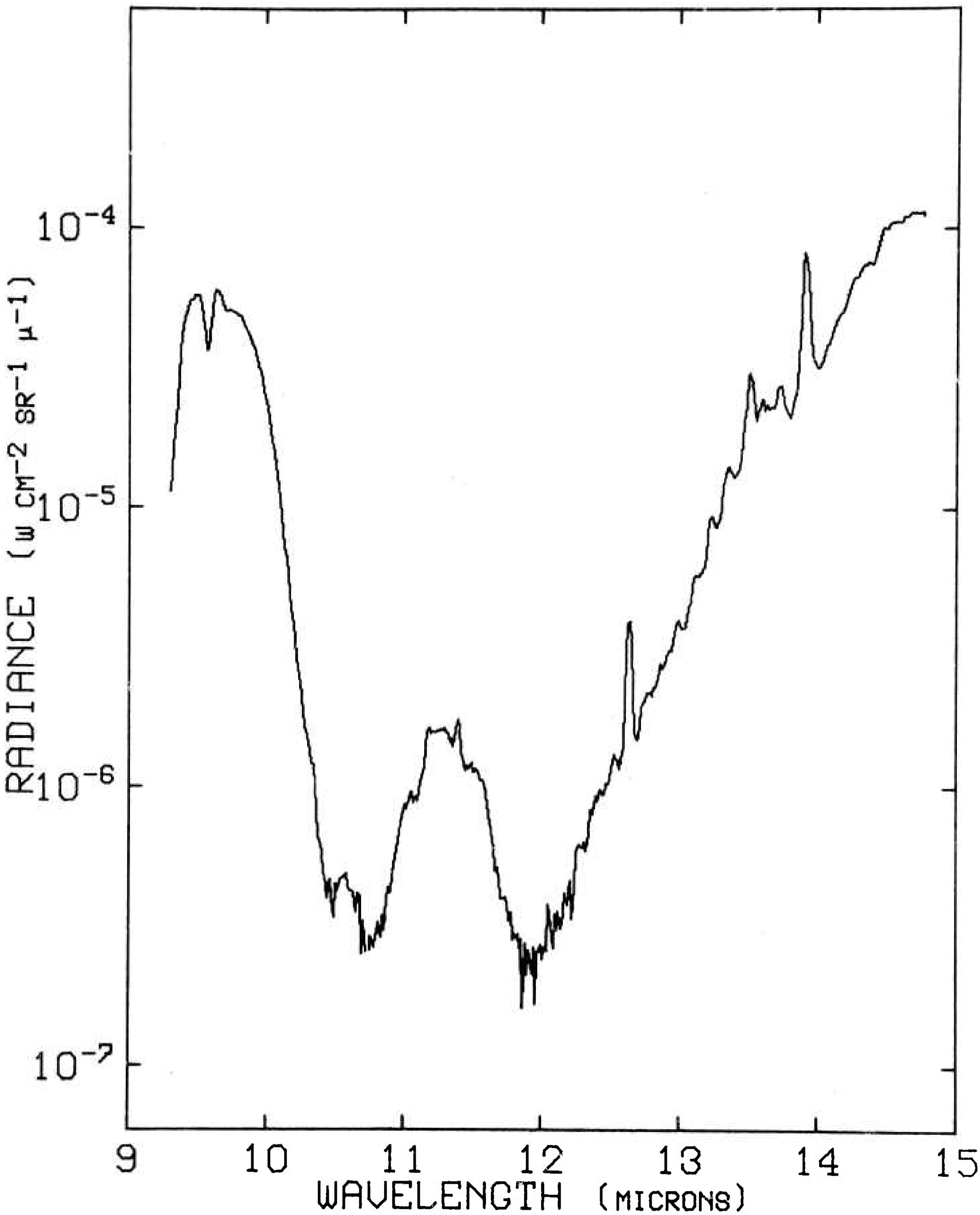

Figure 46. Radiance vs Wavelength at 55.8 kft and 0251 ADT, 12 September 1971.

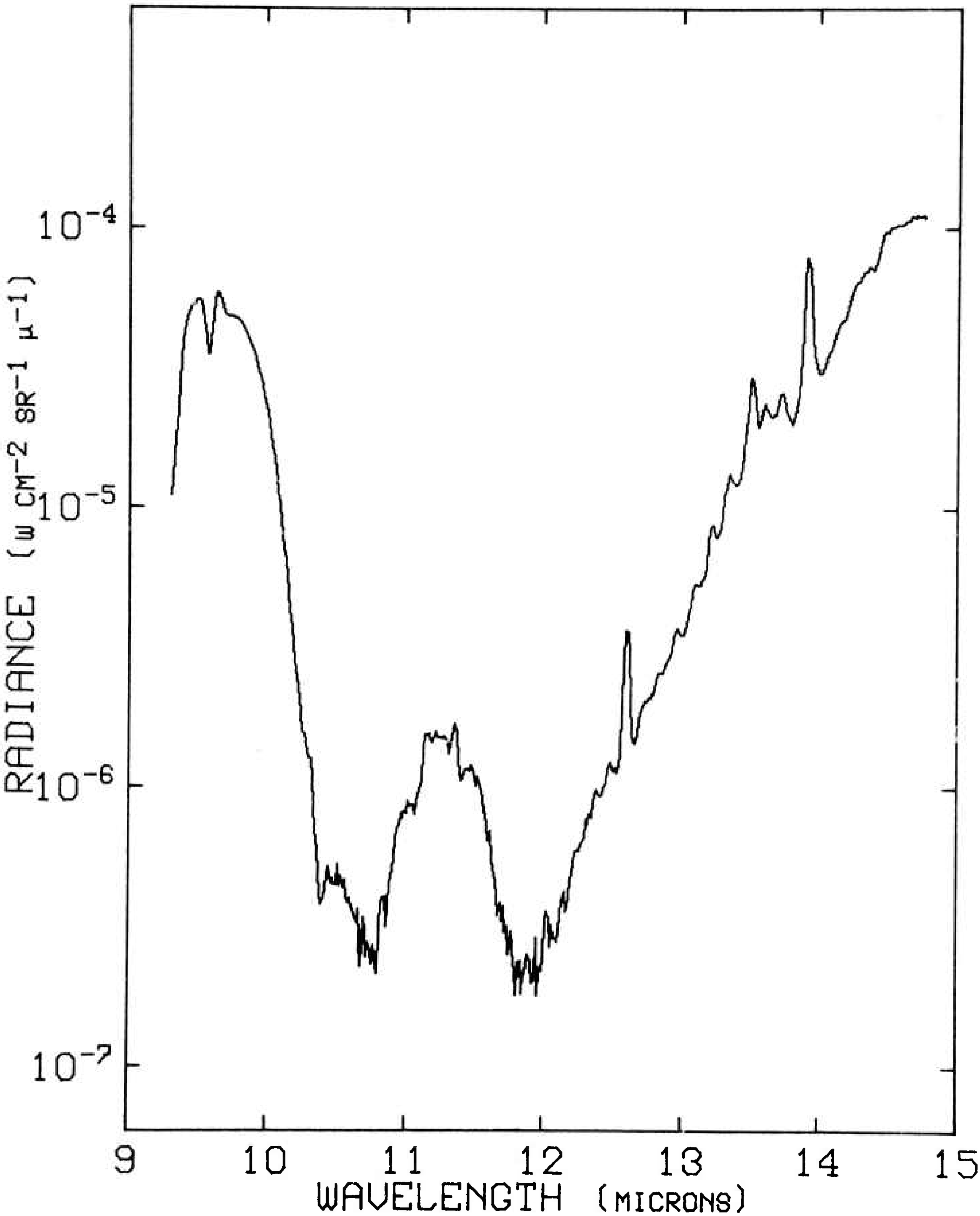

Figure 47. Radiance vs Wavelength at 57.0 kft and 0253 ADT, 12 September 1971.

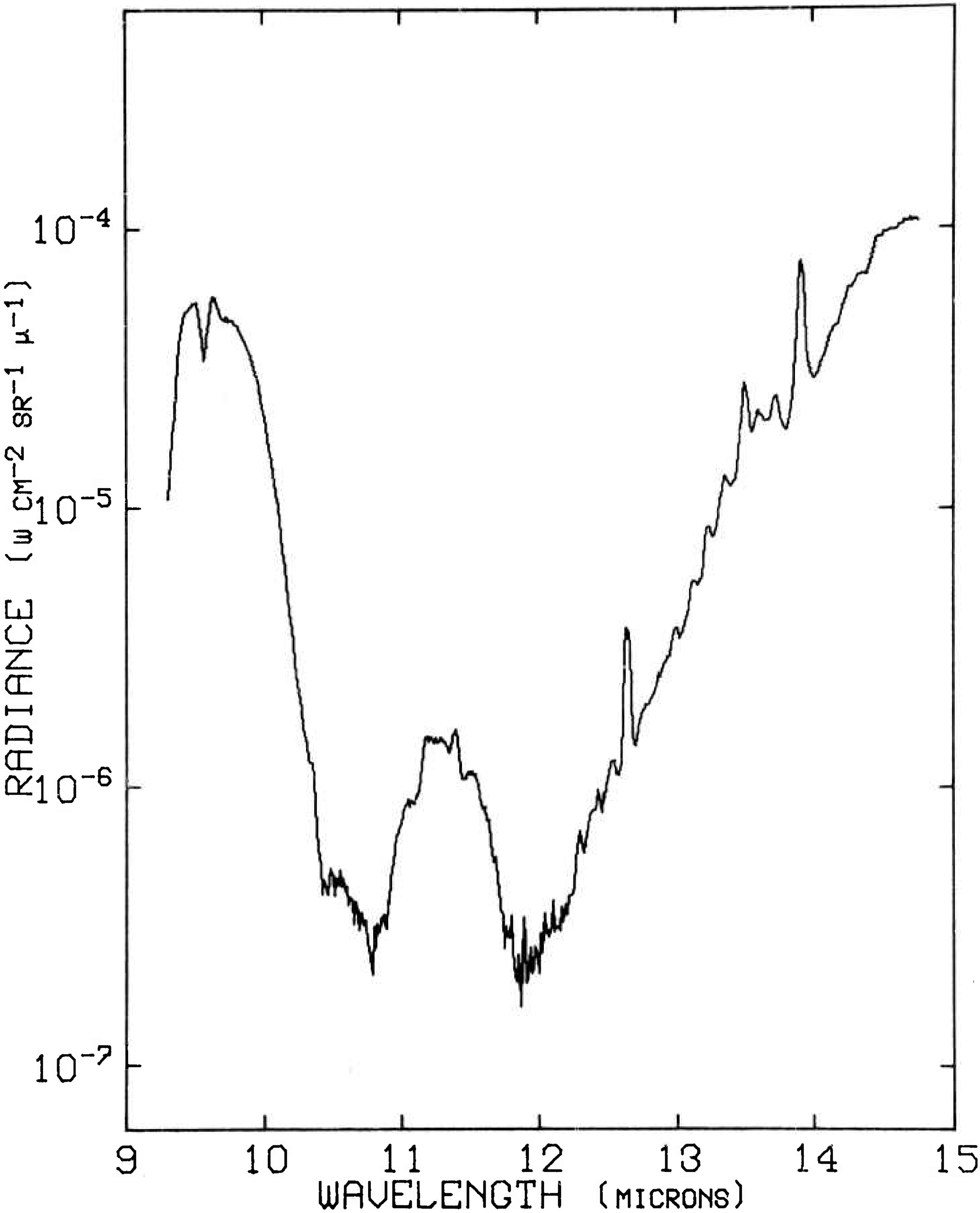

Figure 48. Radiance vs Wavelength at 58.1 kft and 0255 ADT, 12 September 1971.

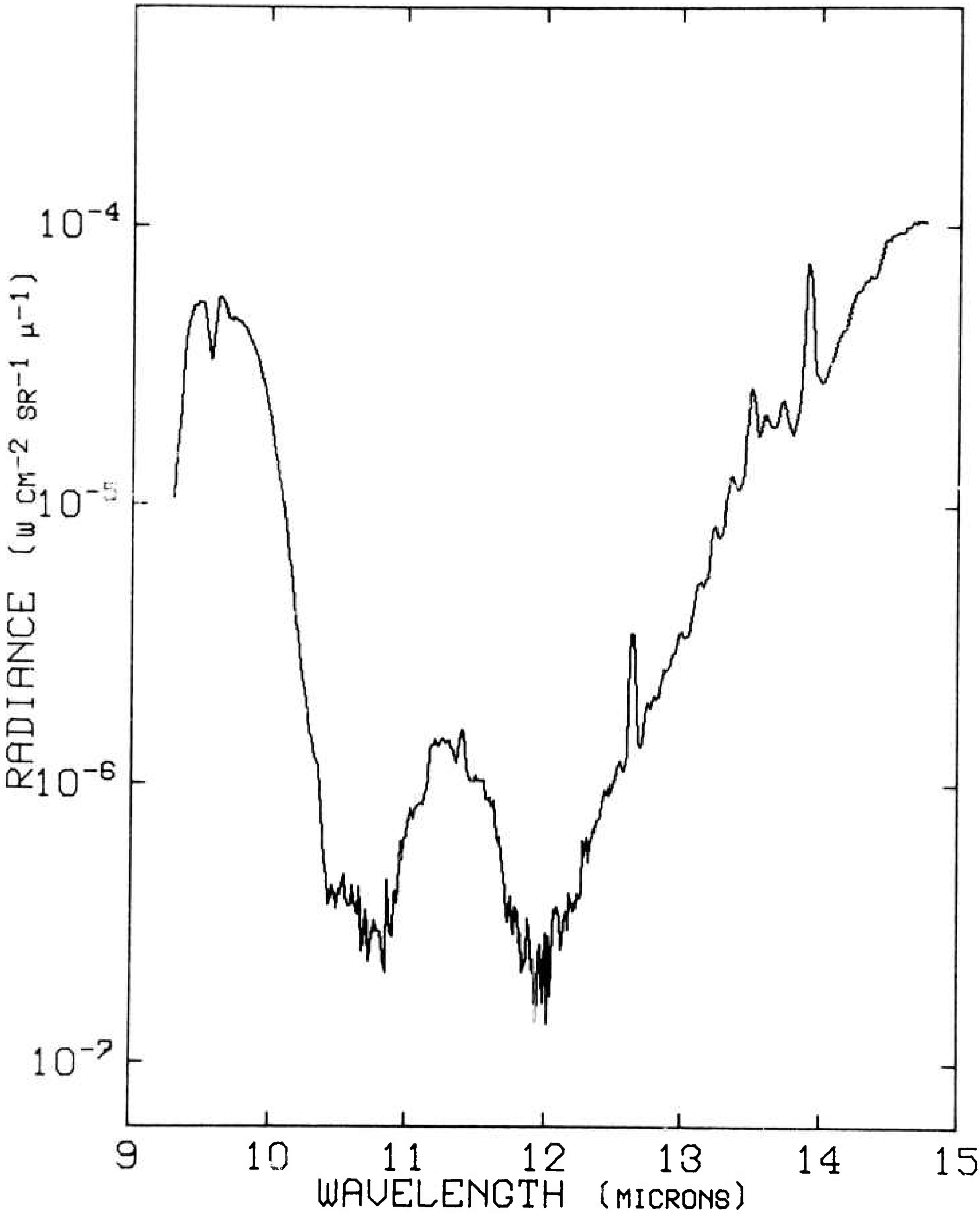

Figure 49. Radiance vs Wavelength at 59.3 kft and 0257 ADT, 12 September 1971.

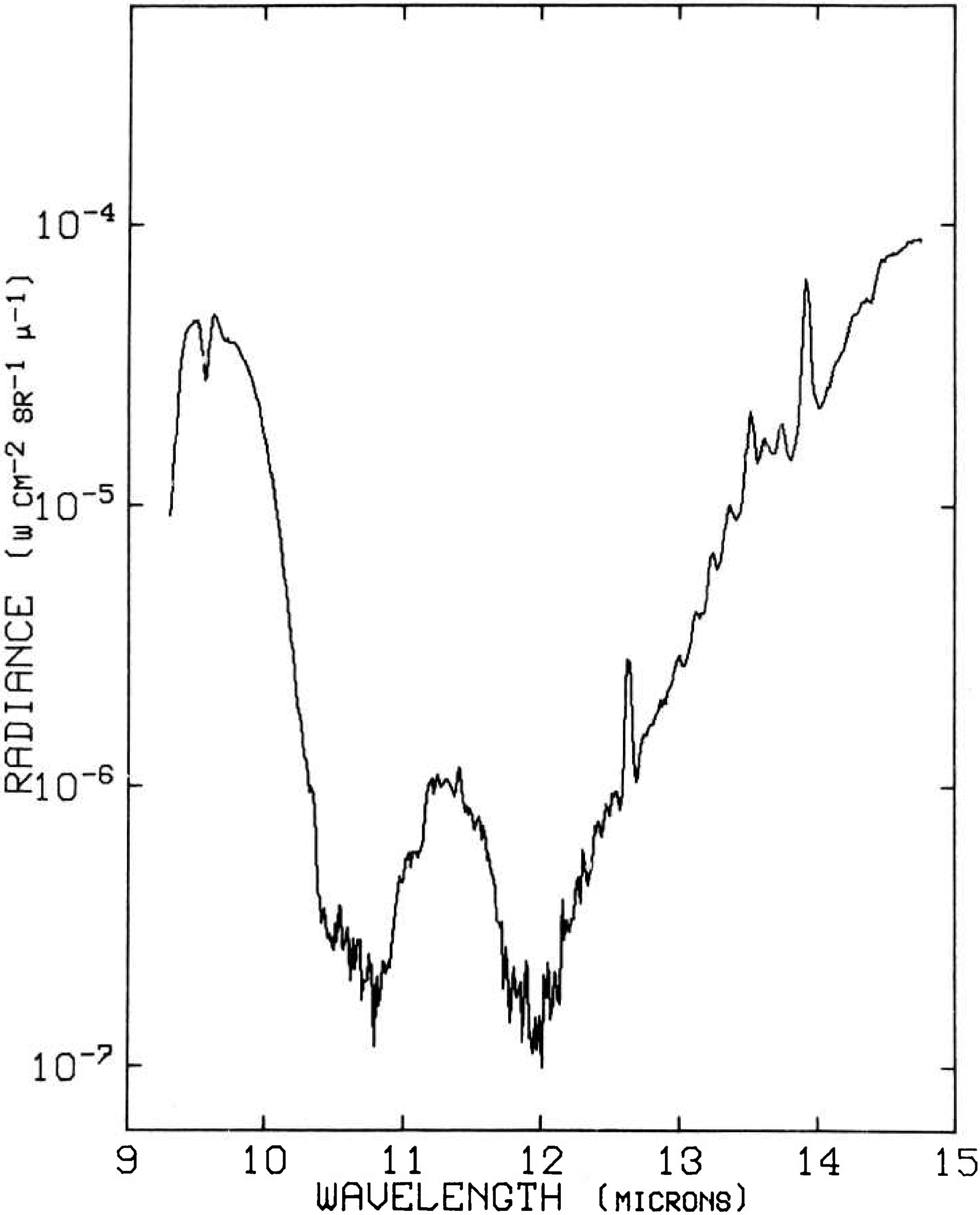

Figure 50. Radiance vs Wavelength at 63.8 kft and 0304 ADT, 12 September 1971.

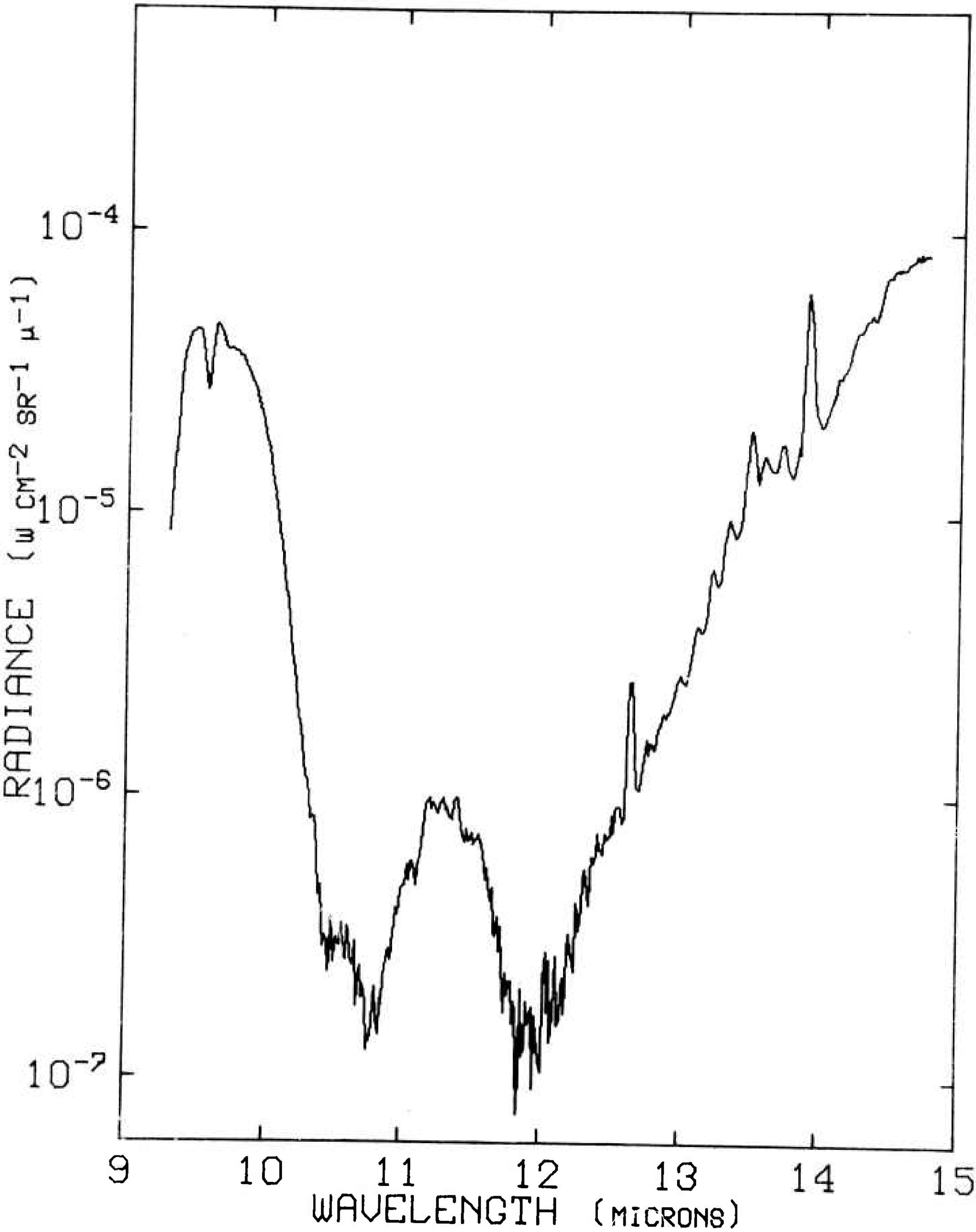

Figure 51. Radiance vs Wavelength at 65.0 kft and 0306 ADT, 12 September 1971.

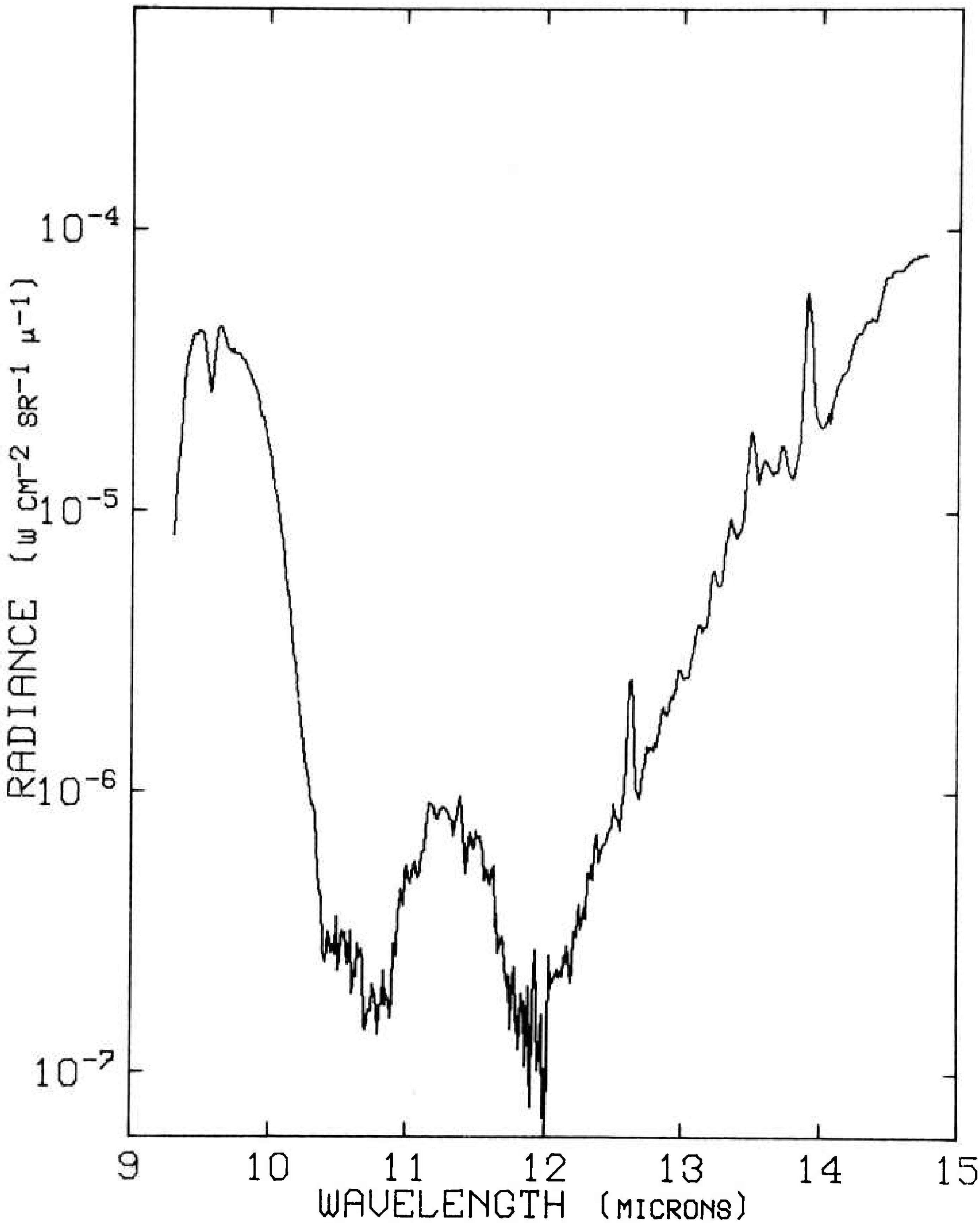

Figure 52. Radiance vs Wavelength at 66.1 kft and 0308 ADT, 12 September 1971.

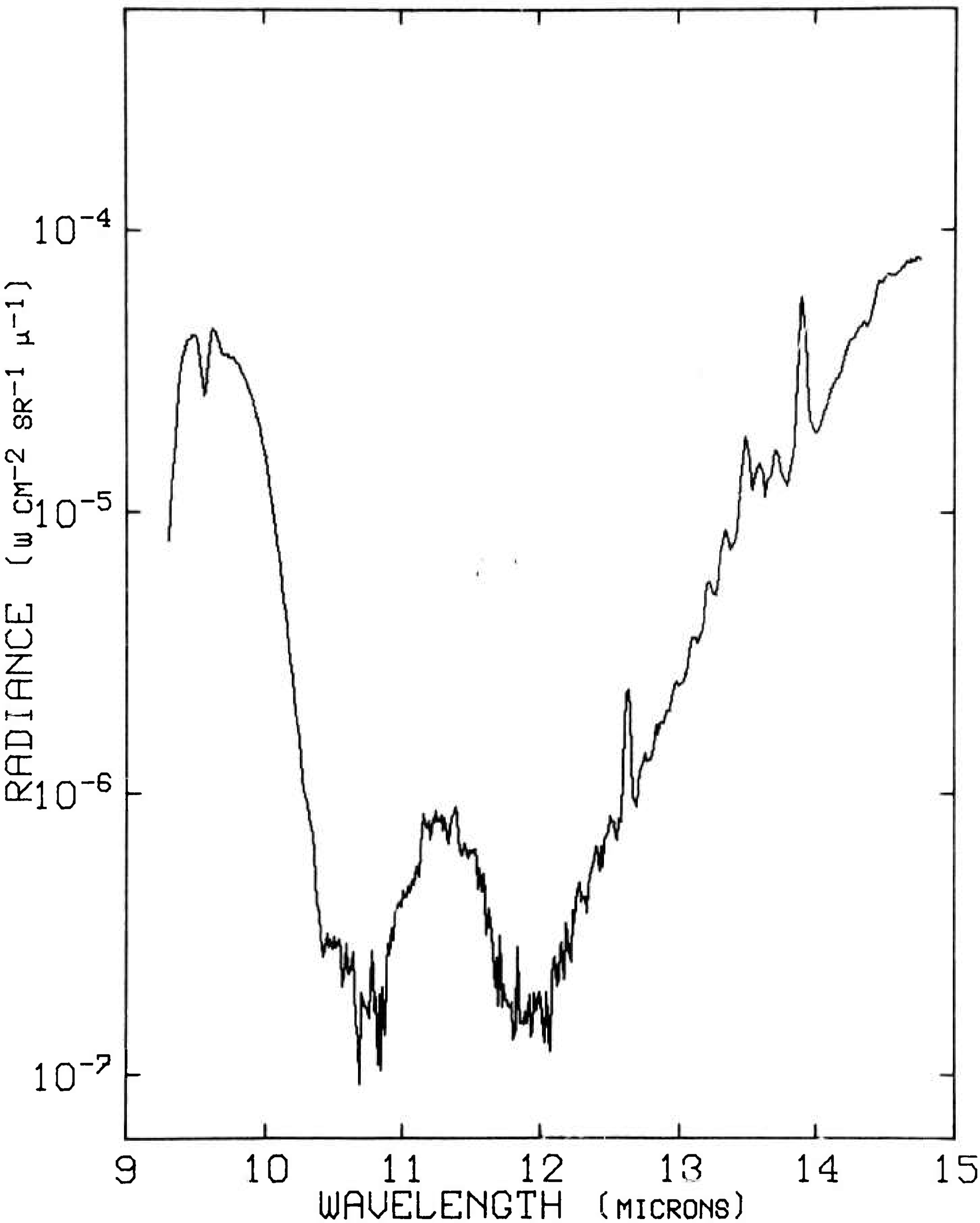

Figure 53. Radiance vs Wavelength at 67.2 kft and 0310 ADT, 12 September 1971.

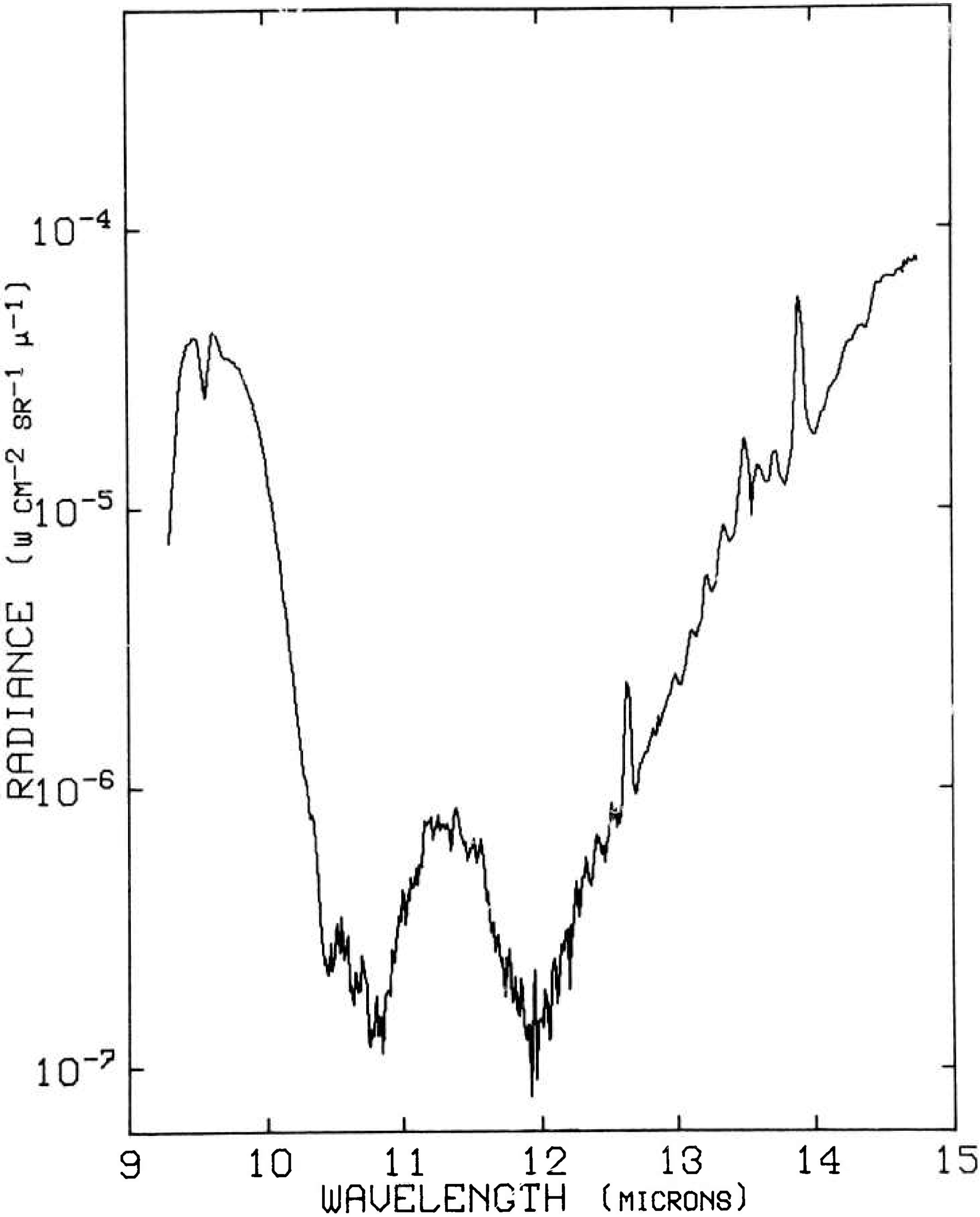

Figure 54. Radiance vs Wavelength at 68.2 kft and 0312 ADT, 12 September 1971.

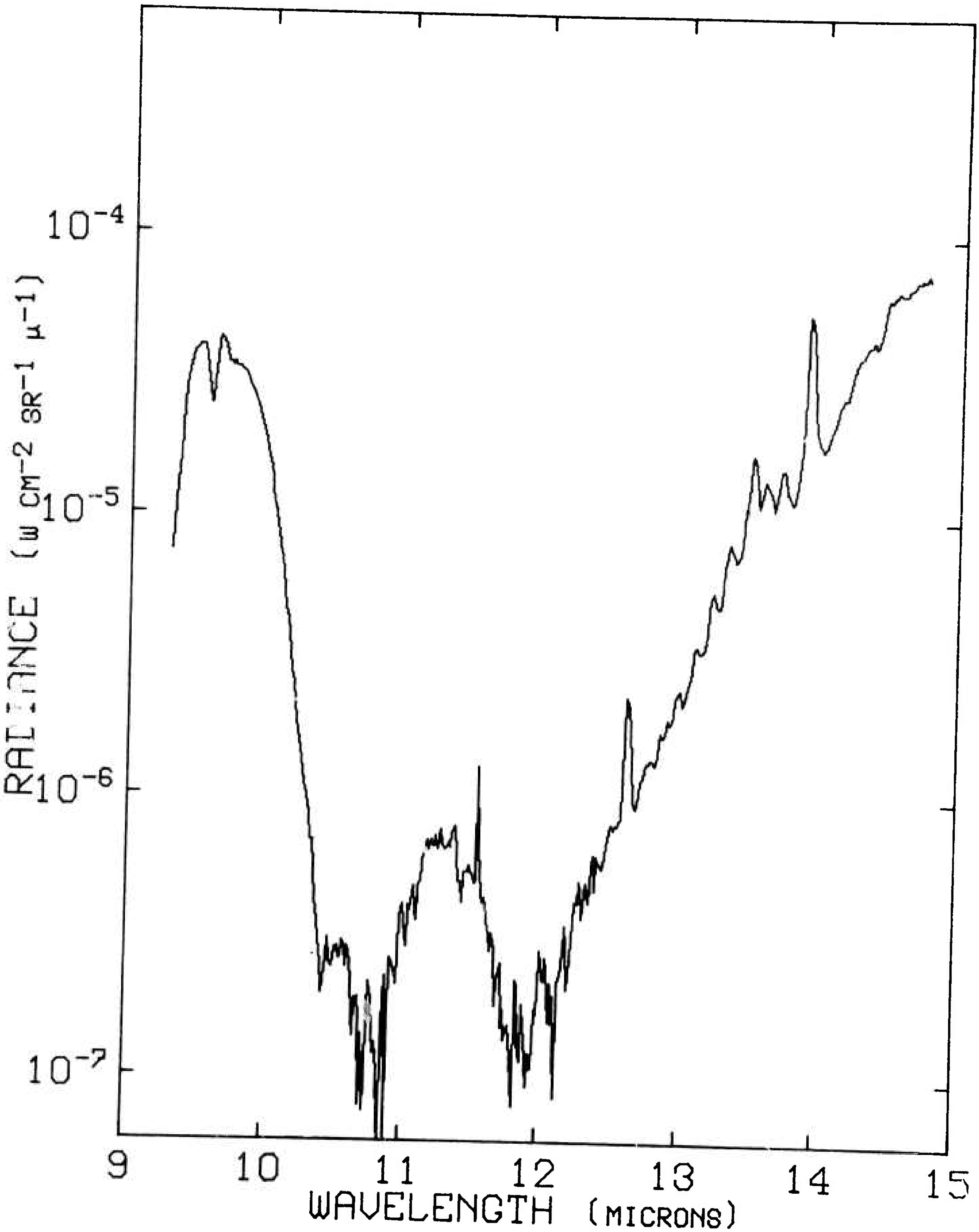

Figure 55. Radiance vs Wavelength at 69.3 kft and 0314 ADT, 12 September 1971.

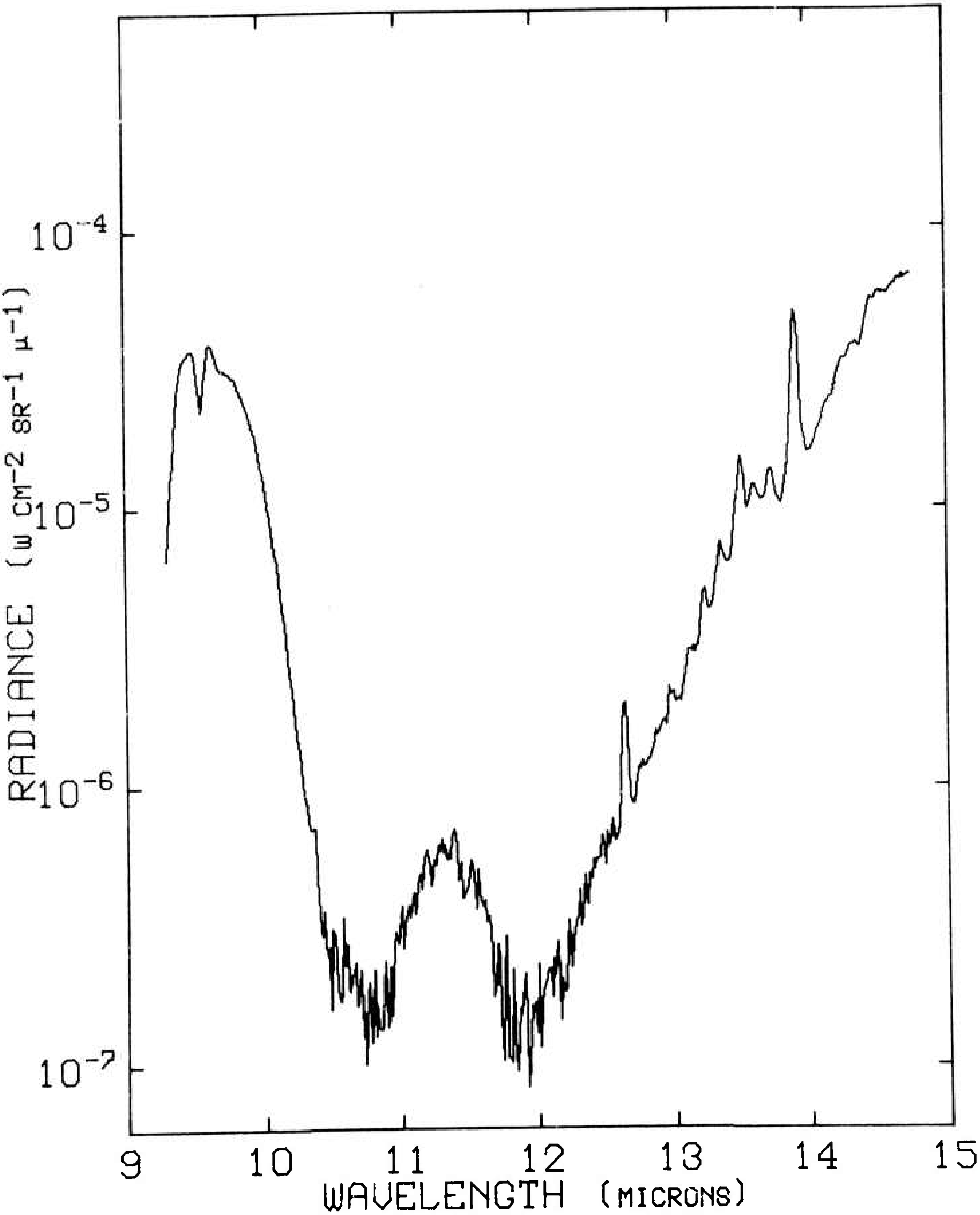

Figure 56. Radiance vs Wavelength at 72.2 kft and 0320 ADT, 12 September 1971.

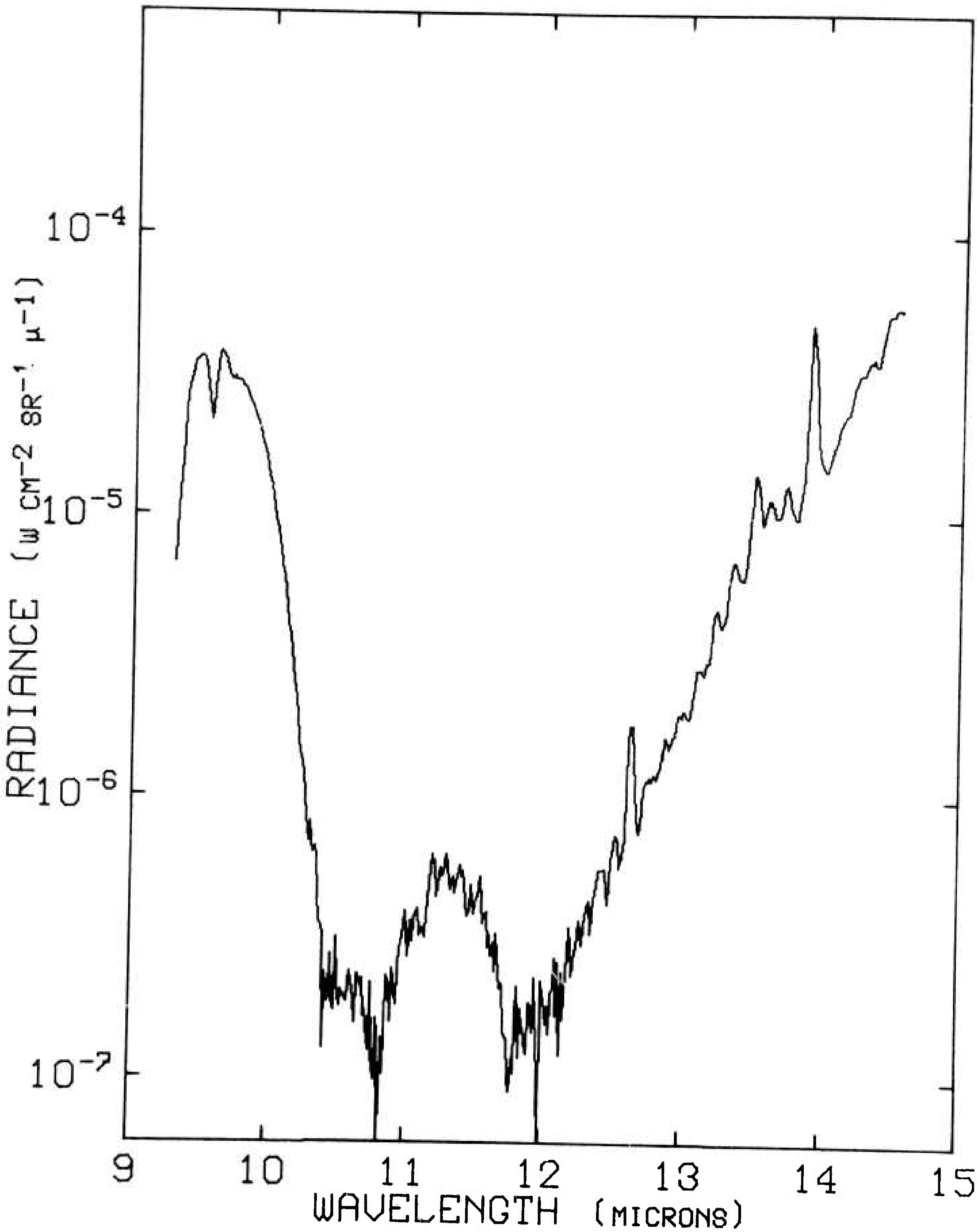

Figure 57. Radiance vs Wavelength at 73.4 kft and 0322 ADT, 12 September 1971.

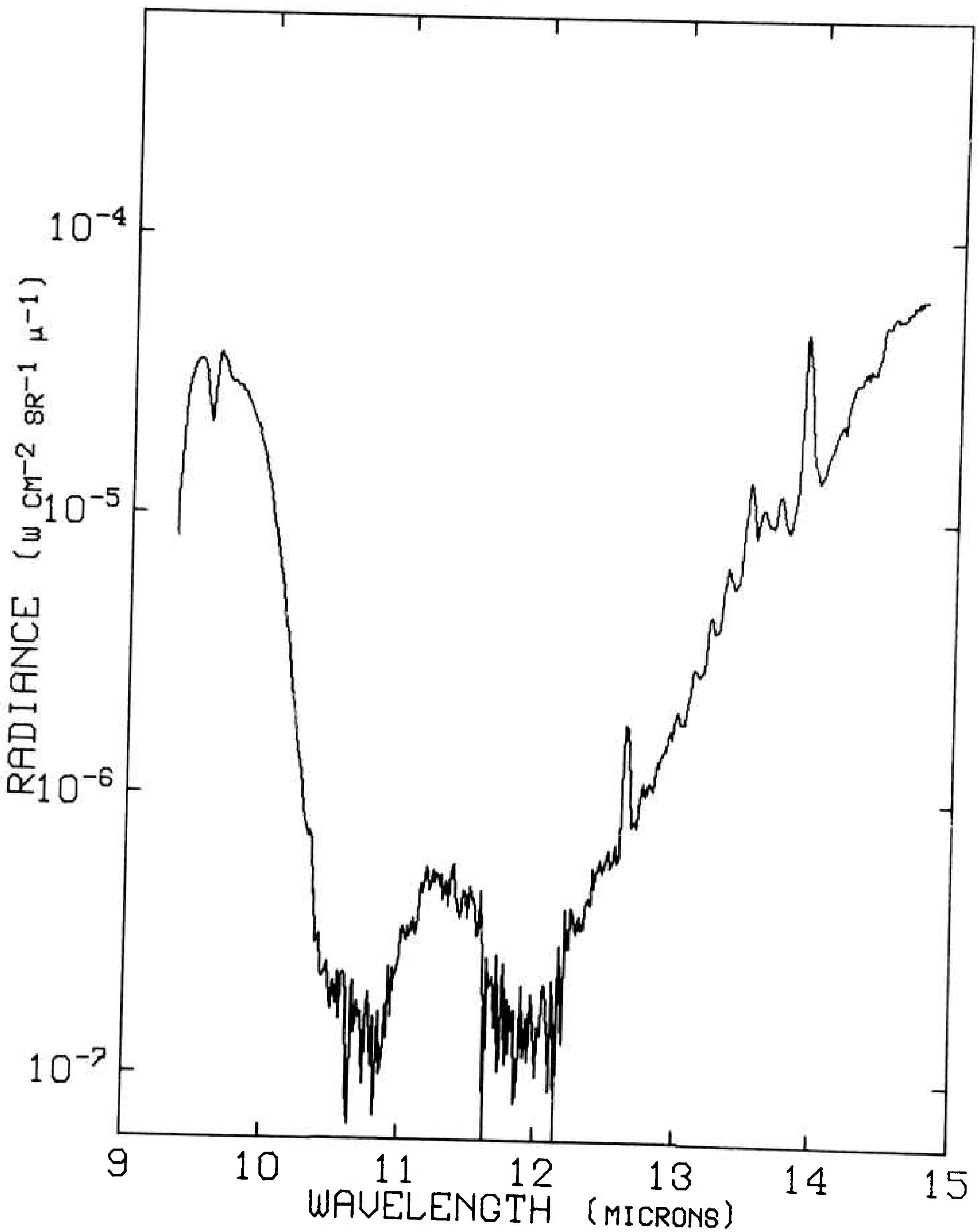

Figure 58. Radiance vs Wavelength at 74.4 kft and 0324 ADT, 12 September 1971.

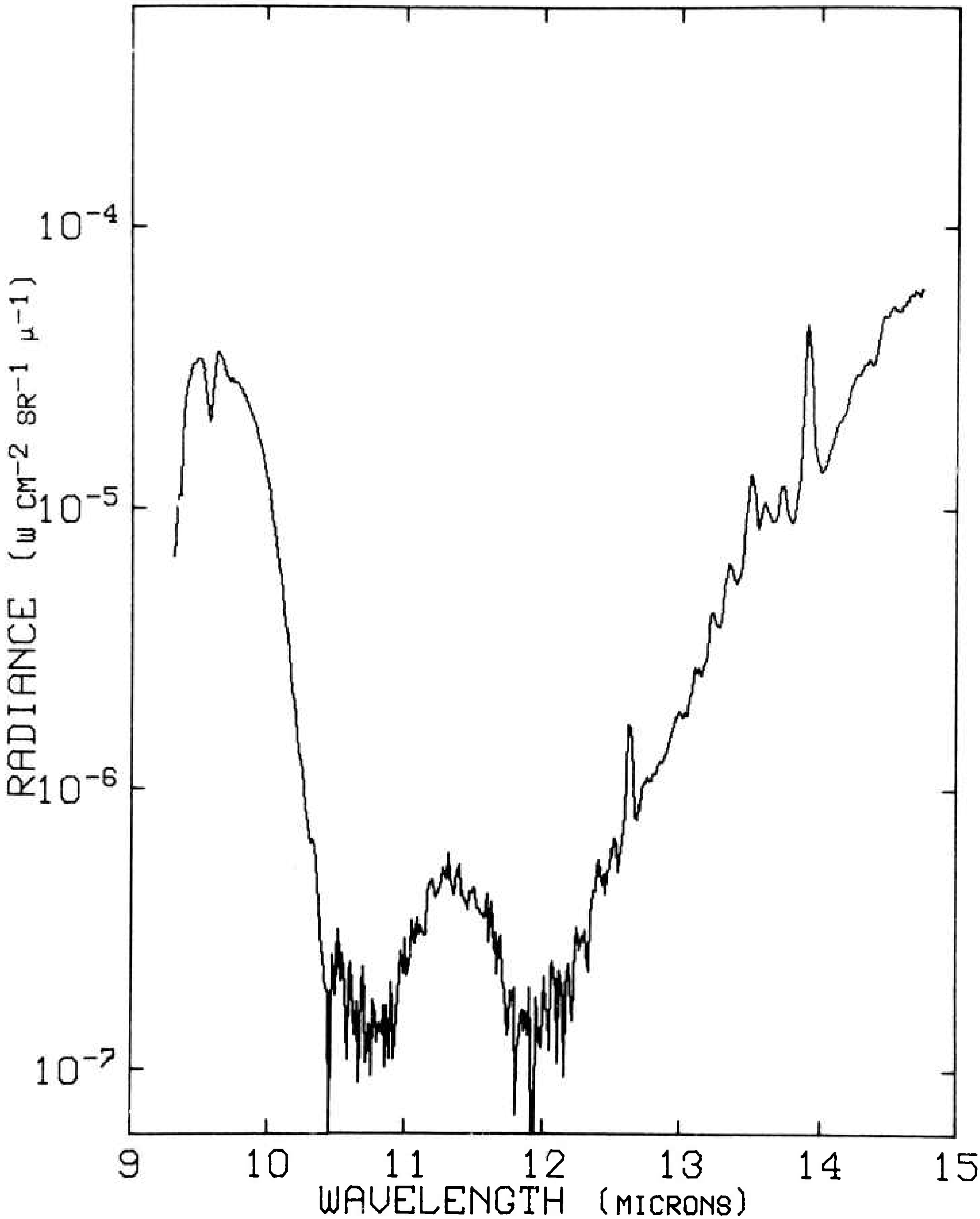

Figure 59. Radiance vs Wavelength at 75.5 kft and 0326 ADT, 12 September 1971.

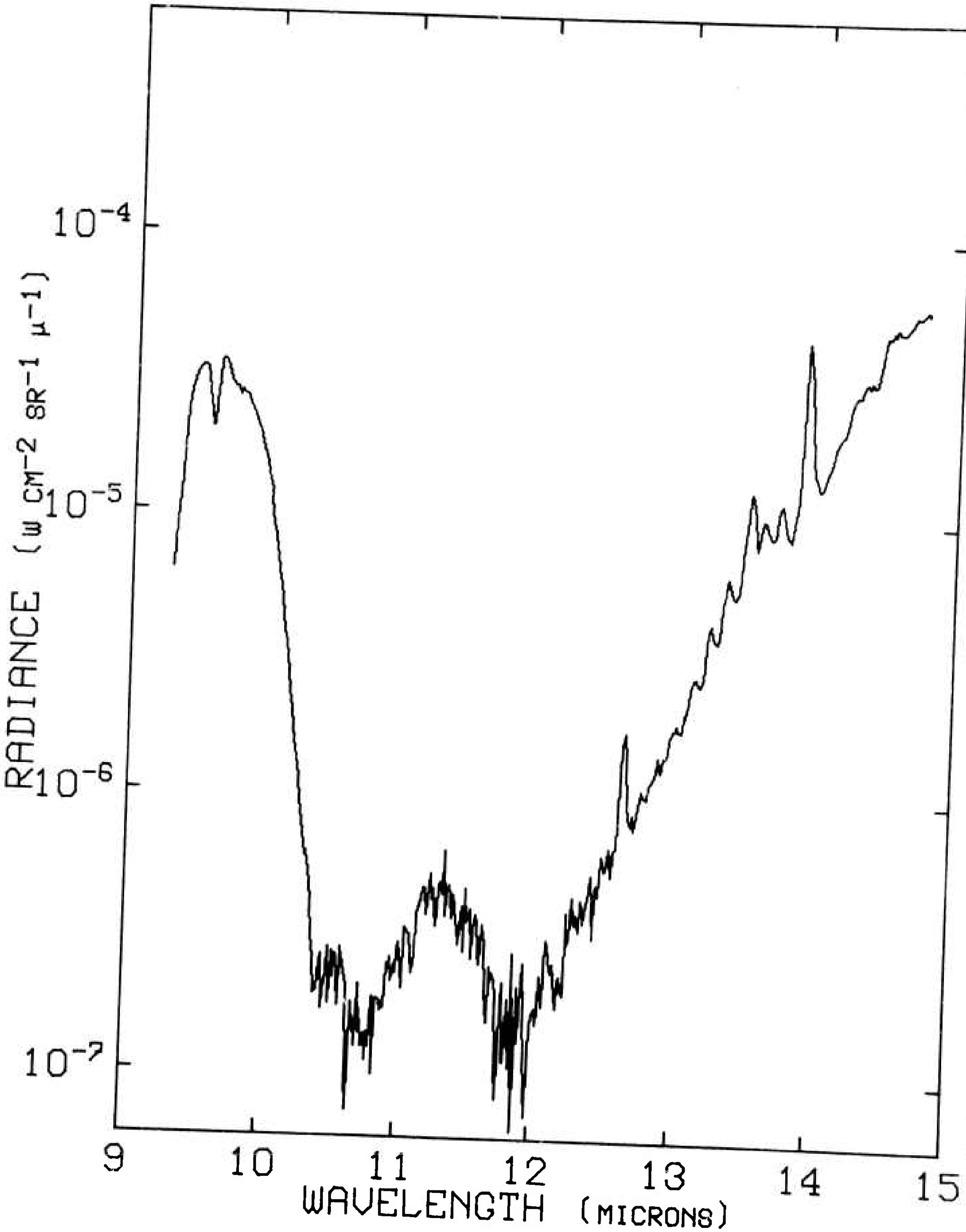

Figure 60. Radiance vs Wavelength at 76.8 kft and 0328 ADT, 12 September 1971.

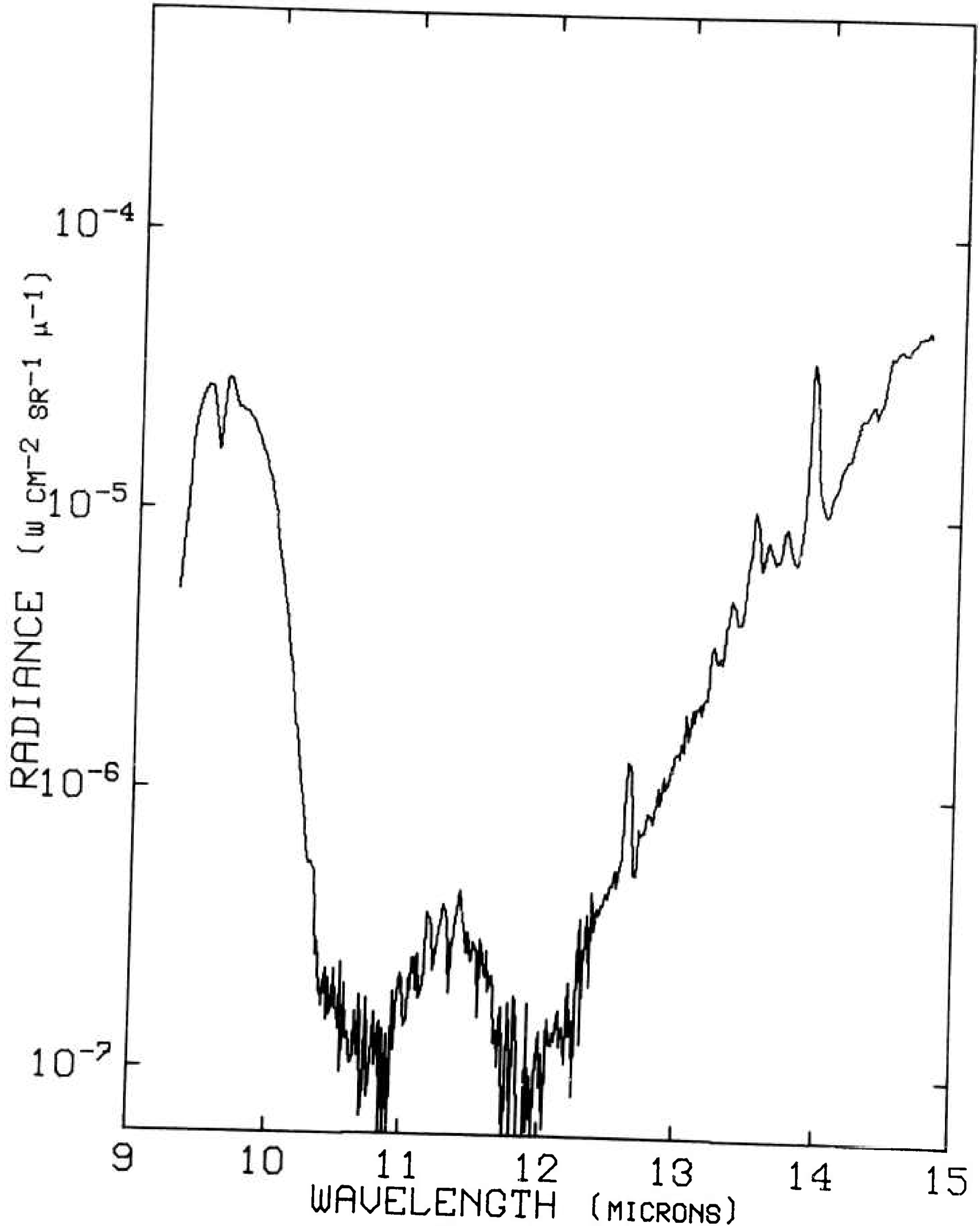

Figure 61. Radiance vs Wavelength at 80.9 kft and 0335 ADT, 12 September 1971.

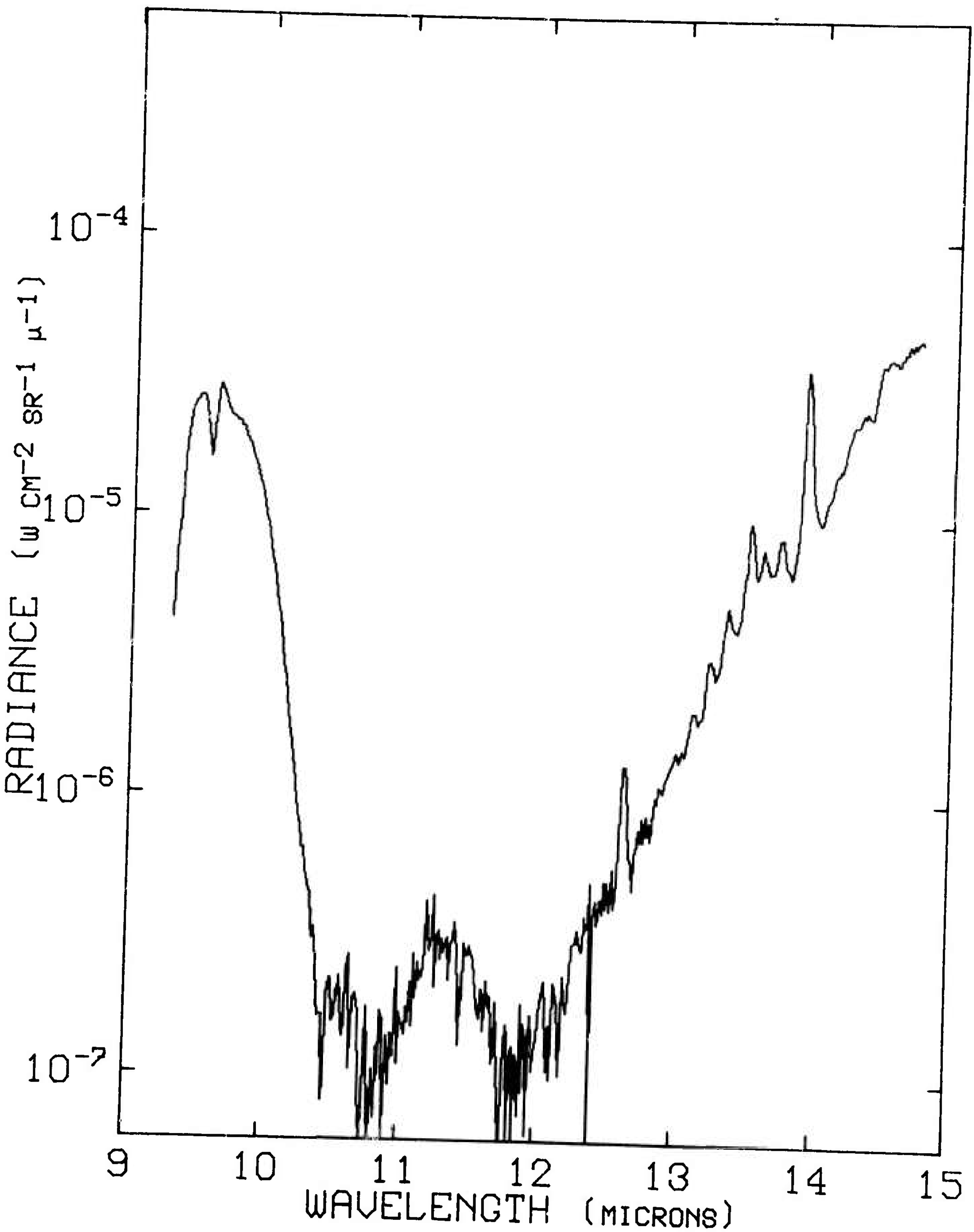

Figure 62. Radiance vs Wavelength at 82.2 kft and 0337 ADT, 12 September 1971.

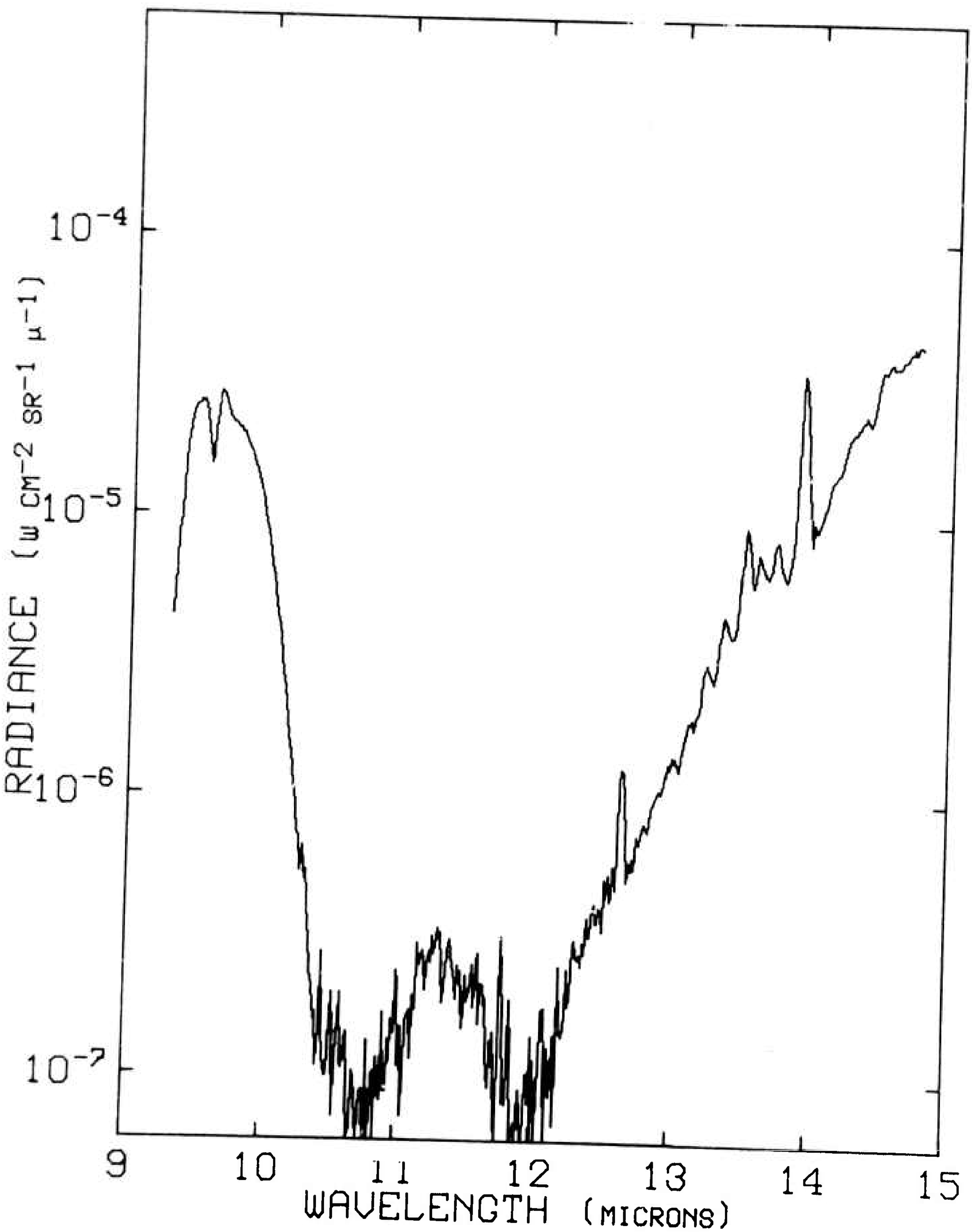

Figure 63. Radiance vs Wavelength at 83.6 kft and 0339 ADT, 12 September 1971.

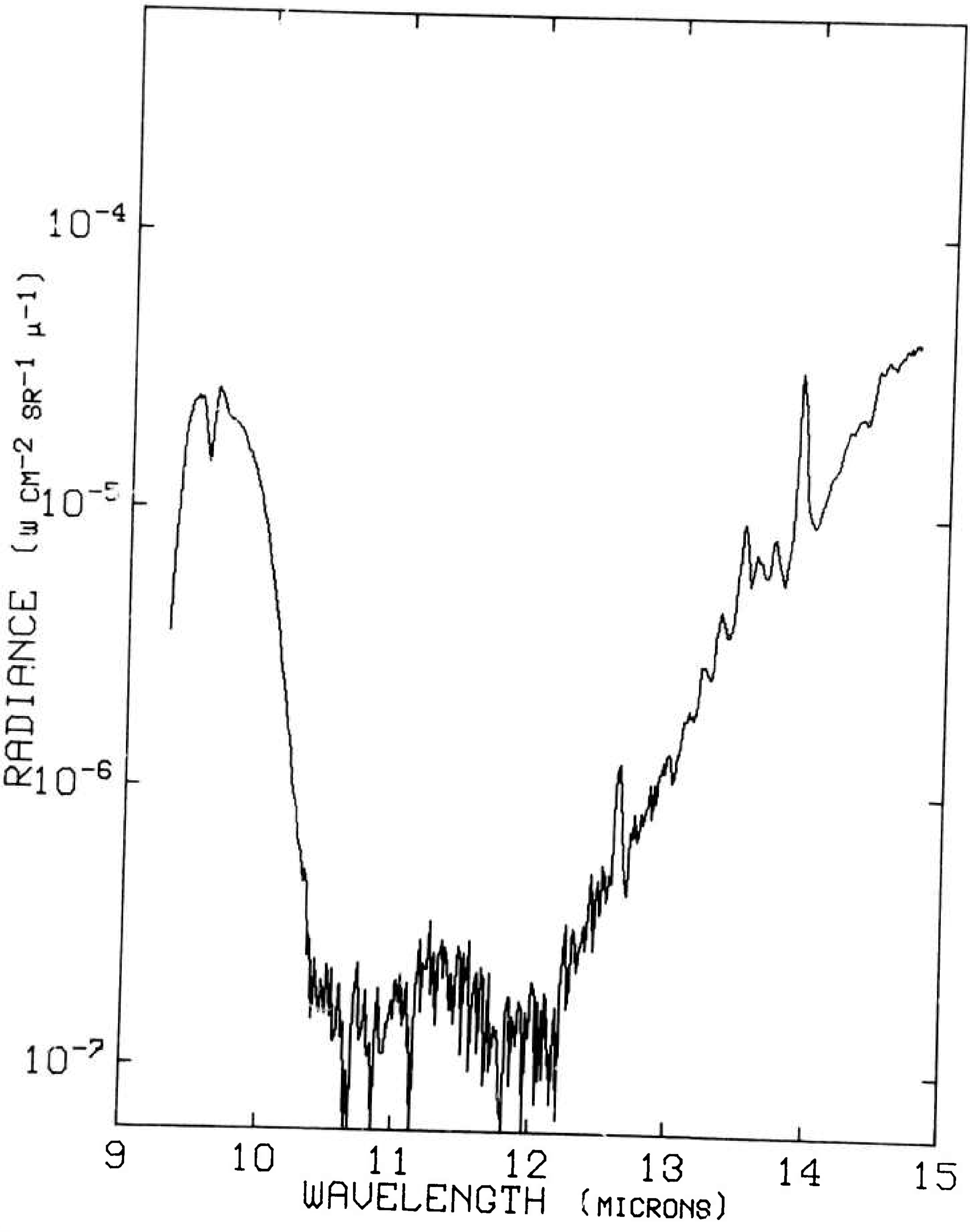

Figure 64. Radiance vs Wavelength at 84.6 kft and 0341 ADT, 12 September 1971.

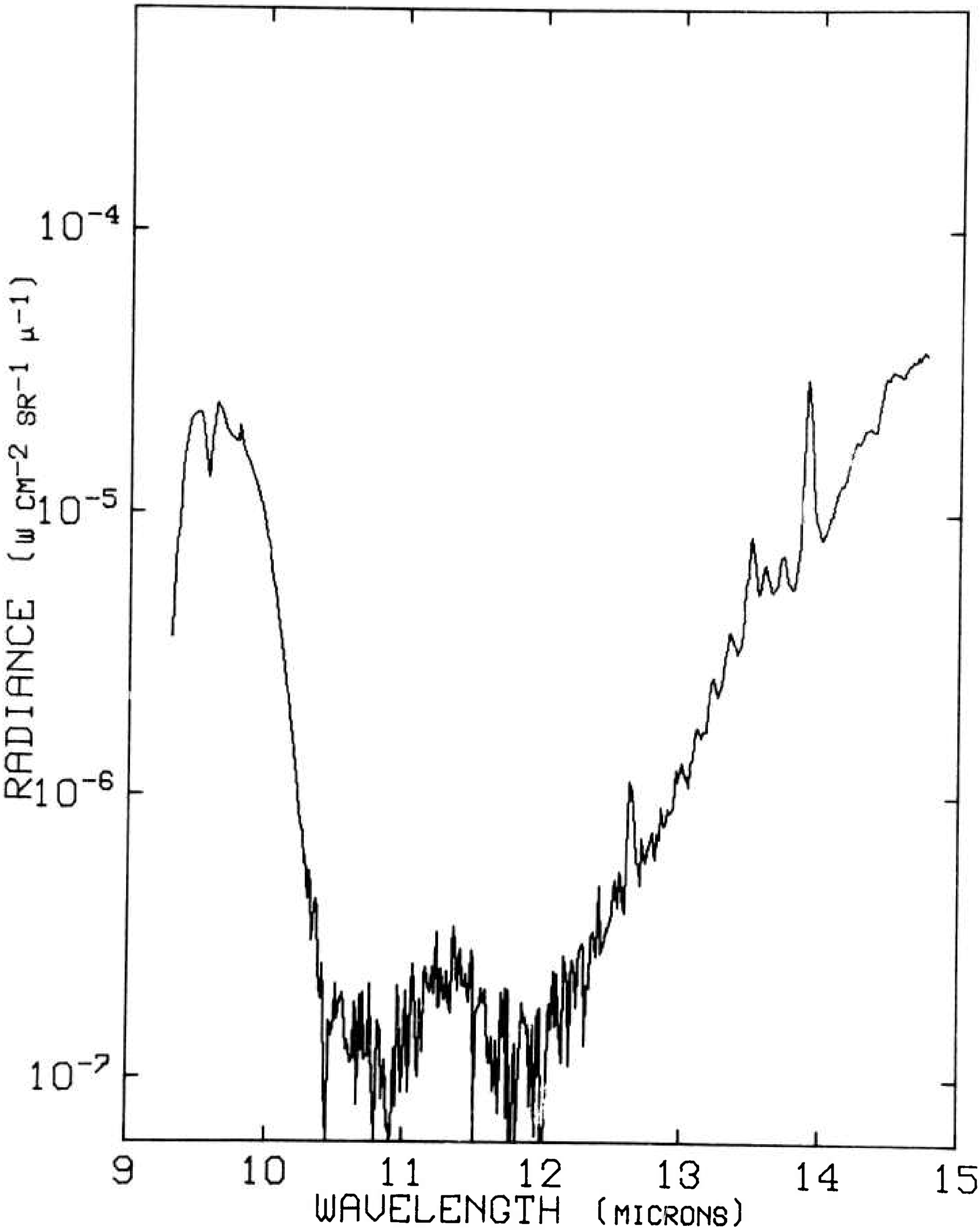

Figure 65. Radiance vs Wavelength at 87.1 kft and 0347 ADT, 12 September 1971.

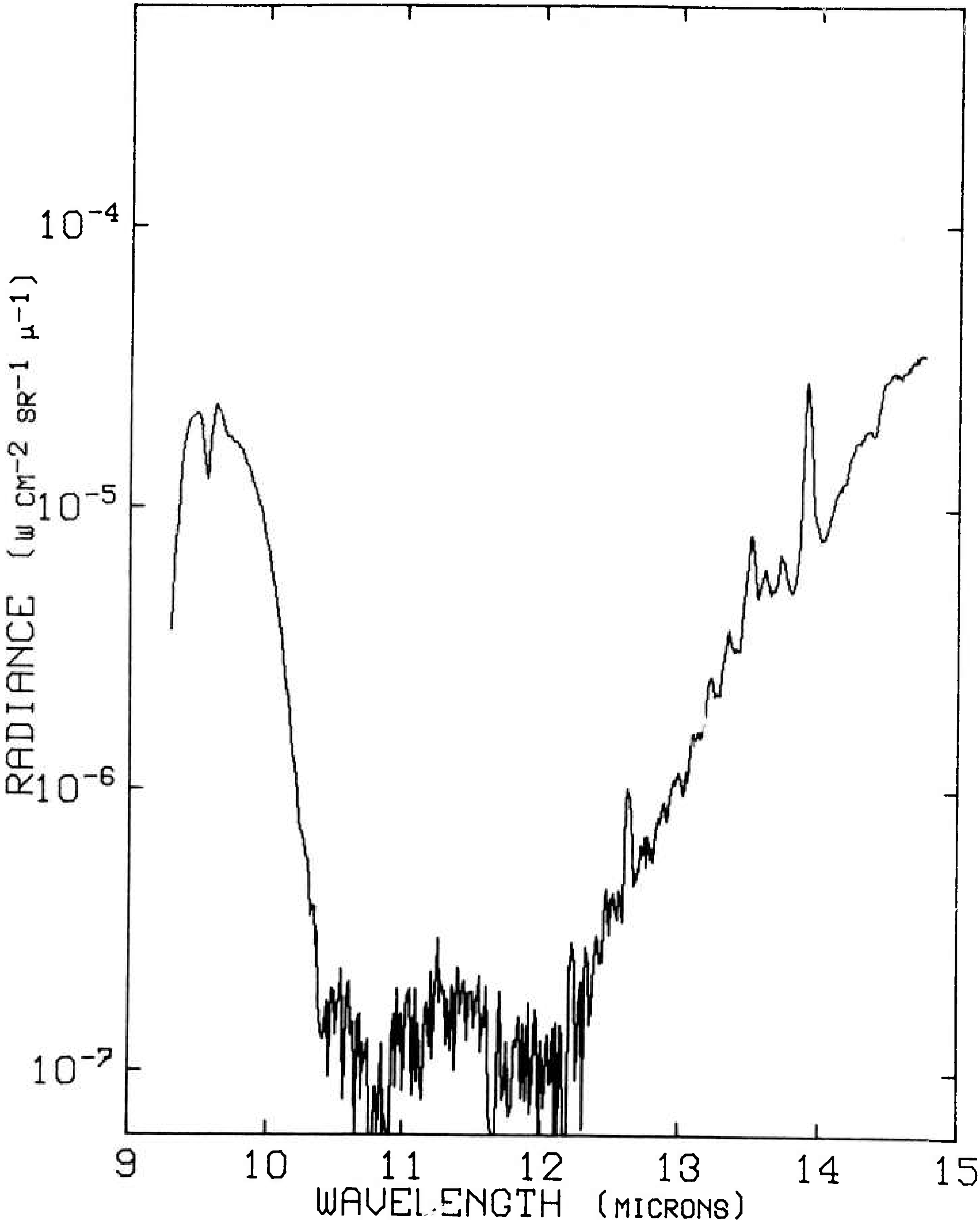

Figure 66. Radiance vs Wavelength at 88.5 kft and 0349 ADT, 12 September 1971.

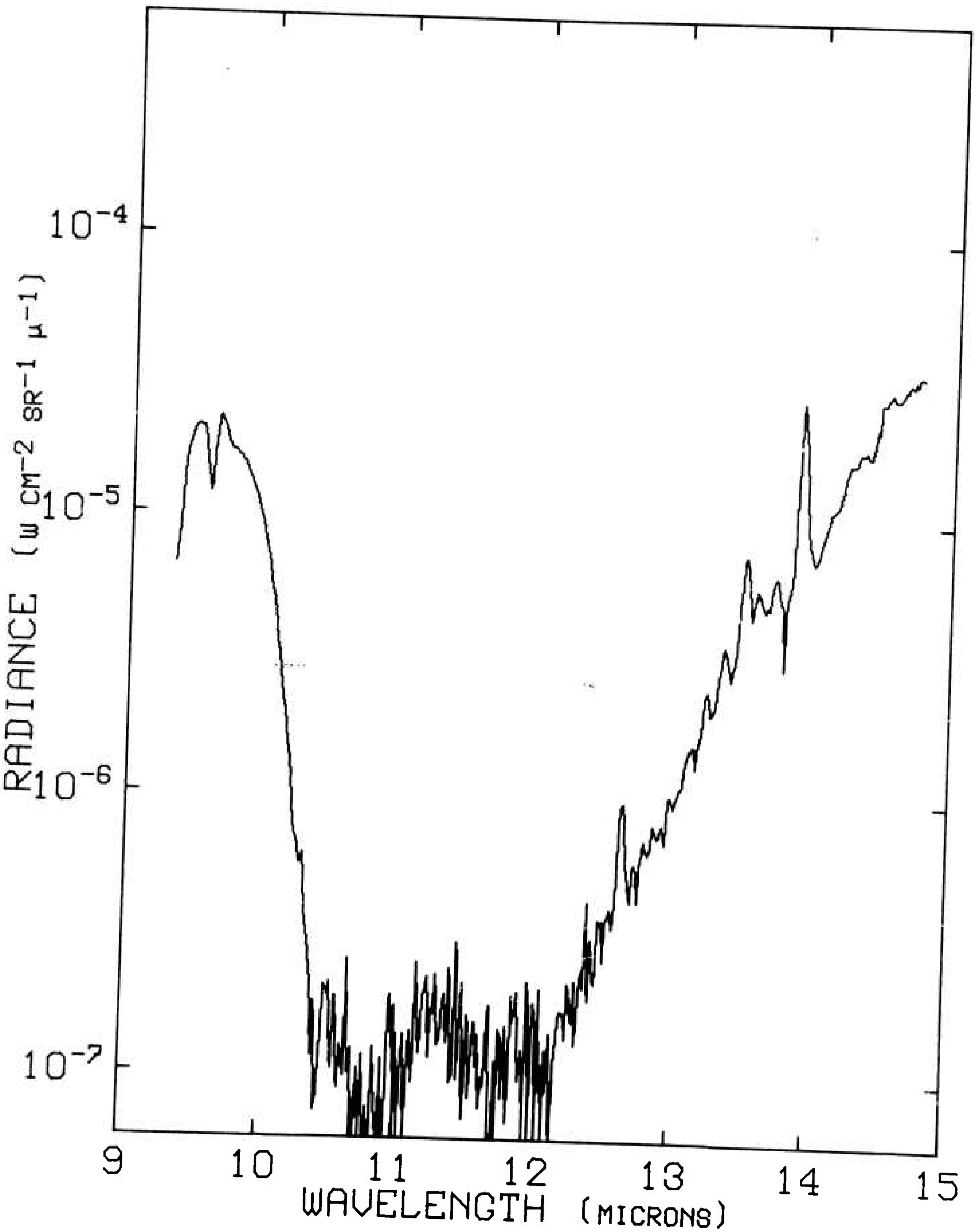

Figure 67. Radiance vs Wavelength at 89.9 kft and 0351 ADT, 12 September 1971.

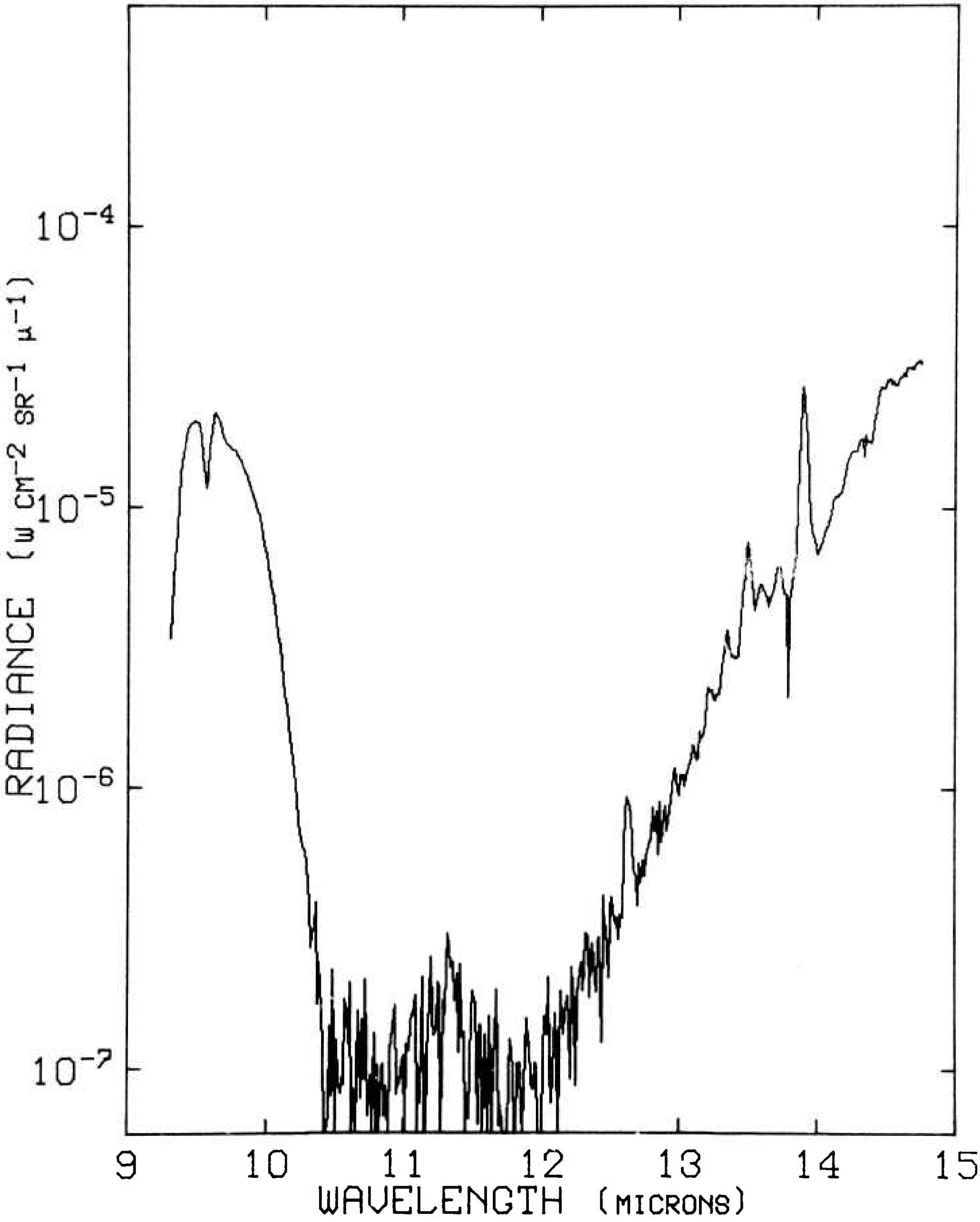

Figure 68. Radiance vs Wavelength at 90.5 kft and 0353 ADT, 12 September 1971.

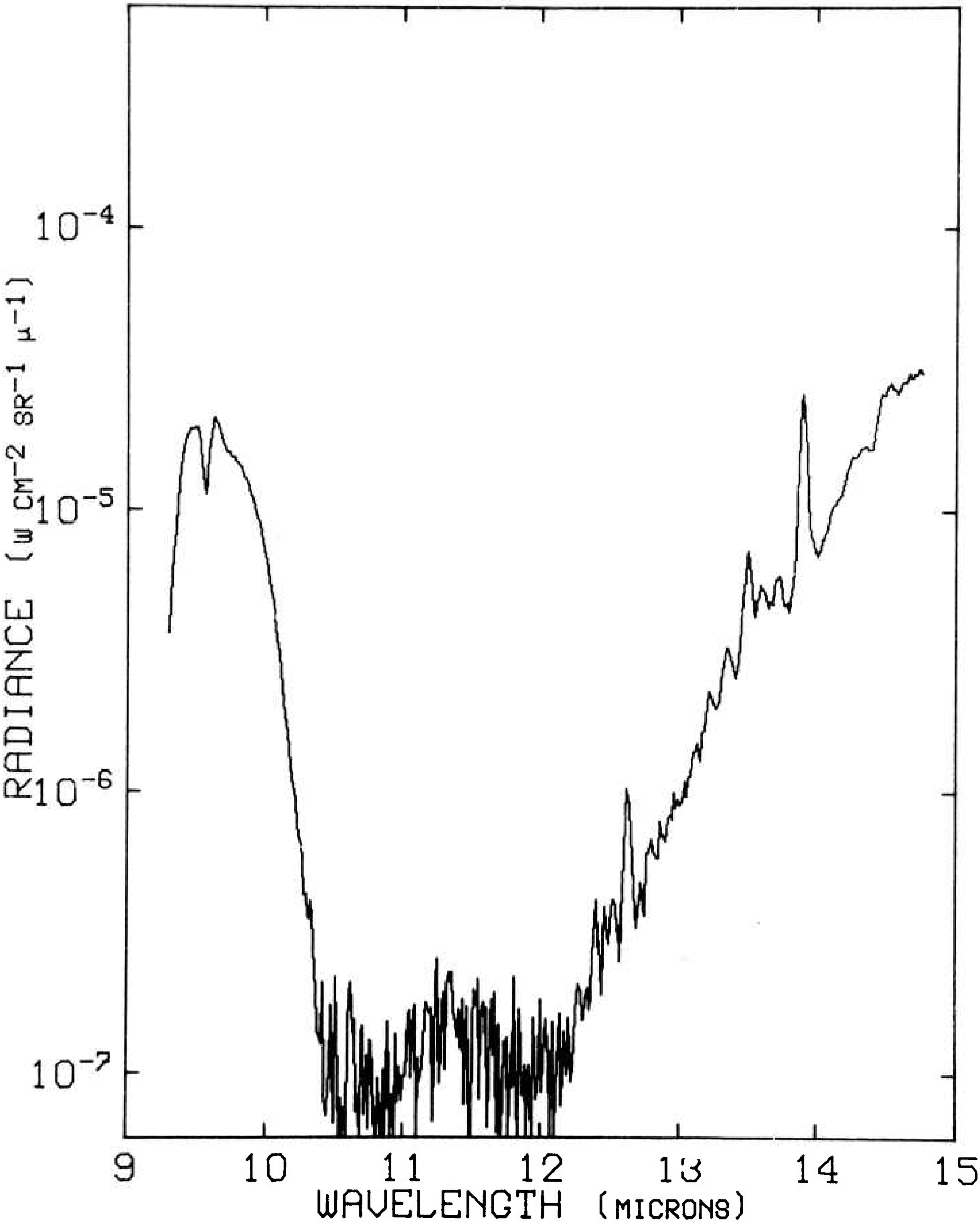

Figure 69. Radiance vs Wavelength at 91.3 kft and 0355 ADT, 12 September 1971.

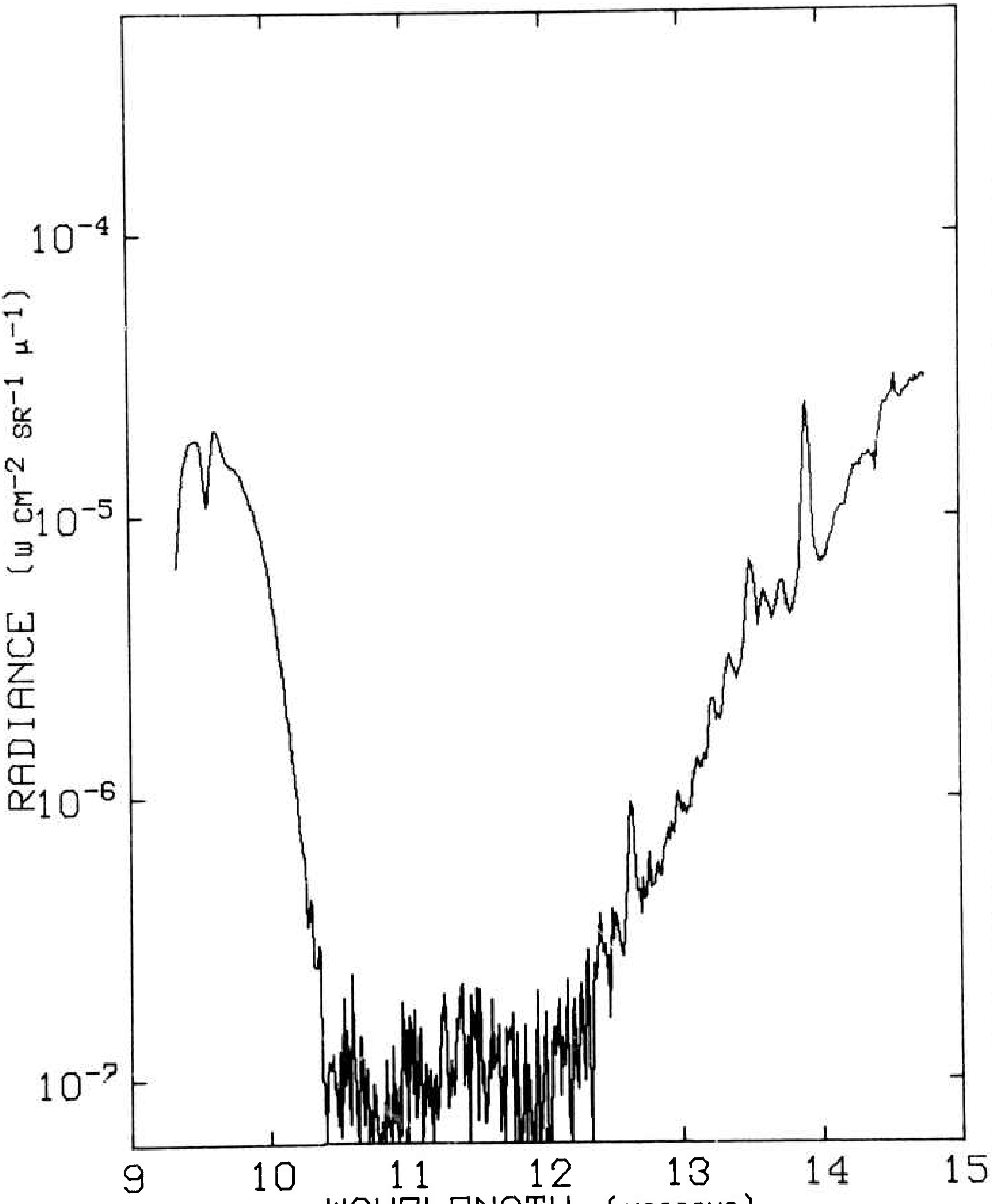

Figure 70. Radiance vs Wavelength at 92.3 kft and 0357 ADT, 12 September 1971.

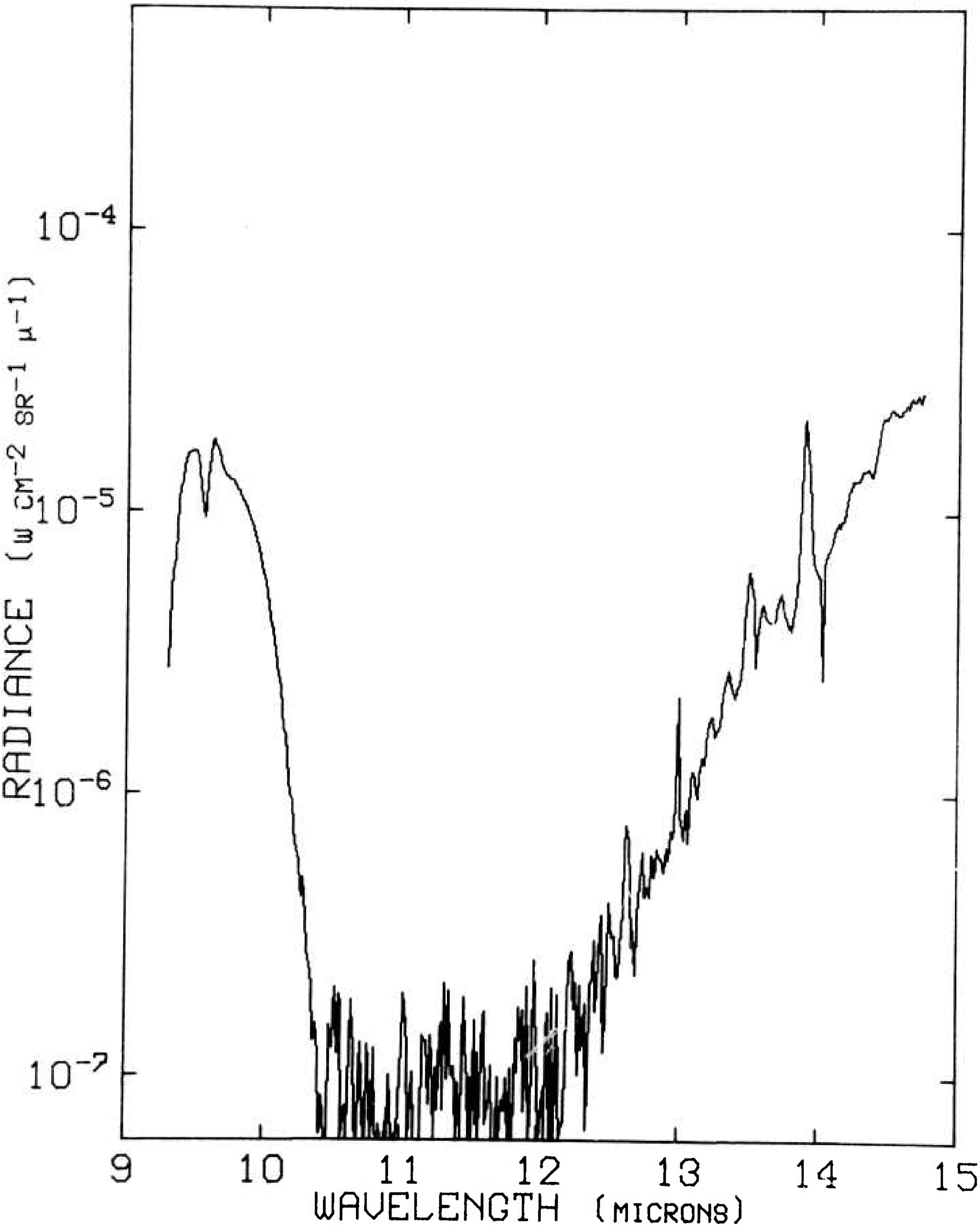

Figure 71. Radiance vs Wavelength at 95.2 kft and 0408 ADT, 12 September 1971.

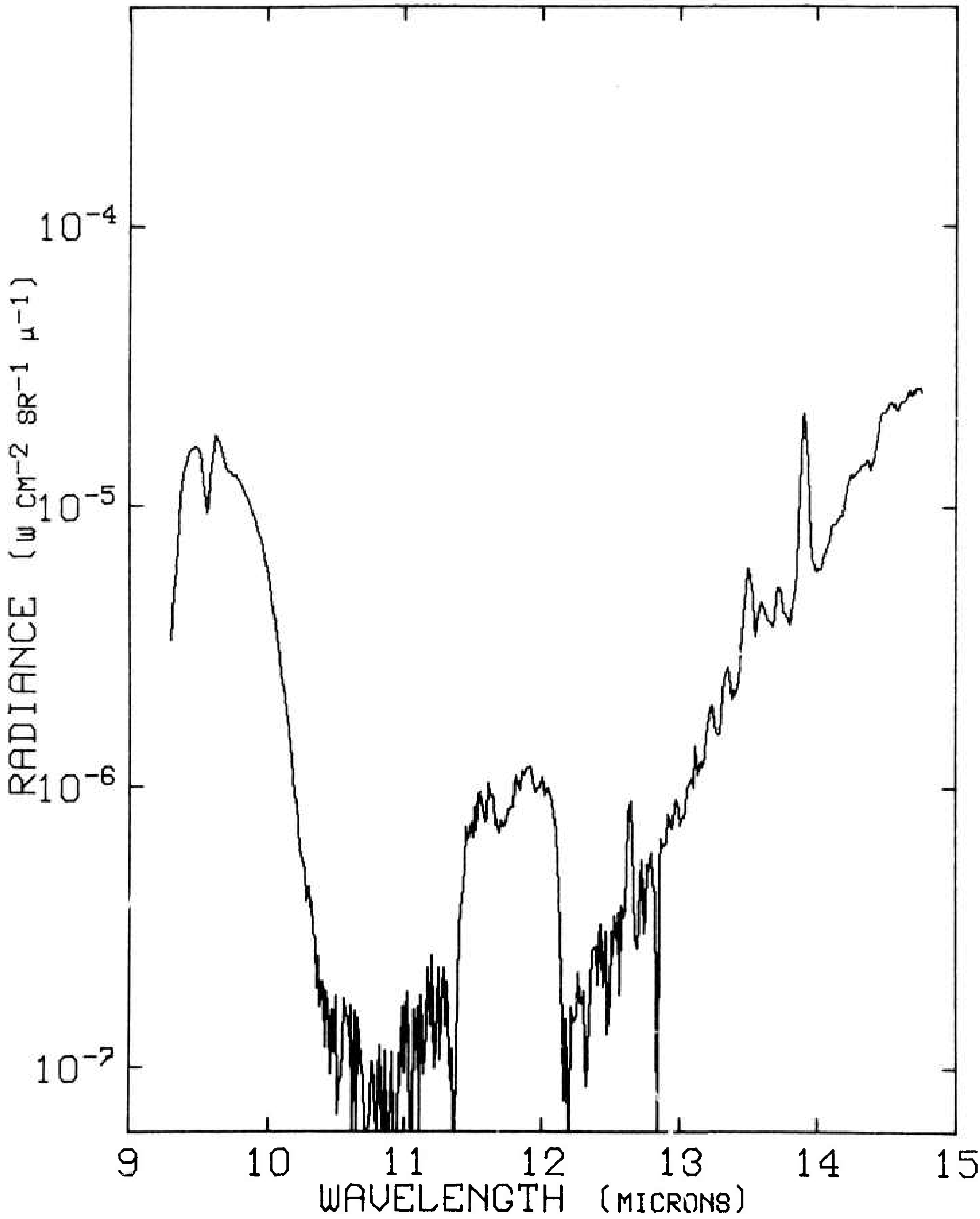

Figure 72. Radiance vs Wavelength at 95.2 kft and 0410 ADT, 12 September 1971.

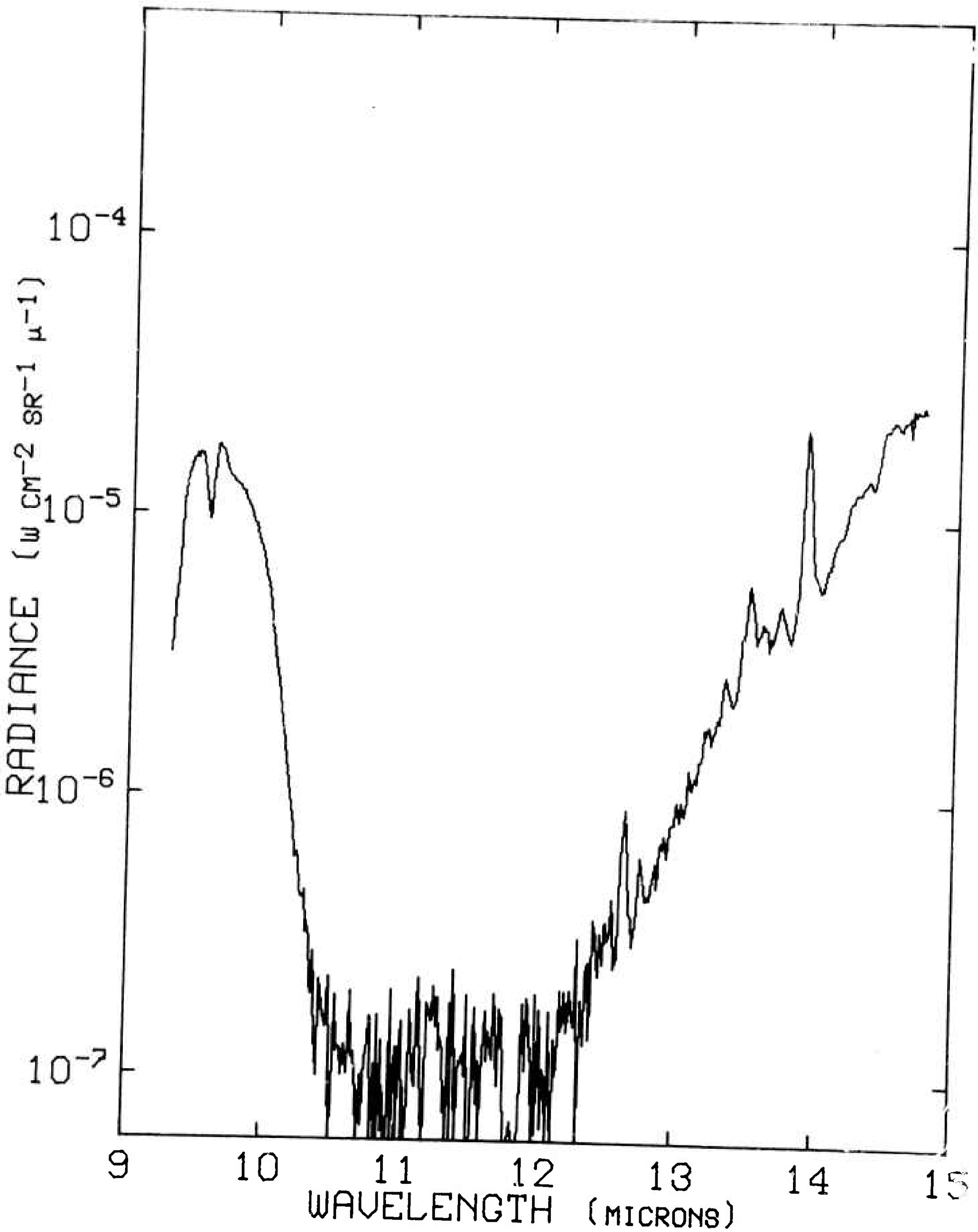

Figure 73. Radiance vs Wavelength at 95.2 kft and 0412 ADT, 12 September 1971.

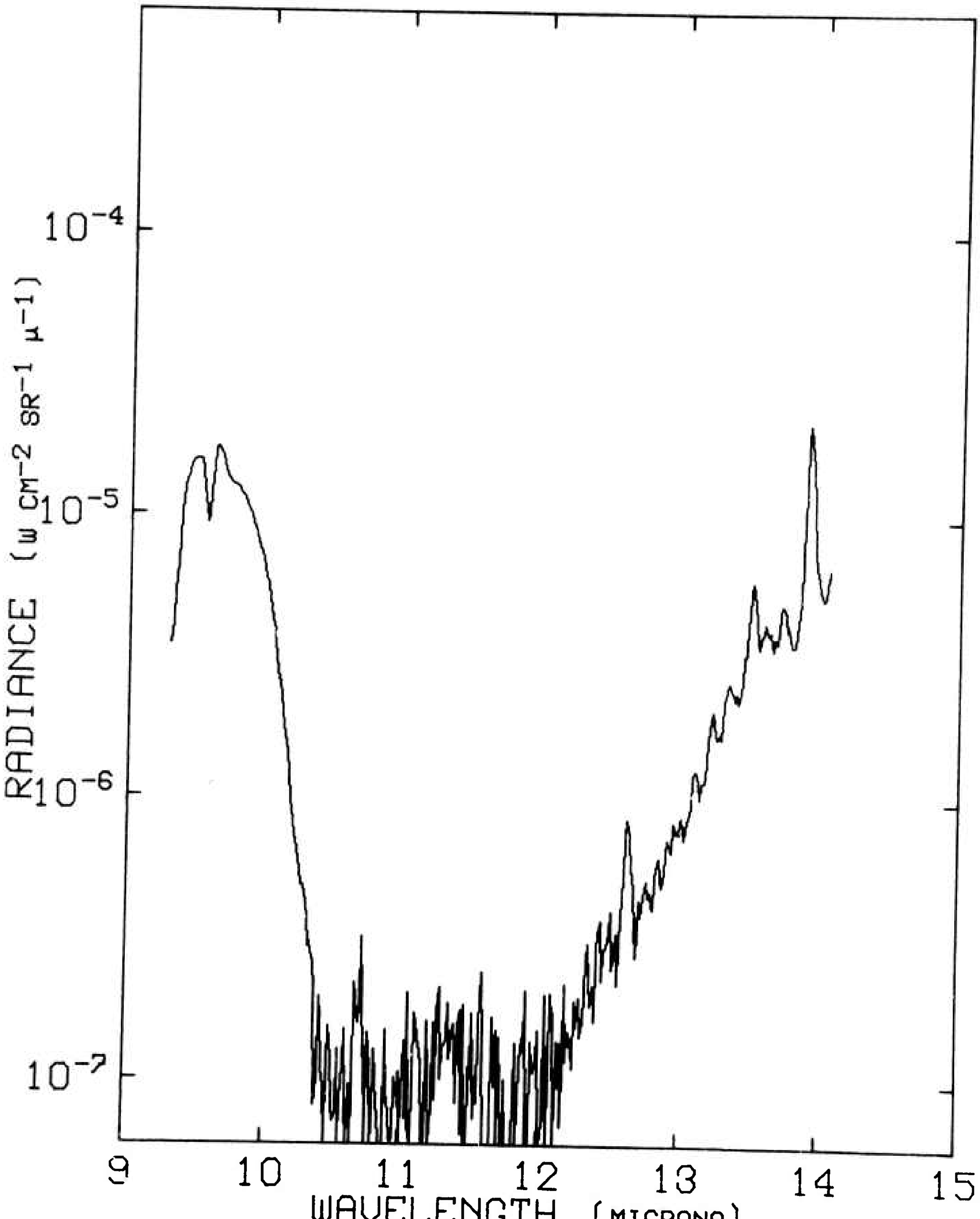

Figure 74. Radiance vs Wavelength at 95.4 kft and 0414 ADT, 12 September 1971.

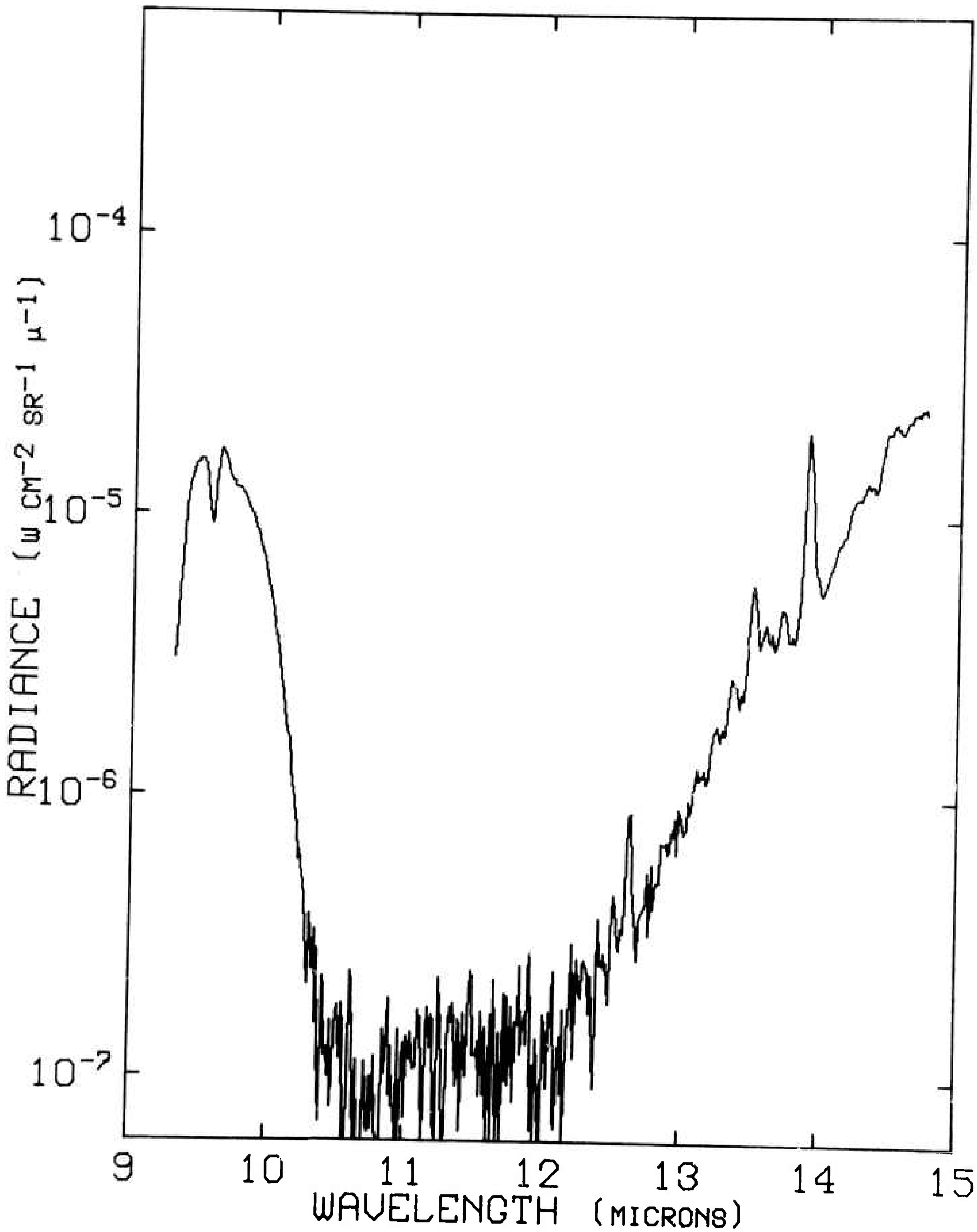

Figure 75. Radiance vs Wavelength at 95.4 kft and 0420 ADT, 12 September 1971.

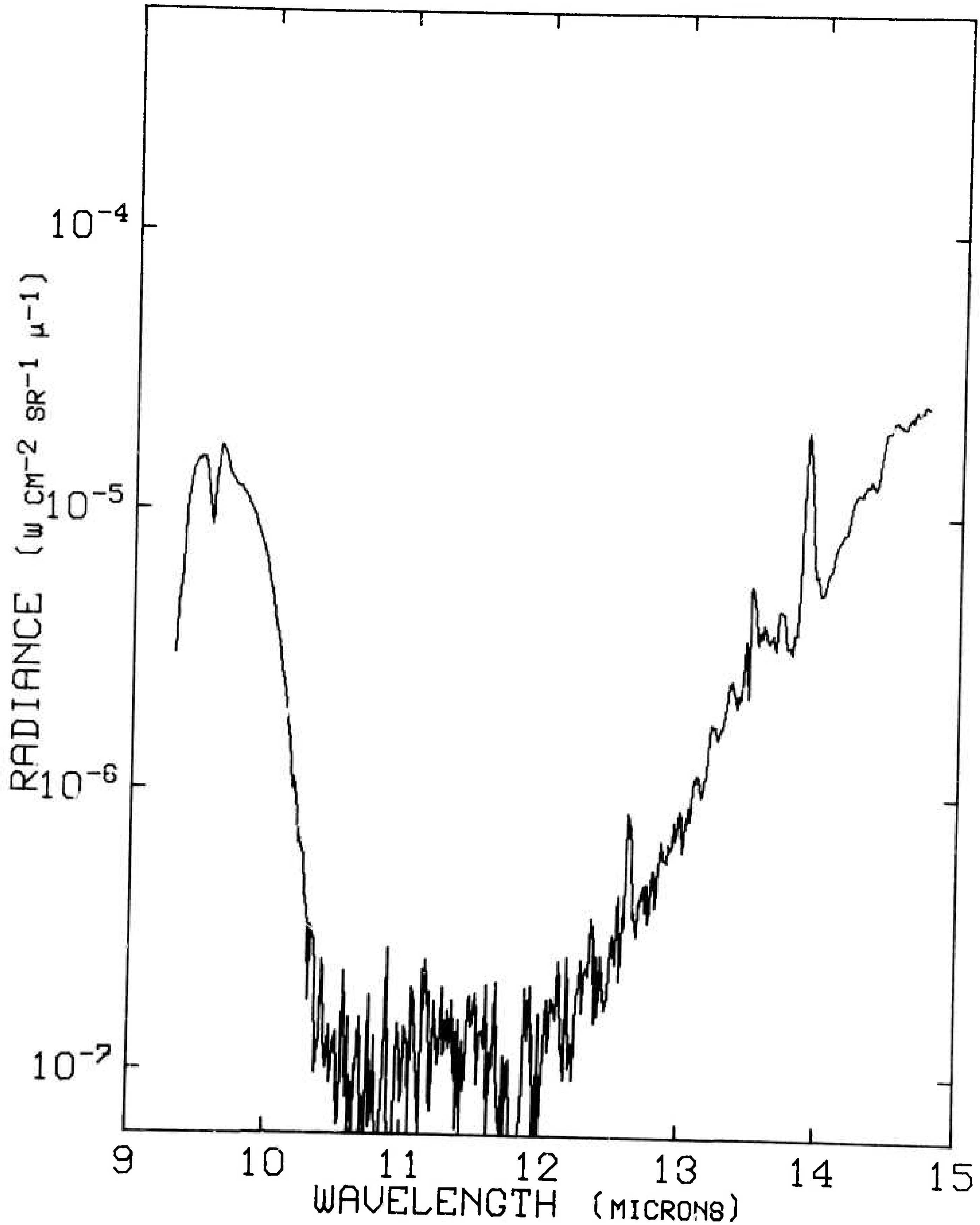

Figure 76. Radiance vs Wavelength at 95.4 kft and 0422 ADT, 12 September 1971.

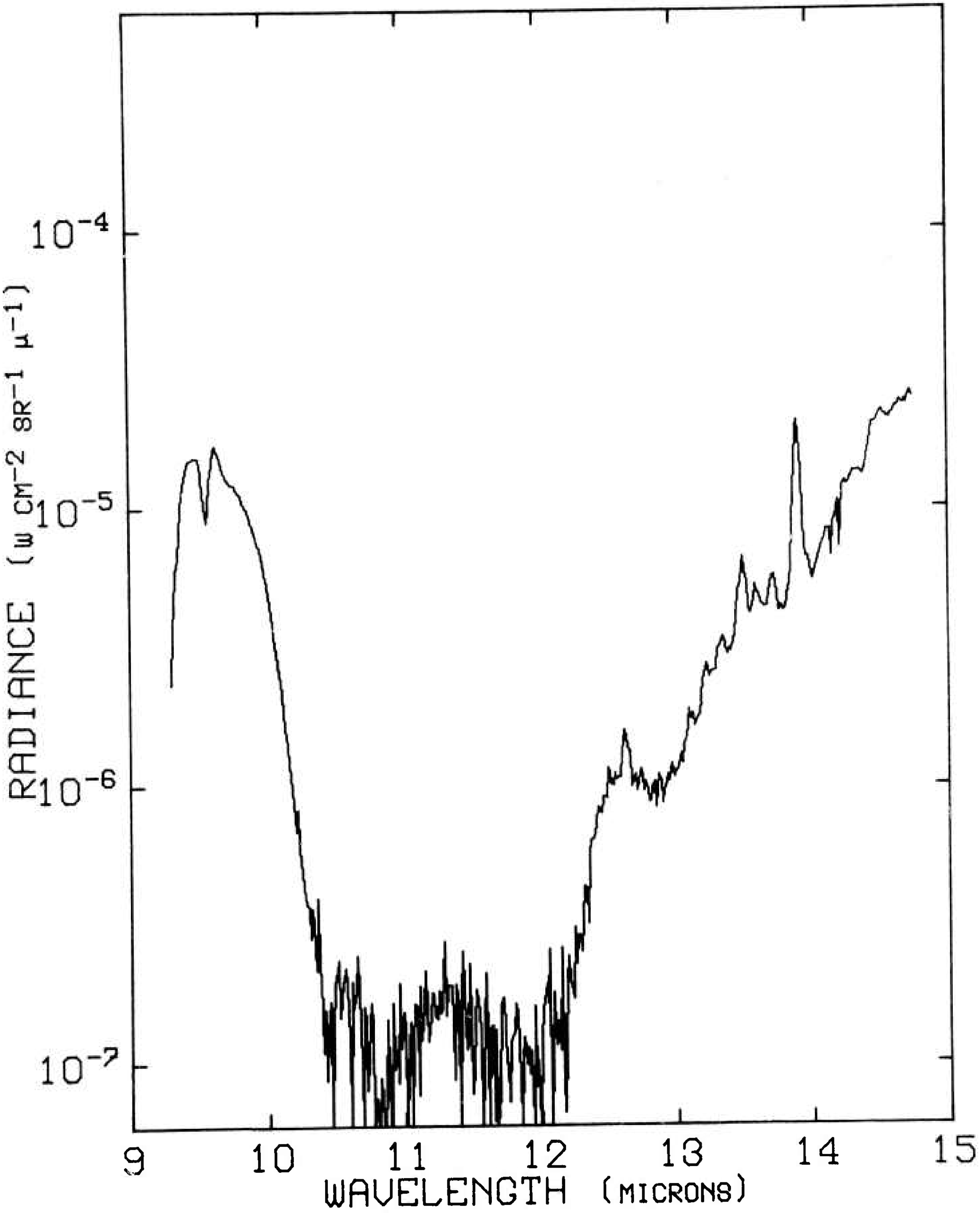

Figure 77. Radiance vs Wavelength at 95.4 kft and 0424 ADT, 12 September 1971.

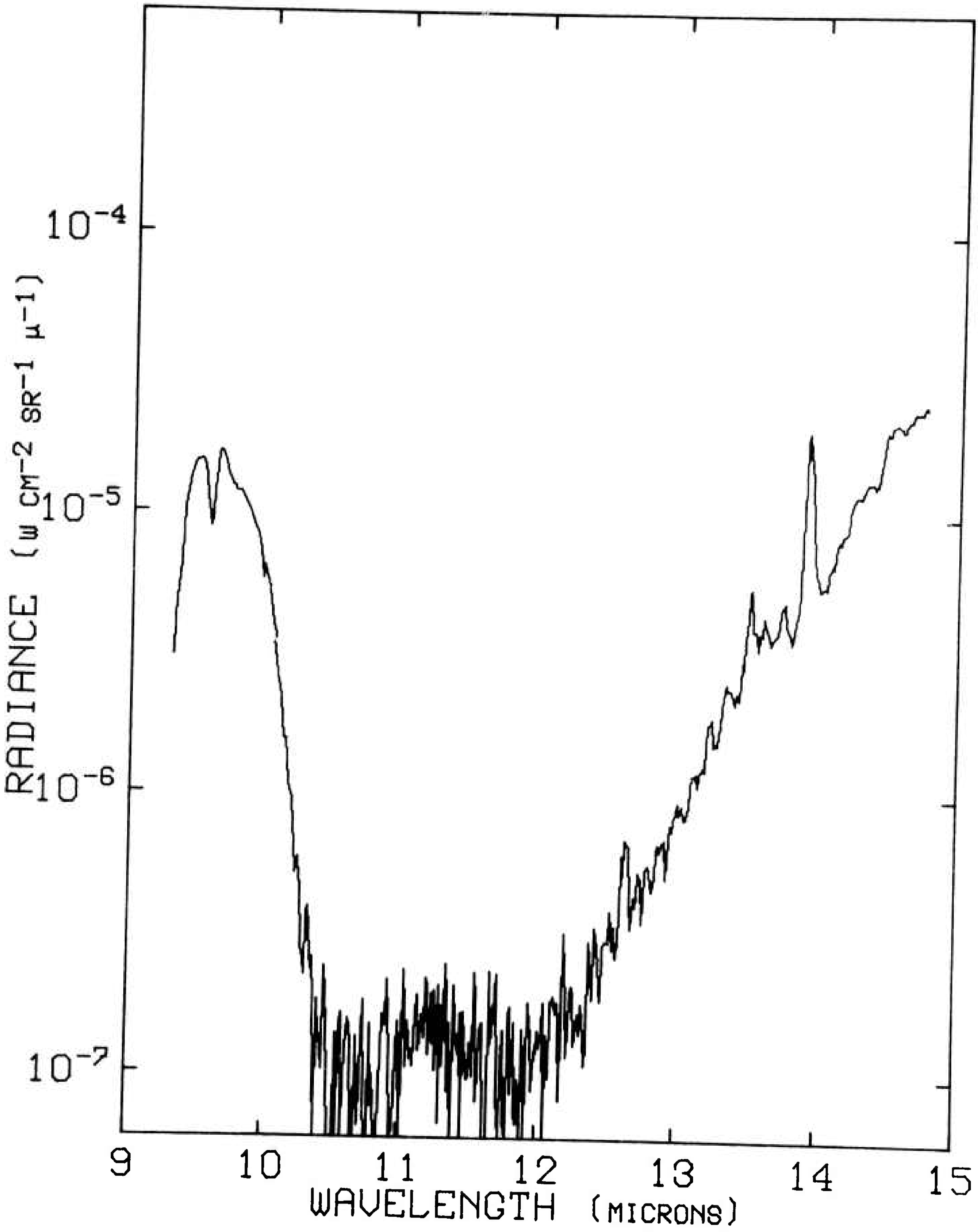

Figure 78. Radiance vs Wavelength at 95.4 kft and 0425 ADT, 12 September 1971.

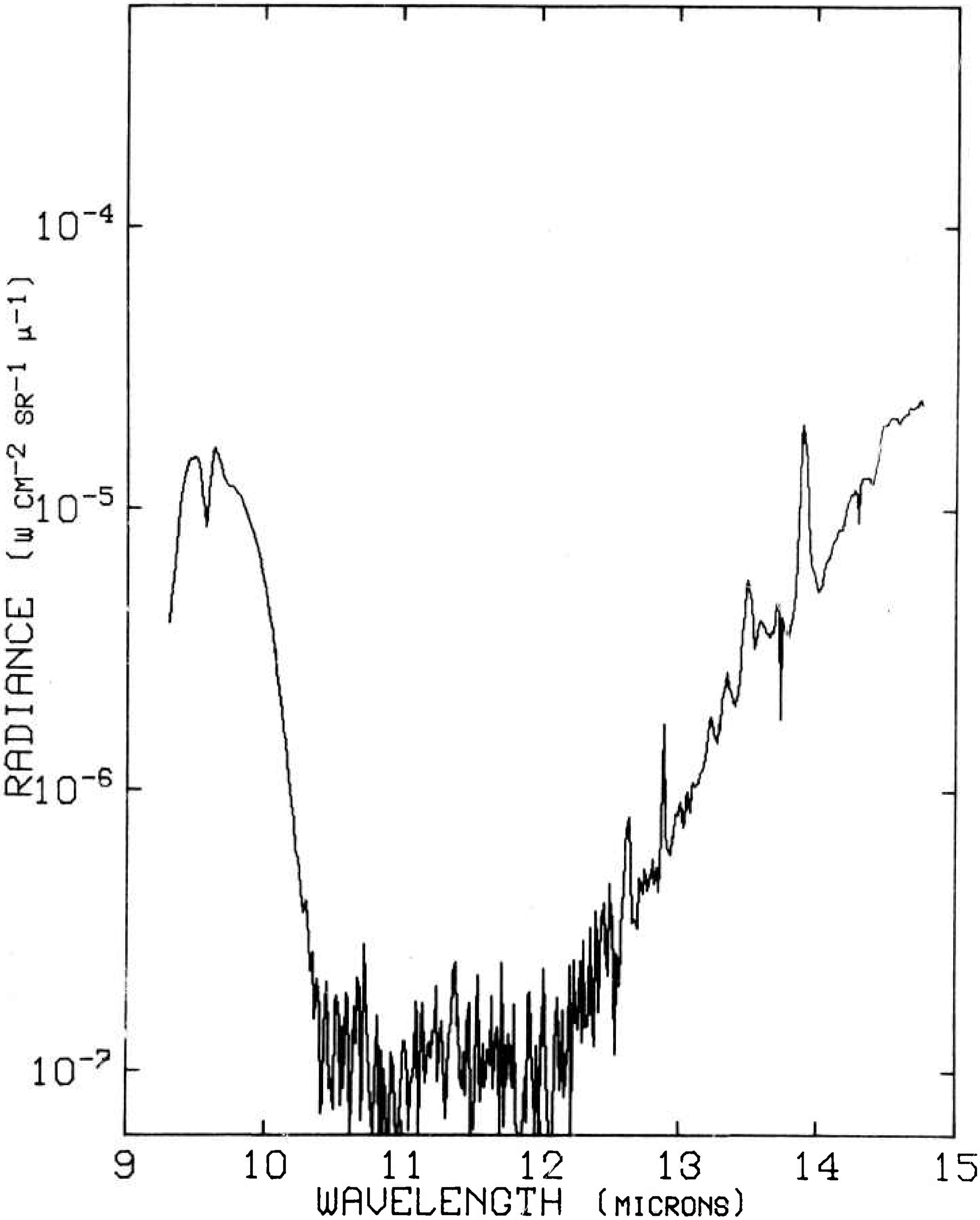

Figure 79. Radiance vs Wavelength at 95.4 kft and 0427 ADT, 12 September 1971.

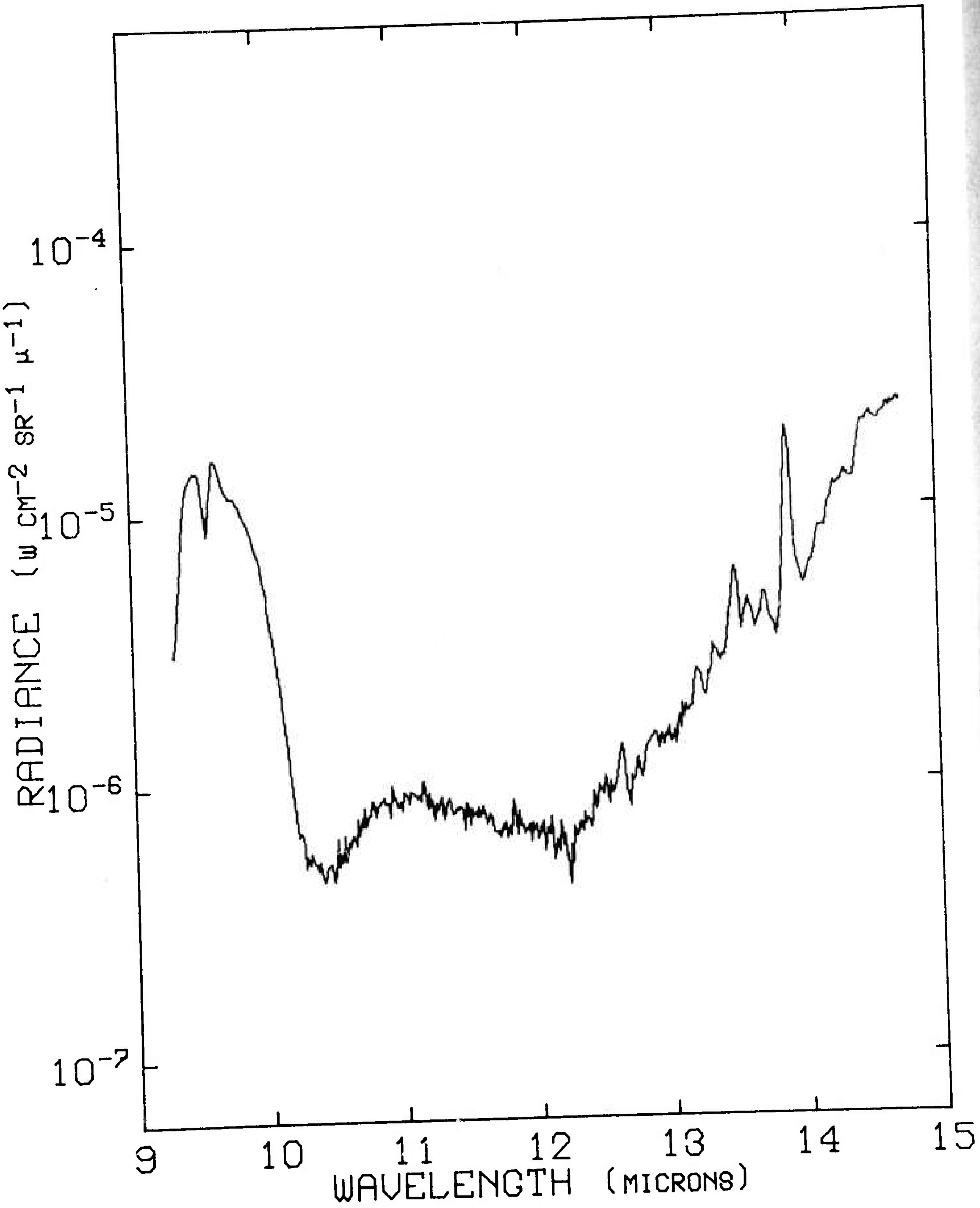

Figure 80. Radiance vs Wavelength at 95.4 kft and 0429 ADT, 12 September 1971.

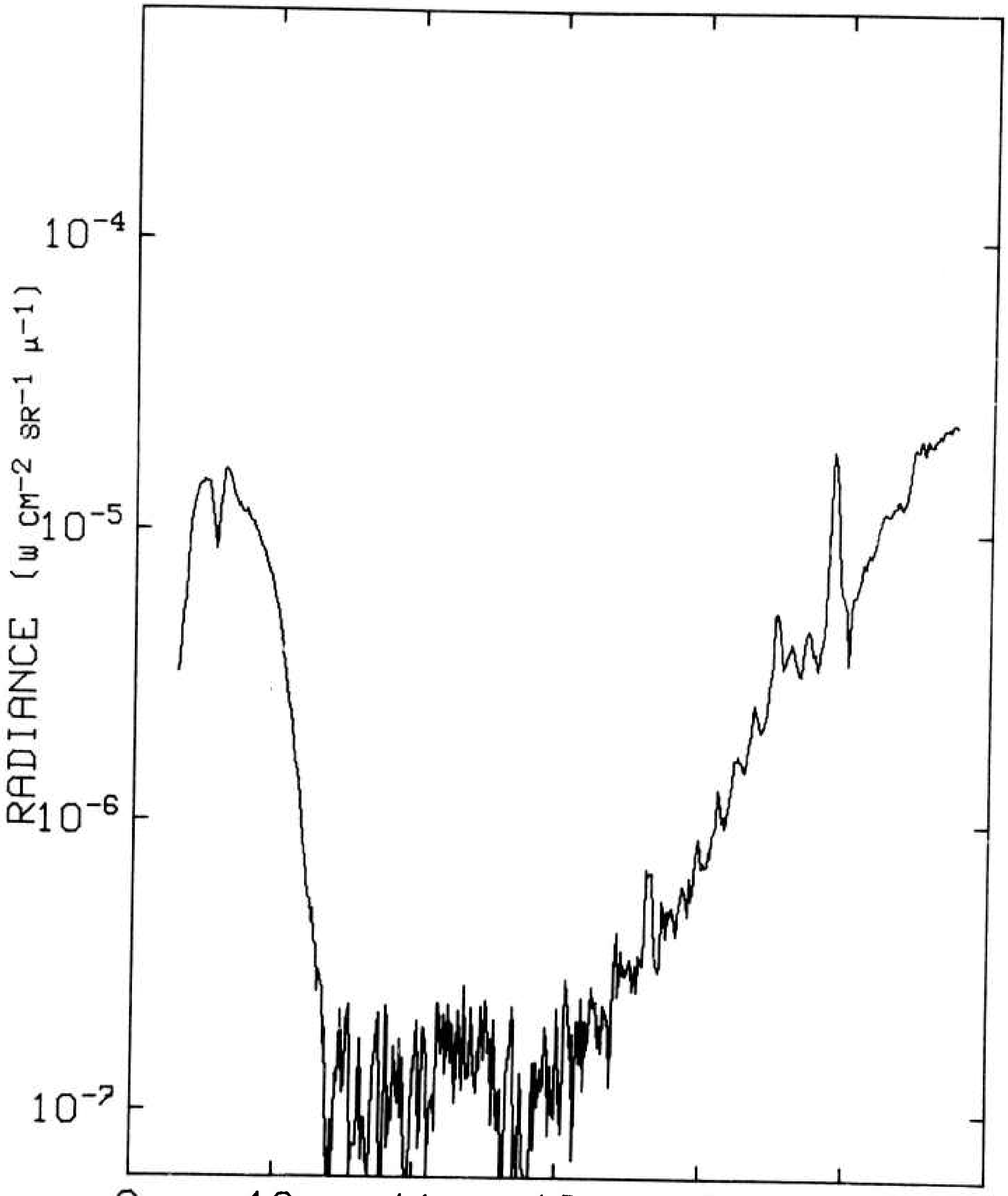

Figure 81. Radiance vs Wavelength at 95.4 kft and 0431 ADT, 12 September 1971.

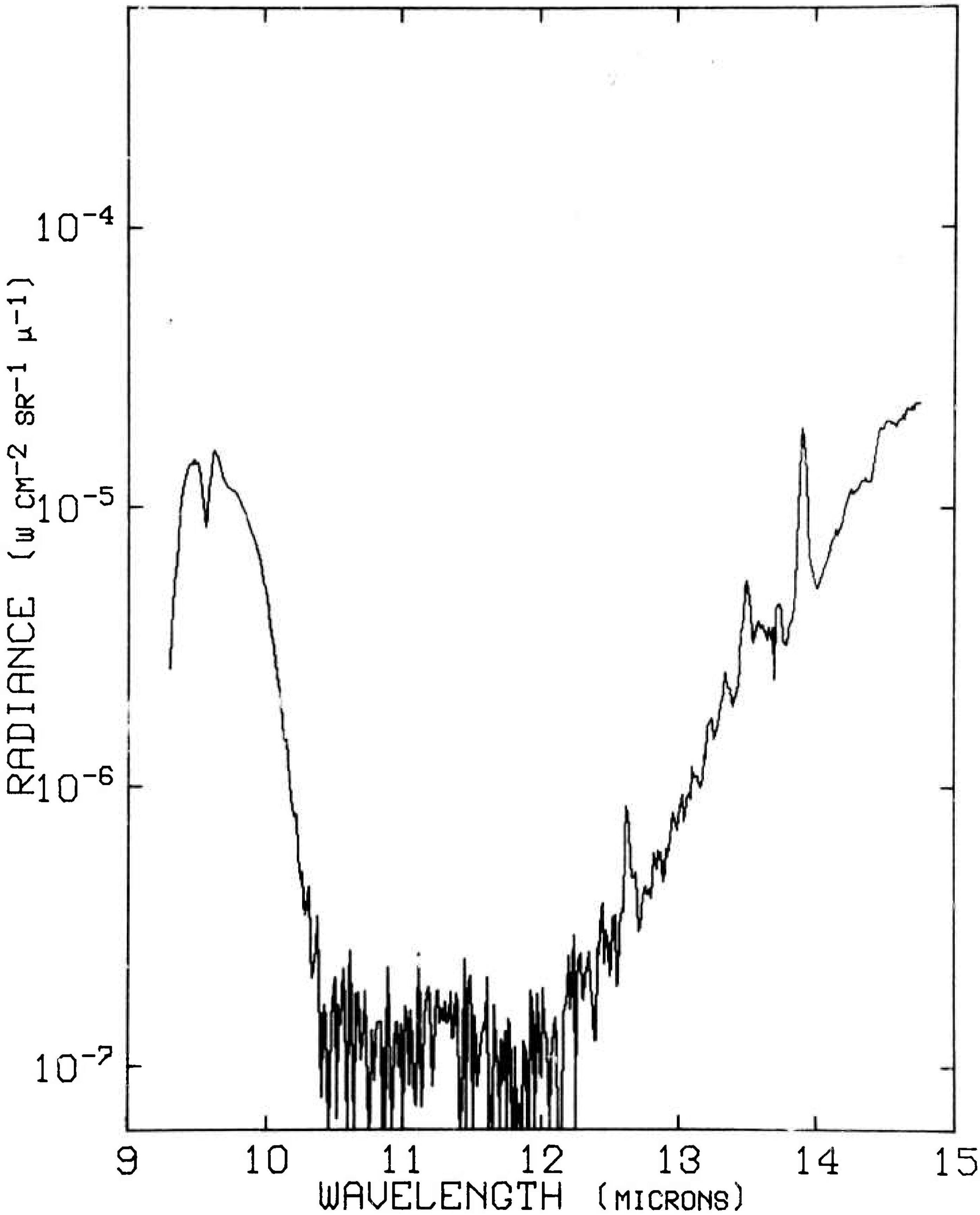

Figure 82. Radiance vs Wavelength at 95.4 kft and 0433 ADT, 12 September 1971.

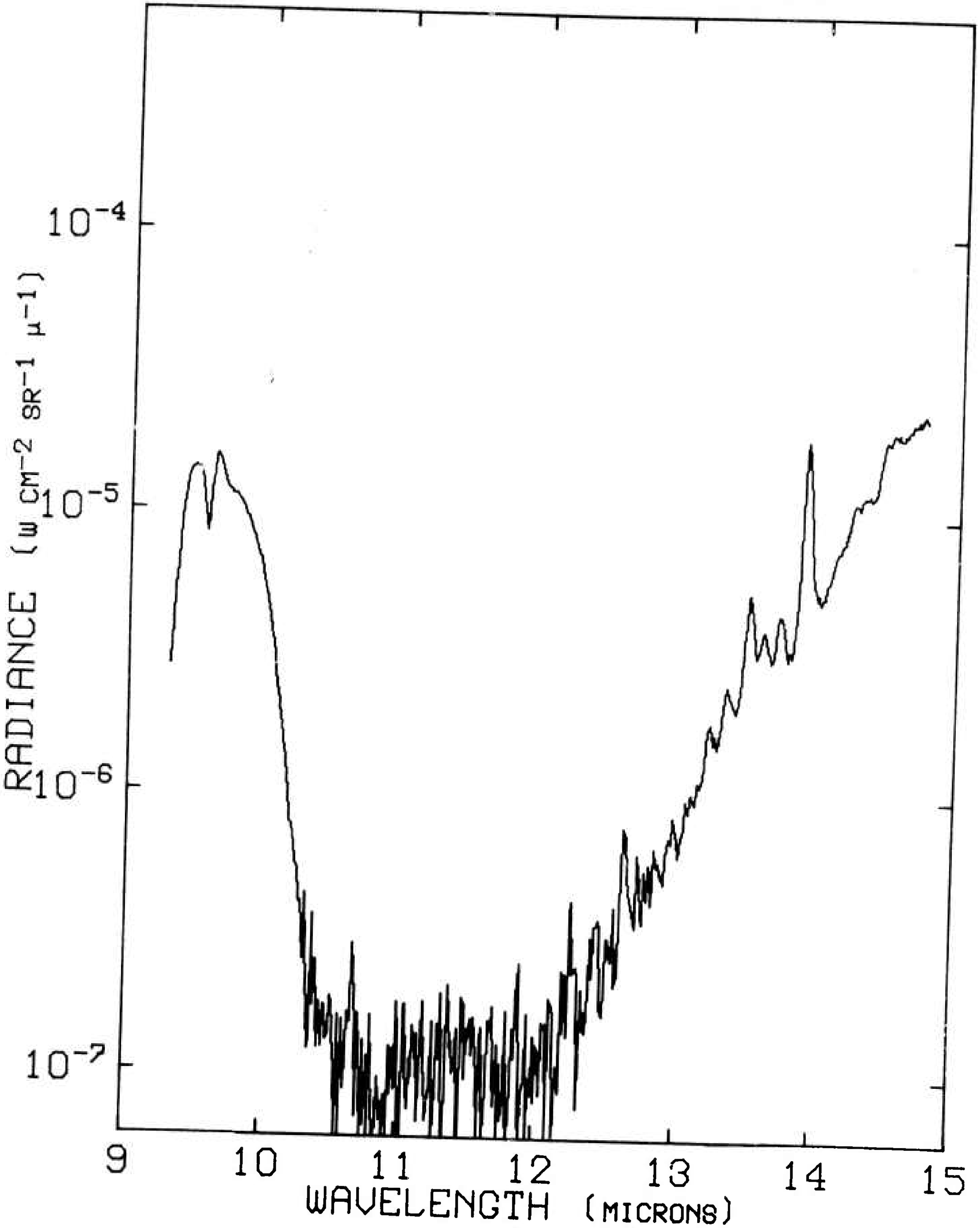

Figure 83. Radiance vs Wavelength at 95.4 kft and 0435 ADT, 12 September 1971.

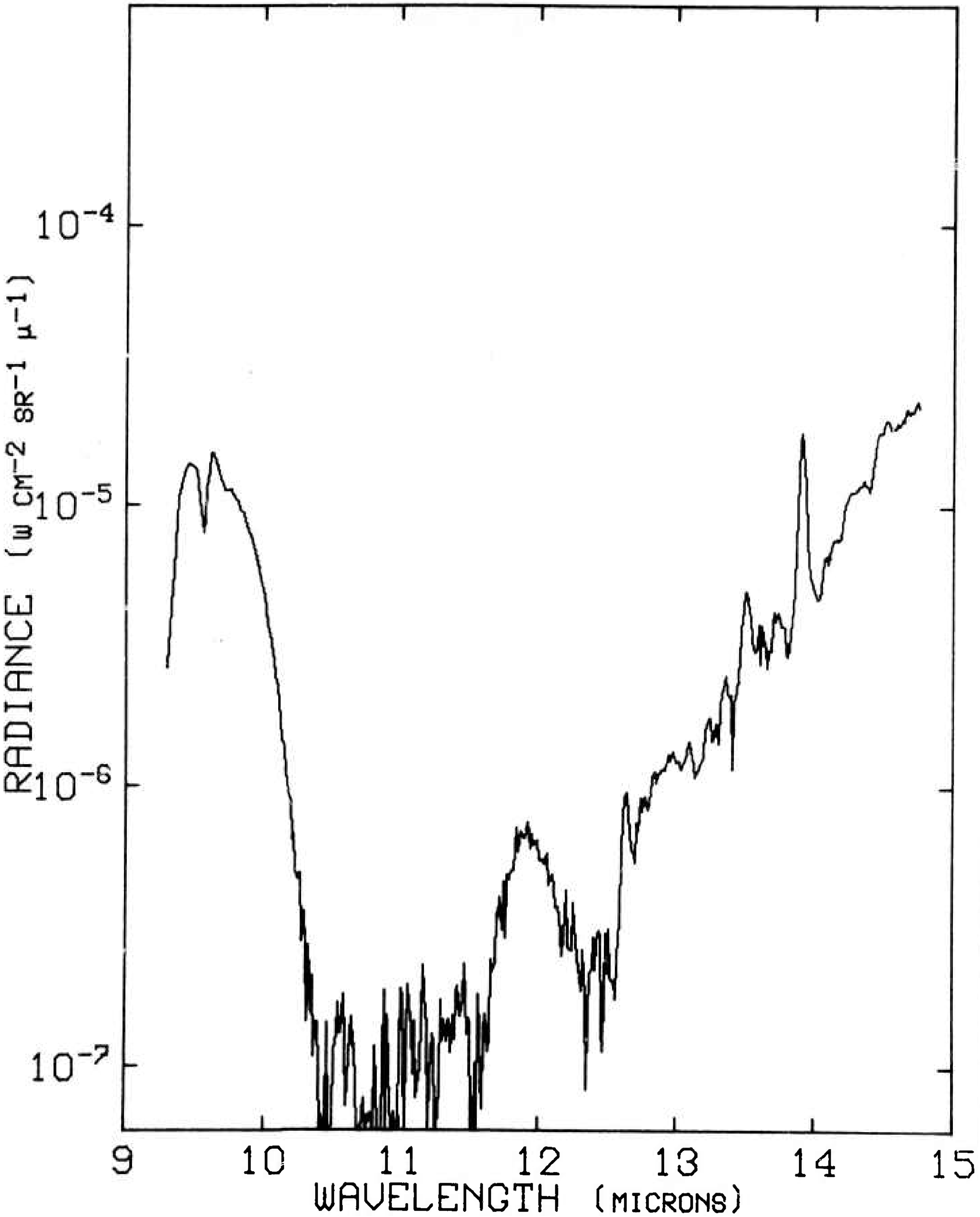

Figure 84. Radiance vs Wavelength at 95.4 kft and 0437 ADT, 12 September 1971.

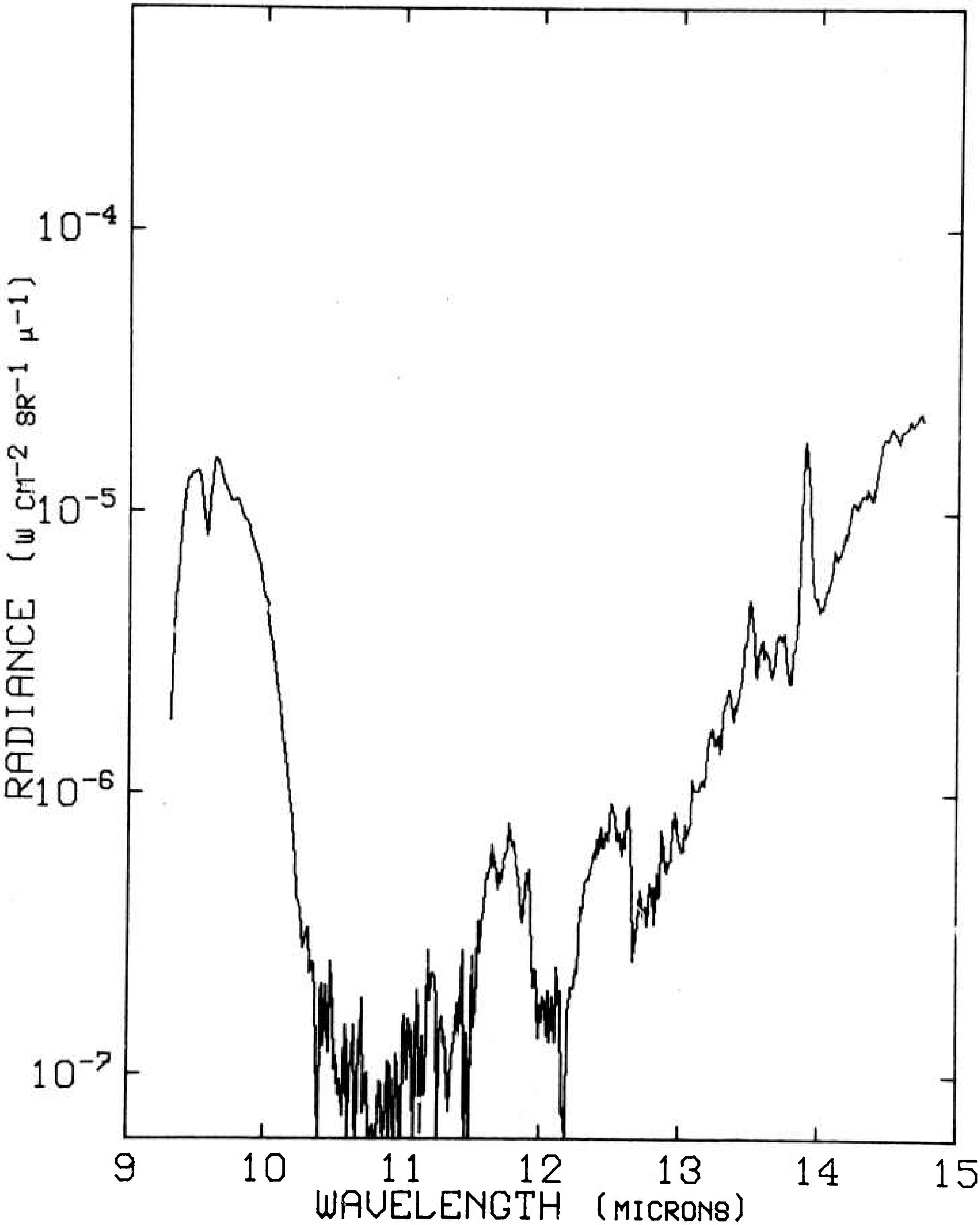

Figure 85. Radiance vs Wavelength at 95.4 kft and 0439 ADT, 12 September 1971.

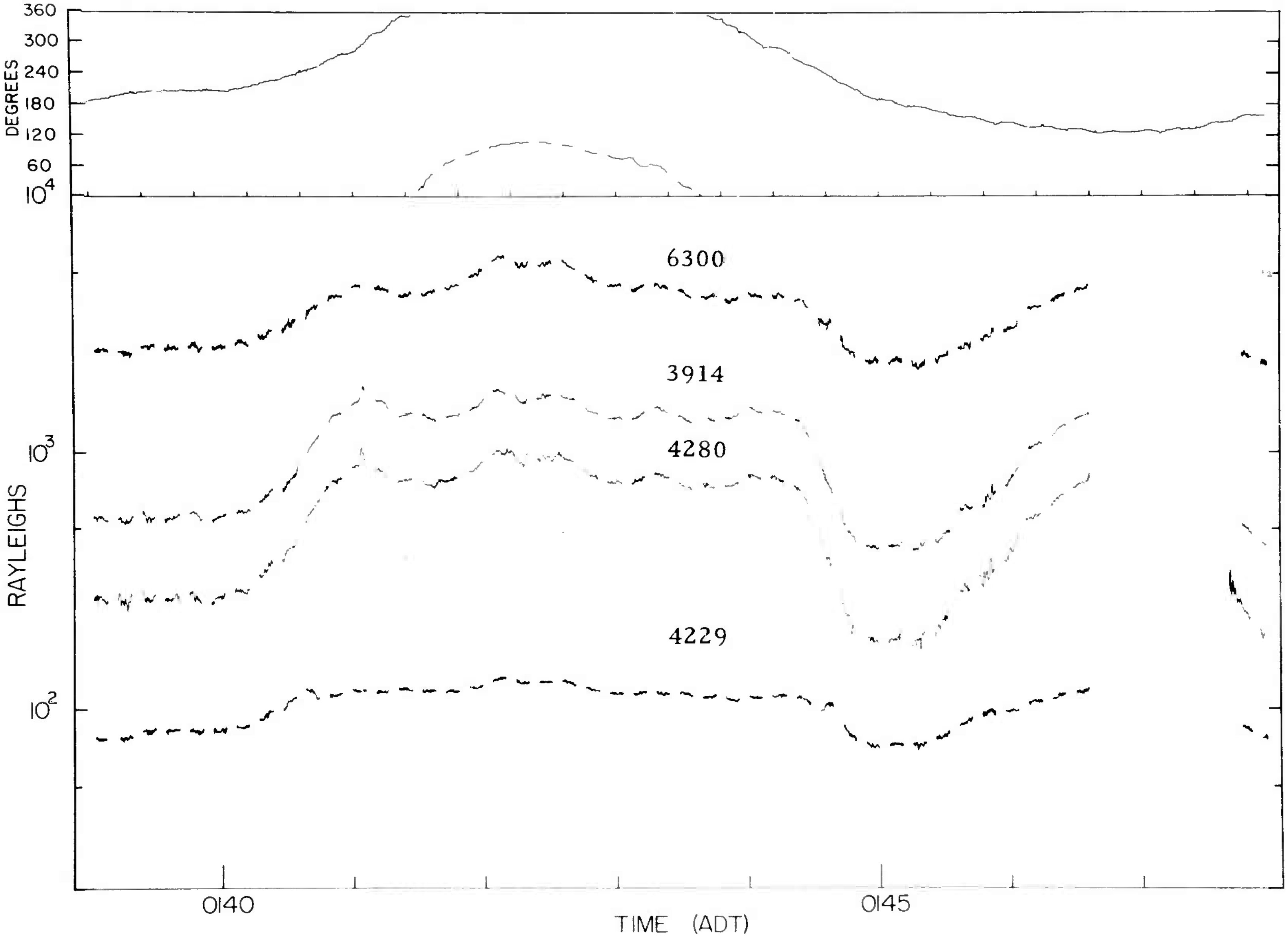

Figure 86. Auroral activity vs time for 12 September 1971.

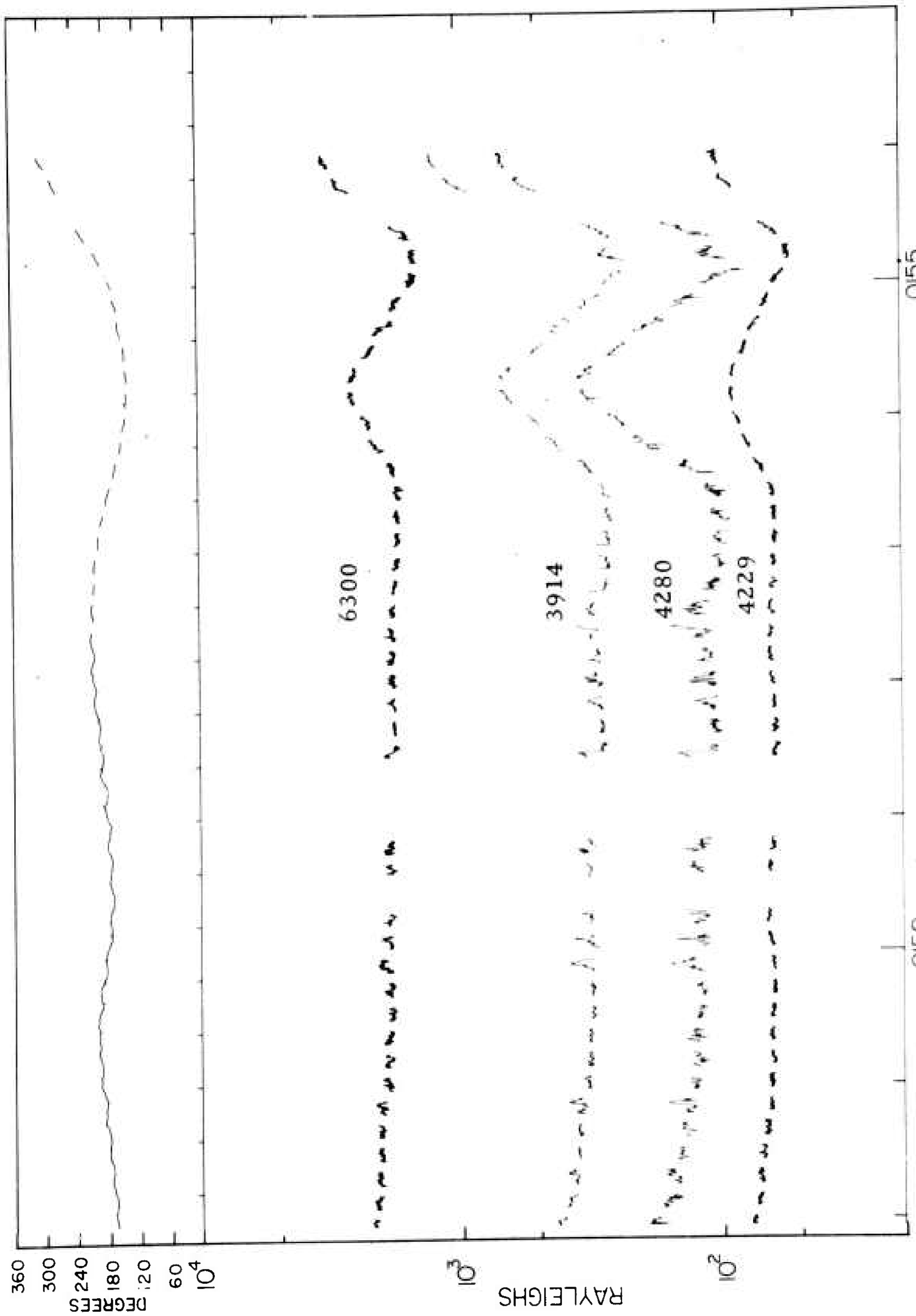

Figure 87. Auroral activity vs time for 12 September 1971.

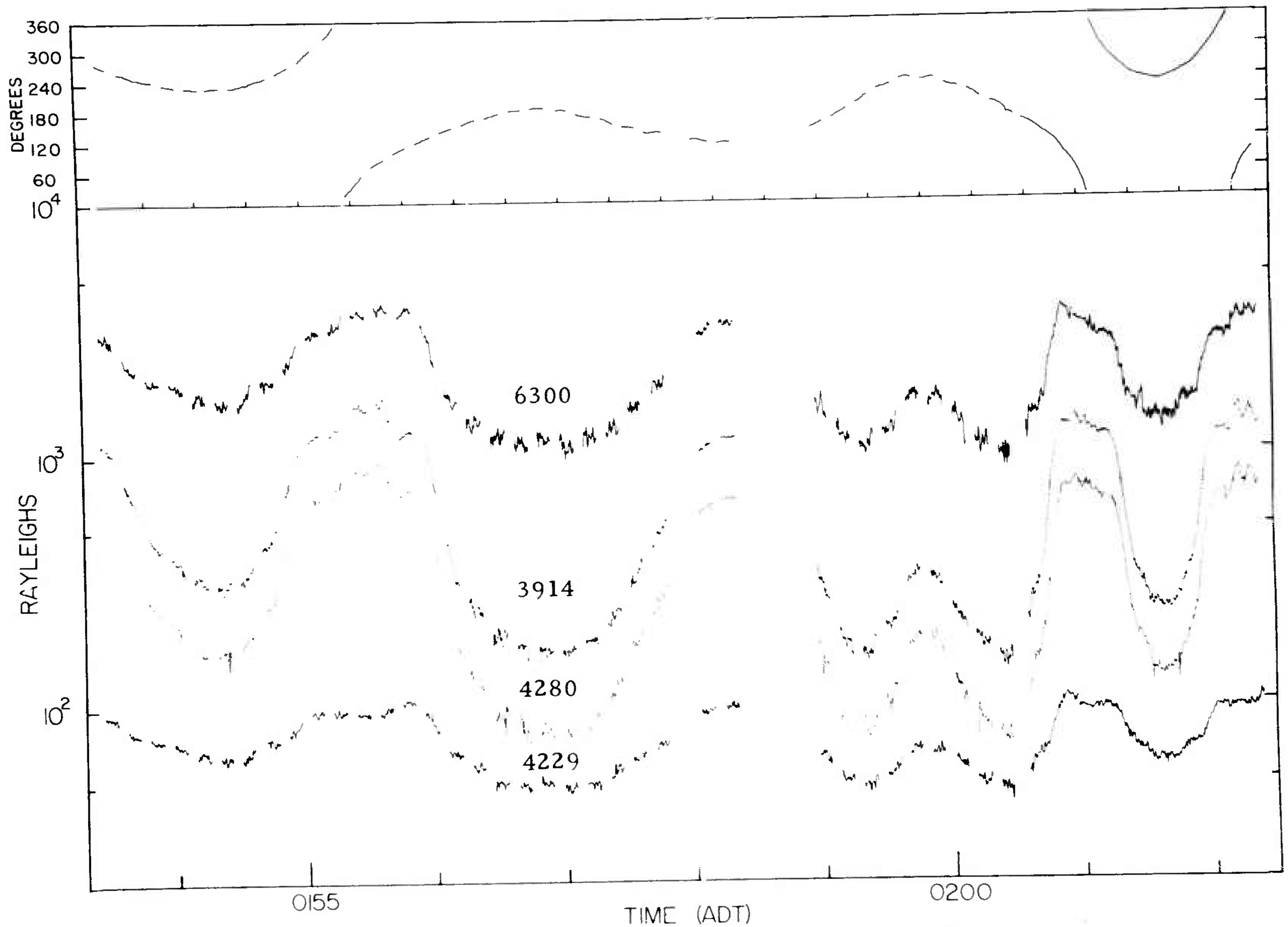

Figure 88. Auroral activity vs time for 12 September 1971.

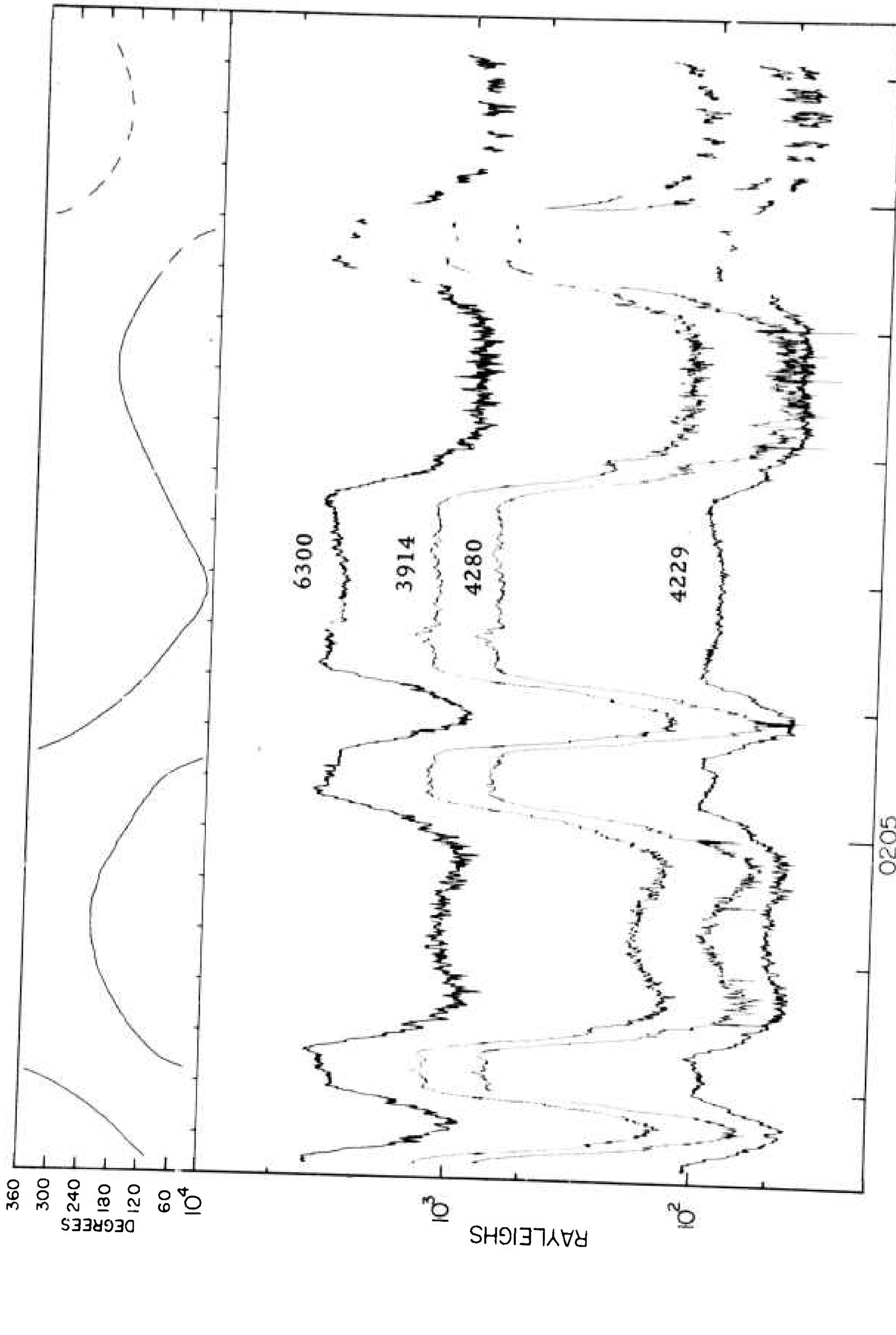

Figure 89. Auroral activity vs time for 12 September 1971.

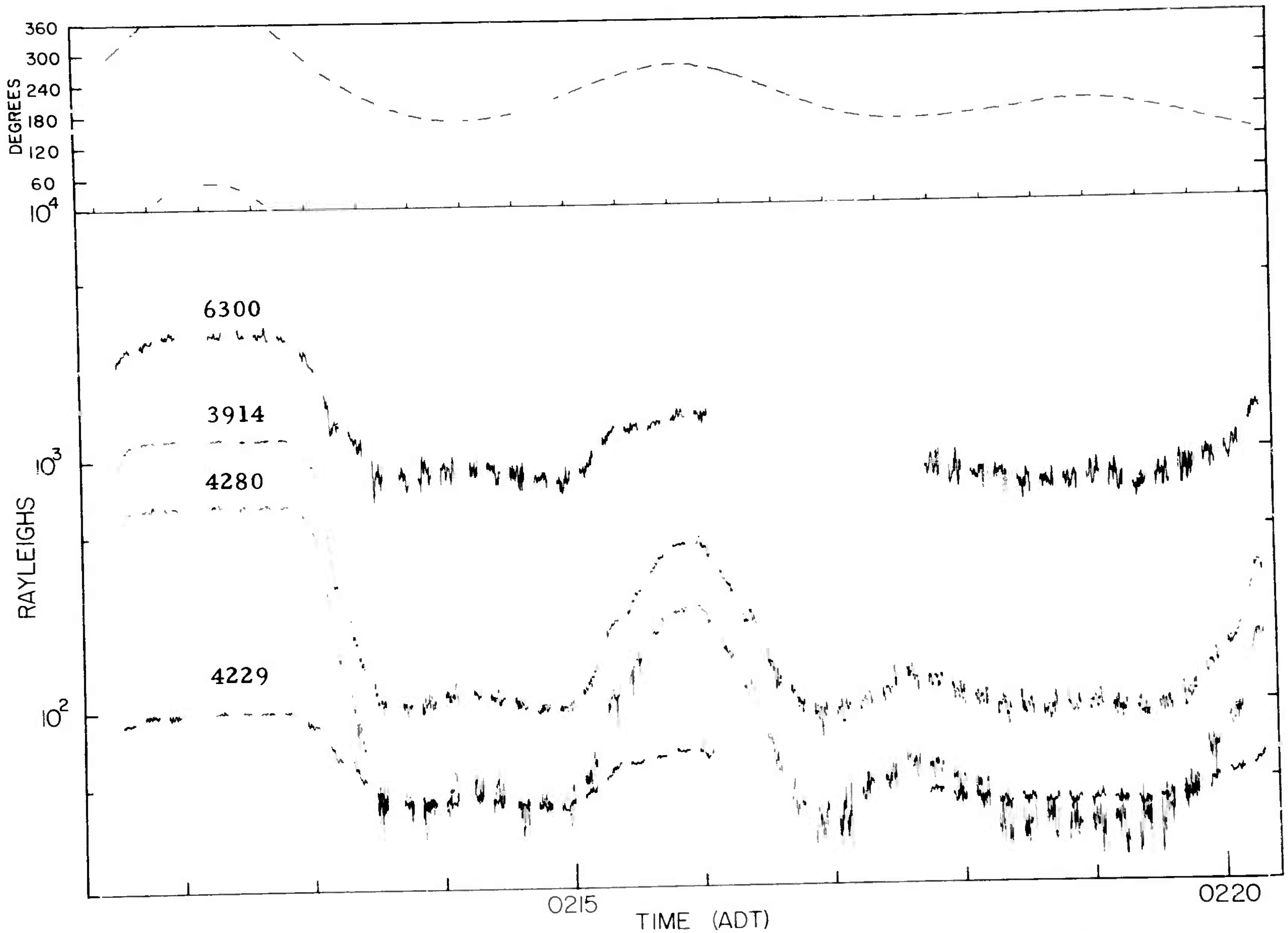

Figure 90. Auroral activity vs time for 12 September 1971.

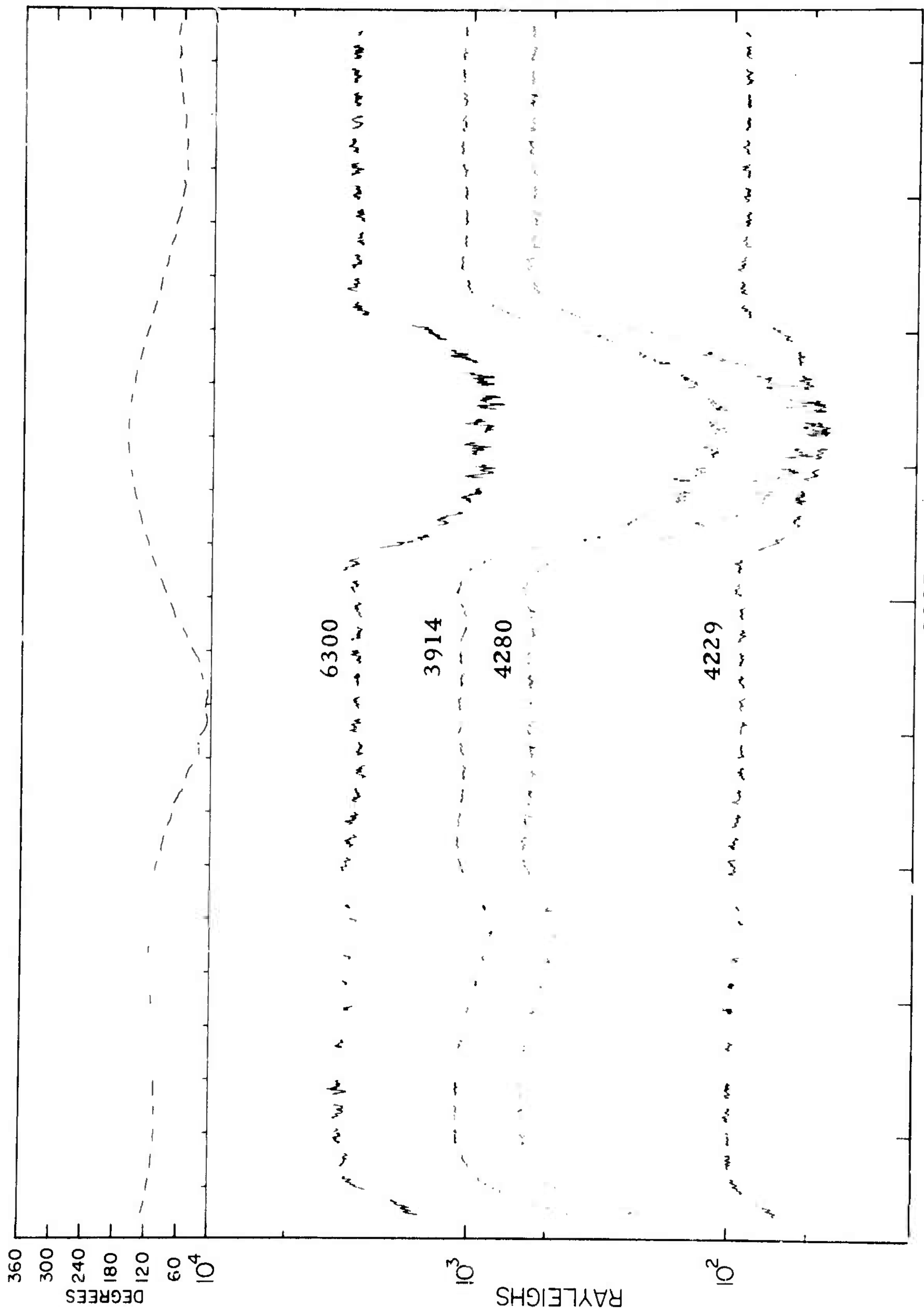

Figure 91. Auroral activity vs time for 12 September 1971.

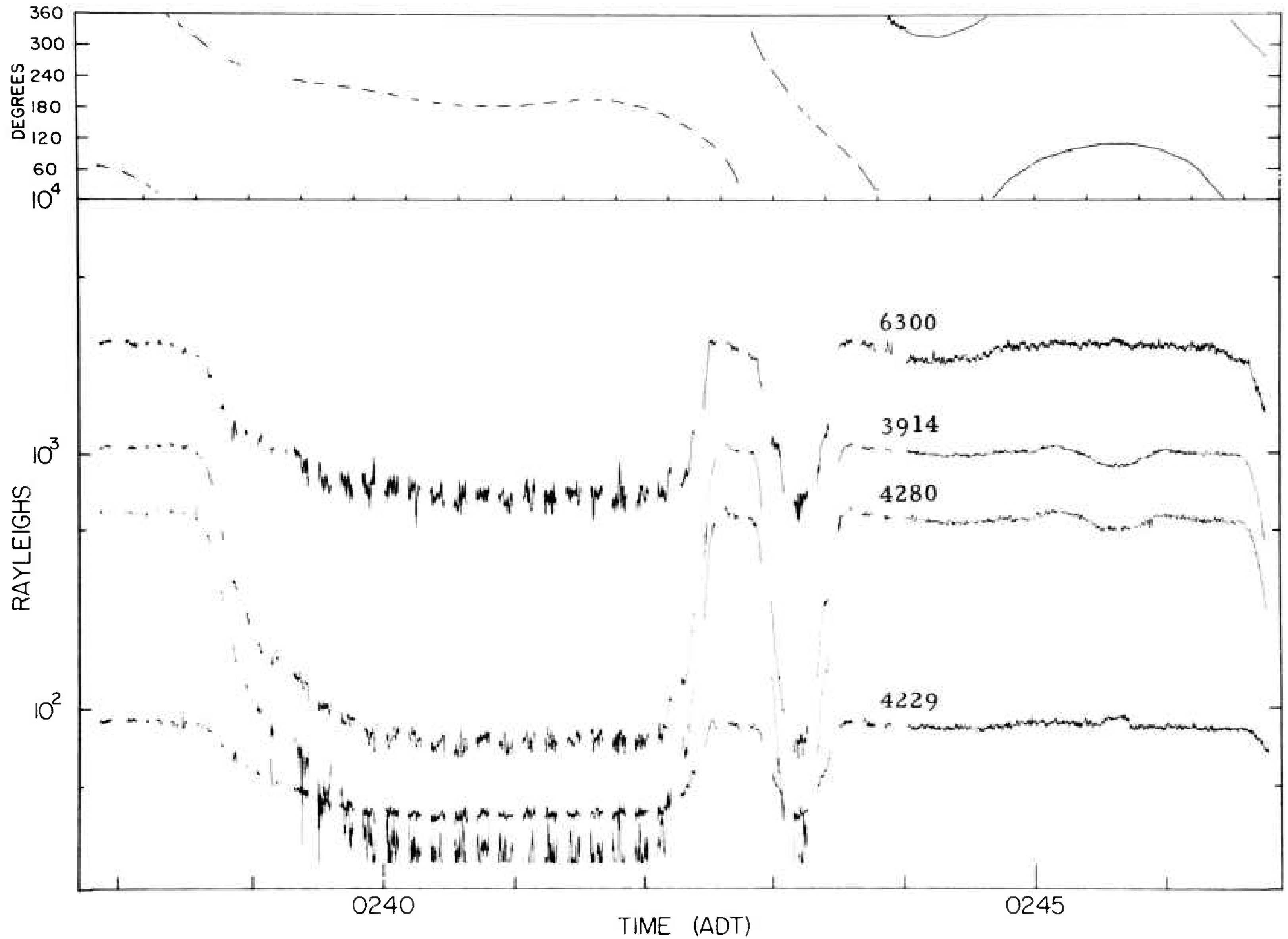

Figure 92. Auroral activity vs time for 12 September 1971.

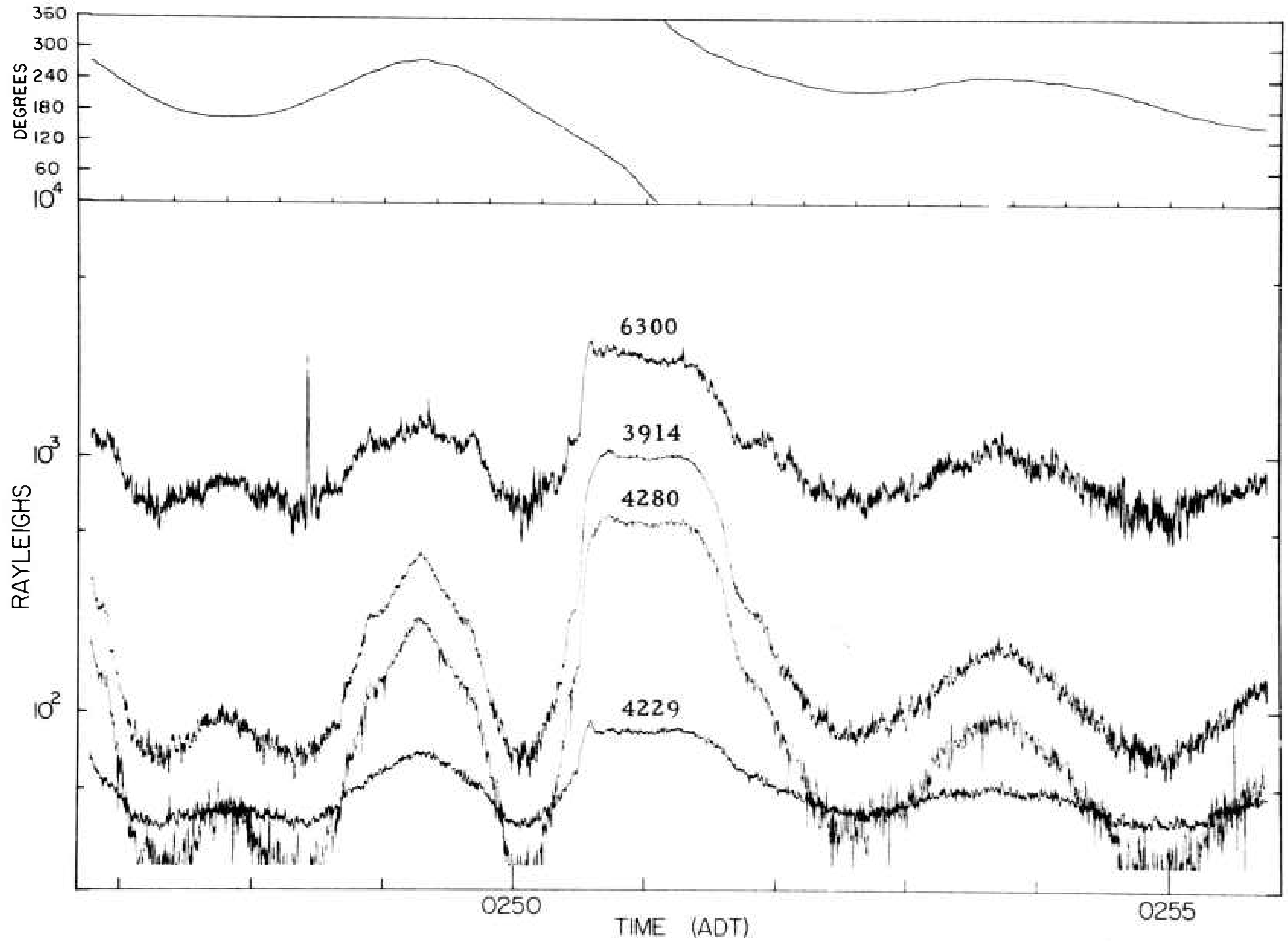

Figure 93. Auroral activity vs time for 12 September 1971.

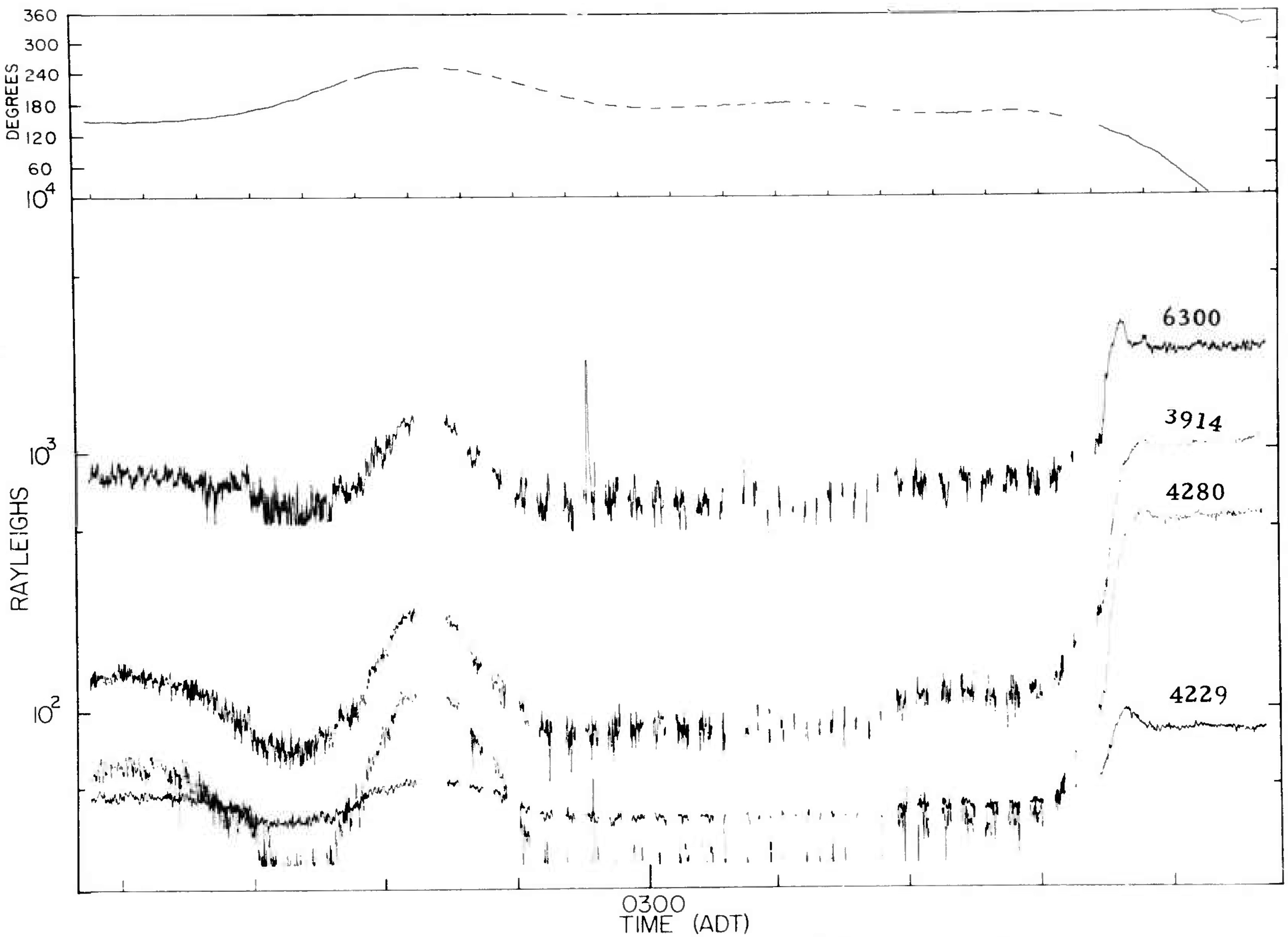

Figure 94. Auroral activity vs time for 12 September 1971.

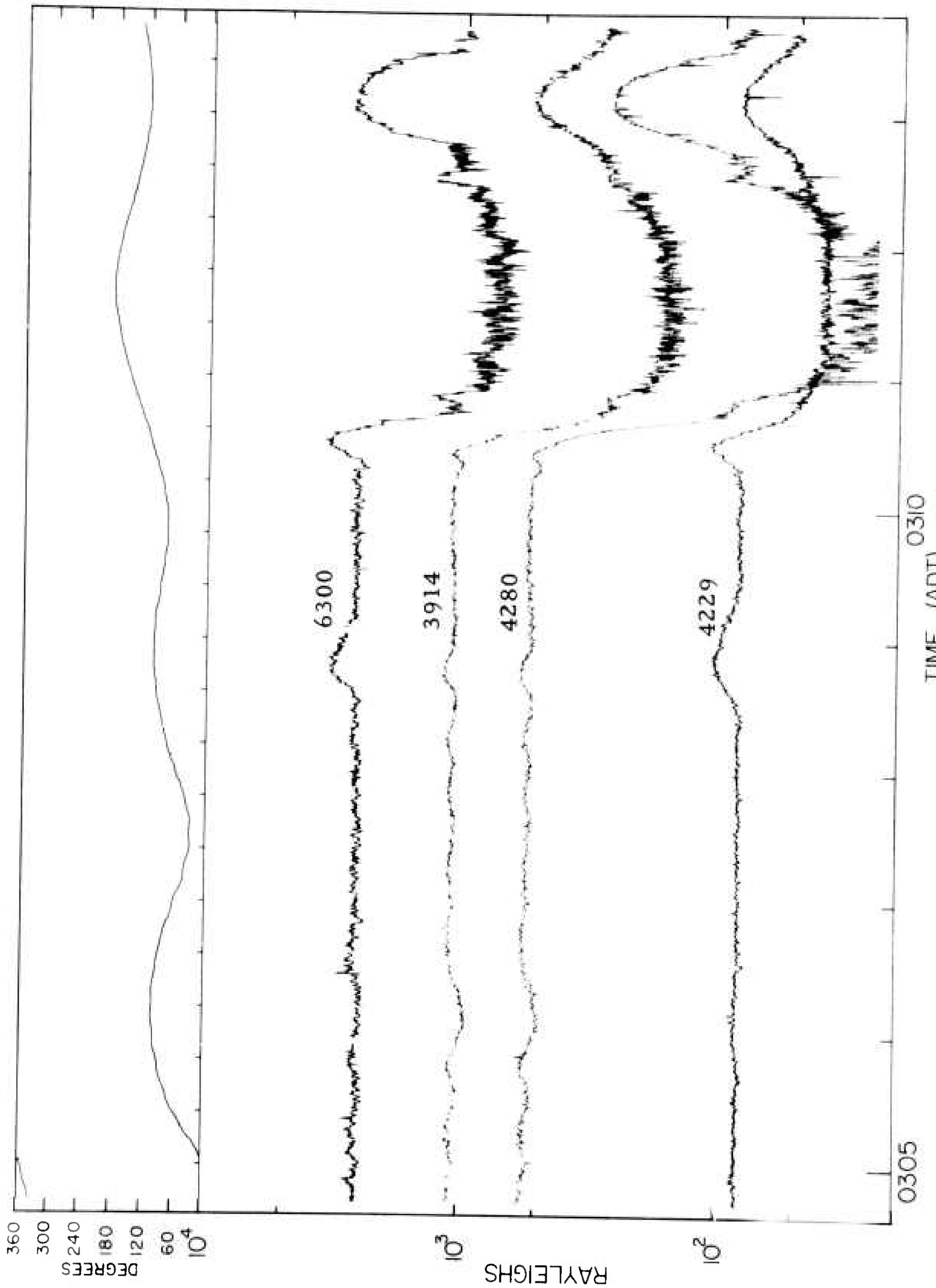

Figure 95. Auroral activity vs time for 12 September 1971.

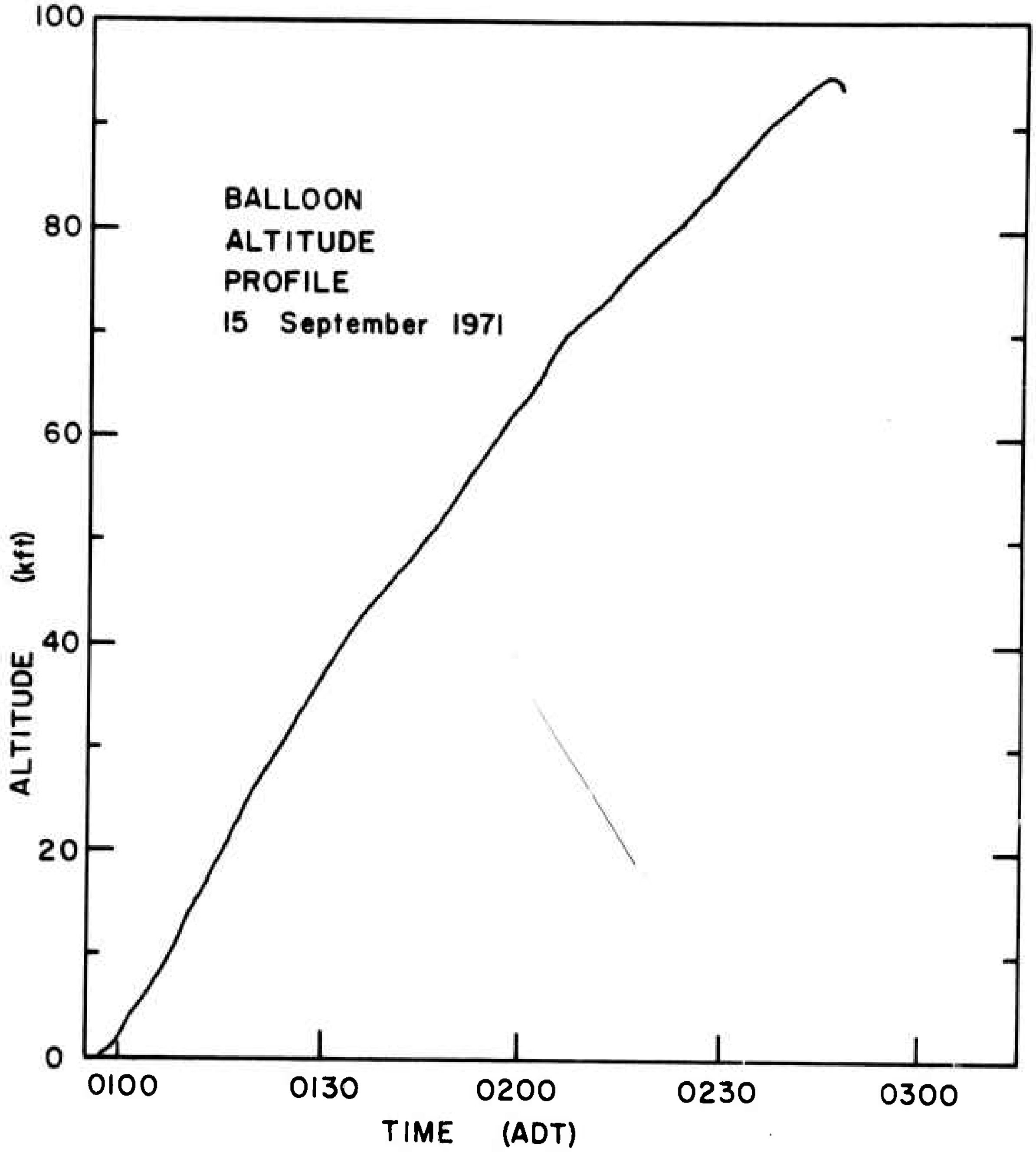

Figure 96. Time vs Altitude Profile of 15 September 1971 Balloon.

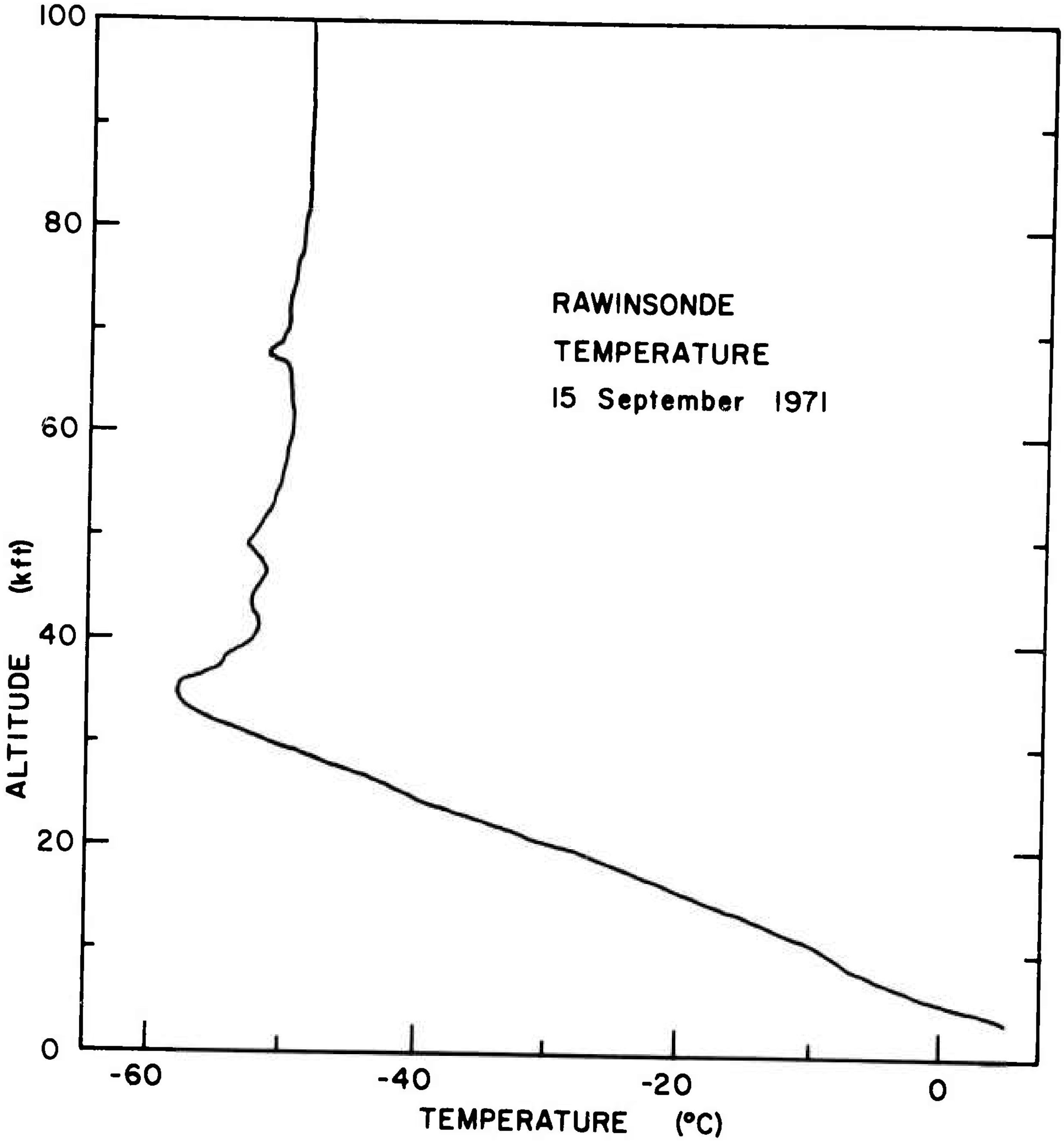

Figure 97. Rawinsonde Temperature vs Altitude for 15 September. 1971, Fairbanks, Alaska.

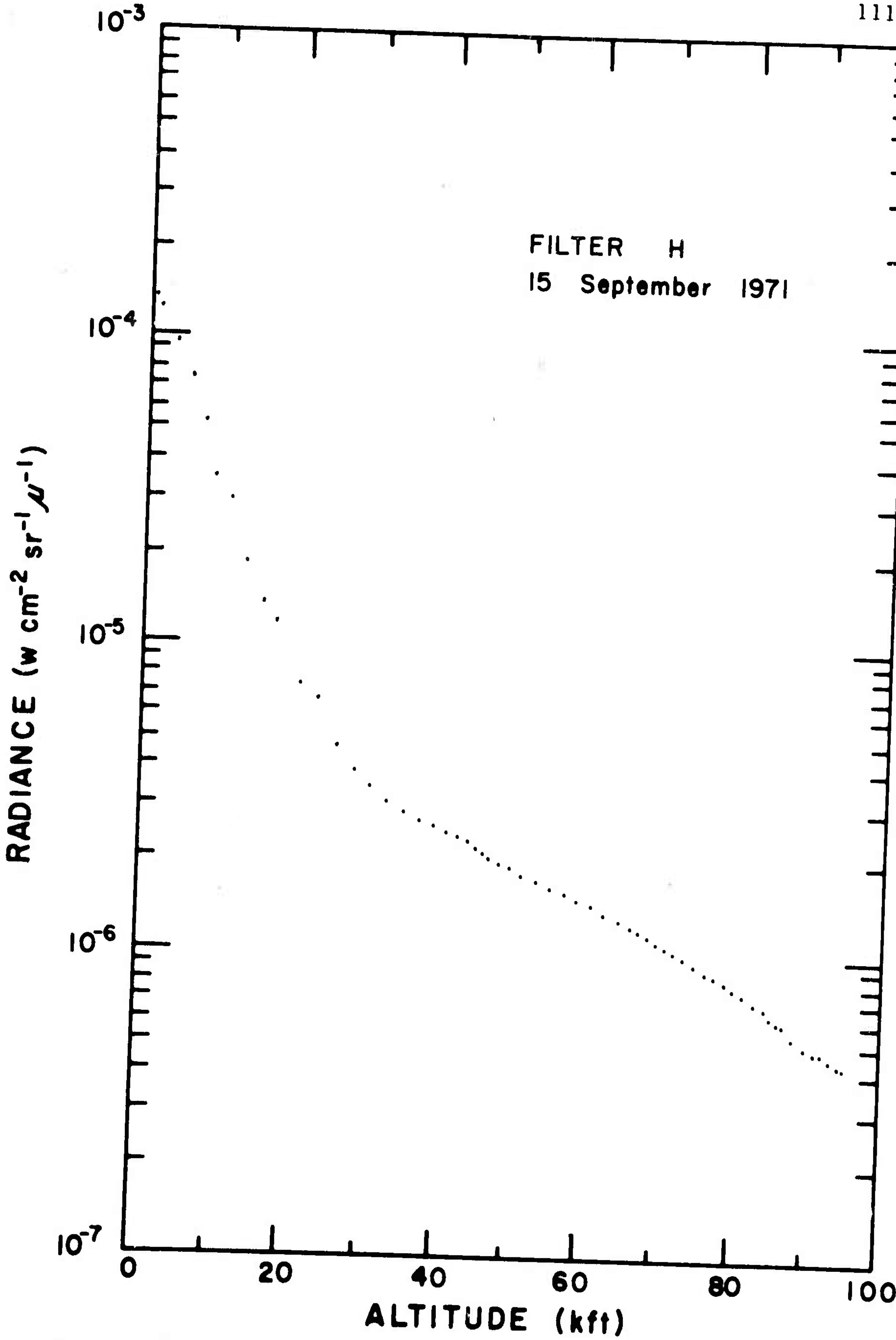

Figure 98. Radiance vs Altitude for Filter H, 15 September 1971.

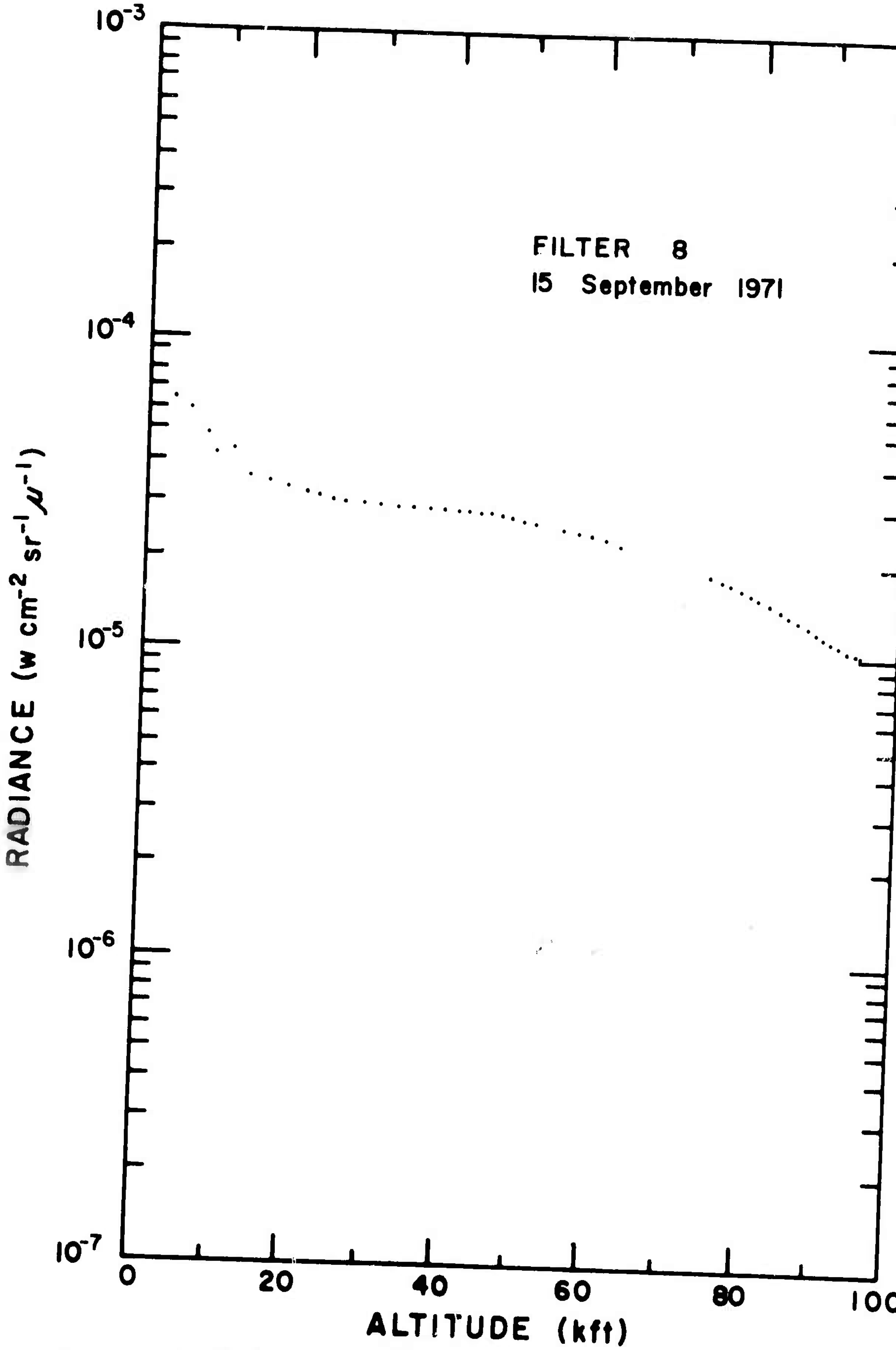

Figure 99. Radiance vs Altitude for Filter 8, 15 September 1971.

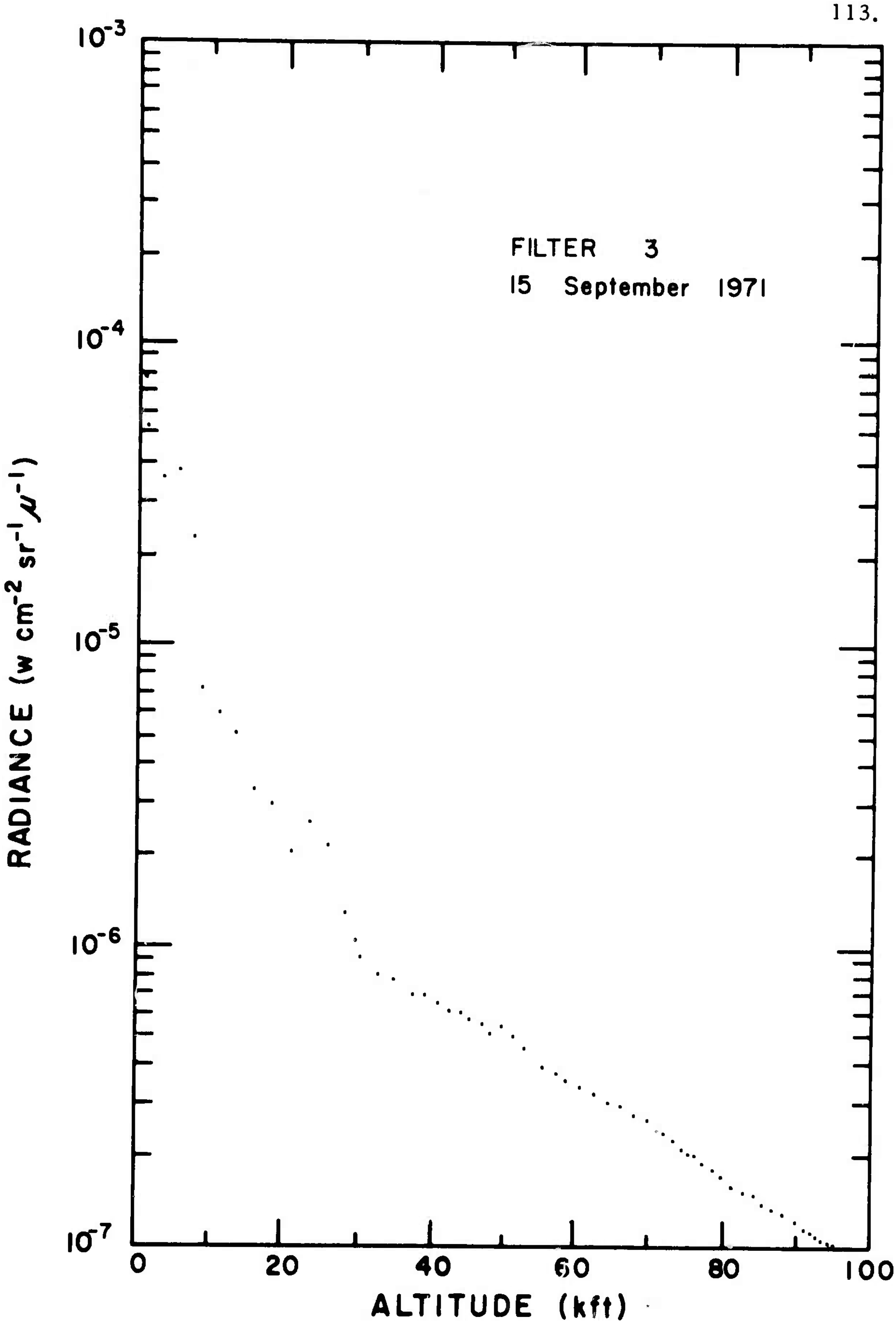

Figure 100. Radiance vs Altitude for Filter 3, 15 September 1971.

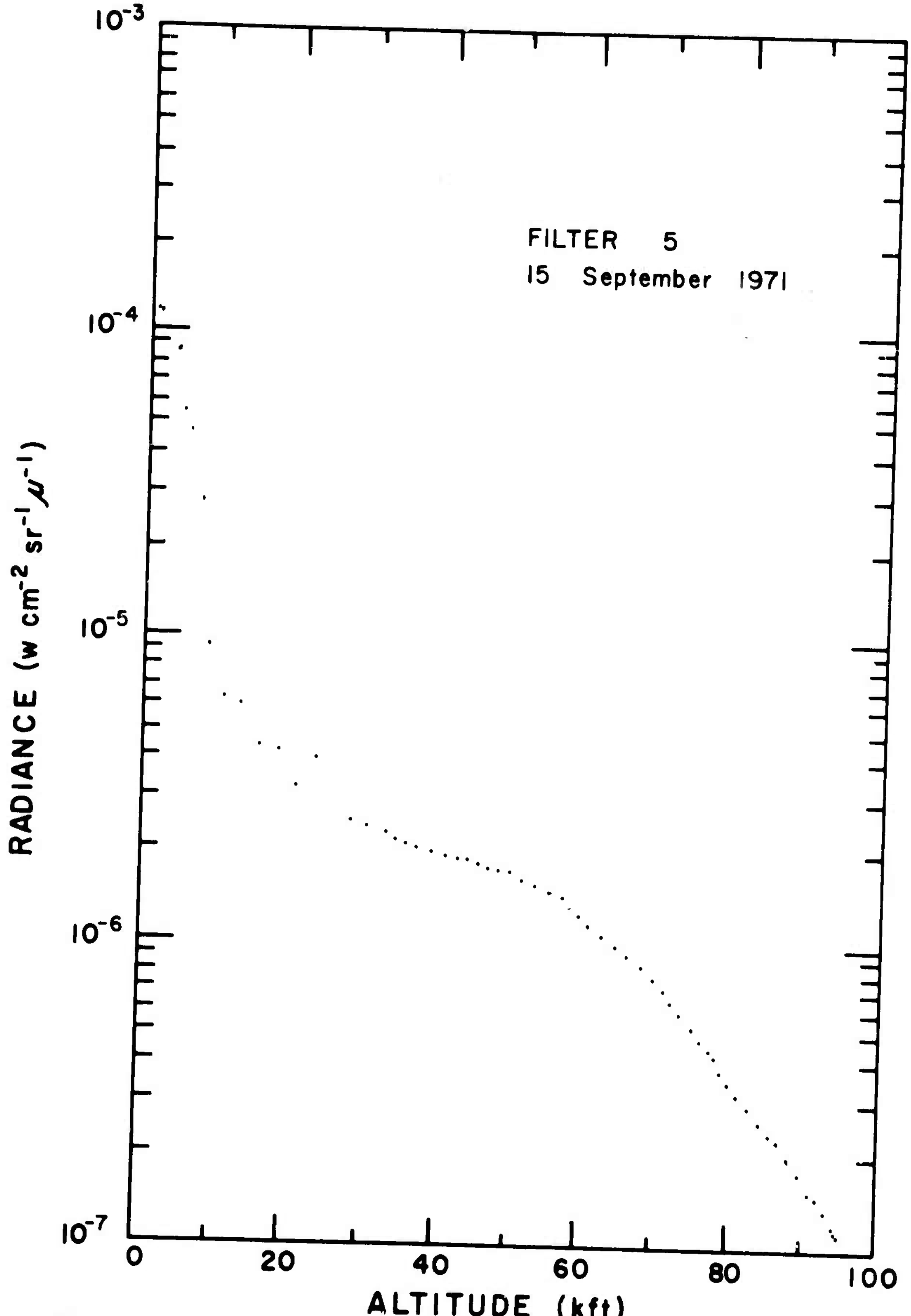

Figure 101. Radiance vs Altitude for Filter 5, 15 September 1971.

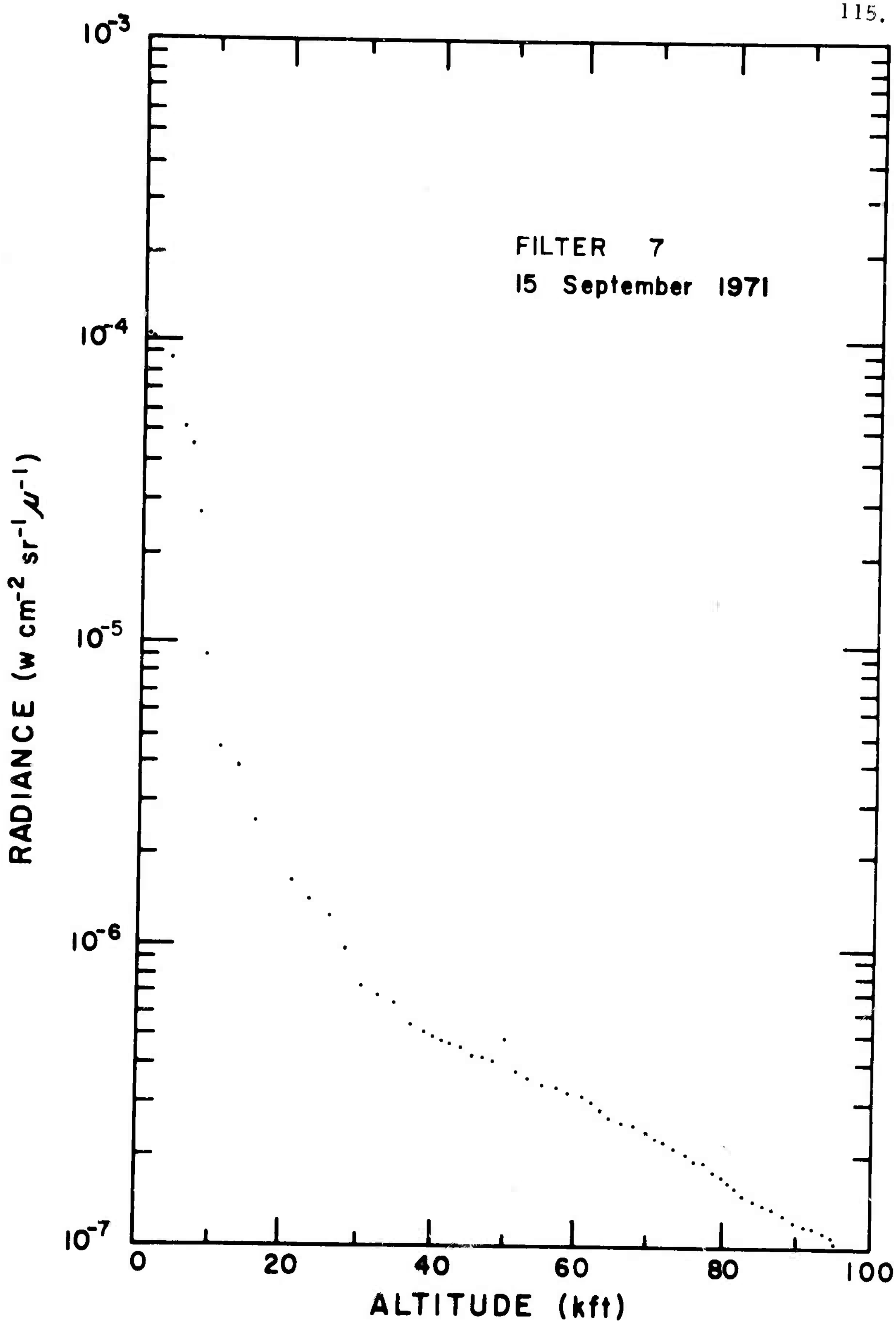

Figure 102. Radiance vs Altitude for Filter 7, 15 September 1971.

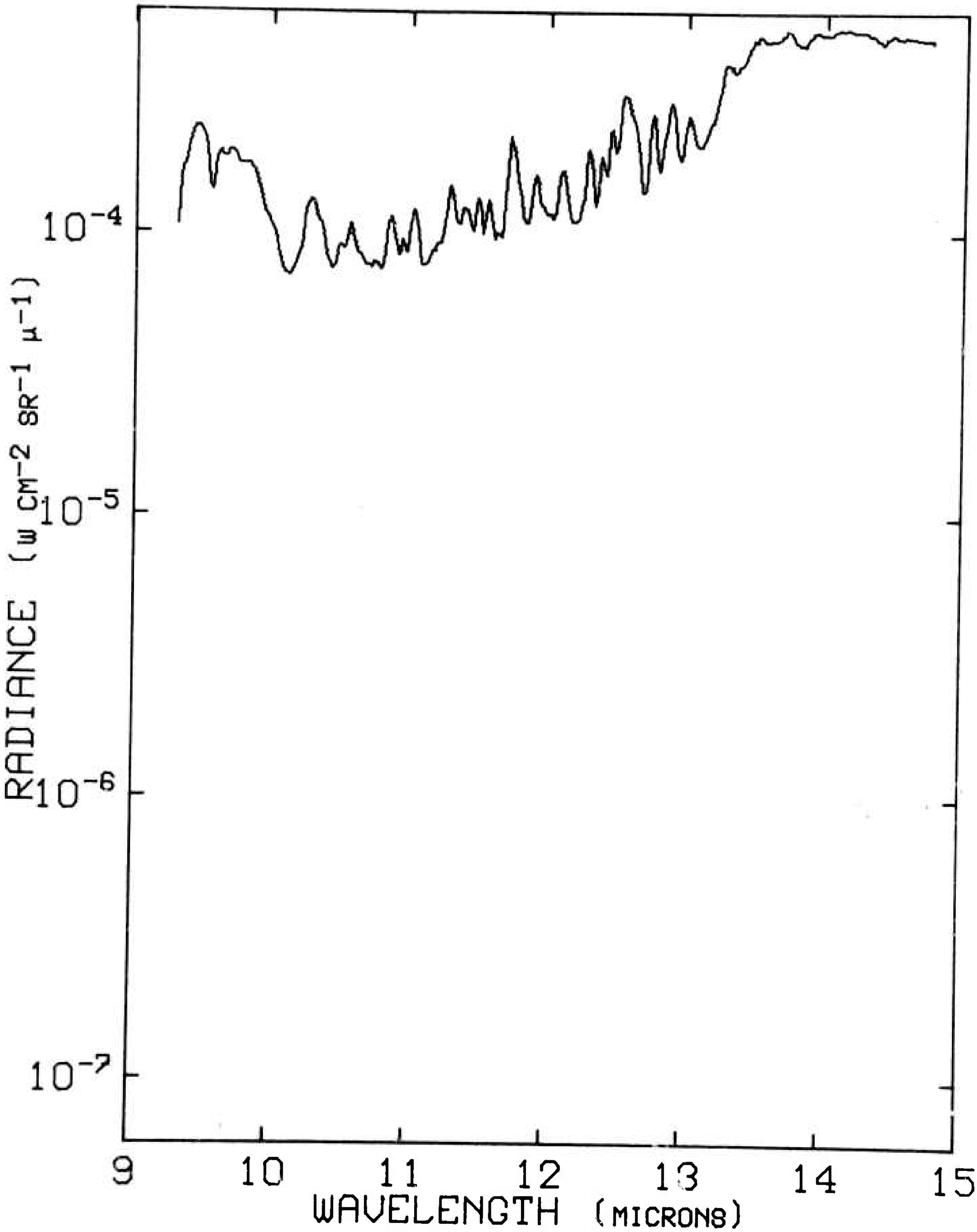

Figure 103. Radiance vs Wavelength at 0.4 kft and 0051 ADT, 15 September 1971.

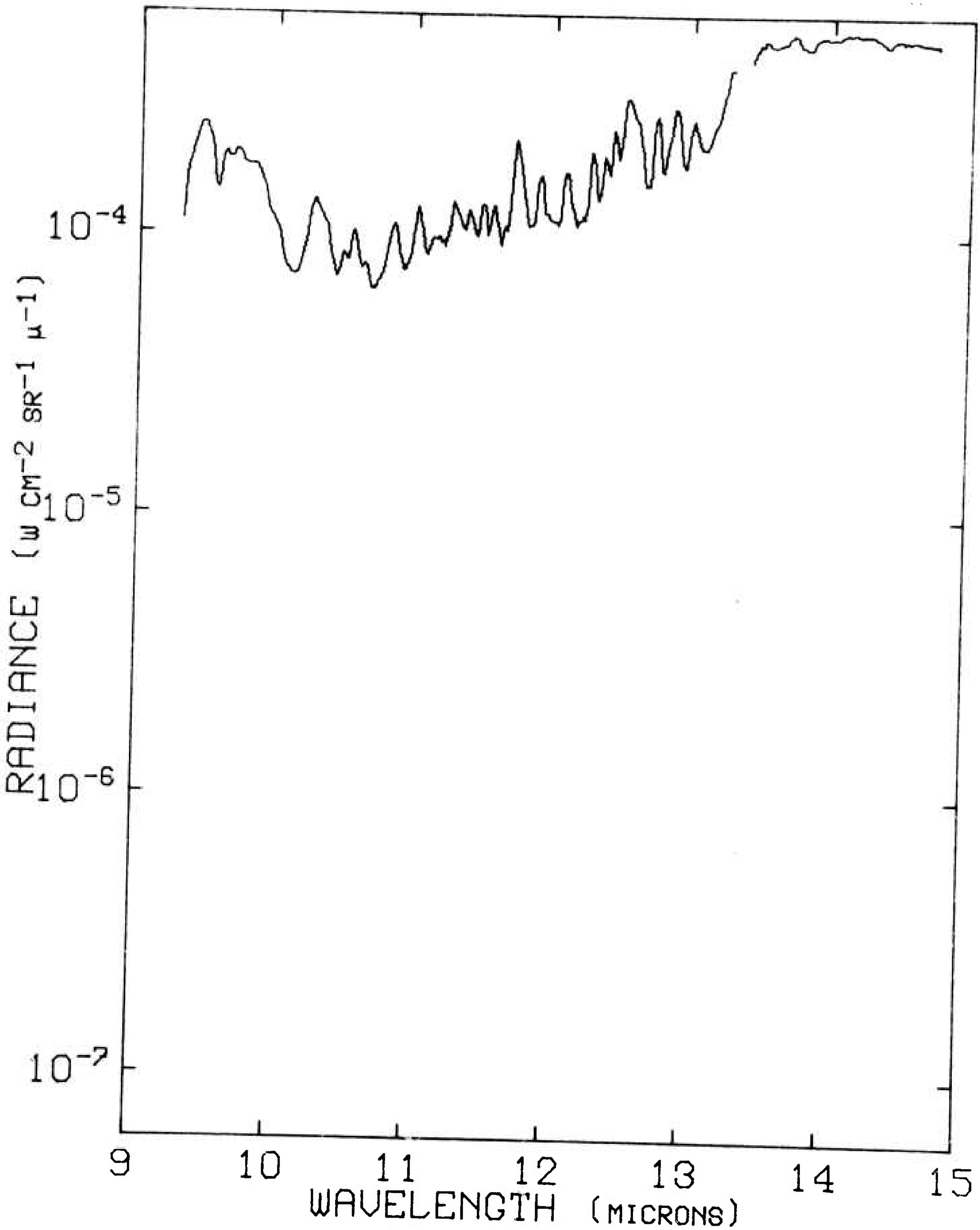

Figure 104. Radiance vs Wavelength at 0.4 kft and 0053 ADT, 15 September 1971.

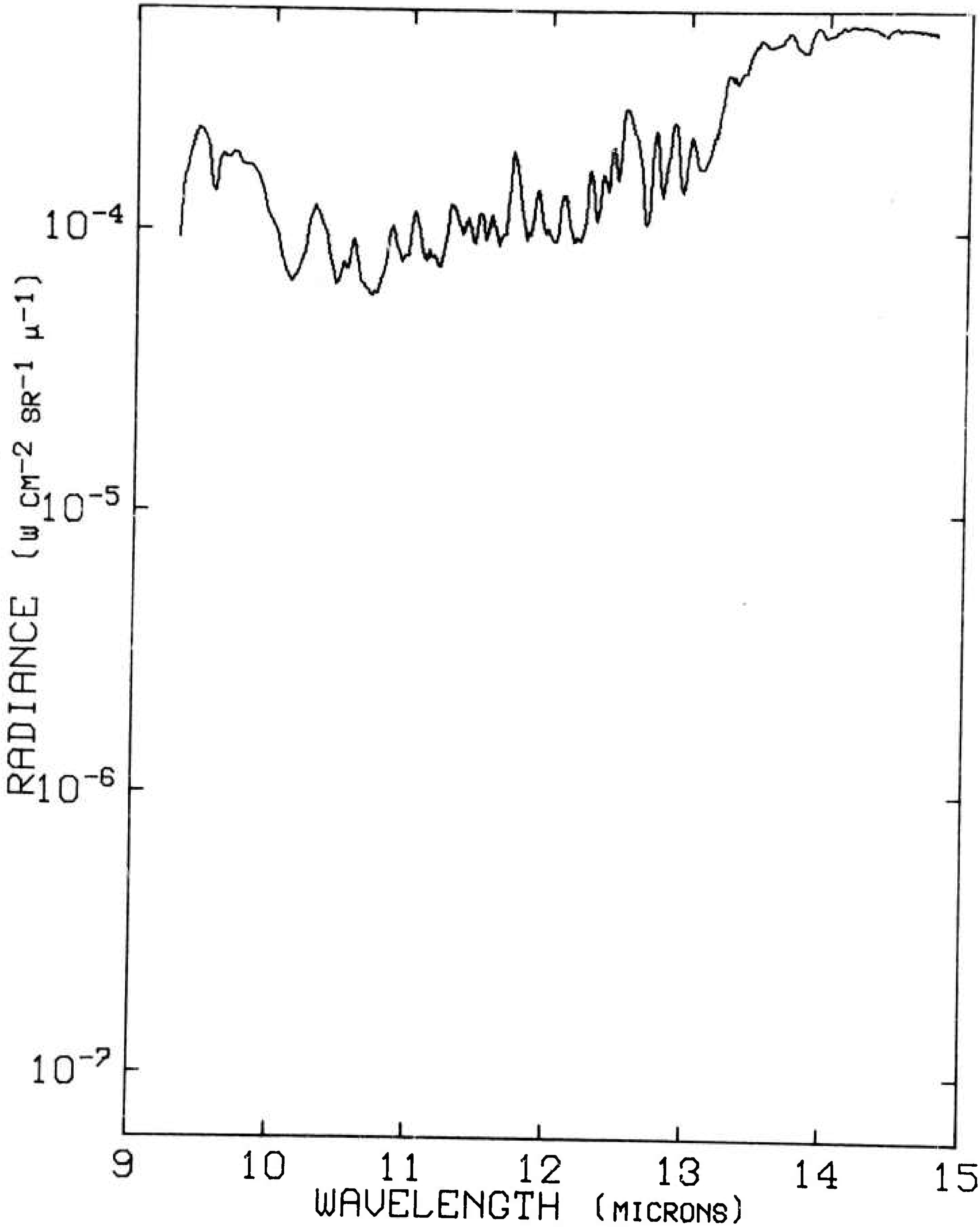

Figure 105. Radiance vs Wavelength at 1.2 kft and 0059 ADT, 15 September 1971.

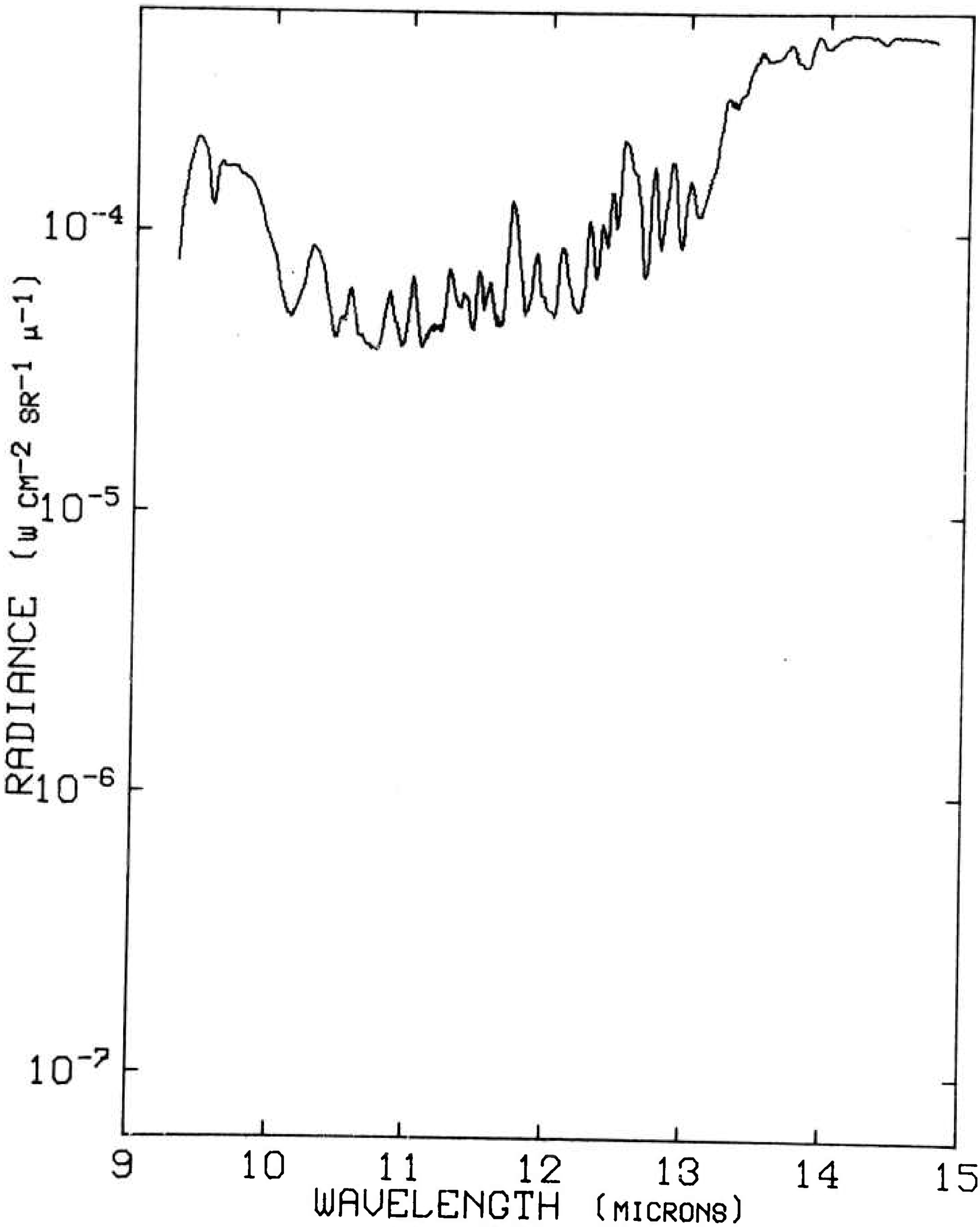

Figure 106. Radiance vs Wavelength at 3.4 kft and 0101 ADT, 15 September 1971.

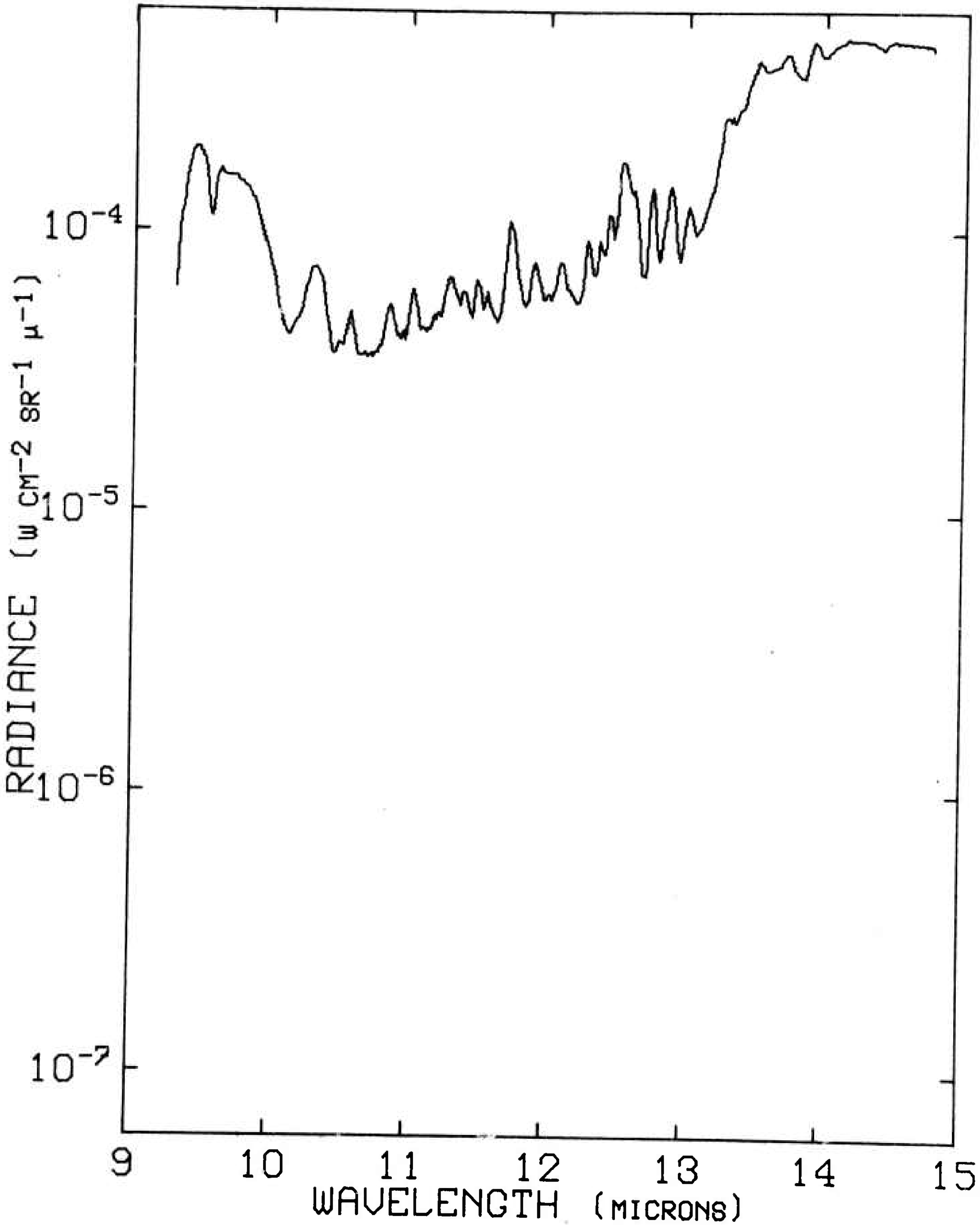

Figure 107. Radiance vs Wavelength at 5.6 kft and 0103 ADT, 15 September 1971.

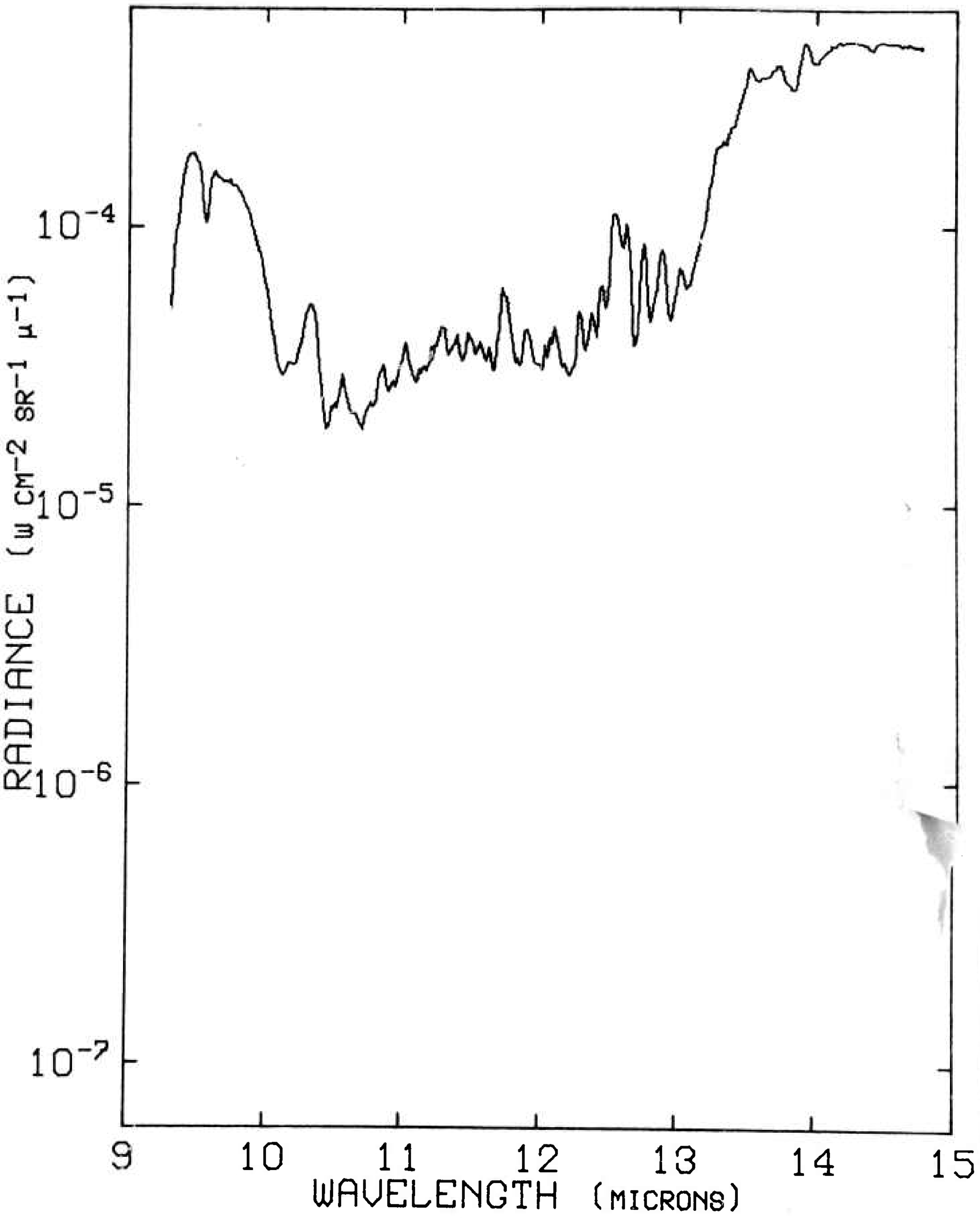

Figure 108. Radiance vs Wavelength at 7.7 kft and 0105 ADT, 15 September 1971.

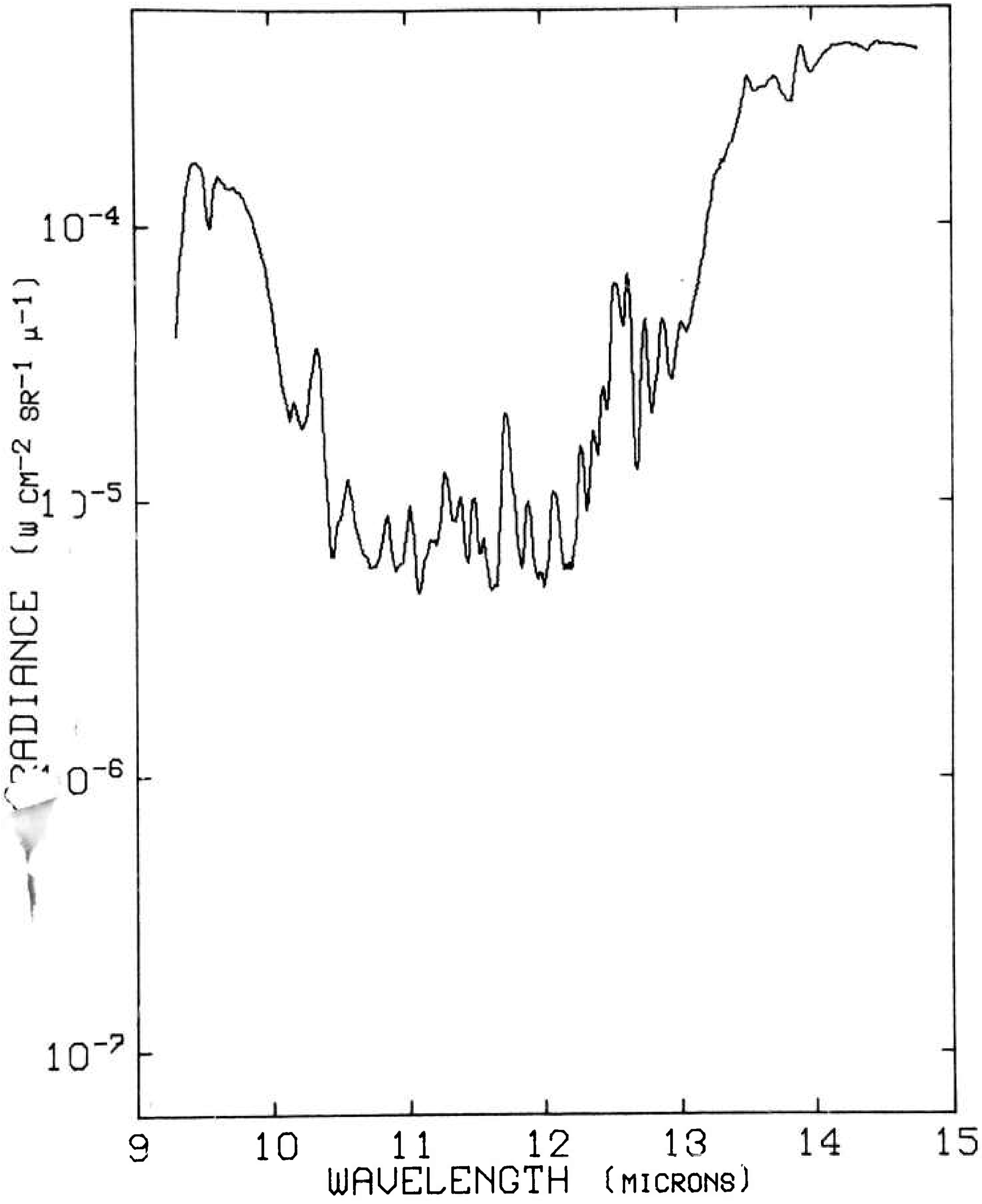

Figure 109. Radiance vs Wavelength at 9.0 kft and 0107 ADT, 15 September 1971.

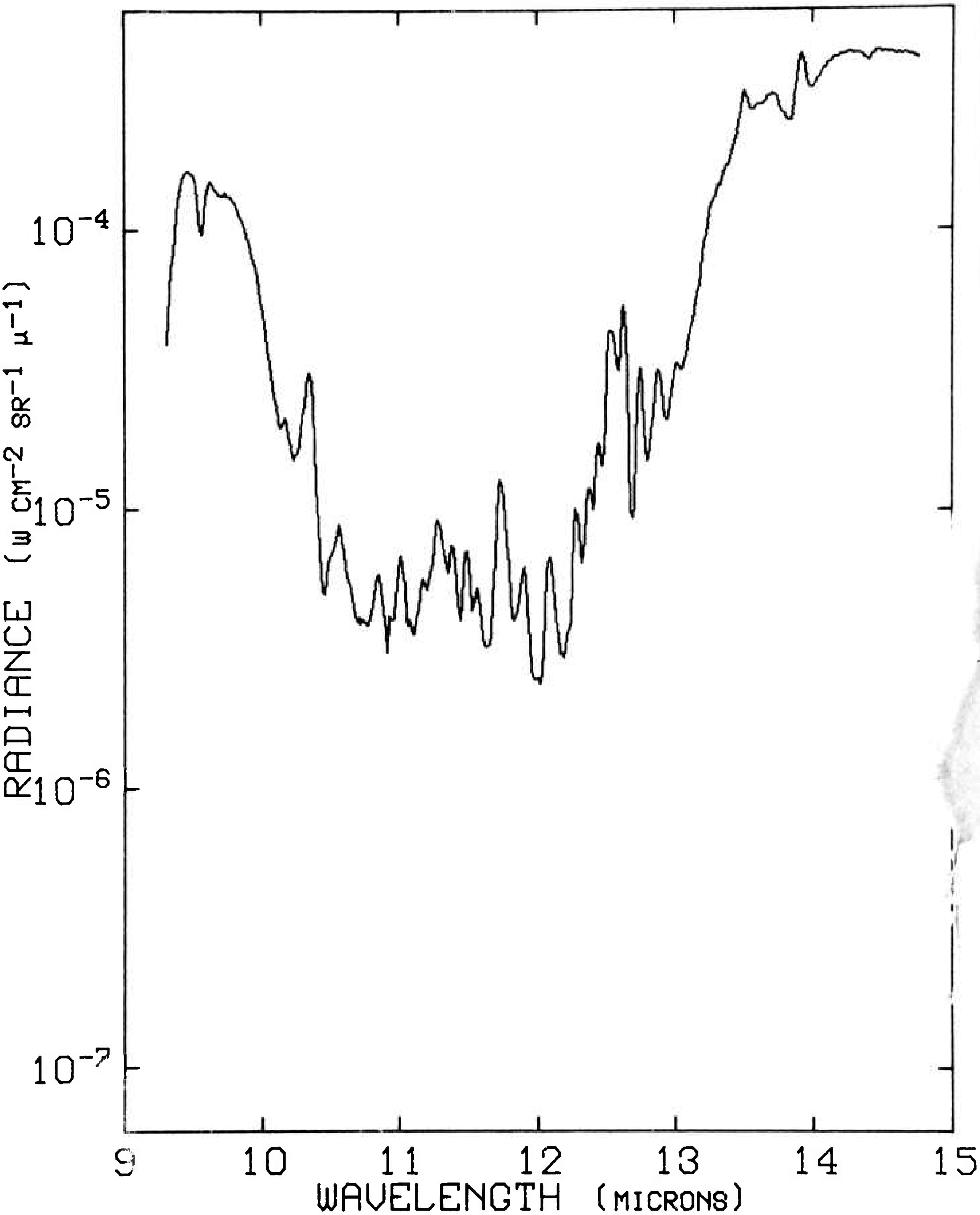

Figure 110. Radiance vs Wavelength at 11.2 kft and 0108 ADT, 15 September 1971.

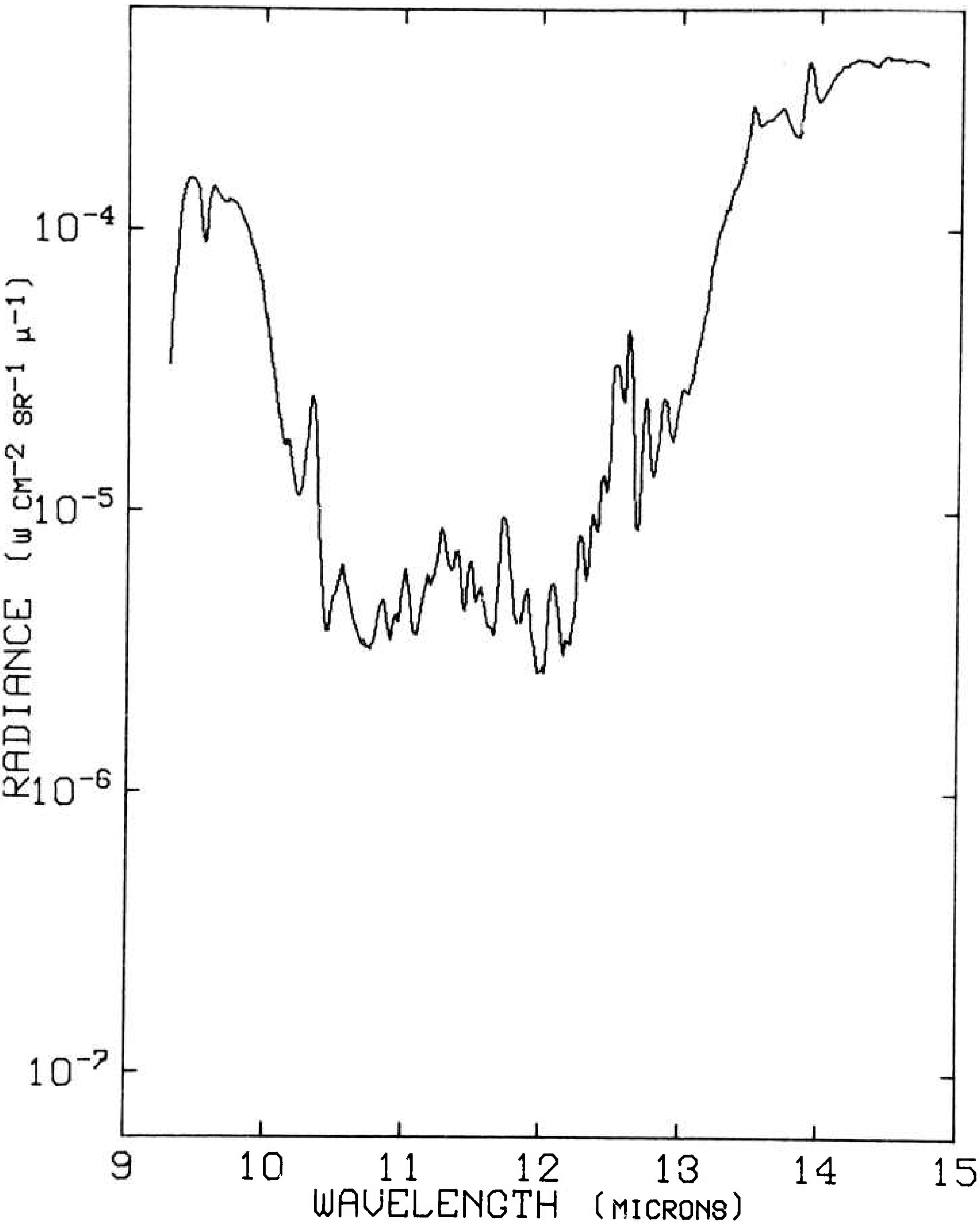

Figure 111. Radiance vs Wavelength at 13.6 kft and 0110 ADT, 15 September 1971.

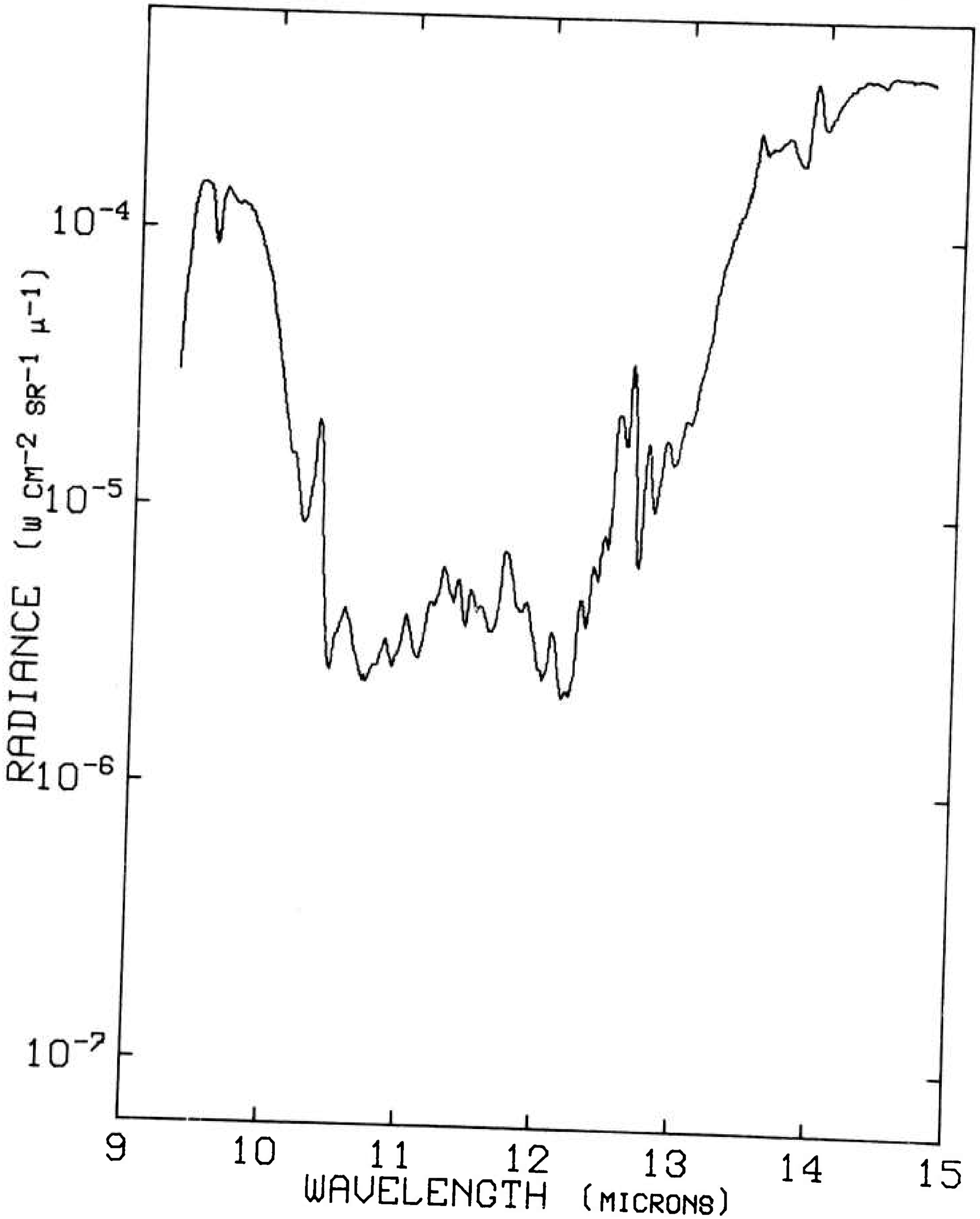

Figure 112. Radiance vs Wavelength at 16.0 kft and 0112 ADT, 15 September 1971.

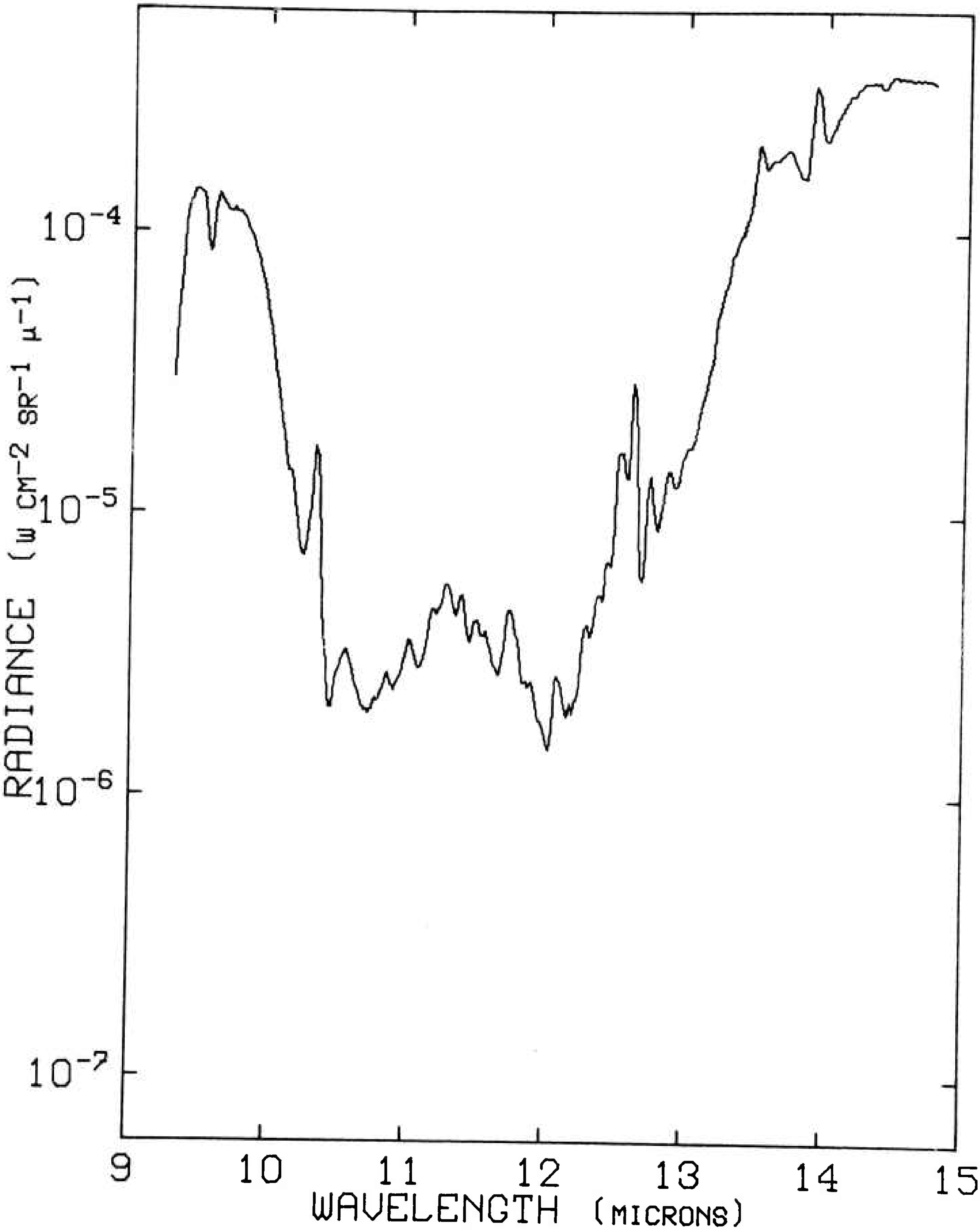

Figure 113. Radiance vs Wavelength at 18.5 kft and 0114 ADT, 15 September 1971.

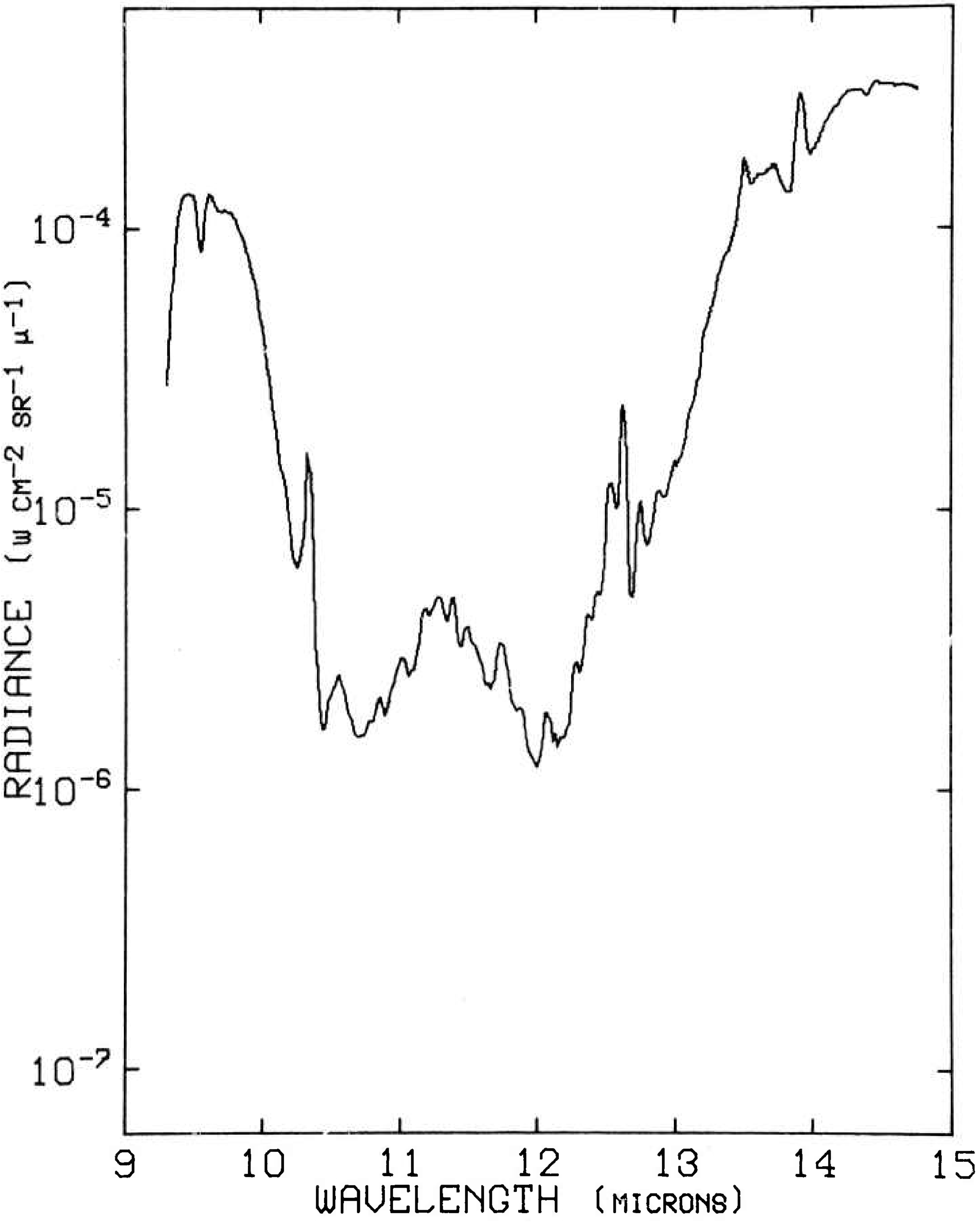

Figure 114. Radiance vs Wavelength at 21.1 kft and 0116 ADT, 15 September 1971.

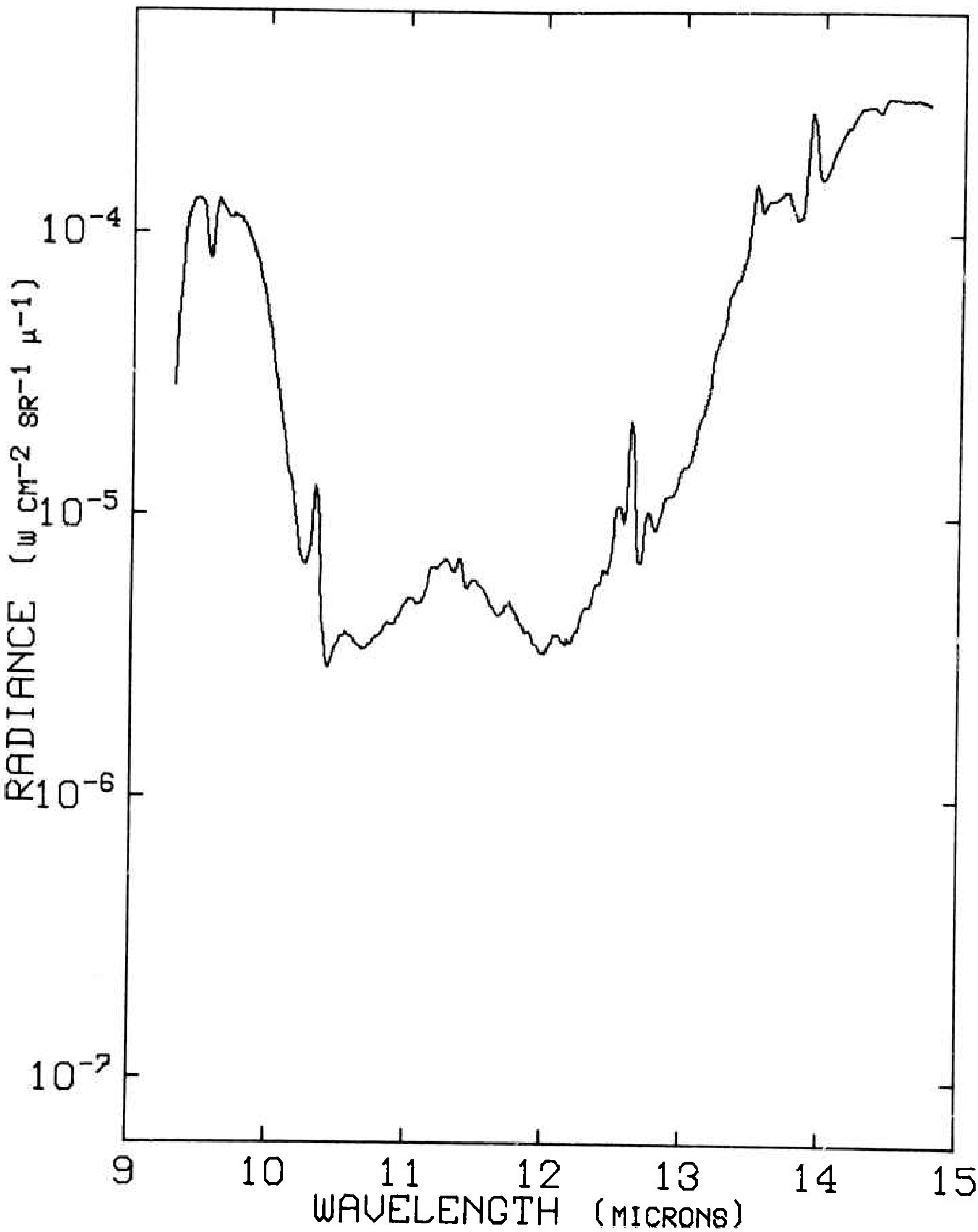

Figure 115. Radiance vs Wavelength at 23.7 kft and 0118 ADT, 15 September 1971.

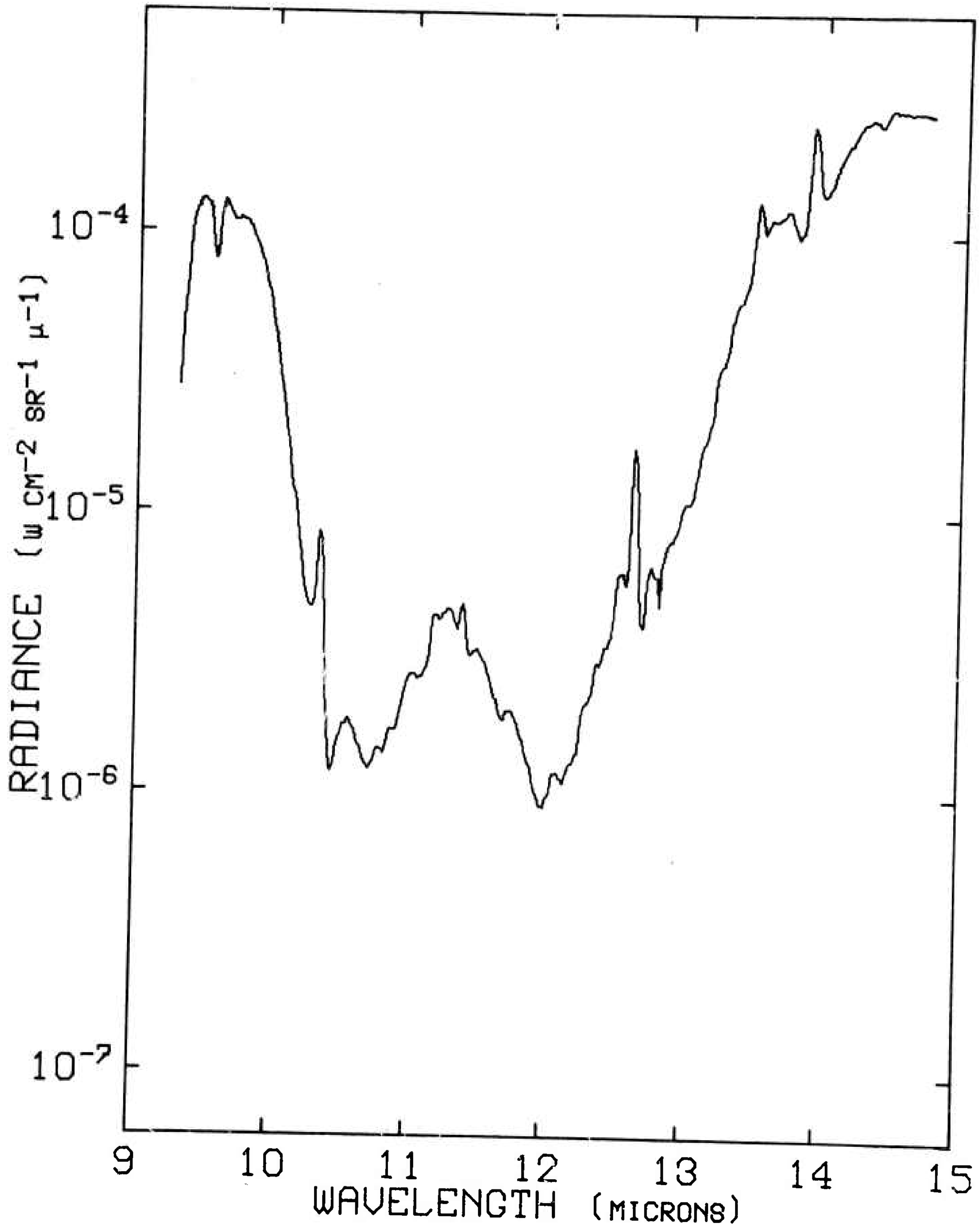

Figure 116. Radiance vs Wavelength at 26.2 kft and 0120 ADT, 15 September 1971.

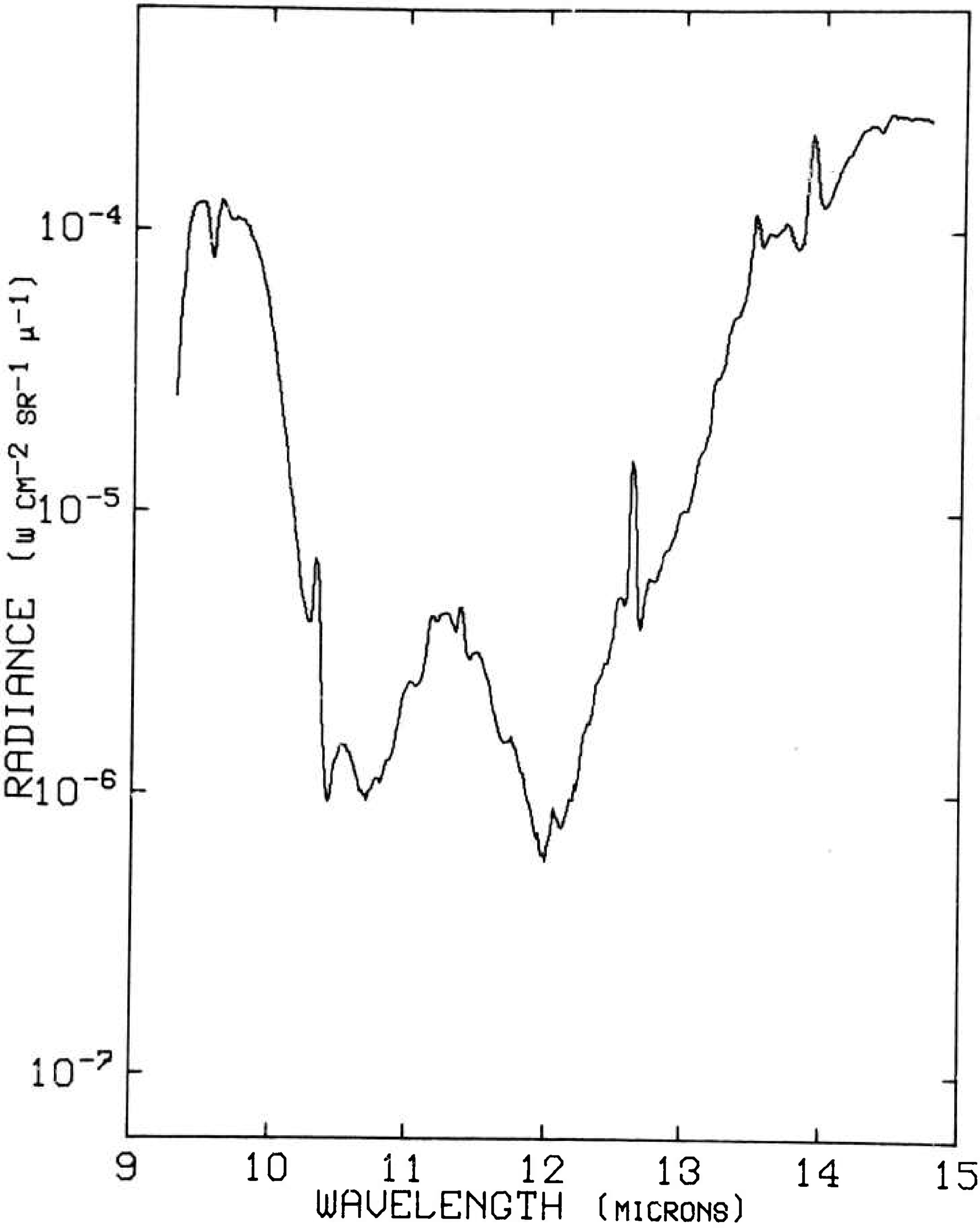

Figure 117. Radiance vs Wavelength at 28.4 kft and 0122 ADT, 15 September 1971.

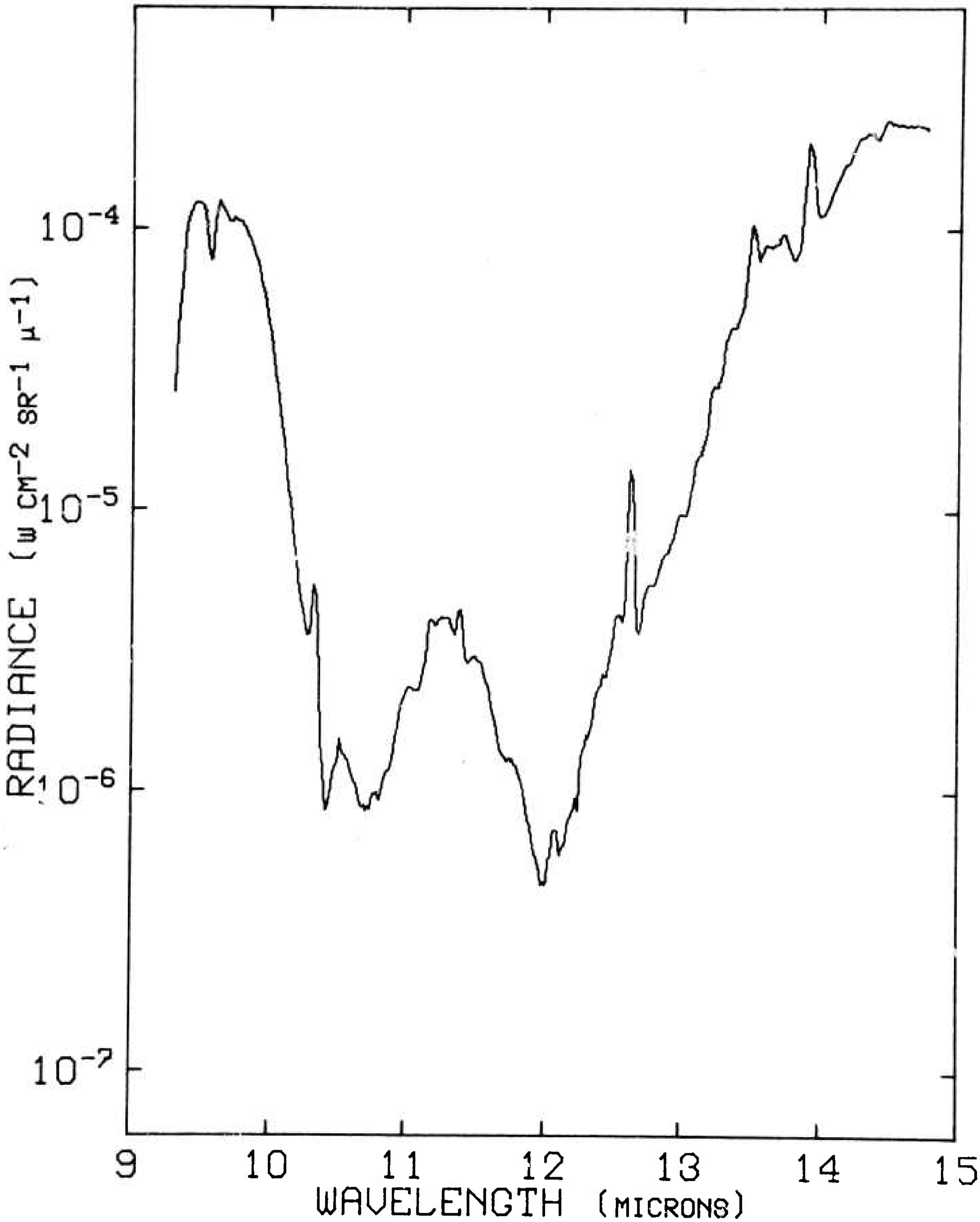

Figure 118. Radiance vs Wavelength at 30.6 kft and 0124 ADT, 15 September 1971.

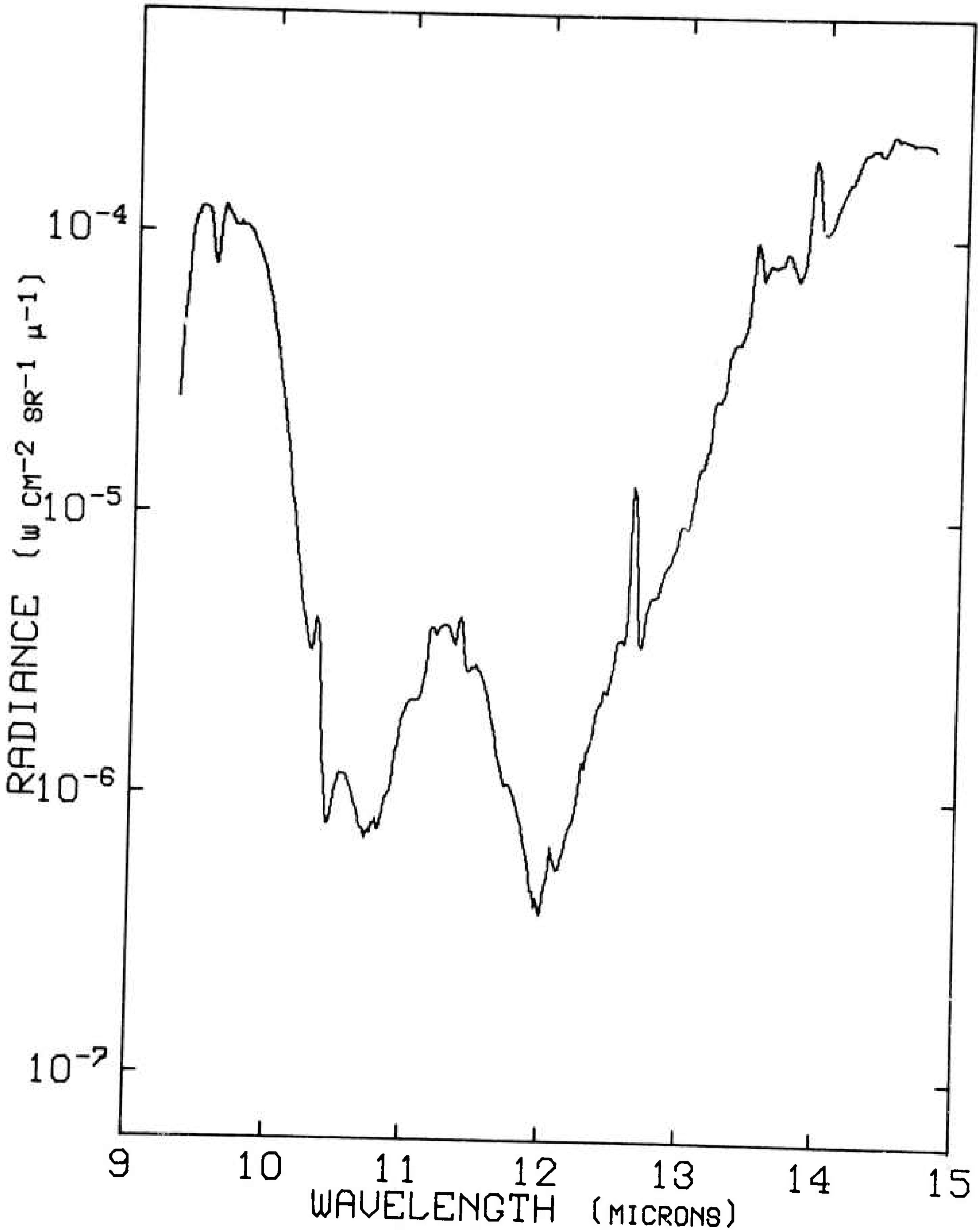

Figure 119. Radiance vs Wavelength at 32.9 kft and 0126 ADT, 15 September 1971.

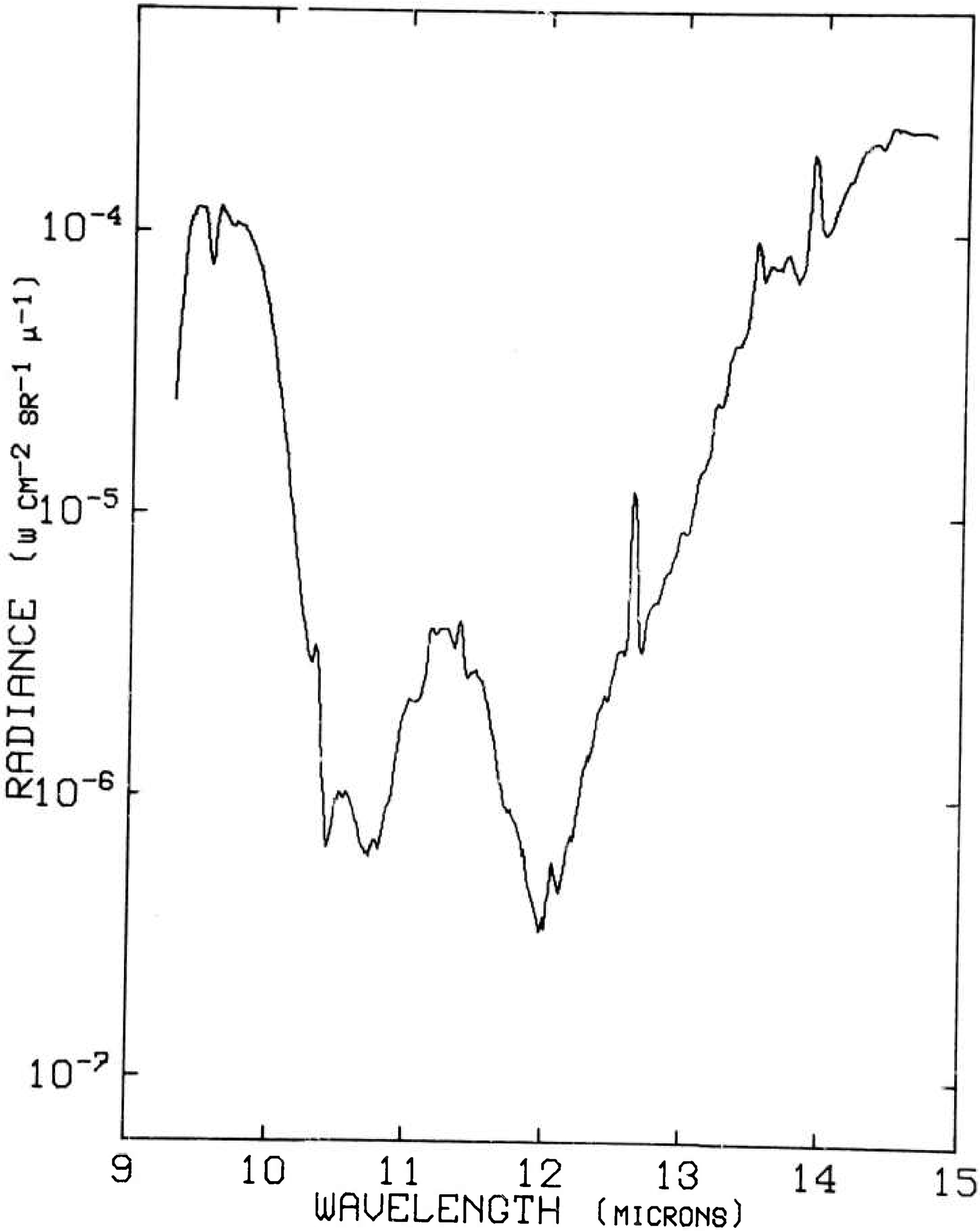

Figure 120. Radiance vs Wavelength at 35.1 kft and 0128 ADT, 15 September 1971.

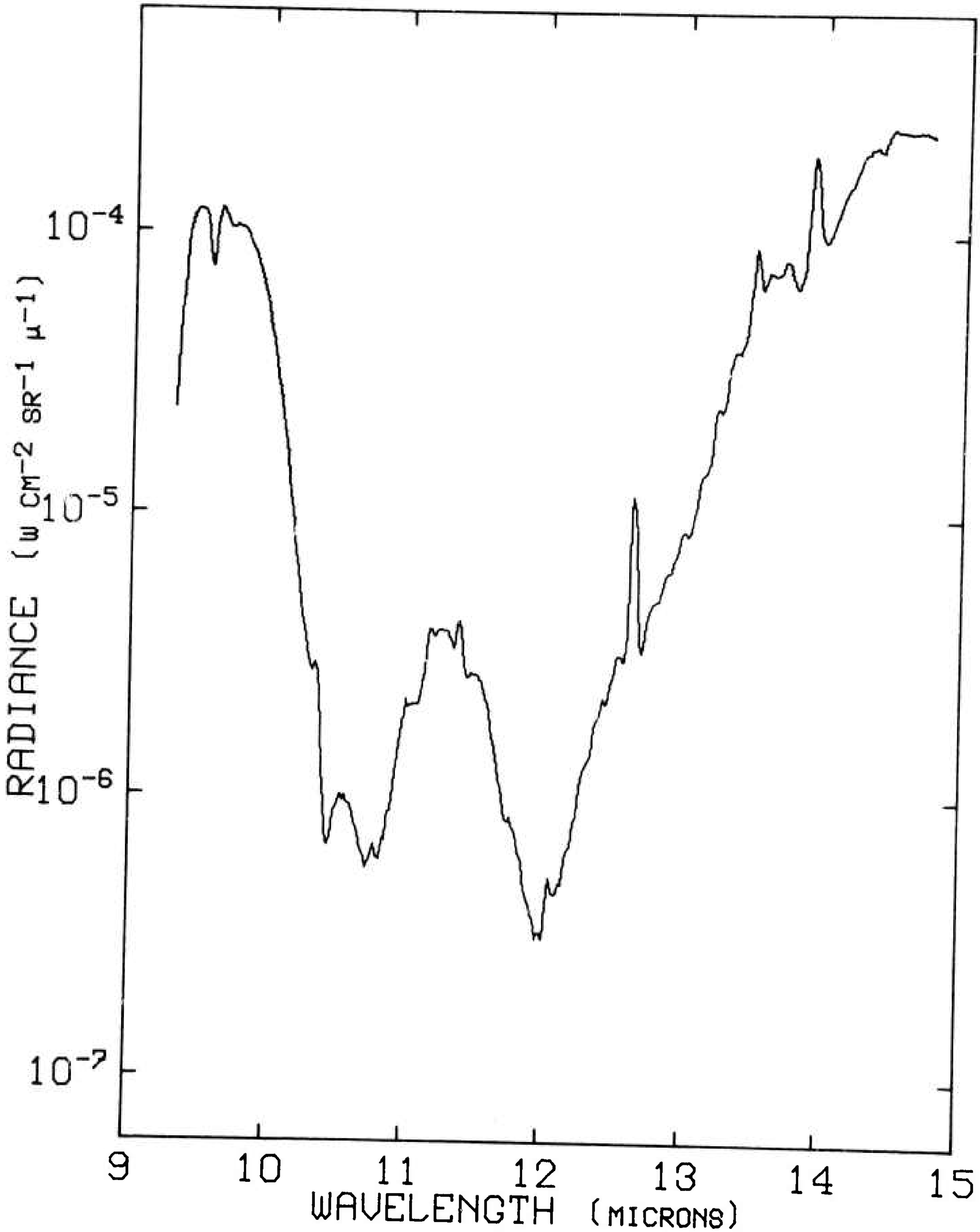

Figure 121. Radiance vs Wavelength at 37.3 kft and 0130 ADT, 15 September 1971.

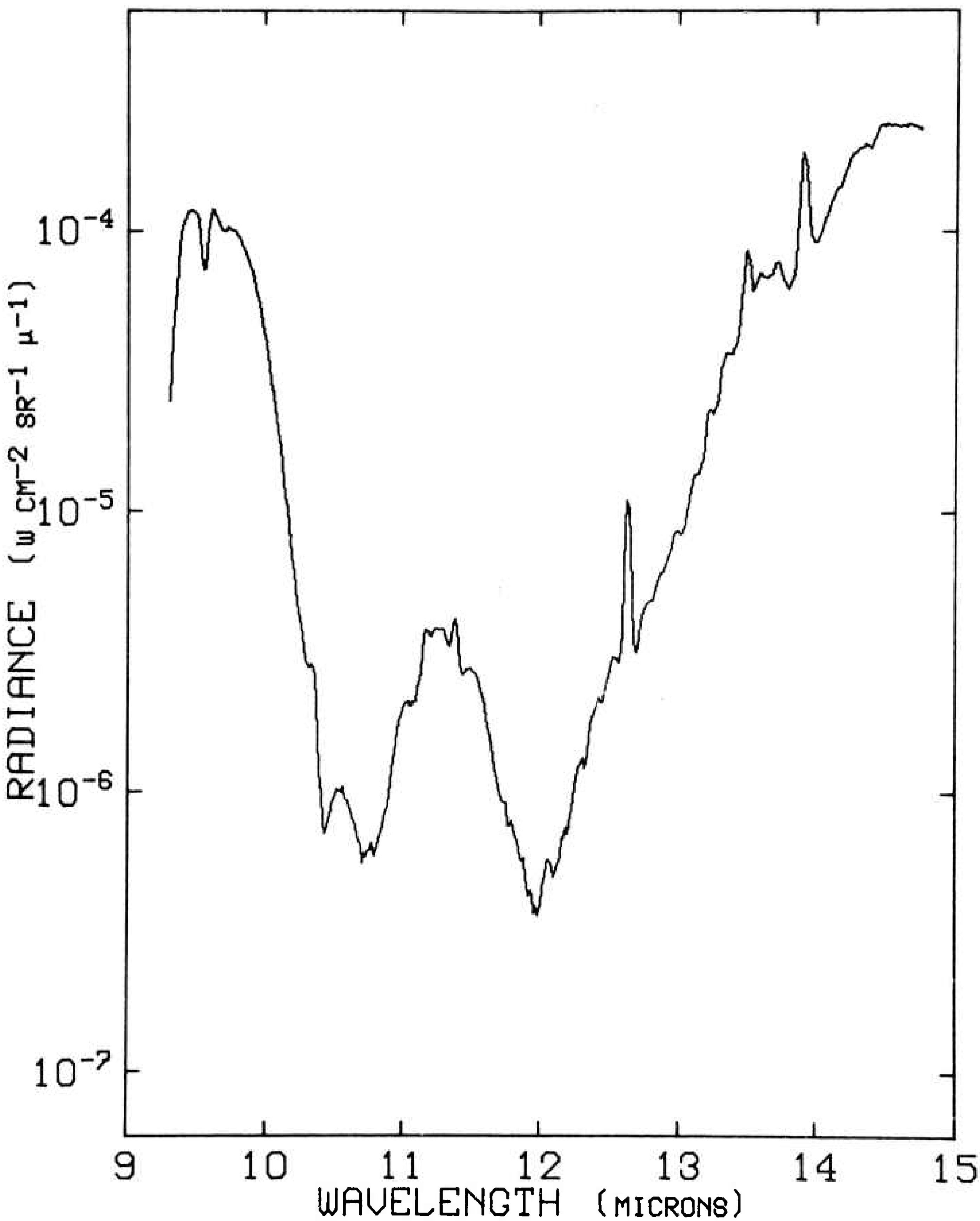

Figure 122. Radiance vs Wavelength at 39.3 kft and 0132 ADT, 15 September 1971.

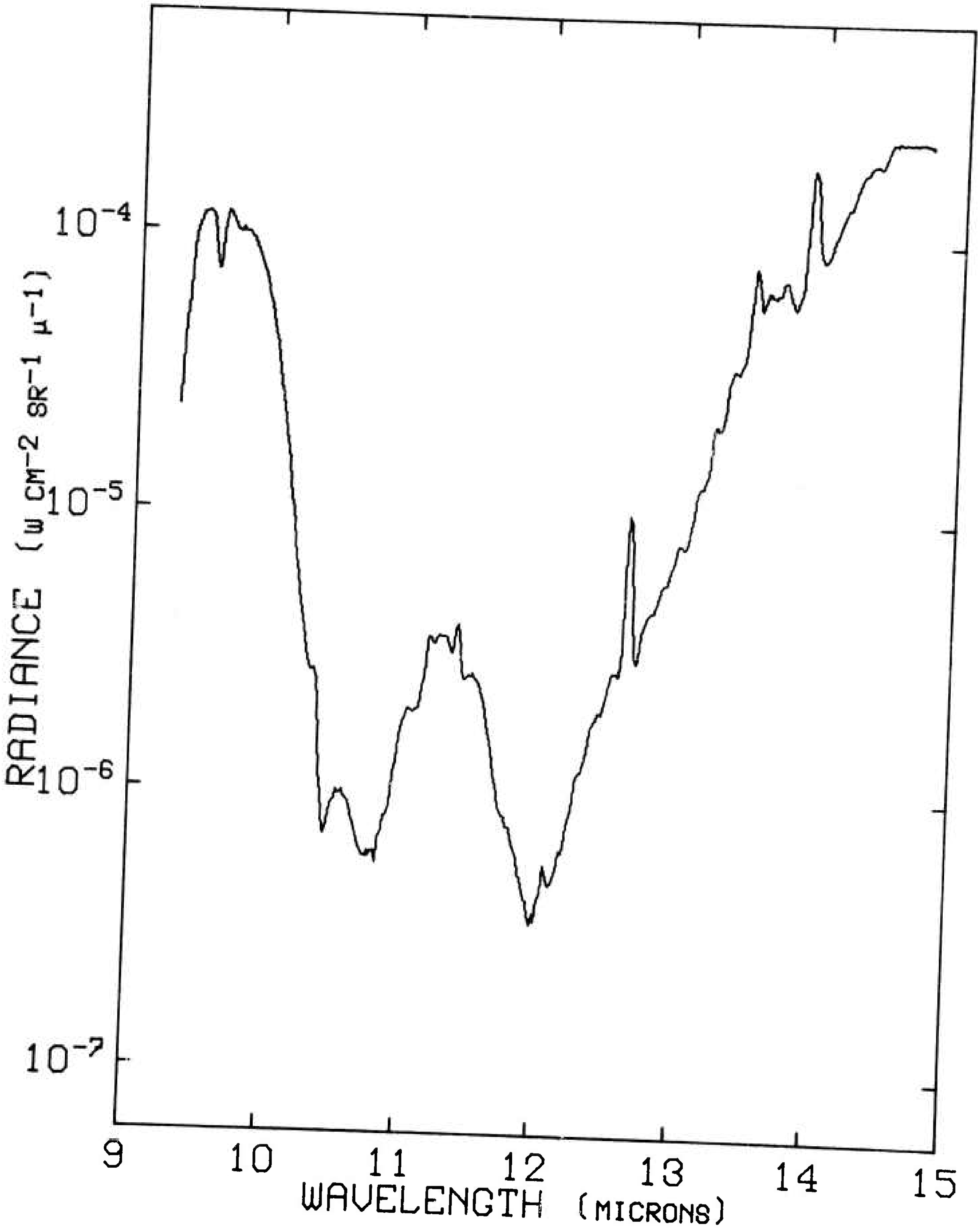

Figure 123. Radiance vs Wavelength at 40.9 kft and 0134 ADT, 15 September 1971.

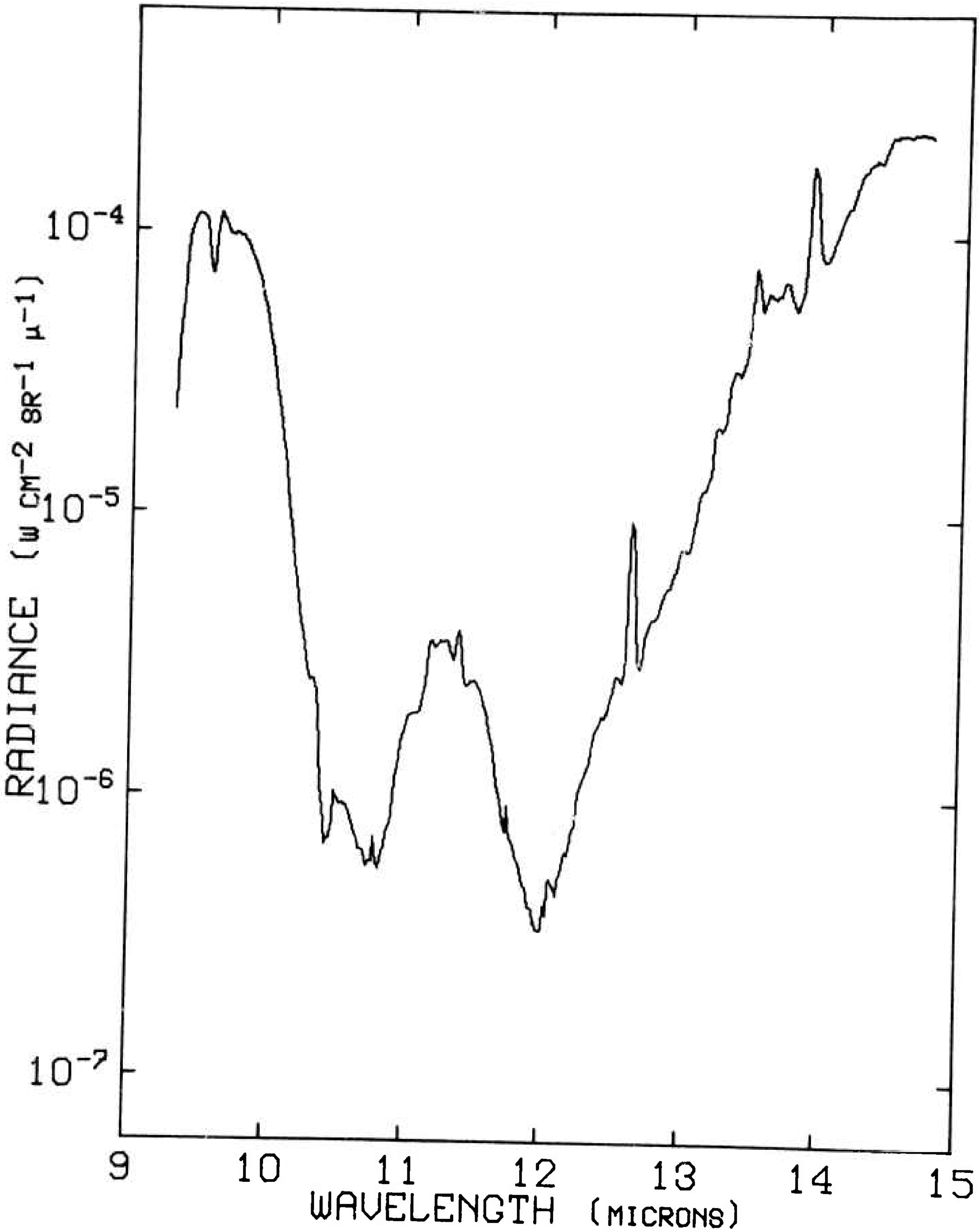

Figure 124. Radiance vs Wavelength at 42.5 kft and 0135 ADT, 15 September 1971.

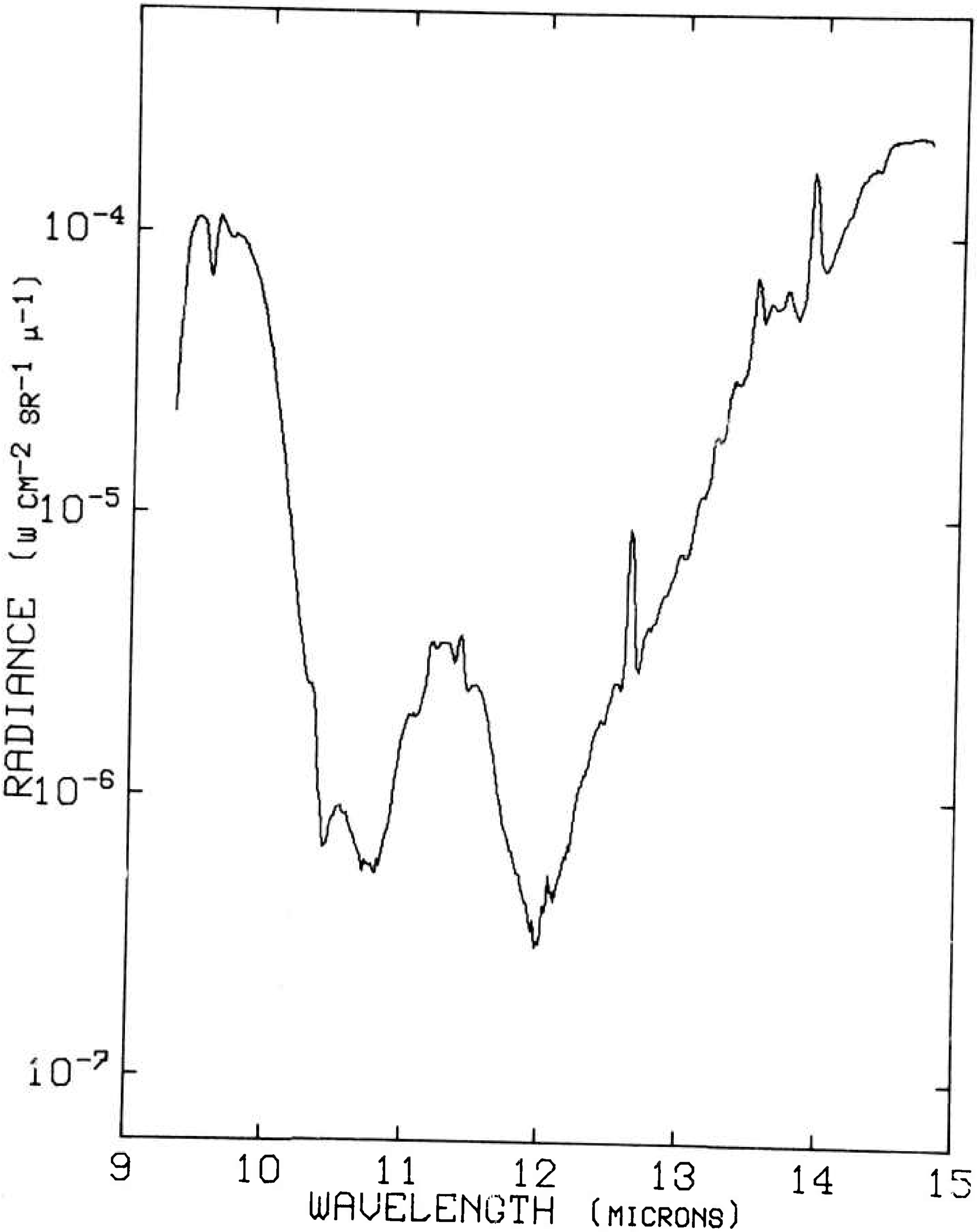

Figure 125. Radiance vs Wavelength at 44.0 kft and 0137 ADT, 15 September 1971.

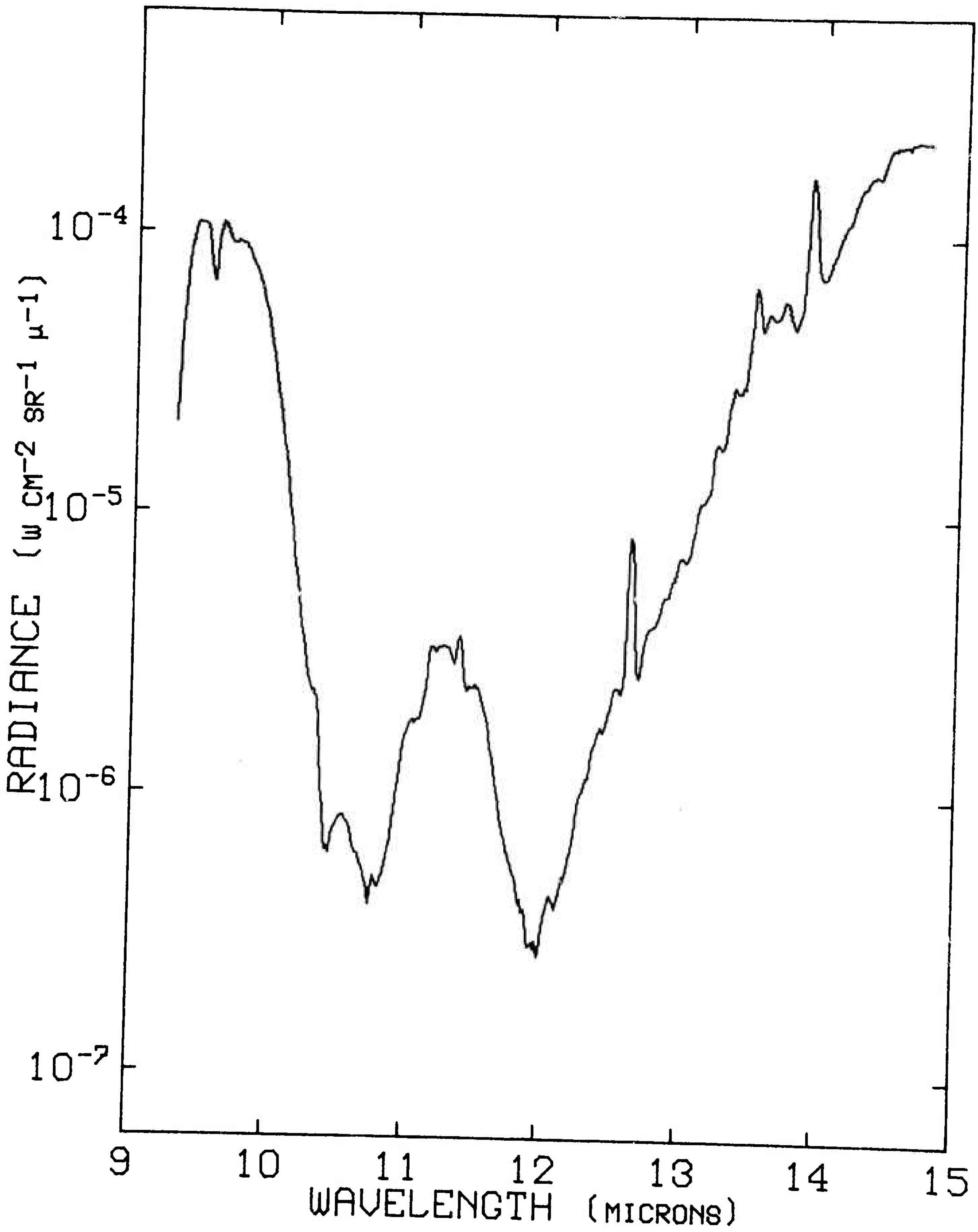

Figure 126. Radiance vs Wavelength at 45.4 kft and 0139 ADT, 15 September 1971.

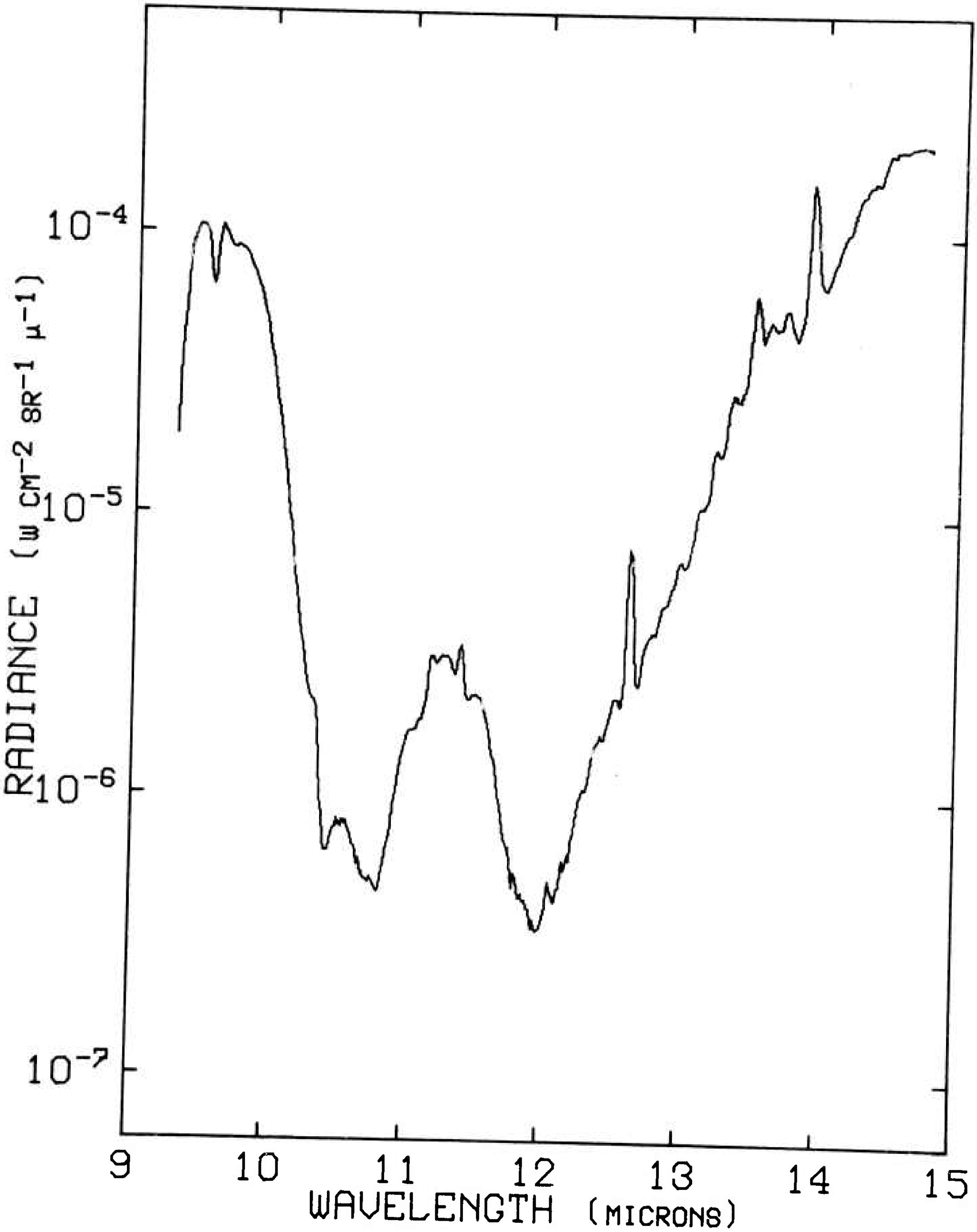

Figure 127. Radiance vs Wavelength at 46.9 kft and 0141 ADT, 15 September 1971.

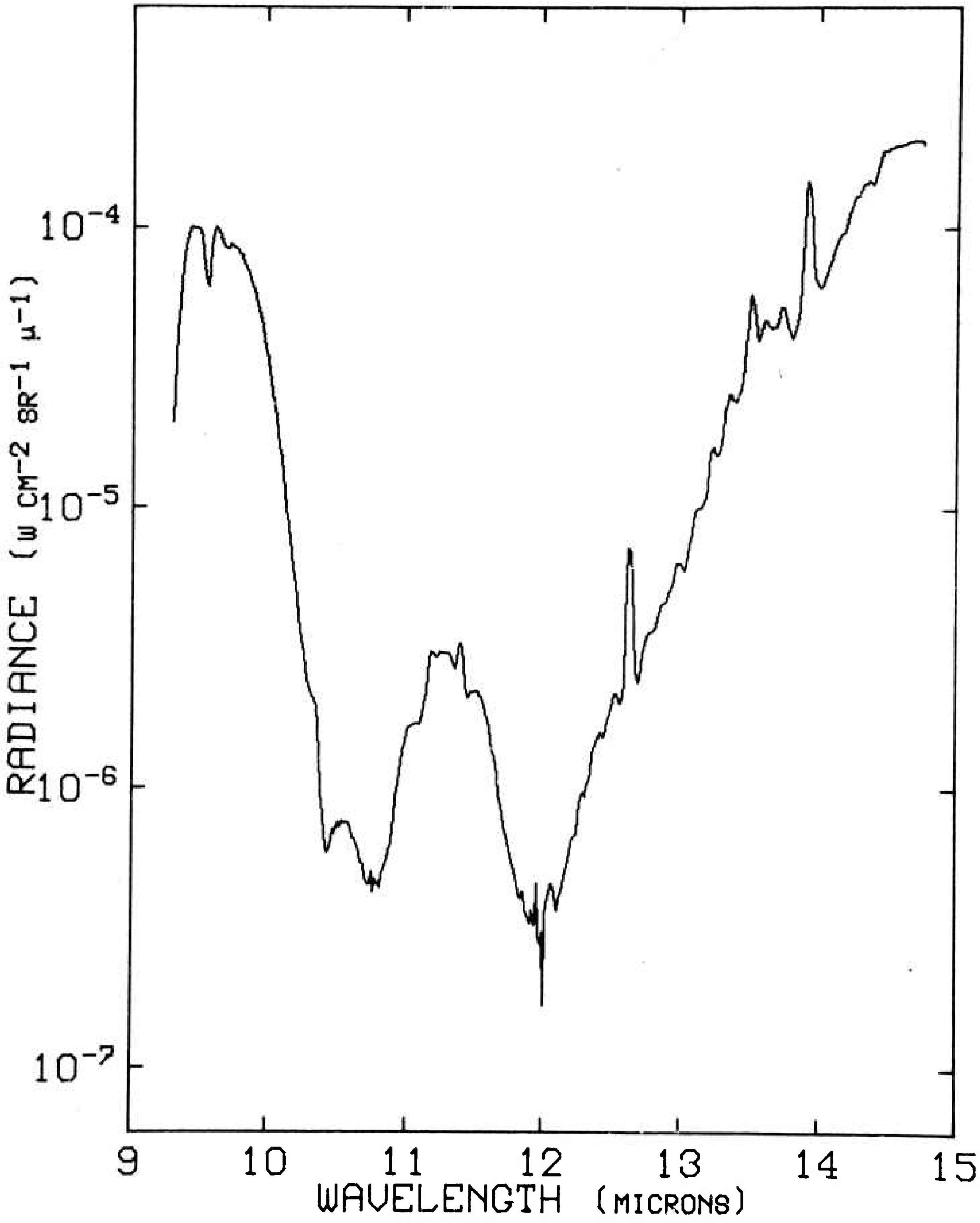

Figure 128. Radiance vs Wavelength at 48.3 kft and 0143 ADT, 15 September 1971.

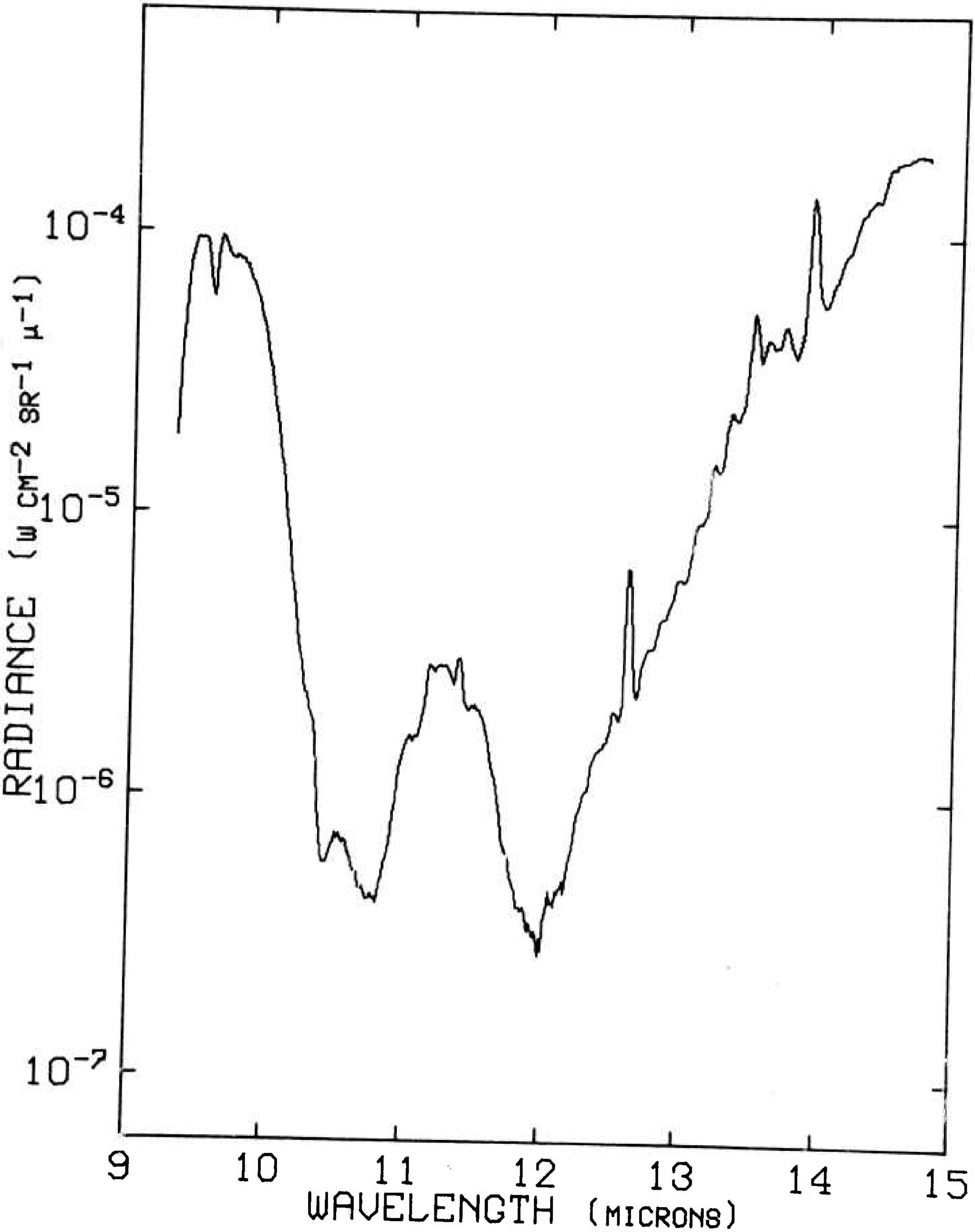

Figure 129. Radiance vs Wavelength at 49.8 kft and 0145 ADT, 15 September 1971.

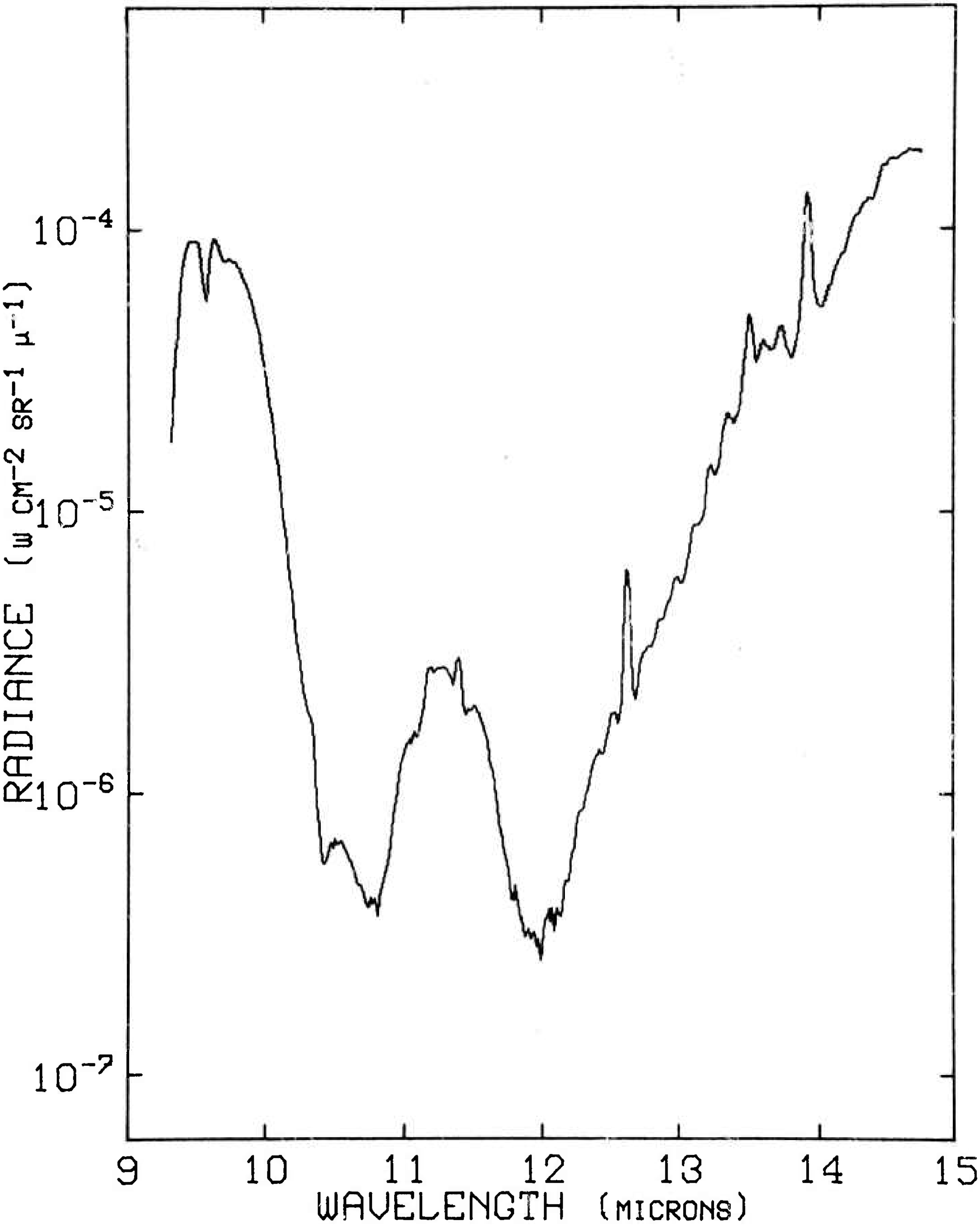

Figure 130. Radiance vs Wavelength at 51.5 kft and 0147 ADT, 15 September 1971.

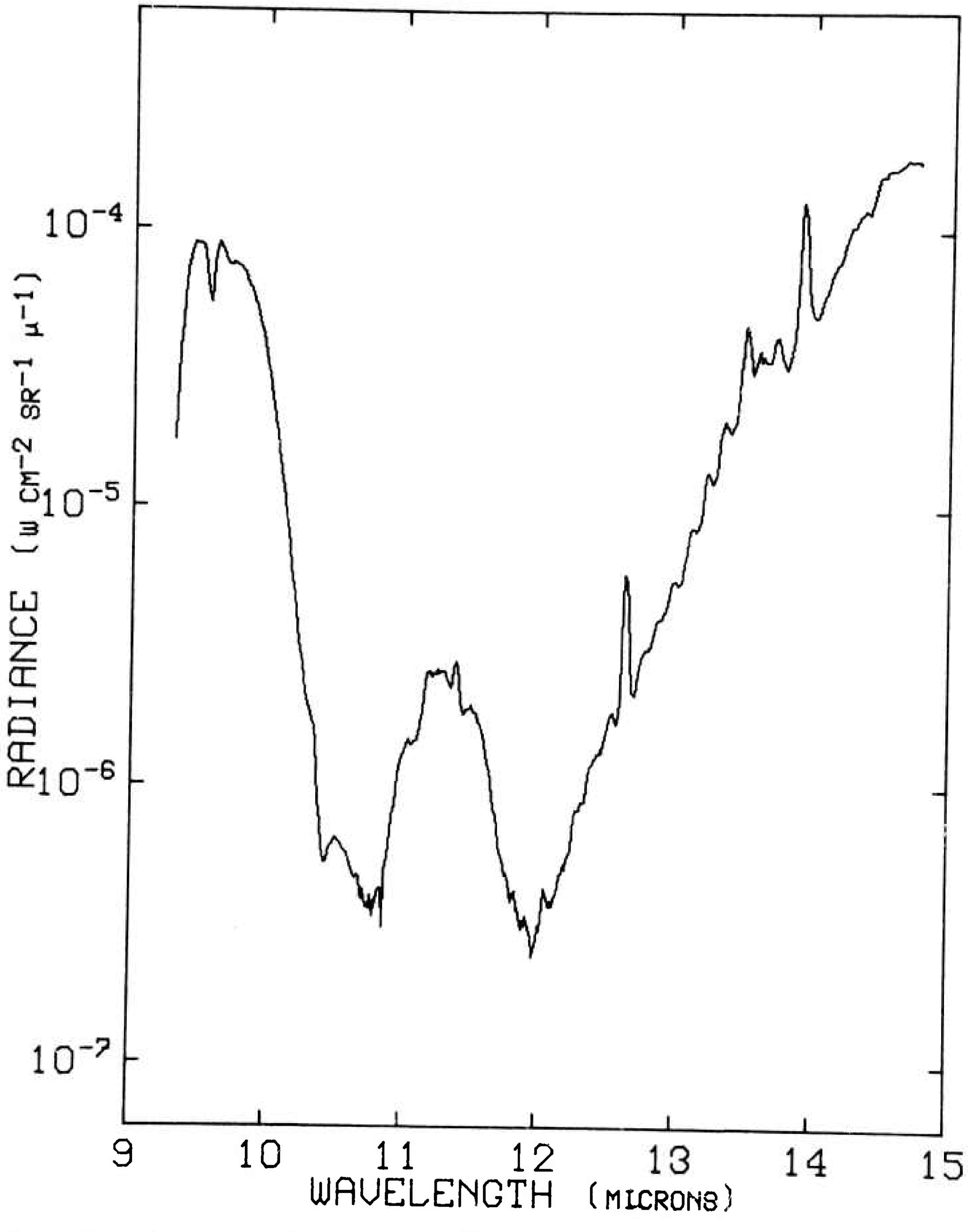

Figure 131. Radiance vs Wavelength at 53.4 kft and 0149 ADT, 15 September 1971.

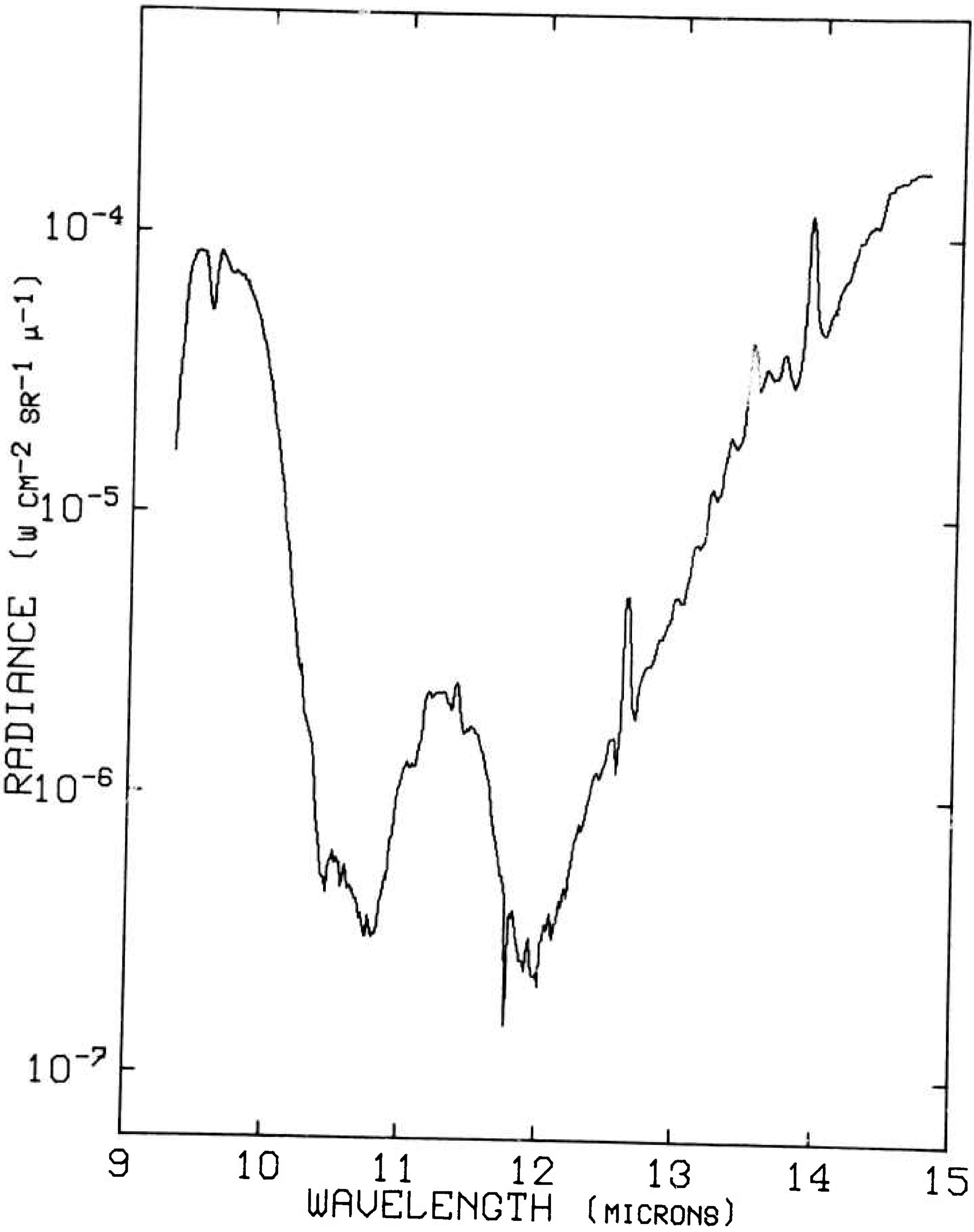

Figure 132. Radiance vs Wavelength at 55.3 kft and 0151 ADT, 15 September 1971.

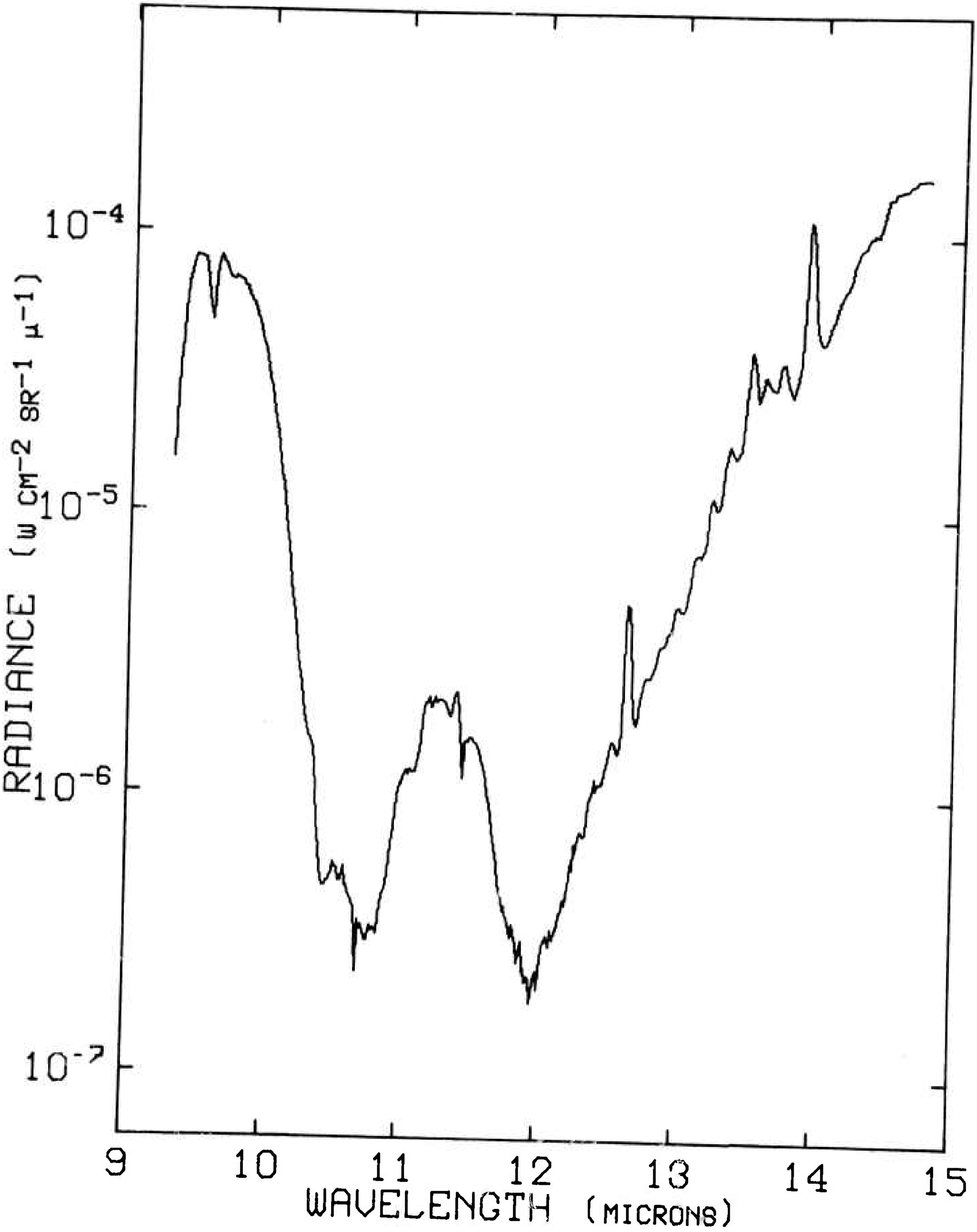

Figure 133. Radiance vs Wavelength at 57.2 kft and 0153 ADT, 15 September 1971.

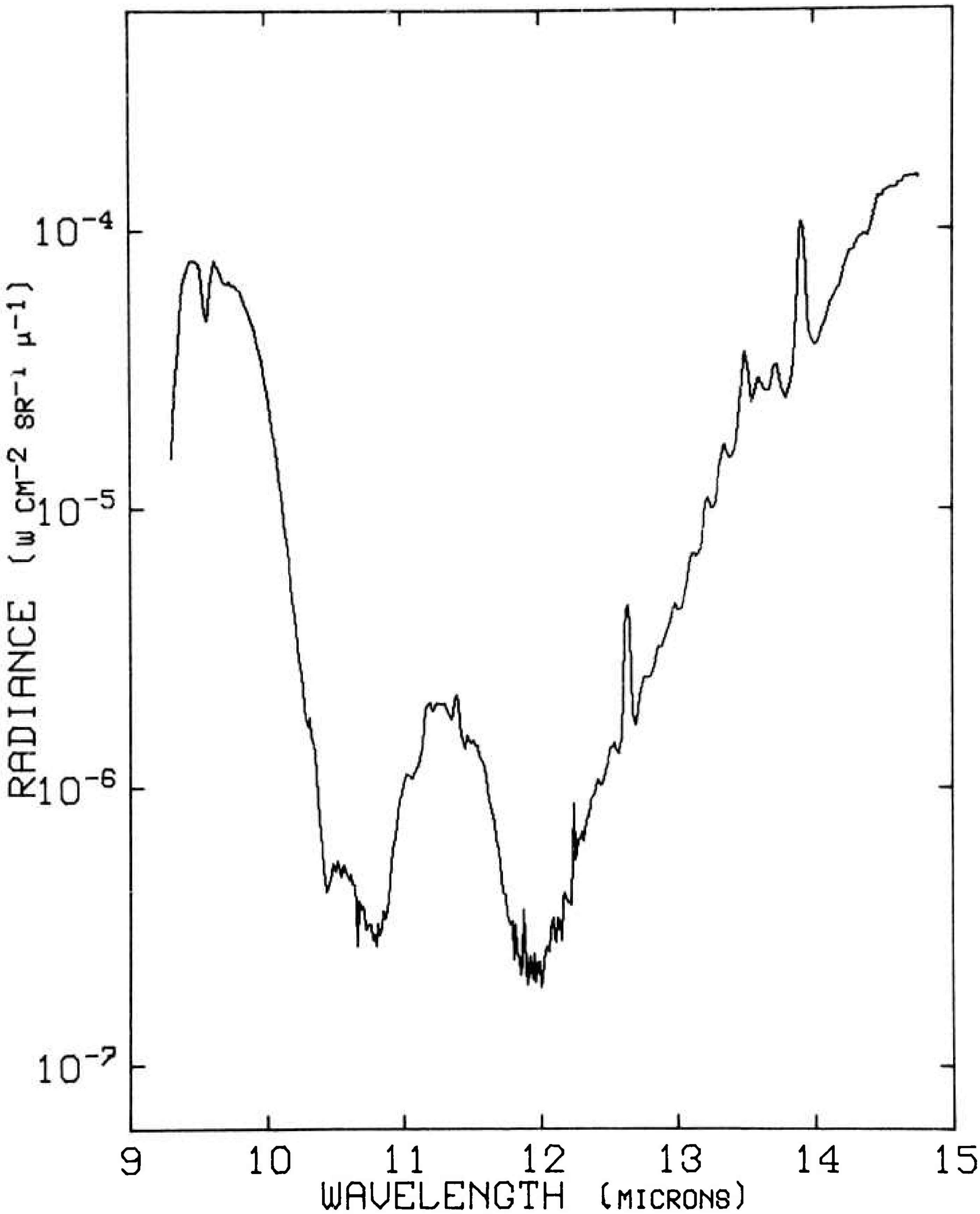

Figure 134. Radiance vs Wavelength at 58.8 kft and 0155 ADT, 15 September 1971.

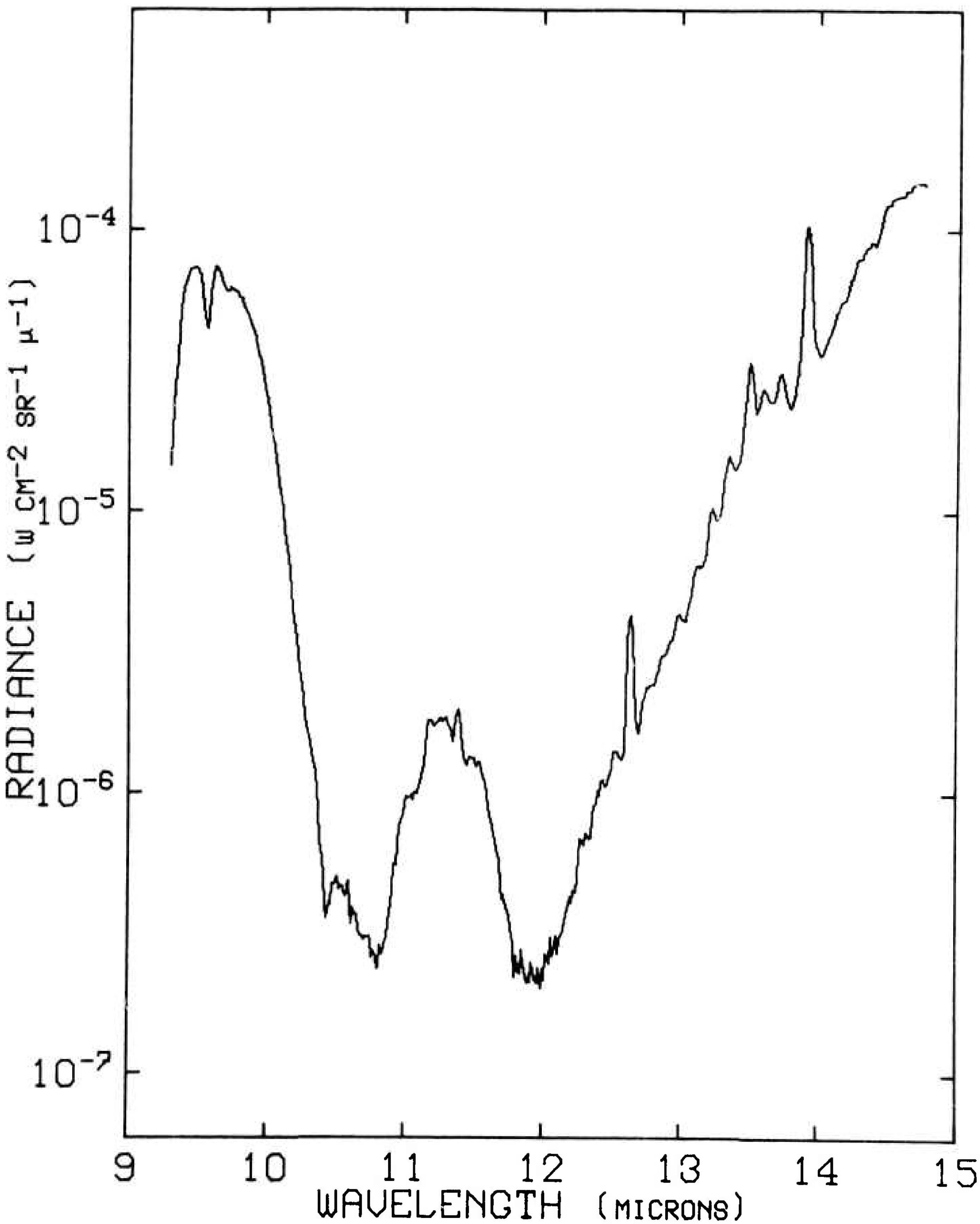

Figure 135. Radiance vs Wavelength at 60.8 kft and 0157 ADT, 15 September 1971.

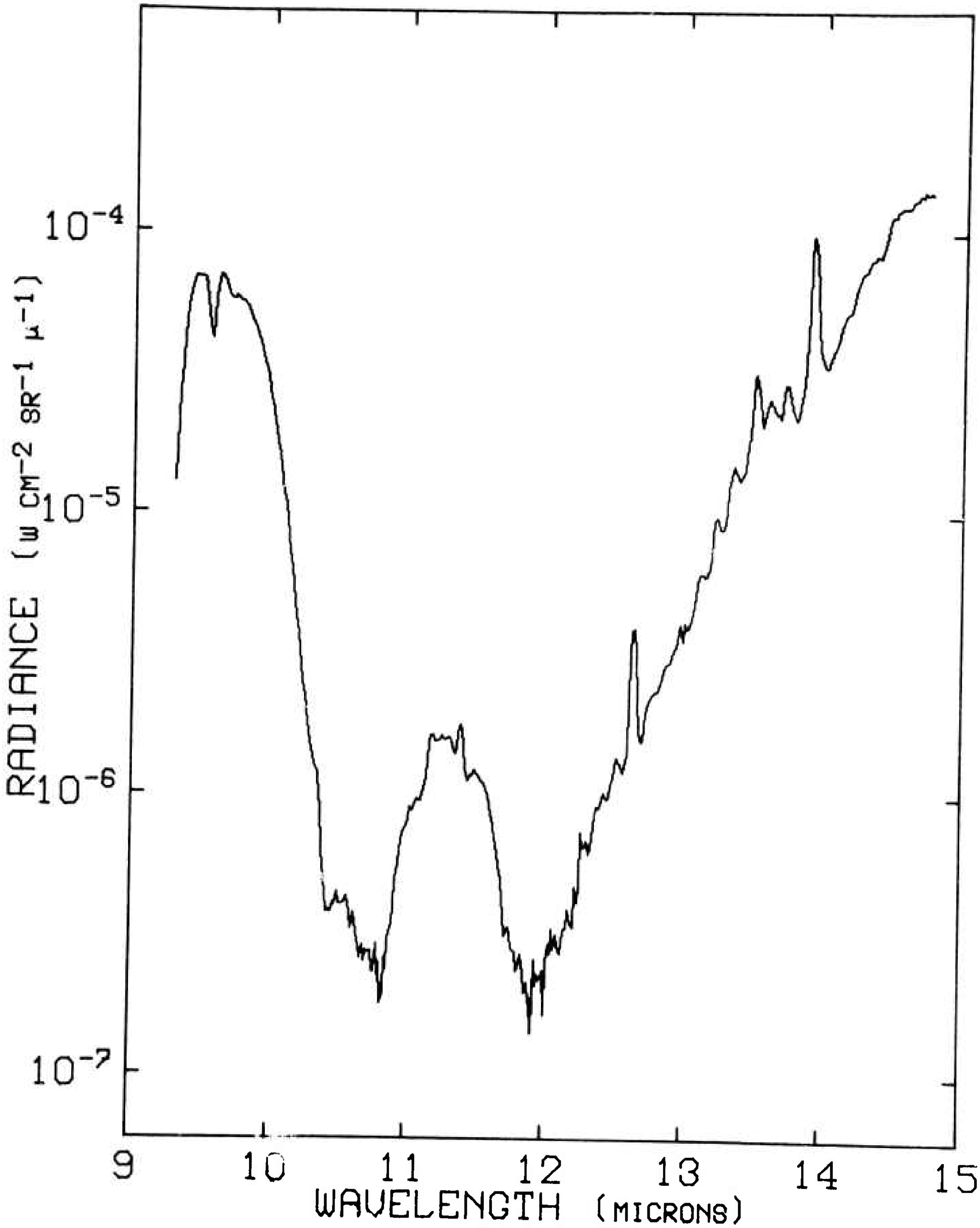

Figure 136. Radiance vs Wavelength at 62.6 kft and 0159 ADT, 15 September 1971.

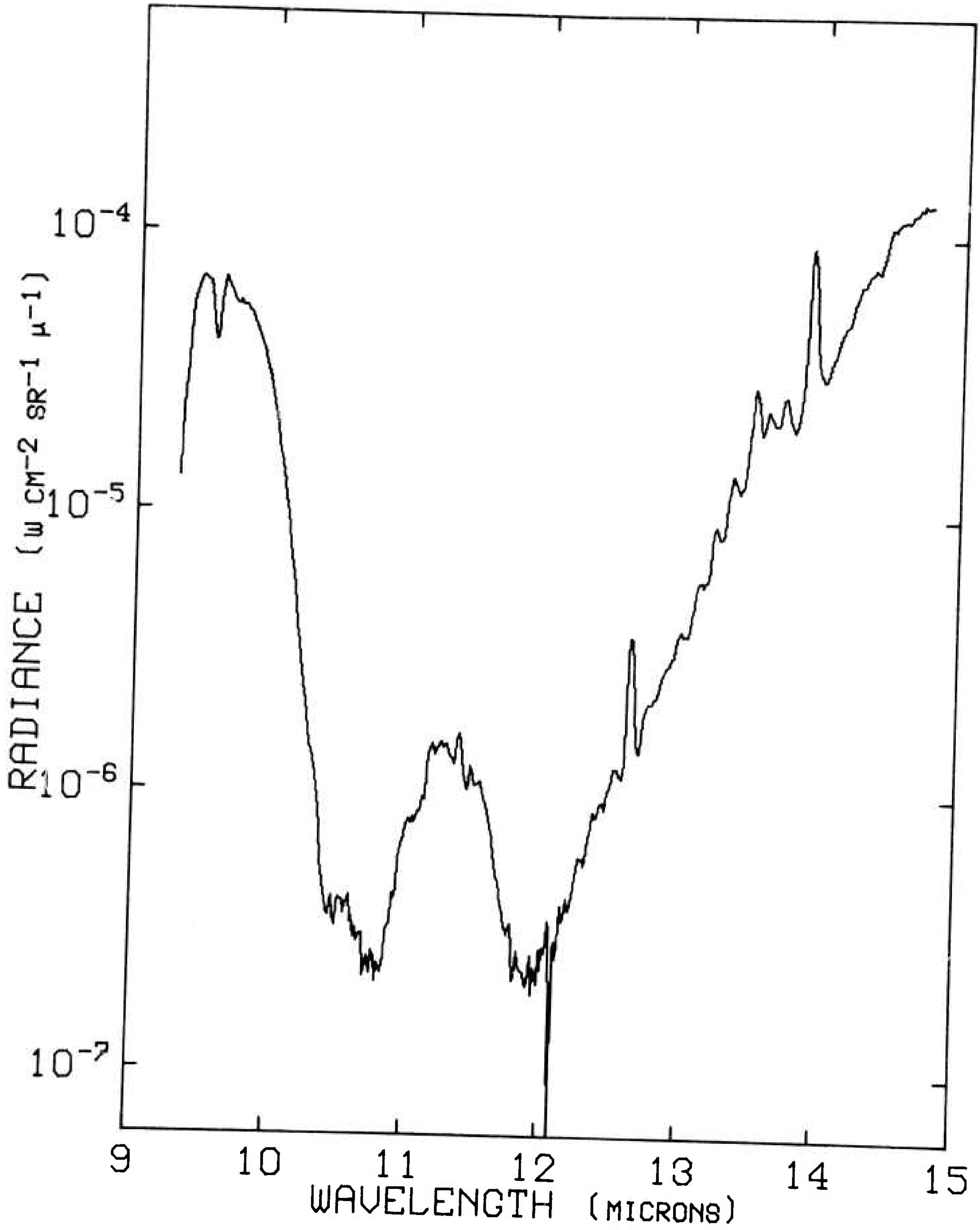

Figure 137. Radiance vs Wavelength at 64.4 kft and 0201 ADT, 15 September 1971.

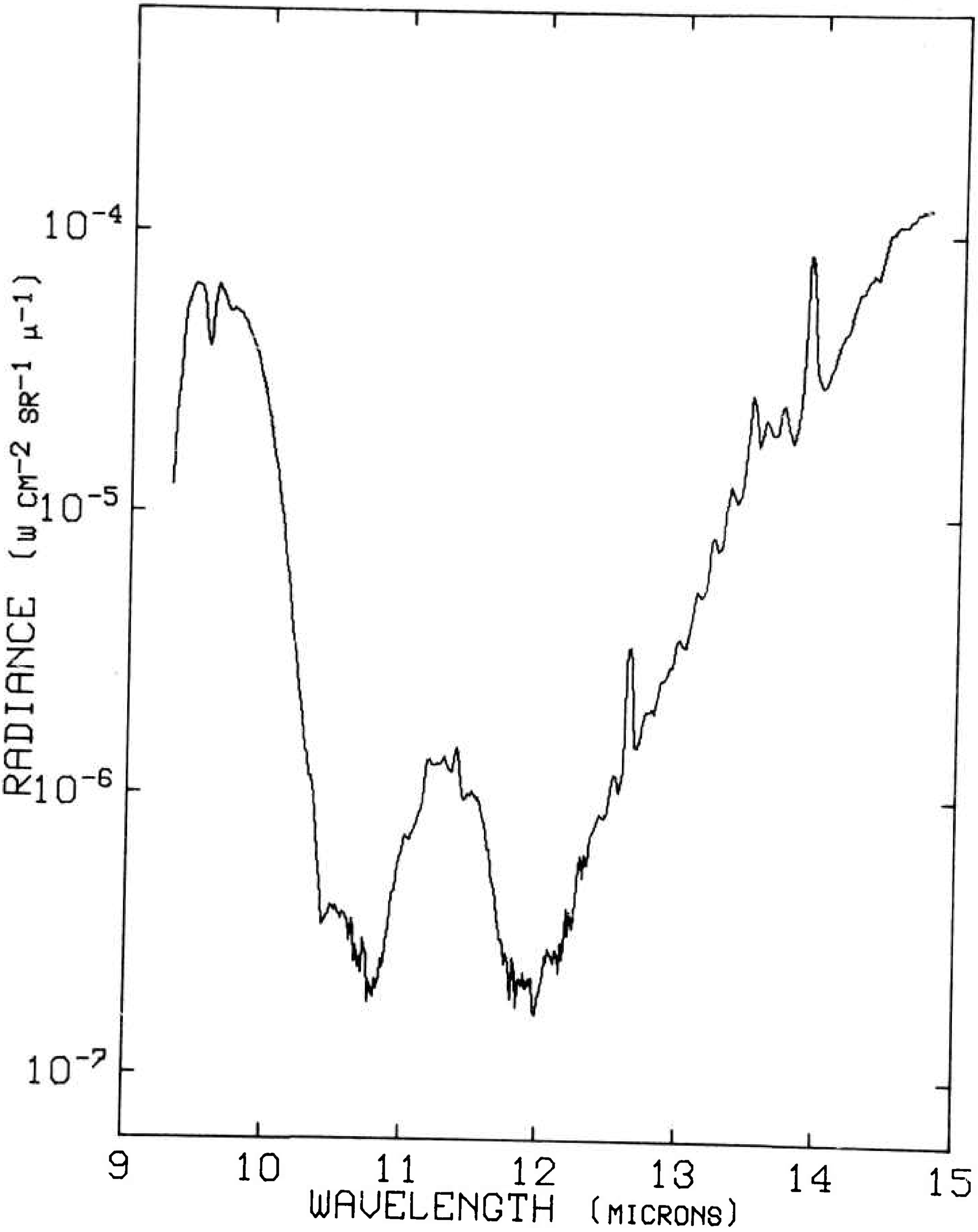

Figure 138. Radiance vs Wavelength at 66.1 kft and 0203 ADT, 15 September 1971.

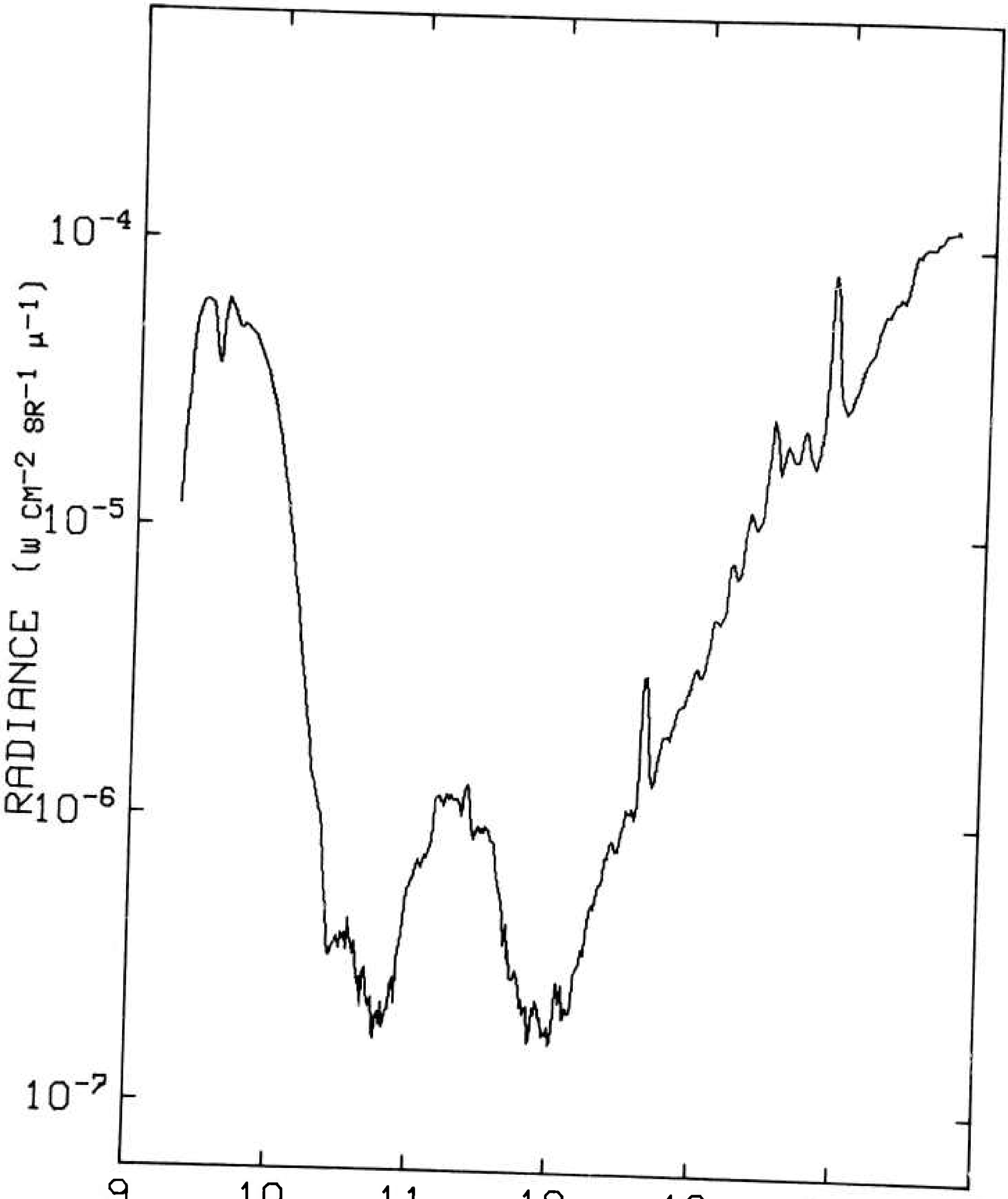

Figure 139. Radiance vs Wavelength at 67.9 kft and 0204 ADT, 15 September 1971.

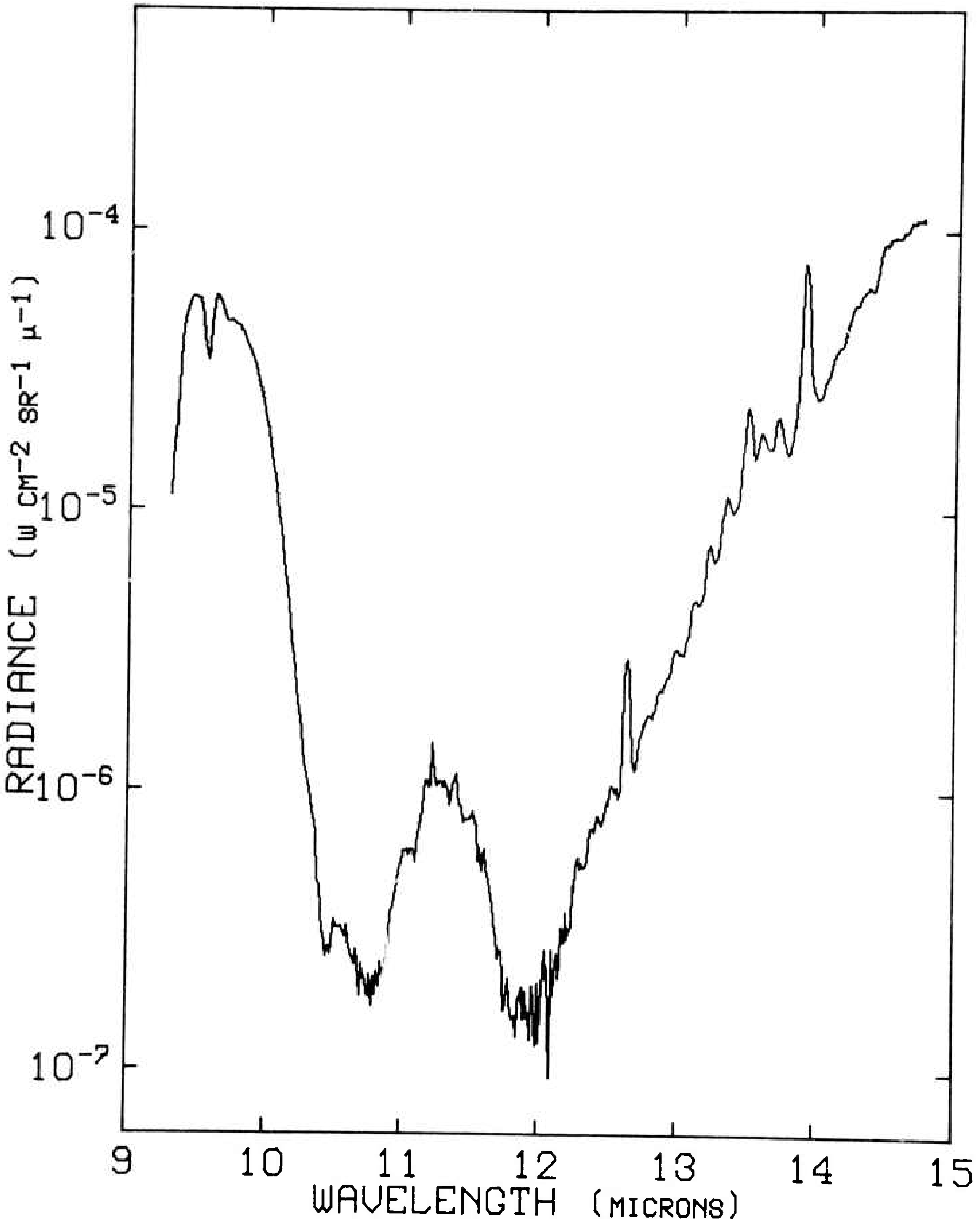

Figure 140. Radiance vs Wavelength at 69.6 kft and 0206 ADT, 15 September 1971.

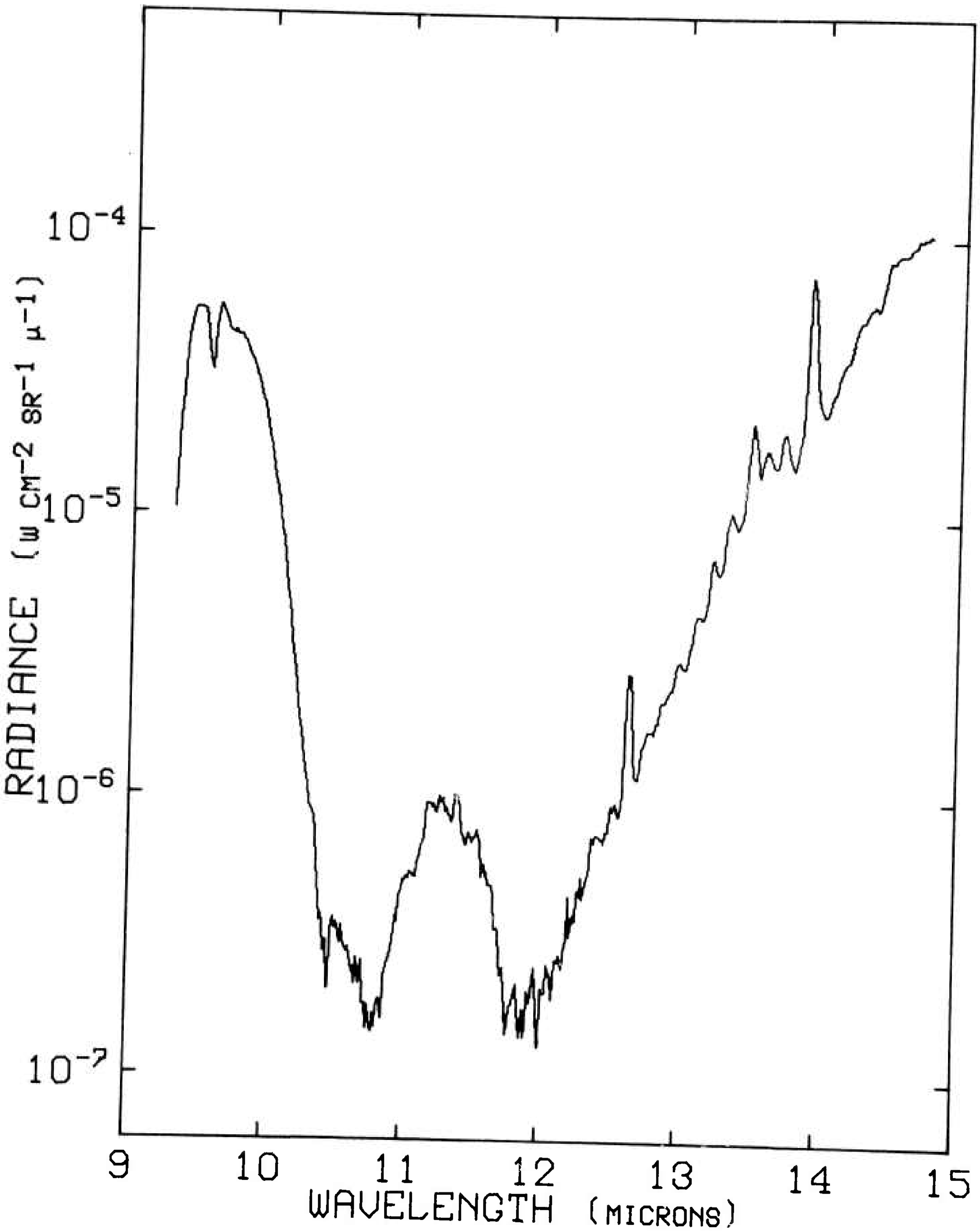

Figure 141. Radiance vs Wavelength at 70.9 kft and 0208 ADT, 15 September 1971.

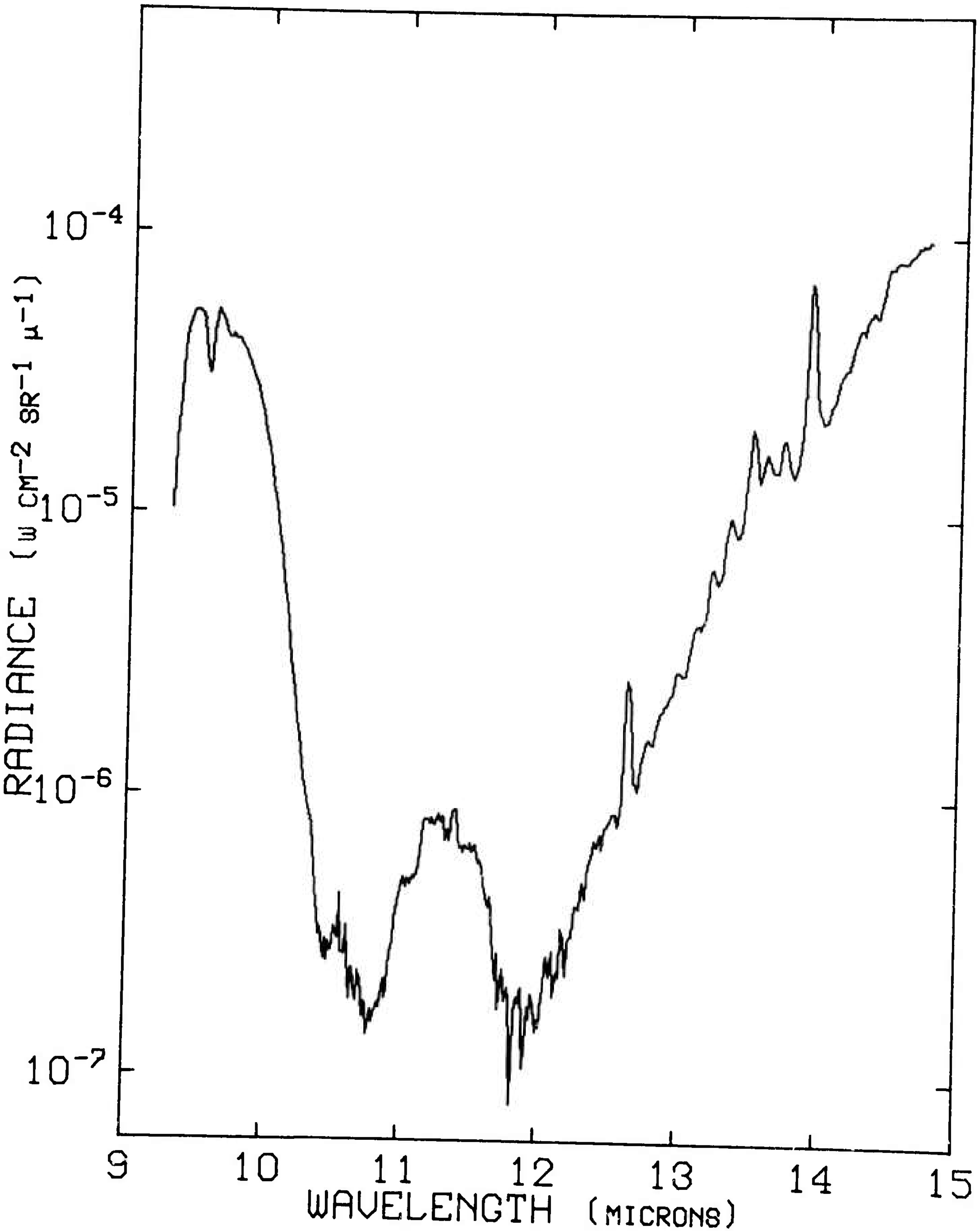

Figure 142. Radiance vs Wavelength at 71.8 kft and 0210 ADT, 15 September 1971.

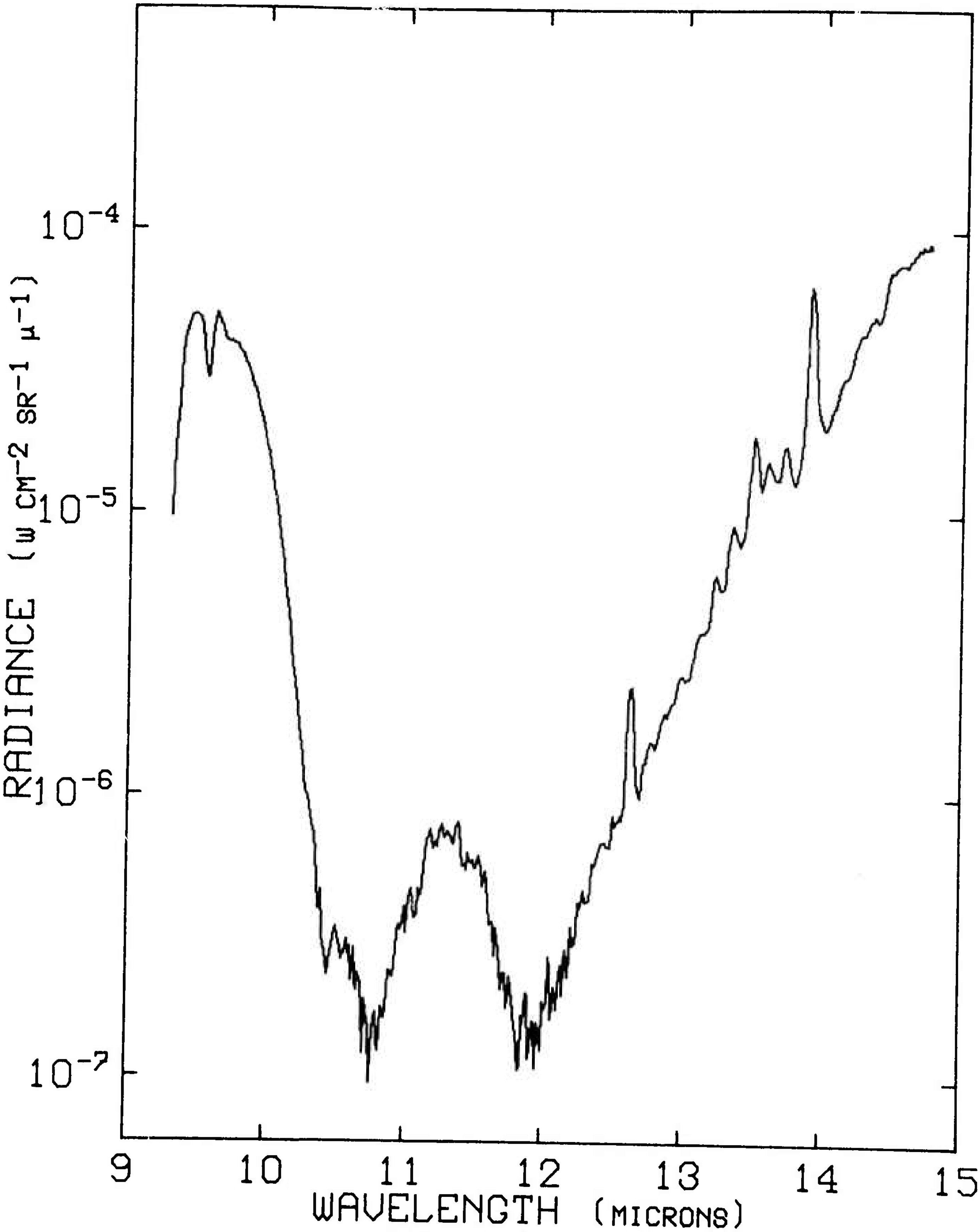

Figure 143. Radiance vs Wavelength at 73.3 kft and 0212 ADT, 15 September 1971.

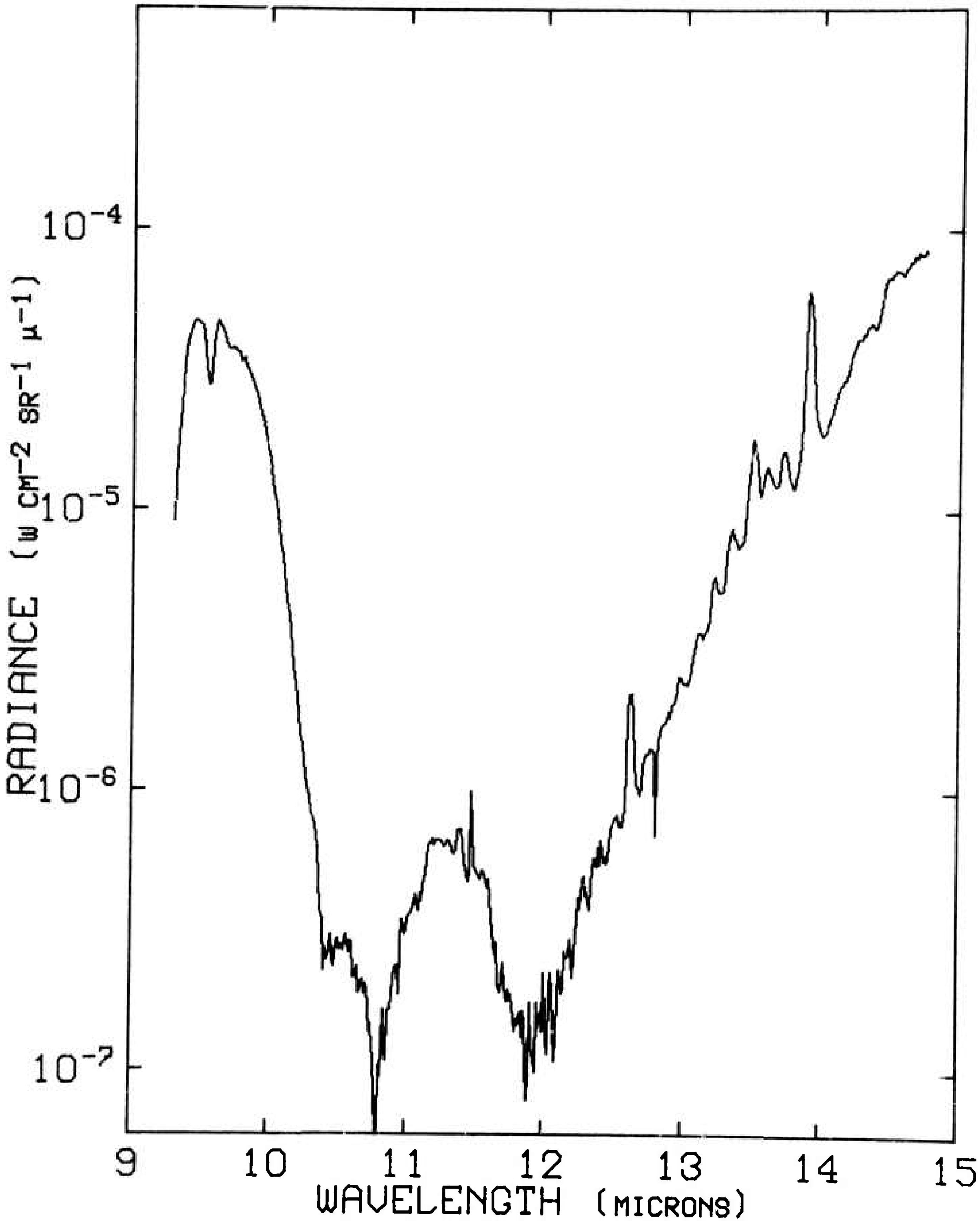

Figure 144. Radiance vs Wavelength at 74.8 kft and 0214 ADT, 15 September 1971.

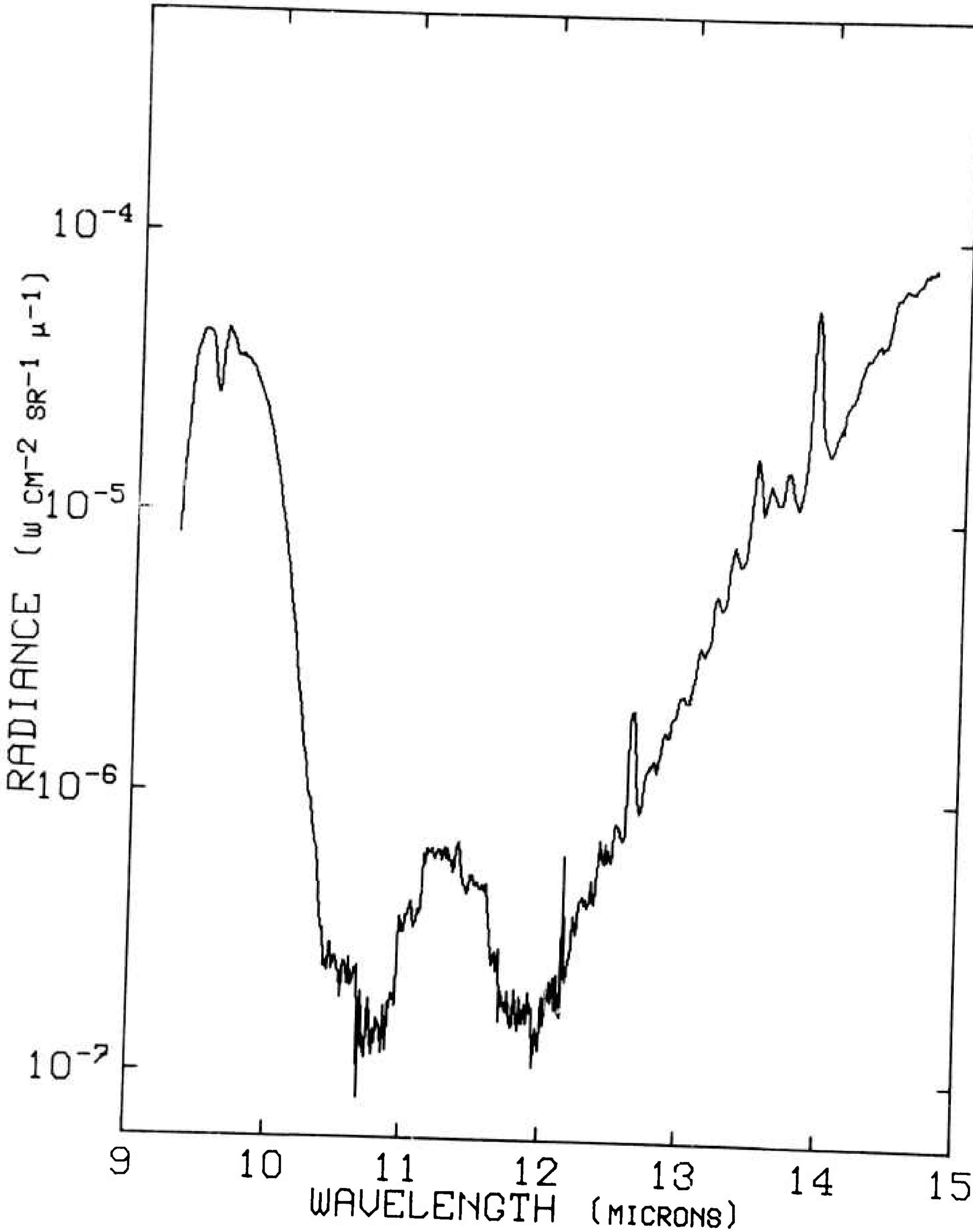

Figure 145. Radiance vs Wavelength at 76.1 kft and 0216 ADT, 15 September 1971.

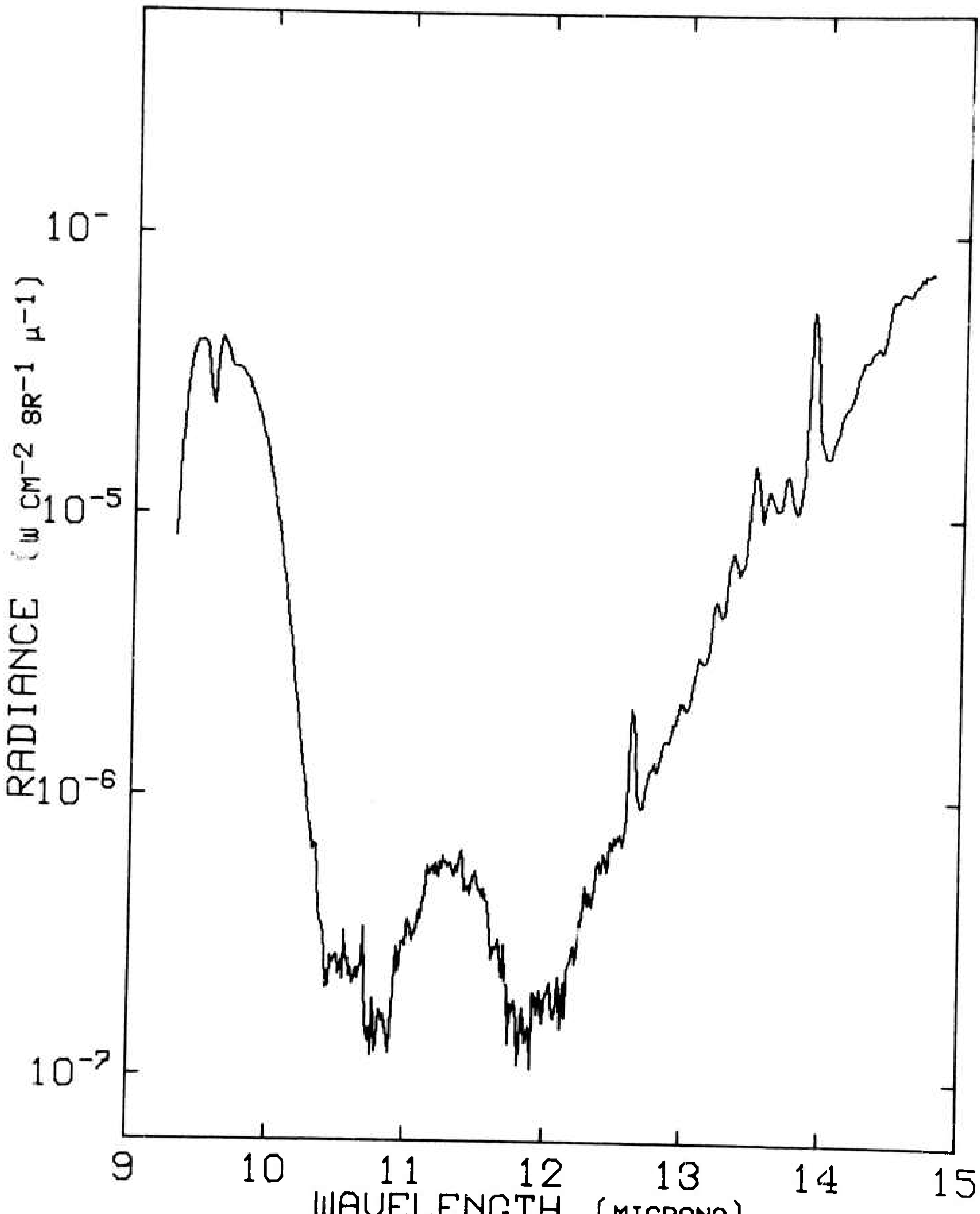

Figure 146. Radiance vs Wavelength at 77.2 kft and 0218 ADT, 15 September 1971.

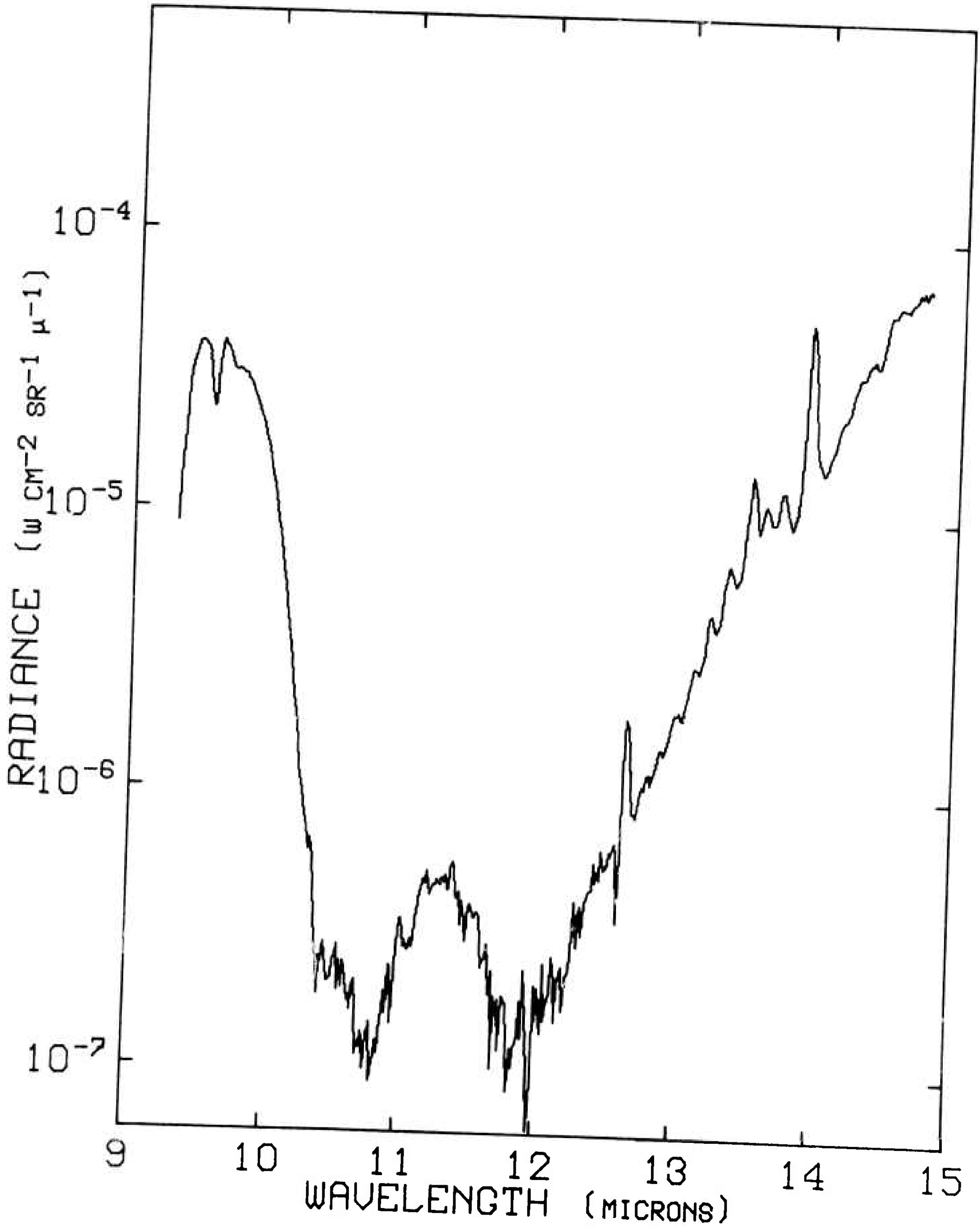

Figure 147. Radiance vs Wavelength at 78.7 kft and 0220 ADT, 15 September 1971.

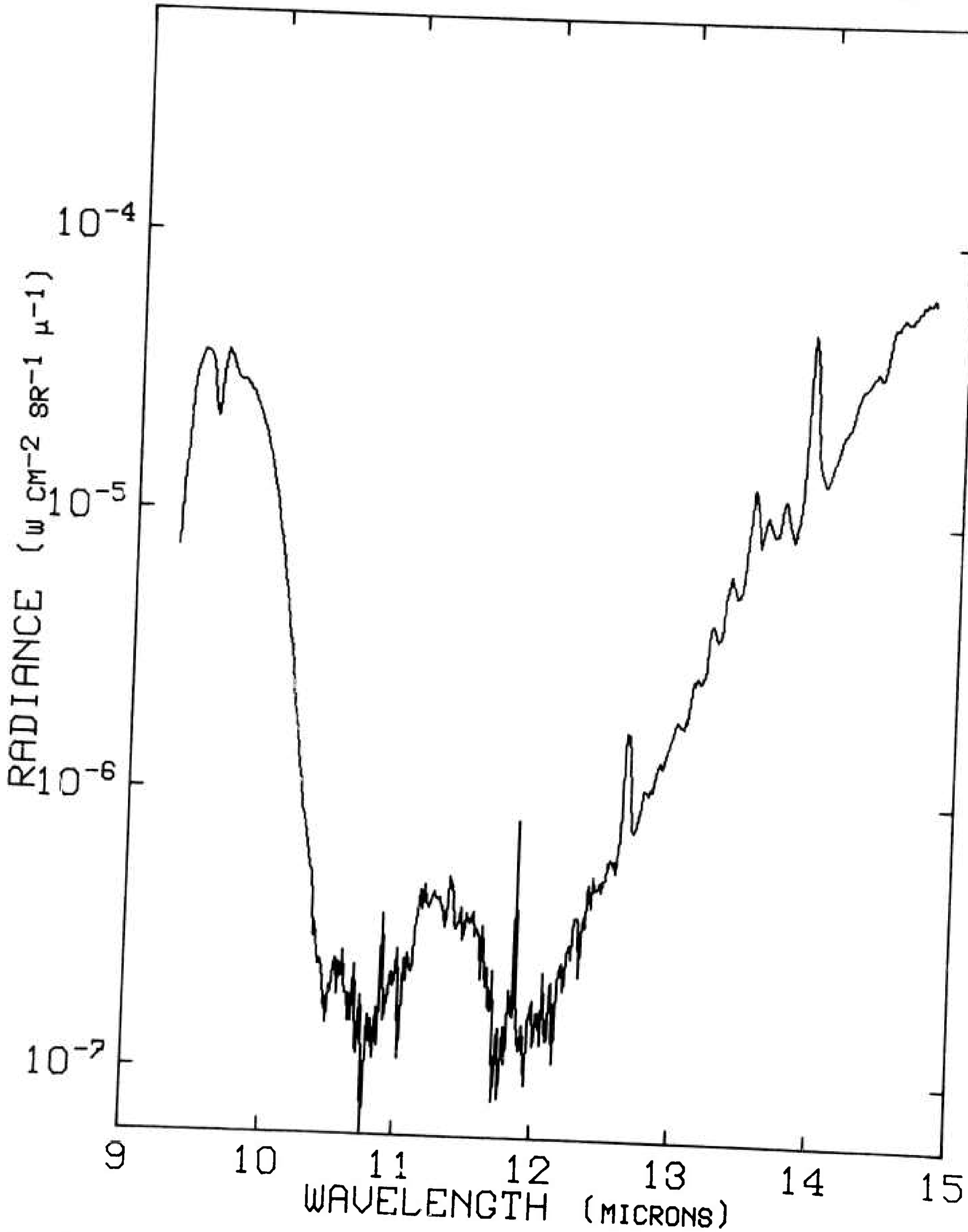

Figure 148. Radiance vs Wavelength at 79.8 kft and 0222 ADT, 15 September 1971.

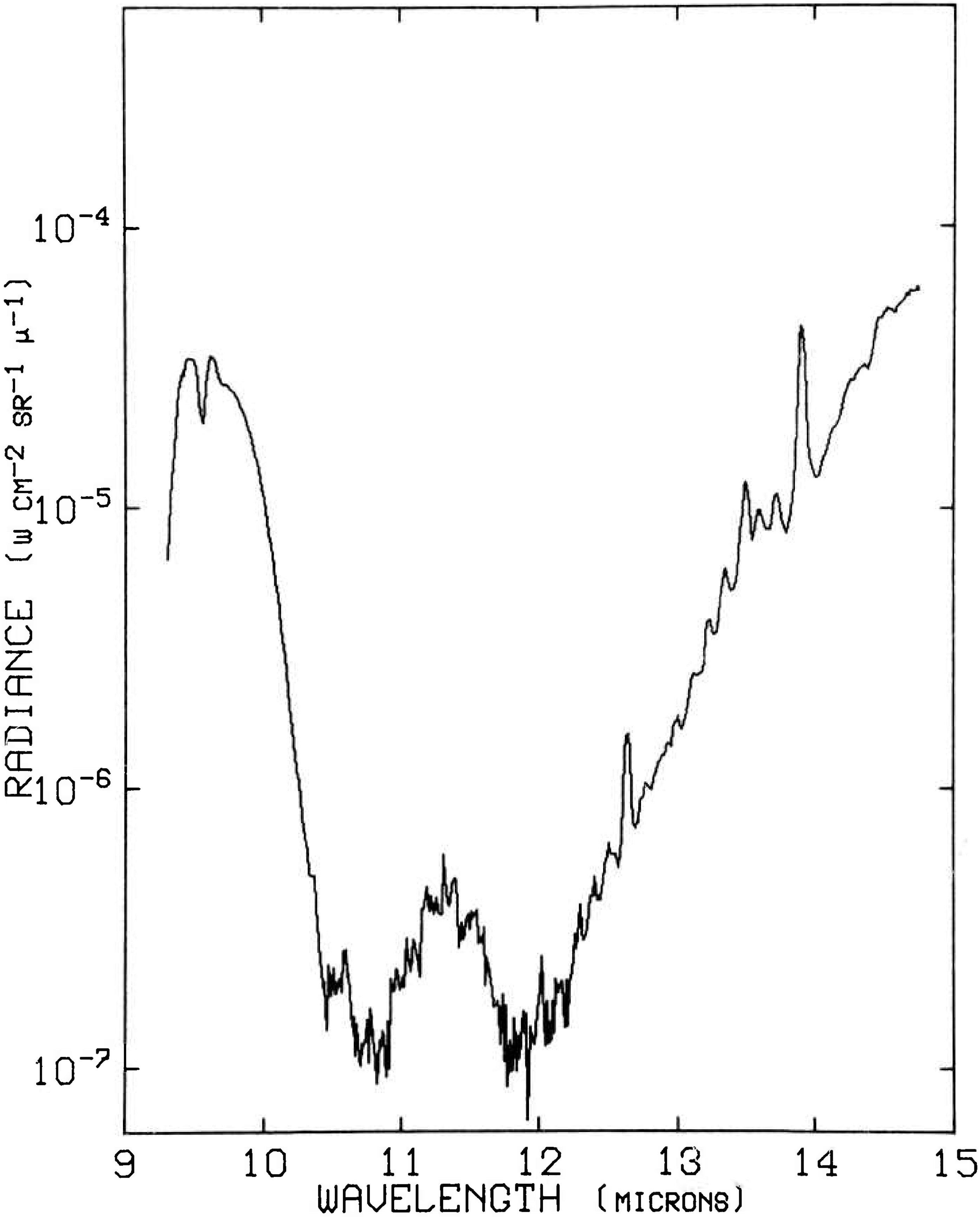

Figure 149. Radiance vs Wavelength at 81.1 kft and 0224 ADT, 15 September 1971.

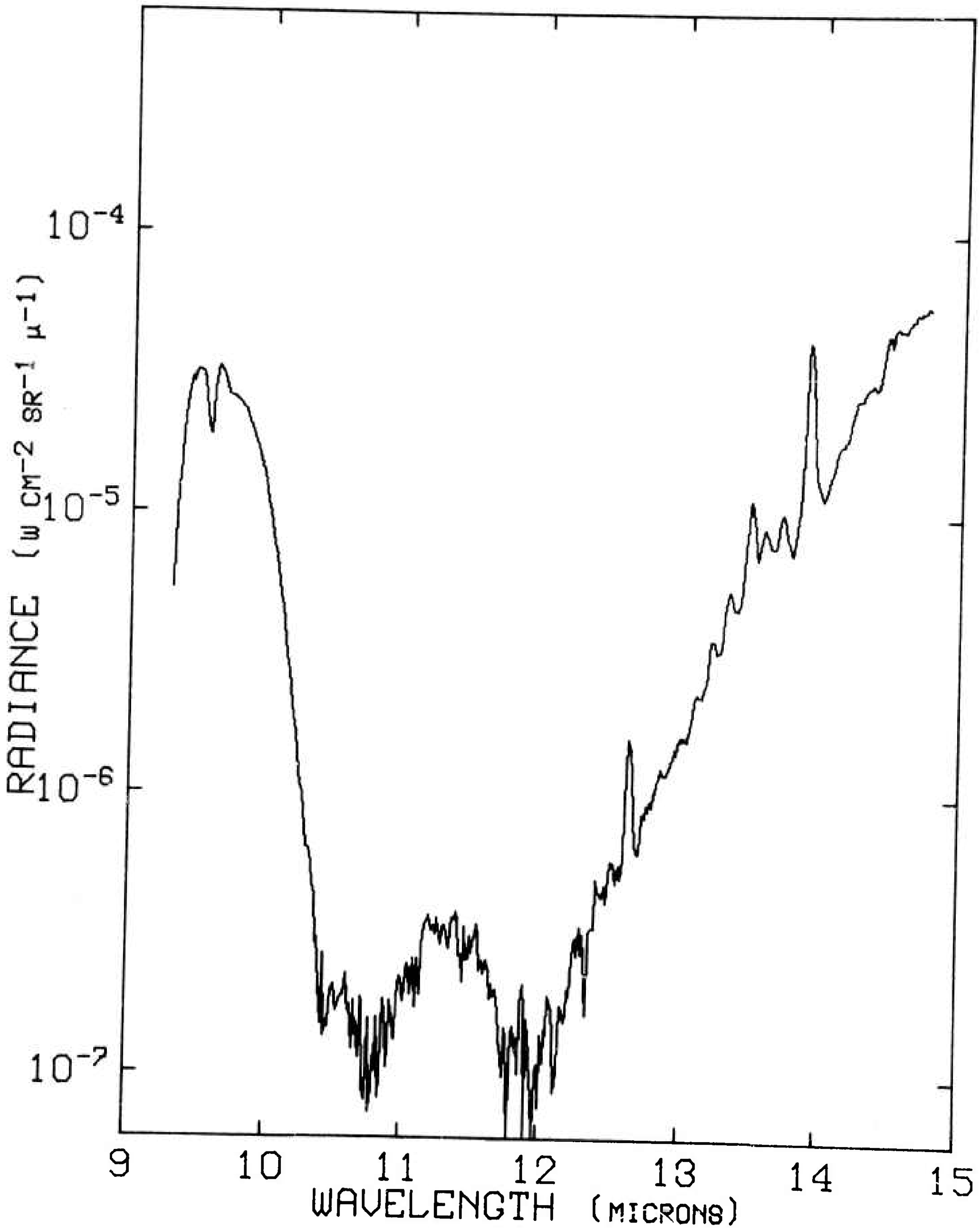

Figure 150. Radiance vs Wavelength at 82.6 kft and 0226 ADT, 15 September 1971.

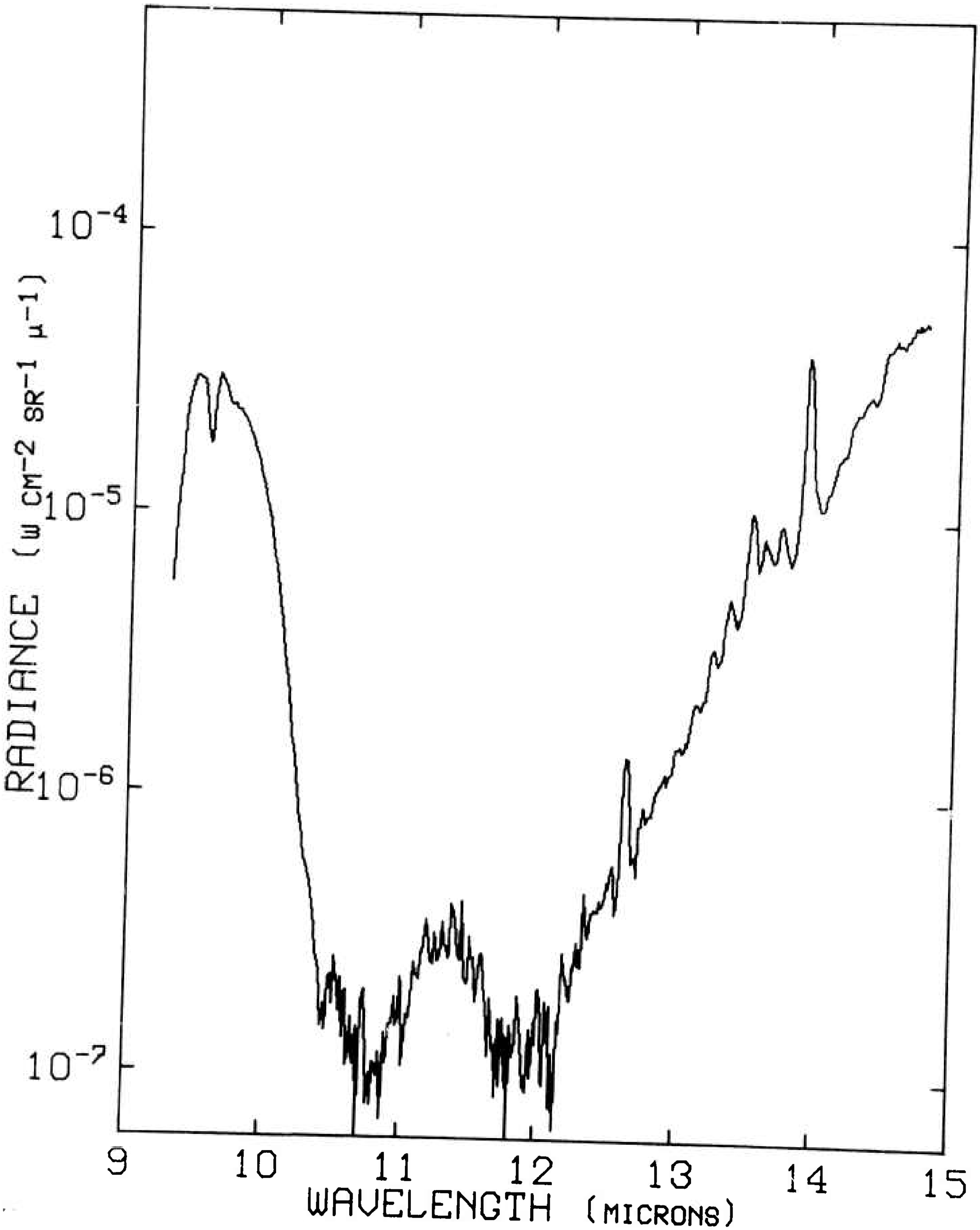

Figure 151. Radiance vs Wavelength at 84.1 kft and 0228 ADT, 15 September 1971.

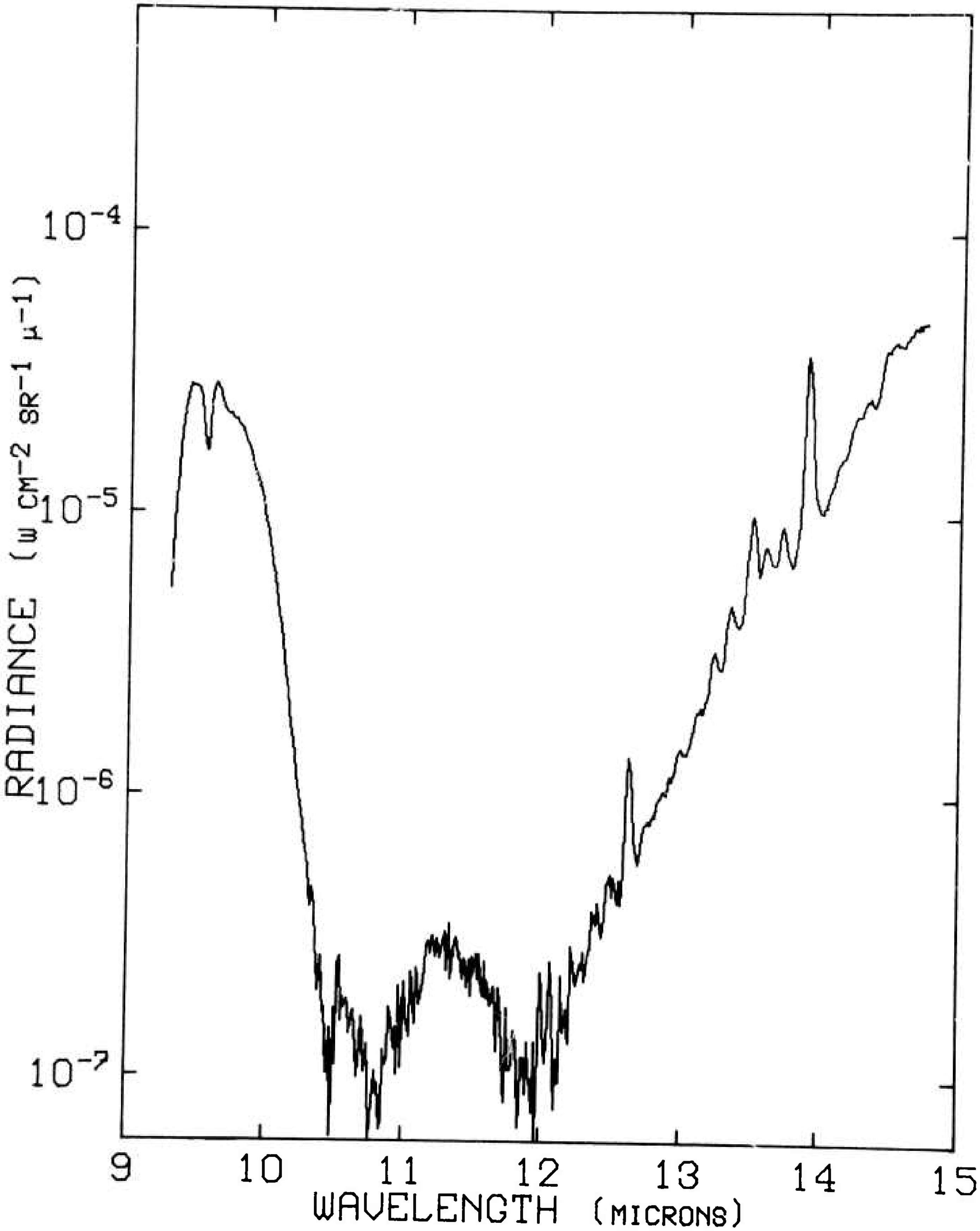

Figure 152. Radiance vs Wavelength at 85.3 kft and 0230 ADT, 15 September 1971.

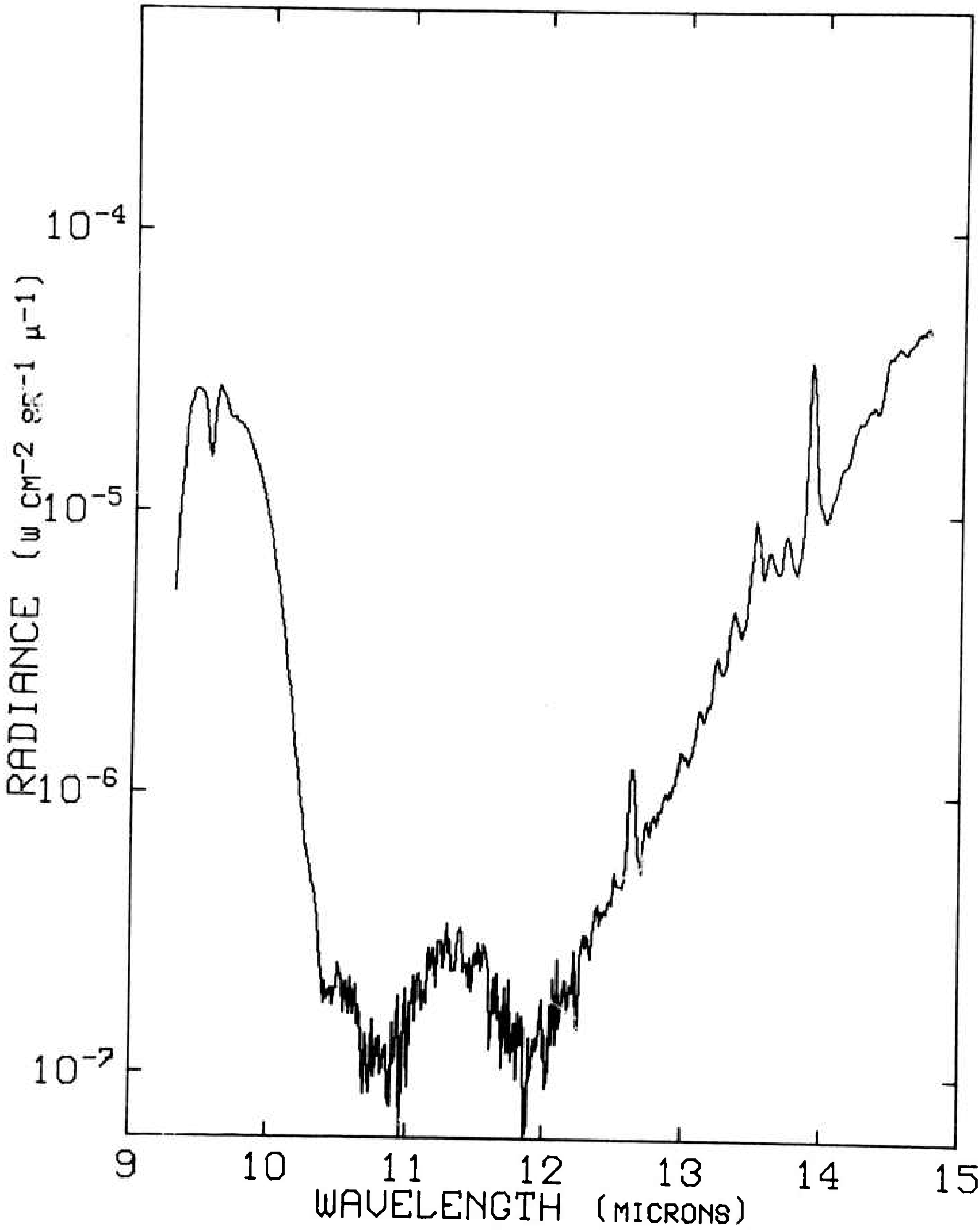

Figure 153. Radiance vs Wavelength at 86.5 kft and 0231 ADT, 15 September 1971.

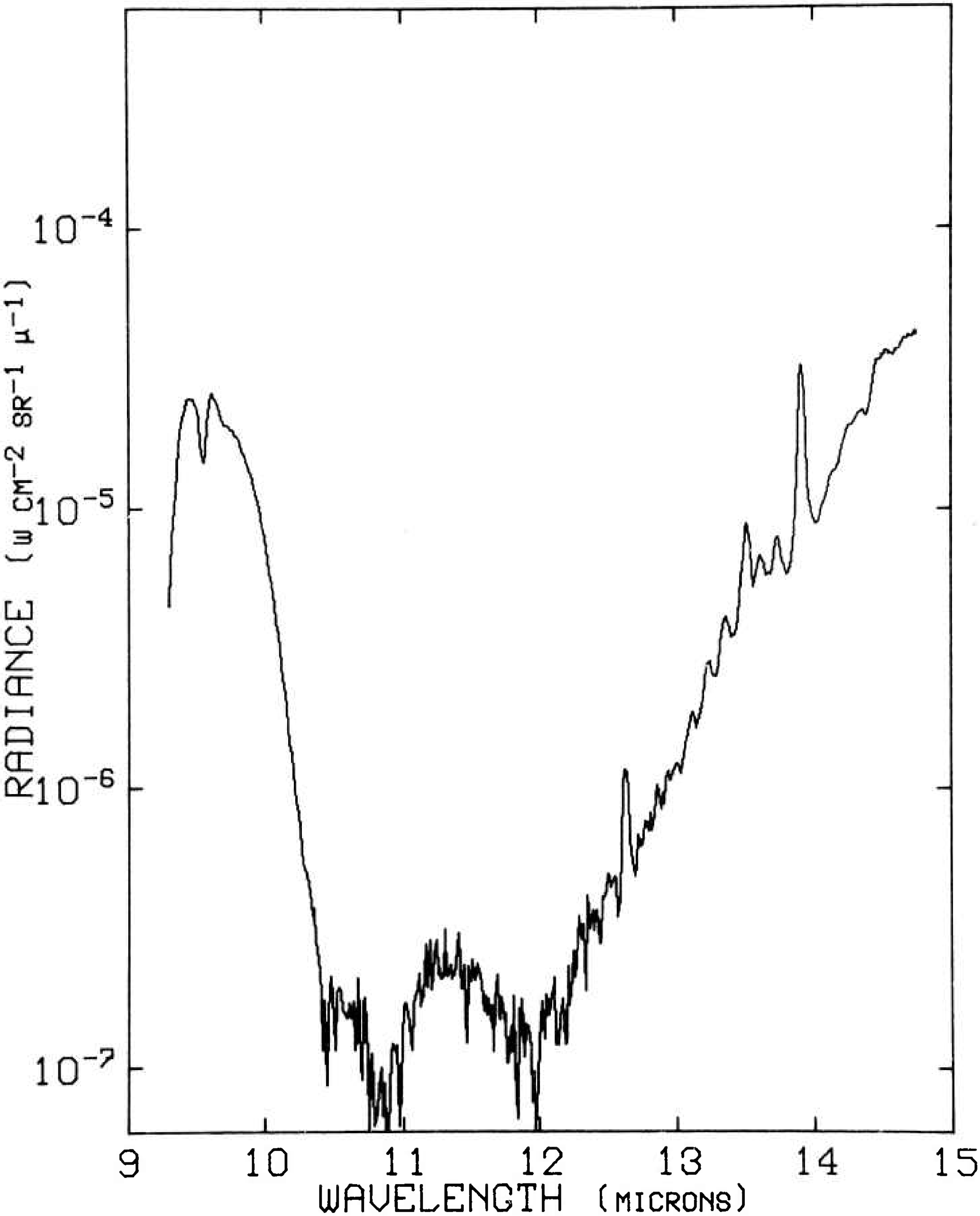

Figure 154. Radiance vs Wavelength at 87.9 kft and 0233 ADT, 15 September 1971.

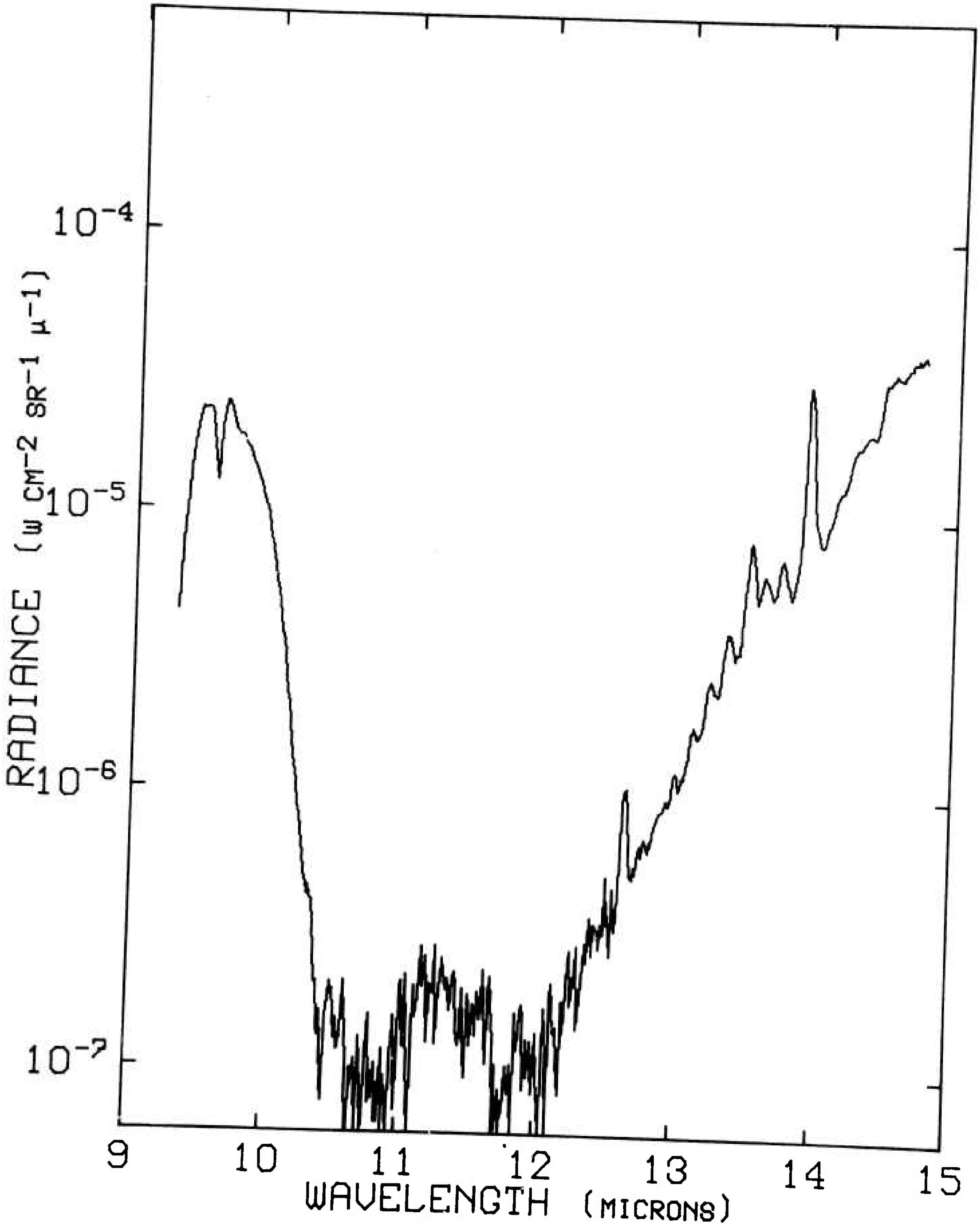

Figure 155. Radiance vs Wavelength at 89.6 kft and 0235 ADT, 15 September 1971.

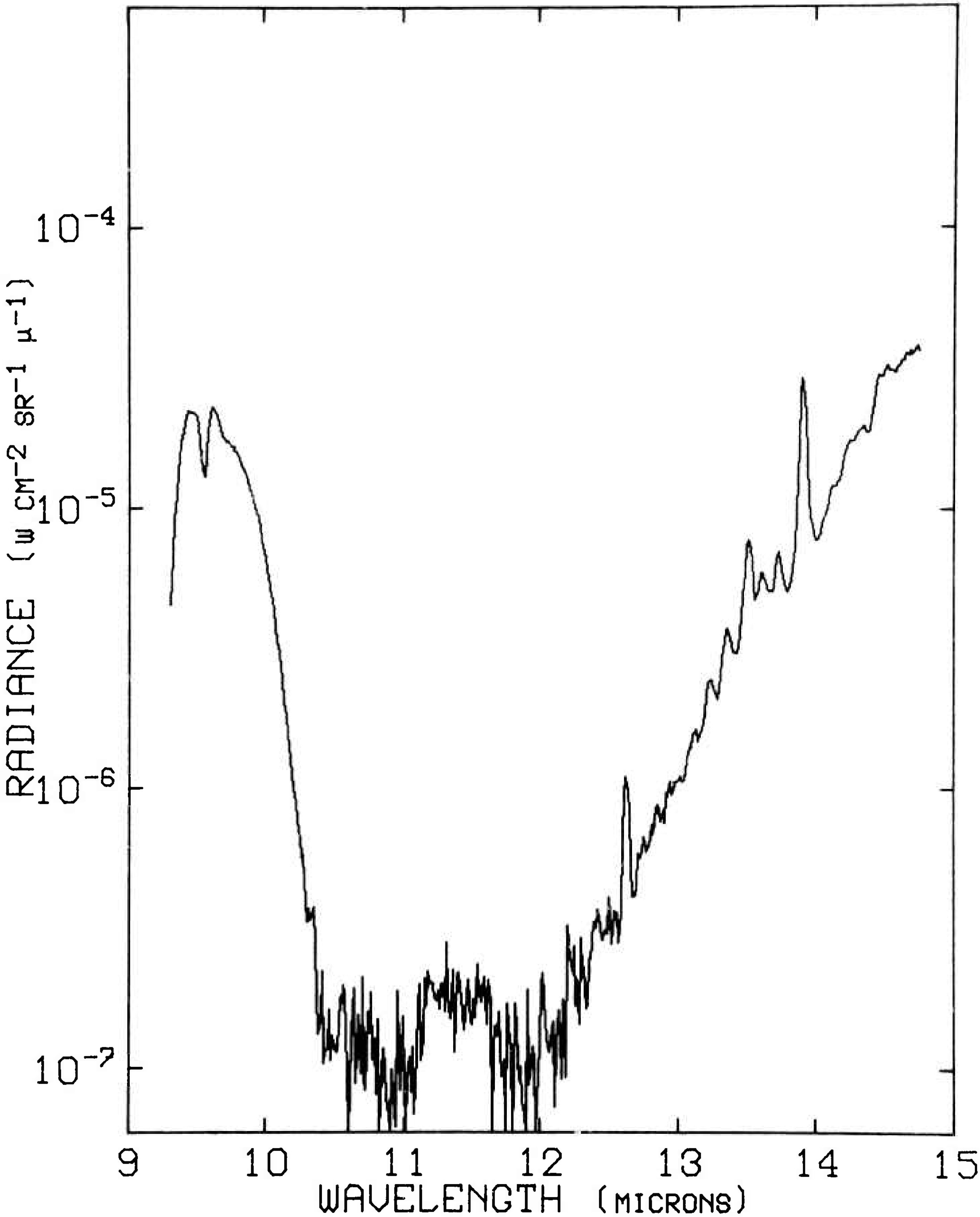

Figure 156. Radiance vs Wavelength at 90.9 kft and 0237 ADT, 15 September 1971.

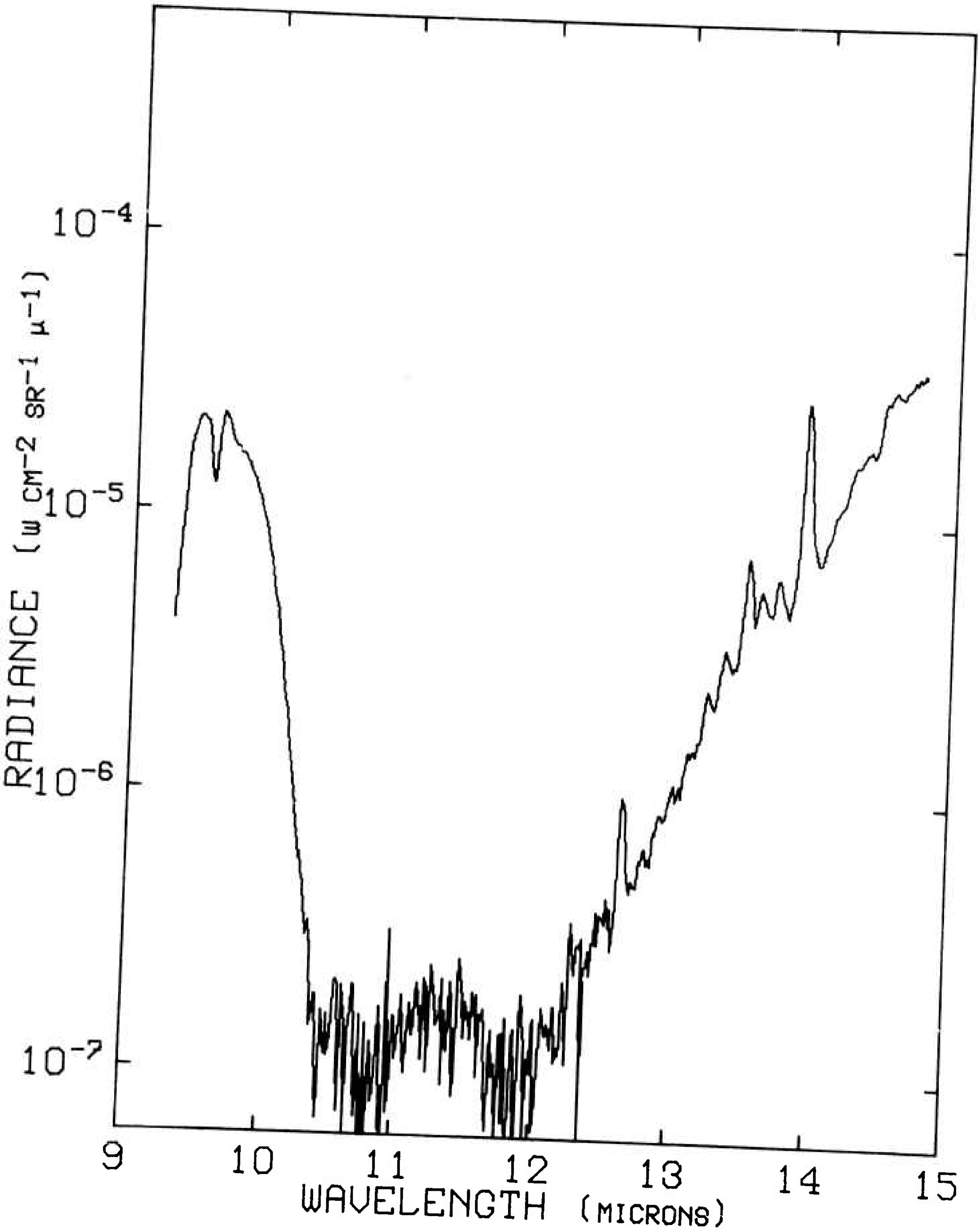

Figure 157. Radiance vs Wavelength at 91.8 kft and 0239 ADT, 15 September 1971.

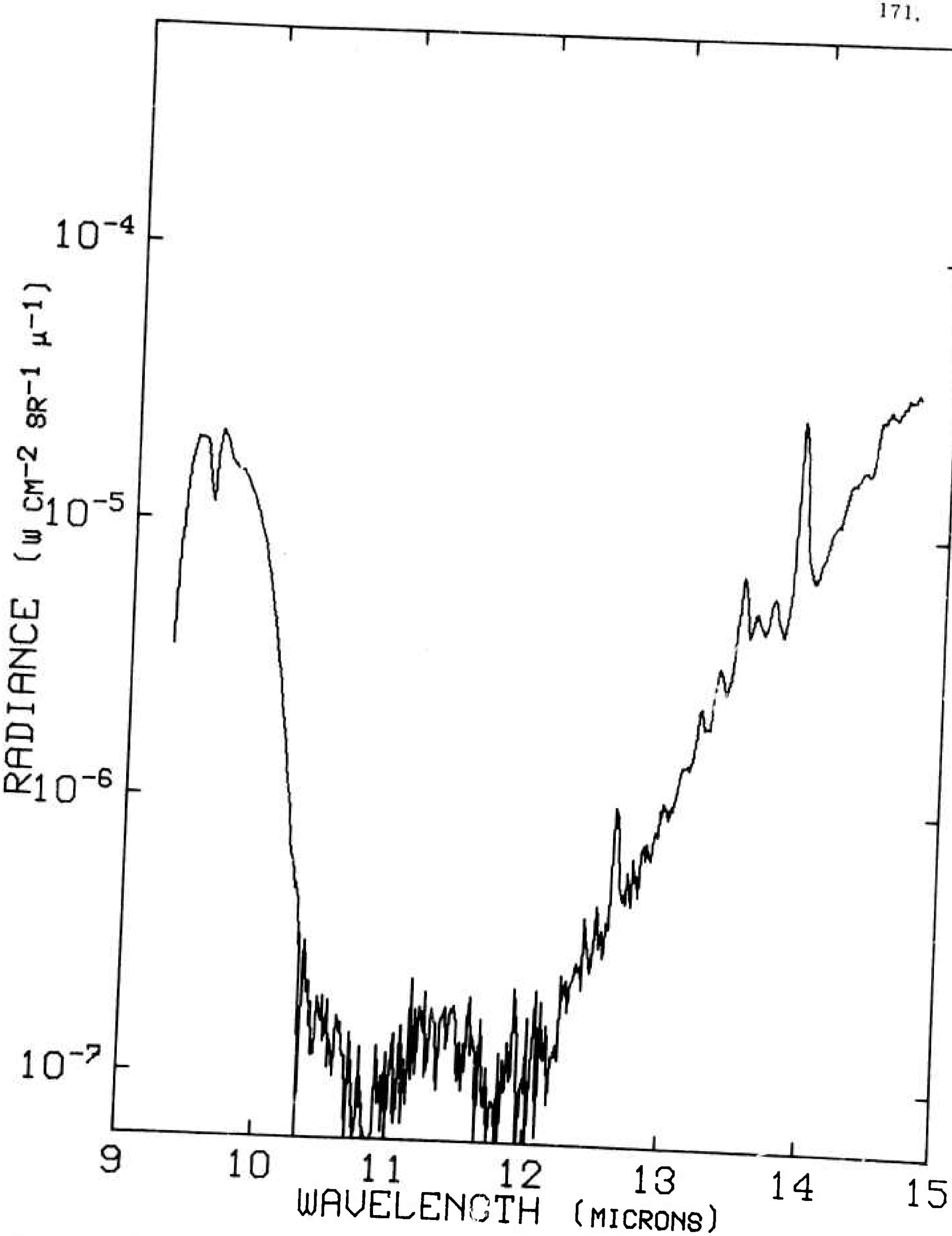

Figure 158. Radiance vs Wavelength at 93.2 kft and 0241 ADT, 15 September 1971.

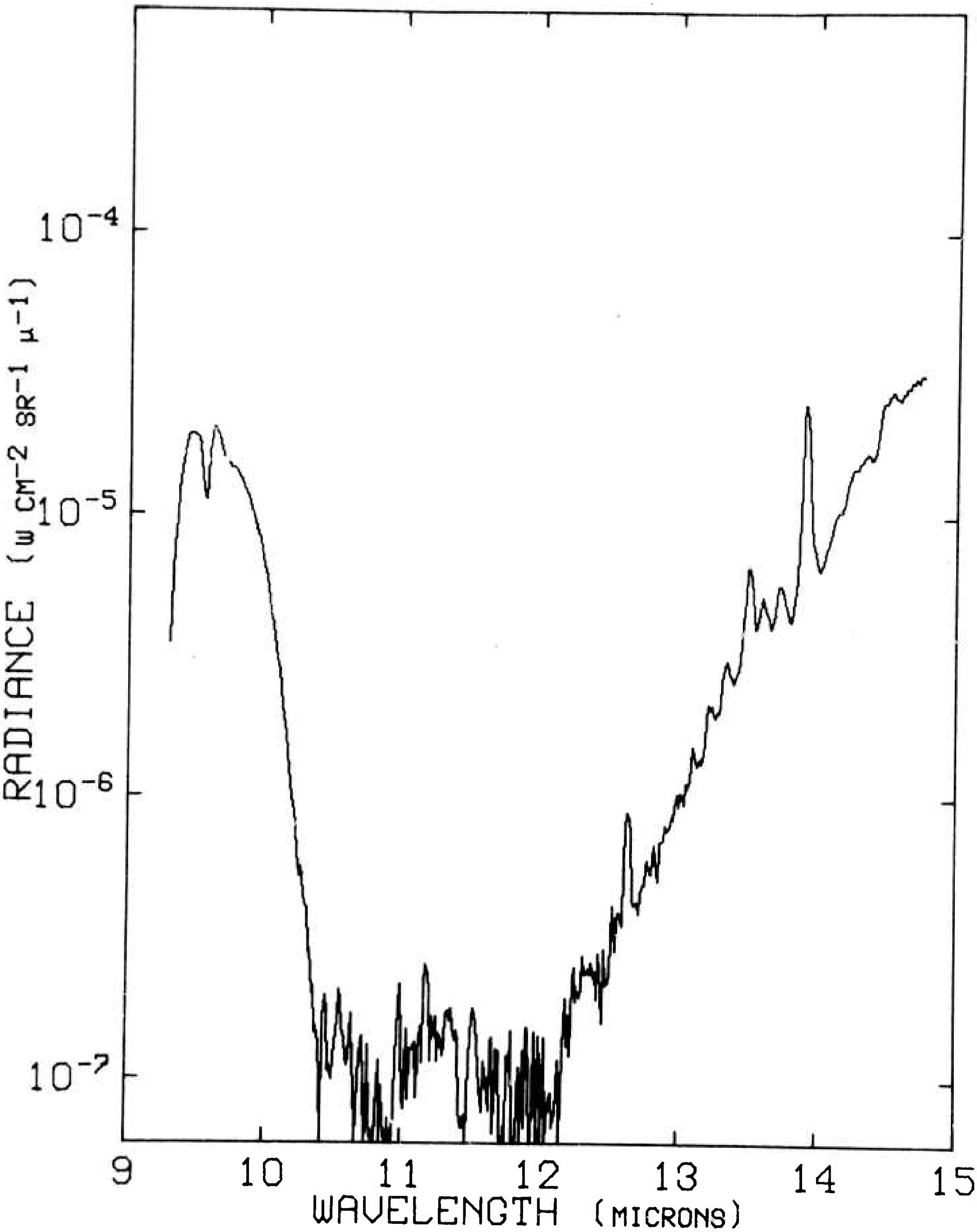

Figure 159. Radiance vs Wavelength at 94.3 kft and 0243 ADT, 15 September 1971.

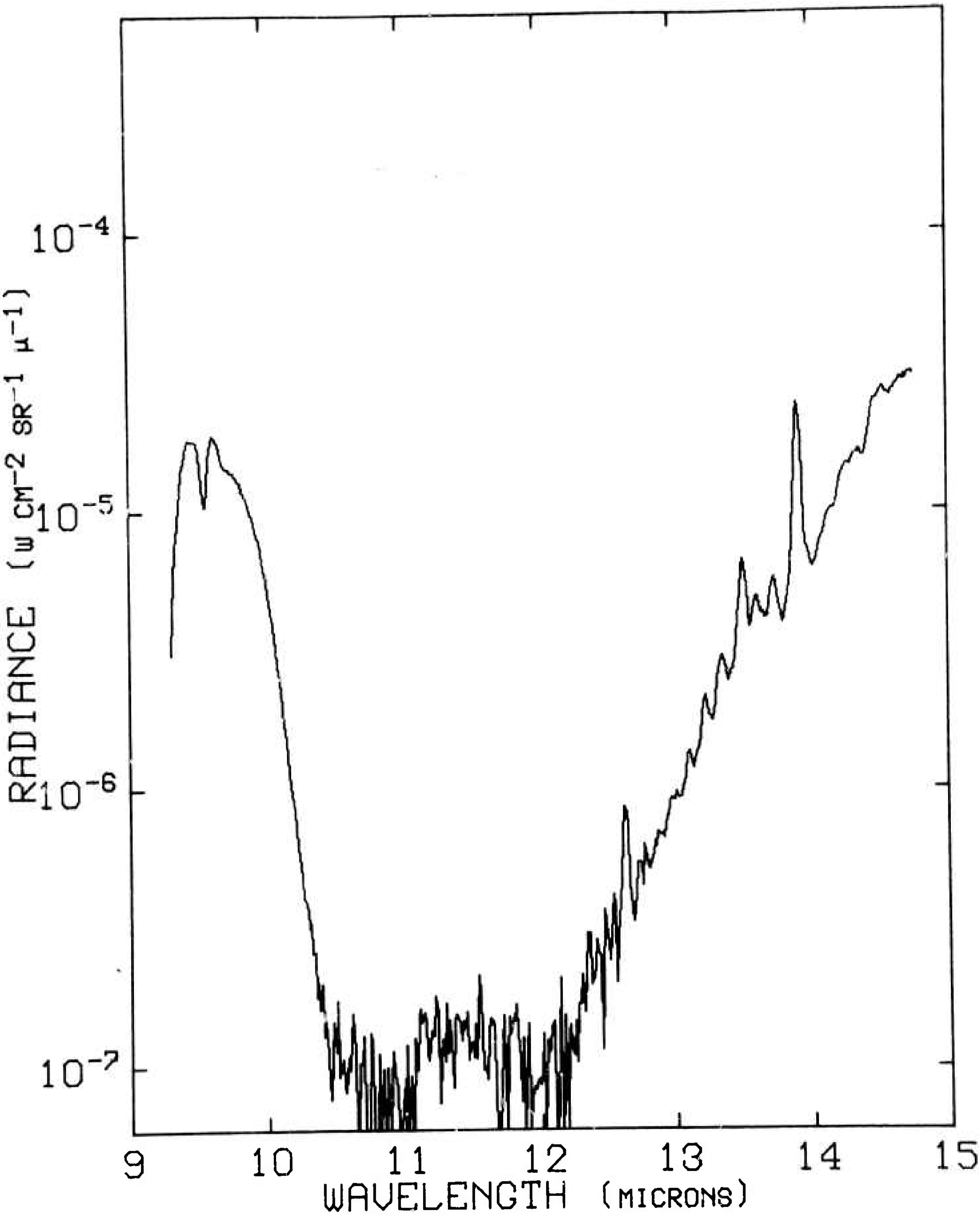

Figure 160. Radiance vs Wavelength at 94.8 kft and 0245 ADT, 15 September 1971.

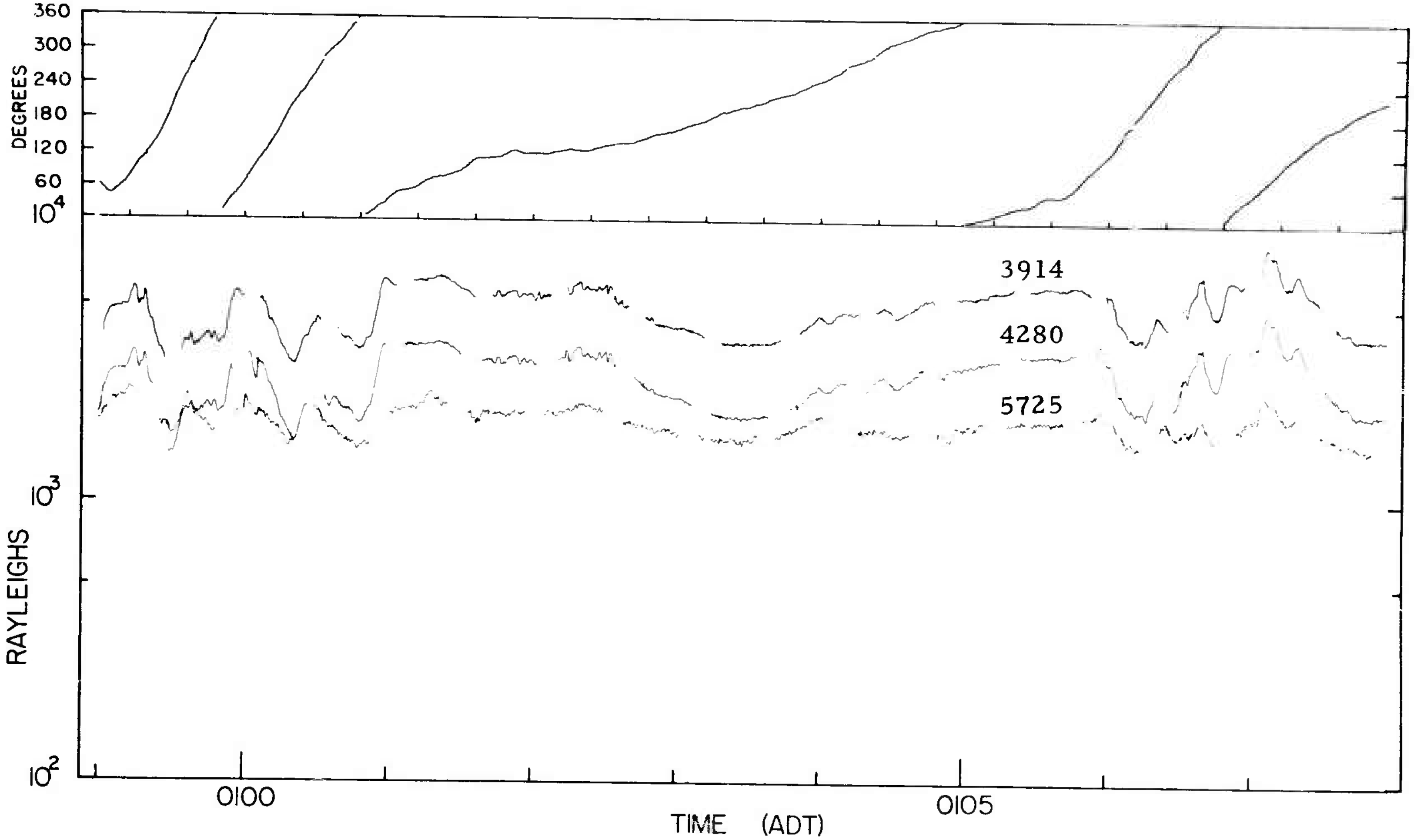

Figure 161. Auroral activity vs time for 15 September 1971.

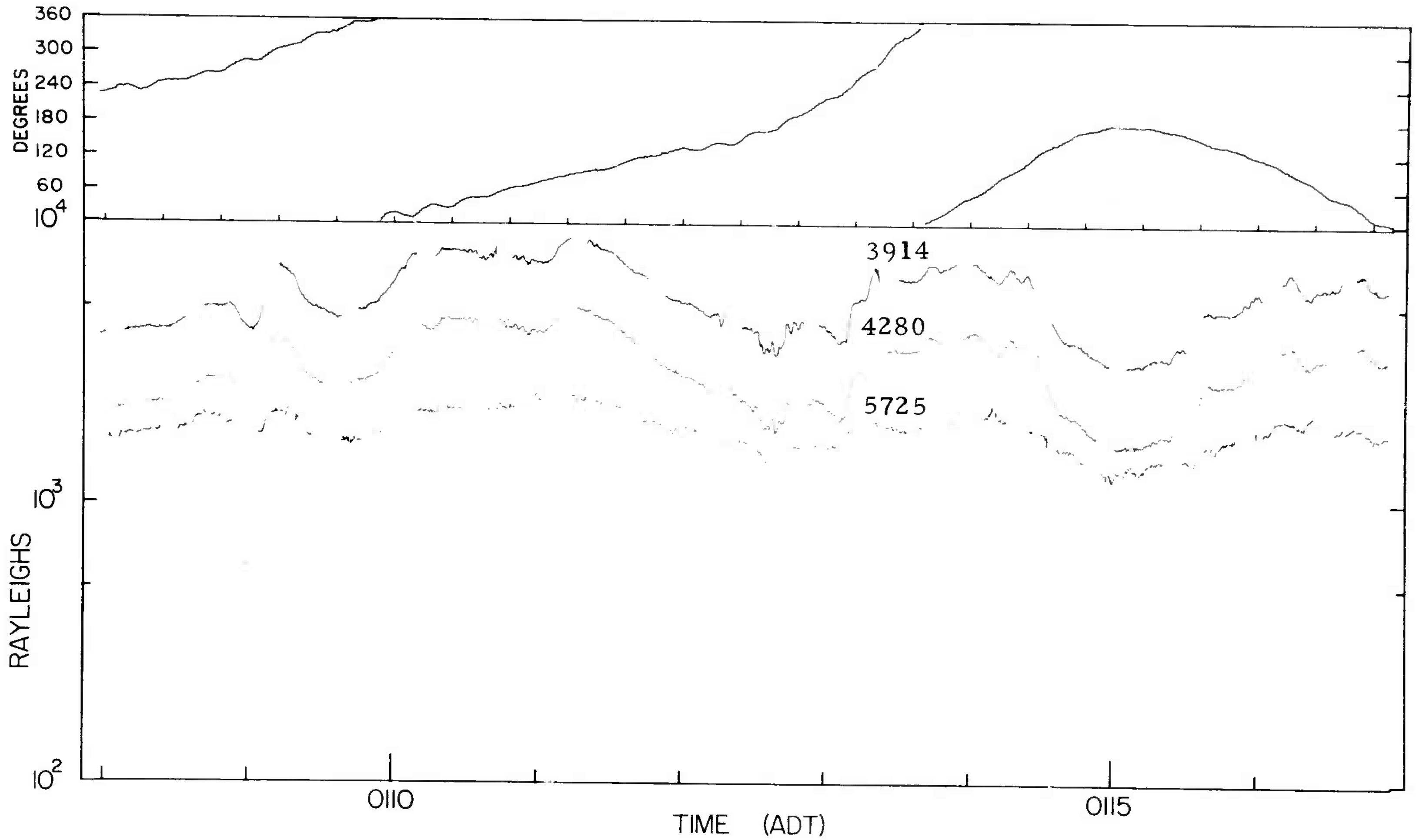

Figure 162. Auroral activity vs time for 15 September 1971.

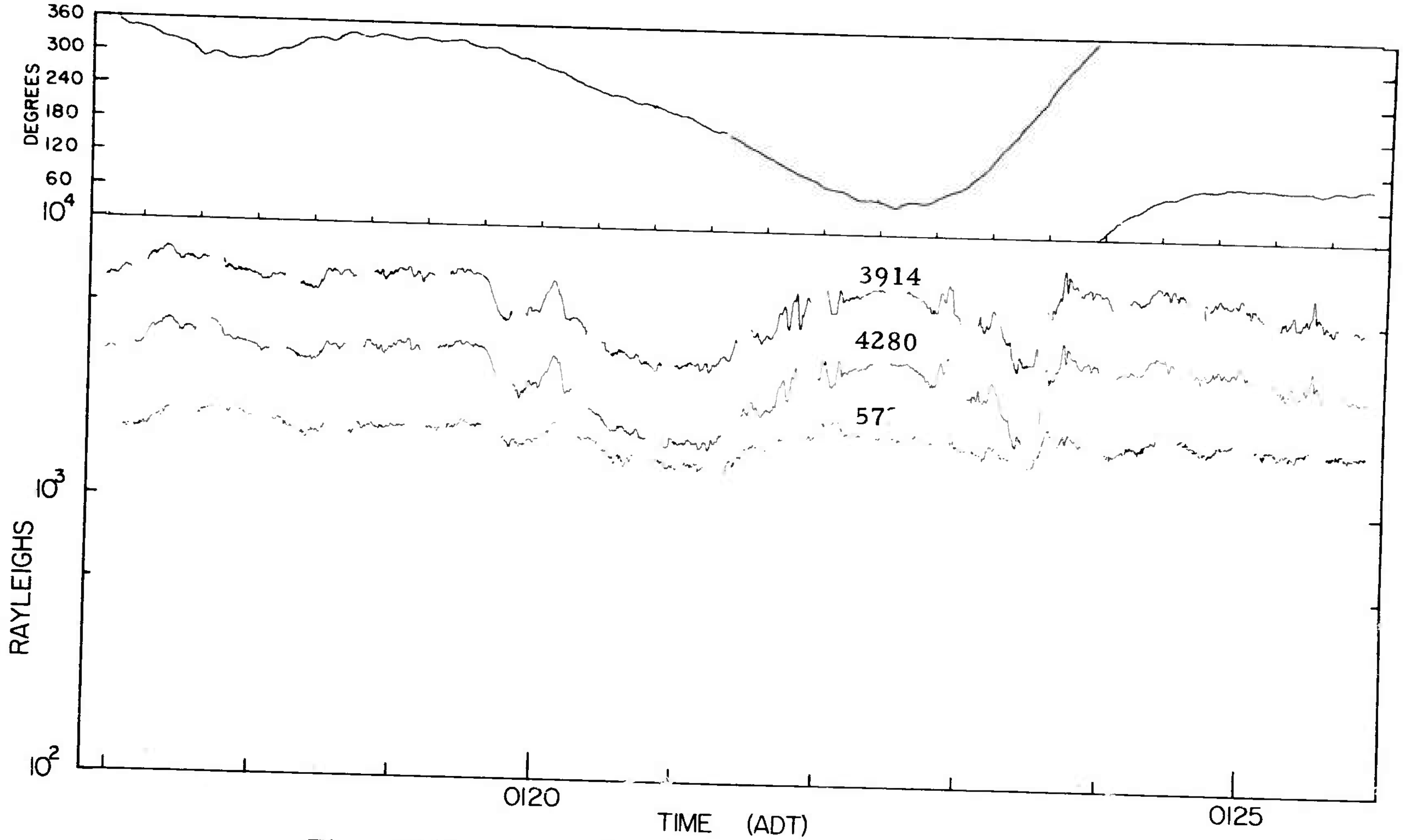

Figure 163. Auroral activity vs time for 15 September 1971.

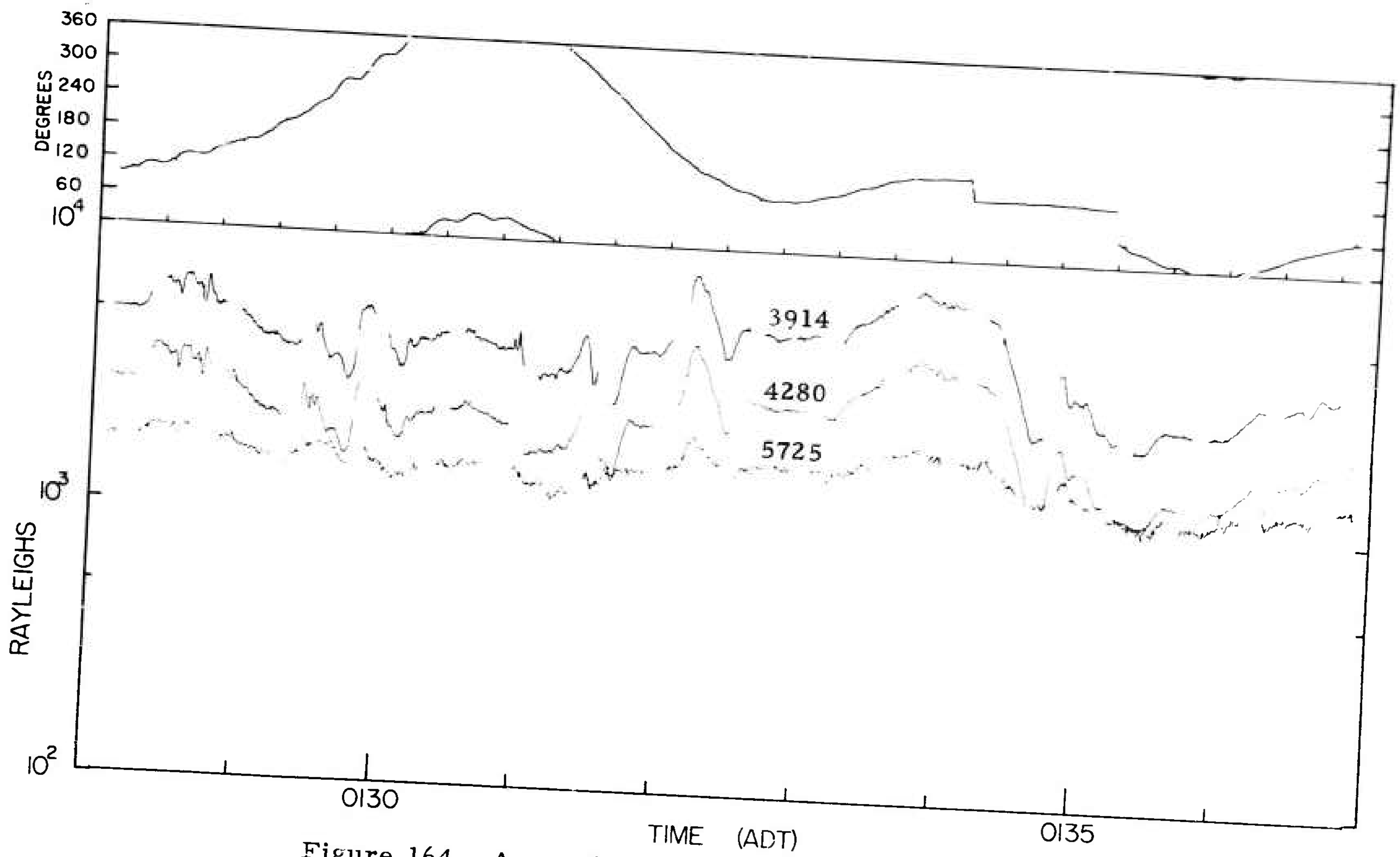

Figure 164. Auroral activity vs time for 15 September 1971.

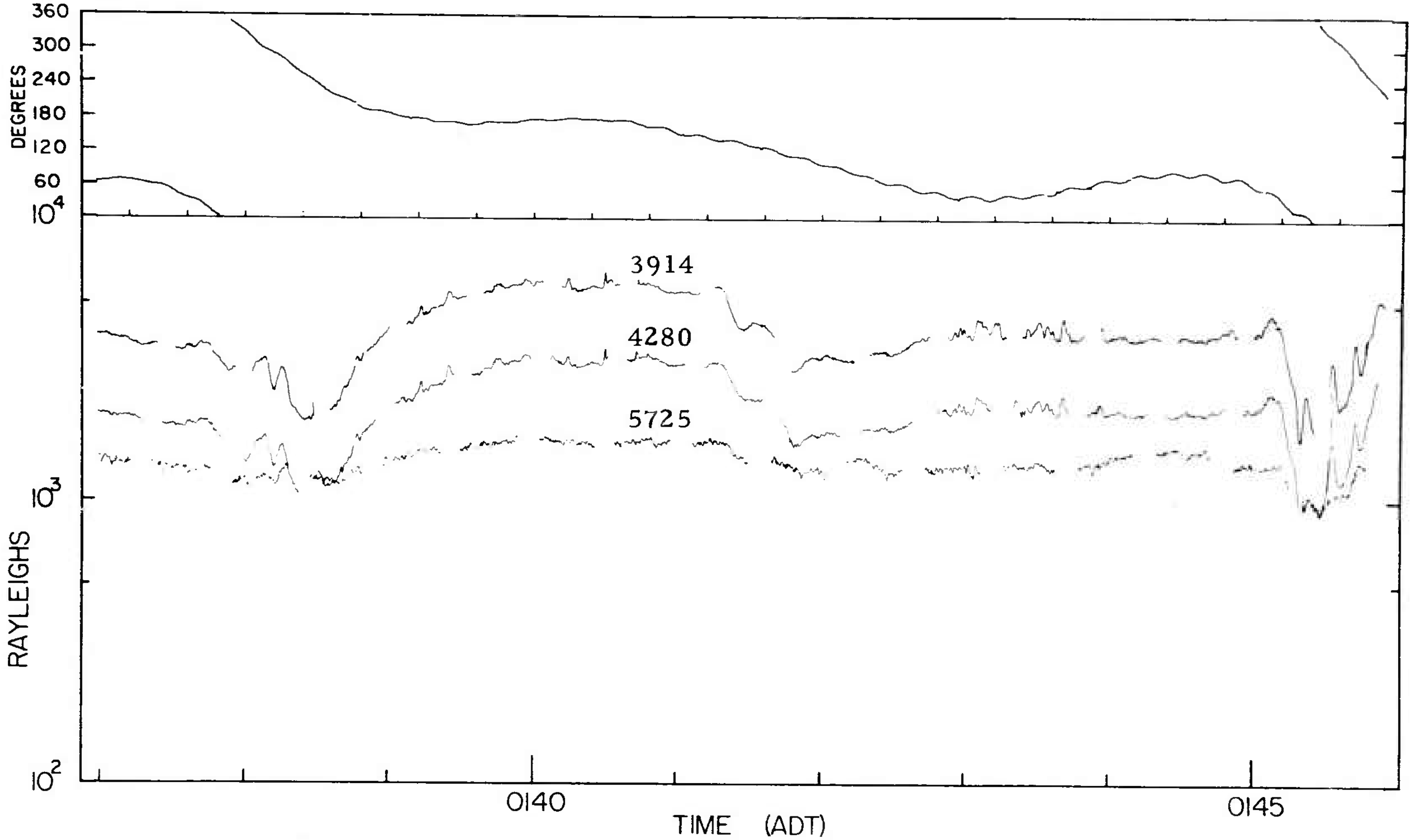

Figure 165. Auroral activity vs time for 15 September 1971.

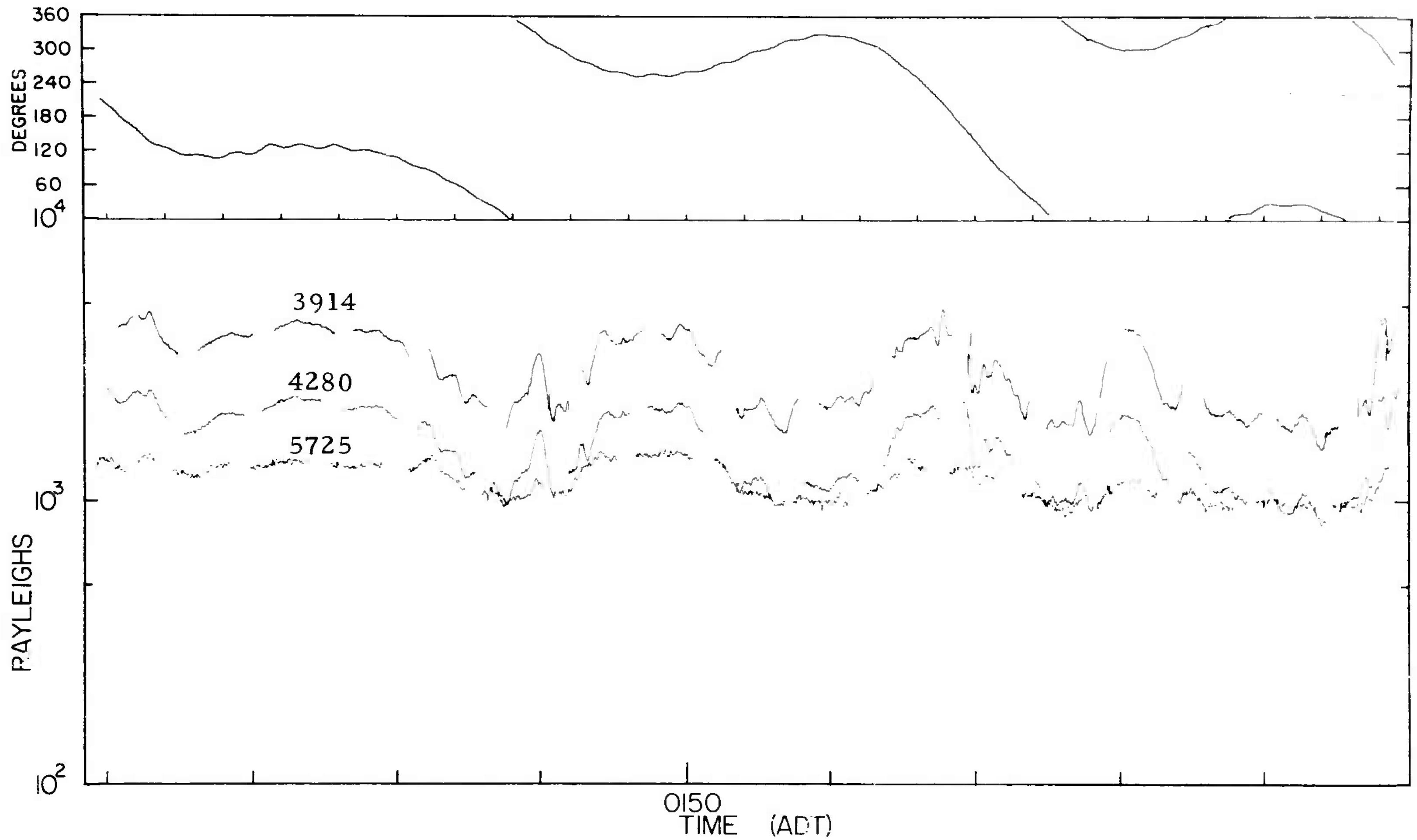

Figure 166. Auroral activity vs time for 15 September 1971.

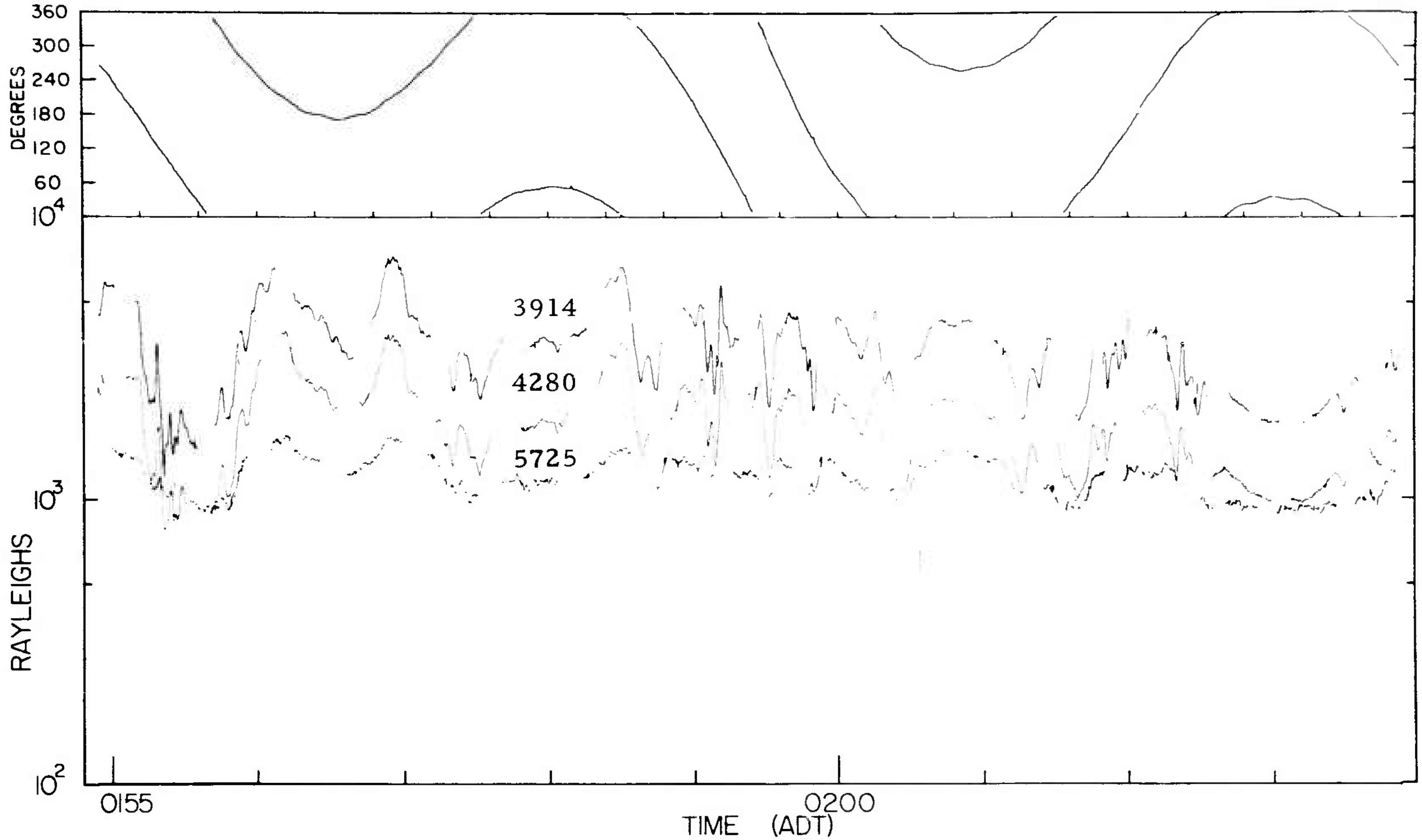

Figure 167. Auroral activity vs time for 15 September 1971.

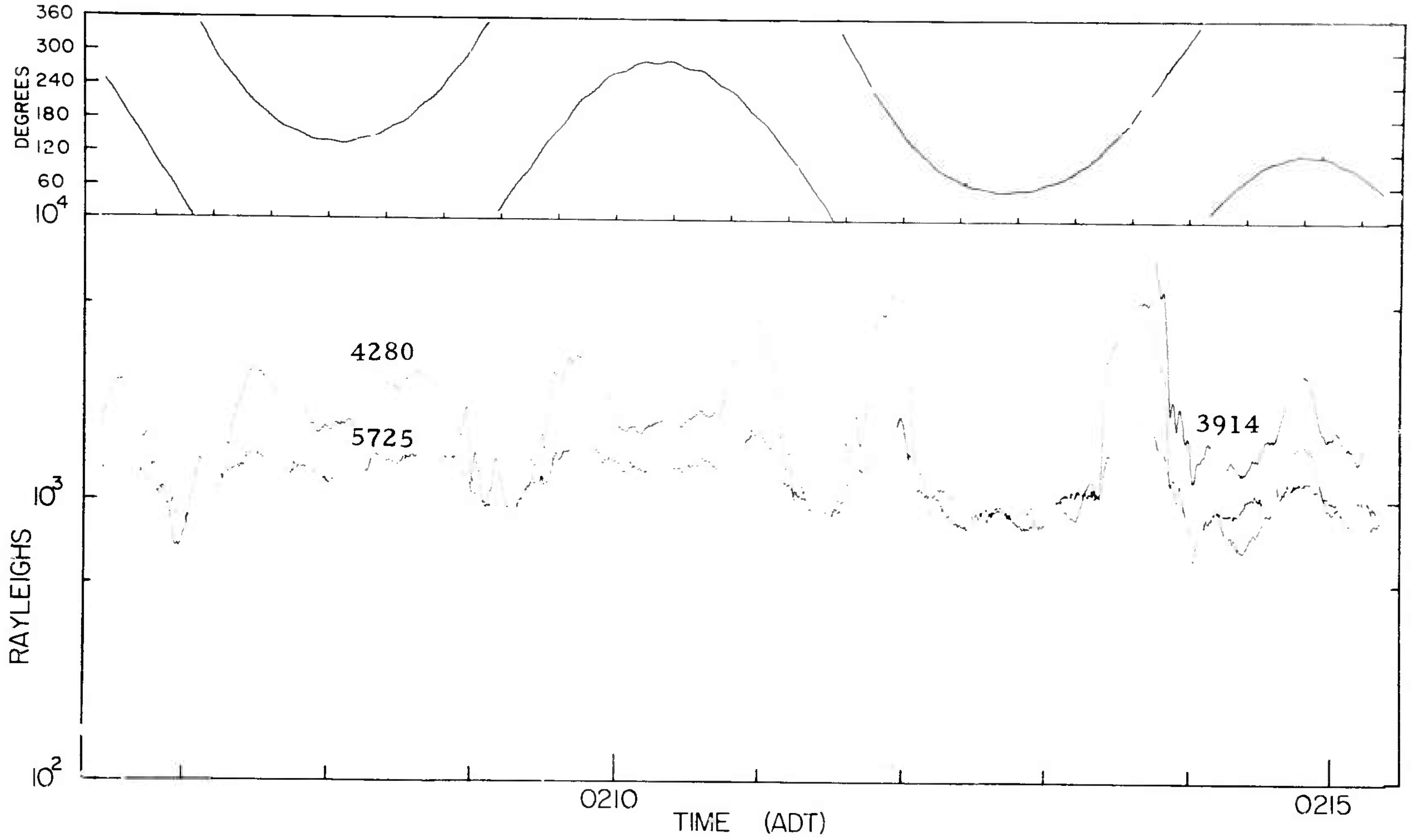

Figure 168. Auroral activity vs time for 15 September 1971.

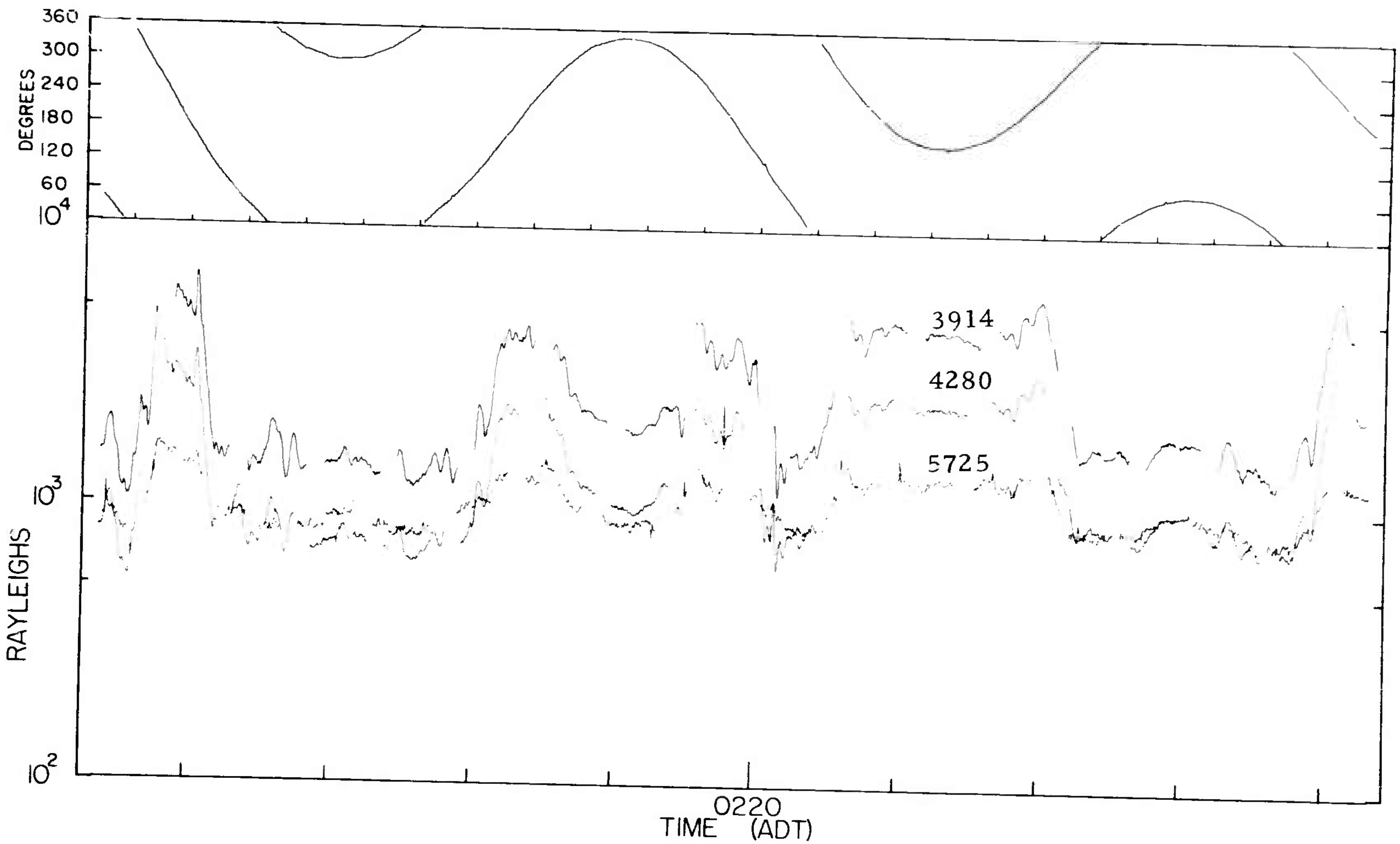

Figure 169. Auroral activity vs time for 15 September 1971.

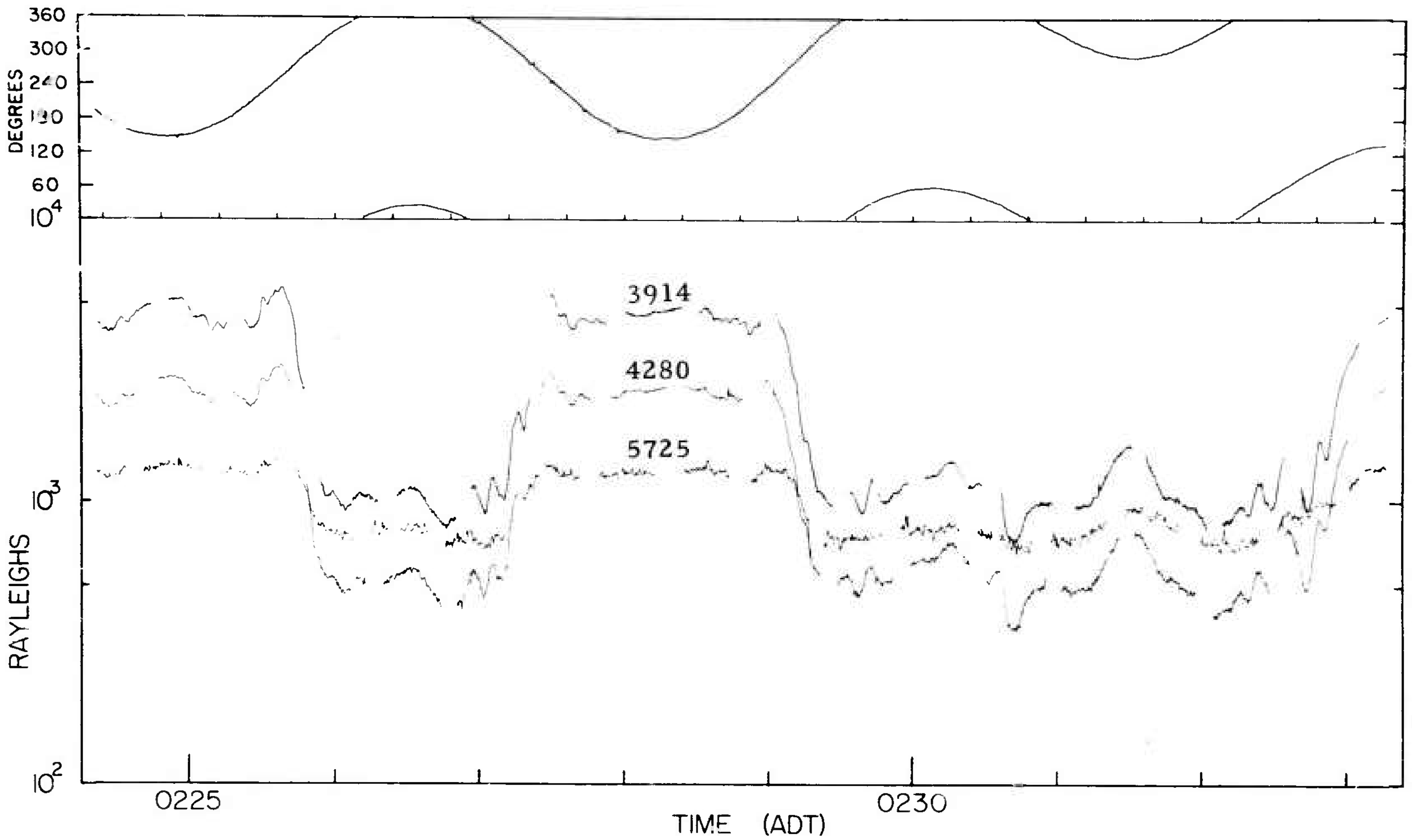

Figure 170. Auroral activity vs time for 15 September 1971.

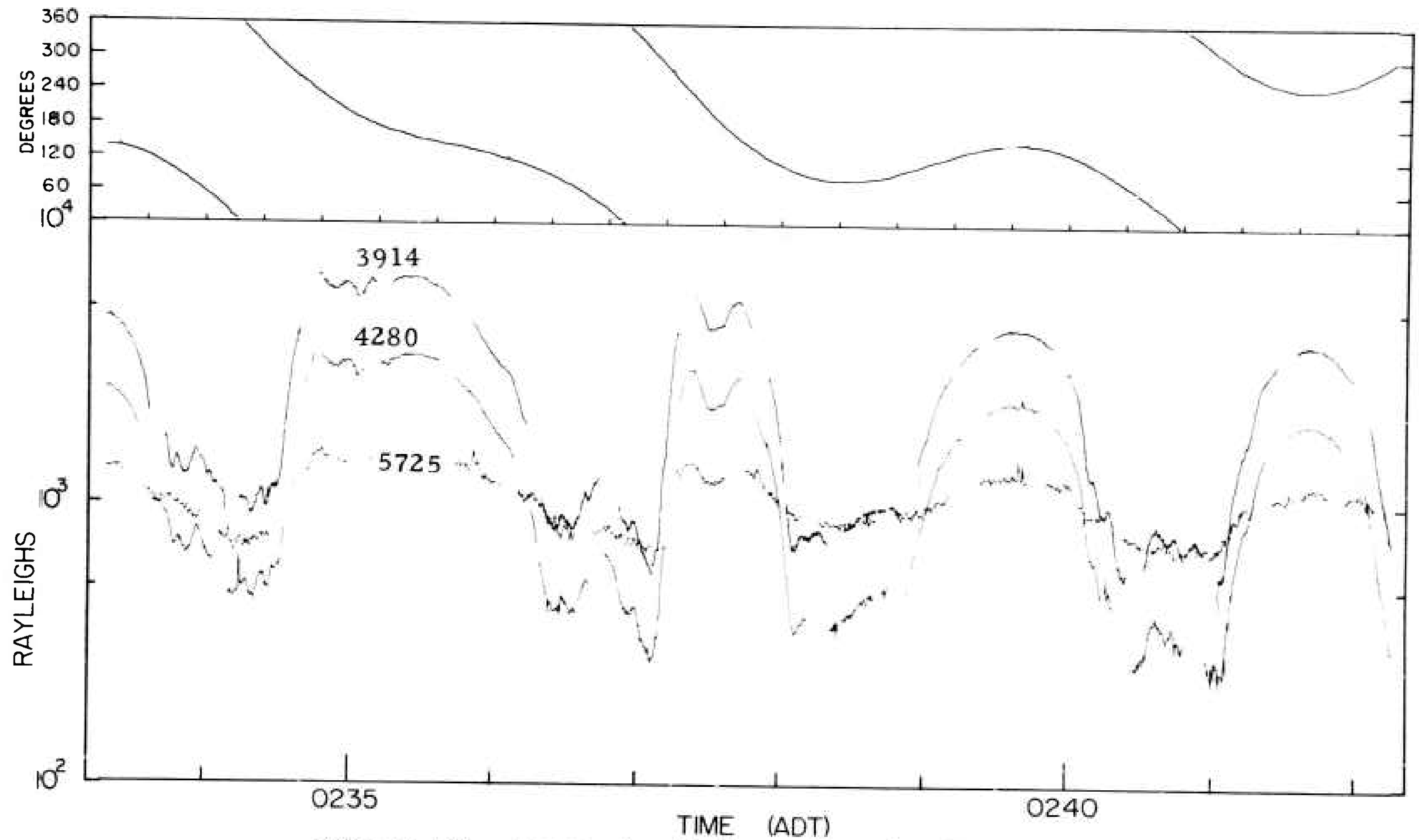

Figure 171. Auroral activity vs time for 15 September 1971.

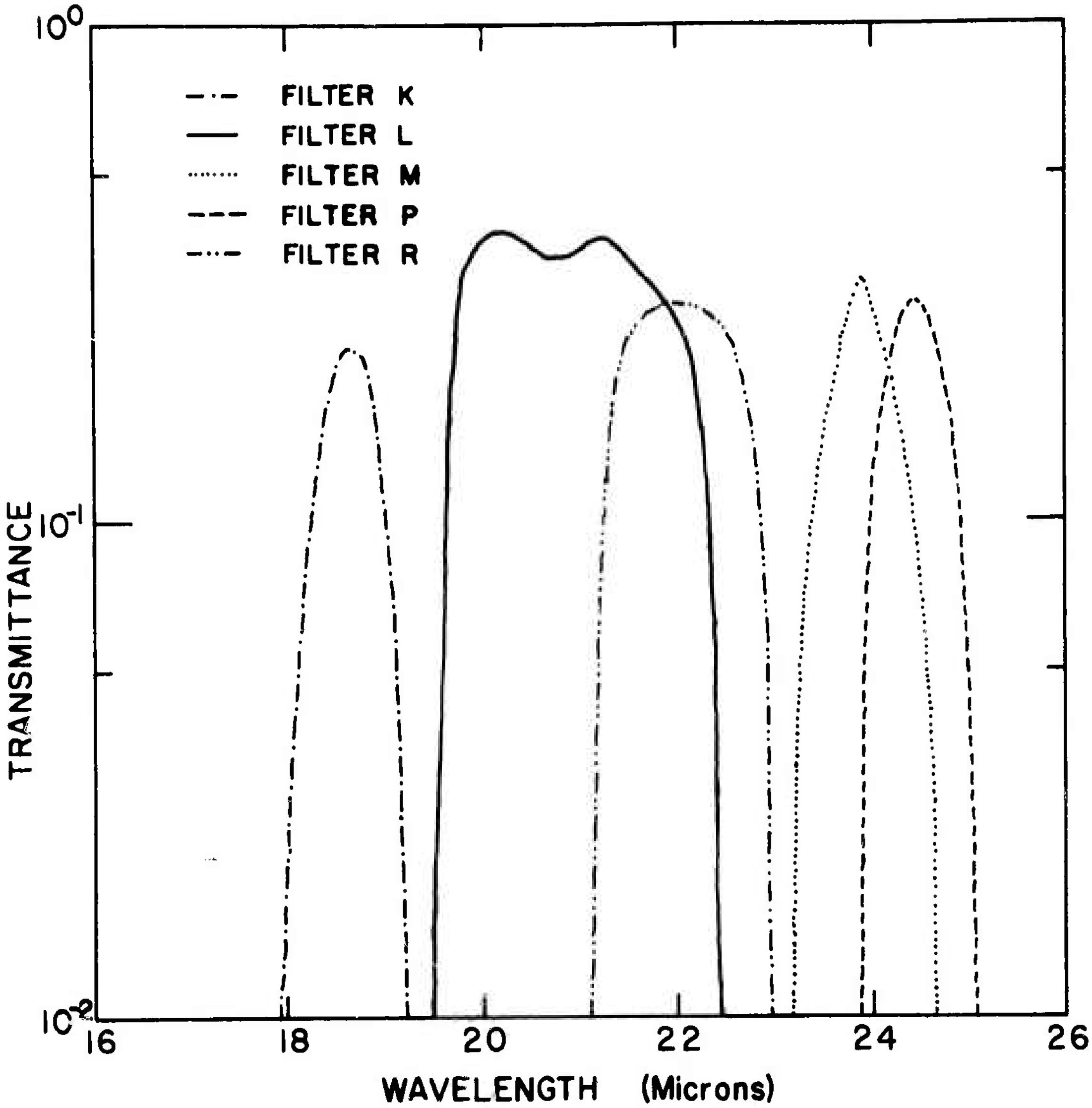

Figure 172. D. U. Filter Radiometer Curves for 23 September 1971, Fairbanks, Alaska.

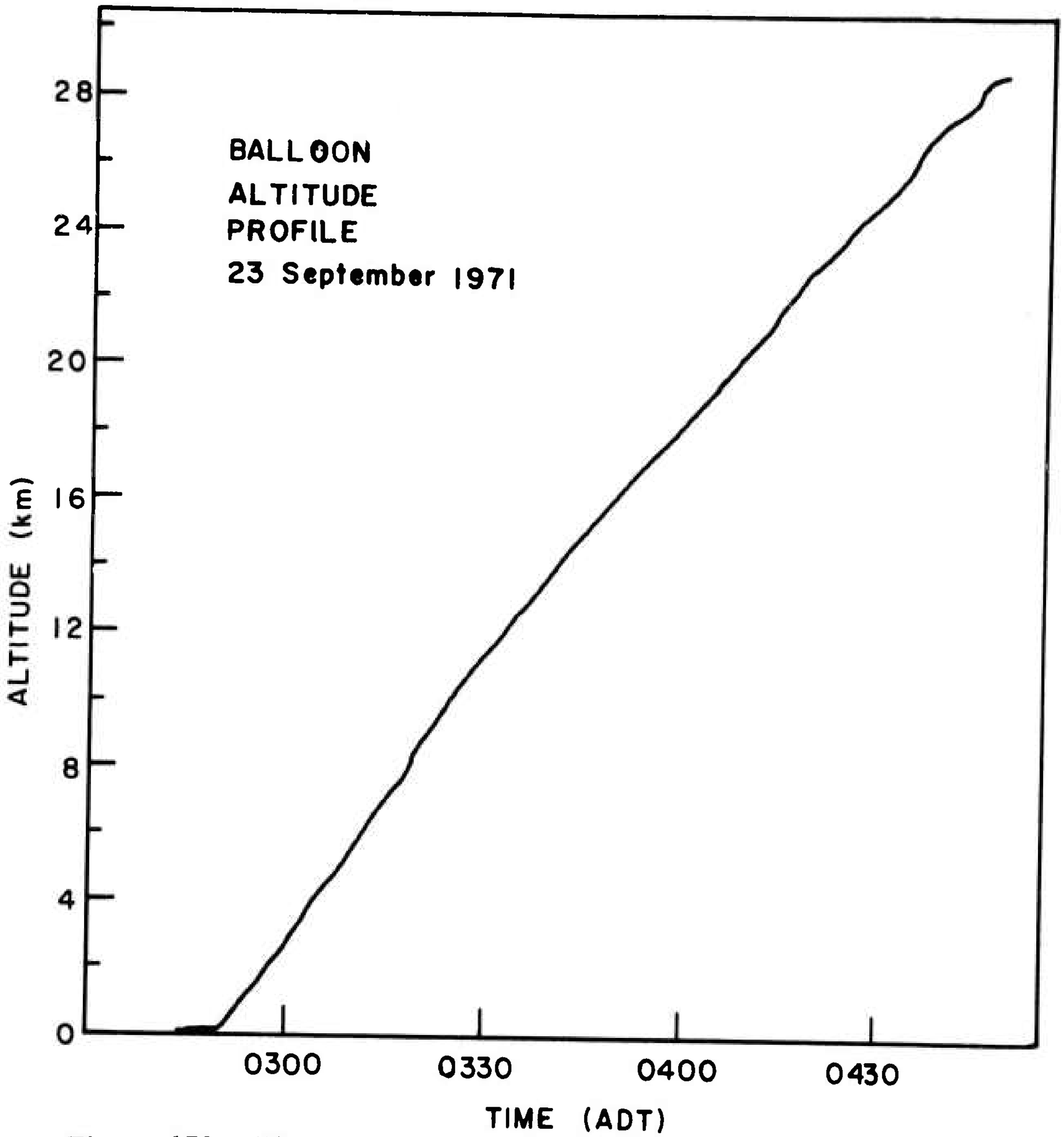

Figure 173. Time vs Altitude Profile of 23 September 1971 Balloon.

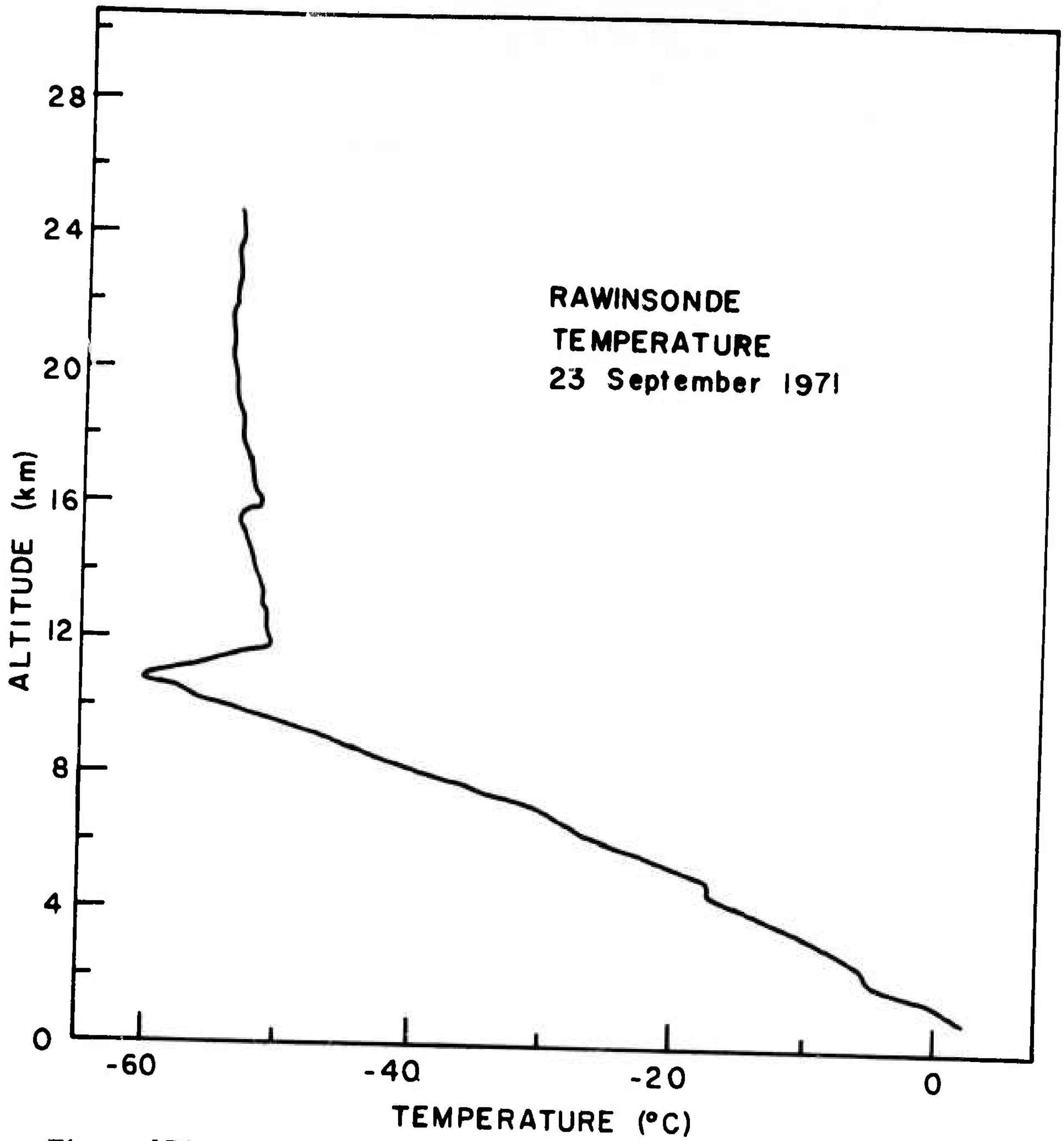

Figure 174. Rawinsonde Temperature vs Altitude for 23 September 1971, Fairbanks, Alaska.

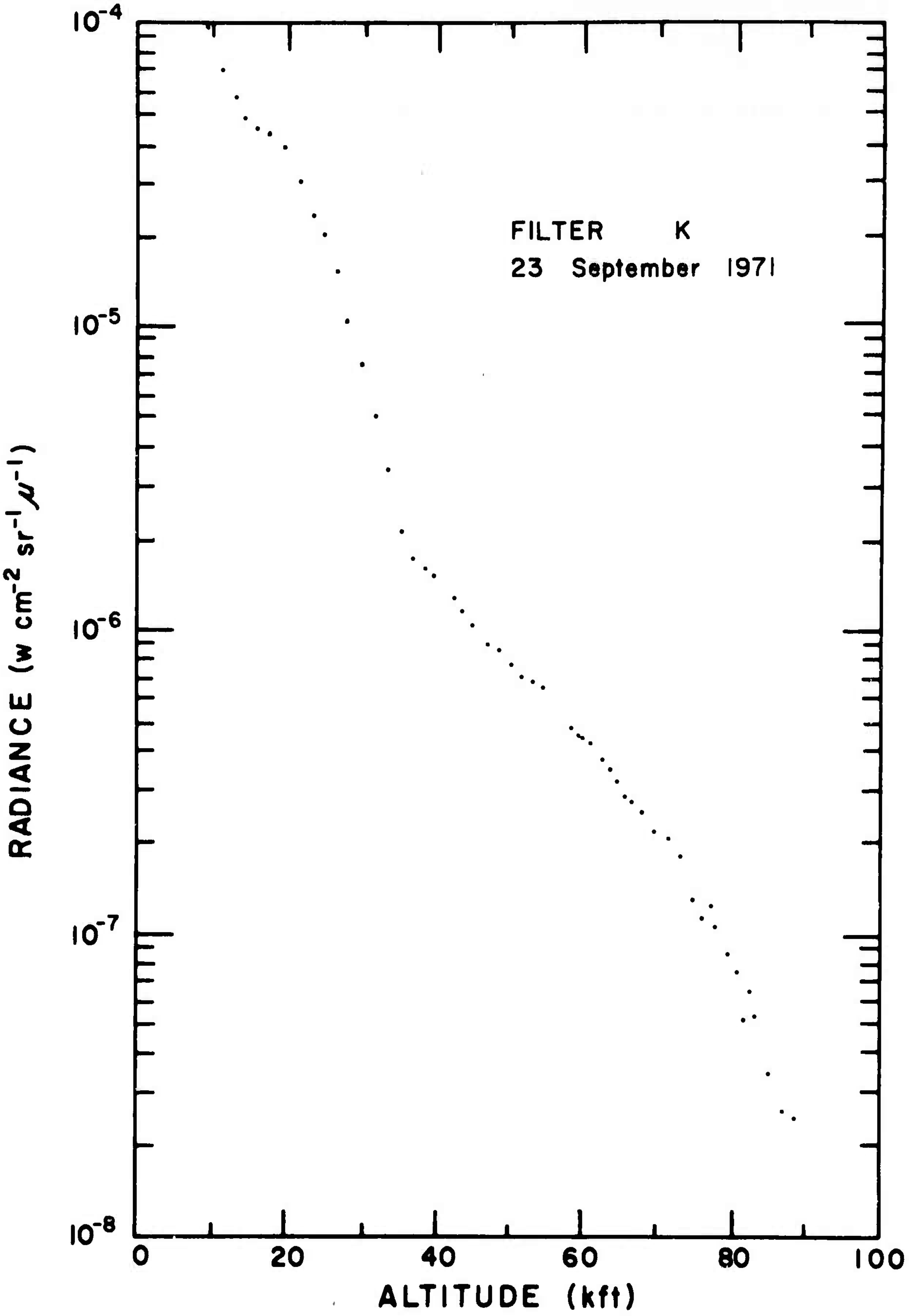

Figure 175. Radiance vs Altitude for Filter K, 23 September 1971.

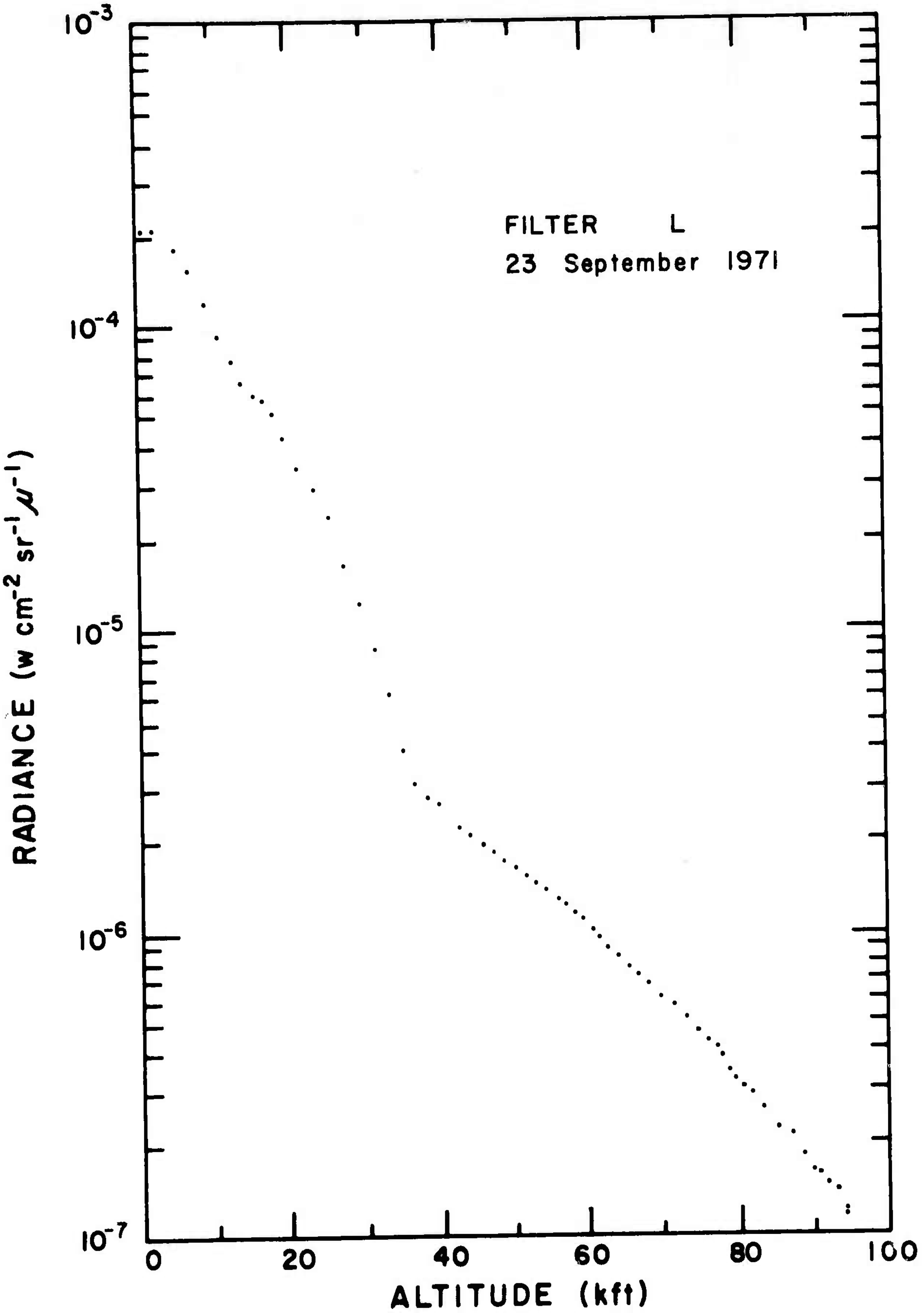

Figure 176. Radiance vs Altitude for Filter L, 23 September 1971.

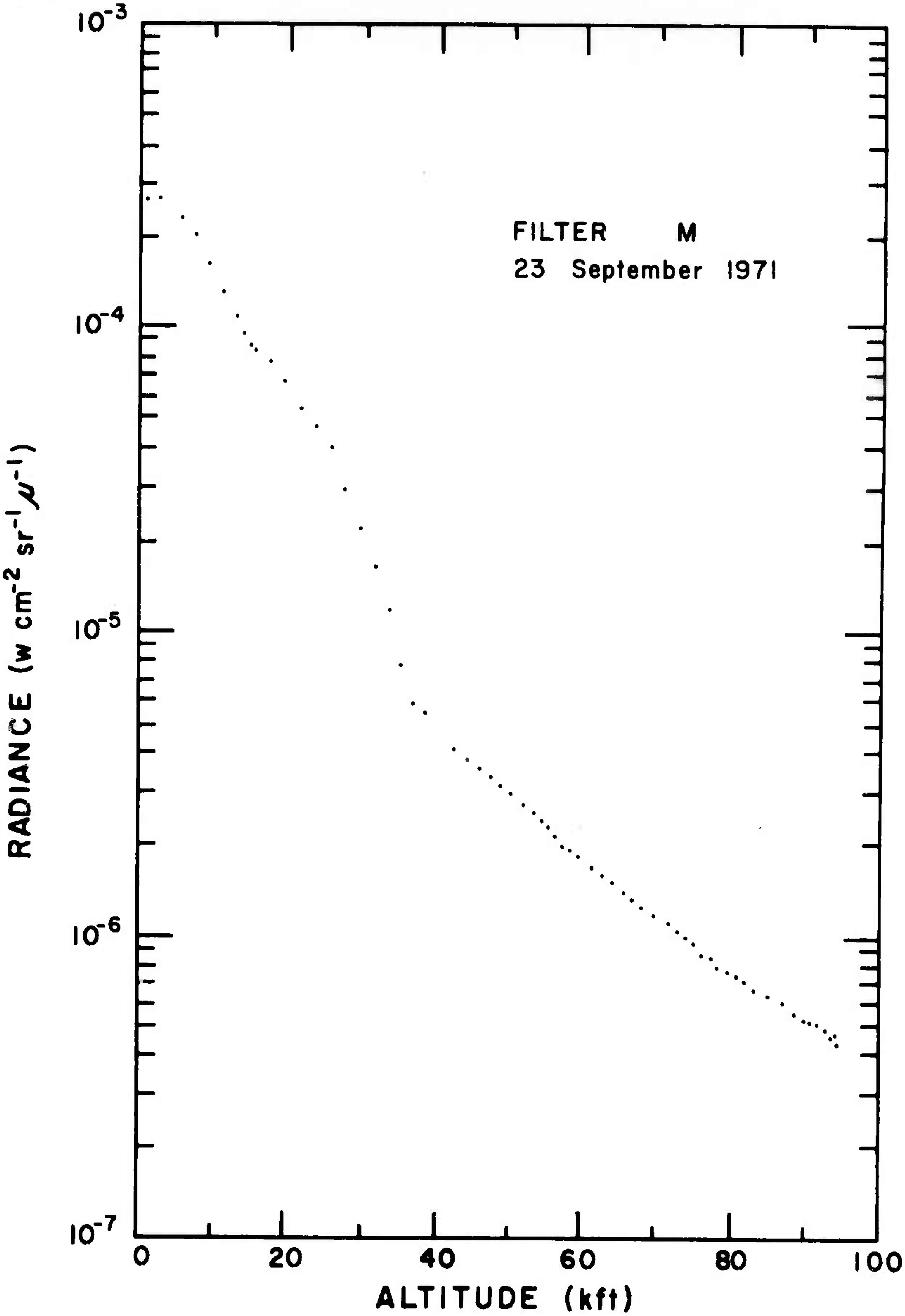

Figure 177. Radiance vs Altitude for Filter M, 23 September 1971.

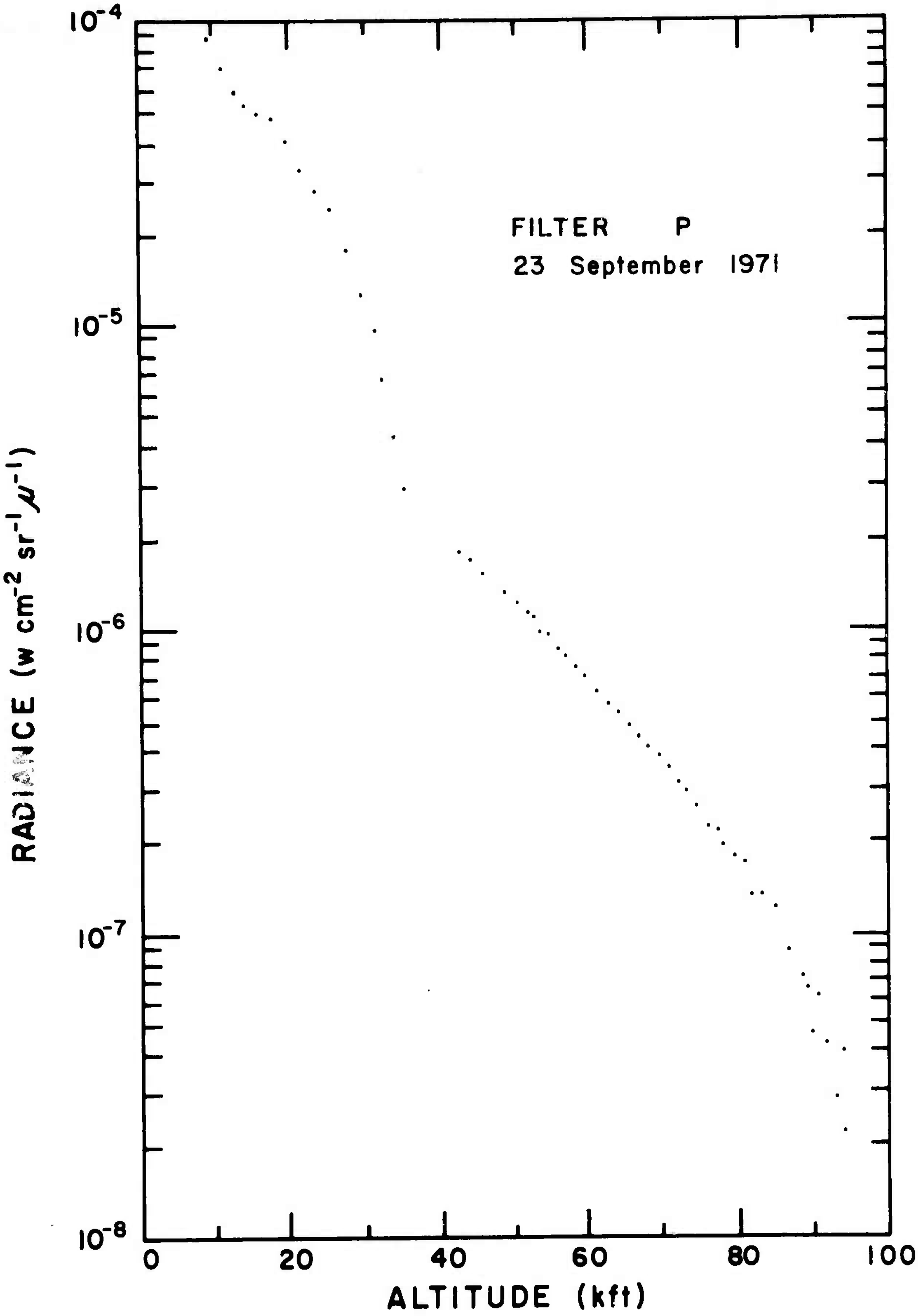

Figure 178. Radiance vs Altitude for Filter P, 23 September 1971.

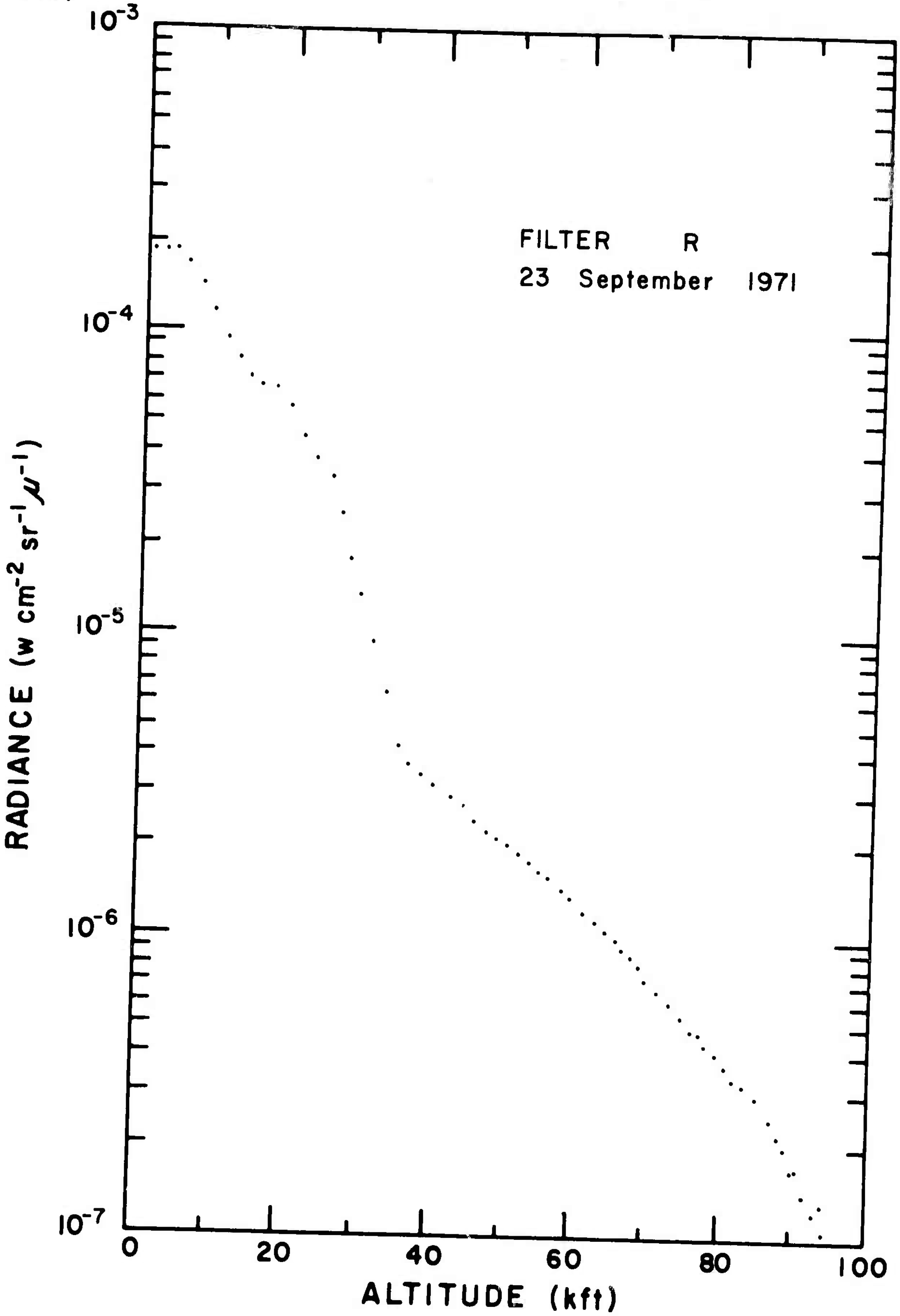

Figure 179. Radiance vs Altitude for Filter R, 23 September 1971.

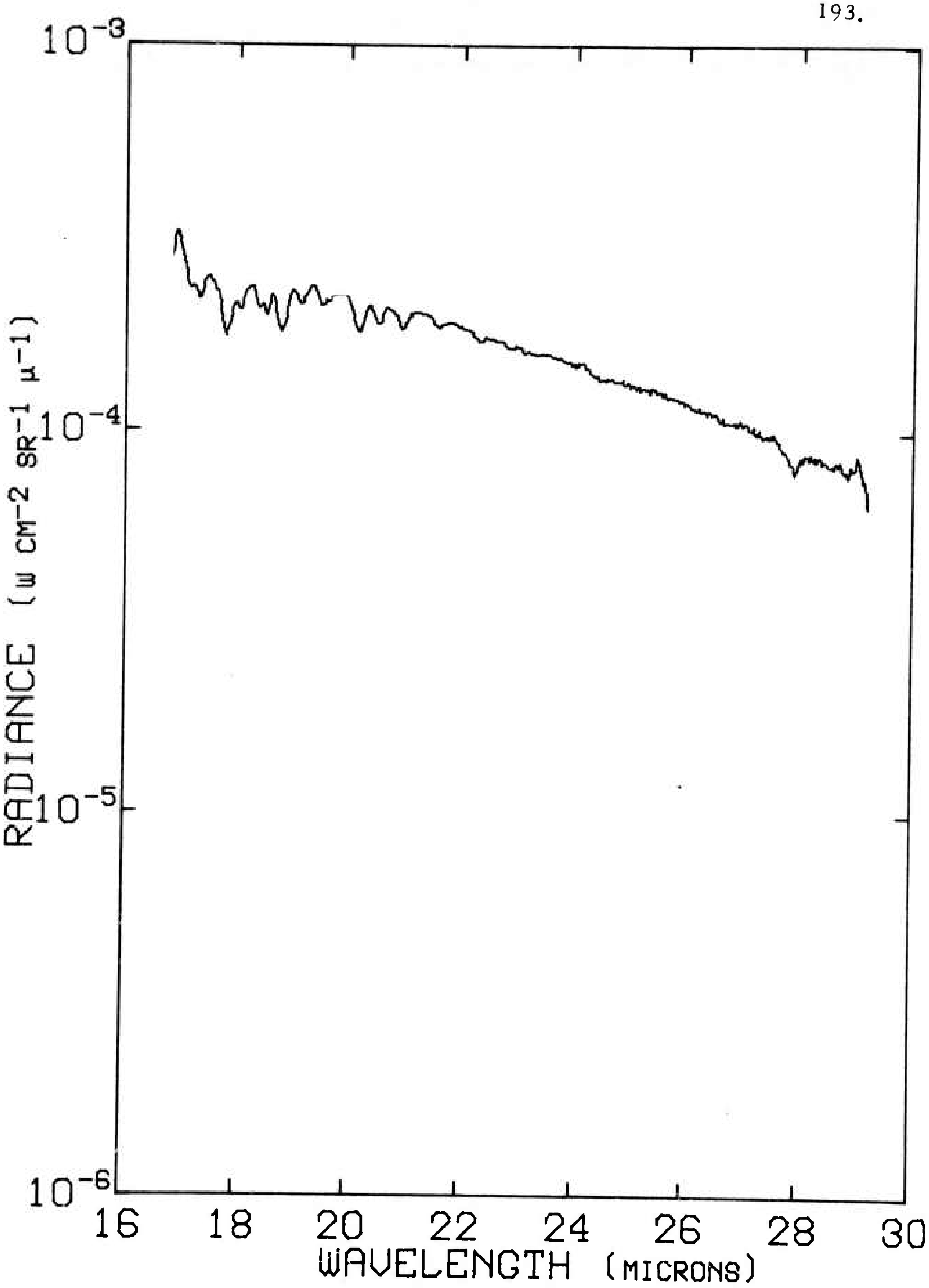

Figure 180. Radiance vs Wavelength at 3.8 kft and 0254 ADT, 23 September 1971.

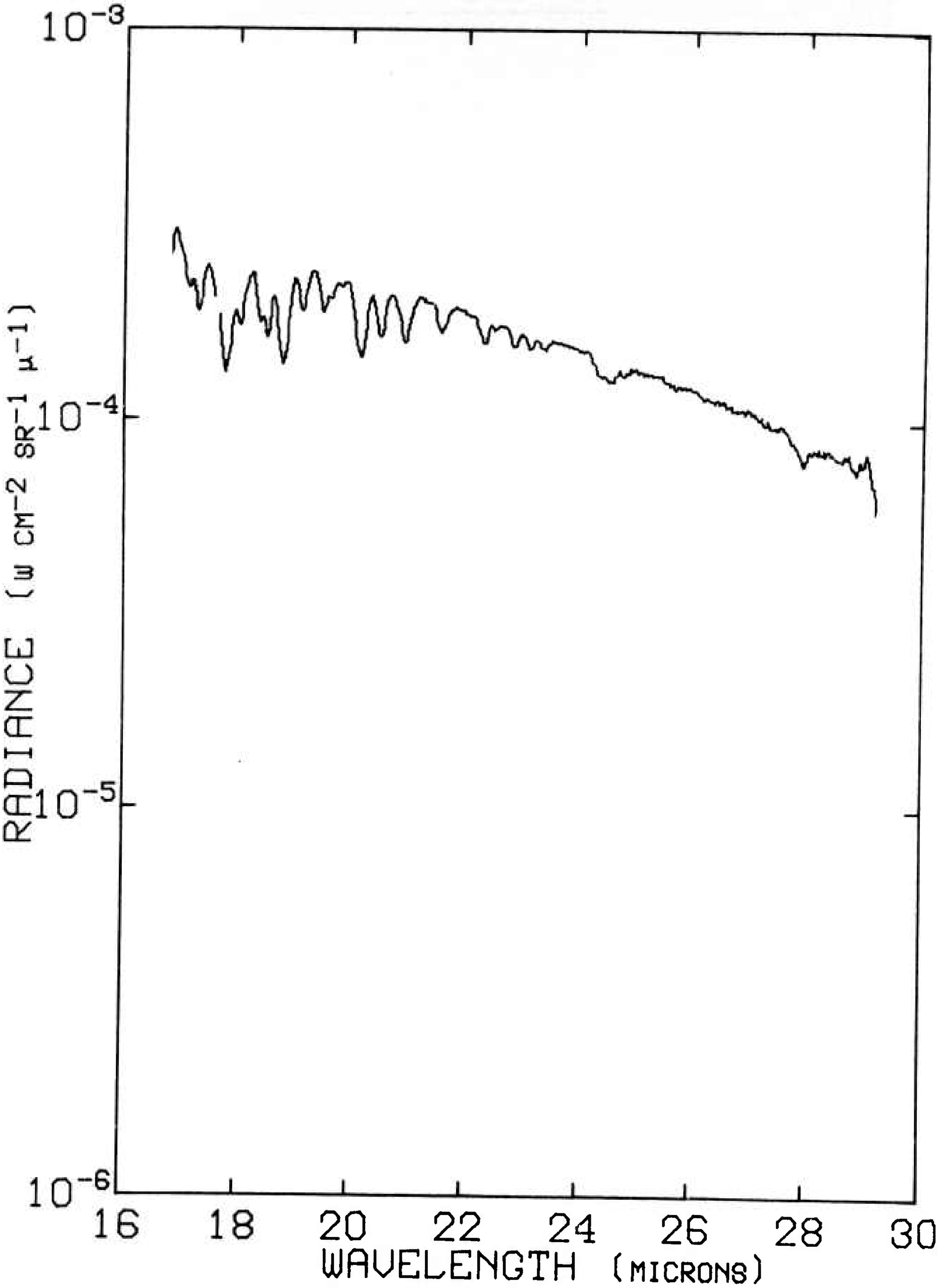

Figure 181. Radiance vs Wavelength at 5.5 kft and 0256 ADT, 23 September 1971.

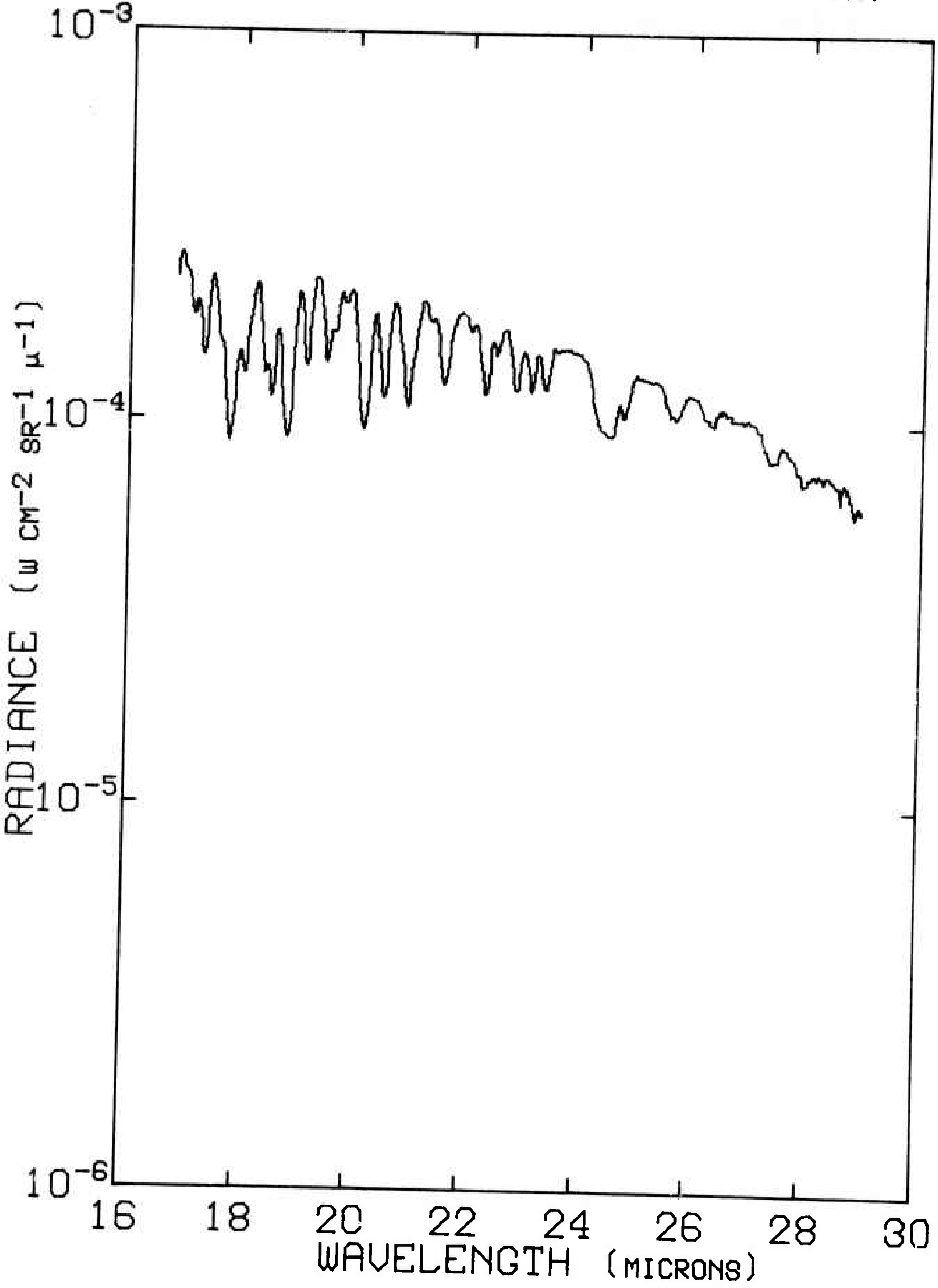

Figure 182. Radiance vs Wavelength at 7.3 kft and 0258 ADT, 23 September 1971.

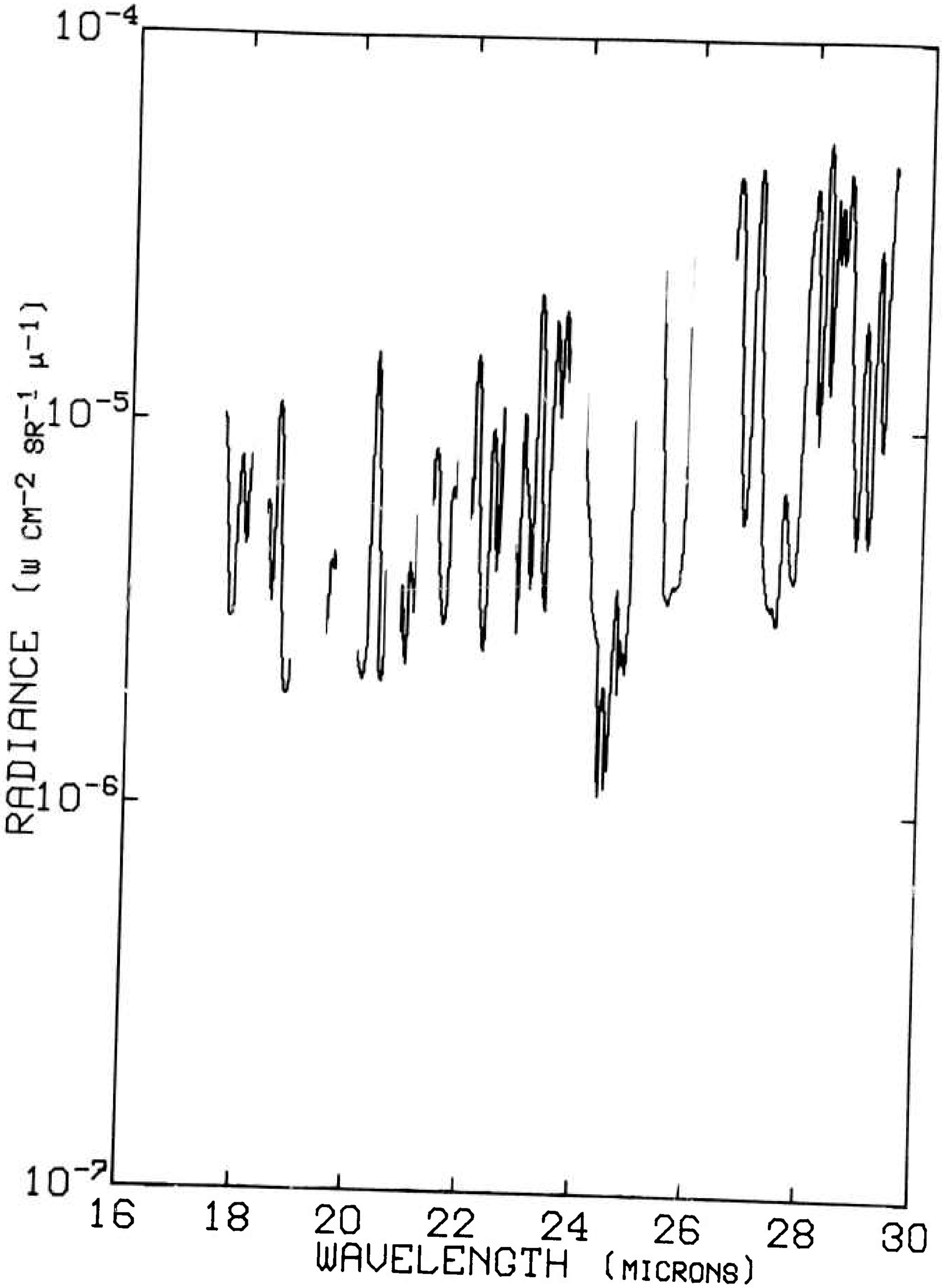

Figure 183. Radiance vs Wavelength at 29.5 kft and 0321 ADT, 23 September 1971.

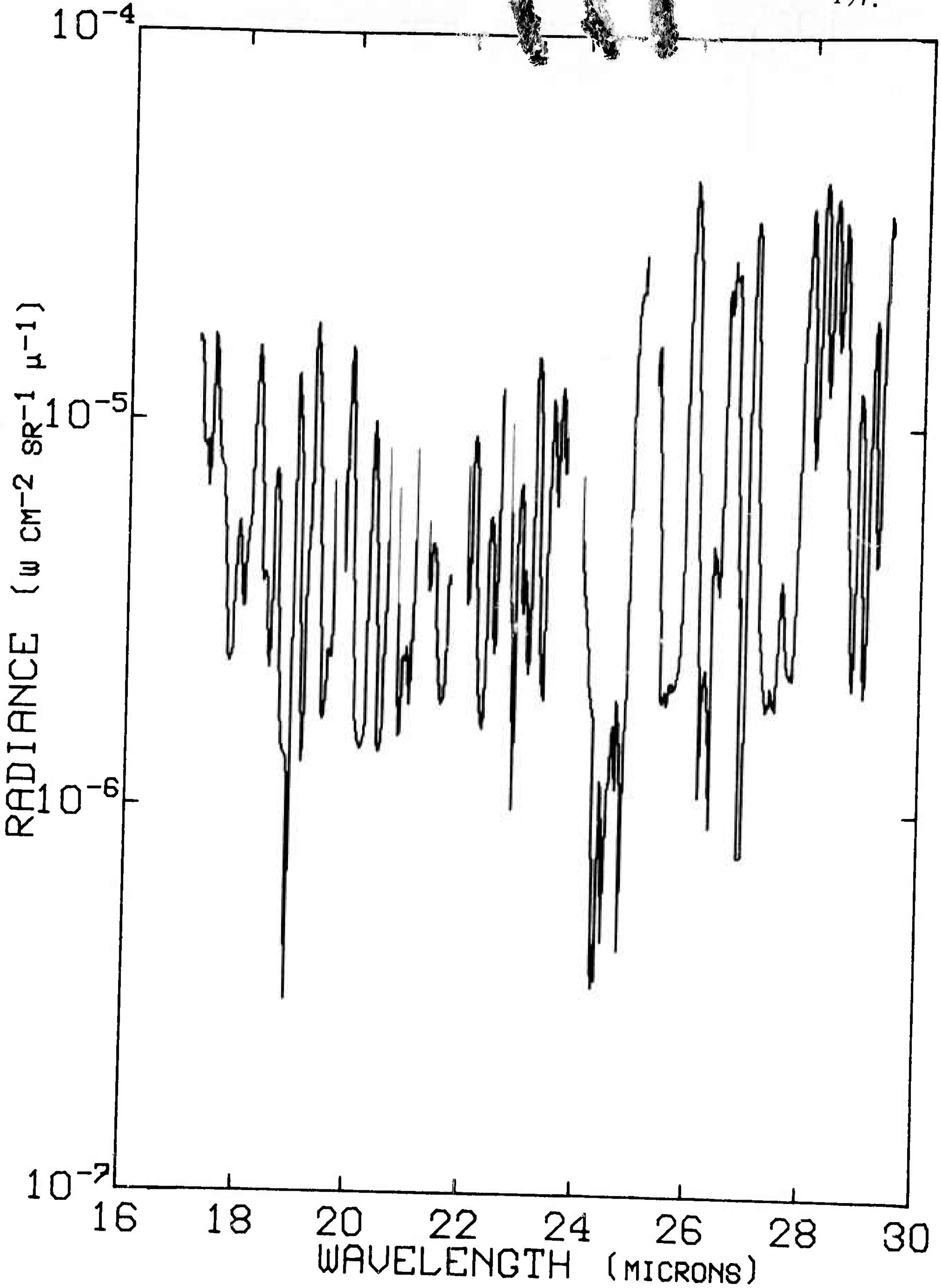

Figure 184. Radiance vs Wavelength at 31.4 kft and 0323 ADT, 23 September 1971.

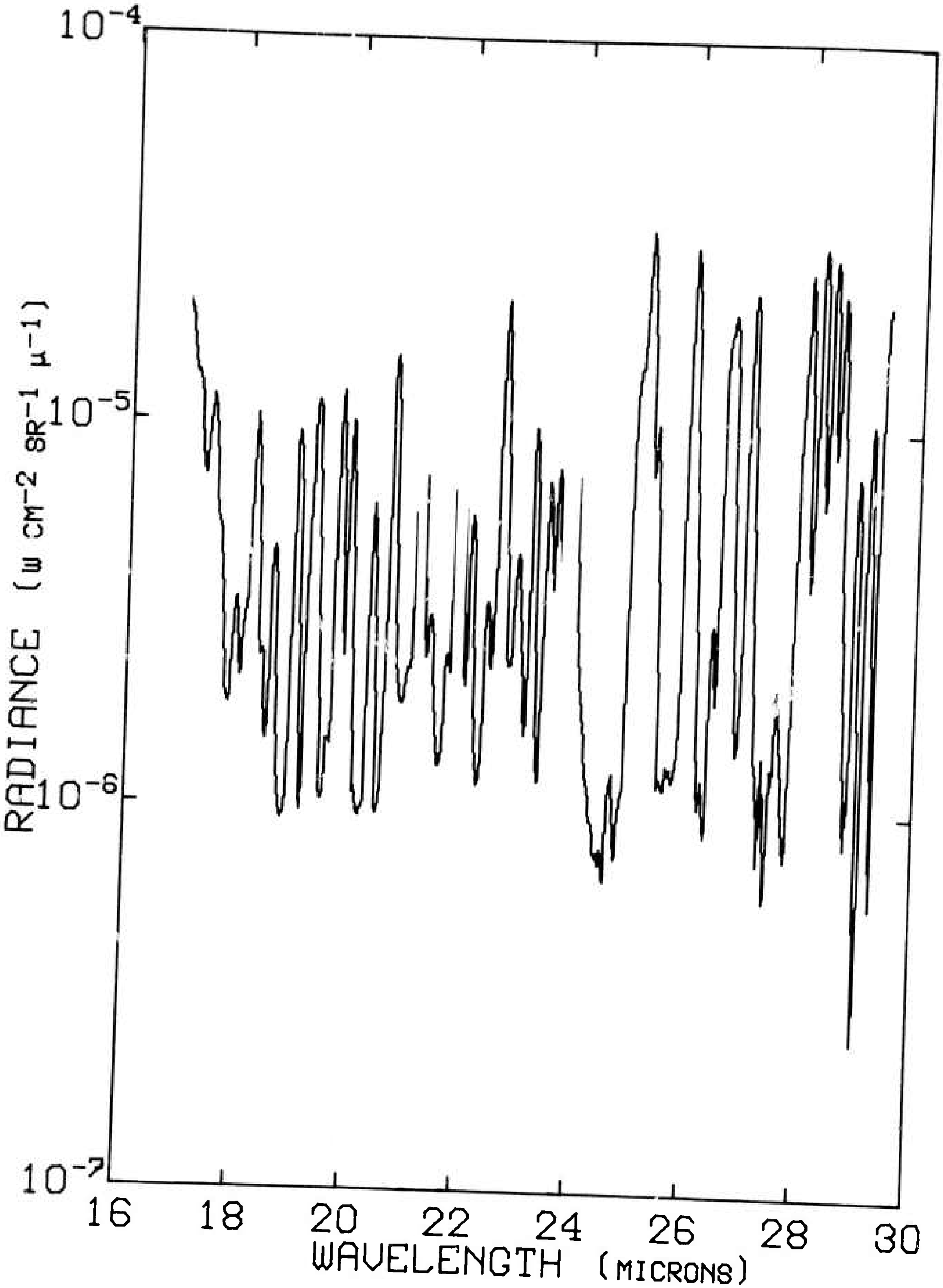

Figure 185. Radiance vs Wavelength at 33.2 kft and 0325 ADT, 23 September 1971.

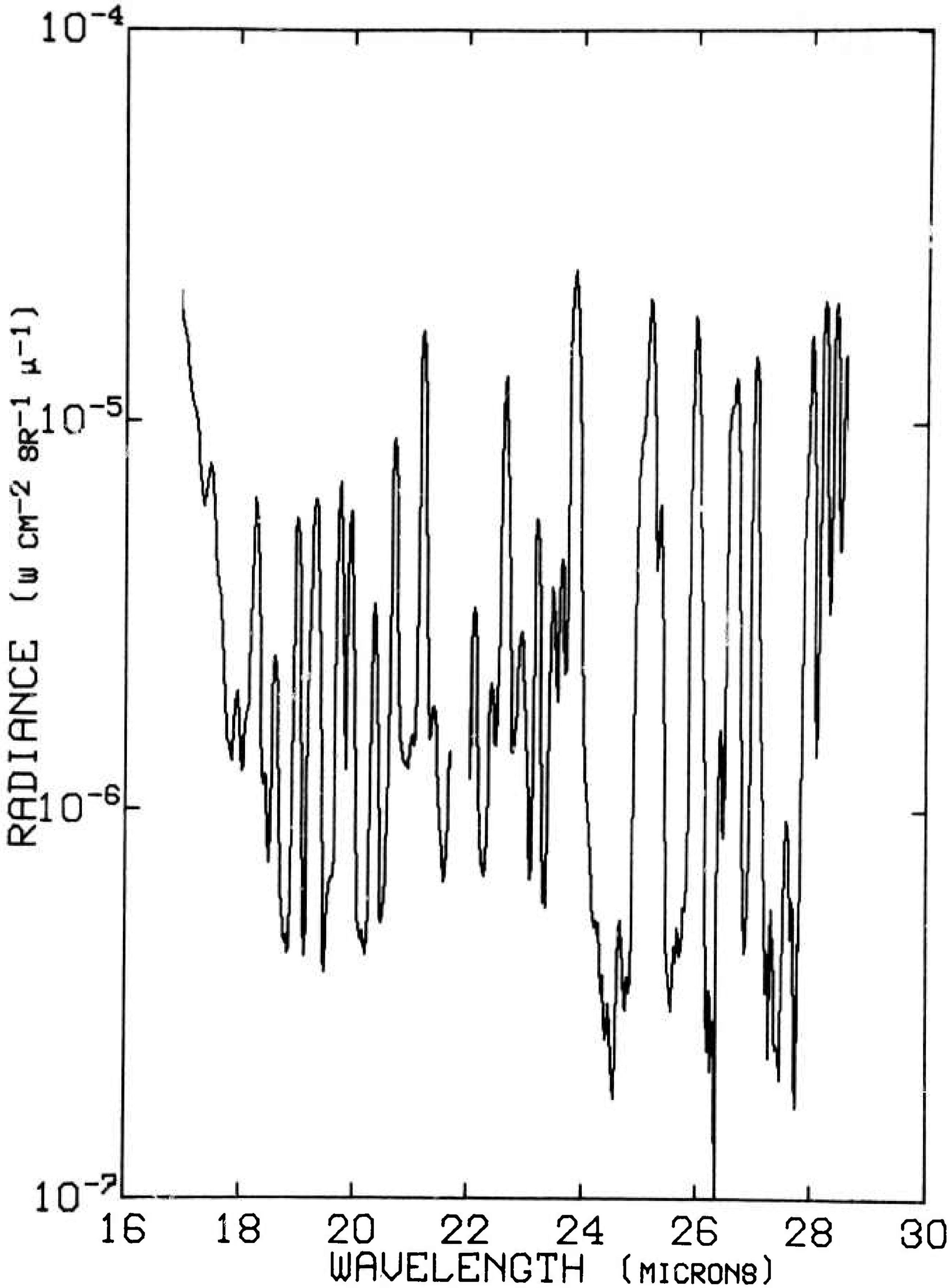

Figure 186. Radiance vs Wavelength at 35.0 kft and 0327 ADT, 23 September 1971.

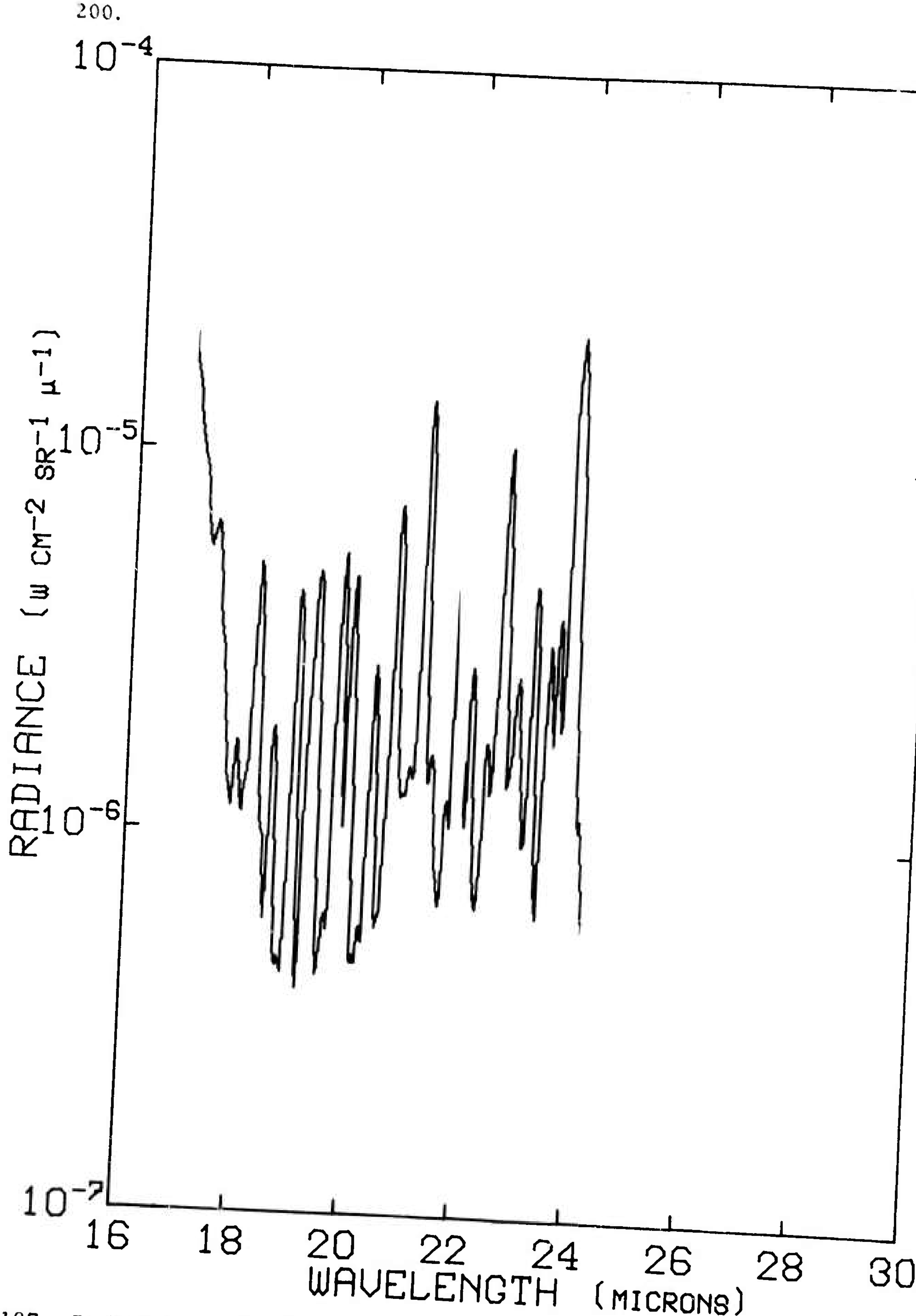

Figure 187. Radiance vs Wavelength at 36.6 kft and 0329 ADT, 23 September 1971.

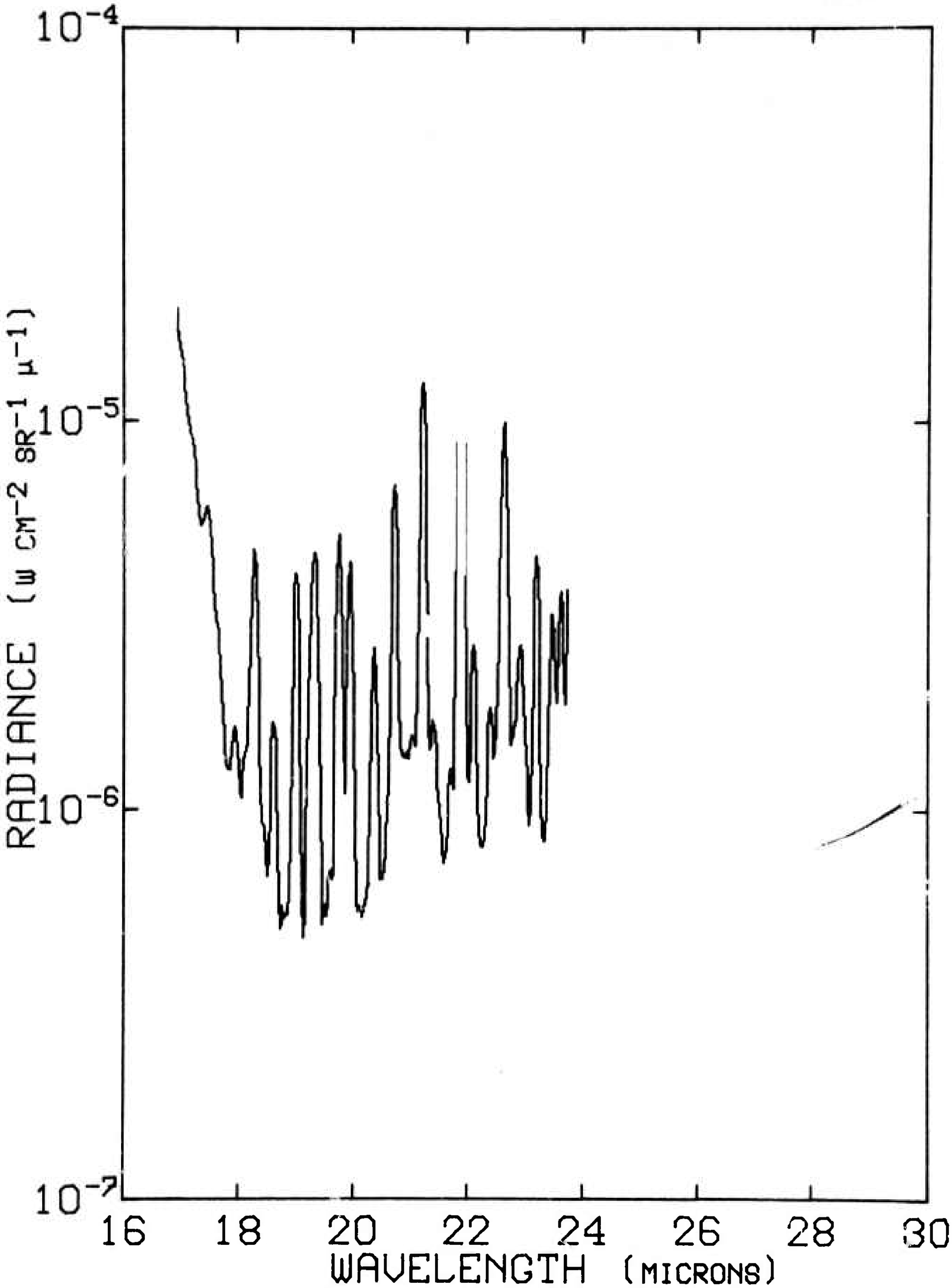

Figure 188. Radiance vs Wavelength at 38.2 kft and 0331 ADT, 23 September 1971.

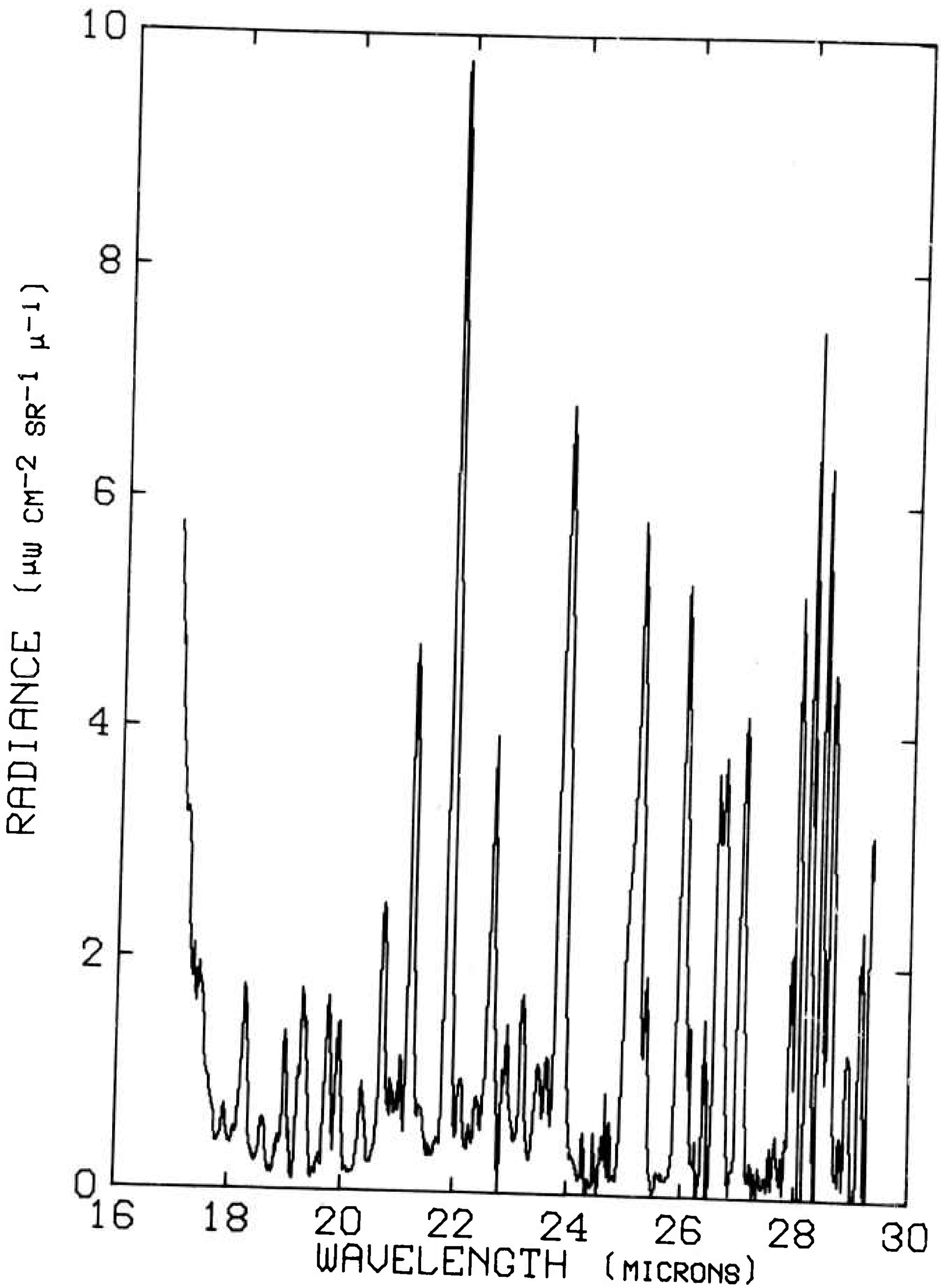

Figure 189. Radiance vs Wavelength at 59.6 kft and 0359 ADT, 23 September 1971.

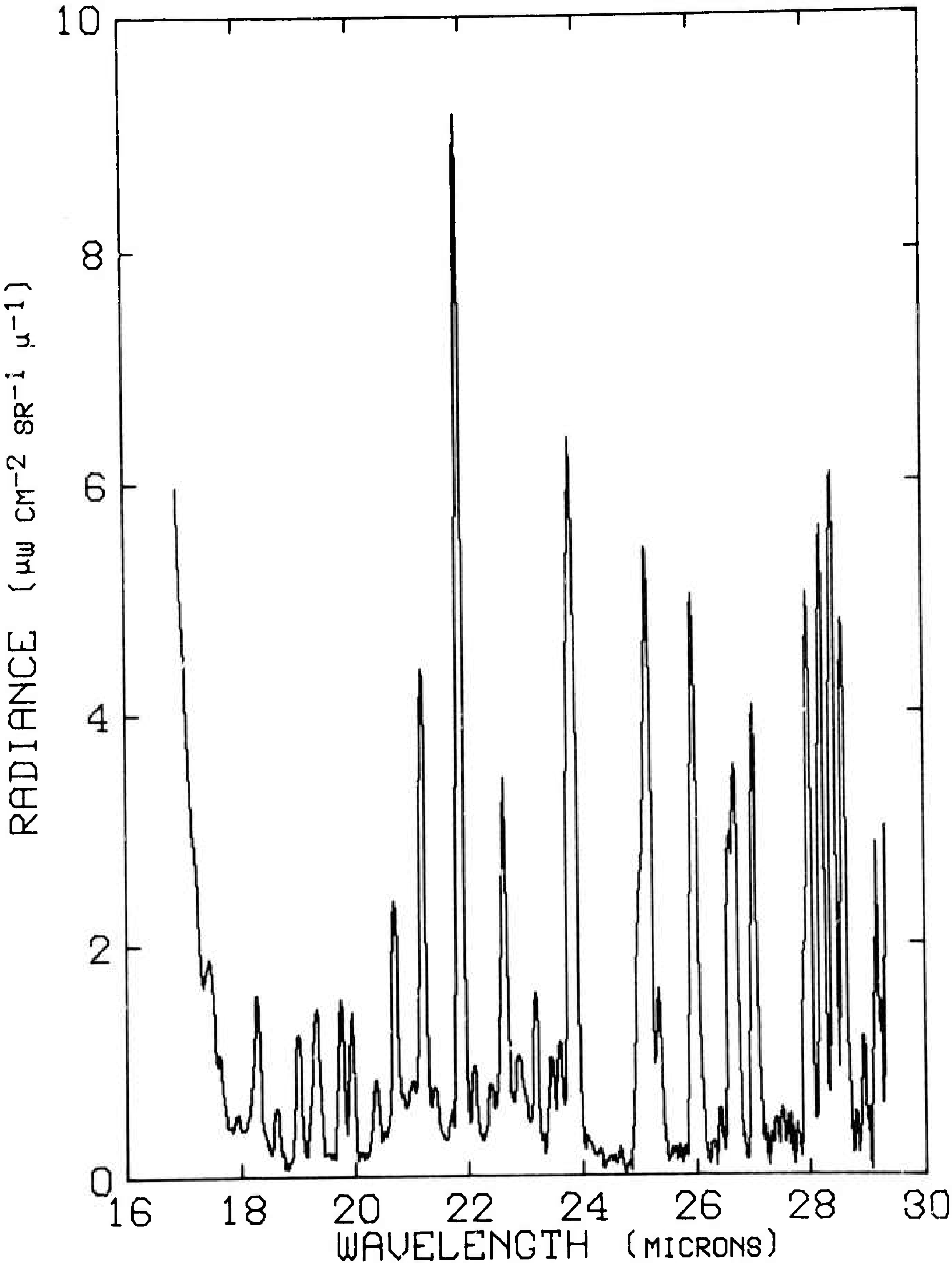

Figure 190. Radiance vs Wavelength at 61.0 kft and 0401 ADT. 23 September 1971.

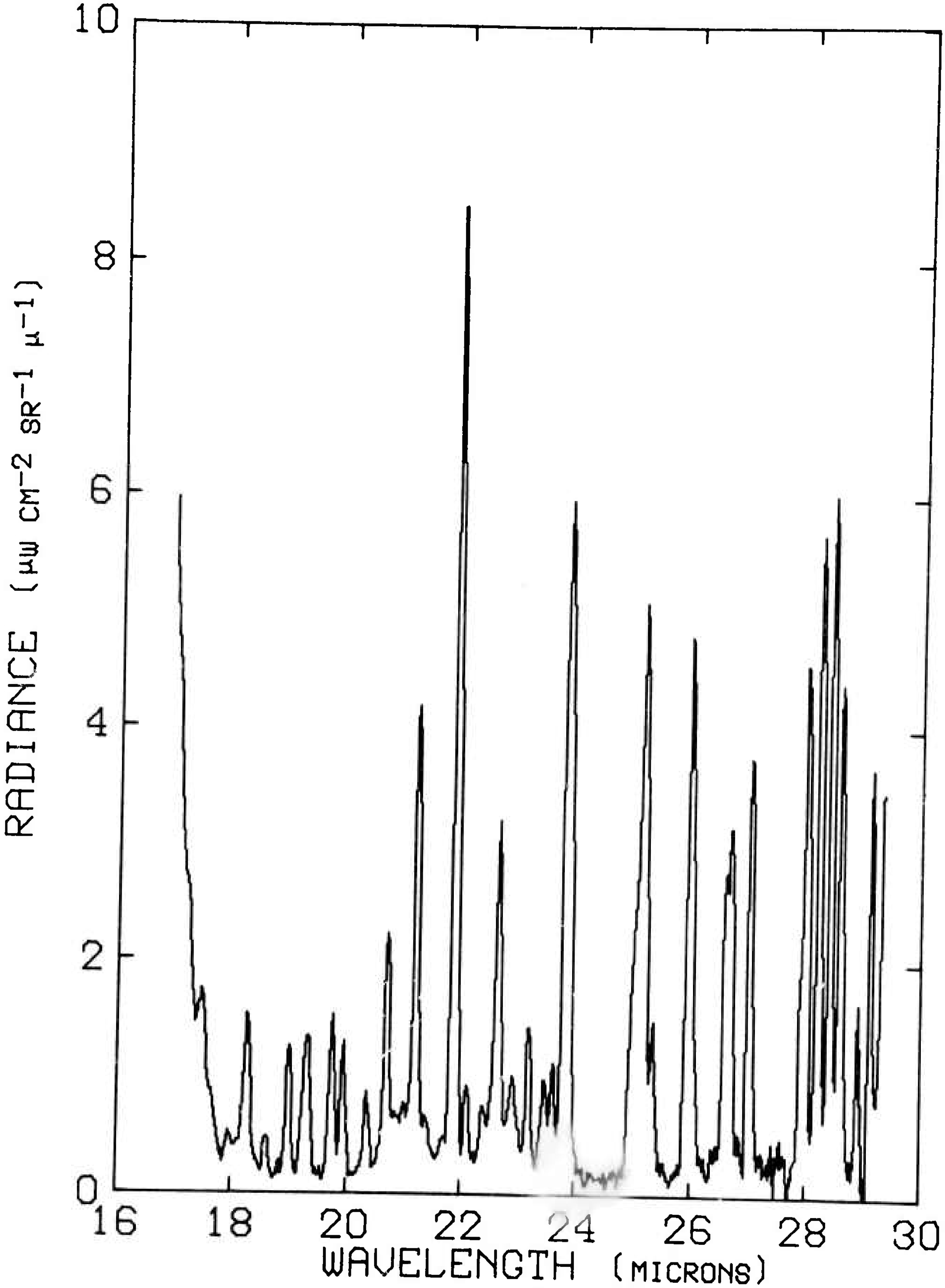

Figure 191. Radiance vs Wavelength at 62.5 kft and 0403 ADT, 23 September 1971.

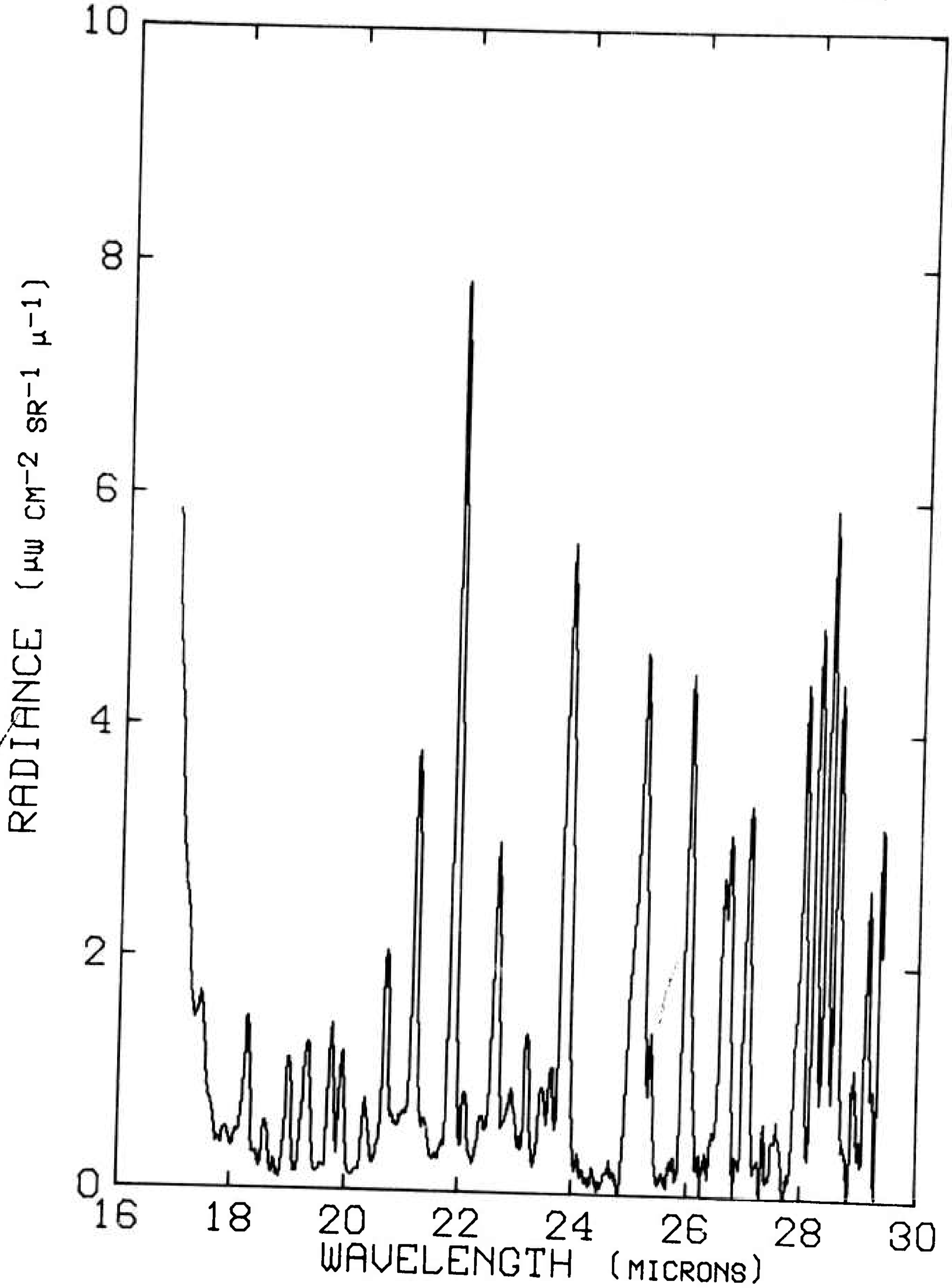

Figure 192. Radiance vs Wavelength at 64.0 kft and 0405 ADT, 23 September 1971.

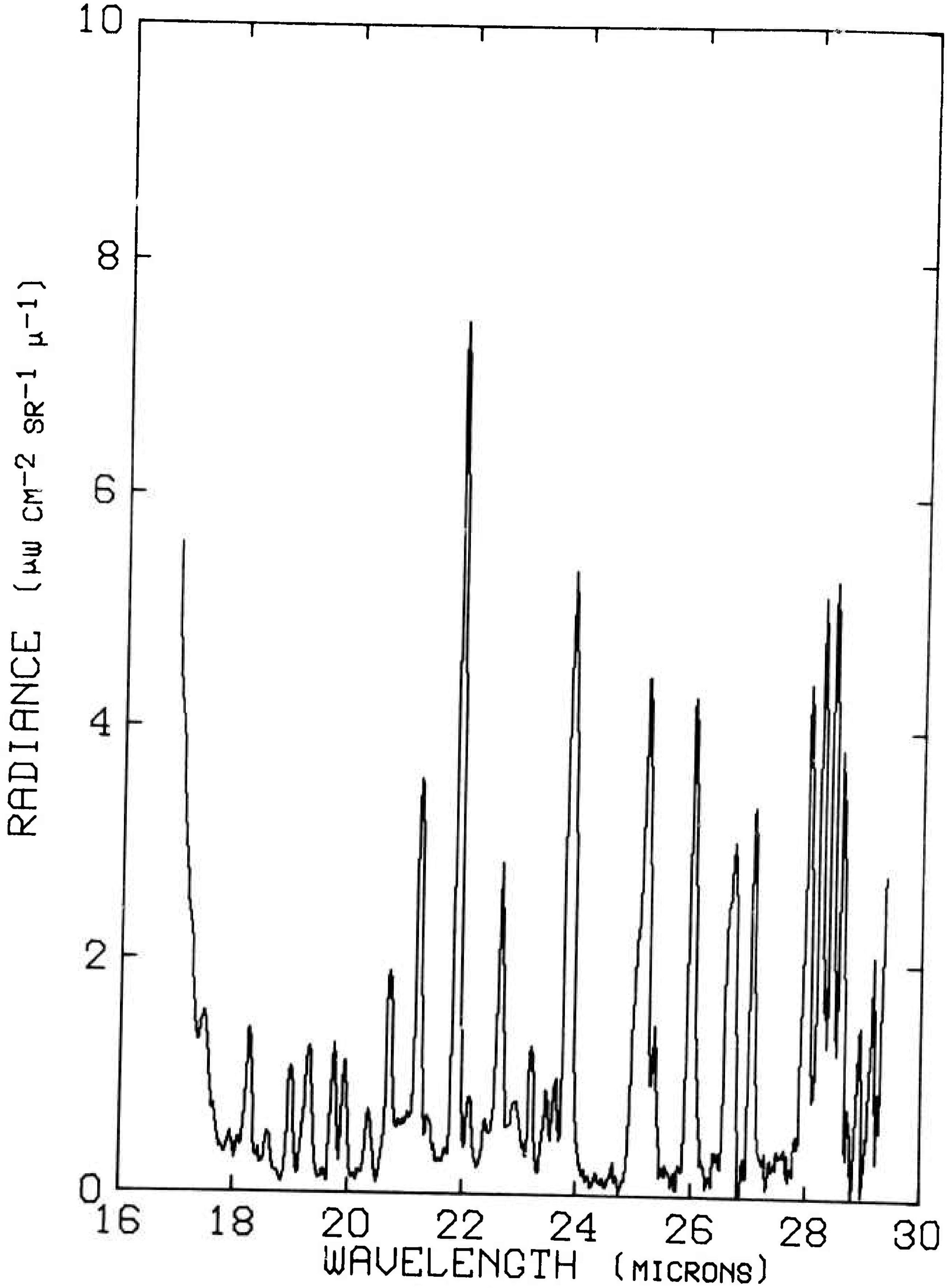

Figure 193. Radiance vs Wavelength at 65.5 kft and 0407 ADT, 23 September 1971.

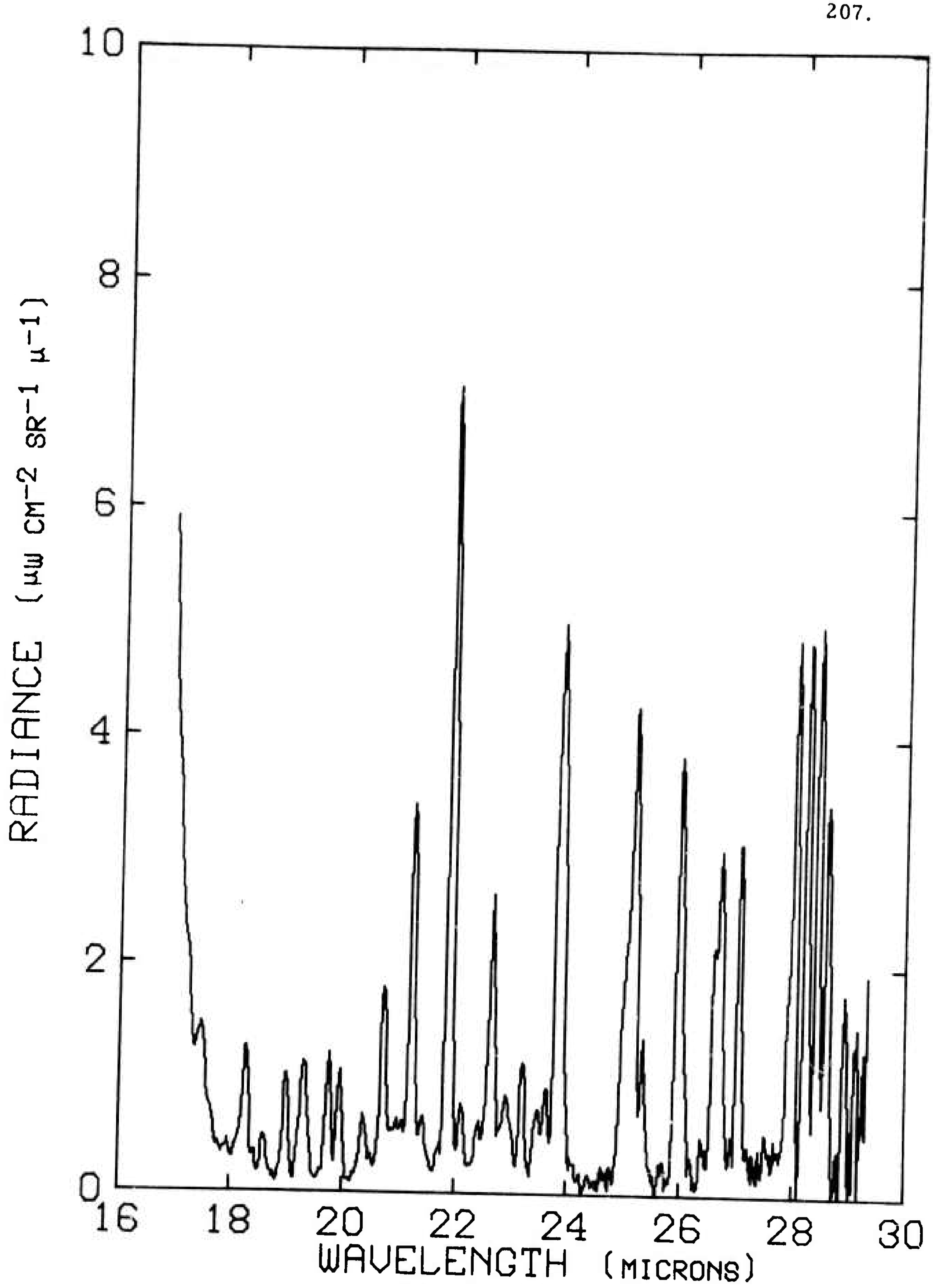

Figure 194. Radiance vs Wavelength at 66.5 kft and 0408 ADT, 23 September 1971.

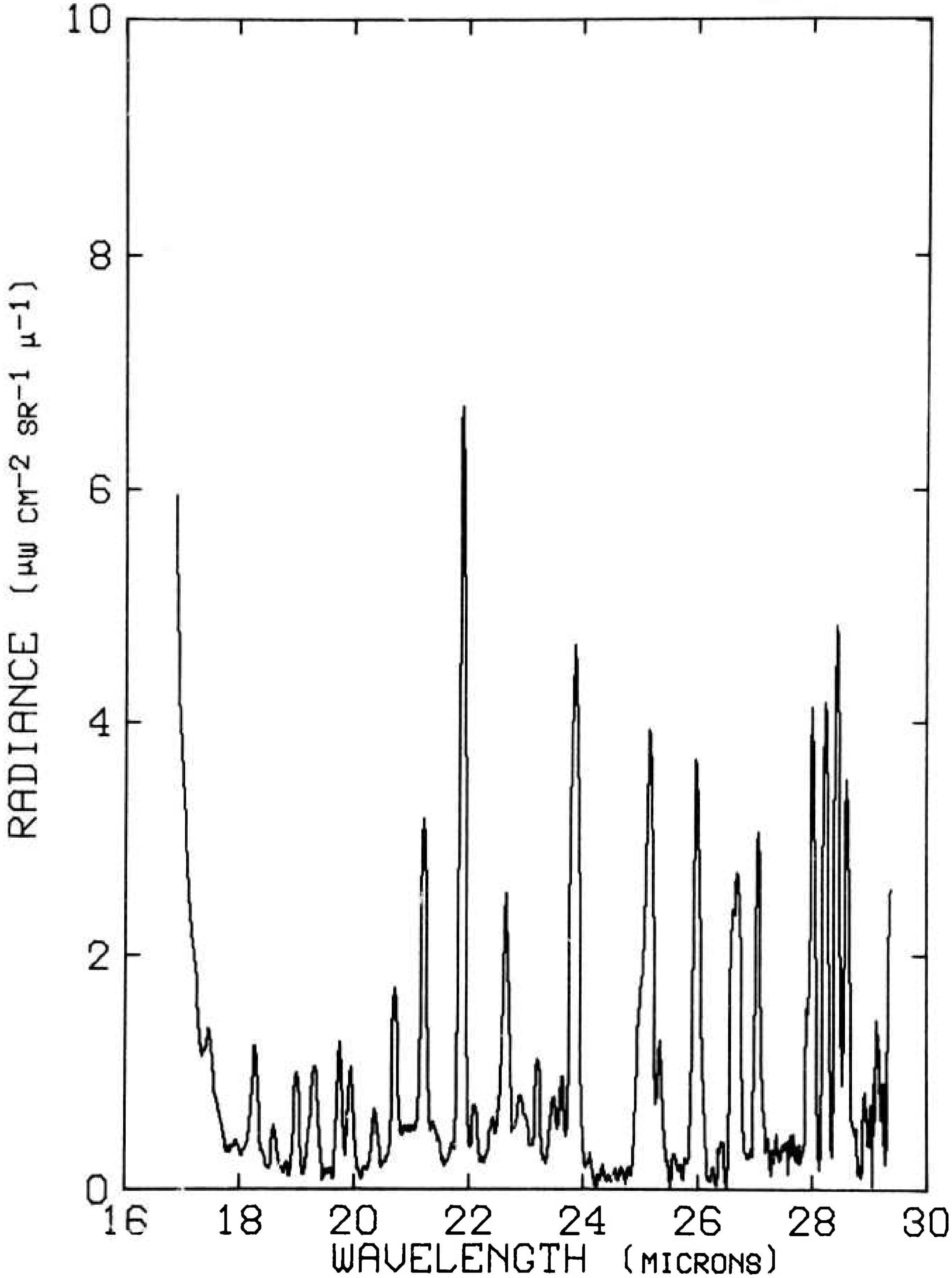

Figure 195. Radiance vs Wavelength at 67.9 kft and 0410 ADT, 23 September 1971.

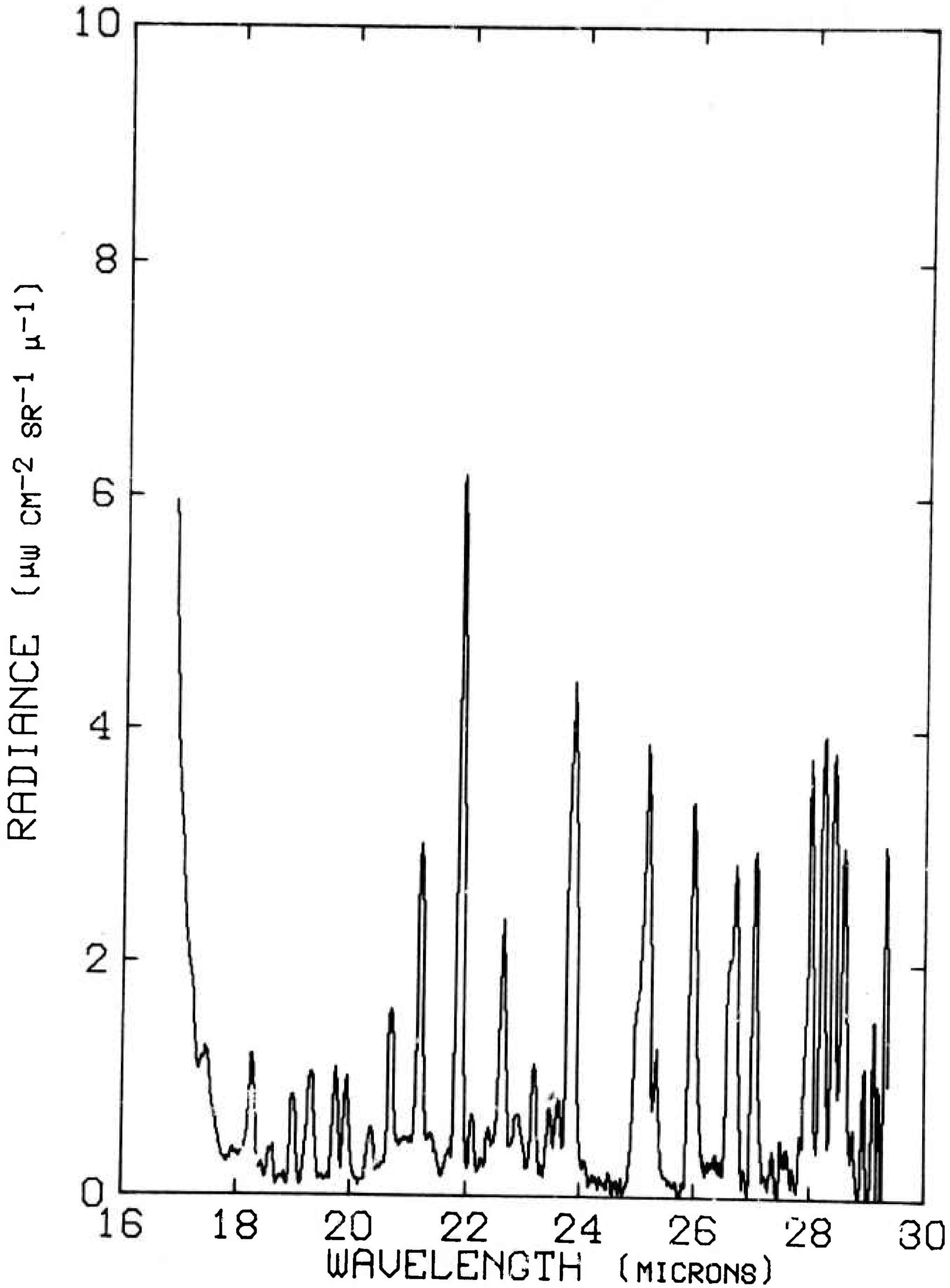

Figure 196. Radiance vs Wavelength at 69.5 kft and 0412 ADT, 23 September 1971.

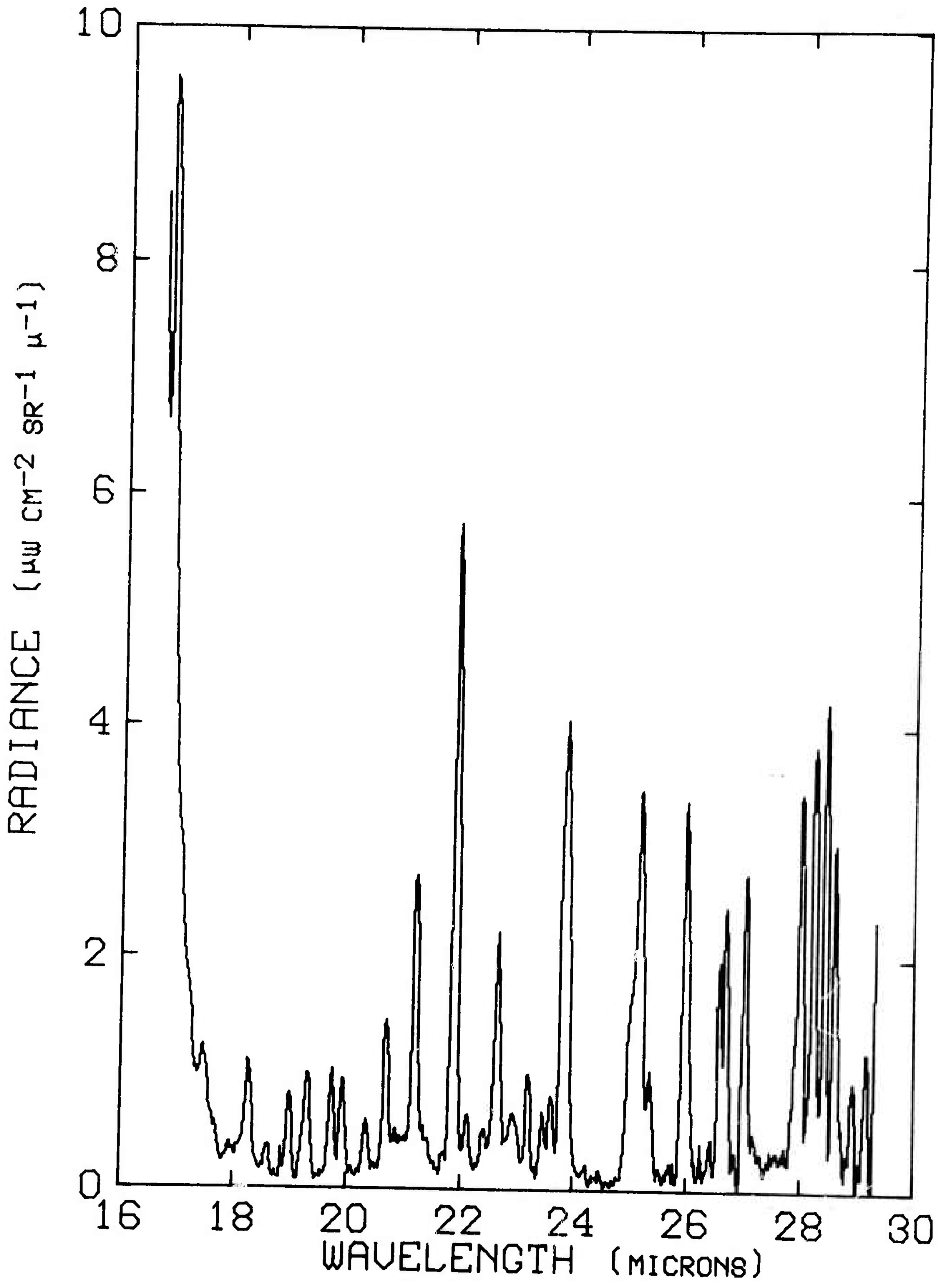

Figure 197. Radiance vs Wavelength at 71.4 kft and 0414 ADT, 23 September 1971.

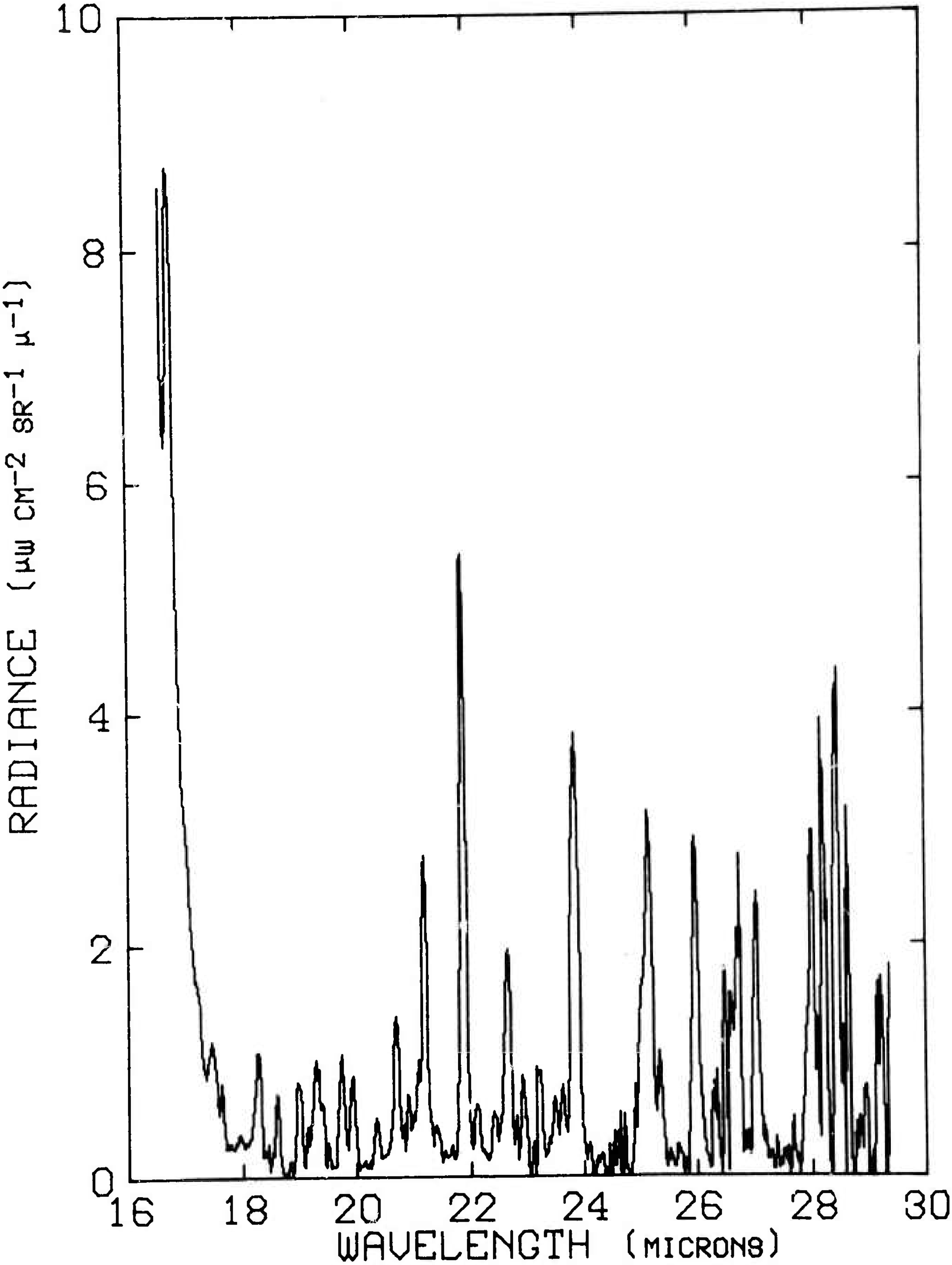

Figure 198. Radiance vs Wavelength at 72.9 kft and 0416 ADT, 23 September 1971.

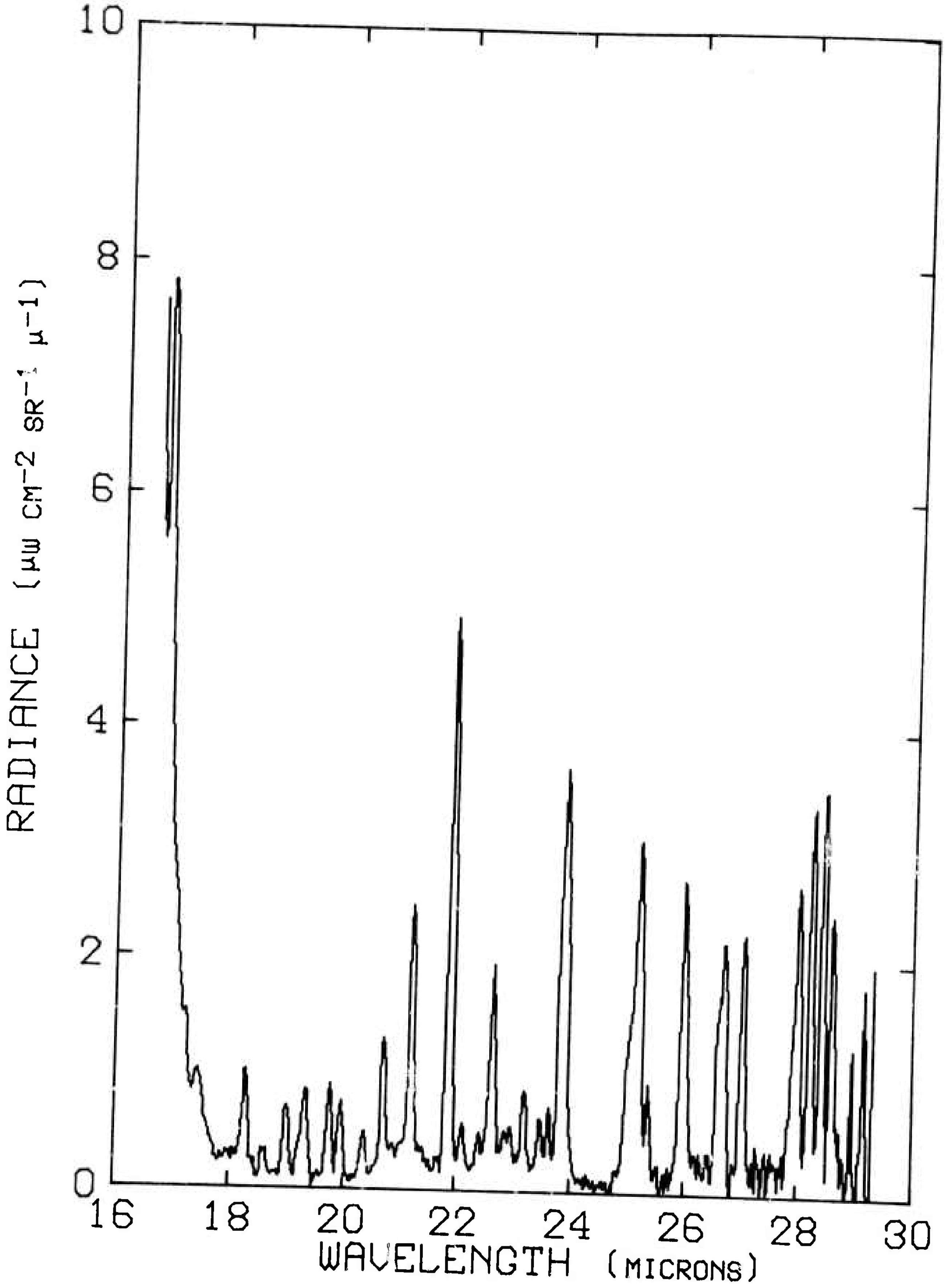

Figure 199. Radiance vs Wavelength at 74.5 kft and 0418 ADT, 23 September 1971.

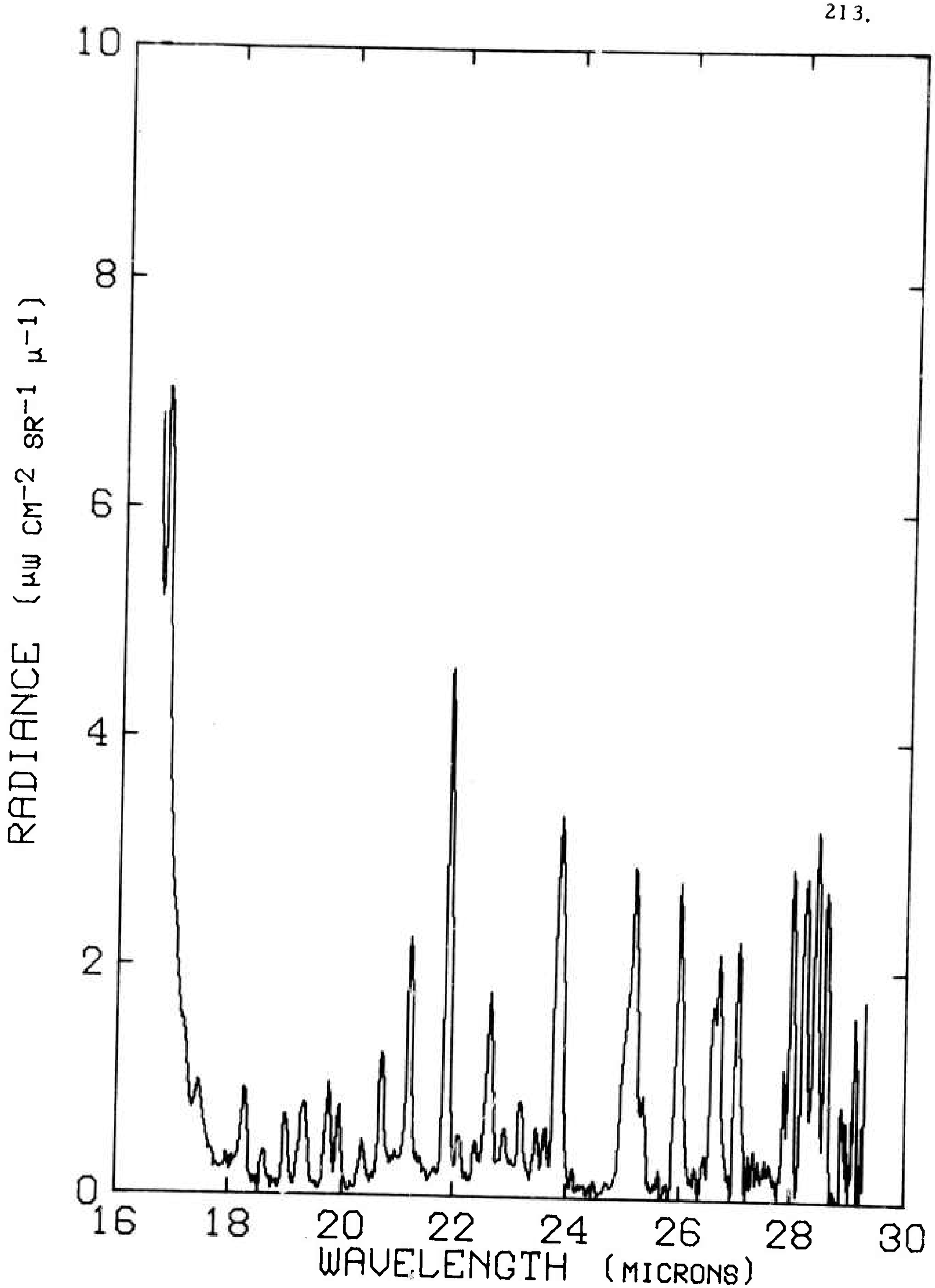

Figure 200. Radiance vs Wavelength at 75.9 kft and 0420 ADT, 23 September 1971.

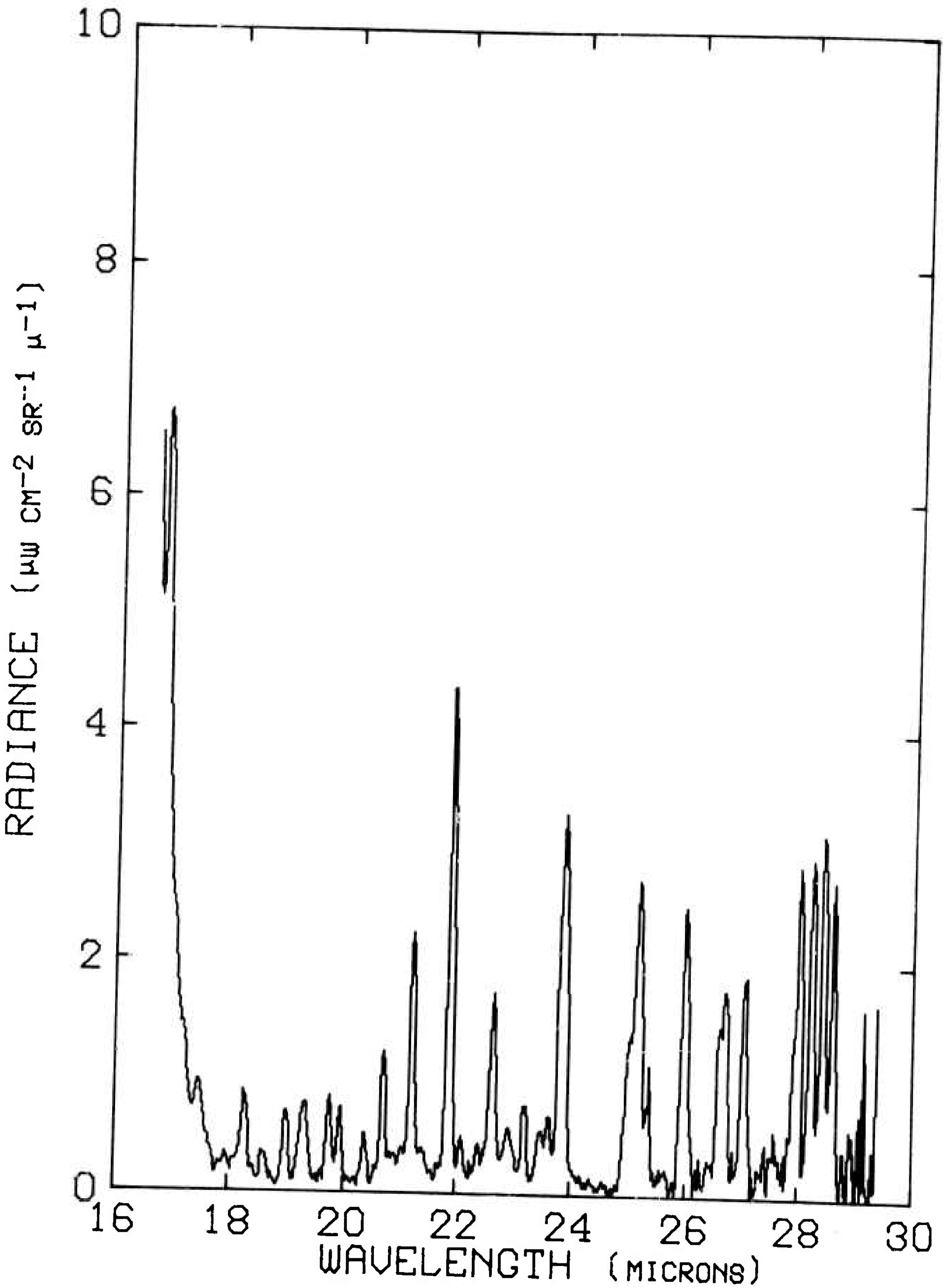

Figure 201. Radiance vs Wavelength at 77.1 kft and 0422 ADT, 23 September 1971.

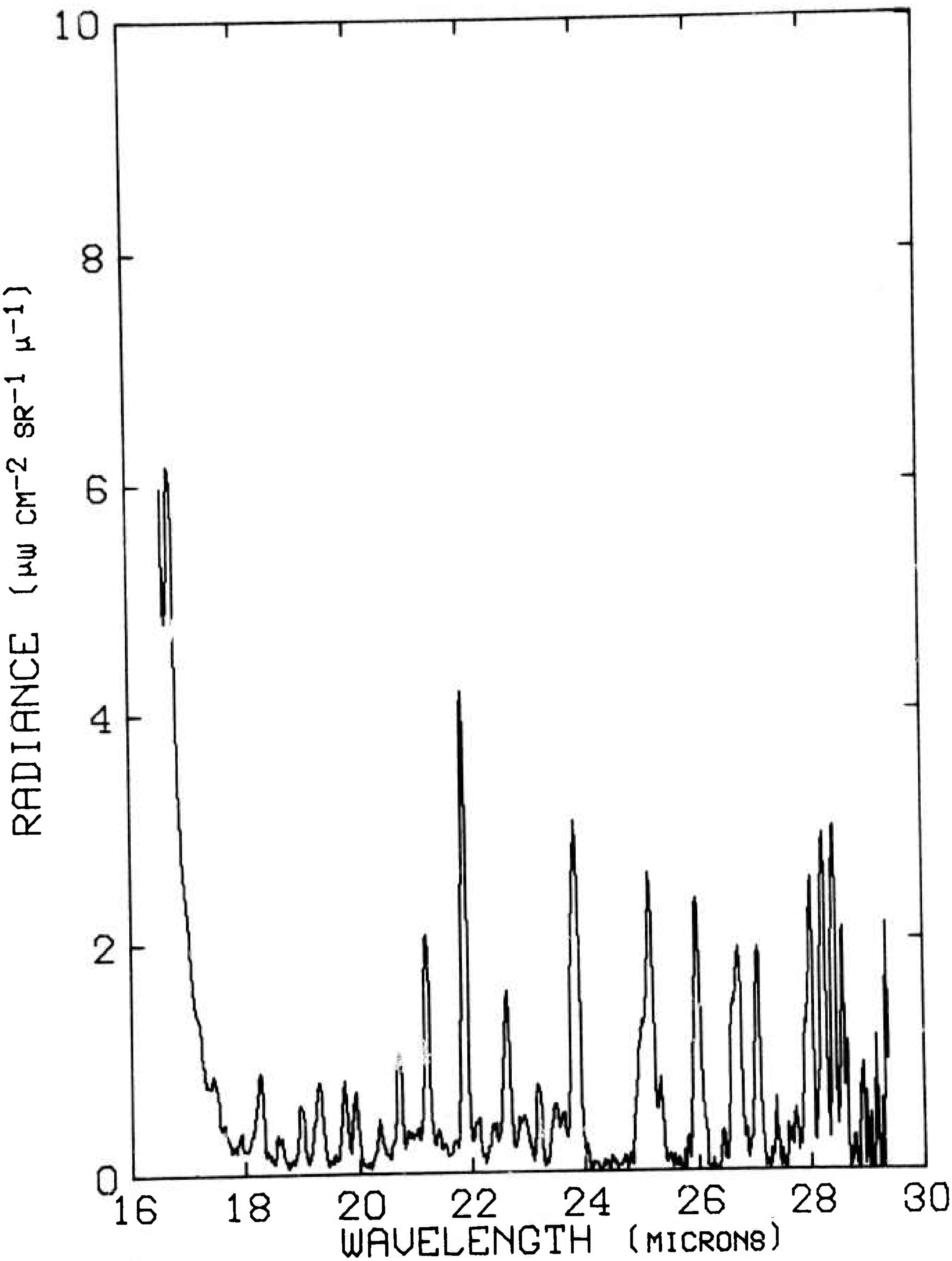

Figure 202. Radiance vs Wavelength at 77.7 kft and 0423 ADT, 23 September 1971.

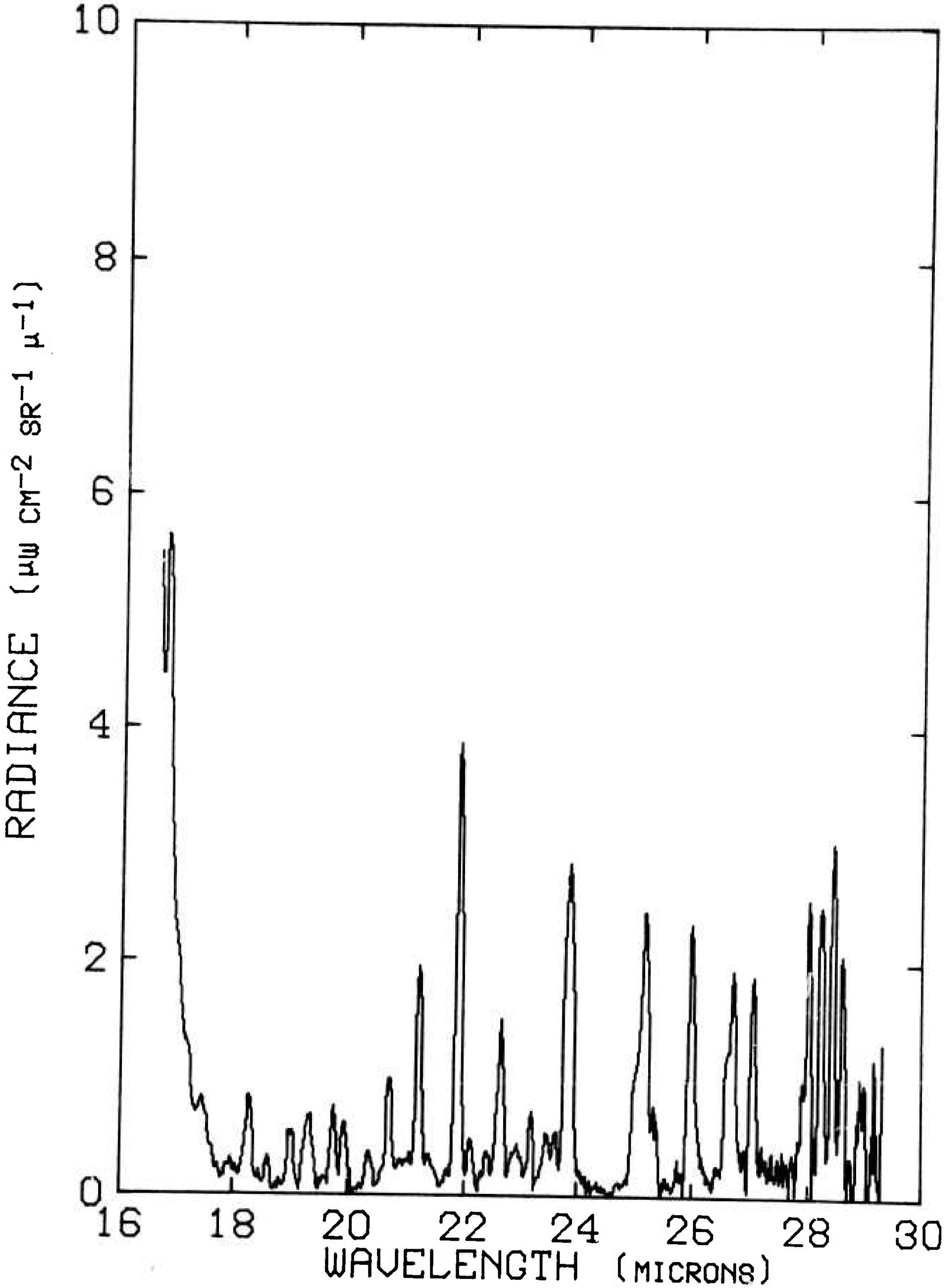

Figure 203. Radiance vs Wavelength at 79.6 kft and 0425 ADT, 23 September 1971.

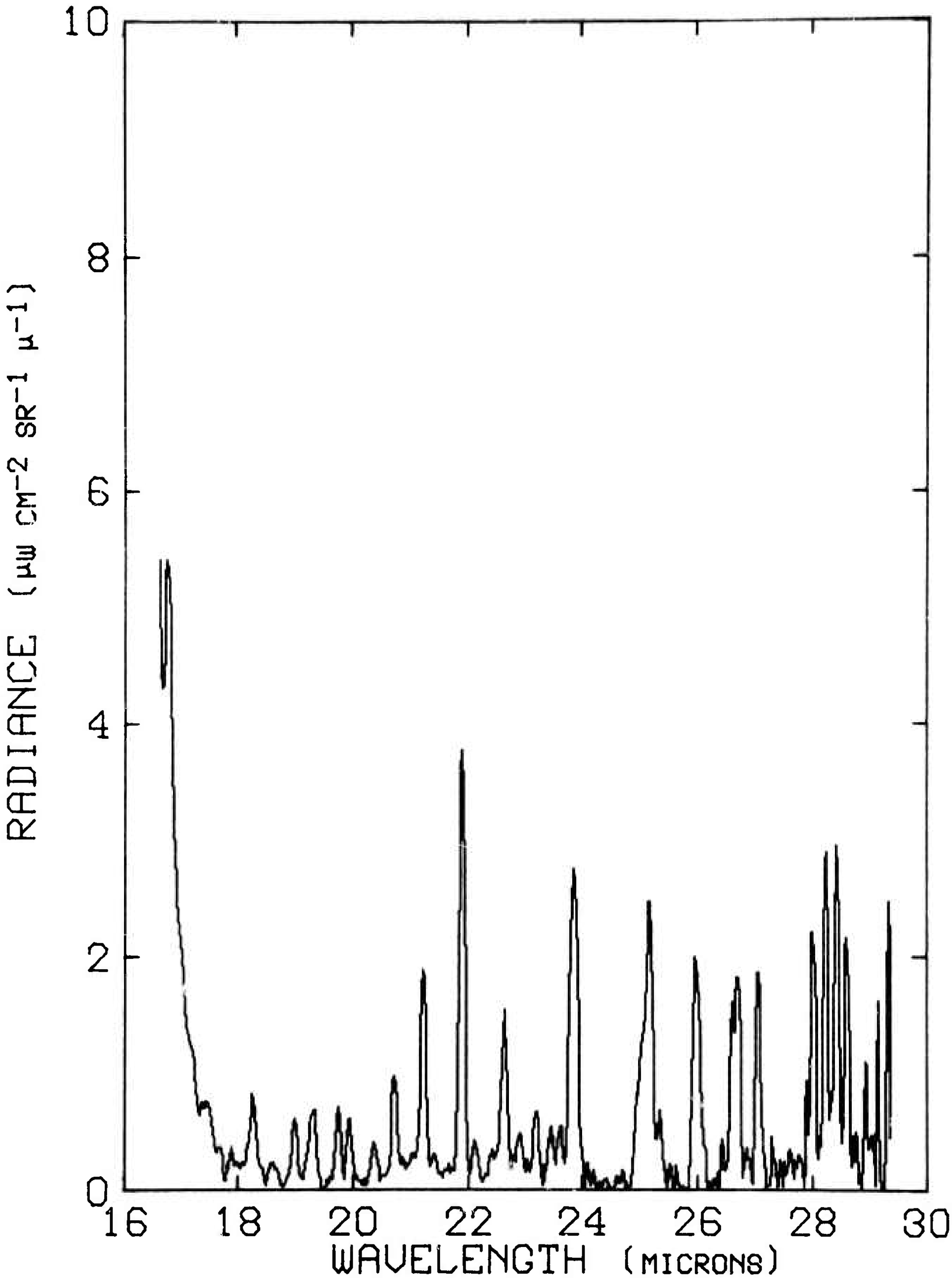

Figure 204. Radiance vs Wavelength at 80.6 kft and 0427 ADT, 23 September 1971.

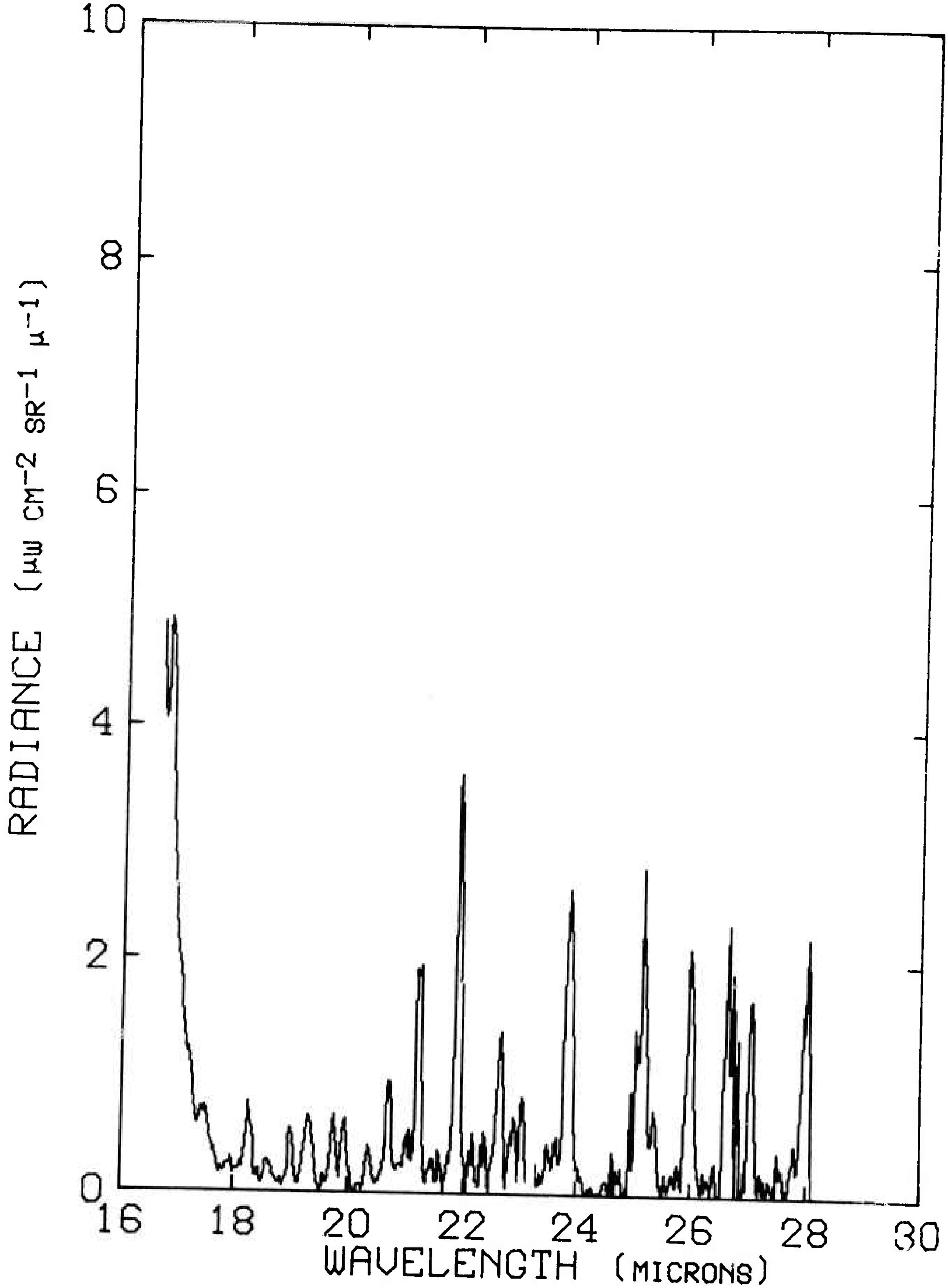

Figure 205. Radiance vs Wavelength at 81.7 kft and 0429 ADT, 23 September 1971.

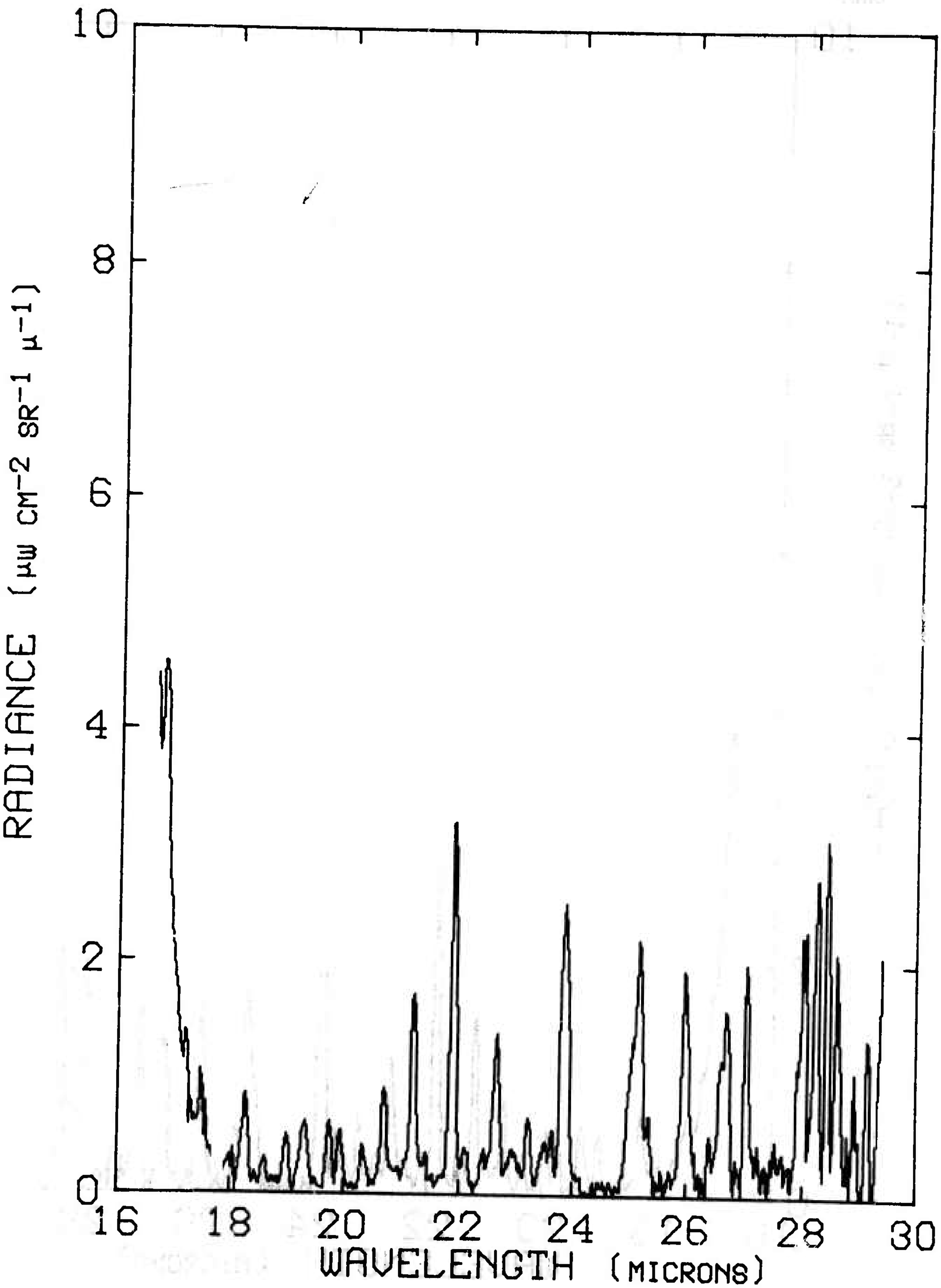

Figure 206. Radiance vs Wavelength at 83.0 kft and 0431 ADT, 23 September 1971.

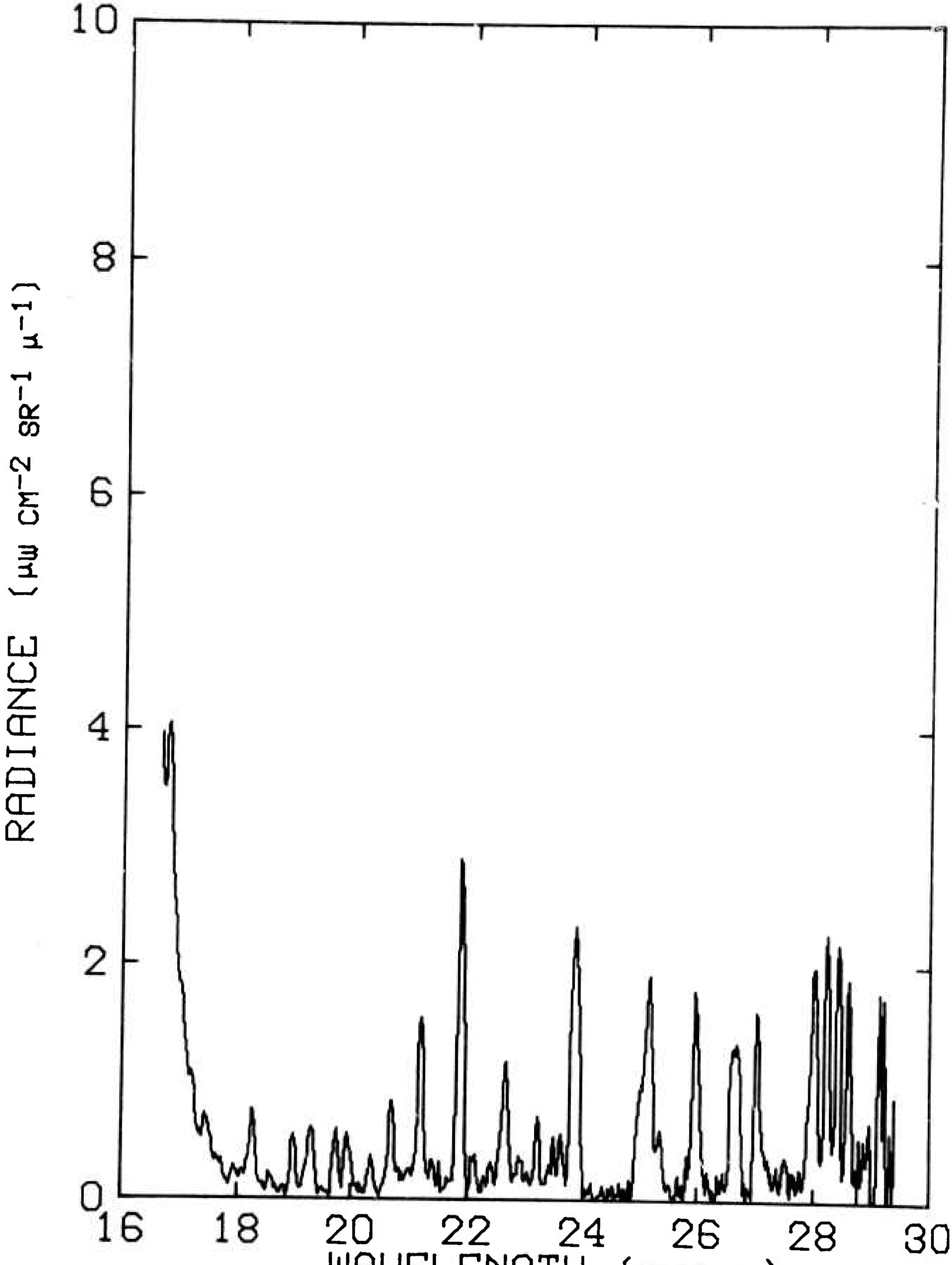

Figure 207. Radiance vs Wavelength at 84.8 kft and 0433 ADT, 23 September 1971.

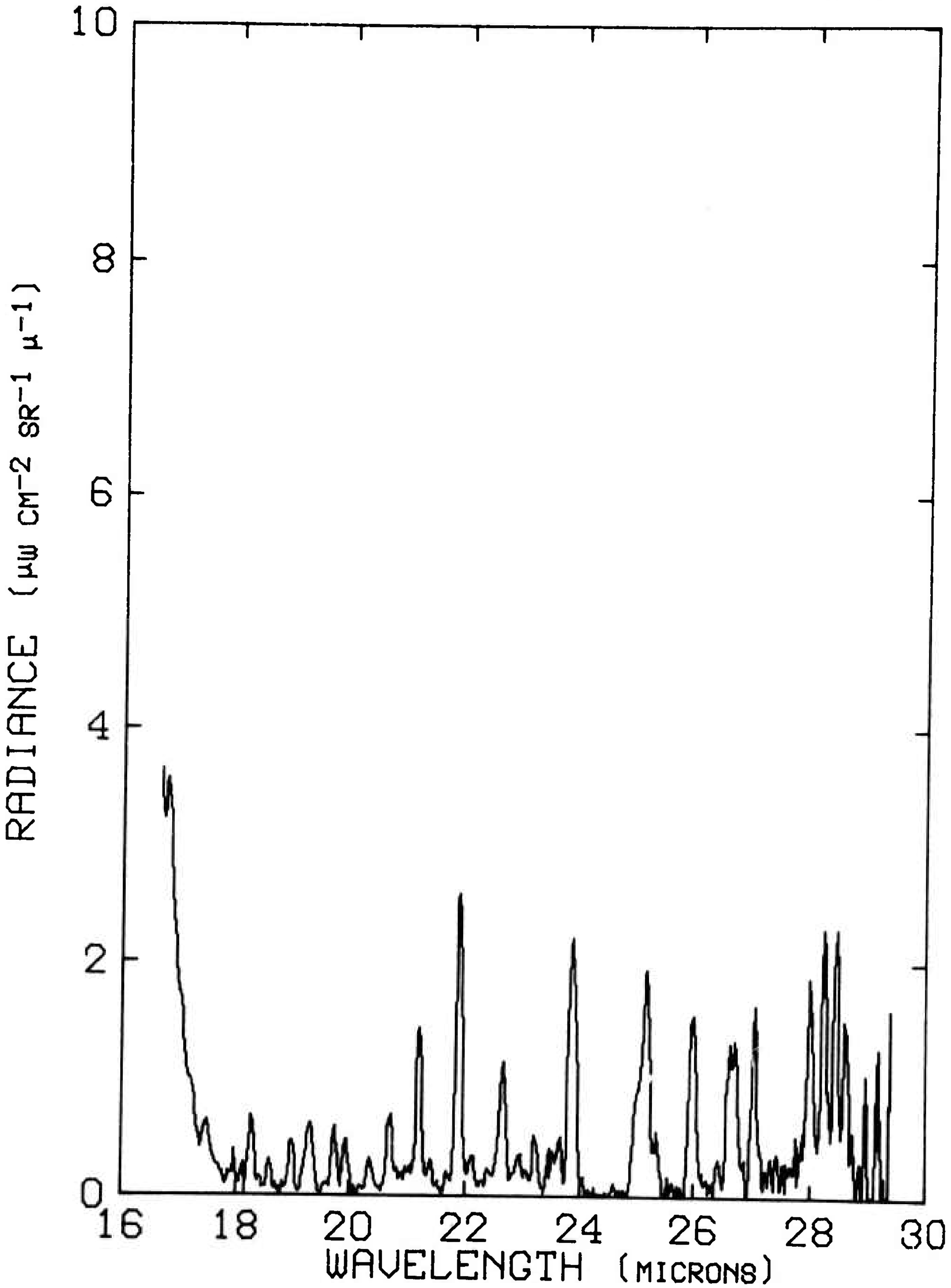

Figure 208. Radiance vs Wavelength at 86.8 kft and 0435 ADT, 23 September 1971.

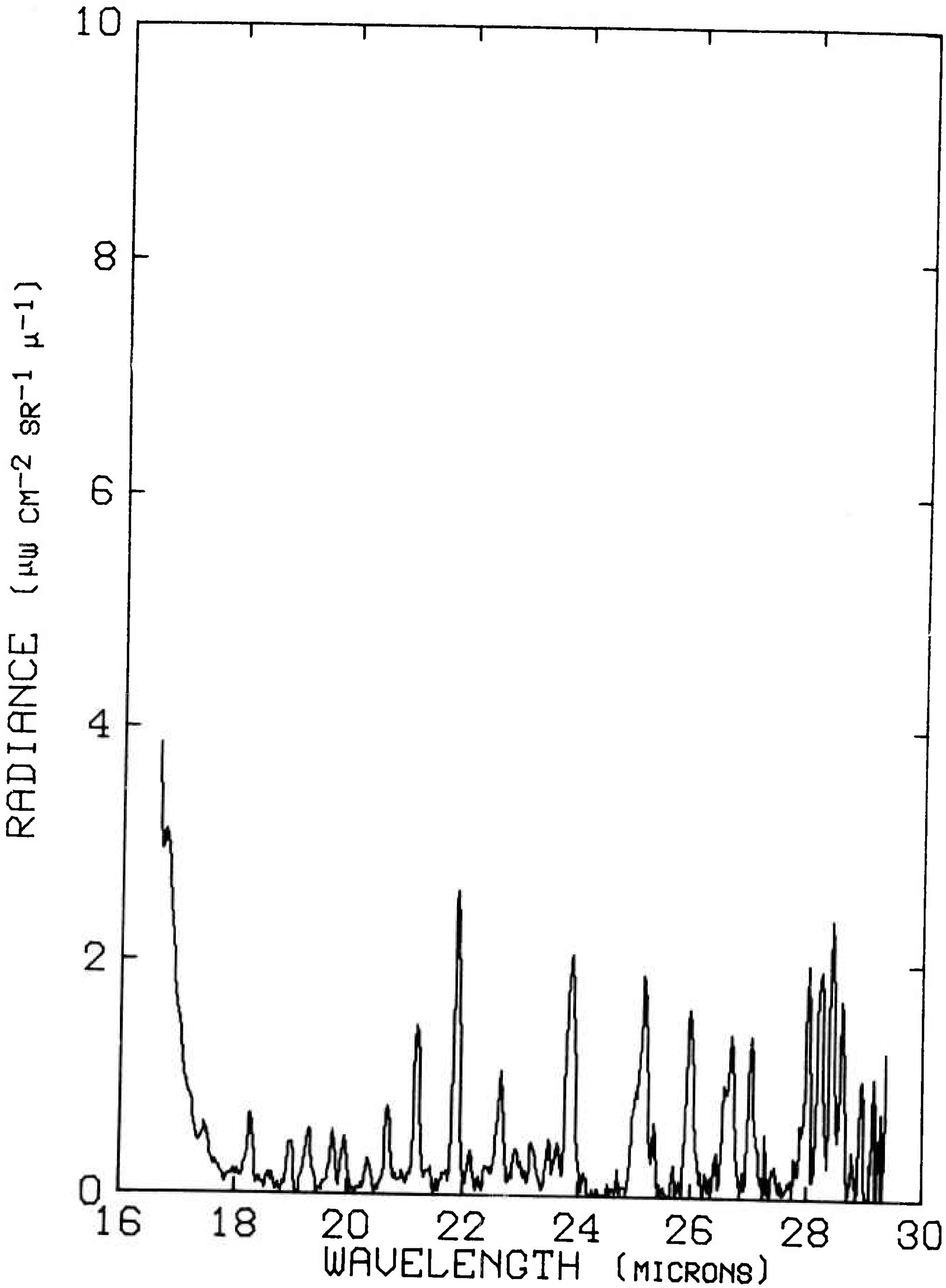

Figure 209. Radiance vs Wavelength at 88.5 kft and 0437 ADT, 23 September 1971.

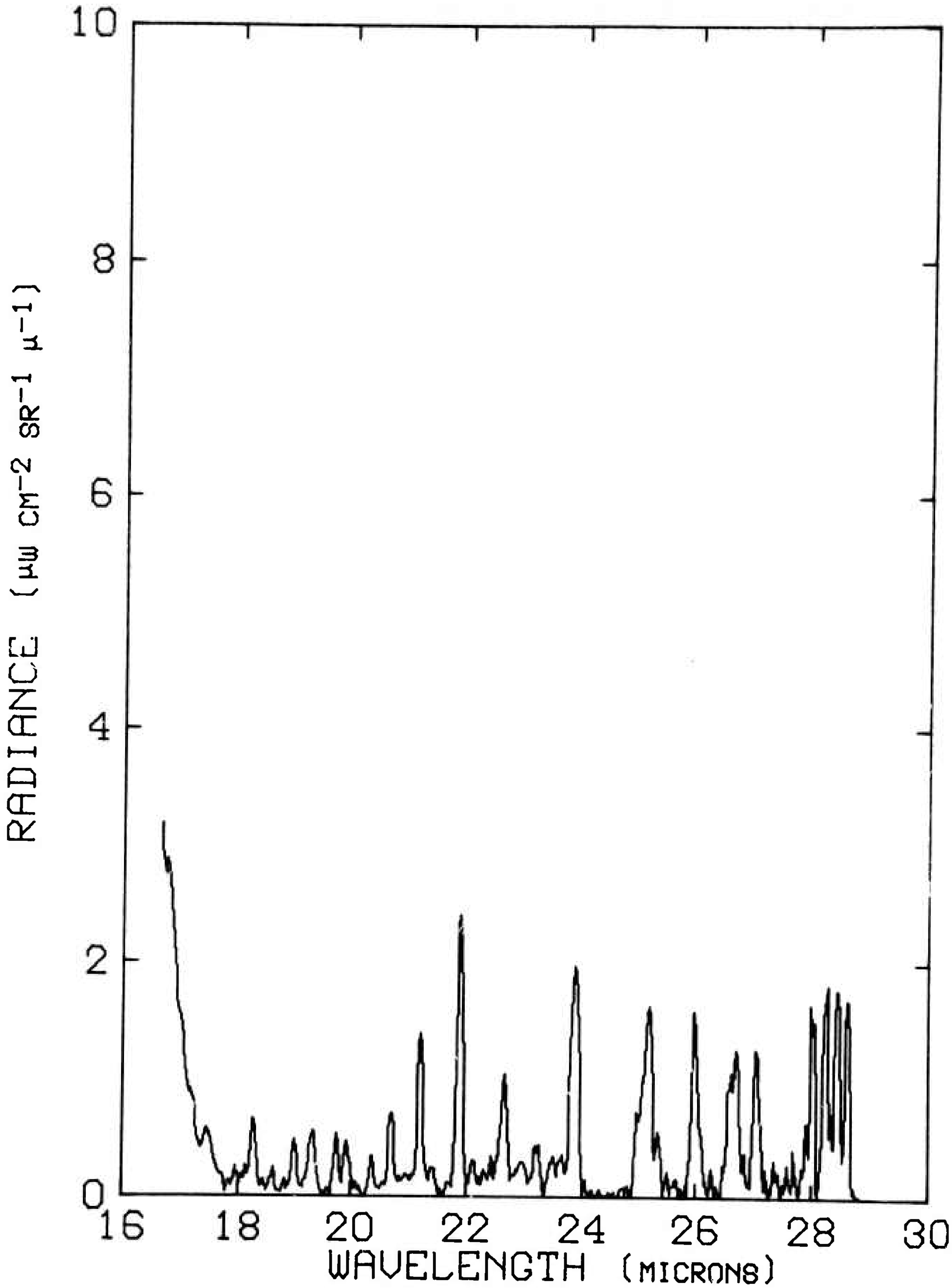

Figure 210. Radiance vs Wavelength at 89.8 kft and 0439 ADT, 23 September 1971.

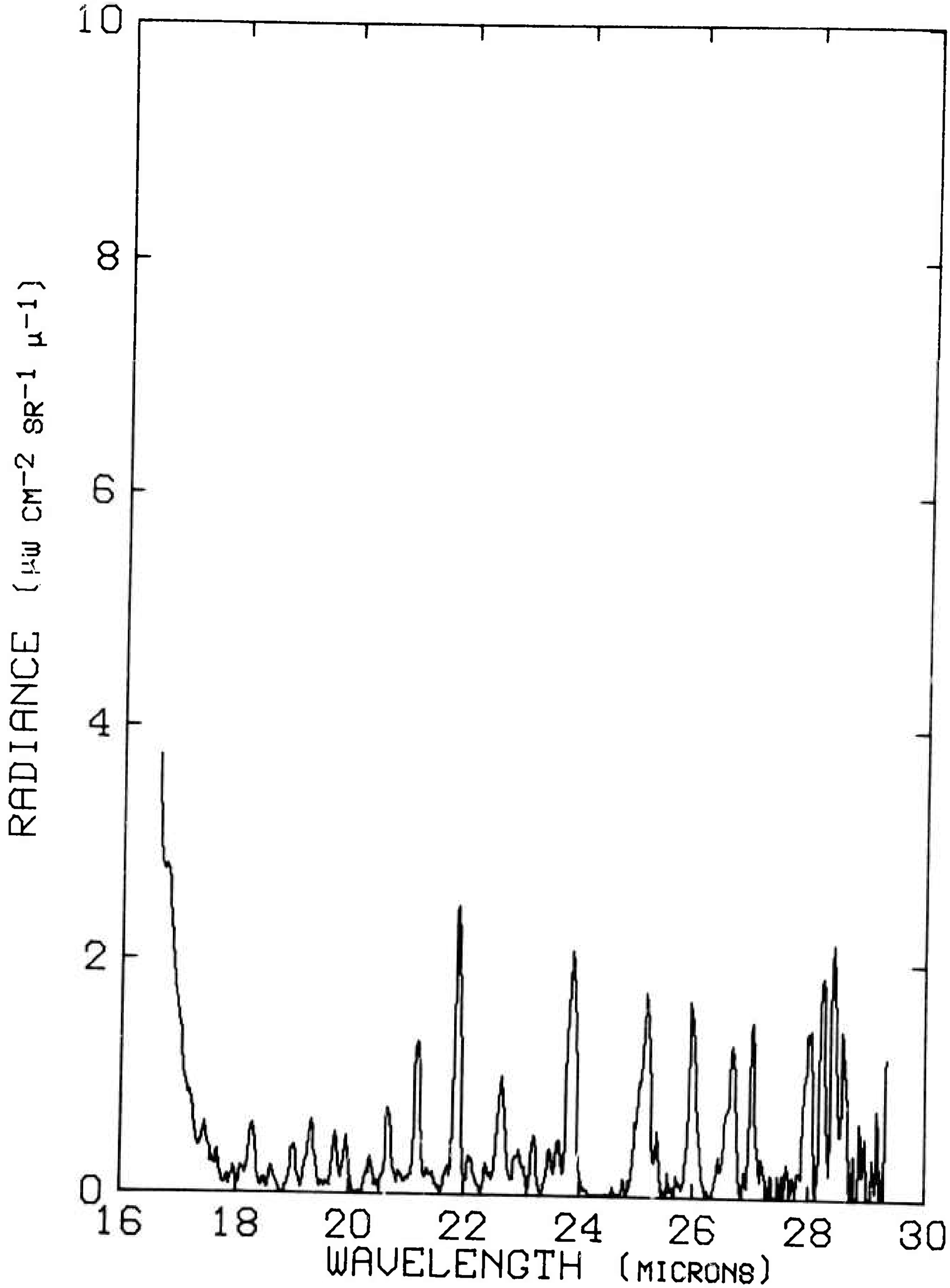

Figure 211. Radiance vs Wavelength at 90.4 kft and 0441 ADT, 23 September 1971.

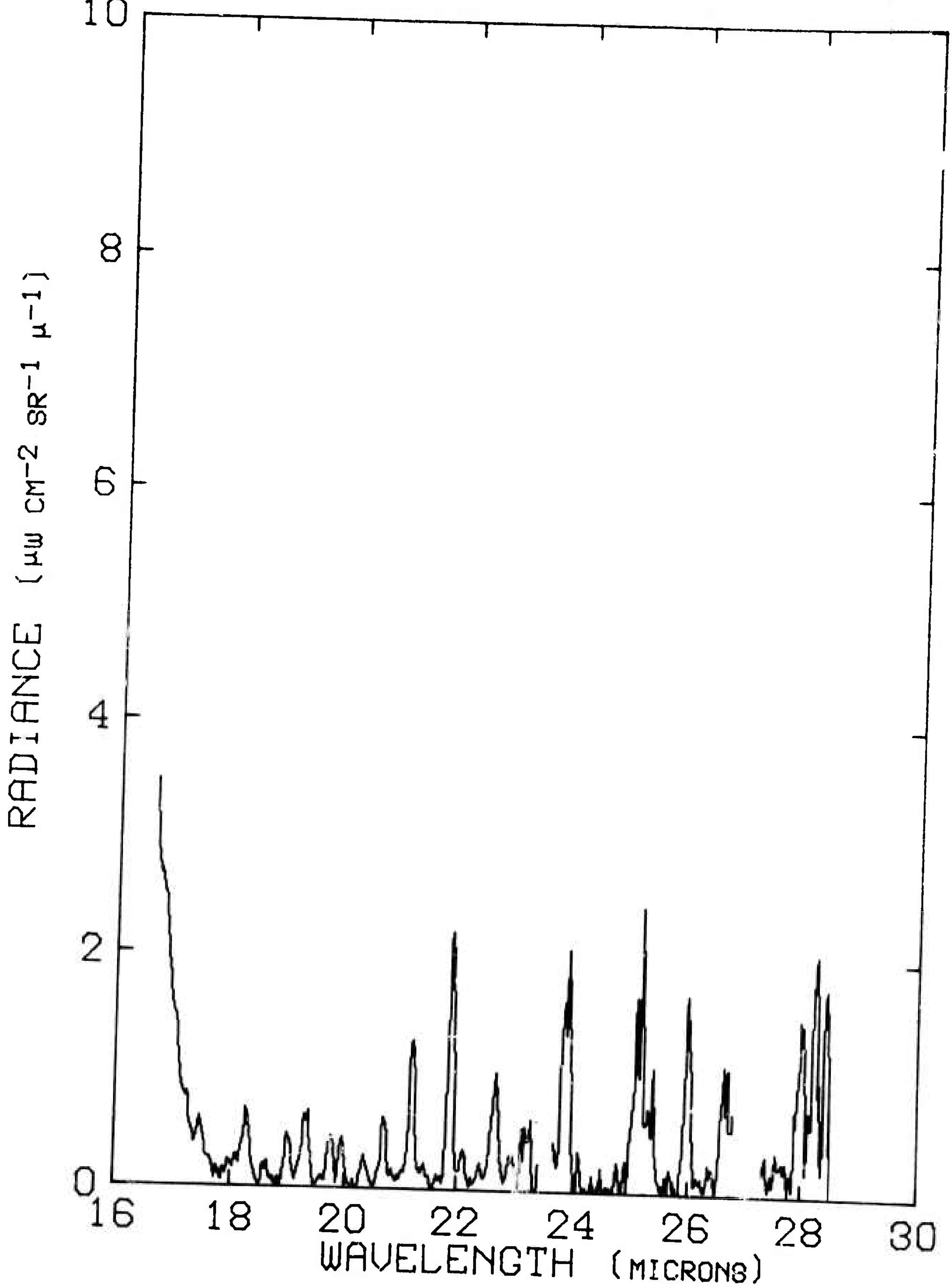

Figure 212. Radiance vs Wavelength at 91.5 kft and 0443 ADT, 23 September 1971.

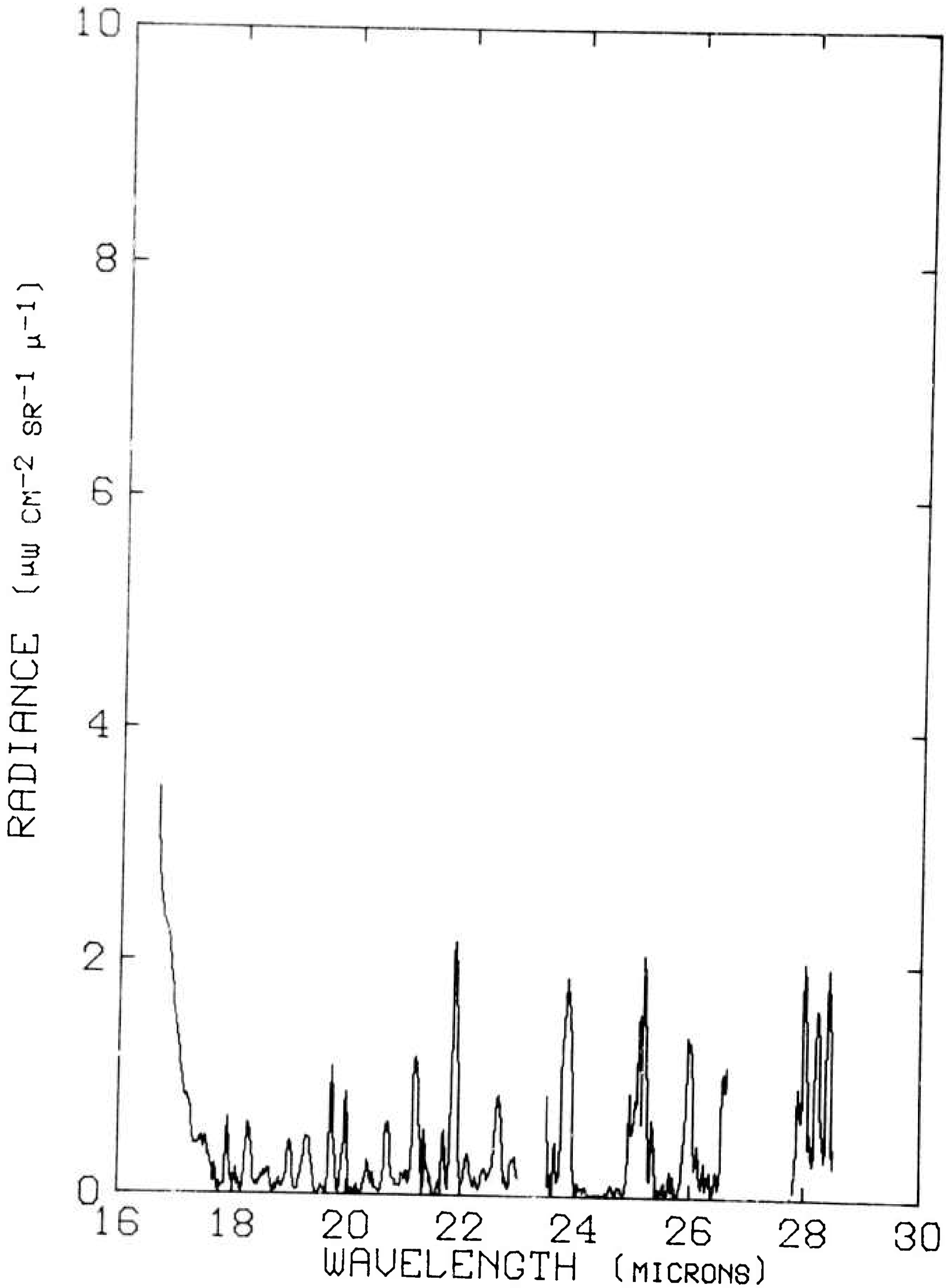

Figure 213. Radiance vs Wavelength at 93.0 kft and 0444 ADT, 23 September 1971.

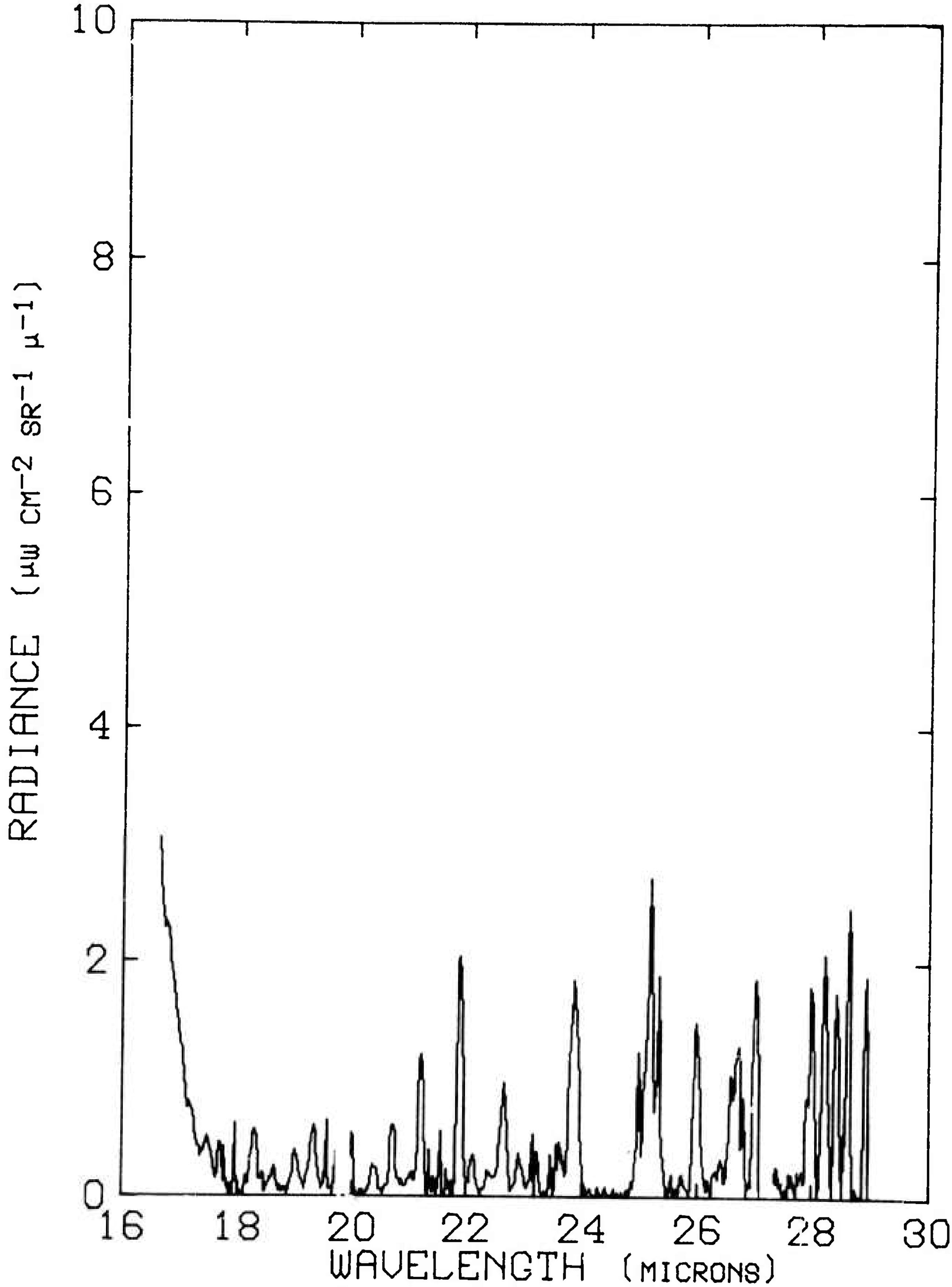

Figure 214. Radiance vs Wavelength at 94.0 kft and 0446 ADT, 23 September 1971.

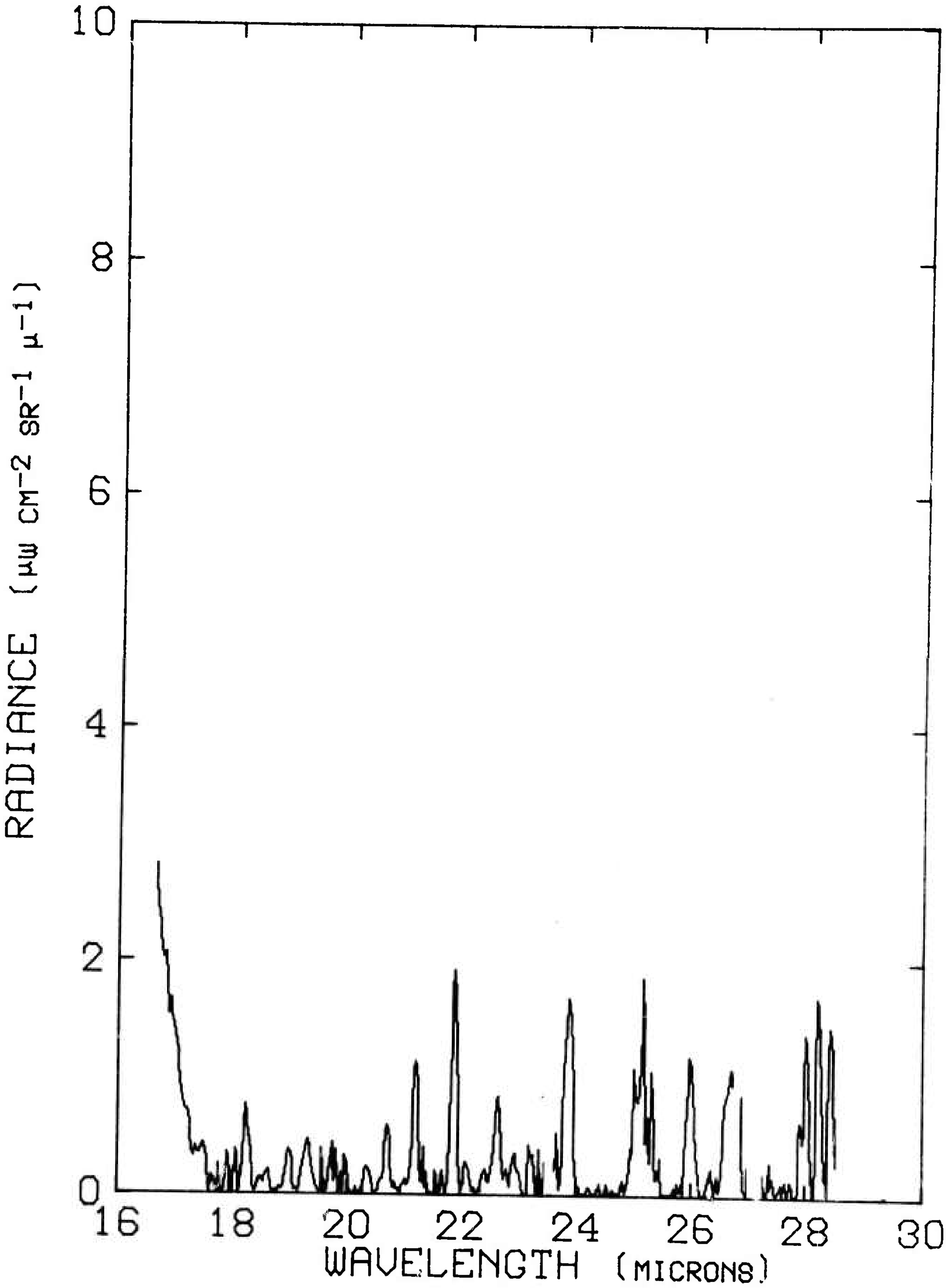

Figure 215. Radiance vs Wavelength at 94.2 kft and 0448 ADT, 23 September 1971.

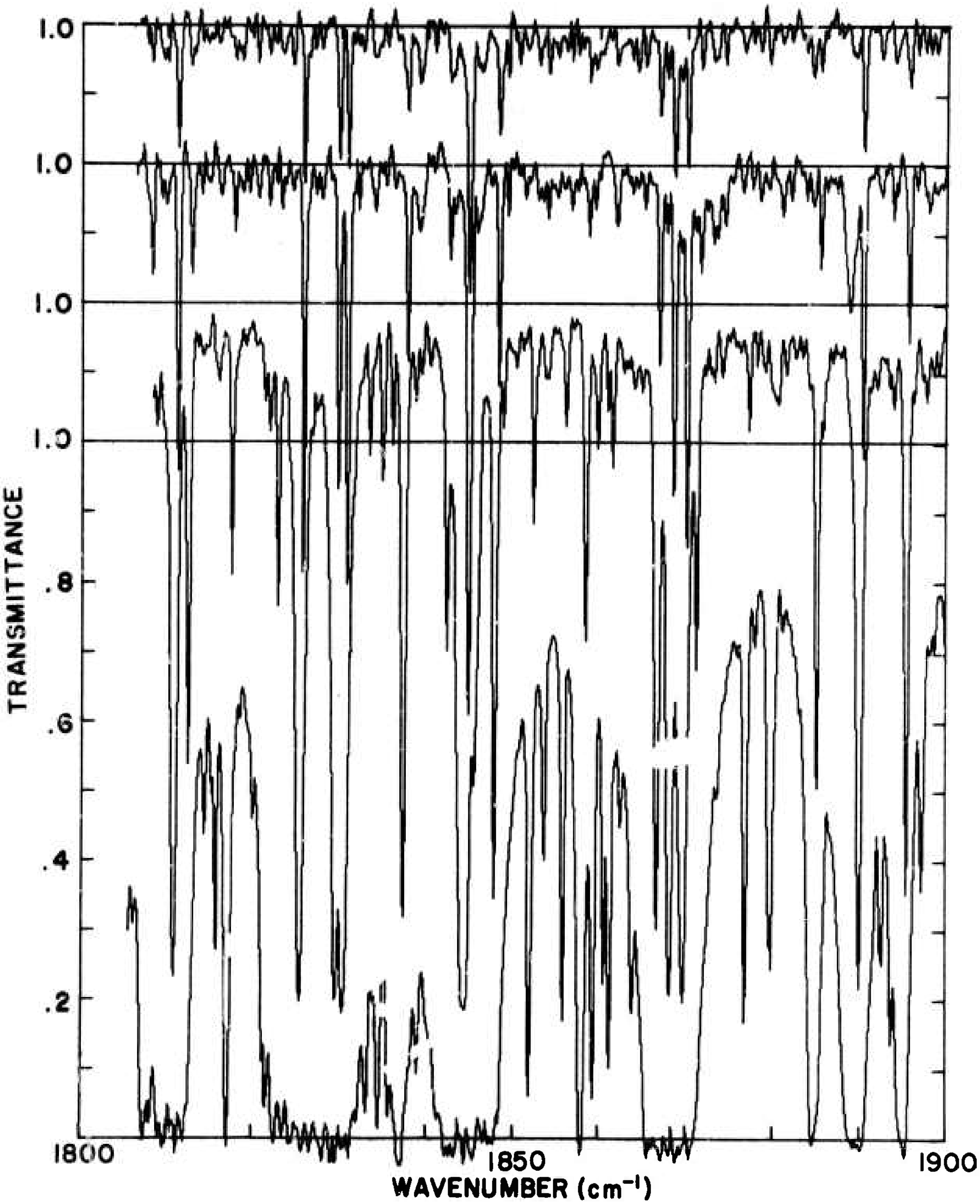

Figure 216. Atmospheric transmittance vs wavenumber at 5.8, 27.6, 42.1 and 68.6 kft with the lowest altitude on the bottom and 0.2 offset in transmittance between each spectrum.

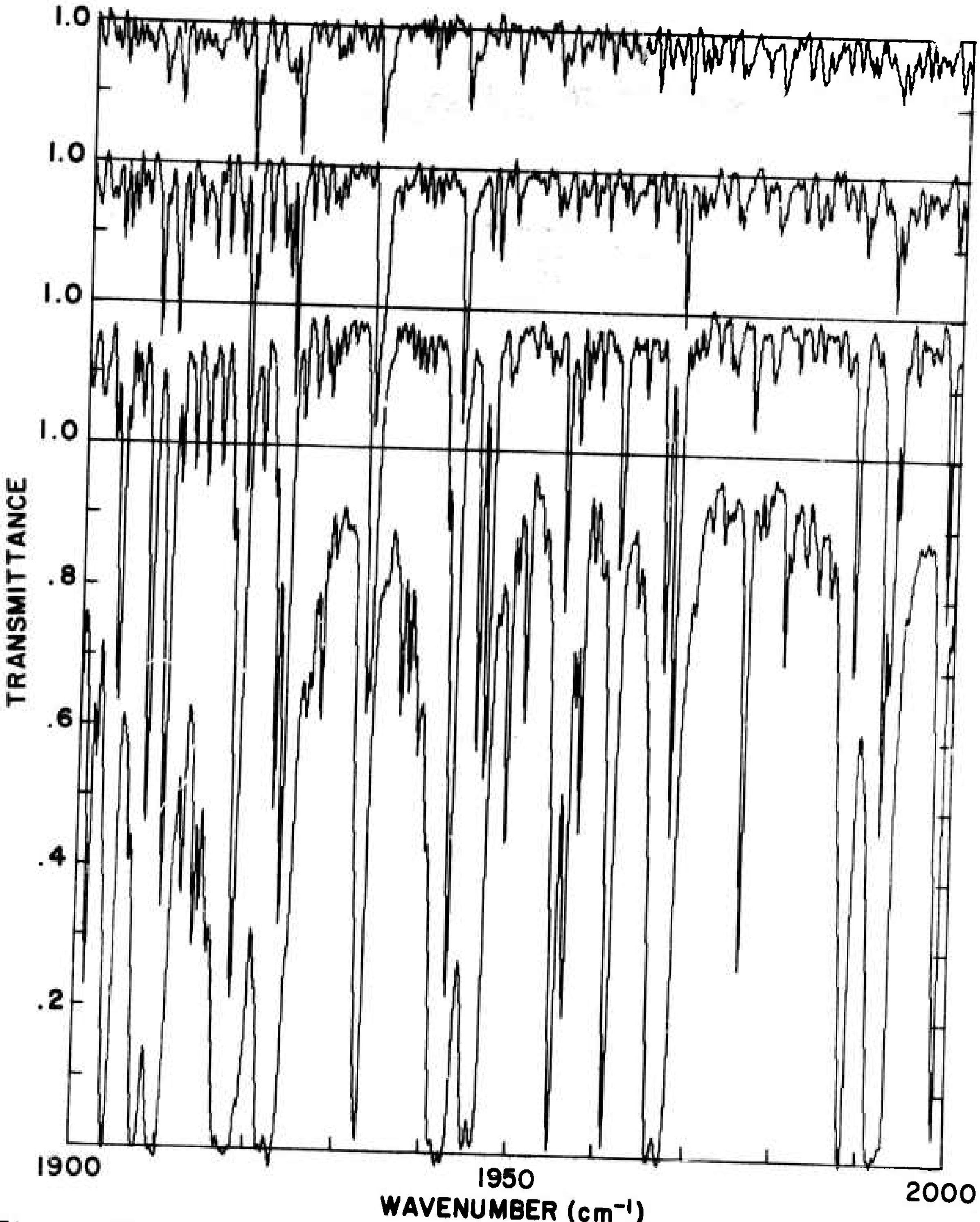

Figure 217. Atmospheric transmittance vs wavenumber at 5.8, 27.6, 42.1 and 68.6 kft with the lowest altitude on the bottom and 0.2 offset in transmittance between each spectrum.

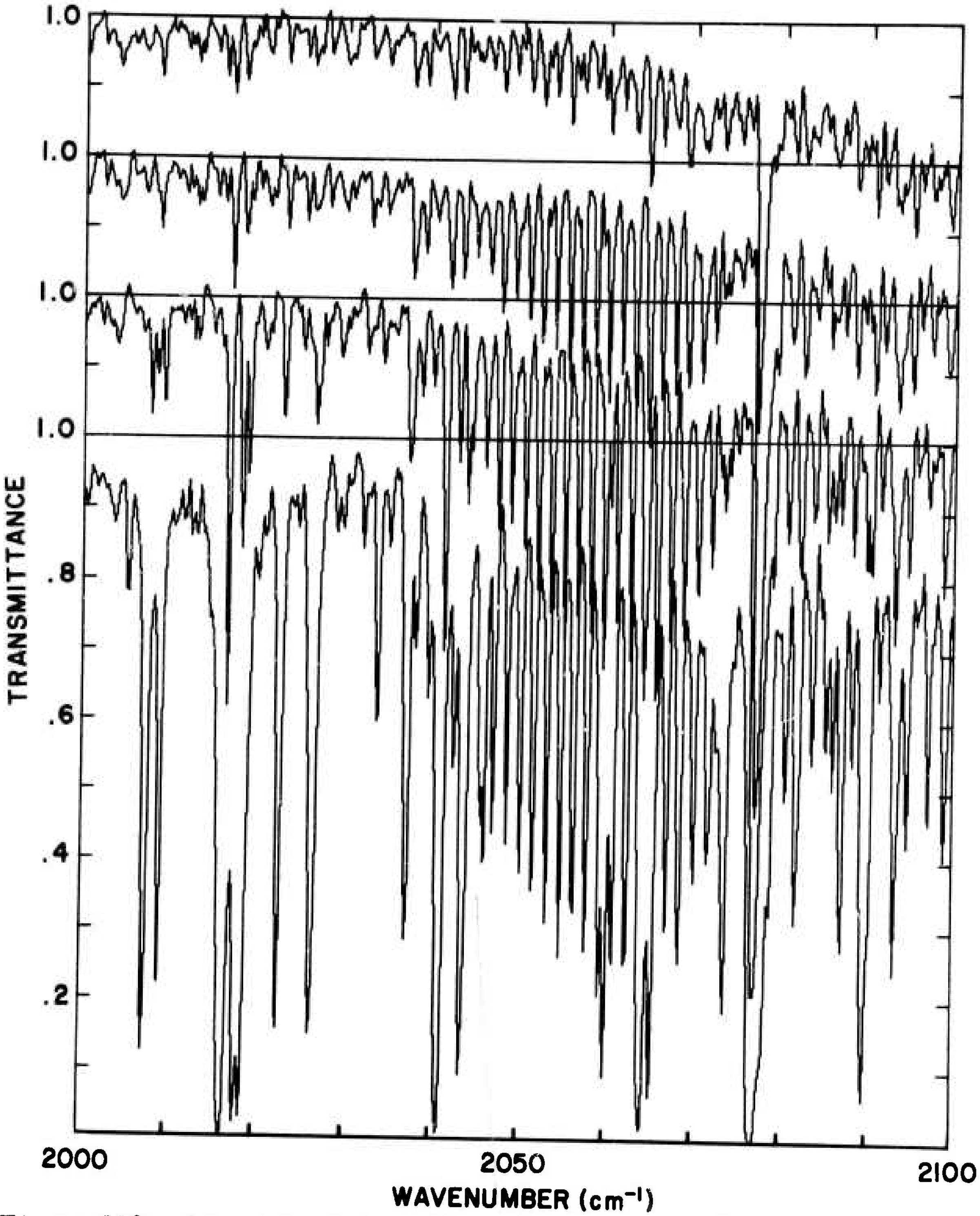

Figure 218. Atmospheric transmittance vs wavenumber at 5.8, 27.6, 42.1 and 68.6 kft with the lowest altitude on the bottom and 0.2 offset in transmittance between each spectrum.

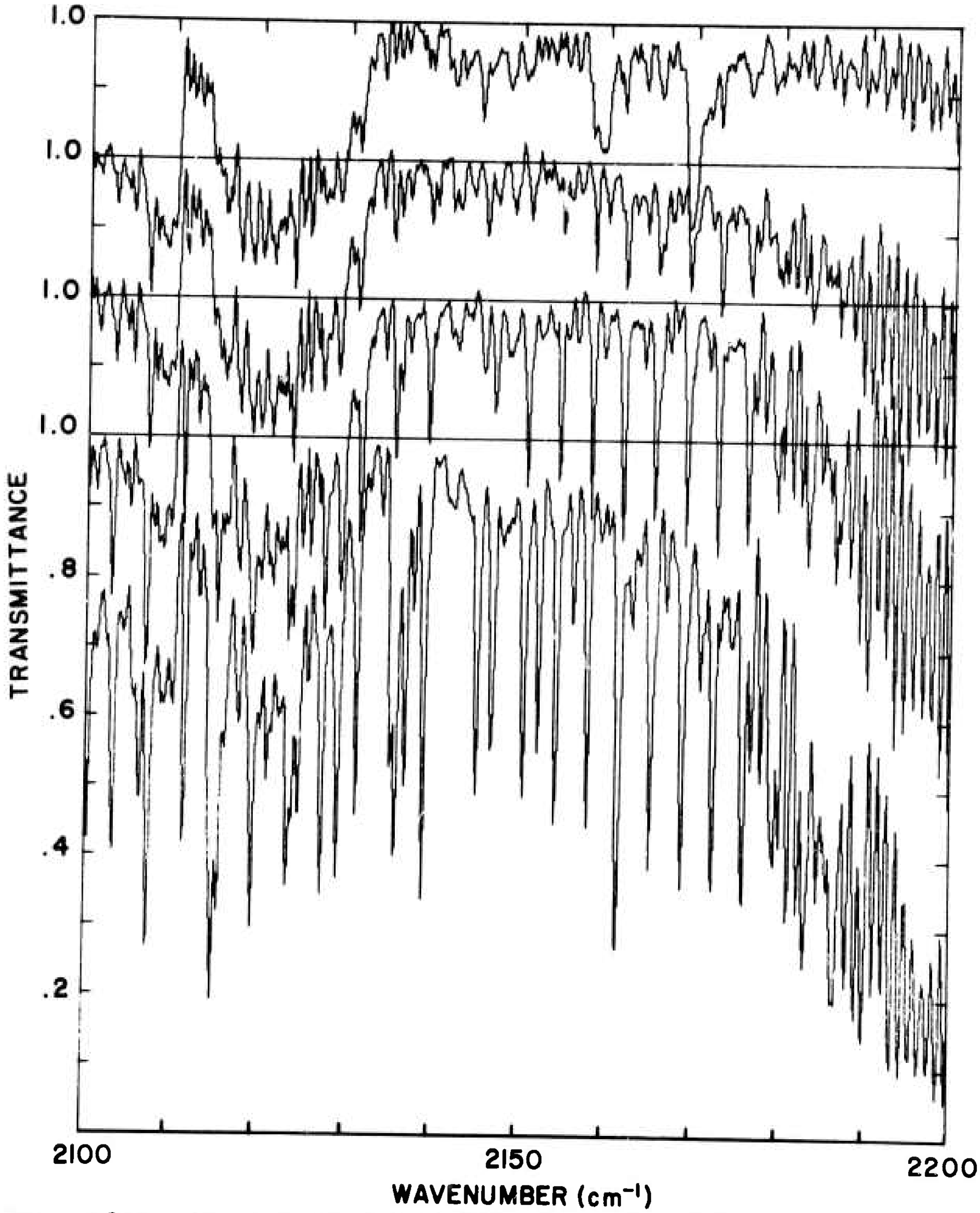

Figure 219. Atmospheric transmittance vs wavenumber at 5.8, 27.6, 42.1 and 68.6 kft with the lowest altitude on the bottom and 0.2 offset in transmittance between each spectrum.

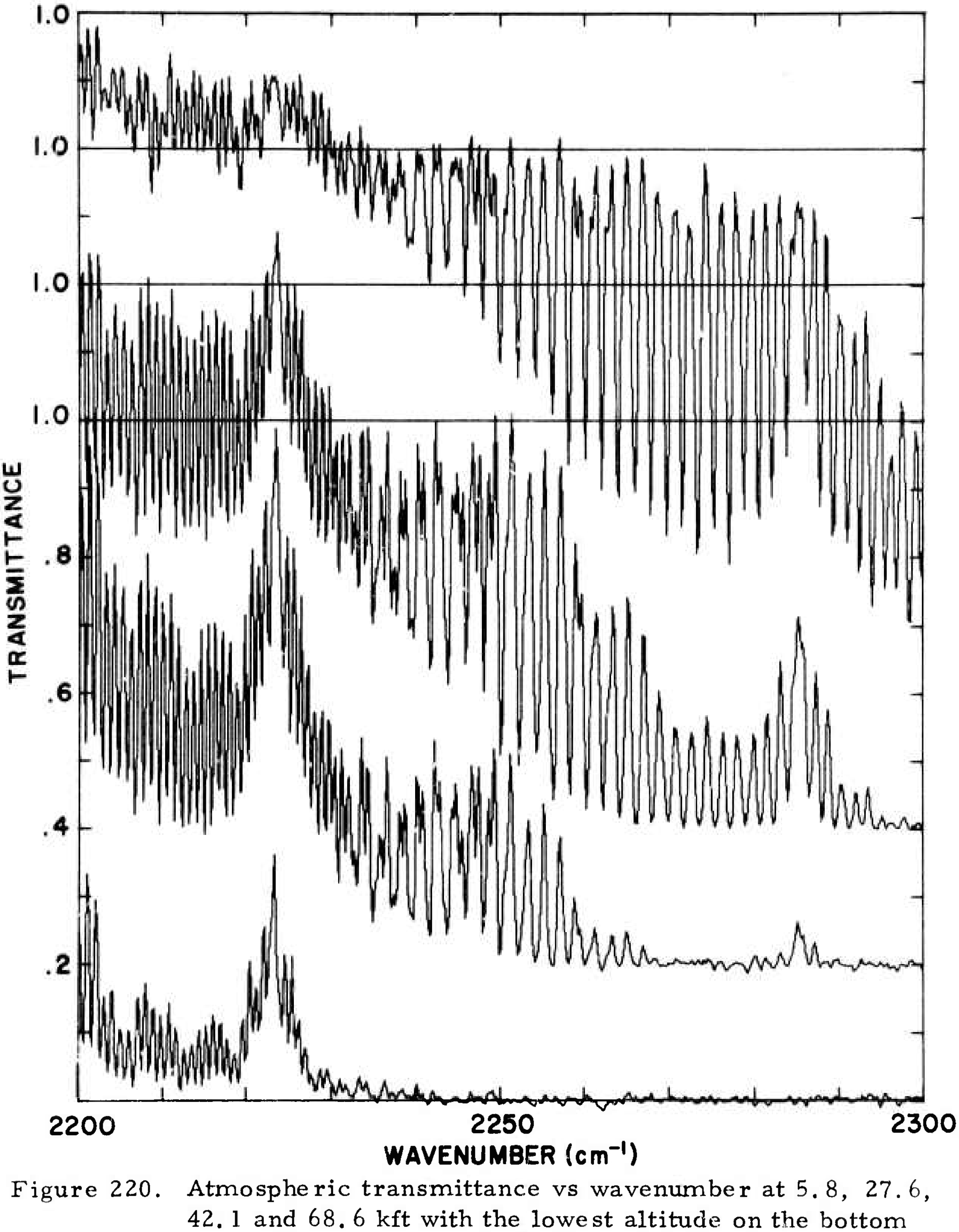

Figure 220. Atmospheric transmittance vs wavenumber at 5.8, 27.6, 42.1 and 68.6 kft with the lowest altitude on the bottom and 0.2 offset in transmittance between each spectrum.

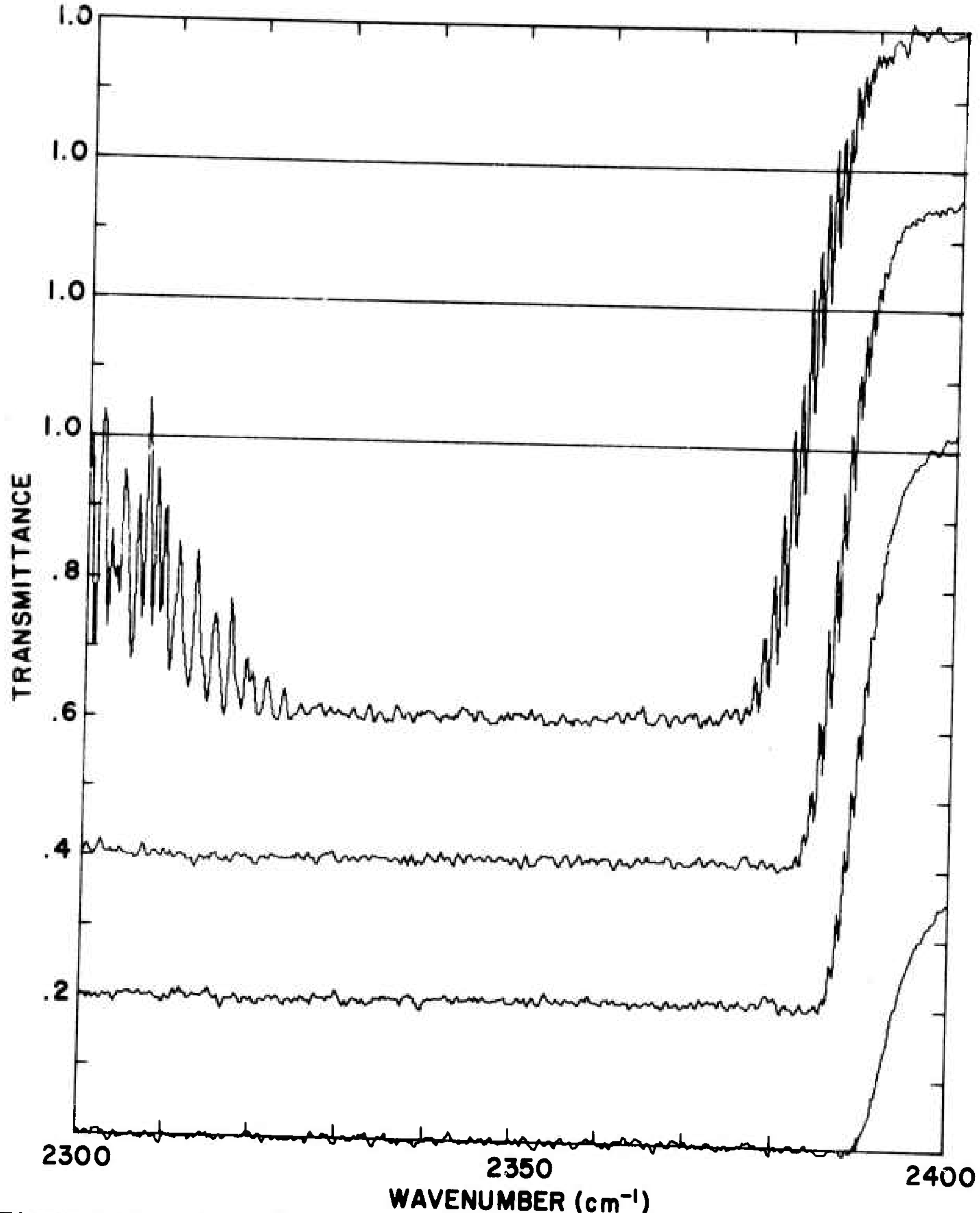

Figure 221. Atmospheric transmittance vs wavenumber at 5.8, 27.6, 42.1 and 68.6 kft with the lowest altitude on the bottom and 0.2 offset in transmittance between each spectrum.

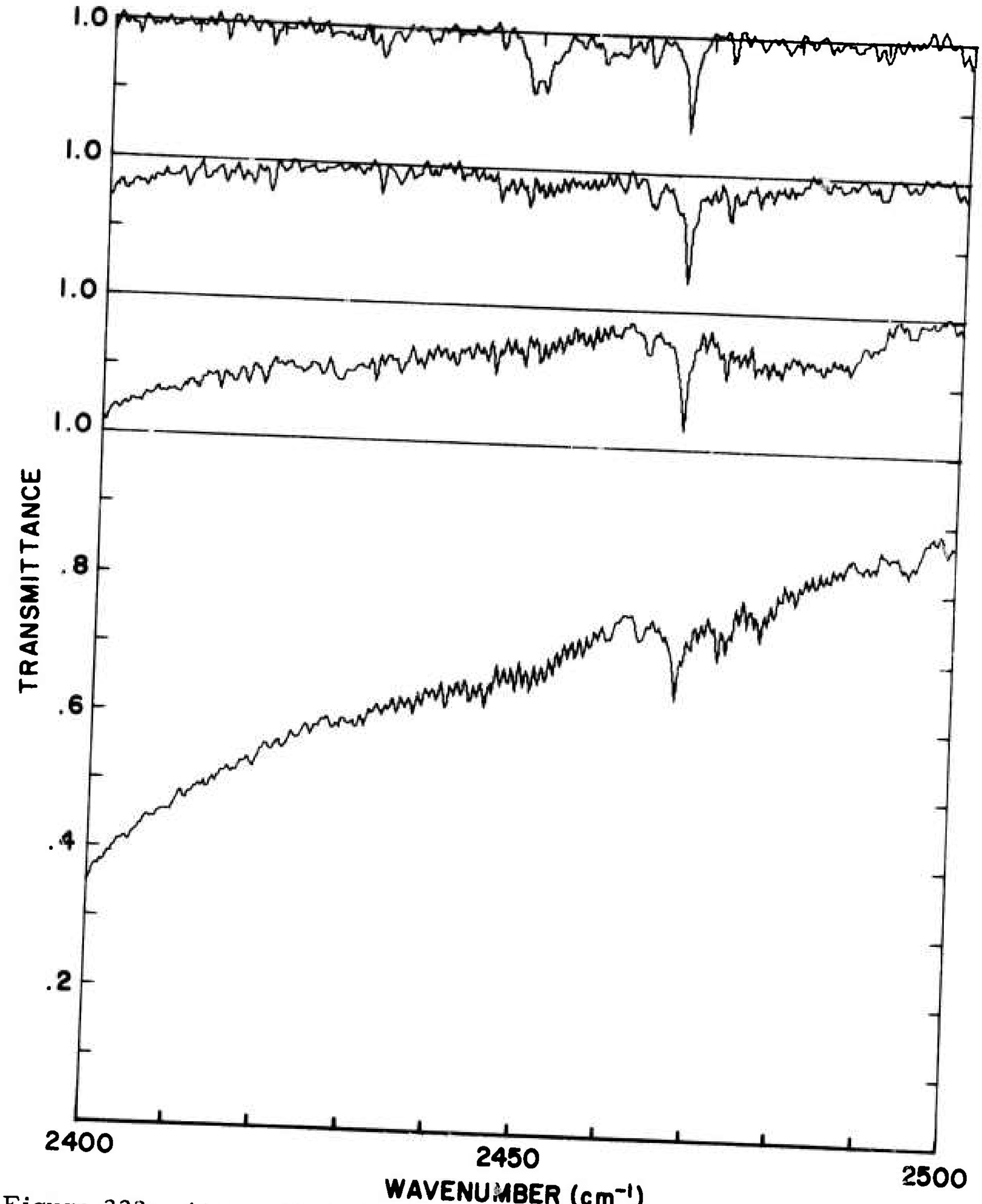

Figure 222. Atmospheric transmittance vs wavenumber at 5.8, 27.6, 42.1 and 68.6 kft with the lowest altitude on the bottom and 0.2 offset in transmittance between each spectrum.

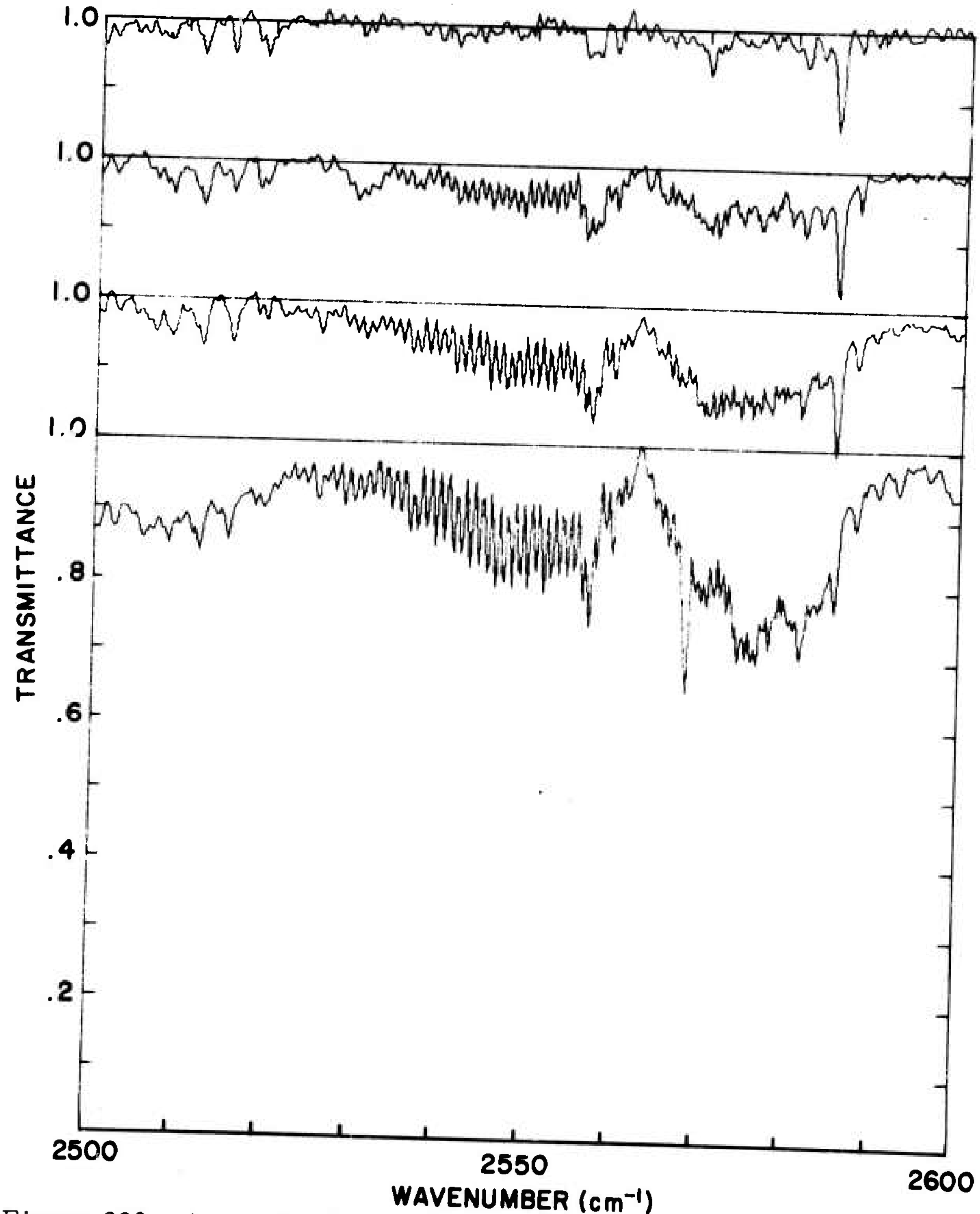

Figure 223. Atmospheric transmittance vs wavenumber at 5.8, 27.6, 42.1 and 68.6 kft with the lowest altitude on the bottom and 0.2 offset in transmittance between each spectrum.

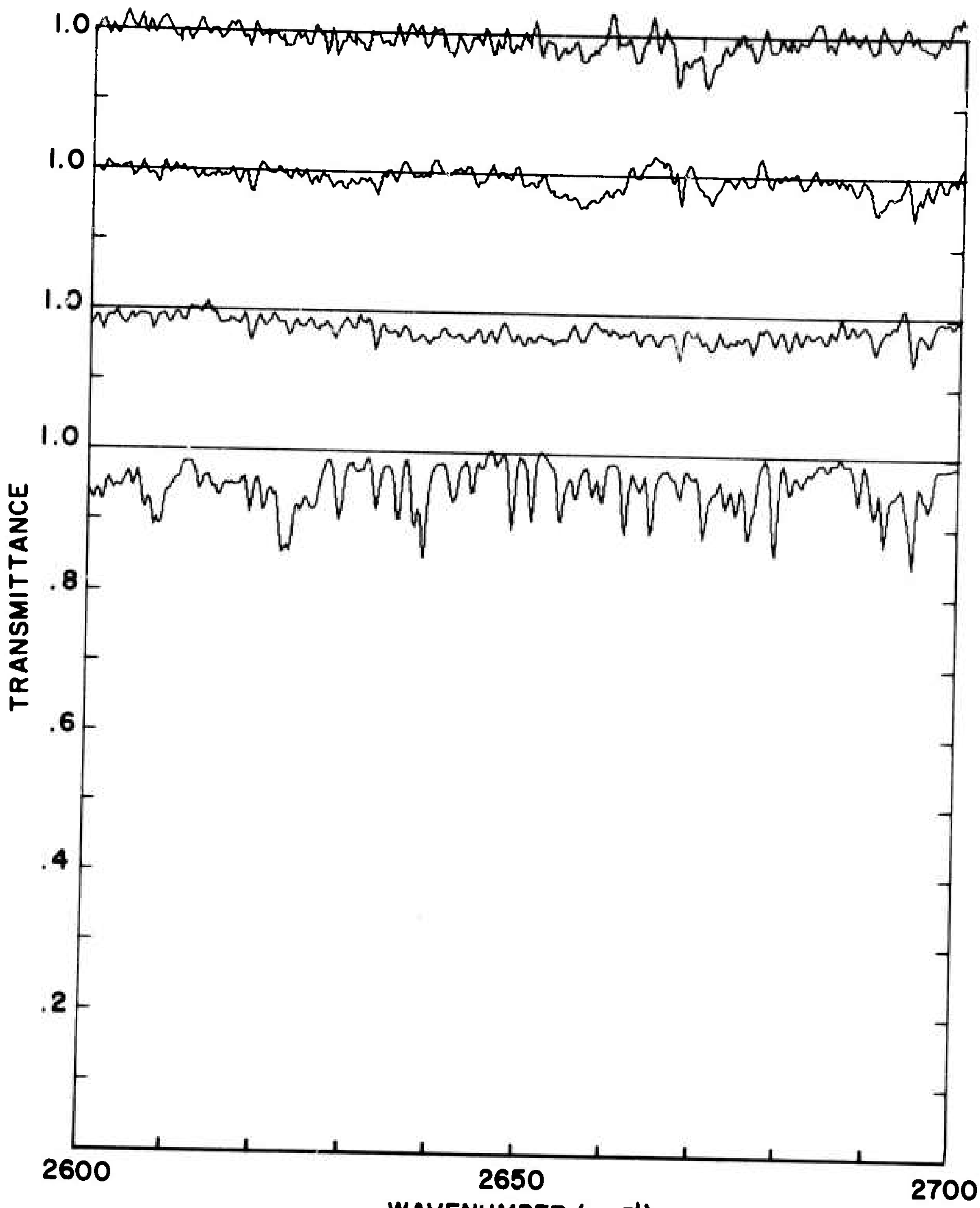

Figure 224. Atmospheric transmittance vs wavenumber at 5.8, 27.6, 42.1 and 68.6 kft with the lowest altitude on the bottom and 0.2 offset in transmittance between each spectrum.

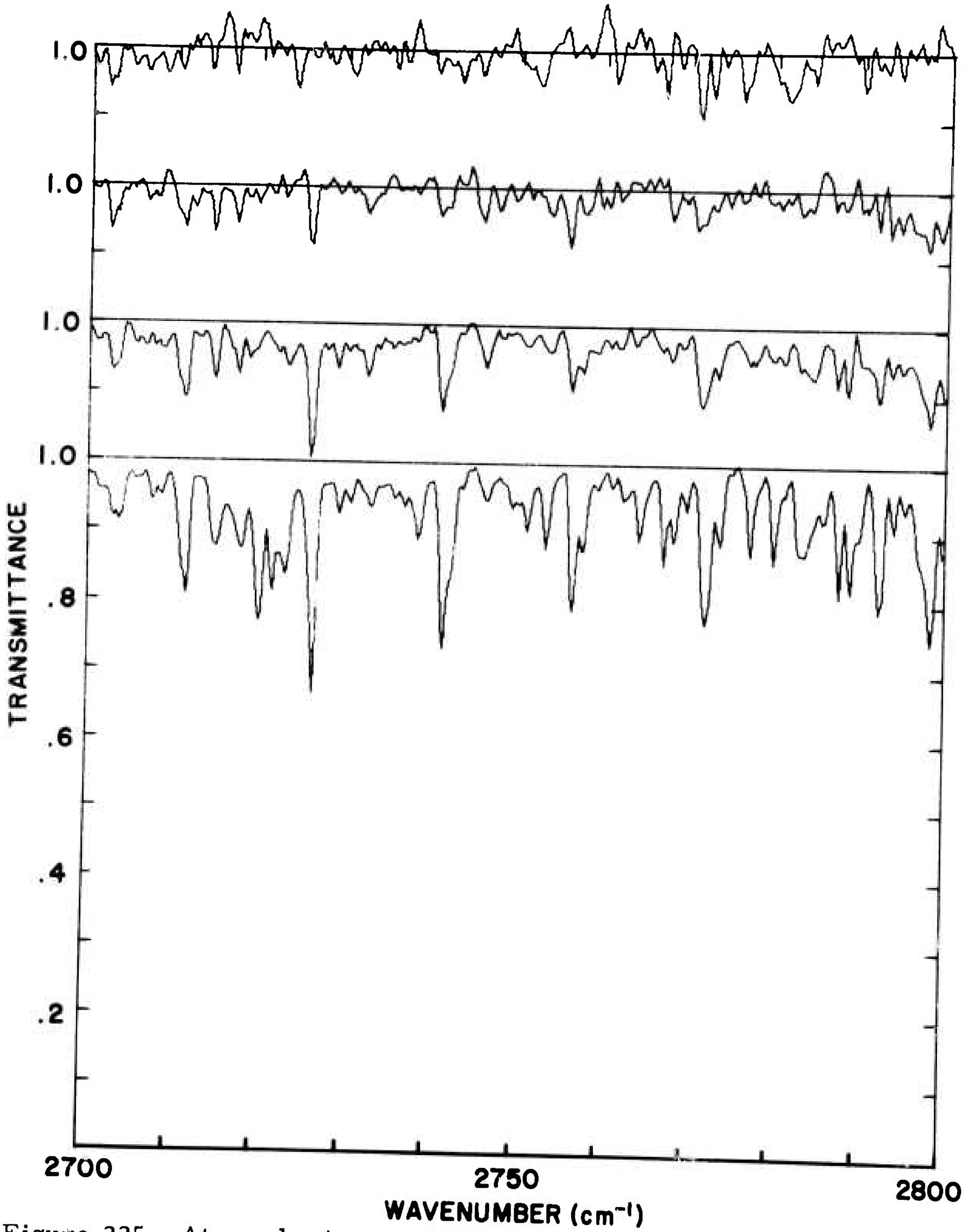

Figure 225. Atmospheric transmittance vs wavenumber at 5.8, 27.6, 42.1 and 68.6 kft with the lowest altitude on the bottom and 0.2 offset in transmittance between each spectrum.

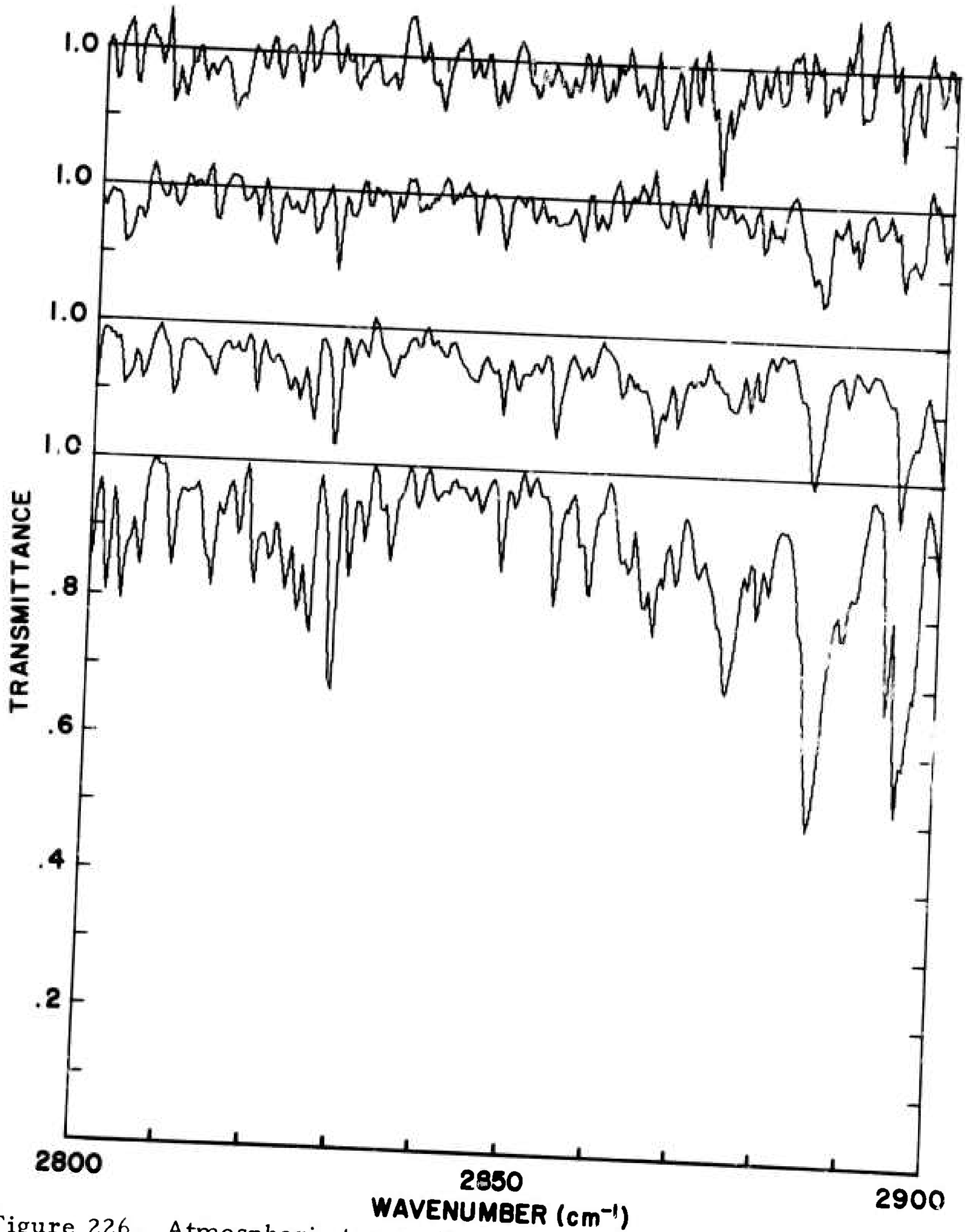

Figure 226. Atmospheric transmittance vs wavenumber at 5.8, 27.6, 42.1 and 68.6 kft with the lowest altitude on the bottom and 0.2 offset in transmittance between each spectrum.

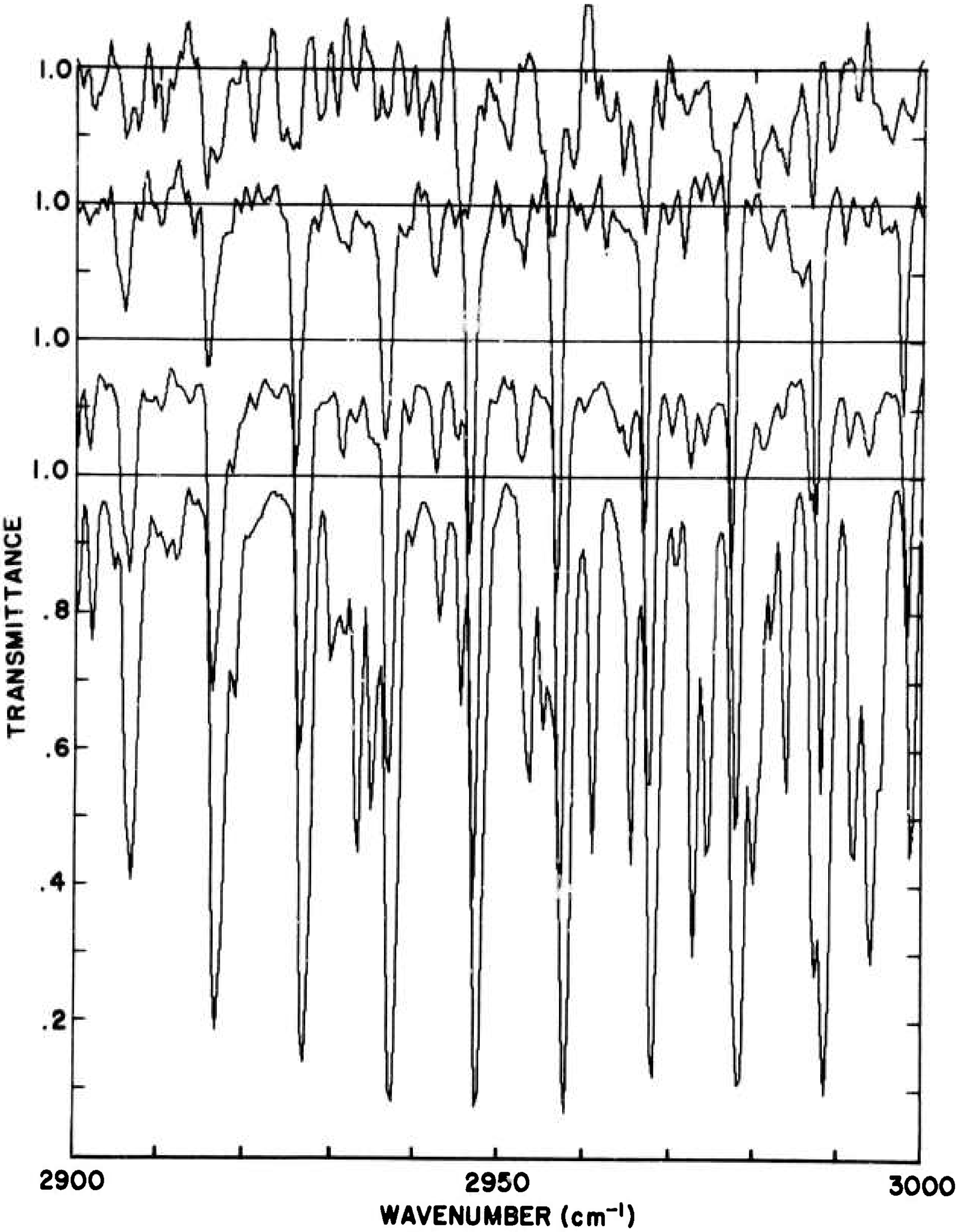

Figure 227. Atmospheric transmittance vs wavenumber at 5.8, 27.6, 42.1 and 68.6 kft with the lowest altitude on the bottom and 0.2 offset in transmittance between each spectrum.

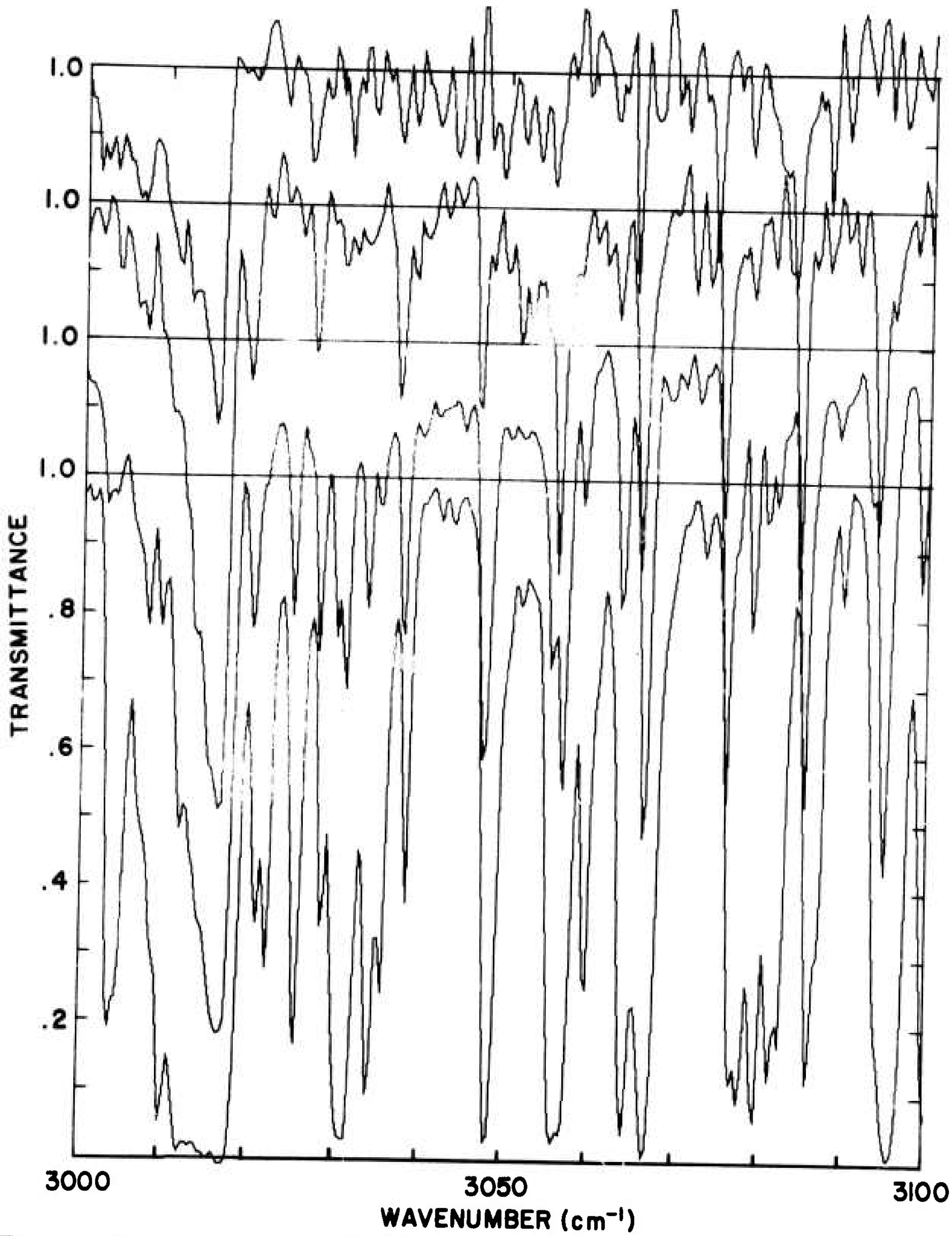

Figure 228. Atmospheric transmittance vs wavenumber at 5.8, 27.6, 42.1 and 68.6 kft with the lowest altitude on the bottom and 0.2 offset in transmittance between each spectrum.

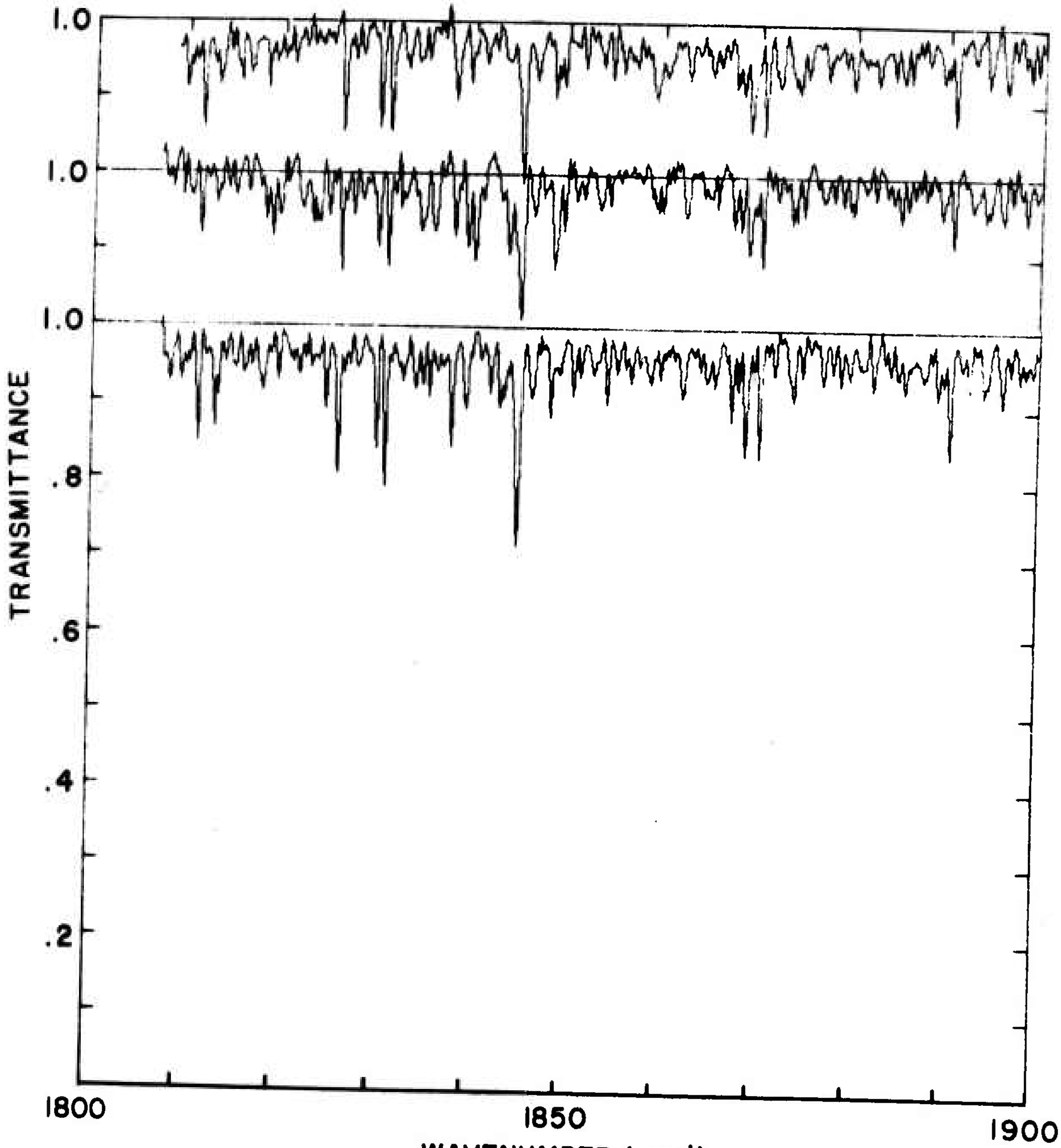

Figure 229. Atmospheric transmittance vs wavenumber near 100 kft for Zenith angles from top to bottom of 78.9, 83.3 and 89.2 with 0.2 offset in transmittance between each spectrum.

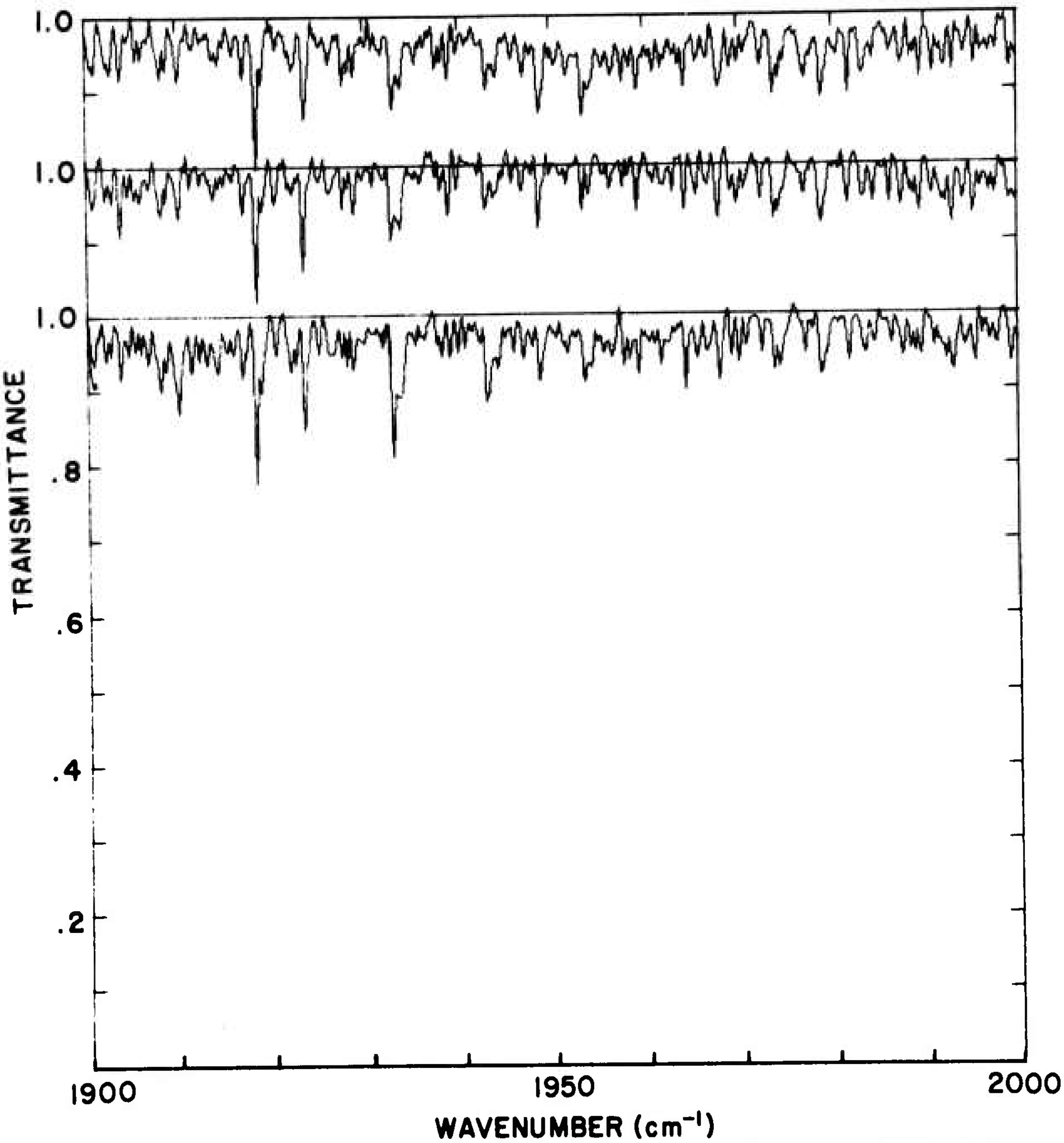

Figure 230. Atmospheric transmittance vs wavenumber near 100 kft for Zenith angles from top to bottom of 78.9, 83.3 and 89.2 with 0.2 offset in transmittance between each spectrum.

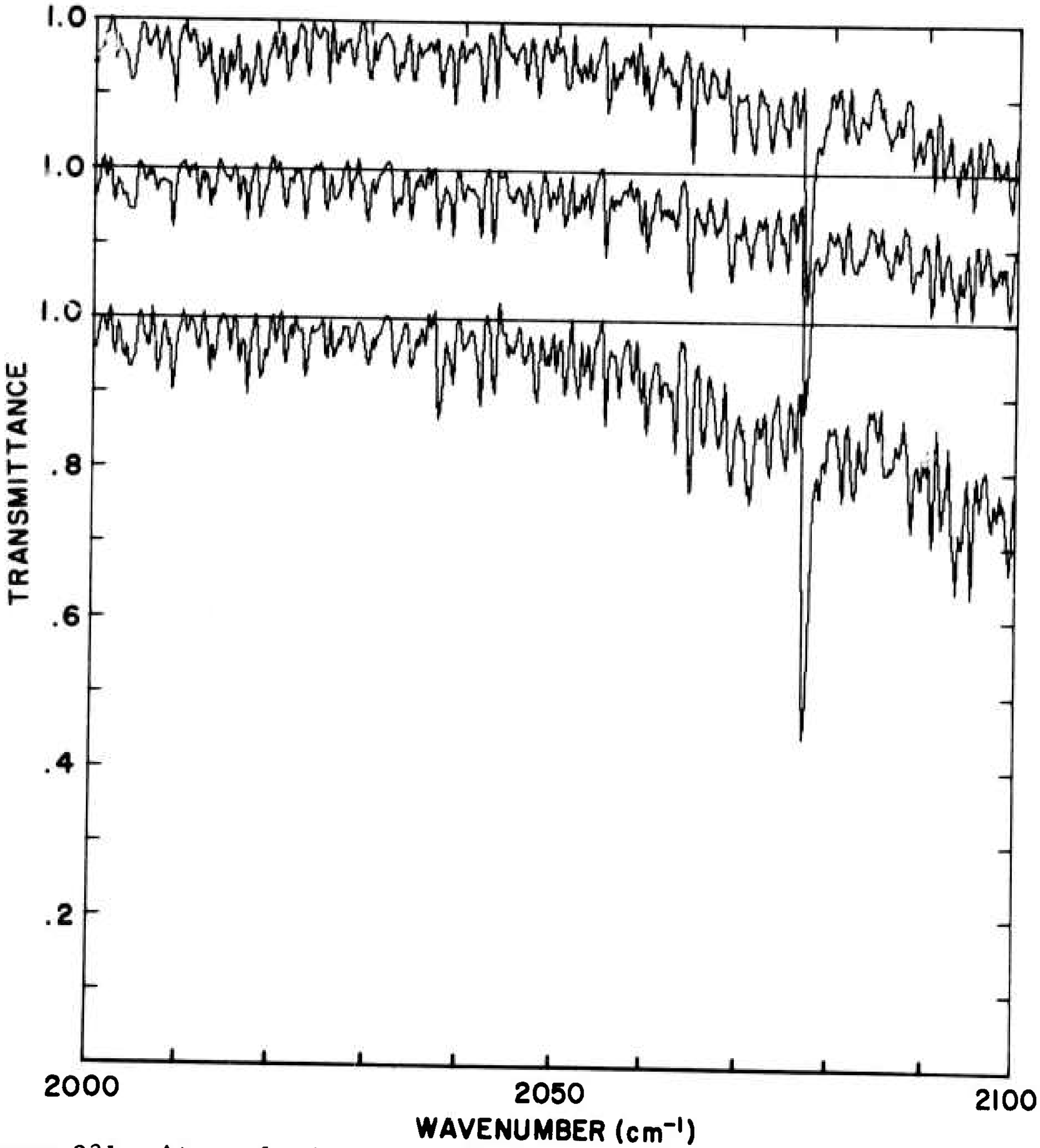

Figure 231. Atmospheric transmittance vs wavenumber near 100 kft for Zenith angles from top to bottom of 78.9, 83.3 and 89.2 with 0.2 offset in transmittance between each spectrum.

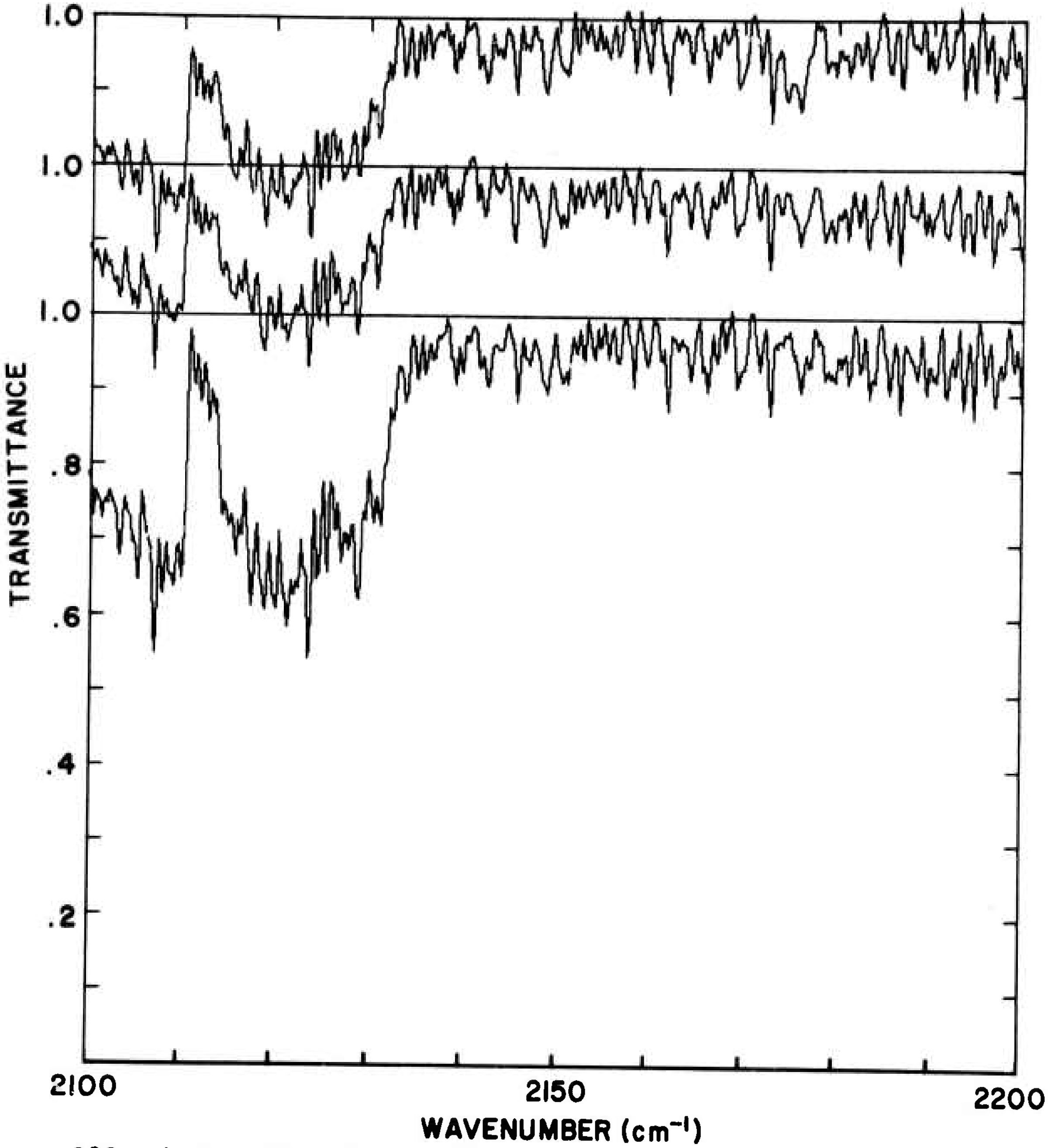

Figure 232. Atmospheric transmittance vs wavenumber near 100 kft for Zenith angles from top to bottom of 78.9, 83.3 and 89.2 with 0.2 offset in transmittance between each spectrum.

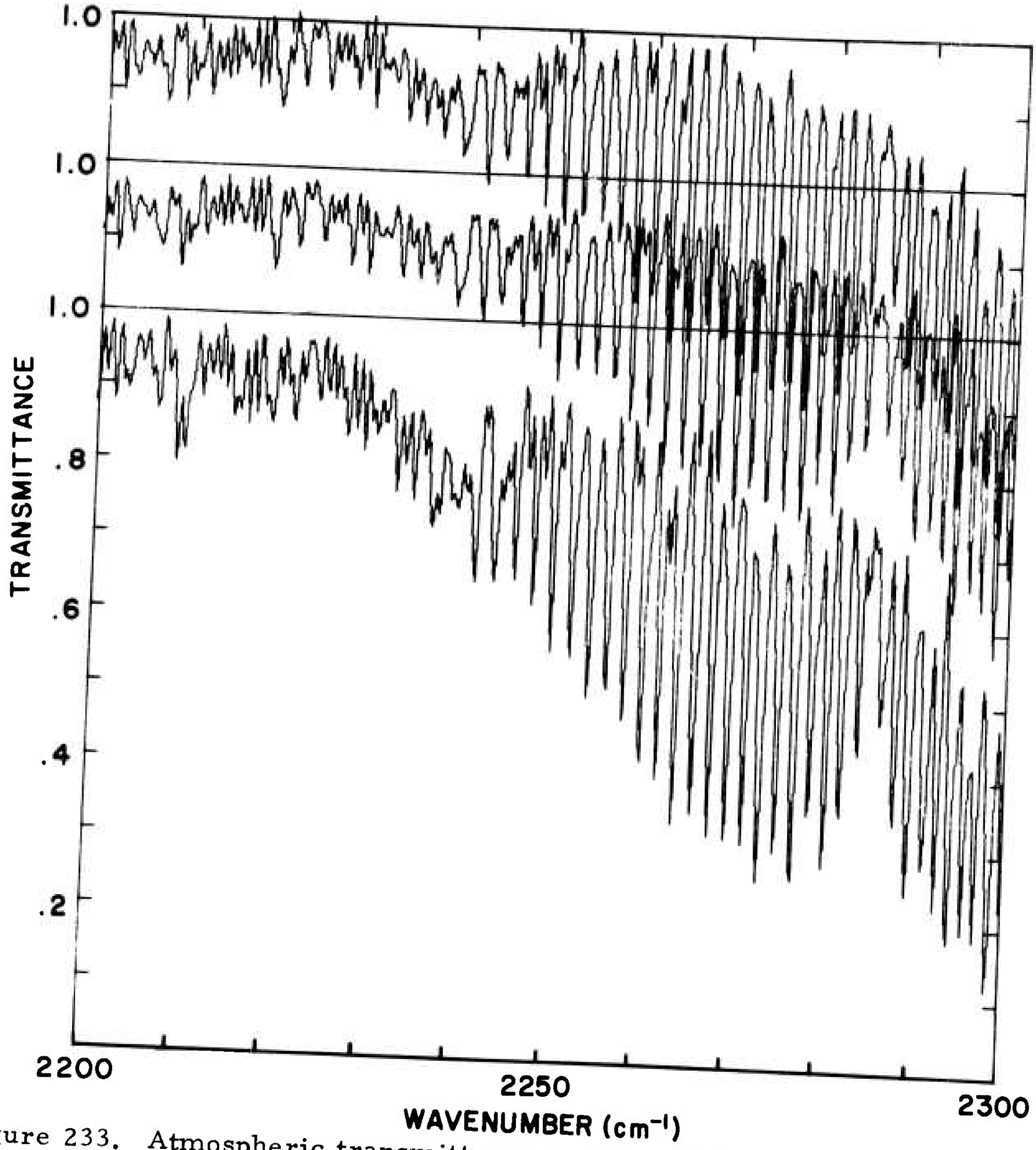

Figure 233. Atmospheric transmittance vs wavenumber near 100 kft for Zenith angles from top to bottom of 78.9, 83.3 and 89.2 with 0.2 offset in transmittance between each spectrum.

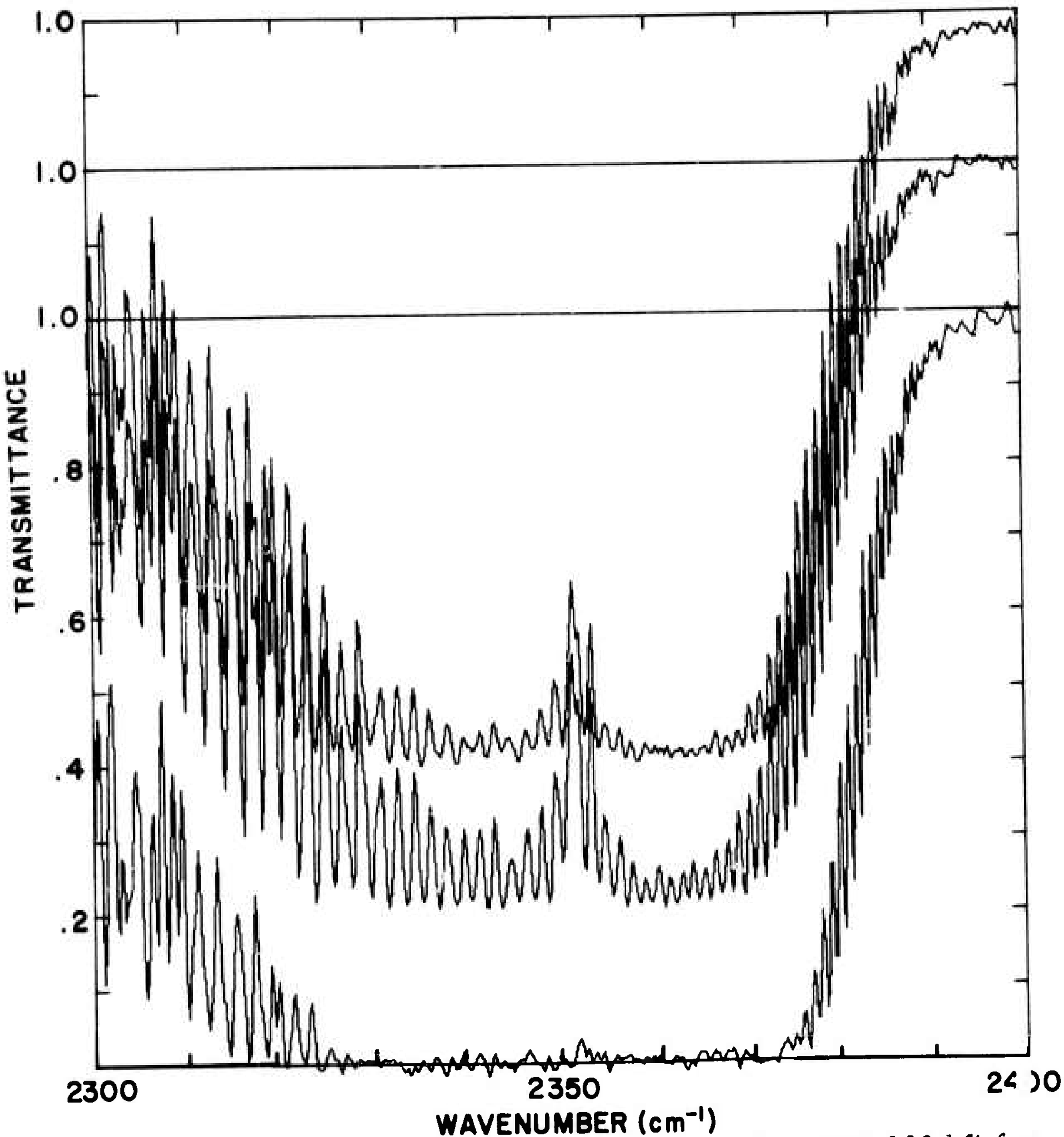

Figure 234. Atmospheric transmittance vs wavenumber near 100 kft for Zenith angles from top to bottom of 78.9, 83.3 and 89.2 with 0.2 offset in transmittance between each spectrum.

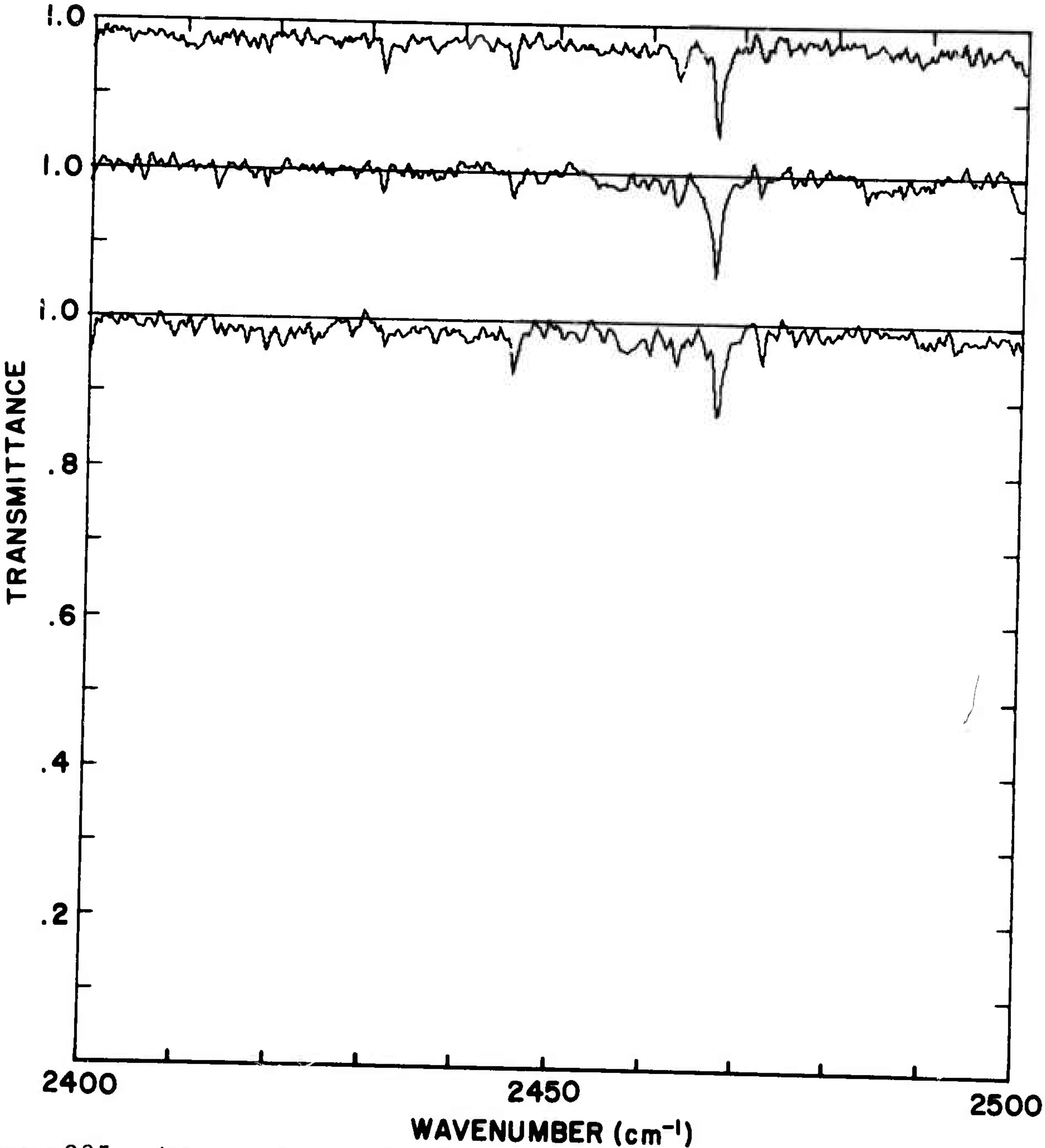

Figure 235. Atmospheric transmittance vs wavenumber near 100 kft for Zenith angles from top to bottom of 78.9, 83.3 and 89.2 with 0.2 offset in transmittance between each spectrum.

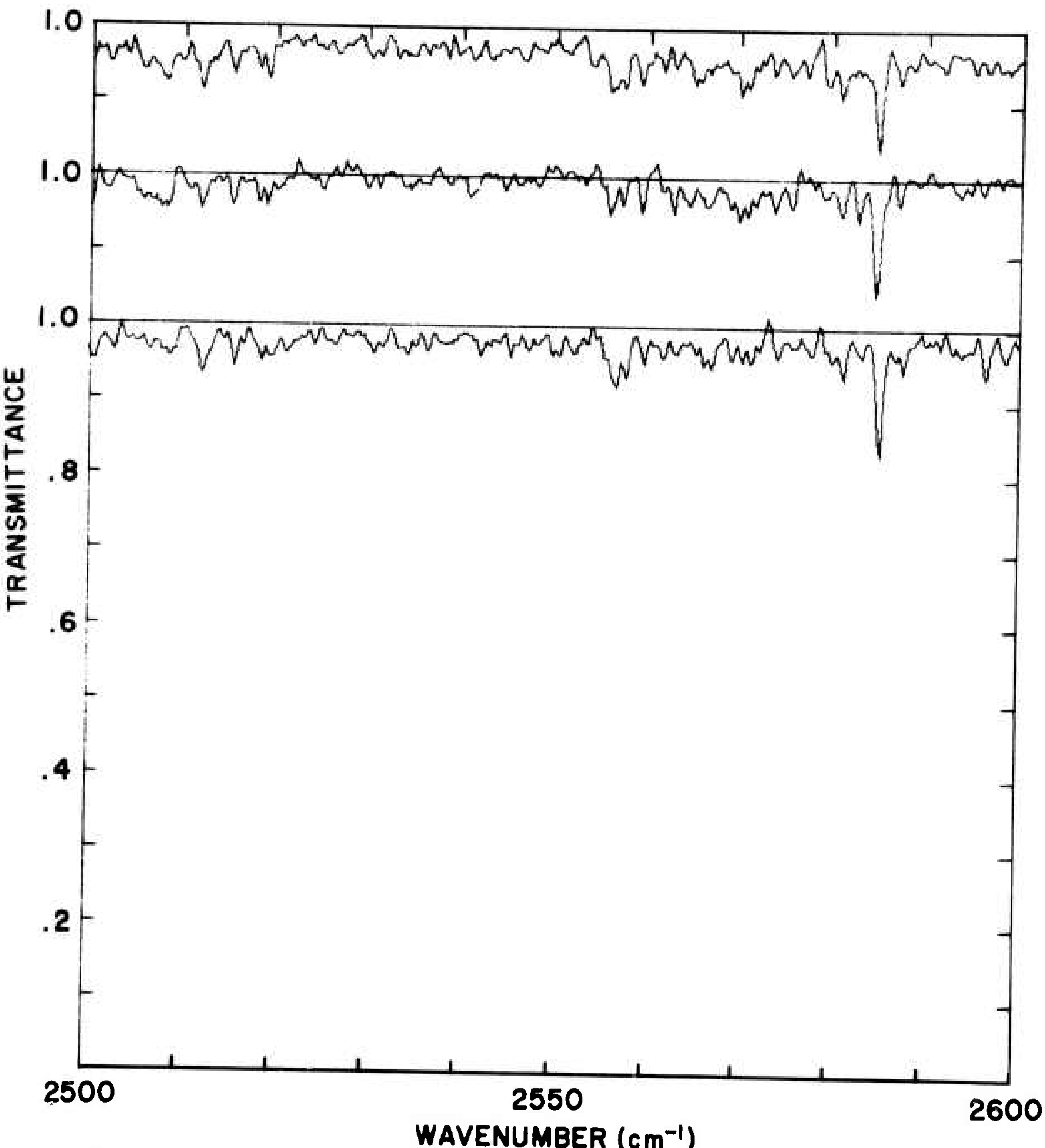

Figure 236. Atmospheric transmittance vs wavenumber near 100 kft for Zenith angles from top to bottom of 78.9, 83.3 and 89.2 with 0.2 offset in transmittance between each spectrum.

Unclassified
Security Classification

DOCUMENT CONTROL DATA - R & D

(Security classification of title, body of abstract and indexing annotation must be entered when the overall report is classified)

1. ORIGINATING ACTIVITY (Corporate author) University of Denver Department of Physics Denver, Colorado 80210	2a. REPORT SECURITY CLASSIFICATION Unclassified 2b. GROUP

3. REPORT TITLE

ATMOSPHERIC EMISSION AT HIGH LATITUDES

4. DESCRIPTIVE NOTES (Type of report and inclusive dates)
Scientific Final: 1 April 1971 to 1 April 1972. Approved 13 July 1972

5. AUTHOR(S) (First name, middle initial, last name)
David G. Murcray, D. Boyd Barker, James N. Brooks, John J. Kosters, Frank H. Murcray, Walter J. Williams

6. REPORT DATE	7a. TOTAL NO. OF PAGES	7b. NO. OF REFS
June 1972	258	1

8a. CONTRACT OR GRANT NO. F19628-71-C-0171 ARPA No. 1366	9a. ORIGINATOR'S REPORT NUMBER(S)
b. PROJECT NO. 8692 Task # n/a Work Unit # n/a	
c. DoD Element 62301D	9b. OTHER REPORT NO(S) (Any other numbers that may be assigned this report)
d. DoD Subelement n/a	AFCRL-72-0353

10. DISTRIBUTION STATEMENT
B-Distribution limited to U.S. Government agencies only; Test and Evaluation, 11 July 1972. Other requests for this document must be referred to AFCRL(OPI) L.G. Hanscom Field, Bedford, Massachusetts 01730

11. SUPPLEMENTARY NOTES This research was supported by the Defense Advanced Research Projects Agency	12. SPONSORING MILITARY ACTIVITY Air Force Cambridge Research Lab (OP) L.G. Hanscom Field Bedford, Massachusetts 01730

13. ABSTRACT

The primary emphasis under this contract has been to obtain infrared emission measurements during known auroral activity. Three balloon flights were made from Fairbanks, Alaska to accomplish this. On two of these flights moderate auroral activity occurred, but there was no enhancement in the emission spectrum from 9-14μm. The time of night that these measurements were made was several hours earlier than the time when observations of enhanced infrared emission were made on 13 September 1969.

A total of six balloon flights was conducted during the contract period. Data from four of these flights is presented in this report and a summary of the data reports covering the other two flights is also included.

DD FORM 1 NOV 65 1473

Unclassified
Security Classification

Unclassified

Security Classification

14. KEY WORDS	LINK A		LINK B		LINK C	
	ROLE	WT	ROLE	WT	ROLE	WT
Infrared Aurora						
Atmospheric Emission						
Atmospheric Transmittance						

Security Classification